eCAM Evidence-Based Complementary and Alternative Medicine

Chemical Basis of Traditional Medicines and New Potential Applications

Guest Editors: Chunlin Long, Shi-Biao Wu, and William C. S. Cho

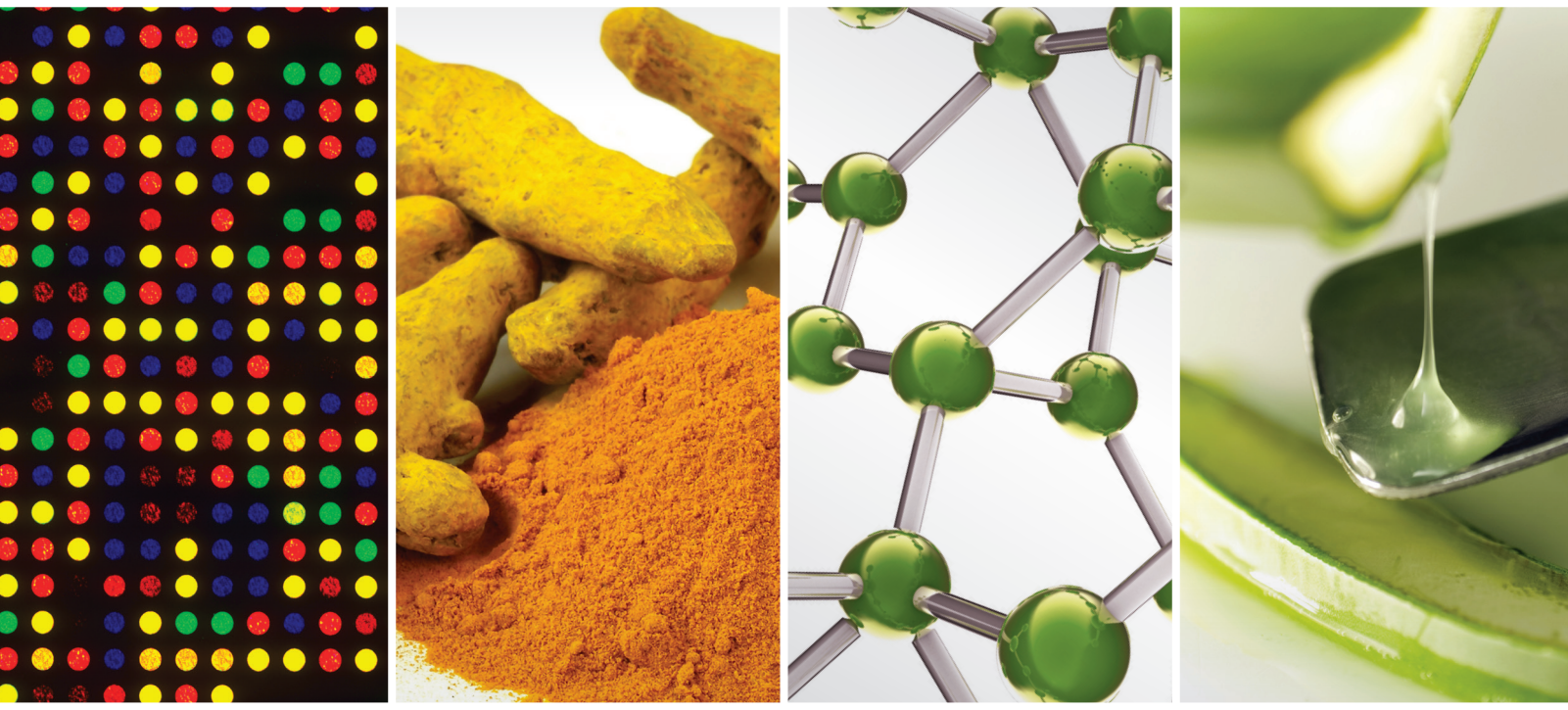

Chemical Basis of Traditional Medicines and New Potential Applications

Evidence-Based Complementary
and Alternative Medicine

Chemical Basis of Traditional Medicines and New Potential Applications

Guest Editors: Chunlin Long, Shi-Biao Wu,
and William C. S. Cho

Editorial Board

Contents

Hindawi Publishing Corporation
Evidence-Based Complementary and Alternative Medicine
Volume 2014, Article ID 723502, 2 pages
http://dx.doi.org/10.1155/2014/723502

Editorial

Chemical Basis of Traditional Medicines and New Potential Applications

Chunlin Long,[1,2] Shi-Biao Wu,[3] and William C. S. Cho[4]

[1] *College of Life and Environmental Sciences, Minzu University of China, Beijing 100081, China*
[2] *Kunming Institute of Botany, Chinese Academy of Sciences, Kunming 650201, China*
[3] *Department of Biological Sciences, Lehman College, The City University of New York, Bronx, NY 10468, USA*
[4] *Department of Clinical Oncology, Queen Elizabeth Hospital, Kowloon, Hong Kong*

Correspondence should be addressed to Chunlin Long; long@mail.kib.ac.cn

Received 12 October 2014; Accepted 12 October 2014; Published 21 December 2014

Traditional medicines such as Chinese medicine, Ayurveda, Unani, and ethnomedicines have globally been practiced by billions of people for many centuries. In the rural areas of developing countries, traditional medicine is often the only accessible and affordable treatment available. Even in developed countries the use of traditional medicine is gaining popularity, where western medicine is generally available. In Asian and African countries, 80% populations depend on traditional medicines for primary health care according to the World Health Organization. A lot of famous pharmaceutical drugs are derived from traditional medicines (e.g., artemisinin from traditional Chinese medicine *Artemisia annua*). Plants, animals, microbes, and minerals used in traditional medicines are enormous. Only the species number of traditionally used medicinal plants was estimated to be between 10,000 and 53,000.

Although studies on traditional medicines have become a popular research trend worldwide, only a very small proportion of traditional medicines had been investigated focusing on their chemical components and biological activities. There are still a huge number of traditional medicinal species which are not investigated chemically. For the tropical plant species, for example, only 1% of them had been screened. As for the polypharmaceuticals with more than two species, especially in traditional Chinese medicine, less chemical studies had been completed. They are being used by millions of people every day. Therefore, further investigations of chemical basis of traditional medicines will be necessary and urgent. It will be also very important in the future to gain a better understanding of the chemical basis of these traditional medicines, demonstrate their activity, understand their mechanism of action, develop new potential applications, and discover new drugs based on the studies of traditional medicines.

We received more than 30 papers after the call for papers was released in October 2013. Finally, only 18 high-quality peer-reviewed papers were included in this special issue. In addition to one review article, 17 papers are original research articles.

The traditional medicinal plants are often selected for pharmacological studies, followed by isolation and identification of their chemical constituents. In this special issue, some plants are famous traditional herbal medicines such as *Panax notoginseng*, *Angelica sinensis*, *Carthamus tinctorius*, and *Oldenlandia diffusa* (*Hedyotis diffusa*). Some are less well-known but important in local ethnic communities (e.g., *Selaginella moellendorffii*, *Elephantopus scarber*, *Melastoma malabathricum, Dicranostigma leptopodum*, and *Rabdosia japonica* var. *glaucocalyx*). Besides the medicinal plants, other natural medicinal sources, such as Czech propolis, have also been included in this issue.

Whether the processed or prepared medicines (e.g., Chinese traditional patent medicine and Chinese medicinal formula) are mixed with other materials or not demonstrated different biological activities from their original herbs. Their chemical basis and mechanism of action should be revealed. Paeoniae Radix (processed roots of *Paeonia lactiflora*),

Fuzheng Fangai pill (composed of *Codonopsis pilosula*, *Astragalus,* and other 4 species), Tianshu capsule (composed of *Ligusticum chuanxiong* and *Gastrodia elata*), and Sihuangxiechai decoction (composed of *Astragalus* and other 15 species) are included in this special issues. The research results pharmacologically supported their customary uses of these traditional medicines.

It is impressive to note that an important traditional medicinal plant, Huangqi (*Astragalus mongholicus* and/or *A. membranaceus*), appeared in 4 papers in this issue (L. Shi et al., Y. Gao et al., S. Liu et al., and X. P. Huang et al.). Both its secondary metabolites and polysaccharide showed multiple pharmacological activities such as immunomodulatory and neuroprotective effects, anti-inflammation, and antivirus. Further studies on Huangqi may endow this traditional medicine with more new potential applications.

Jatropha is ethnobotanically and ethnopharmacologically an important group in Euphorbiaceae, including *J. curcas* and *J. gossypiifolia*. To compare with other *Jatropha* species, few studies have isolated chemical compounds from *J. gossypiifolia*. However, it should be prioritized for bioprospecting.

We believe that this special issue will provide readers with ideas and information in the fields of traditional medicines. Because of the great diversity of traditional medicines, the chemical basis and biological activity should be massively investigated in next decades so as to examine the safety, action mechanisms, new applications, and development potentials of traditional medicines.

Chunlin Long
Shi-Biao Wu
William C. S. Cho

Hindawi Publishing Corporation
Evidence-Based Complementary and Alternative Medicine
Volume 2014, Article ID 580745, 11 pages
http://dx.doi.org/10.1155/2014/580745

Research Article

Chemical Profiling of an Antimigraine Herbal Preparation, Tianshu Capsule, Based on the Combination of HPLC, LC-DAD-MS^n, and LC-DAD-ESI-IT-TOF/MS Analyses

Juanjuan Liang,[1,2] Huimin Gao,[1,2] Liangmian Chen,[1,2] Wei Xiao,[3] Zhenzhong Wang,[3] Yongyan Wang,[1] and Zhimin Wang[1,2]

[1] *Institute of Chinese Materia Medica, China Academy of Chinese Medical Sciences, Beijing 100700, China*
[2] *National Engineering Laboratory for Quality Control Technology of Chinese Herbal Medicine, Beijing 100700, China*
[3] *Jiangsu Kanion Pharmaceut Co. Ltd., Lianyungang 222001, China*

Correspondence should be addressed to Huimin Gao; huimin_gao@126.com and Zhimin Wang; zhmw123@263.net

Received 17 April 2014; Revised 28 June 2014; Accepted 30 June 2014; Published 20 July 2014

Academic Editor: Shi-Biao Wu

Chemical profiling is always the first task in the standardization and modernization of Traditional Chinese Medicine. HPLC and LC-MS were employed to find out the common chromatographic peaks in various batches of Tianshu Capsule (TSC) and the contribution of the characteristic peaks from individual herbs to the whole chromatographic profile of TSC sample. A total of 38 constituents were identified in TSC sample based on the comparison of retention time and UV spectra with authentic compounds as well as by summarized MS fragmentation rules and matching of empirical molecular formula with those of published components. This is the first systematic report on the chemical profiling of the commercial TSC product, which provides the sufficiently chemical evidence for the global quality evaluation of TSC products.

1. Introduction

Traditional Chinese Medicine (TCM) is getting more attention all over the world due to its exact clinical practice, especially prescription application, which comprehensively highlights the quintessence of the theory of traditional Chinese medical science. *Da Chuan Xiong Fang* (DCXF), a well-known and extensively used TCM decoction for the treatment of migraine, first appeared in *Xuan Ming Lun Fang,* a famous formula book written by Wansu Liu who lived in Jin Dynasty (1115–1234). It is composed of two herbs, namely, Chuanxiong (*Chuanxiong rhizoma*) and Tianma (*Gastrodiae rhizoma*), with a crude weight ratio of 4 : 1. Eight dosage forms of DCXF such as capsule, tablet, dripping-pill, honeyed pill, oral liquid, and granule, have been authorized to Chinese market. Tianshu Capsule (TSC), as a representative of DCXF preparations, is widely used in clinics for treating the blood stasis type of headache and migraine [1, 2].

Phytochemical and pharmacological investigations showed that phenols, organic acids, phthalides, and nitrogen-containing compounds were the major active ingredients of DCXF [3]. Several qualitative analyses have been reported concerning main types of constituents in DCXF [4–7]. One study described the identification of 17 different constituents in the 50% EtOH extract of DCXF by LC-Q-TOF/MS, containing gastrodin, parishin C, ferulic acid, guanosine, adenosine, palmitic acid, and 11 phthalide compounds [4]. Another similar study identified 3 compounds of Chuanxiong (ferulic acid, senkyunolide I, and senkyunolide H) and 8 constituents of Tianma (gastrodin, s-(4-hydroxybenzyl)-glutathione, parishin, parishin B, parishin C, p-hydroxybenzaldehyde, etc.) by using the HPLC-DAD-MS^n coupling technique, respectively [5]. Continuous reports from the second research group confirmed that 10 different compounds, including 6 original substances of Chuanxiong and 4 original ones of Tianma,

were detected in the rat plasma after the gavage of DCXF active components [6, 7]. However, all these investigations mentioned above were carried out based on the samples of the 50% EtOH extract of the mixture of both herbs (4 : 1) or active components of single crude herb. No systematic reports could be available involving the chemical profiling of the commercial finished products derived from DCXF. TSC was produced from both crude herbs by employing the various pharmaceutical engineering technologies and the complex manufacturing processes such as extraction, concentration, and preparation. The accumulating studies showed that decocting could induce chemical changes of medicinal herbs or combinatorial formula [8]. It is well-known that ferulic acid and some of the phthalides such as *Z*-ligustilide and dimeric phthalide are unstable at high temperature [9, 10]. Therefore, during the preparation of TSC, these thermolabile components may undertake chemical transformation, consequently leading to the difference of chemical compositions of finished products with DCXF decoction. Understanding the chemical profiles of TSC samples would be helpful in selecting suitable chemical markers for the quality control and pharmacokinetic study. In this work, a combination of HPLC, LC-DAD-MS^n, and LC-DAD-ESI-IT-TOF/MS analyses was employed to find out and identify the common components in various batches of commercial TSC samples. The contribution of the characteristic peaks from individual herb to the whole chemical profiling of TSC was also discussed. A total of 38 constituents were identified or tentatively characterized, among which the water-soluble compounds with higher polarity from *Gastrodiae rhizoma* are detected in TSC samples for the first time.

2. Materials and Methods

2.1. Materials and Reagents. Five batches of Tianshu Capsules and related crude herbal materials (*Chuanxiong rhizoma and Gastrodiae rhizoma*) were provided by *Kanion Pharmaceutical* (Lianyungang, China). The reference substances of gastrodin (Lot. 110807-200205), 5-hydroxymethyl-2-furfural (5-HMF, Lot. 111626-201007), ferulic acid (Lot. 0773-9607), and *Z*-ligustilide (Lot. 111737-201102) were purchased from the National Institutes for Food and Drug Control (Beijing, China). Parishin B (174972-79-3), parishin C (174972-80-6), and parishin (62499-28-9) were from the collection of Dr. Li Wang, Dalian Institute of Chemical Physics, Chinese Academy of Sciences (Dalian, China). The purity for each of these compounds was over 98% by HPLC assay and their structures were shown in Figure 1. HPLC grade methanol (Fisher, Fair Lawn, NJ, USA) and ultrapure water were used for HPLC analyses. All other chemical reagents were of analytical grade from Beijing Chemical Corporation (Beijing, China).

2.2. Sample Preparation

2.2.1. TSC Sample. 1.0 g of pulverized contents of TSC samples was extracted with aqueous methanol (MeOH-H_2O, 1 : 1, 25 mL) by ultrasonication (250 w, 40 kHz) for 30 min at room temperature, and the extract was then centrifuged for 10 min at 14800 rpm. A volume of 10 μL of the supernatant was used for HPLC and LC-DAD-MS^n analysis.

2.2.2. Extraction of Chuanxiong Rhizoma, Gastrodiae Rhizoma, and DCXF. The ethanolic and aqueous extracts of individual herb (*Chuanxiong rhizoma* and *Gastrodiae rhizoma*) and the mixture of both herbs (w/w, 4 : 1, DCXF) were prepared according to the manufacturing processes of TSC (Figure S1 in the Supplementary Material available online at http://dx.doi.org/10.1155/2014/580745) described in the current Chinese pharmacopoeia. The ethanolic and aqueous extracts were diluted with aqueous methanol (MeOH-H_2O, 1 : 1) to the concentration of 0.05 g·mL^{-1} and then centrifuged for 10 min at 14800 rpm. Each of the supernatants was used for HPLC and LC-MS analyses.

2.2.3. Reference Solution. Stock solutions with a concentration of about 0.010 mg·mL^{-1} were prepared by dissolving an accurately weighed amount of each reference substance in aqueous methanol (MeOH-H_2O, 1 : 1). The mixture of 7 reference solutions was prepared from the stock solutions.

2.3. Qualitative HPLC Analyses of 5 Batches of TSC Samples. The analyses were performed on a Shimadzu HPLC system (Shimadzu, Japan) equipped with a LC-20AT binary pump, a DGU-20A5 degasser, a SIL-20AC autosampler, a CTO-20AC column oven, and a SPD-M20A photodiode array detector. The samples were separated on a Phenomenex Luna C_{18} column (5 μm, 4.6 × 250 mm). The mobile phase consisted of methanol (A) and water containing 0.1% formic acid (B) using a gradient program as follows: 0 min, 15% A; 5 min, 15% A; 55 min, 95% A; 60 min, 95% A. The flow rate was 1.0 mL·min^{-1} and the column temperature was set at 30°C. The PDA detector recorded UV spectra in the range from 190 nm to 400 nm and HPLC chromatogram was monitored at 276 nm.

2.4. Comparison of Typical TSC Sample and Its Related Crude Herbal Materials as Well as DCXF by HPLC and LC-MS. TSC sample and its related crude herbal material, *Chuanxiong rhizoma* and *Gastrodiae rhizoma* as well as DXCF, were analyzed under the same chromatographic conditions by HPLC and LC-MS to find the contribution of individual herb to the whole chemical profile of TSC sample. The HPLC system was the same as those in Section 2.3. LC-MS analyses were performed using an Agilent 6130 Quadrupole LC-MS (Agilent, Waldbronn, Germany) connected to an Agilent 1200 HPLC system (Agilent, Waldbronn, Germany). The parameters for MS analysis in the positive and negative ion mode were as follows: nebulizer, 35 psi; ionization voltage, 3500 V; dry temperature, 350°C; flow rate of carrier gas, 9.0 L·min^{-1}. Full-scan mass spectra were acquired in the range of 100–800 *m/z*.

2.5. LC-DAD-ESI-IT-MS^n Analysis of Typical TSC Sample. To comprehensively identify the chemical constituents in

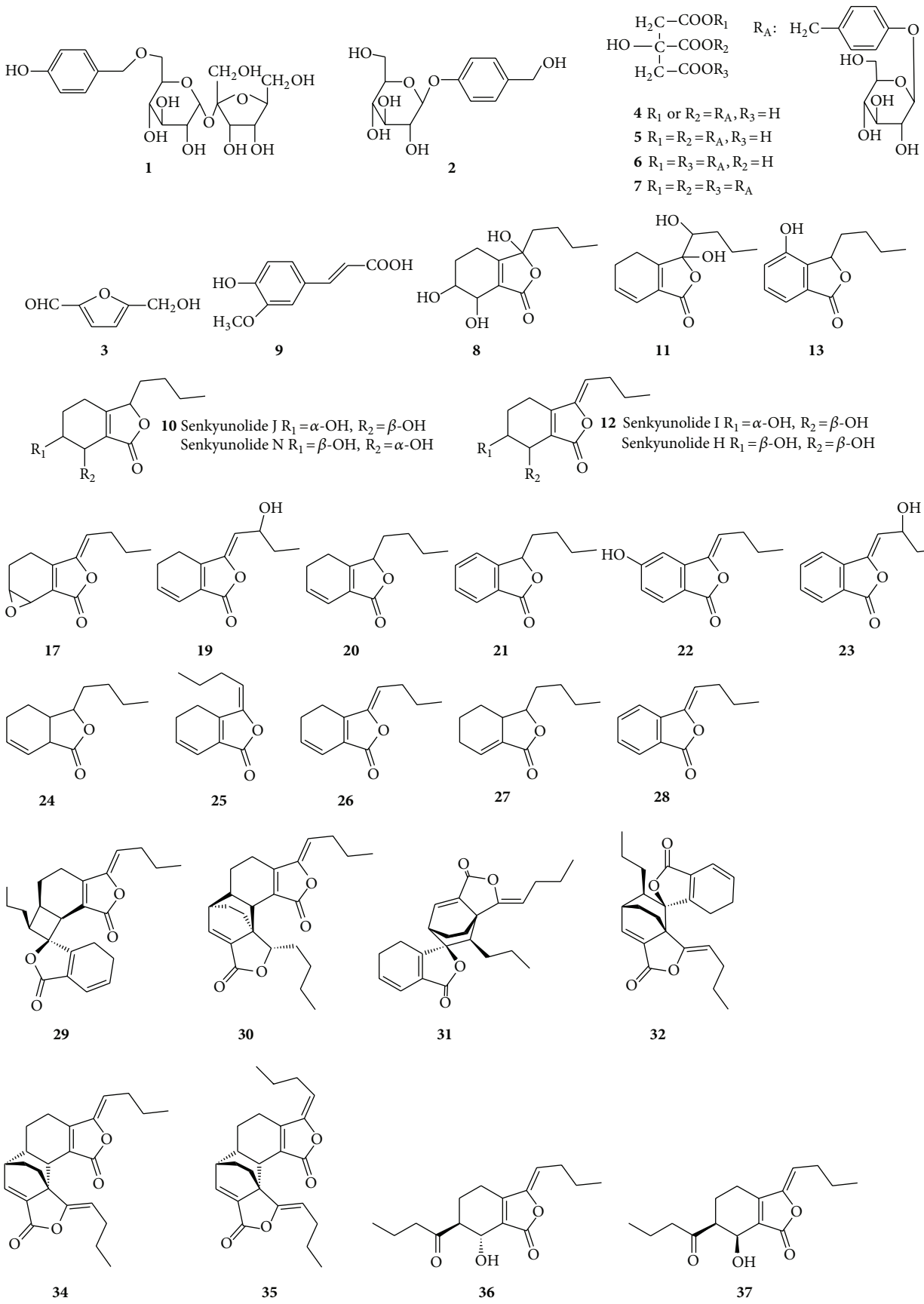

Figure 1: The structures of the identified compounds in TSC sample.

TSC sample by the fragmentation rules, a LC-DAD-ESI-IT-MS^n experiment was performed using an Agilent 6320 ion-trap spectrometer (Agilent, Waldbronn, Germany) connected to an Agilent 1200 HPLC system (Agilent, Waldbronn, Germany). The HPLC conditions were the same as those described in Section 2.3. The LC effluent was introduced into an electrospray ionization source after a postcolumn split ratio of 2 : 1. The parameters for MS analysis in the positive ion mode were as follows: nebulizer, 45 psi; ionization voltage, 4000 V; dry temperature, 350°C; flow rate of carrier gas, 12.0 L·min^{-1}. Full-scan mass spectra were acquired in the range of 100–800 *m/z*. The optimized parameters for MS/MS analysis were as follows: collision energy, 1.5 V; nitrogen was used as the collision gas. MS^n spectra of pure substances were obtained using the same parameters as mentioned above.

2.6. LC-DAD-ESI-IT-TOF/MS of Analysis of Typical TSC Sample. To confirm the elemental composition of precursor ions and their fragments with high-accurate mass, a LC-ESI-IT-TOF/MS experiment was performed on a Shimadzu LC-MS-IT-TOF instrument equipped with a Shimadzu UFLCXR HPLC system (Shimadzu, Kyoto, Japan). The HPLC system consisted of a CBM-20A controller, two LC-20AD binary pumps, an SPD-M20A diode array detector, an SIL-20AC autosampler, a CTO-20A column oven, and a DGU-20A3 degasser. The HPLC conditions were the same as those for HPLC-DAD-ESI-MS^n analysis. The LC effluent was directed into the ESI source as a rough split ratio of 3 : 1. The optimized MS conditions were as follows: positive and negative ion mode; electrospray voltage, +4.5 kV/−3.5 kV; detector voltage, 1.65 kV; curved desolvation line (CDL) temperature, 200°C; heat block temperature, 200°C; nebulizing gas (N_2), 1.5 L·min^{-1}; drying gas (N_2), 10 L·min^{-1}; scan range, *m/z* 100–1100 for MS^1, 100–800 for MS^2, and 100–500 for MS^3. The ultrahigh purity argon was used as the collision gas for collision-induced dissociation (CID) experiments, and the collision energy was set at 50% for MS^2 and MS^3; ion accumulated time was 30 ms. The MS^n data were collected in an automatic mode and the software could automatically select precursor ions for MS^n analysis according to criteria settings. Accurate mass determination was corrected using the external standard method. The data acquisition and analysis were performed by LC-MS Solution Version 3.6 software (Shimadzu, Kyoto, Japan).

3. Results and Discussion

3.1. Qualitative Analyses of TSC and Its Related Crude Herbal Materials by HPLC and LC-MS. Under the HPLC conditions as described in the current Chinese Pharmacopoeia [1], 5 batches of TSC samples, together with the reference compounds, were examined and their HPLC chromatograms were shown in Figure S2. High similarity in the number, type, and amount of chemical constituents was observed in the HPLC profiles of different batches of TSC samples. General chromatographic profile was obtained by Similarity Evaluation System for Chromatographic Fingerprint of Traditional Chinese Medicine software and characteristic peaks were found in the HPLC profile of each individual sample.

In order to identify the origin of these characteristic peaks from individual herbs, a comparative study was carried out by using various extracts of herbs and TSC samples. Accordingly, the possible individual contribution from the corresponding herbs to the general chromatographic profile was found. Compared with the HPLC profiles of the ethanolic and aqueous extracts of *Chuanxiong rhizoma and Gastrodiae rhizoma* (Figure S3), 29 of 38 peaks occurring in HPLC profile of TSC sample were contributed by *Chuanxiong rhizoma* and other 9 peaks came from G*astrodiae rhizoma* (Figures S4 ~ S10). In addition to the comparison of retention time and on-line UV spectra with those of reference compounds gastrodin, 5-HMF, parishin B, parishin C, parishin, ferulic acid, and *Z*-ligustilide, the precursor ions obtained by the positive and negative LC-MS (Figure 2) such as $[M+H]^+$, $[M+NH_4]^+$, $[M+Na]^+$, and $[M-H]^-$ further confirmed the contribution of the characteristic peaks from individual herbs to the chromatographic profile of TSC sample (Table 1).

3.2. Identification of Chemical Constituents in TSC by LC-DAD-EST-IT-MS^n and LC-DAD-ESI-IT-TOF/MS. The combination of LC-DAD-ESI-IT-MS^n and LC-DAD-ESI-IT-TOF/MS experiments was employed for the identification of chemical constituents in TSC sample, and, as a result, a total of 38 compounds was identified or tentatively characterized. The structures of the identified compounds are shown in Figure 1 and their chromatographic and mass spectrometric data are shown in Tables 2 and 3. The total ion chromatograms (TICs) of TSC sample are shown in Figures S11 and S12, respectively. Among the identified constituents, 7 compounds (**2**, **3**, **5**, **6**, **7**, **9,** and **26**) were unambiguously identified as gastrodin, 5-HMF, parishin B, parishin C, parishin, ferulic acid, and *Z*-ligustilide based on the direct comparison of their retention times, UV spectra, and mass spectra with those of the authentic compounds. Furthermore, 31 compounds were tentatively characterized according to their UV spectra, empirical molecular formula, and mass fragmentation pathways as well as their eluted sequence from ODS column reported in the literature [11–14] and acquired in the present experiments.

3.2.1. Fragmentation Characteristic of Reference Compounds. In the present HPLC and MS conditions, characteristic MS adduct ions were observed for phenolic glycosides, organic acid, and phthalide derivatives. Phenolic glycosides and organic acids could be well-detected in positive and negative ionization mode and adduct ions such as $[M+H]^+$, $[M+NH_4]^+$, $[M+Na]^+$, and $[2M+Na]^+$ or $[M-H]^-$ and $[M+HCOO]^-$ were found, whereas phthalides were only detected in positive mode and mainly showed the abundant $[M+H]^+$, $[M+Na]^+$, and $[2M+Na]^+$ ions. The fragmentation characteristic of reference compounds was similar as those described in the literature [11, 14, 15]. For example, gastrodin, the glucoside of *p*-hydroxybenzyl alcohol, mainly showed characteristic product ions at *m/z* 123 and 161 corresponding to the elimination of a molecule of glucose and a molecule of

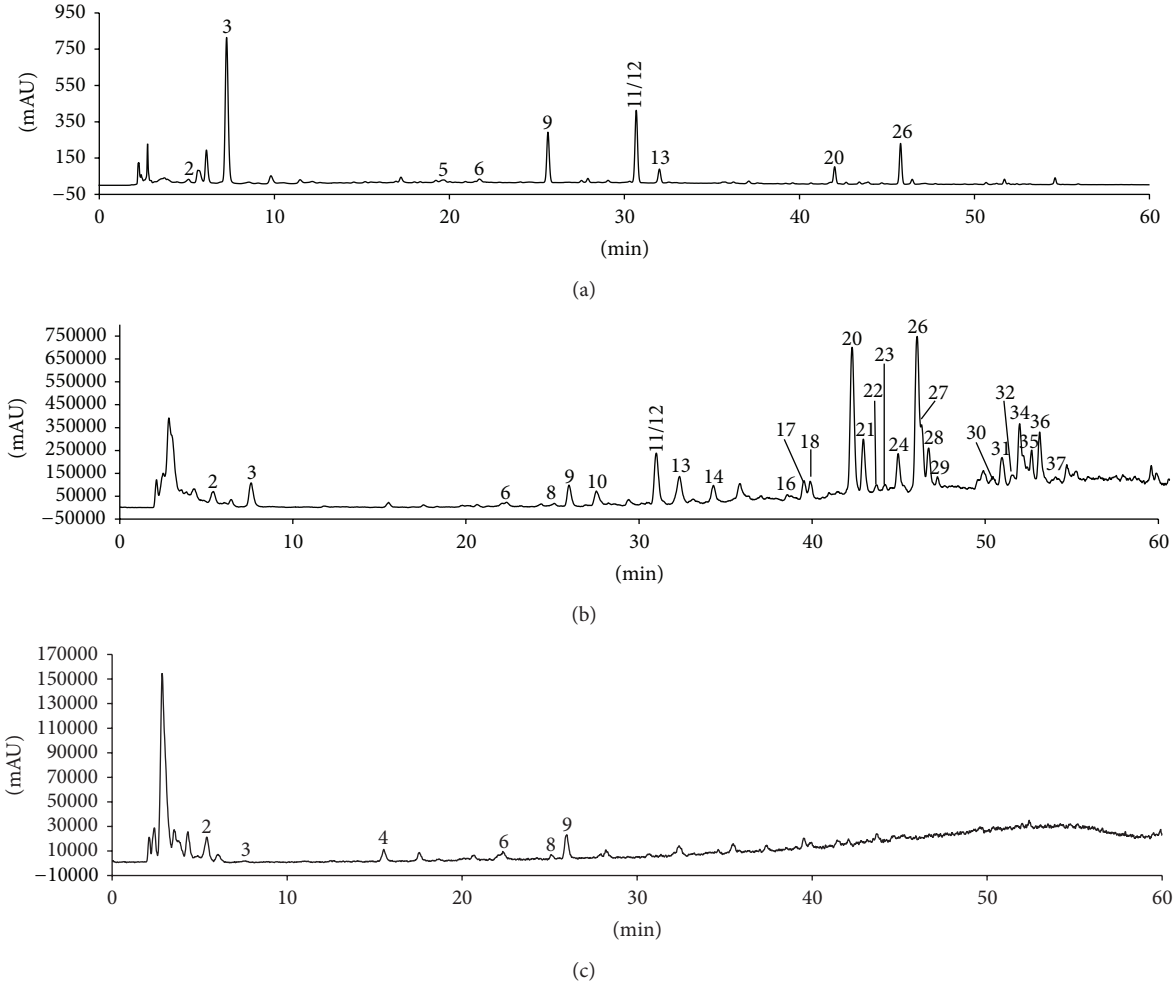

Figure 2: HPLC and TIC of typical TSC sample obtained using an Agilent 6130 Quadrupole LC-MS connected to an Agilent 1200 HPLC system. (a) HPLC (276 nm), (b) (+) TIC, and (c) (−) TIC.

p-hydroxybenzyl alcohol from *m/z* 285 $[M\text{-}H]^-$, respectively. Parishin B and C, the gastrodin derivatives with citric acid, mainly indicated the fragmentation of the ester glucoside bond and the neutral loss of gastrodin residue (268 Da) corresponding to the ion at *m/z* 459. The ions at *m/z* 441, 423, 397, and 379 were also observed, which were related to elimination of H_2O and CO_2 from the tertiary alcoholic hydroxyl group and the free carboxylic groups produced by breaking of the ester glucoside bond. Phthalides mainly displayed two pathways: side-chain cleavage with loss of alkenes and ring-opening followed by elimination of H_2O and CO. These series of characteristic ion rules would be beneficial to elucidate the chemical constituents in TSC sample.

3.2.2. Identification of Phenolics Derivatives in TSC Sample. Compounds **1** and **2** gave the same on-line UV spectrum which is in accordance with that of gastrodin. The structure of **2** was identified as gastrodin based on the comparison of retention time, UV spectrum, and characteristic fragment ions with those of authentic compound as well as accurate molecular weight. The molecular weight of **1** was deduced as 448 from the sodium adduct ion at *m/z* 471 $[M+Na]^+$ detected in positive mode and deprotonated molecular ion at *m/z* 447 $[M\text{-}H]^-$ in negative mode, respectively. A prominent neutral loss of 162 Da, corresponding to the loss of hexose, and disaccharide residue ions at *m/z* 323 were observed in MS^2 of the $[M\text{-}H]^-$ ion at *m/z* 447. The loss of 124 Da was assigned to *p*-hydroxybenzyl alcohol just like the characteristic loss of gastrodin. Therefore, compound **1** was identified as elatoside, namely, 6′-(*p*-hydroxybenzyl methyl)-gastrabiose, which was previously isolated from the rhizome of *G. elata* [16].

Compounds **4**, **5**, **6,** and **7** gave the adduct ions $[M+Na]^+$ and $[M+NH_4]^+$ in positive LC-MS and $[M\text{-}H]^-$ in negative LC-MS experiments as well as UV spectra, which were similar to those of gastrodin derivatives. Compounds **5** and **6** had the same $[M\text{-}H]^-$ ions at *m/z* 727, which produced the prominent fragment ion at *m/z* 459 in the MS^2, due to loss of gastrodin residue (268 Da) as well as other ions at *m/z* 441, 423, 397, and 379. Combining with retention time and addition of reference substances, **5** and **6** were identified as parishin B and C. Similarly, compound **4** was assigned to parishin E

Table 1: Retention time (t_R), UV, and LC-MS data of the identified compounds in Tianshu Capsule and related crude materials.

Number	t_R/min	UV λ_{max}/nm	MW	$[M-H]^-$	$[M+H]^+$	$[M+NH_4]^+$	$[M+Na]^+$	$[2M+Na]^+$	$[M+HCOO]^-$	Tianma	Chuanxiong	Identified compounds
2	5.403	221, 276	286			304			331	+	−	Gastrodin
3	7.736	230, 283	126		127	144	149			+	−	5-HMF
4	15.579	225	460	459		478	483			+	−	Parishin E/G
5	20.691	221, 272	728	727		746	751			+	−	Parishin B
6	22.220	221, 274	728	727		746	751			+	−	Parishin C
8	25.080	218	242	241	243		265	507		−	+	3-Butyl-3,6,7-trihydroxy-4,5,6,7 -tetrahydrophthalide
9	25.567	220, 236, 323	194	193	195		217			+	+	ferulic acid
10	27.529	220, 330	226		227		249	475		−	+	Senkyunolide J/N
11	30.667	280	224		225		247	471		−	+	4,5-Dihydro-3,1′-dihydroxy-3 -butylphthalide
13	32.436	275	206	205	207					−	+	4-hydroxyl-3-butylphthalide
14	34.299	325	396		397					+	+	unidentified
16	38.635	220, 270	222	221	223		245			−	+	Senkyunolide D or 4,7-dihydroxy-3-butylidenephthalide
17	39.502	230, 310	206	205	207		229		435	−	+	*Z*-6,7-Epoxyligustilide
18	39.898	280	208	207	209		231		439	−	+	Senkyunolide K/G
19	41.465	220	206	205	207		229		435	−	+	Senkyunolide F
20	42.332	220, 240, 325	192		193		215	407		+	+	Senkyunolide A
21	42.956	226, 280	190		191	208	213	403		−	+	Butylphthalide
22	43.717	218, 270	204	203	205		227	431	249	−	+	Senkyunolide C
23	44.147	210, 285, 330	204	203	205		227	431	249	−	+	Senkyunolide E
24	44.949	220, 270, 330	194		195		217	411		−	+	Cnidilide
26	45.831	205, 280, 328	190		191		213	403		−	+	Ligustilide
27	46.394	220	194		195		217	411		−	+	Neocnidilide
28	46.653	210, 275, 330	188		189	206	211	399		−	+	3-Butylidenephthalide
29	47.231	225, 280, 310	380		381	398	403			−	+	Riligustilide
30	50.042	276	382		383	399	405			−	+	Senkyunolide P
31	50.476	220, 280	380		381	398	403			−	+	3′,6,8′,3a-Biligustilide
32	50.970	220, 280	380		381	398	403			−	+	Tokinolide B
33	51.065	230, 279	382		383	400	405			−	+	Unidentified
34	51.962	220, 275	380		381		403			−	+	Levistolide A
35	52.267	220, 285	380		381					−	+	3′*Z*-3,3′a,8,6′a-Biligustilide
36	52.693	220, 280	278		279	301	579			−	+	Senkyunolide M
37	53.134	220, 280	278		279	301	579			−	+	Senkyunolide Q
38	53.852	225, 278	382		383	400	405	383		−	+	Unidentified

Table 2: Retention time (t_R), UV, and MS^n data obtained by LC-DAD-ESI-IT-MS^n of the identified compounds in Tianshu Capsule.

Number	t_R/min	Identified compounds	UV λ_{max}/nm	$[M + Na]^+$	$[M + H]^+$	$[2M + Na]^+$	Main product ions	$[M - H]^-$	$[M + HCOO]^-$	Main product ions
1	6.3	Gastrodin glucose (448)	221, 276	471				447	493	323[M – H-$C_7H_8O_2$]$^-$, 285[M – H-glc]$^-$, 179
2	6.3	Gastrodin (286)	220, 269	309			185[M + Na-$C_7H_8O_2$]$^+$	285	331	161[M – H-$C_7H_8O_2$]$^-$, 123[M – H-glc]$^-$
3	8.1	5-HMF (126)	230, 283		127		109[M + H-H_2O]$^+$	125		
5	20.3	Parishin B (728)	221, 272	751			483[M + Na-268]$^+$, 215[483-268]$^+$	727		459, 441, 423, 397, 379, 217
6	21.8	Parishin C (728)	221, 274	751			483[M + Na-268]$^+$, 215[483-268]$^+$	727		459, 441, 423, 397, 379, 217
7	23.4	Parishin (996)	221, 271					995		727[M – H-268]$^-$
9	26.0	Ferulic acid (194)	220, 236, 323		195		177[M + H-H_2O]$^+$, 145[177-CH_3OH]$^+$			
10	27.4	Senkyunolide J/N (226)	220, 330	249		475	209[M + H-H_2O]$^+$, 191[M + H-2H_2O]$^+$, 163[M + H-2H_2O-28]$^+$			
11	30.4	4,5-Dihydro-3,1′-dihydroxy -3-butylphthalide (224)	280	247			207[M + H-H_2O]$^+$, 189[M + H-2H_2O]$^+$, 165, 121			
12	31.6	Senkyunolide I/H (224)	276	247			207[M + H-H_2O]$^+$, 189[M + H-2H_2O]$^+$, 161[189-H_2O]$^+$, 133[189-56]$^+$			
15	37.0	Unidentified (316)	230, 276, 280	339	317		299[M + H-H_2O]$^+$, 281[M + H-2H_2O]$^+$, 271[M + H-H_2O-28]$^+$, 243	315		
17	37.8	*Z*-6,7-Epoxyligustilide (206)	230	229		413	189[M + Na-H_2O]$^+$, 171[189-H_2O]$^+$			
18	38.1	Senkyunolide K/G (208)	233, 280	231		439	191[M + H-H_2O]$^+$, 173[191 – H_2O]$^+$, 149[191-42]$^+$, 135[191-56]$^+$			
20	40.2	Senkyunolide A (192)	280	215	193	407	175[M + H-H_2O]$^+$, 147, 119, 105			
21	40.7	Butylphthalide (190)	232, 275	213	191	403	173[M + H-H_2O]$^+$, 145, 117			
24	42.6	Cnidilide (194)	238, 279, 327	217						
25	43.3	*E*-Ligustilide (190)	281, 327	213	191	403	173[M + H-H_2O]$^+$, 130			
26	43.5	*Z*-Ligustilide (190)	237, 260, 312	213	191	403	173[M + H-H_2O]$^+$, 145[173-28]$^+$ 130, 117, 105			
28	44.0	3-Butylidenephthalide (188)	230, 277, 326	211	189		171[M + H-H_2O]$^+$, 153[171-H_2O]$^+$			
29	47.4	Riligustilide (380)	275	403	381		213[2M + Na-190]$^+$, 191, 173			
30	47.5	Senkyunolide P (382)	278	405	383		192[M + H-190]$^+$			
31	47.8	3′,6,8′,3a-Biligustilide (380)	278, 363	403	381		213[2M + Na-190]$^+$, 191[M + H-190]$^+$, 145, 117			
32	48.0	Tokinolide B (380)	278	403	381		213[2M + Na-190]$^+$, 191[M + H-190]$^+$			
33	48.2	Unidentified (382)	230, 279	405	383		193[M + H-190]$^+$			
34	48.5	Levistolide A (380)	276	403	381		213[2M + Na-190]$^+$, 191[M + H-190]$^+$, 145, 117			
35	48.8	Senkyunolide O (380)	278	403	381		173[191-H_2O]$^+$, 191[M + H-190]$^+$, 145, 117			
36	49.0	Senkyunolide M (278)	279	301	279		245[M + Na-56]$^+$, 189, 171			
37	49.4	Senkyunolide Q (278)	278	301	279		245[M + Na-56]$^+$, 189, 171			
38	49.9	Unidentified (382)	225, 278	405	383					

Table 3: Retention time (t_R) and MS data obtained by LC-DAD-ESI-IT-TOF/MS of the identified compounds in the sample of Tianshu Capsule.

Number	t_R/min	Identified compounds	Formula	Mea. mass/m/z	Calc. mass/m/z	Error/ppm	Other precursor ions	Main product ions
3	7.6	5-HMF (126)	$C_6H_6O_3$	127.0384$[M + H]^+$	127.0390$[M + H]^+$	−4.72	149.0240$[M + Na]^+$	
5	19.8	Parishin B (728)	$C_{32}H_{40}O_{19}$	727.2123$[M - H]^-$	727.2091$[M - H]^-$	4.40		
6	21.5	Parishin C (728)	$C_{32}H_{40}O_{19}$	727.2132$[M - H]^-$	727.2091$[M - H]^-$	5.64		
8	24.5	3-Butyl-3,6,7-trihydroxy-4,5,6,7-tetrahydrophthalide (242)	$C_{12}H_{18}O_5$	241.1090$[M - H]^-$	241.1081$[M - H]^-$	3.72		223.0885$[M - H\text{-}H_2O]^-$, 197.1142, 179.1107, 141.0930, 123.0854
				243.1220$[M + H]^+$	243.1227$[M + H]^+$	2.88	265.1060$[M + Na]^+$	
9	25.3	Ferulic acid (194)	$C_{10}H_{10}O_4$	195.0649$[M + H]^+$	195.0652$[M + H]^+$	−1.54	217.0458$[M + Na]^+$	
10	27.0	Senkyunolide J/N (226)	$C_{12}H_{18}O_4$	227.1259$[M + H]^+$	227.1278$[M + H]^+$	−3.37	249.1082$[M + Na]^+$	209.1177$[M + H\text{-}H_2O]^+$, 191.1026$[M + H\text{-}2H_2O]^+$
11	30.3	4,5-Dihydro-3,1′-dihydroxy-3-butylphthalide (224)	$C_{12}H_{16}O_4$	225.1105$[M + H]^+$	225.1121$[M + H]^+$	−7.11		
12	31.6	Senkyunolide I/H (224)	$C_{12}H_{16}O_4$	225.1105$[M + H]^+$	225.1121$[M + H]^+$	−7.11		
15	37.8	Unidentified (316)	$C_{18}H_{20}O_5$	317.1380$[M + H]^+$	317.1384$[M + H]^+$	−1.26	339.1210$[M + Na]^+$	299.1378$[M + H\text{-}H_2O]^+$, 271.1343$[M + H\text{-}H_2O\text{-}28]^+$
16	37.8	4,7-Dihydroxy-3-butylidenephthalide or senkyunolide D (222)	$C_{12}H_{14}O_4$	223.0986$[M + H]^+$	223.0965$[M + H]^+$	9.41	245.0774$[M + Na]^+$	
17	38.7	*Z*-6,7-Epoxyligustilide (206)	$C_{12}H_{14}O_3$	207.1008$[M + H]^+$	207.1016$[M + H]^+$	3.66	229.0824$[M + Na]^+$	189.0856$[M + H\text{-}H_2O]^+$, 133.0318
18	39.1	Senkyunolide K/G (208)	$C_{12}H_{16}O_3$	209.1167$[M + H]^+$	209.1172$[M + H]^+$	−2.39	231.0974$[M + Na]^+$	191.1091$[M + H\text{-}H_2O]^+$, 119.0819
19	40.6	Senkyunolide F (206)	$C_{12}H_{14}O_3$	207.1009$[M + H]^+$	207.1016$[M + H]^+$	3.38	229.0815$[M + Na]^+$	189.0911$[M + H\text{-}H_2O]^+$, 161.0959
				205.0874$[M - H]^-$	205.0870$[M - H]^-$	1.95	411.1821$[2M - H]^-$	161.0976$[M - H\text{-}44]^-$, 106.0421
20	41.4	Senkyunolide A (192)	$C_{12}H_{16}O_2$	193.1219$[M + H]^+$	193.1223$[M + H]^+$	−2.07	215.1027$[M + Na]^+$, 407.2196$[2M + Na]^+$	175.1119$[M + H\text{-}H_2O]^+$, 147.1155, 105.0718
21	42.1	Butylphthalide (190)	$C_{12}H_{14}O_2$	191.1061$[M + H]^+$	191.1067$[M + H]^+$	−3.14	213.0872$[M + Na]^+$, 403.1888$[2M + Na]^+$	173.0989$[M + H\text{-}H_2O]^+$, 145.1049$[M + H\text{-}H_2O\text{-}28]^+$
22	42.9	Senkyunolide C (204)	$C_{12}H_{12}O_3$	205.0847$[M + H]^+$	205.0859$[M + H]^+$	−5.85	227.0685$[M + Na]^+$, 431.1431$[2M + Na]^+$	187.0763$[M + H\text{-}H_2O]^+$, 169.0757$[M + H\text{-}2H_2O]^+$, 141.0699$[169\text{-}28]^+$
23	43.4	Senkyunolide E (204)	$C_{12}H_{12}O_3$	205.0843$[M + H]^+$	205.0859$[M + H]^+$	−7.80	227.0663$[M + Na]^+$	
24	44.1	Cnidilide (194)	$C_{12}H_{18}O_2$	195.1372$[M + H]^+$	195.1380$[M + H]^+$	−4.10	217.1185$[M + Na]^+$	177.1323$[M + H\text{-}H_2O]^+$, 149.1340$[M + H\text{-}H_2O\text{-}28]^+$
25	44.1	*E*-Ligustilide (190)	$C_{12}H_{14}O_2$	191.1061$[M + H]^+$	191.1067$[M + H]^+$	−3.14	213.0871$[M + Na]^+$	
26	45.2	*Z*-Ligustilide (190)	$C_{12}H_{14}O_2$	191.1056$[M + H]^+$	191.1067$[M + H]^+$	−5.76	213.0859$[M + Na]^+$, 403.1901$[2M + Na]^+$	173.0984$[M + H\text{-}H_2O]^+$, 145.0999$[M + H\text{-}H_2O\text{-}28]^+$, 117.0690
27	45.5	Neocnidilide (194)	$C_{12}H_{18}O_2$	195.1372$[M + H]^+$	195.1380$[M + H]^+$	−4.10	217.1179$[M + Na]^+$	177.1323$[M + H\text{-}H_2O]^+$, 149.1306$[M + H\text{-}H_2O\text{-}28]^+$, 121.0998
28	45.8	3-Butylidenephthalide (188)	$C_{12}H_{12}O_2$	189.0907$[M + H]^+$	189.0910$[M + H]^+$	−1.59	211.0720$[M + Na]^+$	171.0817$[M + H\text{-}H_2O]^+$, 153.0800$[M + H\text{-}H_2O\text{-}H_2O]^+$, 143.0882$[M + H\text{-}H_2O\text{-}28]^+$, 129.0724
29	46.2	Riligustilide (380)	$C_{24}H_{28}O_4$	381.2058$[M + H]^+$	381.2060$[M + H]^+$	−0.52	403.1872$[M + Na]^+$, 191.1060, 213.0875	
30	48.9	Senkyunolide P (382)		383.2220$[M + H]^+$	383.2217$[M + H]^+$		405.2031$[M + Na]^+$	193.1212$[M/2 + H]^+$
31	49.2	3′,6,8′,3a-Biligustilide (380)	$C_{24}H_{28}O_4$	381.2058$[M + H]^+$	381.2060$[M + H]^+$	−0.52	403.1885$[M + Na]^+$, 191.1091	
32	49.8	Tokinolide B (380)	$C_{24}H_{28}O_4$	381.2037$[M + H]^+$	381.2060$[M + H]^+$	−6.03	403.1878$[M + Na]^+$, 191.1062	
33	49.9	Unidentified (382)		383.2220$[M + H]^+$	383.2217$[M + H]^+$		405.2040$[M + Na]^+$	193.1214$[M/2 + H]^+$
34	50.3	Levistolide A (380)	$C_{24}H_{28}O_4$	381.2064$[M + H]^+$	381.2060$[M + H]^+$	1.05	403.1887$[M + Na]^+$, 191.1054	
35	50.8	Senkyunolide O (380)	$C_{24}H_{28}O_4$	381.2061$[M + H]^+$	381.2060$[M + H]^+$	0.26	403.1879$[M + Na]^+$, 191.1057	191.1051$[M/2 + H]^+$
36	51.4	Senkyunolide M (278)		279.1582$[M + H]^+$			301.1402$[M + Na]^+$, 579.2952$[2M + Na]^+$	
37	52.0	Senkyunolide Q (278)		279.1596$[M + H]^+$			301.1381$[M + Na]^+$, 579.2952$[2M + Na]^+$	
38	52.7	Unidentified (382)		383.2217$[M + H]^+$	383.2217$[M + H]^+$	0.00	405.2008$[M + Na]^+$	365.2115, 347.1905, 193.1201$[M/2 + H]^+$

or its positional isomer parishin G with identical molecular mass of 460 [17]. Compound **7** had the molecular mass of 996 and exhibited consecutive loss of gastrodin residue (268 Da), and, therefore, it was identified as parishin, a conjugate of one citric acid and three gastrodins.

3.2.3. Identification of Phthalide Derivatives in TSC Sample. The molecular formula of compound **8**, detected from individual herb *Chuanxiong rhizoma*, was calculated as $C_{12}H_{18}O_5$ by $[M+H]^+$ ion at *m/z* 243.1220 and $[M-H]^-$ ion at *m/z* 241.1090 in its LC-IT-TOF/MS experiment. It had the same molecular weight of 242 as those of known compounds, senkyunolide L and 3-butyl-3,6,7-trihydroxy-4,5,6,7-tetrahydrophthalide, present in *Chuanxiong rhizoma*; however, compound **8** could not be senkyunolide L ($C_{12}H_{15}ClO_3$) because both had the different element composition [18]. The fragmentation ion of **8** at *m/z* 197.1142, which was derived from a retro-Diels-Alder cleavage of the $[M-H-H_2O]^-$ ion at *m/z* 223.0885, suggested that the structure of **8** was proposed as 3-butyl-3,6,7-trihydroxy-4,5,6,7-tetrahydrophthalide.

Compound **10** displayed $[M+H]^+$ ion at *m/z* 227.1259, suggesting the molecular formula of $C_{12}H_{18}O_4$. The fragment ions at *m/z* 209 and 191 in the MS^2, indicating consecutive loss of H_2O, supported that **10** was a dihydroxylated derivative of ligustilide. UV and MS data of **10** were in accordance with those of senkyunolide J and senkyunolide N, but the stereochemistry information of two hydroxy groups could not be provided. Thus, **10** was tentatively assigned as one of senkyunolide J and senkyunolide N. Compounds **11** and **12** gave the same $[M-H]^-$ ions at *m/z* 224 and their molecular formula was established as $C_{12}H_{18}O_4$ according to the $[M+H]^+$ ion at *m/z* 225.1105. However, both constituents had different fragmentation rules. The MS^2 of **11** displayed the fragment ions at *m/z* 207, 189 and the characteristic ion at *m/z* 165, which were similar to those of 4,5-dihydro-3,1′-dihydroxy-3-butylphthalide [15], whereas **12** showed elimination of two H_2O followed by side-chain cleavage. Therefore, **11** was deduced as 4,5-dihydro-3,1′-dihydroxy-3-butylphthalide and **12** could be one of senkyunolide I and senkyunolide H [14, 15].

Compounds **13**, **17,** and **19** have the same molecular formula of $C_{12}H_{14}O_3$ and were tentatively characterized as 4-hydroxy-3-butylphthalide, *Z*-6,7-epoxyligustilide, and senkyunolide F. Compared with monohydroxy phthalide derivatives **13** and **19**, the instable structure of **17** resulted in the ion at *m/z* 189 as base peak observed in MS^1, suggesting loss of H_2O from the $[M-H]^-$ ion at *m/z* 207. Senkyunolide A **20** and *Z*-ligustilide **26** as main constituents were identified and butylphthalide **21**, senkyunolide C **22**, senkyunolide E **23**, *E*-ligustilide **24,** and 3-butylidenephthalide **28** were characterized as minor constituents. For the compounds **20**, **21**, **24,** and **26**, the neutral loss of CO (28 Da) and side-chain cleavage (56 Da) from $[M+H-H_2O]^+$ were the common fragmentation rules.

Compound **16** ($C_{12}H_{14}O_3$) was tentatively proposed to 4,7-dihydroxy-3-butylidenephthalide or senkyunolide D. Compound **18** was assigned as senkyunolide K or senkyunolide G. These compounds and their isomers could not be differentiated by available MS data.

Five dimeric ligustilides **29**, **31**, **32**, **34,** and **35**, which produced the protonated ion $[M+H]^+$ at *m/z* 381, were detected in extracted ion chromatograms. They showed the base peak at *m/z* 403 $[M+Na]^+$ in MS^1 and the fragment ion at *m/z* 191 $[M+H-190]^+$ as base peak in MS^2 by the loss of a RDA fragment (145 Da) followed by the loss of H_2O and HCOOH (46 Da). Comprehensively considering the information described in the literature [14], they were tentatively identified as riligustilide, 3′,6,8′,3a-biligustilide, tokinolide B, levistolide A, and senkyunolide O, respectively. Three compounds, indicating the protonated ion $[M+H]^+$ at *m/z* 383, were detected in extracted ion chromatograms; however, only senkyunolide P was previously reported in *Chuanxiong Rhizoma*. Thus, compound **30** was tentatively characterized as senkyunolide P and the other compounds (**33** and **38**) were still indefinite based on the available information.

In the modernization of TCM, chemical profiling is always the first task. It is of importance for development of the suitable quality standard and control strategy, study of pharmacokinetics, and interpretation of therapeutic character of TCM [19, 20]. As a marketed product in China, the quality control system of TSC is still to be improved and its pharmacokinetics and action mechanism are not completely clear. Usually, gastrodin, ferulic acid, and 6,7-dihydroxyligustilide are selected as marker compounds for the quality control or the pharmacokinetic study of Tianshu Capsule [1, 21, 22]. The present investigation provides more chemical information for the selection of the marker compounds and the improvement of quality control. It also tells the pharmacokinetic scientists and ethnopharmacologists which compounds in TSC samples are worth further evaluation. In addition to gastrodin and ferulic acid, more efforts should be made to the group of phthalide derivatives such as major constituents, senkyunolide I/H **12**, 4-hydroxy-3-butylphthalide **13**, senkyunolide A **20,** and *Z*-ligustilide **26** as well as their dimers. Additionally, it is worth noting that 5-HMF **3**, a potent toxic compound, was found as main peak in the chemical profile of TSC samples. This compound originated from the crude material *Gastrodiae rhizoma* and its content in TSC samples was up to 2.67 $mg \cdot g^{-1}$ [23]. If it is necessary to develop its limit standard in TSC product or not, more study are expected. Also, ligustrazine is not detected in TSC sample, even in the extracted ion chromatogram, which could result from its very low amount in crude herbal material (about 0.01~0.02%), although, actually, it is often considered as one of active components in *Chuanxiong rhizoma*.

4. Conclusions

In this study, HPLC analysis was employed to find out the common chromatographic peak in various batches of TSC samples. The contribution of the characteristic peaks from individual herbs to the whole chromatographic profile was discussed based on comparative HPLC and LC-MS analyses. A total of 38 constituents were identified based on the comparison of retention time and UV spectra with authentic

compounds as well as by summarized MS fragmentation rules and matching empirical molecular formula with those of published components. The present investigation provided the good basis for monitoring the manufacturing processes and improving quality control of TSC products.

Conflict of Interests

The authors declare that there is no conflict of interests regarding the publication of this paper.

Acknowledgments

This research work was supported by China Postdoctoral Science Foundation (2012M510731) and State Key Laboratory of New-tech for Chinese Medicine Pharmaceutical Process (SKL2010M0204). Meanwhile great thanks are due to Dr. Feng Ji from Shimadzu (China) Co., Ltd., Beijing Office, for measuring the LC-DAD-ESI-IT-TOF/MS experiments.

References

[1] Chinese Pharmacopoeia Commission, *Chinese Pharmacopoeia*, vol. 1, China Medical Science Press, Beijing, China, 2010.

[2] W. Xia, M. J. Zhu, Z. Zhang et al., "Effect of Tianshu capsule in treatment of migraine: a meta-analysis of randomized control trials," *Journal of Traditional Chinese Medicine*, vol. 33, no. 1, pp. 9–14, 2013.

[3] L. Wang, J. M. Zhang, Y. L. Hong, Y. Feng, M. W. Chen, and Y. T. Wang, "Phytochemical and pharmacological review of Da Chuanxiong formula: a famous herb pair composed of Chuanxiong Rhizoma and Gastrodiae Rhizoma for headache," *Evidence-Based Complementary and Alternative Medicine*, vol. 2013, Article ID 425369, 16 pages, 2013.

[4] S. M. Ni, D. W. Qian, E. X. Shang, J. A. Duan, J. M. Guo, and Y. P. Tang, "Analysis of Chemical composition of Da chuanxiong Fang by ultra performance liquid chromatography-electrospray ionization quadrupole time of flight/mass spectrometry," *Chinese Journal of Experimental Traditional Medical Formulae*, vol. 16, no. 1, pp. 40–45, 2010.

[5] L. Shen, X. Lin, S. Liang et al., "Characterization on central ingredients of active components in dachuanxiong fang based on HPLC-DAD-MSn," *Chinese Journal of Experimental Traditional Medical Formulae*, vol. 18, no. 7, pp. 128–134, 2012.

[6] Y. F. Wei, X. Lin, N. Zhang, and Y. Feng, "UPLC-MS analysis of constituents of *Dachuanxiong Fang* active parts absorbed into blood," *Zhongguo Zhongyao Zazhi*, vol. 36, no. 9, pp. 1245–1248, 2011.

[7] Y. Wei, N. Zhang, X. Lin, and Y. Feng, "Release characteristics in vitro and pharmacokinetics of *Da Chuanxiong Fang* multiunit drug delivery system in rats," *Acta Pharmaceutica Sinica*, vol. 46, no. 9, pp. 1150–1155, 2011.

[8] X. L. Zhang, L. F. Liu, L. Y. Zhu et al., "A high performance liquid chromatography fingerprinting and ultra high performance liquid chromatography coupled with quadrupole time-of-flight mass spectrometry chemical profiling approach to rapidly find characteristic chemical markers for quality evaluation of dispensing granules, a case study on Chuanxiong Rhizoma," *Journal of Pharmaceutical and Biomedical Analysis*, vol. 88, pp. 391–400, 2014.

[9] X. Z. Zhang, H. B. Xiao, Q. Xu, X. L. Li, J. N. Wang, and X. M. Liang, "Characterization of phthalides in Ligusticum chuanxiong by liquid chromatographic-atmospheric pressure chemical ionization-mass spectrometry," *Journal of Chromatographic Science*, vol. 41, no. 8, pp. 428–433, 2003.

[10] S. Li, R. Yan, Y. Tam, and G. Lin, "Post-harvest alteration of the main chemical ingredients in *Ligusticum chuanxiong* HORT. (Rhizoma Chuanxiong)," *Chemical and Pharmaceutical Bulletin*, vol. 55, no. 1, pp. 140–144, 2007.

[11] L. Wang, H. B. Xiao, X. M. Liang, and L. Wei, "Identification of phenolics and nucleoside derivatives in *Gastrodia elata* by HPLC-UV-MS," *Journal of Separation Science*, vol. 30, no. 10, pp. 1488–1495, 2007.

[12] T. Yi, K. S. Leung, G. H. Lu, and H. Zhang, "Comparative analysis of *Ligusticum chuanxiong* and related umbelliferous medicinal plants by high performance liquid chromatography-electrospray ionization mass spectrometry," *Planta Medica*, vol. 73, no. 4, pp. 392–398, 2007.

[13] R. Yan, S. L. Li, H. S. Chung, Y. Tam, and G. Lin, "Simultaneous quantification of 12 bioactive components of *Ligusticum chuanxiong* Hort. by high-performance liquid chromatography," *Journal of Pharmaceutical and Biomedical Analysis*, vol. 37, no. 1, pp. 87–95, 2005.

[14] T. Yi, K. S. Leung, G. H. Lu, K. Chan, and H. Zhang, "Simultaneous qualitative and quantitative analyses of the major constituents in the rhizome of Ligusticum chuanxiong using HPLC-DAD-MS," *Chemical and Pharmaceutical Bulletin*, vol. 54, no. 2, pp. 255–259, 2006.

[15] Q. Wu and X. W. Yang, "GC-MS analysis of essential oil from rhizomes of *Ligusticum chuanxiong* cultivated in GAP Base for Chinese Medicinal Materials of China," *China Journal of Chinese Materia Medica*, vol. 33, no. 3, pp. 276–280, 2008.

[16] L. Ning, *Studies on the constituents of Gastrodia elata and three medicinal plants belongs to Curculigo [Doctoral thesis]*, Kunming Institute of Botany, Chinese Academy of Sciences, Kunming, China, 2004.

[17] L. Wang, H. Xiao, L. Yang, and Z. T. Wang, "Two new phenolic glycosides from the rhizome of *Gastrodia elata*," *Journal of Asian Natural Products Research*, vol. 14, no. 5, pp. 457–462, 2012.

[18] M. Kobayashi and H. Mitsuhashi, "Studies on the constituents of umbelliferea plants X VII structure of three new ligustilide derivatives from *Ligusticum wallichii*," *Chemical & Pharmaceutical Bulletin*, vol. 35, no. 12, pp. 4789–4792, 1987.

[19] Z. Q. Shi, D. F. Song, R. Q. Li et al., "Identification of effective combinatorial markers for quality standardization of herbal medicines," *Journal of Chromatography A*, vol. 1345, pp. 78–85, 2014.

[20] Z. Hu, J. Yang, C. Cheng et al., "Combinatorial metabolism notably affects human systemic exposure to ginsenosides from orally administered extract of *Panax notoginseng* roots (Sanqi)," *Drug Metabolism and Disposition*, vol. 41, no. 7, pp. 1457–1469, 2013.

[21] H. F. Zhang, X. H. Chen, Y. S. Huo, and K. S. Bi, "RP-HPLC simultaneous determination of the contents of gastrodin , ferulic acid and 6,7-dihydroxyligustilide in Tianshu capsules under a changed UV wavelengths," *Journal of Shenyang Pharmaceutical University*, vol. 29, no. 6, pp. 443–447, 2012.

[22] H. Zhang, L. Sun, X. Chen, Y. Huo, B. Yan, and K. Bi, "Simultaneous quantification of 6,7-di-hydroxyligustilide and gastrodin in rat plasma by LC-MS: application to pharmacokinetic study of Tianshu capsule," *Latin American Journal of Pharmacy*, vol. 31, no. 1, pp. 112–119, 2012.

[23] J. J. Liang, H. M. Gao, L. M. Chen et al., "Simultaneous determination of three constituents in Tiansu Capsule by HPLC," *Chinese Journal of Experimental Traditional Medical Formulae*, vol. 19, no. 17, pp. 81–84, 2013.

Hindawi Publishing Corporation
Evidence-Based Complementary and Alternative Medicine
Volume 2014, Article ID 437803, 7 pages
http://dx.doi.org/10.1155/2014/437803

Research Article

Effect of *Flos carthami* Extract and α_1-Adrenergic Antagonists on the Porcine Proximal Ureteral Peristalsis

San-Yuan Wu,[1,2] Kee-Ming Man,[1,2,3,4,5] Jui-Lung Shen,[6] Huey-Yi Chen,[2,7] Chiao-Hui Chang,[2] Fuu-Jen Tsai,[2,7] Wen-Tsong Hsieh,[2] Daniel Winardi,[2] Yuan-Ju Lee,[8] Kao-Sung Tsai,[2,7] Yu-Ning Lin,[2] Yung-Hsiang Chen,[2,7] and Wen-Chi Chen[2,7]

[1] *Department of Anesthesiology, Tungs' Taichung MetroHarbor Hospital, Taichung 435, Taiwan*
[2] *Graduate Institute of Integrated Medicine, Institute of Chinese Medicine, School of Chinese Medicine, Department of Pharmacology, Research Center for Chinese Medicine and Acupuncture, China Medical University, Taichung 404, Taiwan*
[3] *Department of Medicinal Botanicals and Health Applications, Da-Yeh University, Changhua 515, Taiwan*
[4] *Department of Life Sciences, National Chung Hsing University, Taichung 402, Taiwan*
[5] *Graduate Institute of Geriatric Medicine, Anhui Medical University, Hefei 230032, China*
[6] *Department of Dermatology, Taichung Veterans General Hospital, Taichung 407, Taiwan*
[7] *Departments of Obstetrics and Gynecology, Medical Genetics and Pediatrics, Dermatology, Medical Research, and Urology, China Medical University Hospital, Taichung 404, Taiwan*
[8] *Department of Urology, National Taiwan University Hospital, Taipei 100, Taiwan*

Correspondence should be addressed to Yung-Hsiang Chen; d87a03@ym.edu.tw
and Wen-Chi Chen; wgchen@mail.cmu.edu.tw

Received 10 March 2014; Revised 8 May 2014; Accepted 8 May 2014; Published 9 July 2014

Academic Editor: Shi-Biao Wu

Traditional Chinese medicine (TCM) has been proposed to prevent urolithiasis. In China, *Flos carthami* (FC, also known as *Carthamus tinctorius*) (Safflower; Chinese name: Hong Hua/紅花) has been used to treat urological diseases for centuries. We previously performed a screening and confirmed the *in vivo* antilithic effect of FC extract. Here, *ex vivo* organ bath experiment was further performed to study the effect of FC extract on the inhibition of phenylepinephrine (PE) (10^{-4} and 10^{-3} M) ureteral peristalsis of porcine ureters with several α_1-adrenergic antagonists (doxazosin, tamsulosin, and terazosin) as experimental controls. The results showed that doxazosin, tamsulosin, and terazosin dose (approximately $4.5 \times 10^{-6} - 4.5 \times 10^{-1}$ μg/mL) dependently inhibited both 10^{-4} and 10^{-3} M PE-induced ureteral peristalsis. FC extract achieved 6.2% ± 10.1%, 21.8% ± 6.8%, and 24.0% ± 5.6% inhibitions of 10^{-4} M PE-induced peristalsis at doses of 5×10^3, 1×10^4, and 2×10^4 μg/mL, respectively, since FC extract was unable to completely inhibit PE-induced ureteral peristalsis, suggesting the antilithic effect of FC extract is related to mechanisms other than modulation of ureteral peristalsis.

1. Introduction

Ureteral stones can obstruct the ureter and cause severe colicky pain as a sequence of hydronephrosis and increased intrarenal pressure [1–3]. The clinical symptoms of renal colic include acute colicky pain, urinary frequency, dysuria, nausea, and vomiting. As the stone migrates downward from the kidney or upper ureter to the distal ureter, treatment involves measures to relieve pain, encouraging water intake, and administering some medications [4, 5]. Spontaneous expulsion is expected within 4 weeks if the stone is <6 mm in diameter [6]. For situations other than those requiring urgent treatment, such as larger stone size, infection, intractable pain, renal function deterioration, or solitary kidney, many treatments are available to induce spontaneous stone passage.

Drugs commonly used to treat colic include nonsteroidal anti-inflammatory drugs (NSAIDs), narcotics, antidiuretics, calcium channel blockers, and α-blockers. Several clinical trials of highly selective α-blockers are promising for improving spontaneous ureteral stone expulsion [7]. However,

the efficacy of these treatments remains controversial. Studies by Wang et al. found that tamsulosin improved the success rate of medical expulsion therapy (MET) of stones in selected patients [8]. A systematic review by Singh et al. recommended the use of α-antagonists or calcium channel blockers to facilitate ureteral stone expulsion [9]. A meta-analysis by Woolley concluded that tamsulosin may be useful for enhancing ureteric stone expulsion [10]. However, tamsulosin treatment did not demonstrate improvements in the rate of stone expulsion in patients with distal ureteral stones that are $\leq$7 mm in diameter. Tamsulosin treatment was shown to have a supportive analgesic effect in a randomised, double-blind, placebo-controlled trial by Hermanns et al. [11]. A study of Mexican patients by Ochoa-Gómez et al. did not find that tamsulosin had greater efficacy than conventional treatment [12]. Nevertheless, the effect of other nonselective α-blockers on MET remains to be determined.

The effect of α-blockers on MET is mediated through ureteral peristalsis. The ureter has differential distribution of α-adrenergic receptors. Blocking receptor action may relax the ureteral peristalsis that is believed to facilitate stone expulsion. Davenport et al. studied the relaxation effect of selective α_{1A}-adrenergic antagonists on human ureteral activity [13]. Hernandez et al. investigated ureteral peristalsis in porcine ureter and described some useful methods [14]. In this study, we used porcine ureteral smooth muscle samples to study the effect of some potential drugs useful for MET.

Traditional Chinese Medicine (TCM) [15–17] has been proposed to play a role in the prevention of urolithiasis [18]. *Flos carthami* (FC, also known as *Carthamus tinctorius*) (Safflower; Chinese name: Hong Hua/紅花) has been used to treat urological diseases for centuries in China [19]. We previously confirmed the *in vivo* antilithic effect of FC extract [20]; here, we assessed the possible effect of FC extract on the inhibition of ureteral peristalsis. α-adrenergic receptors are found on arteries and in the urinary tract. However, few animal [21] and clinical studies have assessed the effect of FC extract on ureter. The purpose of this study was to investigate the inhibitory effect of FC extract on peristalsis in an *ex vivo* porcine ureteral model in organ bath experiment.

2. Materials and Methods

2.1. Porcine Ureter. Porcine ureters from healthy animals were kindly provided by the slaughterhouse in Taichung City. The ureteral samples were immediately put into a flask of preoxygenated Krebs' solution (pH 7.4) at 4°C after the pigs were slaughtered in the house.

2.2. Ureteral Peristalsis Measurement. The method for measuring ureteral contraction was previously described by Hernandez et al. with modifications (Figure 1) [14, 22]. Briefly, the ureteral samples were cut longitudinally into 1 cm strips. The system used open-ended Perspex tissue baths with a volume of 5 mL to allow exchange with physiological solution.

Tension transducers (Gould 2600 polygraph, Gould Instruments, Cleveland, OH, USA) were used to convert the mechanical tension of the sample into a voltage signal. The tension transducer is suspended by a retort stand vertically above the tissue bath [23], and fine cotton sutures attach the muscle specimen to the transducer; the opposite end of the sample was fixed within the tissue bath. The specimens were continuously irrigated with Krebs' solution with gas (95% oxygen + 5% carbon dioxide). Nonporous tubing connected the Krebs' solution to the tissue baths via a peristaltic pump delivering 1 mL/min to each tissue bath (Minipuls 2, Gilson Inc., Middleton, WI, USA). The tubing passed through a water bath set at 37°C to ensure that the perfusate was at body temperature by the time it reached the tissue bath. The tension transducer responses were recorded on polygraph paper.

We simultaneously assessed cut ureteral samples in each experiment. The ureteral rings were irrigated with Krebs' solution for 1 h to allow equilibration, during that time 5 g of tension was applied. Any spontaneous activity was recorded. Viability was determined by applying 80 mM potassium-enriched Krebs' solution to produce near-maximal contraction. Potassium-enriched solutions were prepared by substituting potassium for sodium [24]. Any unresponsive ureteral samples (unchanged on polygraph during baseline tension) were discarded.

The tension generated with 80 mM potassium-enriched Krebs' solution was used as the control value. The drugs were added to 80 mM potassium-enriched Krebs' solution in increasing concentrations and applied consecutively with a 10 min washout with Krebs' solution between each concentration. Phenylepinephrine (PE) was used to induce ureteral peristalsis at concentrations of 10^{-4} M and 10^{-3} M. The inhibitory effects of drugs were compared with the effects elicited by PE.

2.3. Drug Preparation. Only one drug was applied to each ureteral sample to prevent any risk of cross-reactivity. The maximum tone achieved at 3 min was recorded and expressed as a percentage of that recorded with potassium-enriched solution alone. Before testing the drug solutions, 80 mM potassium solution (prepared in double-distilled (dd) water) was applied to ureteral specimens. The maximum tone generated did not increase on repeated application of 80 mM potassium solution.

The following drugs were tested: water extracts of FC, doxazosin, terazosin, (two nonselective α_{1A}-adrenoceptor antagonists), and tamsulosin (selective α_{1A}-adrenoceptor antagonist). The tested concentrations of all α-blockers were 10^{-10} M, 10^{-9}, 10^{-8}, 10^{-7}, and 10^{-6} M (approximately equal to 4.5×10^{-6}–4.5×10^{-1} μg/mL) dissolved in dd water. All chemical agents were obtained from Sigma-Aldrich Inc. (St. Louis, MO, USA).

We used herbal powder of FC extract provided by the Koda pharmaceutical company (Taoyun, Taiwan). FC powder quality including high-performance liquid chromatography finger print, thin layer chromatography, and heavy metal quantification was examined by the Medical and Pharmaceutical Industry Technology and Development Centre (Taiwan) [20]. The highest stock dose of FC extract was the maximal dissolved dose in dd water (2.0 g/mL water), and the low and medium doses were 0.5 and 1.0 g/mL, respectively. For each experiment, 50 μL was added to the

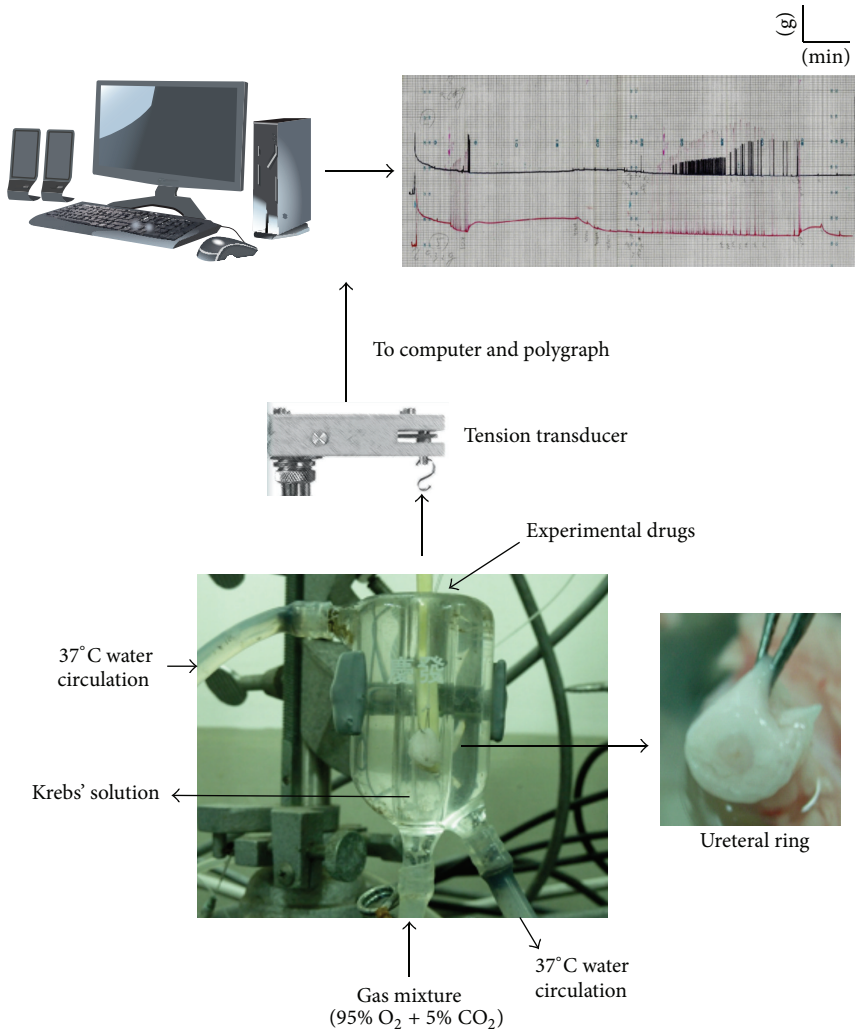

Figure 1: A schematic diagram of a porcine ureteral ring preparation in an organ bath.

5 mL organ bath (final concentration: 5×10^3, 1×10^4, and 2×10^4 μg/mL, resp.).

The inhibitory effect on peristalsis frequency was determined by comparing the values after treatment with those observed at baseline. The percentage of inhibition was calculated by comparing the frequency from baseline to the induction period (3 min interval). Each test was repeated in quadruplicate, and the results are expressed as mean ± standard error of the mean (SEM).

Percentage of inhibition = (baseline frequency − induction frequency)/baseline frequency × 100%. The concentration of 50% inhibition (IC_{50}) was calculated to compare the doses of tested agents. IC_{50} was calculated with a linear curve and the equation for a line is ($Y = aX + b$), where "a" and "b" are the constants of the equation, "Y" is the inhibition of peristalsis (%), and "X" is the drug concentration (μg/mL).

2.4. Statistical Analyses. The significance of differences in mean values among groups was determined with analysis of variance. The data are expressed as means ± SEM. Differences were considered statistically significant if $P < 0.05$. All analyses were performed with the Statistical Package for the Social Science (SPSS for Windows, release 15.0, SPSS Inc., Chicago, IL, USA).

3. Results

3.1. Effects of Nonselective α-Blockers: Doxazosin, Tamsulosin, and Terazosin. A total of 100 ureteral samples were used in this study, and 88 were viable for the experiment. Ureteral peristalsis was recorded on polygraph paper. All tested α_1-adrenoceptor antagonists exerted an inhibitory effect on PE-induced ureteral peristalsis. Doxazosin (Figure 2), tamsulosin (Figure 3), and terazosin (Figure 4) dose dependently inhibited both 10^{-4} and 10^{-3} M PE-induced ureteral peristalsis.

3.2. Effects of FC Extract. FC-mediated inhibition was observed in 10^{-4} M PE-treated samples, and the levels of inhibition were 6.2 ± 10.1%, 21.8 ± 6.8%, and 24.0 ± 5.6% for the doses of 5×10^3, 1×10^4, and 2×10^4 μg/mL, respectively.

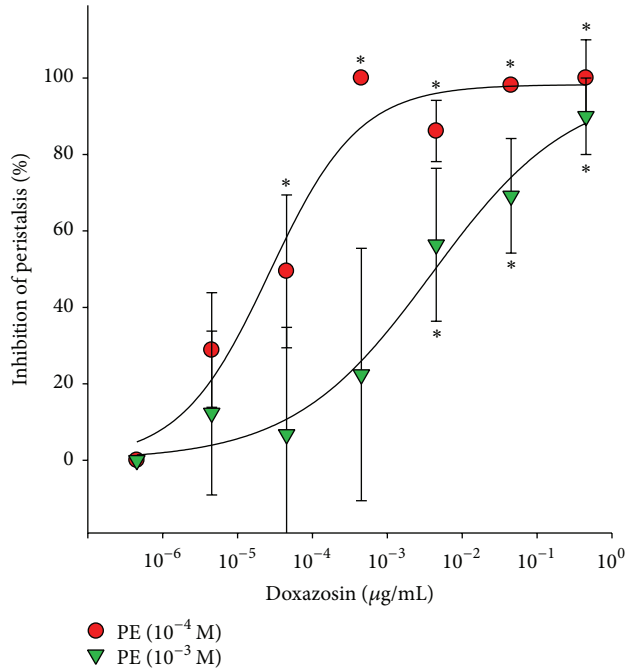

FIGURE 2: Inhibitory effect of doxazosin on porcine ureteral peristalsis. Graphic representation of concentration-response curves. The calculated data were presented as mean ± SEM for at least four different experiments. $^{*}P < 0.05$ compared to control group.

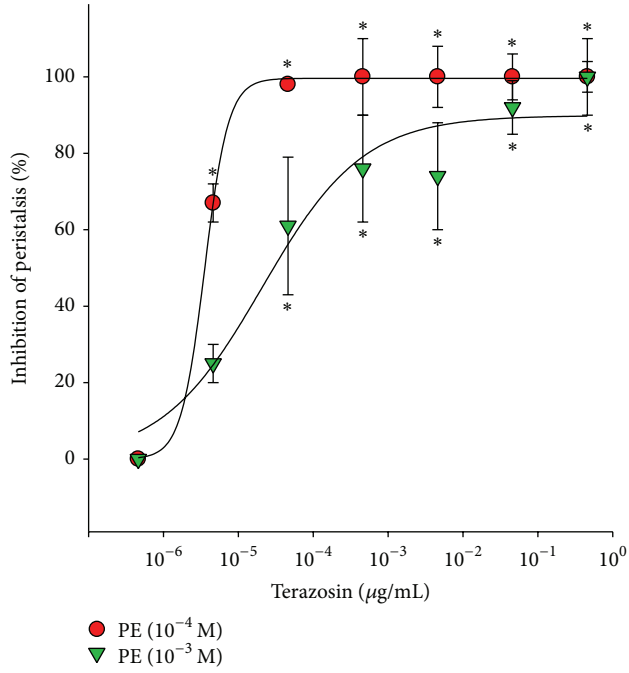

FIGURE 4: Inhibitory effect of terazosin on porcine ureteral peristalsis. Graphic representation of concentration-response curves. The calculated data were presented as mean ± SEM for at least four different experiments. $^{*}P < 0.05$ compared to control group.

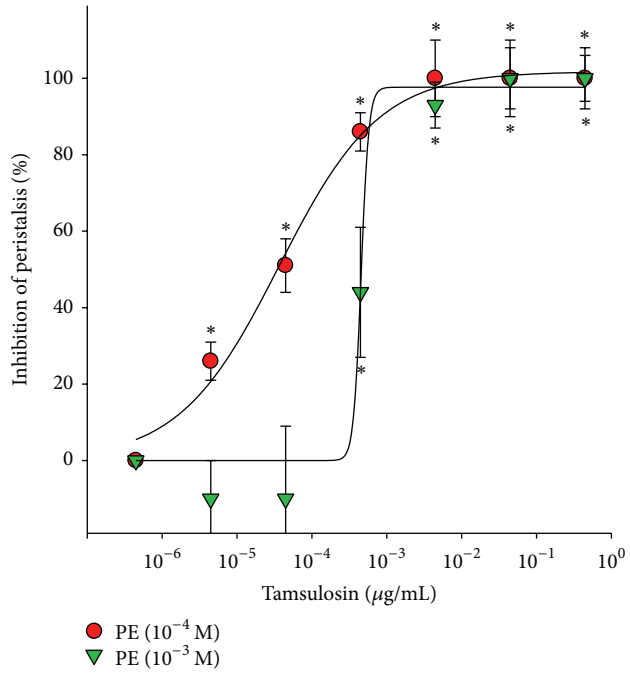

FIGURE 3: Inhibitory effect of tamsulosin on porcine ureteral peristalsis. Graphic representation of concentration-response curves. The calculated data were presented as mean ± SEM for at least four different experiments. $^{*}P < 0.05$ compared to control group.

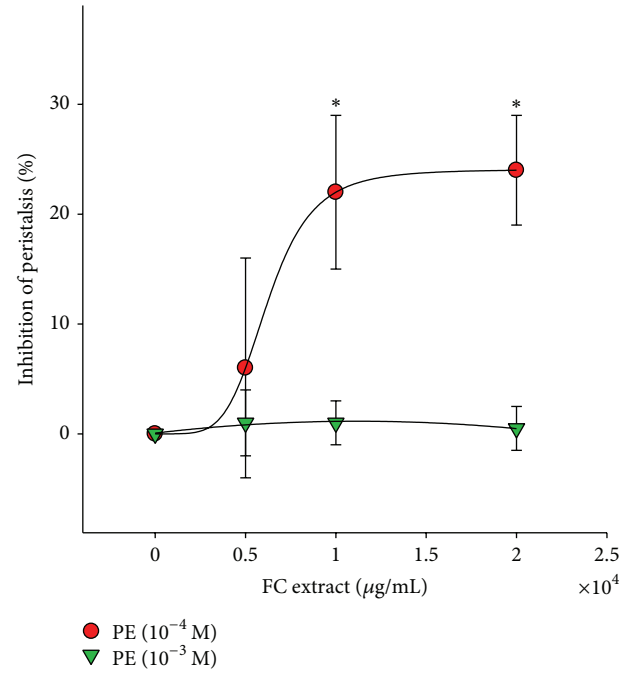

FIGURE 5: Effect of FC extract on porcine ureteral peristalsis. Graphic representation of concentration-response curves. The calculated data were presented as mean ± SEM for at least four different experiments. $^{*}P < 0.05$ compared to control group.

Table 1: The concentration of 50% inhibition (IC_{50}) of tested agents on the porcine proximal ureteral peristalsis.

IC_{50} (μg/mL)	Doxazosin	Tamsulosin	Terazosin	FC extract
PE (10^{-4} M)	2.9×10^{-5}	3.7×10^{-5}	3.9×10^{-6}	—
PE (10^{-3} M)	5.1×10^{-3}	4.9×10^{-4}	3.2×10^{-5}	—

FC: *Flos carthami*.
PE: phenylepinephrine.

However, FC extract did not have an inhibitory effect on 10^{-3} M PE-induced ureteral peristalsis (Figure 5). The IC_{50} of tested agents on the porcine proximal ureteral peristalsis is shown in Table 1.

4. Discussion

The results indicate that the tested agents inhibited PE-induced ureteral peristalsis in isolated porcine proximal ureter. Terazosin and tamsulosin had greater inhibitory effects than doxazosin. By contrast, FC extract only showed a weak inhibitory effect at concentrations of PE (10^{-4} M), with up to 24.0% inhibition at the highest dose. FC extract was ineffective at the higher concentration of PE (10^{-3} M)-induced ureteral peristalsis.

We used three α-blockers as experimental controls, and all of them exerted dose-dependent inhibitory effects on ureteral peristalsis. There are numerous studies describing the inhibitory effect that α-blockers have on distal ureteral peristalsis. Although there is a lack of innervation of the ureter, stimulation of α_1 adrenergic receptors may enhance its contraction. Therefore, α-blockers are hypothesised to have pharmacological effects that facilitate ureteral stone passage. Currently, α-blockers such as tamsulosin, terazosin, and doxazosin are used to treat lower urinary tract symptoms, and several clinical trials have suggested that these agents are helpful for MET. A randomised clinical trial by Červenàkov et al. indicated that tamsulosin increases stone expulsion rate [25].

Zaytoun et al. also studied the effects of tamsulosin and doxazosin as adjunctive therapies following shock wave treatment for renal stones in a randomised controlled clinical trial [26]. They found that both α-blockers decreased the time of stone expulsion, the amount of analgesic use, and the number of colics but did not find increased rates of stone expulsion. Tamsulosin more effectively decreased the number of colic episodes and decreased analgesic doses compared to doxazosin. This trial lasted up to 12 weeks and enrolled patients with renal stones <2 cm; they did not specifically assess ureteral stones, and it is possible that the α-blockers affected the entire ureter. MET has been studied extensively in recent years. Most reports confirmed that α-blockers facilitate stone passage spontaneously without shock wave treatment, especially in the distal ureter.

We investigated the effects of FC extract and α-blockers on proximal porcine ureter, which is less studied than the distal segment. Only a few reports have measured autonomic receptors in ureteral smooth muscle. Furthermore, it is difficult to maintain stable spontaneous contractions in the ureter, and either electrical field stimulation or high concentrations of KCl are utilized to induce ureteral contractions in many *in vitro* ureteral pharmacological examinations. We avoided these confounding variables by employing spiral ureteral strips, which generate spontaneous contractions.

The existence of α_1-, α_2-, and β-adrenoceptors and muscarinic cholinergic receptors were demonstrated in the canine ureter using radio-ligand techniques. The density of α_1-receptor-binding sites was significantly greater than that of other receptors examined. Morita et al. showed that the sympathetic nervous system is more involved than the parasympathetic nervous system in canine ureteral contractile activities and that α- and β-receptors in canine ureteral smooth muscle are comprised mainly of the α_1- and β-subtypes. Their results also suggested that prostaglandins directly affect canine ureteral contraction [27].

There are several reports on the use of TCM in the management of urinary stone disease [18]; the pharmacological effects include increased urinary volume, decreased crystal formation, and decreased secretion of promoter [28]. Purportedly, TCM treatments have fewer side effects than other antilithic treatments. We previously studied FC extract in a rat model and found a positive effect on the prevention of stone occurrence. However, delayed blood coagulation was also found [20]. This indicated that a large dose of single agent was inappropriate for the treatment of stone disease. There were fewer studies on the inhibition of ureteral peristalsis for MET; the present study of a TCM compound on the treatment of MET indicated a positive effect.

FC extract exerted inhibitory effects on the peristalsis of porcine proximal ureter, especially at the highest dose. Because FC extract was difficult to dissolve, further study is needed to achieve a dose that would match the effects achieved by α-blockers. Traditionally, a single herbal drug is not used to treat disease [29–31]; rather, most treatments are formulas. In addition, our previous work indicated that FC extract also affects blood coagulation [32]. For these reasons, increased dose of FC extract might be inappropriate for the treatment of stone disease. However, we believe that a combination of FC extract with another herbal medicine might be effective for MET.

This study has inherent advantages and limitations. First, the porcine ureter was useful in that we were able to obtain a large amount of viable samples. The experimental period time was short, and the results were easily observed and calculated. However, pig ureters may be not an ideal model for humans. For example, the variation (SEM) is so high in lower concentration of both data of α-adrenergic antagonists and FC extract. It may be caused because of the variances of the individual animal tissues. Second, the concentration of FC extract was limited, and we were unable to induce an inhibitory effect that was comparable with those achieved with α-blockers. Page et al. studied the effects of oral alfuzosin on ureteral pressure and peristalsis in a distally obstructed porcine ureter. They showed the increase in ureteral pressure and peristaltic rate with distal ureteral obstruction. Alfuzosin appears to decrease the delta pressure in the distal ureter

during obstruction; even statistical significance was not reached [33]. The opposite might be because of the difference between *in vivo* porcine study with oral administration of alfuzosin and *ex vivo* organ bath study. Further assessment of FC extract on MET should include oral administration in an animal model to increase the available dose. Moreover, a number of components in FC extract have been isolated, such as safflor yellow and carthamin [34]. Further studies on these effective constituents using this approach would be beneficiary.

5. Conclusions

In conclusion, all the tested α-blockers exerted inhibitory effects on porcine ureteral peristalsis in a dose-dependent manner. However, FC extract did not achieve the same inhibitory effect as the α-blockers. The present work assessed the effect of FC extract on ureter, which might provide clue for future mechanism of TCM studies. Since FC extract was unable to match the effects of α-blockers on inhibiting PE-induced ureteral peristalsis, suggesting the antilithic effect of FC extract is related to mechanisms other than modulation of ureteral peristalsis.

Conflict of Interests

The authors declare that they have no conflict of interests.

Acknowledgments

This study is supported in part by Taiwan Ministry of Health and Welfare Clinical Trial and Research Center of Excellence (DOH102-TD-B-111-004), Taiwan Ministry of Science and Technology (NSC102-2314-B-039-025), China Medical University (CMU) Hospital (CMU99-COL-01), and CMU under the Aim for Top University Plan of the Taiwan Ministry of Education. San-Yuan Wu and Kee-Ming Man contributed equally to this study. The authors thank the guest editor Professor Wu and the three anonymous reviewers for their constructive comments, which helped them to improve the paper.

References

[1] R. B. de Oliveira, E. B. Coelho, M. R. Rodrigues et al., "Effect of the *Copaifera langsdorffii* desf. leaf extract on the ethylene glycol-induced nephrolithiasis in rats," *Evidence-Based Complementary and Alternative Medicine*, vol. 2013, Article ID 131372, 10 pages, 2013.

[2] A. Premgamone, P. Sriboonlue, S. Maskasem, W. Ditsataporn-charoen, and B. Jindawong, "Orthosiphon versus placebo in nephrolithiasis with multiple chronic complaints: a randomized control trial," *Evidence-Based Complementary and Alternative Medicine*, vol. 6, no. 4, pp. 495–501, 2009.

[3] A. L. Shirfule, V. Racharla, S. S. Y. H. Qadri, and A. L. Khandare, "Exploring antiurolithic effects of gokshuradi polyherbal ayurvedic formulation in ethylene-glycol-induced urolithic rats," *Evidence-Based Complementary and Alternative Medicine*, vol. 2013, Article ID 763720, 9 pages, 2013.

[4] Y. Chen, H. Liu, H. Chen et al., "Ethylene glycol induces calcium oxalate crystal deposition in Malpighian tubules: a Drosophila model for nephrolithiasis/urolithiasis," *Kidney International*, vol. 80, no. 4, pp. 369–377, 2011.

[5] W. Chen, S. Wu, H. Liu et al., "Identification of melamine/cyanuric acid-containing nephrolithiasis by infrared spectroscopy," *Journal of Clinical Laboratory Analysis*, vol. 24, no. 2, pp. 92–99, 2010.

[6] D. M. Coll, M. J. Varanelli, and R. C. Smith, "Relationship of spontaneous passage of ureteral calculi to stone size and location as revealed by unenhanced helical CT," *The American Journal of Roentgenology*, vol. 178, no. 1, pp. 101–103, 2002.

[7] S. K. Singh, M. M. Agarwal, and S. Sharma, "Medical therapy for calculus disease," *BJU International*, vol. 107, no. 3, pp. 356–368, 2011.

[8] C. Wang, S. Huang, and C. Chang, "Efficacy of an α 1 blocker in expulsive therapy of lower ureteral stones," *Journal of Endourology*, vol. 22, no. 1, pp. 41–45, 2008.

[9] A. Singh, H. J. Alter, and A. Littlepage, "A systematic review of medical therapy to facilitate passage of ureteral calculi," *Annals of Emergency Medicine*, vol. 50, no. 5, pp. 552–563, 2007.

[10] B. Woolley, "Towards evidence based emergency medicine: best BETs from the Manchester Royal Infirmary. Use of tamsulosin in patients with urinary calculi to increase spontaneous stone passage," *Emergency Medicine Journal*, vol. 24, no. 10, pp. 725–726, 2007.

[11] T. Hermanns, P. Sauermann, K. Rufibach, T. Frauenfelder, T. Sulser, and R. T. Strebel, "Is there a role for tamsulosin in the treatment of distal ureteral stones of 7 mm or less? Results of a randomised, double-blind, placebo-controlled trial," *European Urology*, vol. 56, no. 3, pp. 407–412, 2009.

[12] R. Ochoa-Gómez, E. Prieto-Díaz-Chávez, B. Trujillo-Hernández, and C. Vásquez, "Tamsulosin does not have greater efficacy than conventional treatment for distal ureteral stone expulsion in Mexican patients," *Urological Research*, vol. 39, no. 6, pp. 491–495, 2011.

[13] K. Davenport, A. G. Timoney, and F. X. Keeley, "A comparative in vitro study to determine the beneficial effect of calcium-channel and α1-adrenoceptor antagonism on human ureteric activity," *BJU International*, vol. 98, no. 3, pp. 651–655, 2006.

[14] M. Hernandez, D. Prieto, U. Simonsen, L. Rivera, M. V. Barahona, and A. Garcia-Sacristan, "Noradrenaline modulates smooth muscle activity of the isolated intravesical ureter of the pig through different types of adrenoceptors," *British Journal of Pharmacology*, vol. 107, no. 4, pp. 924–931, 1992.

[15] P. Huang, H. Tsai, C. Wang et al., "Moderate intake of red wine improves ischemia-induced neovascularization in diabetic mice—roles of endothelial progenitor cells and nitric oxide," *Atherosclerosis*, vol. 212, no. 2, pp. 426–435, 2010.

[16] J. Shen, K. Man, P. Huang et al., "Honokiol and magnolol as multifunctional antioxidative molecules for dermatologic disorders," *Molecules*, vol. 15, no. 9, pp. 6452–6465, 2010.

[17] C. Lin, Y. Lin, P. Huang, H. Tsai, and Y. Chen, "Inhibition of endothelial adhesion molecule expression by *Monascus purpureus*-fermented rice metabolites, monacolin K, ankaflavin, and monascin," *Journal of the Science of Food and Agriculture*, vol. 91, no. 10, pp. 1751–1758, 2011.

[18] R. Miyaoka and M. Monga, "Use of traditional Chinese medicine in the management of urinary stone disease," *International Brazilian Journal of Urology*, vol. 35, no. 4, pp. 396–405, 2009.

[19] S. P. Mahamuni, R. D. Khose, F. Menaa, and S. L. Badole, "Therapeutic approaches to drug targets in hyperlipidemia," *BioMedicine*, vol. 2, no. 4, pp. 137–146, 2012.

[20] W. C. Lin, M. T. Lai, H. Y. Chen et al., "Protective effect of Flos carthami extract against ethylene glycol-induced urolithiasis in rats," *Urological Research*, vol. 40, no. 6, pp. 655–661, 2012.

[21] W.-C. Chen, W.-Y. Lin, H.-Y. Chen et al., "Melamine-induced urolithiasis in a *Drosophila* model," *Journal of Agricultural and Food Chemistry*, vol. 60, no. 10, pp. 2753–2757, 2012.

[22] T. J. Jerde, R. Saban, and S. Y. Nakada, "Evaluation of ureteric contraction: a comparison among ring, spiral-cut and longitudinal segments," *BJU International*, vol. 83, no. 1, pp. 95–100, 1999.

[23] H.-Y. Chen, W.-Y. Lin, Y.-H. Chen, W.-C. Chen, F.-J. Tsai, and C.-H. Tsai, "Matrix metalloproteinase-9 polymorphism and risk of pelvic organ prolapse in Taiwanese women," *European Journal of Obstetrics Gynecology and Reproductive Biology*, vol. 149, no. 2, pp. 222–224, 2010.

[24] P.-L. Liu, J.-R. Tsai, C.-C. Chiu et al., "Decreased expression of thrombomodulin is correlated with tumor cell invasiveness and poor prognosis in nonsmall cell lung cancer," *Molecular Carcinogenesis*, vol. 49, no. 10, pp. 874–881, 2010.

[25] I. Červenàkov, J. Fillo, J. Mardiak, M. Kopečný, J. Šmirala, and P. Lepieš, "Speedy elimination of ureterolithiasis in lower part of ureters with the alpha 1-blocker - Tamsulosin," *International Urology and Nephrology*, vol. 34, no. 1, pp. 25–29, 2002.

[26] O. M. Zaytoun, R. Yakoubi, A. R. M. Zahran et al., "Tamsulosin and doxazosin as adjunctive therapy following shockwave lithotripsy of renal calculi: randomized controlled trial," *Urological Research*, vol. 40, no. 4, pp. 327–332, 2012.

[27] T. Morita, M. Ando, K. Kihara, and H. Oshima, "Function and distribution of autonomic receptors in canine ureteral smooth muscle," *Neurourology and Urodynamics*, vol. 13, no. 3, pp. 315–321, 1994.

[28] S. K. Pareta, K. C. Patra, P. M. Mazumder, and D. Sasmal, "Aqueous extract of Boerhaavia diffusa root ameliorates ethylene glycol-induced hyperoxaluric oxidative stress and renal injury in rat kidney," *Pharmaceutical Biology*, vol. 49, no. 12, pp. 1224–1233, 2011.

[29] W. L. Liao and F. J. Tsai, "Personalized medicine: a paradigm shift in healthcare," *BioMedicine*, vol. 3, no. 2, pp. 66–72, 2013.

[30] F.-J. Tsai, "Biomedicine brings the future nearer," *BioMedicine*, vol. 1, no. 1, p. 1, 2011.

[31] M. C. Yin, "Biomedicine offers advanced medical findings," *BioMedicine*, vol. 2, no. 1, part 1, 2012.

[32] W. Lin, M. Lai, H. Chen et al., "Protective effect of Flos carthami extract against ethylene glycol-induced urolithiasis in rats," *Urological Research*, vol. 40, no. 6, pp. 655–661, 2012.

[33] J. B. Page, S. Humphreys, D. Davenport, P. Crispen, and R. Venkatesh, "Second prize: *in-vivo* physiological impact of alpha blockade on the porcine ureter with distal ureteral obstruction," *Journal of Endourology*, vol. 25, no. 3, pp. 391–396, 2011.

[34] J. Asgarpanah and N. Kazemivash, "Phytochemistry, pharmacology and medicinal properties of Carthamus tinctorius L," *Chinese Journal of Integrative Medicine*, vol. 19, no. 2, pp. 153–159, 2013.

Hindawi Publishing Corporation
Evidence-Based Complementary and Alternative Medicine
Volume 2014, Article ID 965429, 8 pages
http://dx.doi.org/10.1155/2014/965429

Research Article

Inhibitory Effect of Sihuangxiechai Decoction on Ovalbumin-Induced Airway Inflammation in Guinea Pigs

Xue Ping Huang,[1] En Xue Tao,[2] Zhan Qin Feng,[3] Zhao Lu Yang,[1] and Wei Fen Zhang[3]

[1] *Department of Radiology, Affiliated Hospital of Weifang Medical University, No. 2428, Yuhe Street, Weifang, Shandong 261031, China*
[2] *Universtiy Hospital of Weifang Medical University, Weifang, Shandong 261053, China*
[3] *College of Pharmacy and Biological Science, Weifang Medical University, No. 7166, Baotong West Street, Weifang, Shandong 261053, China*

Correspondence should be addressed to Zhao Lu Yang; wyfyfangliaoke@163.com and Wei Fen Zhang; zwf2024@126.com

Received 14 April 2014; Revised 20 May 2014; Accepted 27 May 2014; Published 2 July 2014

Academic Editor: Shi-Biao Wu

The aim of this study was to investigate the effect of sihuangxiechai decoction on asthmatic Guinea pig model which was sensitized by intraperitoneal (i.p.) injection of ovalbumin (OVA) and challenged by OVA inhalation to induce chronic airway inflammation. Differential cell counts of cytospins were performed after staining with Giemsa solution. The quantity of leukocytes and its classification in bronchoalveolar lavage fluid (BALF) and blood were evaluated by blood cell analyzer and microscope. Histological analysis of the lung was performed by hematoxylin and eosin (H&E) staining. The levels of interleukin-4 (IL-4) and tumor necrosis factor-alpha (TNF-α) in BALF and serum were detected by radioimmunoassay (RIA). The total number of leukocytes in BALF and blood has no significant difference between Sihuangxiechaitang decoction treated group and dexamethasone (DXM) treated group but was significantly lower than those of asthma group. The percentage of eosinophils in lung tissues of sihuangxiechai decoction treated group was significantly lower than that of asthma group. The results demonstrated that the levels of IL-4 and TNF-α in the sihuangxiechai decoction treated group were significantly reduced compared with the asthma group. In conclusion, these findings demonstrate that sihuangxiechai decoction has a protective effect on OVA-induced asthma in reducing airway inflammation and airway hyperresponsiveness (AHR) in a Guinea pig model and may be useful as an adjuvant therapy for the treatment of bronchial asthma.

1. Introduction

Bronchial asthma is the most common chronic respiratory disease which is seriously damaging to people's health. The prevalence of asthma is markedly increasing worldwide, and it has been included to be a significant cause of morbidity and mortality in developed countries [1, 2]. It has been broadly recognized that asthma is characterized by structural alterations in the airways [3] and variable degrees of chronic inflammation which can lead to recurrent episodes of wheezing, breathlessness, chest tightness, and cough. This chronic disease also causes bronchospasm, bronchial mucosal thickening from edema, eosinophilic infiltration, bronchial wall remodeling, and excessive mucus production and can ultimately lead to airway obstruction [4–6]. These reactions have been referred to as airway remodeling, which is considered to occur as a result of an imbalance in the mechanism of airway regeneration and repair. Recent studies indicate that asthma is a chronic inflammatory airway disease that is caused by a variety of cells like eosinophils (Eos), mast cells, neutrophils, T lymphocytes, airway epithelial cells, and a number of cytokines [7]. These cells secrete several chemical mediators, such as major basic protein (MBP), eosinophil cationic protein (ECP), eosinophil peroxidase (EPO), lipid ecosystems, elastase, and Th2 cytokines, such as IL-4 (a switch factor for IgE synthesis), IL-5, and IL-13 [8]. Therefore, these cells are considered as major targets for basic and therapeutic research. Among them, Eos together with Th2 cytokines IL-4, IL-5, and IL-13 may ultimately contribute to AHR in asthma; it can also cause airway inflammation

in the initial and effector phase stages of allergy [9, 10]. Toxic proteins produced and released by Eos could injure airway epithelium directly; then, remodeling is associated with more severe airflow obstruction; therefore, AHR is produced. There is evidence that Eos inflammation of the airway is involved in the risk of exacerbations. Eos has important antigen presenting function. It also could be used as antigen presenting cell (APC) that participates in the pathogenesis of asthma by producing the potent cytokine IL-4. Meanwhile, IL-4 can also promote Th0 differentiation into Th2 and produce a large number of cytokines. Many characteristics of asthma are deemed to reflect consequences of Th2 cell-dominated immune responses to allergens. Furthermore, allergen-specific Th2 cells play a pivotal role in the pathogenesis of asthma. Airway Eos, together with IL-4, IL-5, and IL-13, may directly act on epithelial and smooth muscle cells in airway epithelium to induce mucus hyperproduction, goblet cell hyperplasia, and AHR [7, 11–13]. In addition, IgE plays a crucial role in the propagation of airway inflammation in allergic asthma. It is well known that IgE levels positively correlate with the presence of asthma symptoms, probability for allergic sensitization [14].

Likewise, tumor necrosis factor-alpha (TNF-α) is considered to be a significant proinflammation and the promoter of the airway inflammation in asthma. Both IL-13 and TNF-α are well known as remodeling associated cytokines [15]. Furthermore, asthma inflammation is also induced by cytokines released from TNF-α, which can increase the production of more inflammatory mediators, including IL-8, granulocyte-macrophage colony-stimulating factor (GM-CSF), and other cytokines. Clinical observation and animal experimentation indicated that the content of TNF-α in BALF was elevated when asthma attacks [16–19].

Since the establishment of the doctrine of airway inflammation, anti-inflammatory therapy had an irreplaceable role in asthma. Because of its anti-inflammatory, antiallergy, and other pharmacological effects, glucocorticoids have become the first-line drugs for treating asthma [20]. Although corticosteroids can significantly ameliorate airway inflammation and inhibit Eos infiltration and airway inflammatory mediator release, it cannot change the course of the disease. A lot of practice has proved that traditional Chinese medicine (TCM) has the holism in mind and superiority in synthetic action in the treatment of asthma. In previous report, the compounds of Chinese medicines (*Astragalus membranaceus*, honey-fried herba ephedrae, stir-baked radix scutellariae, rhizoma polygonati, scorpio, centipede, radix bupleuri, and cassia twig) were considered to improve the patient's constitution, regulate immune function, and enhance the anti-inflammatory and antiallergic ability and it has enjoyed satisfied clinical application [21]. For example, *Astragalus membranaceus* (Huangqi) are amongst the most popular health-promoting herbs in China; their use dates back to more than 2000 years and were recorded in *Shen Nong's Materia Medica* written in the Han Dynasty. It has also been used in the treatment of diabetes mellitus, nephritis, leukemia, and uterine cancer [22]. In addition, *Scutellaria baicalensis* is a widely used Chinese herbal medicine that has been used historically in anti-inflammatory and anticancer therapy [23].

In this paper, we investigated the effect of sihuangxiechai decoction applied to allergic diseases. The ovalbumin (OVA) was used to induce asthma Guinea pig model which evaluated the possible effects and mechanisms of sihuangxiechai decoction on inflammation and systemic immune responses. According to the research of quantitative analysis of inflammation and the role of cytokines in OVA-induced asthma Guinea pig model, the aim of this study was to explore the mechanism of Chinese medicine prescriptions on asthma and mine new drugs which could enhance immunity, improve the body's defenses function, enhance the resistance to disease, and provide pharmacodynamics and mechanism of the experimental basis for clinical.

2. Materials and Methods

2.1. Animal. 32 healthy male Guinea pigs (weighing 250 ± 30 g) were purchased from Lukang & Co. (Jining, Shandong, China). The Guinea pigs were housed under standard laboratory conditions for one week. All Guinea pigs were provided with food and tap water *ad libitum*. All experimental procedures were carried out in accordance with the NIH Guidelines for the Care and Use of Laboratory Animals, and animal handling followed the dictates of the National Animal Welfare Law of China [24, 25].

2.2. Materials. Ovalbumin (OVA) was obtained from Sigma Company (Sigma & Co., American) and purchased from Beijing Branch Company after packing. Dexamethasone was purchased from Yongning Pharmaceutical Co., Ltd. (Jinan, Shandong, China), batch number: 0203131. Sihuangxiechai decoction was provided by the pharmacy in our hospital. The radioimmunoassay (RIA) kits of IL-4 and TNF-α were purchased from Science and Technology Development Center of PLA General Hospital. Piston compressor nebulizer was manufactured by San Up S.A. (San Up S.A., Argentina). γ-counter was produced by Shanghai annular company.

2.3. Preparation of Sihuangxiechai Decoction. This formula is a dried decoction of a mixture of 16 medicinal herbs (Table 1). The quality of each crude drug was tested in accordance with the pharmacopoeia of China. The herbs were soaked in cold water, which were dissolved in the 2 times bigger volume of water, boiled for 30 min, filtered, and boiled with slow fire for 20 min, poured out the supernatant fluid about 200 mL. Then the dregs were added in boiling water in the same way with 3 replications. All the liquid was combined and concentrated to 2 g/mL. Moreover, scorpion and centipede were ground into powder and added into the liquid directly.

2.4. Experimental Group and Drug Treatment. The experimental groups ($n = 8$) were randomly divided into four groups as follows: normal group, asthma group, dexamethasone-treated group (DXM group), and traditional Chinese medicine group (TCM group). Except normal group, the remaining groups of animals were induced by intraperitoneal

Table 1: The main component of sihuangxiechai decoction.

Herbal medicine	Mass (g)
Astragalus	9
Honey-fried herba ephedrae	9
Stir-baked radix scutellariae	9
Rhizoma polygonati	9
Scorpio	6
Centipede	6
Radix bupleuri	9

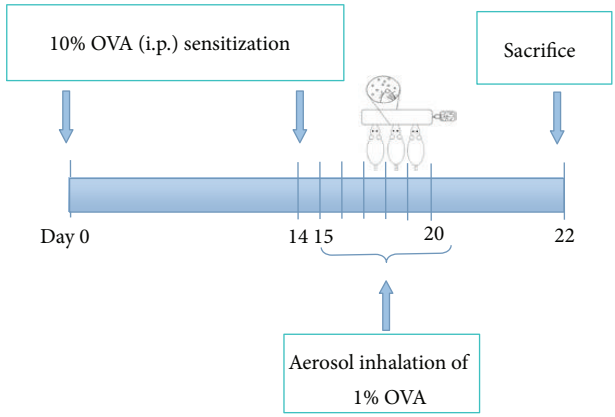

Figure 1: Schematic representation of the experiment procedure. The Guinea pigs were sensitized with intraperitoneal (i.p.) injection of OVA on day 0 and challenged with aerosolized OVA for six consecutive days 14 days later. The animals were sacrificed 24 hours after the last challenge, and tissue samples were collected on day 22.

injection of 1 mL of 10% OVA on day 0. After 14 days, the oversensitized animals showed asthma symptoms while inhaling with an aerosol of 20 min of 1% OVA using piston compressor nebulizer for 6 days every other day (Figure 1). The OVA-sensitized animals were treated with TCM (10 g/kg/day) suspended in NS (0.9%) by oral gavage 30 minutes before the OVA challenge. Normal group and asthma group were treated with only NS (0.9%, 10 g/kg/day) by oral gavage, and the positive control group (DXM group) was treated with DXM (2 mg/kg/day) by intraperitoneal injection (i.p.) before the OVA challenge [26].

2.5. Bronchoalveolar Lavage Fluid (BALF). 24 h after the last OVA challenge, all Guinea pigs were anesthetized by intraperitoneal injection of pentobarbital (50 mg/kg, 3%). Thoracotomy was performed according to standard surgical procedures. BALF was collected by flushing 1 mL of NS (0.9%) into the lung via the trachea immediately after sacrifice. Approximately 0.8 mL of BALF was recovered after three lavages. The BALF was centrifuged (400 g, 4°C, 5 min) and the supernatant was stored at −70°C until measurement of cytokines. Cells from the BALF were washed three times with PBS and the pellet was resuspended in 100 μL of phosphate buffer solution (PBS). Total cell number was counted and differential cell counts of cytospins were performed after staining with Giemsa solution. The cells were differentiated by general leukocyte morphology and 200 cells were counted in each of four random locations.

2.6. Blood Collection. After BALF was collected, the Guinea pigs were euthanized by aortic exsanguination. The artery blood was collected in different tubes with sodium citrate anticoagulant or gel procoagulant for different tests and centrifuged at 4°C (4000 rpm) for 10 min [27]. Subsequently, the serum was stored at −70°C for measurement of cytokines [20].

2.7. Measurement of IL-4 and TNF-α Using Radioimmunoassay (RIA). IL-4 and TNF-α concentrations of each sample were detected by radioimmunoassay (RIA) according to the manufacturer's instructions. Samples and standard products were mixed with IL-4 and TNF-α antibodies and then incubated at 37°C for 20 minutes. After centrifugation (3500 r/min, 4°C), the supernatant in each tube was measured by γ-counts. Finally, according to the standard curve, the concentrations of IL-4 and TNF-α were calculated. All samples and standards were assayed in duplicate.

2.8. Histological Analysis. Prior to the removal of the lung, the lung tissue and trachea were filled intratracheally with fixative (10% formaldehyde) using a ligature around the trachea. Lung tissue was fixed in 10% formaldehyde. The tissues were dehydrated in various concentrations of ethanol and embedded in paraffin. For histopathological examination, 4 μm sections fixed tissues were cut on a microtome (Leica RM 2235, Microsystems Nussloch GmbH, Germany), placed on glass slides, deparaffinized, and stained with H&E for general morphology. Tissue lesion and inflammatory cell infiltration were then examined using microscope [27–29].

2.9. Statistical Analysis. All of the quantitative data analyses were performed using statistical software programs SPSS 17.0. All results were expressed as means ± standard errors of the mean. All statistical significance of differences was assessed by one-way ANOVA followed by Student's t-tests. In all cases, $P < 0.05$ was considered statistically significant.

3. Result

3.1. Effects of TCM on OVA-Induced Total and Differential Leukocytes in BALF. As shown in Table 2, the total number of leukocytes in BALF of asthma group (17.77 ± 1.89) was significantly increased compared with normal group (8.44 ± 1.97, $P < 0.01$) and was significantly higher than those of TCM group (13.62 ± 2.18, $P < 0.01$) and DXM group (12.9 ± 1.57, $P < 0.01$). In addition, the percentage of Eos (Figure 2) in TCM group (14.49 ± 1.92) has no significant difference with DXM group (15.08 ± 2.60, $P > 0.05$) but was significantly lower than that of asthma group (45.05 ± 6.64, $P < 0.01$) and was higher than that of normal group (4.01 ± 1.93, $P < 0.01$). The percentages of neutrophils, epithelial cells, and lymphocytes were remarkably higher in the asthma

Table 2: Counting and classification of leukocytes in BALF by treatment with TCM (%, $\overline{x} \pm S$).

Classification	Normal group	Asthma group	DXM group	TCM group
Leukocyte	8.44 ± 1.97	$17.77 \pm 1.89^{**}$	$12.90 \pm 1.57^{**\Delta\Delta}$	$13.62 \pm 2.18^{**\Delta\Delta}$
Neutrophils	5.08 ± 2.62	$12.34 \pm 2.61^{**}$	$9.31 \pm 0.63^{**\Delta}$	$9.28 \pm 0.98^{**\Delta}$
Epithelial cells	4.32 ± 0.45	$12.35 \pm 1.44^{**}$	$1.74 \pm 0.40^{**\Delta\Delta}$	$1.10 \pm 0.41^{**\Delta\Delta}$
Eosinophilic	4.01 ± 1.93	$45.05 \pm 6.64^{**}$	$15.08 \pm 2.60^{**\Delta\Delta}$	$14.69 \pm 2.92^{**\Delta\Delta}$
Lymphocytes	3.90 ± 0.97	4.20 ± 0.51	$2.60 \pm 1.30^{*\Delta}$	$2.93 \pm 0.43^{*\Delta}$
Macrophage-monocytes	83.04 ± 3.01	$25.42 \pm 6.21^{**}$	$72.00 \pm 5.59^{**\Delta\Delta}$	$73.62 \pm 5.59^{**\Delta\Delta}$

$^{*}P < 0.05$ and $^{**}P < 0.01$ when compared with normal group; $^{\Delta}P < 0.05$ and $^{\Delta\Delta}P < 0.01$ when compared with asthma group.

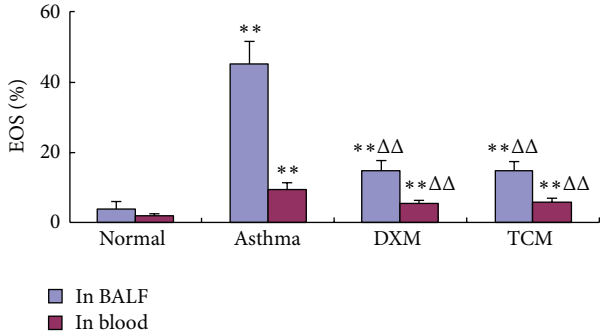

Figure 2: The percentages of EOS in BALF and blood.

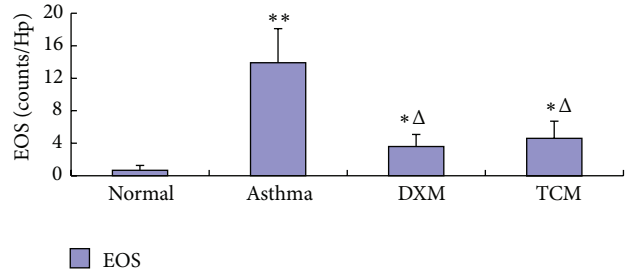

Figure 3: The changes of EOS infiltrating in the lung tissue.

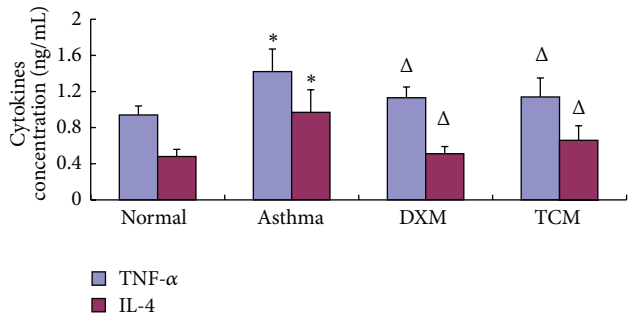

Figure 4: The concentration of TNF-α and IL-4 in serum.

group when compared with TCM group ($P < 0.01$) and DXM group ($P < 0.01$). As a positive control group, DXM group showed a similar suppressive effect on leukocyte influx into BALF, which indicated that TCM group ($P < 0.01$) was more favorable to treat with asthma.

3.2. Effects of TCM on OVA-Induced Total and Differential Leukocytes in Blood. As shown in Table 3, compared with the normal group (10.03 ± 2.74), a total number of leukocytes in blood were significantly increased in asthma group (18.16 ± 2.27, $P < 0.01$) and were significantly higher than that of TCM group (13.40 ± 1.67, $P < 0.05$) and DXM group (13.13 ± 1.42, $P < 0.05$). In addition, the percentage of Eos (Figure 3) in TCM group (5.93 ± 1.12) has no significant difference with DXM group (5.43 ± 1.12, $P > 0.05$) but was significantly lower than that of asthma group (9.70 ± 1.86, $P < 0.01$) and was higher than that of normal group (1.97 ± 0.79, $P < 0.01$). The percentages of neutrophils, epithelial cells, and lymphocytes were remarkably higher in the asthma group when compared with TCM group ($P < 0.01$) and DXM group ($P < 0.01$). As a positive control group, DXM showed a similar suppressive effect on leukocyte influx into BALF, which indicated that TCM group ($P < 0.01$) was more favorable to treat with asthma.

3.3. Effects of TCM on OVA-Induced EOS Airway Inflammation. A large number of Eos infiltrations can be seen through the lung tissue of asthma group (13.9 ±4.21, $P < 0.01$), which were significantly increased compared with the normal group (0.67 ± 0.59, $P < 0.01$) and were significantly higher than that of TCM group (4.6 ± 2.12, $P < 0.01$) and DXM group (3.6 ± 1.49, $P < 0.01$). There was no different from that of DXM group and TCM group (Figure 3).

3.4. The Levels of TNF-α and IL-4 in BALF and Serum. As shown in Figures 4 and 5, the OVA-induced asthma group significantly increased the concentrations of TNF-α and IL-4 in BALF in comparison to the normal group ($P < 0.01$, $P < 0.01$). Moreover, the concentrations of TNF-α and IL-4 in serum of the TCM group (1.14 ± 0.21, 0.66 ± 0.16) were obviously lower than the asthma group ($P < 0.05$, $P < 0.01$) and have no significant difference with DXM group (1.13 ± 0.12, 0.51 ± 0.08).

3.5. Effects of TCM on OVA-Induced EOS in Lung Tissue Biopsy. Lung tissue sections of OVA-induced Guinea pigs were stained with H&E and examined using light microscopy. Histological evaluation of the lung tissue demonstrated that, compared with the normal group, numerous inflammatory cells were observed in the lung interstitium around airways and blood vessels in the asthma group (Figure 6(b)).

Table 3: Counting and classification of leukocytes in blood by treatment with TCM (%, $\overline{x} \pm S$).

Groups	Normal group	Asthma group	DXM group	TCM group
Leukocytes	10.03 ± 2.74	18.16 ± 2.27**	13.13 ± 1.42*Δ	13.40 ± 1.67*Δ
Eosinophils	1.97 ± 0.79	9.70 ± 1.86**	5.43 ± 1.12**ΔΔ	5.93 ± 1.12**ΔΔ
Neutrophils	40.14 ± 8.13	62.66 ± 7.97**	50.67 ± 3.20*ΔΔ	53.33 ± 3.98**Δ
Lymphocytes	47.97 ± 4.06**	27.07 ± 1.98**	43.93 ± 1.57**ΔΔ	60.25 ± 4.65**ΔΔ

*$P < 0.05$ and **$P < 0.01$ when compared with normal group; $^{\Delta}P < 0.05$ and $^{\Delta\Delta}P < 0.01$ when compared with asthma group.

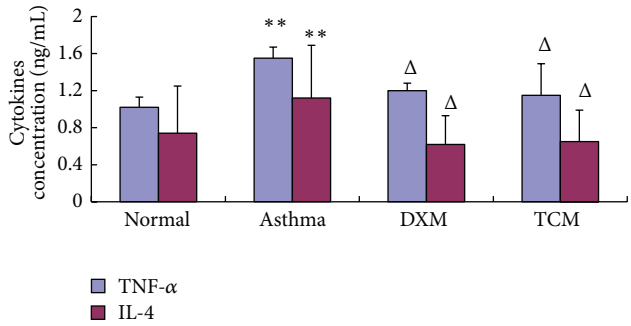

Figure 5: The concentration of TNF-α and IL-4 in BALF.

The results showed that only a few Eos and lymphocytes were distributed in the small bronchus of the normal group (Figure 6(a)). Guinea pigs treated by TCM significantly downregulated the accumulation of mucus in the airways and prevented the accumulation of Eos in BALF after OVA challenge (Figure 6(c)) compared with the asthma group. Likewise, DXM group showed a substantial reduction in inflammation and Eos infiltration into lungs (Figure 6(d)). Mucosal epithelium was tidy and the lung tissue was basically normal without obvious pathology change.

4. Discussion

OVA-induced asthma is a complicated inflammatory disease characterized by reversible airway obstruction, airway remodeling, airway inflammation, and AHR. The accompanying airways inflammation is characterized by infiltration of the airway wall with mast cells, lymphocytes, and Eos in the bronchial epithelium and lamina propriety [20, 30, 31]. In recent years, inhaled corticosteroids, leukotriene receptor antagonists, or β2-agonists are considered the most effective means of reducing airway inflammation, symptoms, and morbidity in patients with asthma. However, these treatments can produce potential negative side effects and do not consistently ameliorate airway inflammation in many asthmatic individuals [26, 32]. Thus, a safe and effective method is needed for the treatment of asthma.

The exact mechanism of herbs medicines on asthma is not entirely clear, but it is considered to be dependent on many persistent inflammatory cells, including infiltrating lymphocytes, Eos, basophils, and macrophages, and activated, and then synthesis and release of various pro-inflammatory mediators and cytokines [7, 20, 33, 34]. In this study, we have demonstrated a correlation between sihuangxiechai decoction and asthma. Dong et al. [27] showed evidences of lung tissue histological assay that various degrees of inflammation appeared in all OVA-induced animals. However, the asthma rats presented with more severe inflammation (inflammatory cell influx) than the treatment groups, and generally more serious inflammation was found in the DXM group than in TCM group. Our data showed that the total number of leukocytes in BALF and blood of asthma group was significantly higher than the other groups ($P < 0.01$), and rats treated with drugs showed substantial decrease compared with asthma rats ($P < 0.01$). This result suggested that sihuangxiechai decoction has an effect on the OVA-induced asthma. In addition, Regal [35] and Holgate et al. [36] concluded that Eos airway inflammation has been shown to be one of the basic features of allergic asthma. In our study, the percentage of Eos infiltrating in TCM group was significantly decreased in BALF and blood after OVA challenge (Figure 2) compared with the asthma group. Likewise, DXM group showed a substantial reduction in inflammation and eosinophilic infiltration into lungs (Figure 6(d)). These findings are consistent with the presented evidence for a significant increase in serum Eos level in TCM group.

Guan et al. [37] demonstrated that adequate assessment of inflammatory cells, cytokines, chemokines, and anti-inflammatory molecules is essential for understanding, monitoring, and treating lung diseases. Additionally, Stow et al. [38] concluded that IL-1β, IL-4, IL-13, and TNF-α have been found to reduce the severity of the inflammatory reaction. Larché et al. [39] and Bisset and Schmid-Grendelmeier [40] showed that allergic asthma is characterized by unbalance of Th1/Th2 cell and recruitment of type-2 T helper (Th2) cells. Th1 cells mainly excrete cytokines like IL-2, IFN-α, and TNF-α; Th2 cells mainly excrete cytokines like IL-4, IL-5, IL-6, IL-9, and IL-13 [27]. Through the manufacture and release of proinflammatory mediators, Eos can amplify the expression of Th1, Th2, and Th17 cytokines and chemokines suggesting that they play a vital role in the adaptive immune responses [41]. Activated Eos can secrete some basic proteins which may also be associated with the pathophysiology of asthma such as MBP, ECP, and EPO [8]. Previous studies have demonstrated that MBP can increase vascular permeability, bronchoconstriction, and airway epithelial damage; then remodeling is associated with more severe airflow obstruction, and AHR made in asthma. In our study, we found that the concentration of IL-4 and TNF-α in BALF or blood of TCM group both was markedly lower than that of asthma groups ($P < 0.05$, $P < 0.01$) and has no significant difference

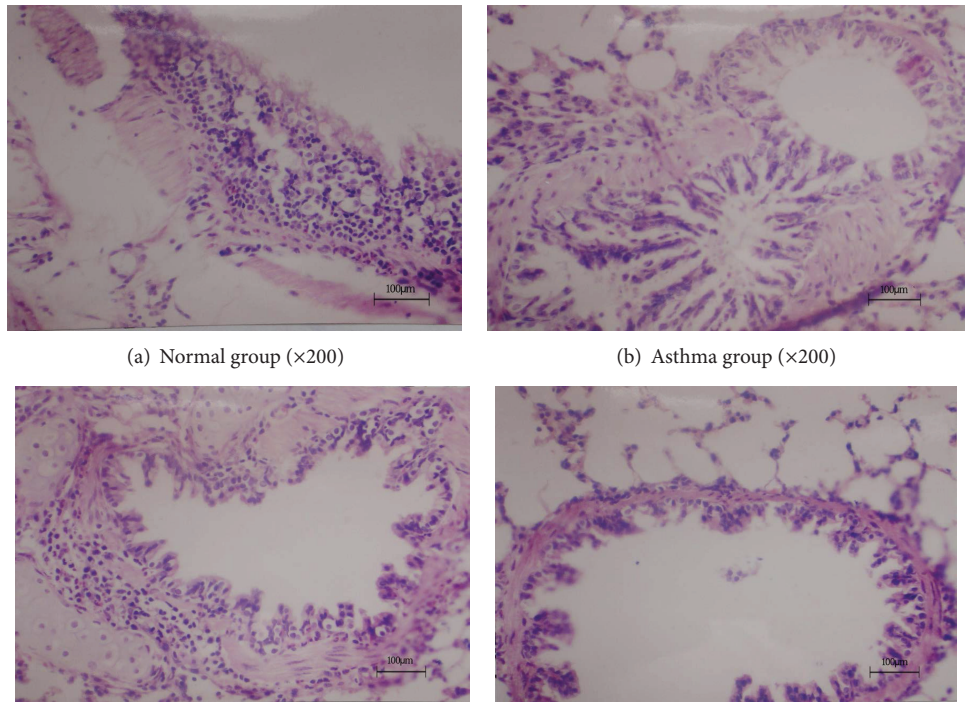

(a) Normal group (×200)

(b) Asthma group (×200)

(c) TCM group (×200)

(d) DXM group (×200)

Figure 6: The airway inflammation in OVA-induced Guinea pigs. Lung tissue sections of OVA-induced/challenged Guinea pigs, stained with H&E and examined using light microscopy (magnification 200x). Scale bar = 100 μm.

with DXM group ($P < 0.05$, $P < 0.05$). These results indicated that IL-4 and TNF-α were involved in the pathogenesis and development of asthma. Furthermore, all these results indicated that sihuangxiechai decoction had an inhibitory effect on the contents of IL-4 and TNF-α.

Sihuangxiechai decoction was composed of Xiaoqinglong decoction, Xiaochaihu decoction, and the powder of scorpion and centipede with the permit addition and subtraction. Huang et al. [42] concluded that Xiaoqinglong decoction and shegan mahuang decoction were widely used in clinic and received good curative effect. In this prescription, *Astragalus* with honey-fried herba ephedrae, stir-baked radix scutellariae, rhizoma polygonati, scorpio, centipede, and radix bupleuri have also been used as a traditional herb with sedative, antispasmodic, stomachic, tonic, diuretic, and topical bactericidal properties in order to enhance the effect of anti-inflammatory, antiallergic, antirheumatism, and immunosuppressive. In our study, inflammatory infiltration cells in or around the bronchus were significantly decreased in the TCM group more than in the asthma group, suggesting that sihuangxiechai decoction has curative effect on the bronchus inflammation of asthma (Figure 6).

In conclusion, this study clearly shows that sihuangxiechai decoction not only has evident antifebrile, antitussive, expectorant, and antiasthmatic effects but also relieves clinical symptoms and signs of asthma. Both of the TCM and DXM groups showed that Eos infiltration was reduced in various degrees and thus confirmed that the prescription can not only reduce Eos counts in peripheral blood but also decrease the possibility of EOS recruiting into airway. Additionally, prescriptions can suppress the damage of toxic proteins which were released by EOS and the formation of AHR. In summary, OVA-induced asthma treated by sihuangxiechai decoction is through multiple mechanisms to achieve their good treatment; at the same time, this method has provided the scientific basis for the application of clinical.

5. Conclusions

This study showed that sihuangxiechai decoction not only reduced the infiltration of leukocytes (especially Eos) but also suppressed histopathological changes such as airway remodeling and AHR. In conclusion, the results demonstrated that sihuangxiechai decoction might be a new potential therapy for the management of asthma in humans and for suppressing airway inflammation in a rat model of bronchial asthma. Further studies should be undertaken to clarify its detailed mechanism of action.

Conflict of Interests

The authors declare that there is no conflict of interests regarding the publication of this paper.

Authors' Contribution

Xue Ping Huang and En Xue Tao contributed equally to this work.

Acknowledgments

The authors are grateful for the generous financial support from the National Key Technology R&D Program of the Ministry of Science and Technology (no. 2013GA740103), the National Natural Science Foundation of China (no. 81370628), Shandong Provincial Natural Science Foundation, China (ZR2012CM025), for grant support, the Scientific and Technological Development Project of Shandong Province (2012YD18063), and Shandong Province Higher Educational Science, Technology Program (J11LF67).

References

[1] M. S. Choi, S. Park, T. Choi et al., "Bee venom ameliorates ovalbumin induced allergic asthma via modulating $CD4^+CD25^+$ regulatory T cells in mice," *Cytokine*, vol. 61, no. 1, pp. 256–265, 2013.

[2] S. S. Braman, "The global burden of asthma," *Chest*, vol. 130, no. 1, supplement, pp. 4S–12S, 2006.

[3] A. M. Vignola, J. Kips, and J. Bousquet, "Tissue remodeling as a feature of persistent asthma," *Journal of Allergy and Clinical Immunology*, vol. 105, no. 6, pp. 1041–1053, 2000.

[4] J. W. Seo, S. C. Cho, S. J. Park et al., "1′-acetoxychavicol acetate isolated from *Alpinia galanga* ameliorates ovalbumin-induced asthma in mice," *PLoS ONE*, vol. 8, no. 2, Article ID e56447, pp. 1–8, 2013.

[5] A. B. Kay, "Allergy and allergic diseases," *The New England Journal of Medicine*, vol. 344, no. 1, pp. 30–37, 2001.

[6] W. W. Busse, H. A. Boushey, S. Buist et al., "National asthma education and prevention program. Expert panel report: guidelines for the diagnosis and management of asthma update on selected topics-2002," *The Journal of Allergy and Clinical Immunology*, vol. 111, supplement 5, no. 3, pp. S141–S219, 2002.

[7] M. M. Wei, X. X. Xie, X. Chu, X. Yang, M. Guan, and D. Wang, "Dihydroartemisinin suppresses ovalbumin-induced airway inflammation in a mouse allergic asthma model," *Immunopharmacology and Immunotoxicology*, vol. 35, no. 3, pp. 382–389, 2013.

[8] T. Ueno Iio, M. Shibakura, K. Iio et al., "Effect of fudosteine, a cysteine derivative, on airway hyperresponsiveness, inflammation, and remodeling in a murine model of asthma," *Life Sciences*, vol. 92, no. 20-21, pp. 1015–1023, 2013.

[9] M. Wei, X. Chu, M. Guan et al., "Protocatechuic acid suppresses ovalbumin-induced airway inflammation in a mouse allergic asthma model," *International Immunopharmacology*, vol. 15, no. 4, pp. 780–788, 2013.

[10] J. J. Lee, D. Dimina, M. P. Macias et al., "Defining a link with asthma in mice congenitally deficient in eosinophils," *Science*, vol. 305, no. 5691, pp. 1773–1776, 2004.

[11] K. Shin, H. C. Chung, D. U. Kim, J. K. Hwang, and S. H. Lee, "Macelignan attenuated allergic lung inflammation and airway hyper-responsiveness in murine experimental asthma," *Life Sciences*, vol. 92, no. 22, pp. 1093–1099, 2013.

[12] S. J. Galli, M. Tsai, and A. M. Piliponsky, "The development of allergic inflammation," *Nature*, vol. 454, no. 7203, pp. 445–454, 2008.

[13] D. W. Cockcroft and B. E. Davis, "Mechanisms of airway hyperresponsiveness," *Journal of Allergy and Clinical Immunology*, vol. 118, no. 3, pp. 551–559, 2006.

[14] D. Z. Hsu, C. T. Liu, P. Y. Chu, Y. H. Li, S. Periasamy, and M. Y. Liu, "Sesame oil attenuates ovalbumin-induced pulmonary edema and bronchial neutrophilic inflammation in mice," *BioMed Research International*, vol. 2013, Article ID 905670, 7 pages, 2013.

[15] H. Bae, Y. Kim, E. Lee et al., "*Vitex rotundifolia* L. Prevented airway eosinophilic inflammation and airway remodeling in an ovalbumin-induced asthma mouse model," *International Immunology*, vol. 25, no. 3, pp. 197–205, 2013.

[16] P. S. Thomas, "Tumour necrosis factor-α: the role of this multifunctional cytokine in asthma," *Immunology and Cell Biology*, vol. 79, no. 2, pp. 132–140, 2001.

[17] P. Carmeliet and R. K. Jain, "Angiogenesis in cancer and other diseases," *Nature*, vol. 407, no. 6801, pp. 249–257, 2000.

[18] D. J. Jackson, A. Sykes, P. Mallia, and S. L. Johnston, "Asthma exacerbations: origin, effect, and prevention," *Journal of Allergy and Clinical Immunology*, vol. 128, no. 6, pp. 1165–1174, 2011.

[19] J. C. Bouchard, D. R. Beal, J. Kim, L. J. Vaickus, and D. G. Remick, "Chemokines mediate ethanol-induced exacerbations of murine cockroach allergen asthma," *Clinical and Experimental Immunology*, vol. 172, no. 2, pp. 203–216, 2013.

[20] S. Abdureyim, N. Amat, A. Umar, B. Berke, N. Moore, and H. Upur, "Anti-inflammatory, immunomodulatory, and heme oxygenase-1 inhibitory activities of Ravan Napas, a formulation of Uighur traditional medicine, in a rat model of allergic asthma," *Evidence-Based Complementary and Alternative Medicine*, vol. 2011, Article ID 725926, 13 pages, 2011.

[21] J. J. Gao, P. P. Song, F. H. Qi, N. Kokudo, X. J. Qu, and W. Tang, "Evidence-based research on traditional Japanese medicine, Kampo, in treatment of gastrointestinal cancer in Japan," *Drug Discoveries & Therapeutics*, vol. 6, no. 1, pp. 1–8, 2012.

[22] E. Bedir, N. Pugh, I. Calis, D. S. Pasco, and I. A. Khan, "Immunostimulatory effects of cycloartane-type triterpene glycosides from Astragalus species," *Biological and Pharmaceutical Bulletin*, vol. 23, no. 7, pp. 834–837, 2000.

[23] T. Kumagai, C. I. Muller, J. C. Desmond, Y. Imai, D. Heber, and H. P. Koeffler, "Scutellaria baicalensis, a herbal medicine: anti-proliferative and apoptotic activity against acute lymphocytic leukemia, lymphoma and myeloma cell lines," *Leukemia Research*, vol. 31, no. 4, pp. 523–530, 2007.

[24] H. Zhao, J. Li, X. He et al., "The protective effect of Yi Shen Juan Bi Pill in arthritic rats with castration-induced kidney deficiency," *Evidence-Based Complementary and Alternative Medicine*, vol. 2012, Article ID 102641, 8 pages, 2012.

[25] C. H. Ma, Z. Q. Ma, Q. Fu et al., "Anti-asthmatic effects of baicalin in a mouse model of allergic asthma," *Phytotherapy Research*, vol. 28, no. 2, pp. 231–237, 2013.

[26] S. Park, S. H. Sohn, and K. H. Jung, "The Effects of maekmoondong-tang on cockroach extract-induced allergic asthma," *Evidence-Based Complementary and Alternative Medicine*, vol. 2014, Article ID 958965, 12 pages, 2014.

[27] F. Dong, C. B. Wang, J. Y. Duan et al., "Puerarin attenuates ovalbumin-induced lung inflammation and hemostatic unbalance in rat asthma model," *Evidence-Based Complementary and Alternative Medicine*, vol. 2014, Article ID 726740, 9 pages, 2014.

[28] T. Eldh, F. Heinzelmann, A. Velalakan, W. Budach, C. Belka, and V. Jendrossek, "Radiation-induced changes in breathing frequency and lung histology of C57BL/6J mice are time- and dose-dependent," *Strahlentherapie und Onkologie*, vol. 188, no. 3, pp. 274–281, 2012.

[29] J. H. Choi, Y. P. Hwang, H. S. Lee, and H. G. Jeong, "Inhibitory effect of Platycodi Radix on ovalbumin-induced airway inflammation in a murine model of asthma," *Food and Chemical Toxicology*, vol. 47, no. 6, pp. 1272–1279, 2009.

[30] M. Wills-Karp, "Immunologic basis of antigen-induced airway hyperresponsiveness," *Annual Review of Immunology*, vol. 17, pp. 255–281, 1999.

[31] J. K. Sont, L. N. A. Willems, E. H. Bel et al., "Clinical control and histopathologic outcome of asthma when using airway hyperresponsiveness as an additional guide to long-term treatment," *The American Journal of Respiratory and Critical Care Medicine*, vol. 159, no. 4, pp. 1043–1051, 1999.

[32] P. Wang, X. Y. Wang, X. Q. Yang, Z. Liu, M. Wu, and G. Li, "Budesonide suppresses pulmonary antibacterial host defense by down-regulating cathelicidin-related antimicrobial peptide in allergic inflammation mice and in lung epithelial cells," *BMC Immunology*, vol. 14, no. 1, article 7, 2013.

[33] K. Amin, D. Lúdvíksdóttir, C. Janson et al., "Inflammation and structural changes in the airways of patients with atopic and nonatopic asthma," *The American Journal of Respiratory and Critical Care Medicine*, vol. 162, no. 6, pp. 2295–2301, 2000.

[34] L. Maddox and D. A. Schwartz, "The pathophysiology of asthma," *Annual Review of Medicine*, vol. 53, pp. 477–498, 2002.

[35] J. F. Regal, "Immunologic effector mechanisms in animal models of occupational asthma," *Journal of Immunotoxicology*, vol. 1, no. 1, pp. 25–37, 2004.

[36] S. T. Holgate, D. E. Davies, S. Puddicombe et al., "Mechanisms of airway epithelial damage: epithelial-mesenchymal interactions in the pathogenesis of asthma," *European Respiratory Journal*, vol. 22, supplement 44, pp. 24S–29S, 2003.

[37] M. C. Guan, W. H. Tang, Z. Xu, and J. Sun, "Effects of selenium-enriched protein from ganoderma lucidum on the levels of IL-1beta and TNF-alpha, oxidative stress, and NF-kappaB activation in ovalbumin-induced asthmatic mice," *Evidence-Based Complementary and Alternative Medicine*, vol. 2014, Article ID 182817, 6 pages, 2014.

[38] J. L. Stow, P. Ching Low, C. Offenhauser, and D. Sangermani, "Cytokine secretion in macrophages and other cells: pathways and mediators," *Immunobiology*, vol. 214, no. 7, pp. 601–612, 2009.

[39] M. Larché, D. S. Robinson, and A. B. Kay, "The role of T lymphocytes in the pathogenesis of asthma," *Journal of Allergy and Clinical Immunology*, vol. 111, no. 3, pp. 450–463, 2003.

[40] L. R. Bisset and P. Schmid-Grendelmeier, "Chemokines and their receptors in the pathogenesis of allergic asthma: progress and perspective," *Current Opinion in Pulmonary Medicine*, vol. 11, no. 1, pp. 35–42, 2005.

[41] S. Esnault, E. A. Kelly, E. A. Schwantes et al., "Identification of genes expressed by human airway eosinophils after an in vivo allergen challenge," *PLoS ONE*, vol. 8, no. 7, Article ID e67560, 2013.

[42] J. M. Huang, W. Tian, D. B. Chen, and S. M. Liu, "Effects of mahuang decoction on allergic airway inflammation in asthmatic mouse," *Chinese Journal of Clinical Rehabilitation*, vol. 9, no. 47, pp. 180–182, 2005.

Hindawi Publishing Corporation
Evidence-Based Complementary and Alternative Medicine
Volume 2014, Article ID 248768, 10 pages
http://dx.doi.org/10.1155/2014/248768

Research Article

Effects of the Czech Propolis on Sperm Mitochondrial Function

Miroslava Cedikova,[1,2] Michaela Miklikova,[1,2] Lenka Stachova,[3] Martina Grundmanova,[4] Zdenek Tuma,[2,5] Vaclav Vetvicka,[6] Nicolas Zech,[7] Milena Kralickova,[1,2] and Jitka Kuncova[2,4]

[1] *Department of Histology and Embryology, Faculty of Medicine in Pilsen, Charles University in Prague, 301 00 Pilsen, Czech Republic*
[2] *Biomedical Centre, Faculty of Medicine in Pilsen, Charles University in Prague, 301 00 Pilsen, Czech Republic*
[3] *Institute of Pharmacology and Toxicology, Faculty of Medicine in Pilsen, Charles University in Prague, 301 00 Pilsen, Czech Republic*
[4] *Department of Physiology, Faculty of Medicine in Pilsen, Charles University in Prague, 301 00 Pilsen, Czech Republic*
[5] *Ist Internal Department, Faculty of Medicine and Teaching Hospital in Pilsen, Charles University in Prague, 301 00 Pilsen, Czech Republic*
[6] *Department of Pathology, University of Louisville, Louisville, KY 40292, USA*
[7] *IVF Centers Prof. Zech - Pilsen, 301 00 Pilsen, Czech Republic*

Correspondence should be addressed to Jitka Kuncova; jitka.kuncova@lfp.cuni.cz

Received 11 April 2014; Revised 2 June 2014; Accepted 6 June 2014; Published 1 July 2014

Academic Editor: Shi-Biao Wu

Propolis is a natural product that honeybees collect from various plants. It is known for its beneficial pharmacological effects. The aim of our study was to evaluate the impact of propolis on human sperm motility, mitochondrial respiratory activity, and membrane potential. Semen samples from 10 normozoospermic donors were processed according to the World Health Organization criteria. Propolis effects on the sperm motility and mitochondrial activity parameters were tested in the fresh ejaculate and purified spermatozoa. Propolis preserved progressive motility of spermatozoa in the native semen samples. Oxygen consumption determined in purified permeabilized spermatozoa by high-resolution respirometry in the presence of adenosine diphosphate and substrates of complex I and complex II (state $OXPHOS_{I+II}$) was significantly increased in the propolis-treated samples. Propolis also increased uncoupled respiration in the presence of rotenone (state ETS_{II}) and complex IV activity, but it did not influence state LEAK induced by oligomycin. Mitochondrial membrane potential was not affected by propolis. This study demonstrates that propolis maintains sperm motility in the native ejaculates and increases activities of mitochondrial respiratory complexes II and IV without affecting mitochondrial membrane potential. The data suggest that propolis improves the total mitochondrial respiratory efficiency in the human spermatozoa in vitro thereby having potential to improve sperm motility.

1. Introduction

Propolis (bee glue) is a natural product that honeybees (*Apis mellifera*) collect from various plants. It is used as building material (filling of cracks and gaps) or for protection against intruders (embalms killed invader insects) [1].

Propolis has been used as a remedy for thousands of years. The term is derived from Greek word *pro-* (meaning in front of) and *polis* (city, community). Its chemical composition depends on the place, time of collection, and plant sources making it highly variable. To date, more than 300 compounds have been detected in various propolis extracts [2, 3]. It is composed mainly of resin (50%) and wax (30%). Other components are pollen (5%), essential and aromatic oils (10%), and minor compounds as flavonoids (quercetin, kaempferol, pinocembrin, apigenin, chrysin, etc.), beta-steroids, terpenes, minerals, and vitamins [1, 4–6]. Propolis is known in folk medicine for its pharmacological effects: antibacterial, antiviral, antifungal, antiparasitic, anti-inflammatory, chemopreventive, immunomodulatory, hepatoprotective, antioxidant,

and antitumor [1, 7]. As a result of these effects, over the past 30 years, propolis has been the subject of intense medical studies.

Infertility affects 10–15% of couples of reproductive age and plenty of unanswered questions remain concerning the physiological mechanisms underlying the successful fertility [8]. Male factor contributes to about 50% of cases of infertility and most of them are still idiopathic [9]. More than 90% of male infertility cases are due to low sperm count (oligozoospermia), poor sperm motility (asthenozoospermia), abnormal sperm morphology (teratozoospermia), or all three. The remaining cases of male infertility can be caused by a number of factors including anatomical problems, hormonal imbalances, and genetic defects.

Appropriate sperm motility is fundamental for reproductive success in mammals since the spermatozoa have to travel a relatively long distance through the female reproductive system by active flagellar motion. The energy for the sperm movement in the form of adenosine triphosphate (ATP) is supplied by two metabolic processes: glycolysis taking place in the cytoplasm or oxidative phosphorylation in the mitochondria found only in the sperm midpiece, where 72–80 helically arranged organelles can be detected. However, the relative contributions of both pathways to the sperm motility in different species are a matter of long-standing debate [10, 11]. Nevertheless, recent experimental data suggest that reduced efficiency of the mitochondrial respiratory activity may contribute to the reduced sperm motility. In asthenozoospermic patients, morphological and functional changes in sperm mitochondria have been described [12, 13].

Until now, the effects of propolis on the mitochondrial morphology and function have been studied particularly in the somatic cells. However, the results of these studies are far from uniform showing both stimulation and inhibition of various mitochondrial functions including oxygen consumption, apoptosis, and mitochondrial membrane potential [14–17]. The aim of our study was to assess the effect of ethanolic extract of propolis (EEP) on the human sperm motility, mitochondrial respiratory activity, and membrane potential to test the putative therapeutic potential of this natural product in the treatment of asthenozoospermia.

2. Methods

2.1. Ethanolic Extract of Propolis Preparation. Propolis was collected using plastic nets in region of West Bohemia (Horni Slavkov—50° 8′17.268″ N, 12° 48′48.992″ E) in September 2012. Propolis was frozen at −20°C and ground in a mill. The resulting powder (10 g) was mixed at room temperature with 70% ethanol (100 mL) for 24 h and then filtered. The filtrate was then made up to 100 mL with 70% ethanol [18]. The sample was kept in darkness at 4°C until analysis. For experiments with live cells, propolis was further diluted resulting in a final ethanol concentration below 1% which is not toxic to cells [19]. The final concentration of propolis chosen for further experiments was 0.01 mg/mL of the corresponding medium.

2.2. High Performance Liquid Chromatography Analysis (HPLC). Qualitative and quantitative chromatographic analyses of phenolics were performed on a HPLC system equipped with a binary pump (Waters 1525), Waters 717 plus Autosampler, and dual UV/VIS detector 2487. Separation was performed on a Symmetry C18 column, particle size 5 μm (150 mm × 4.6 mm), using a mobile phase of 0.08% acetic acid in methanol (A) and 0.1% acetic acid and 10% methanol in water (B). The gradient was 10–47% A (25 min), 47% A (25–40 min), 47–70% A (40–70 min), and 70–100% A (70–80 min) at a flow rate of mobile phase 0.5 mL/min. Injection volume was 10 μL, and column temperature was 30°C.

Spectrophotometric detection was conducted at 280 nm and 330 nm. Identification of polyphenolic compounds was achieved by comparison of retention times with those of commercial pure compounds. All standards were dissolved in dimethyl sulfoxide (Sigma-Aldrich; St. Louis, USA) to give 10 mmol/L standard solutions. Calibration standards were prepared by dilution of the standard solution in ethanol.

Quantitative analysis was carried out by external standard method. Calibration curves showed a linear response of $R^2 > 0.97$ over a concentration range of 5–100 μmol/L. Before the HPLC analysis, the EEP was filtered on teflon syringe microfilter Separon 0.45 μm. The propolis extract was diluted one hundred times for HPLC analysis.

Phenolic compounds were purchased from Sigma-Aldrich (St. Louis, USA) (apigenin, chrysin, genistein, kaempferol, luteolin, naringenin, pinocembrin, galangin and phenolic acids: caffeic, p-coumaric, t-ferulic, t-cinnamic, benzoic, and gallic acid and caffeic acid phenethyl ester). Vanillin was purchased from Merck (Darmstadt, Germany).

2.3. Sperm Sample Preparation. The study design was approved by the Local Ethics Committee of the University Hospital in Pilsen and a written informed consent was obtained from each of the 10 participants included in the study (mean age 24.2 years, SEM ± 2.8).

Ejaculates were collected after 3 days of sexual abstinence in IVF Center Prof. Zech, Pilsen. Semen samples were evaluated by an experienced employee. After liquefaction, they were analyzed according to the World Health Organization criteria 2010 [20]. We investigated semen volume and, under the microscope with phase-contrast optics at magnification ×200, concentration of spermatozoa, motility of spermatozoa and pathologies. Sperm motility was assessed at room temperature in Makler counting chamber. Two hundred spermatozoa per replicate were classified into three motility categories (progressive, nonprogressive, and immotile sperm cells). All samples were considered normozoospermic ejaculates (Table 1).

Fresh ejaculate (0.1 mL) was subjected to experiment with propolis. Propolis or ethanol only (1 μL) was added to 0.1 mL of fresh ejaculate (final concentration of propolis was 0.01 mg/mL) and sperm motility was evaluated after 60 minutes.

The remaining sample was prepared by gradient separation technique and used for experiment with polarographic oxygraph (Oroboros, Innsbruck, Austria) and sperm flow

Table 1: Main sperm parameters of the normozoospermic men (±SEM).

Parameters	Normozoospermic men ($n = 10$)
Volume (mL)	3.18 ± 0.26
Concentration ($\times 10^6$/mL)	81.22 ± 13.97
Progressive motility (%)	62.5 ± 4.4
Pathology morphology (%)	42.00 ± 2.26
Concentration after separation ($\times 10^6$/mL)	158.44 ± 18.09
Progressive motility after separation (%)	86.43 ± 2.10

cytometry evaluation. Sperm number after separation was also determined in the Makler counting chamber.

2.4. The Sperm Density Gradient Separation Technique. The sperm was separated and purified. This was performed using gradient solution media SpermGrad medium (SGm, Vitrolife, Sweden) and SpermRinse medium (SRm, Vitrolife, Sweden). SpermGrad medium was diluted to 90% (0.15 mL SGm : 1.35 mL SRm), 70% (0.09 mL SGm : 0.21 mL SRm) and 50% (0.15 mL SG : 0.15 mL SRm). Into a conical tube 1.5 mL 90%, 0.3 mL 70% and 0.3 mL of a 50% gradient media were layered. Full ejaculate was added and the sample was centrifuged for 20 minutes at 300 g. After removal of the supernatant, 8 mL SRm was added and then the sample was centrifuged 8 minutes at 300 g. After removal of supernatant, the sample was evaluated for the concentration and motility of spermatozoa and ready for injection into the oxygraph.

2.5. High-Resolution Respirometry. Oxygen consumption by purified spermatozoa was measured at 36°C in 2 mL glass chambers of oxygraph Oroboros (Oroboros, Innsbruck, Austria) connected to the computer with DatLab software for data acquisition and analysis (Oroboros, Innsbruck, Austria). The oxygen flux was calculated as a negative time derivative of the oxygen concentration. All values of oxygen fluxes were corrected for instrumental and chemical background measured in separate experiments performed in the same medium without human gametes.

The medium consisting of 0.5 mmol/L ethylene glycol tetraacetic acid, 3 mmol/L $MgCl_2 \cdot 6H_2O$, 60 mmol/L K-lactobionate, 20 mmol/L taurine, 10 mmol/L KH_2PO_4, 20 mmol/L HEPES, 110 mmol/L sucrose, and 1 g/L albumin essentially fatty acid free [21] was stirred at 750 rpm and equilibrated for 60 min with air. After equilibration, oxygen concentration in the chamber corresponded to its concentration in the atmospheric air and solubility in the medium (0.92). The chambers were then closed and the samples of intact spermatozoa were injected into the chambers using Hamilton syringe. Into one of two chambers recording in parallel, propolis (0.01 mg/mL) was injected and the samples were further incubated at 36°C for 20 min. The spermatozoa cell membrane was permeabilized with digitonin (Sigma-Aldrich, St. Louis, USA; 5 μg/mL) and combination of substrates, inhibitors, and uncouplers was sequentially injected into the chambers to measure the respiration through different segments of the electron transport system (Figure 1). (1) Resting respiration with substrates providing electrons to complex I malate (2 mmol/L) and glutamate (10 mmol/L) was measured as a state S2 (non-phosphorylating LEAK state, L_N). (2) Active respiration was induced by 5 mmol/L adenosine diphosphate (ADP; state S3 or OXPHOS). (3) Oxygen consumption was further measured with pyruvate (5 mmol/L) and a substrate of electron transfer flavoprotein (ETF) palmitoyl carnitine (20 μmol/L). (4) Integrity of the mitochondrial inner membrane was checked with cytochrome c (10 μmol/L). (5) Mitochondrial respiration was then increased by succinate, complex II substrate (10 mmol/L). (6) State LEAK was induced again by inhibition of ATP-synthase oligomycin (2 μg/mL). (7) Maximum capacity of the electron-transporting system (state S3u or ETS) was reached by titration of uncoupler trifluorocarbonylcyanide phenylhydrazone (FCCP; 0.05 μmol/L titration steps). (8) After addition of a complex I inhibitor rotenone, the oxygen flux corresponded to maximum capacity of the electron-transporting system with the complex II only. (9) Then, antimycin A (2.5 μmol/L), a complex III inhibitor was injected into the chambers to measure residual oxygen consumption (ROX). (10) N,N,N′,N′-tetramethyl-p-phenylenediamine dihydrochloride (TMPD; 0.5 mmol/L) and ascorbate (2 mmol/L) were injected simultaneously for respirometric assay for cytochrome c oxidase (C IV) activity. In the results, oxygen fluxes recorded in the individual titration steps were corrected for residual oxygen consumption.

The dose-response relationship between the propolis concentration and sperm respiratory activity was tested in another set of experiments, where the final concentrations of propolis 0.001, 0.005, and 0.01 mg/mL were used. Higher dose of propolis was not tested as in experiments running in parallel, higher concentrations of propolis in the incubation medium (0.03 and 0.05 mg/mL) were toxic for mouse embryonic stem cells reducing their growth, survival, and proliferation (unpublished observation).

2.6. Permeability of Cell Membrane in Sperm. Sperm was treated with the impermeable fluorescent dye propidium iodide to check cell membrane permeability for substrates, inhibitors, and uncouplers after treatment by digitonin. Final concentration of propidium iodide was 1 μg/mL.

2.7. Sperm Flow Cytometry Evaluation. Mitochondrial membrane potential ($\Delta\Psi m$) was determined with MitoProbe JC-1 Assay Kit (Life Technologies). Each sperm sample was resuspended in 37°C warm phosphate-buffered saline (PBS) at approximately 1×10^6 cells/mL. Propolis (1 μL) was added to test samples (100 μL) to reach final concentration 0.01 mg/mL. Controls remained without intervention. Samples were incubated in propolis for 60 min and after that were washed with PBS. JC-1 (10 μL of 200 μmol/L) was added for 20 min incubation (37°C, 5% CO_2). Wash with PBS followed (5 min, 1500 rpm). Samples were resuspended in 500 μL PBS and measured on BD FACS CANTO II cytometer (BD Biosciences, New Jersey, USA). Analysis was performed with BD FACS Diva software with 488 nm excitation using

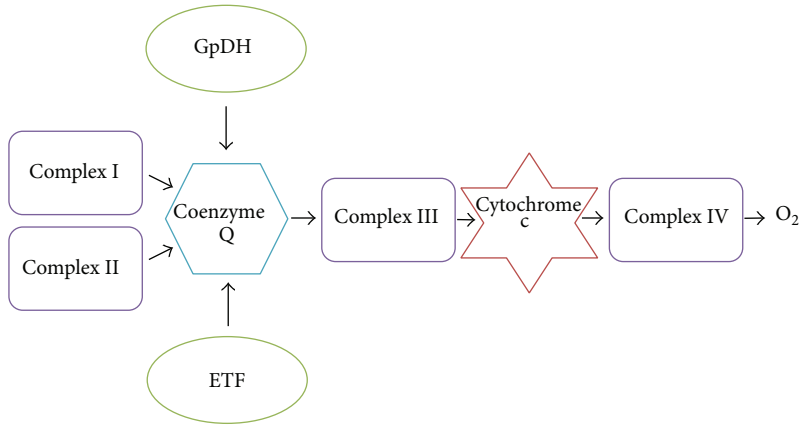

Figure 1: A scheme of an electrotransport convergent system. System is situated on the inner mitochondrial membrane. GpDH = glucose-6-phosphate dehydrogenase; complex I = NADH-Q reductase; complex II = succinate-Q oxidoreductase; complex III = cytochrome reductase; complex IV = cytochrome oxidase; ETF = electron-transporting flavoprotein; O_2 = oxygen.

emission filters appropriate for Alexa Fluor 488 dye and R-phycoerythrin.

2.8. Citrate Synthase Activity. Mitochondrial content in the samples aspirated from each oxygraph chamber was assayed by determination of the citrate synthase activity [22, 23]. The assay medium consisted of 0.1 mmol/L 5,5-dithio-bis-(2-nitrobenzoic) acid, 0.25% Triton-X, 0.5 mmol/L oxalacetate, 0.31 mmol/L acetyl coenzyme A, 5 μmo/L EDTA, 5 mmol/L triethanolamine hydrochloride, and 0.1 mol/L Tris-HCl, pH 8.1 [22]. Two hundred microliters of the mixed and homogenized chamber content was added to 800 μL of the medium. The enzyme activity was measured spectrophotometrically at 412 nm and 30°C over 200 s and expressed in mIU per 10^7 cells.

2.9. Data Analysis and Statistics. Results are presented as mean ± SEM. Statistical differences were analyzed using software package STATISTICA Cz, 8 (StatSoft Inc., Prague, Czech Republic). After testing for the normality of distribution and homogeneity of variances, comparisons were made using Student's t-test, Wilcoxon signed-rank test and analysis of variance (ANOVA) with post hoc tests corrected for multiple comparisons by Bonferroni's method. The results were considered significantly different when $P < 0.05$.

3. Results

3.1. HPLC Analysis. Analyzing the propolis by the HPLC, we were able to identify compounds as t-ferulic acid, p-coumaric acid, vanillin, caffeic acid, t-cinnamic acid, kaempferol, apigenin, and chrysin. Although we analyzed standards of gallic acid, benzoic acid, quercetin, naringenin, luteolin, genistein, pinocembrin, galangin, and caffeic acid phenethyl ester, they were not identified in our propolis sample. Chromatogram of ethanolic extract of the Czech propolis is presented in Figure 2. Detailed results with concentrations of observed substances are shown in Table 2.

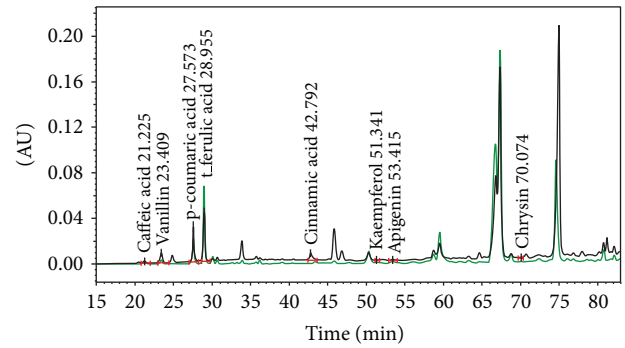

Figure 2: HPLC chromatogram of the Czech propolis extract and the identified compounds/retention time (λ = 280 nm—black line and λ = 330 nm—green line).

3.2. Semen Parameters and Effect of Propolis on Sperm Motility in Fresh Ejaculate. Ten healthy men were included in this study. The mean age was 24.2 years. The general sperm characteristic of the normozoospermic men after ejaculation is shown in Table 1. The effect of propolis on human sperm motility after incubation for 60 minutes is presented in Figure 3. Propolis preserved the progressive motility of spermatozoa in the native semen samples, since the percentage of the progressively motile spermatozoa after incubation with propolis remained nearly the same as in the fresh samples, whereas in the ejaculates without propolis, the progressive motility significantly declined with time ($P = 0.028$). Ethanol alone had no negative effect on sperm motility.

3.3. High Resolution Respirometry. Representative traces of the oxygen consumption in permeabilized spermatozoa with and without propolis 0.01 mg/mL are depicted in Figure 4. Oxygen consumption of intact spermatozoa (0.13 ± 0.01 nmol/(s·IU)) was significantly enhanced by propolis (0.27 ± 0.03 nmol/(s·IU); $P = 0.006$). After permeabilization with digitonin, state 2 determined in the presence of malate

Table 2: Analysis of the ethanolic extract of propolis by the HPLC.

Compound	Rt [min]	Concentration [mg/L of EEP]
Gallic acid	6.0	n.d
Caffeic acid	21.2	**65 ± 11**
Vanillin	23.4	**65 ± 11**
p-Coumaric acid	27.5	**231 ± 10**
t-Ferulic acid	28.9	**514 ± 15**
Benzoic acid	33.6	n.d
Quercetin	42.3	n.d
t-Cinnamic acid	42.7	**29 ± 1**
Naringenin	43.2	n.d.
Luteolin	44.7	n.d
Genistein	45.6	n.d
Kaempferol	51.3	**101 ± 45**
Apigenin	53.4	**73 ± 8**
Chrysin	70.0	**36 ± 5**
Pinocembrin	65.1	n.d.
Galangin	73.1	n.d.
CAPE	71.4	n.d.

(n.d. = nondetected; CAPE = caffeic acid phenethyl ester).

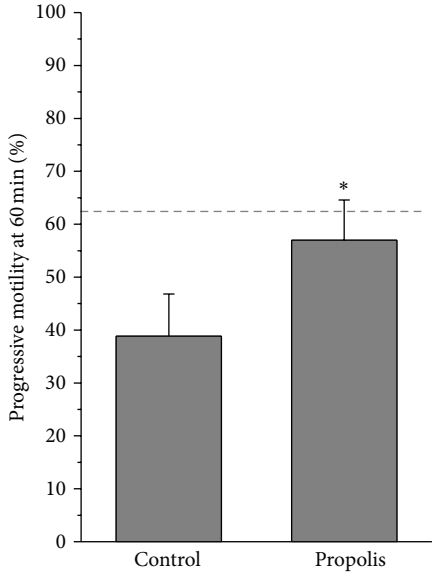

Figure 3: Effect of propolis on sperm motility. Columns represent progressive motility of spermatozoa in native ejaculates after 60 min incubation with propolis extract (mean ± SEM). Dashed line = progressive motility at time 0. $^{*}P < 0.05$, compared to the respective control value.

and glutamate was 0.19 ± 0.04 nmol/(s·IU) in the control samples and it was significantly higher in the propolis-treated sperm samples (0.29 ± 0.05 nmol/(s·IU); $P = 0.014$). State 3, that is, oxygen consumption during oxidative phosphorylation, determined in the presence of ADP and substrates of the complex I, ETF, and complex II is depicted in Figure 5. Propolis significantly increased (by ~50%) $S3_{I+II}$ oxygen flux ($P = 0.003$) suggesting increased activity of the complex II. Propolis did not influence state 4 induced by oligomycin that

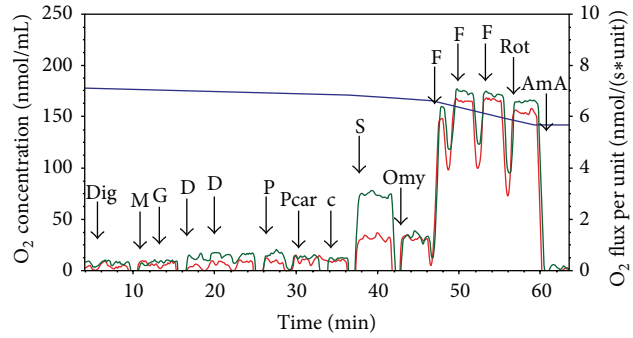

Figure 4: Substrate-uncoupler-inhibitor titration protocol in human spermatozoa. Substrate-uncoupler-inhibitor titration (SUIT) protocol with substrates for complex I, complex II, and electron-transferring flavoprotein (ETF) in human spermatozoa. Red line = oxygen flux expressed per IU citrate synthase activity in the control sample, green line = oxygen flux expressed per IU citrate synthase activity in the sample treated with propolis 0.01 mg/mL, and blue line = oxygen concentration in the oxygraph chamber. Dig = digitonin, M = malate, G = glutamate, D = ADP, P = pyruvate, Pcar = palmitoylcarnitine, c = cytochrome c, S = succinate, Omy = oligomycin, F = FCCP, Rot = rotenone, and AmA = antimycin A.

reached 0.81 ± 0.07 and 0.94 ± 0.09 nmol/(s·IU) in the control and propolis-treated spermatozoa, respectively. Maximum capacity of the electron-transporting system (state S3u) tested for both complexes I and II and in the presence of the complex I inhibitor rotenone was significantly higher after propolis administration (Figure 6). In measurements with TMPD + ascorbate, complex IV respiration was 12.16 ± 2.58 nmol O_2/(s·IU) in the control samples and it was significantly enhanced by propolis to 15.4 ± 3.19 nmol O_2/(s·IU). Absolute ethanol alone (medium for propolis, oligomycin, antimycin A, FCCP, and rotenone) in the volume up to 10 μL did not influence respirometric parameters measured with substrates of complexes I, II, and ETF in the presence of ADP.

Flux control ratios were calculated to estimate the relative efficiency of individual interventions and coupling state of the sperm mitochondria. The ratio $OXPHOS_{I+II}/OXPHOS_I$ was significantly higher in the propolis-treated samples (3.53 ± 0.42) compared to controls (2.8 ± 0.28) suggesting increased efficiency of coupled respiration when complex II was stimulated by succinate. The LEAK control ratio is the ratio of LEAK respiration and ETS capacity; it reached 0.25 ± 0.02 in the control samples and it significantly decreased after propolis to 0.21 ± 0.02 ($P = 0.024$).

The dose-response relationship tested in separate experiments is shown in Figure 7 for state S3 (OXPHOS), where glutamate, malate, pyruvate, succinate, and ADP were present in the medium, and for state S3u (ETS), where mitochondria where uncoupled by FCCP. Propolis dose-dependently increased oxygen consumption, although the extent of its effect was greater for state S3 than for state S3u.

3.4. Permeability of Cell Membrane in Sperm. Addition of 5 μg/mL of digitonin made the sperm cell membrane permeable to dye propidium iodide and for the substrates,

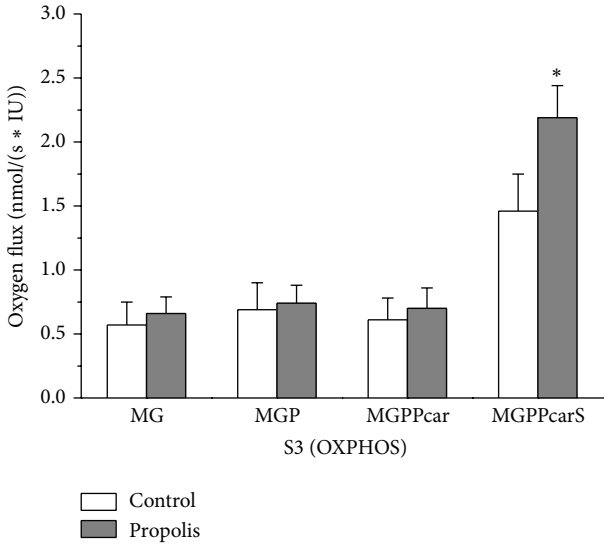

Figure 5: Oxygen consumption rates in the state S3 (OXPHOS) measured under control conditions and with propolis. Oxygen consumption rates in the state S3 (OXPHOS) measured under control conditions (control) and with propolis extract added (propolis) in the presence of ADP and substrates providing electrons to complex I, ETF, and complex II. M = malate, G = glutamate, P = pyruvate, Pcar = palmitoylcarnitine, and S = succinate. Oxygen fluxes were corrected for residual oxygen consumption and expressed per IU citrate synthase activity. $^{*}P < 0.05$, compared to the respective control value.

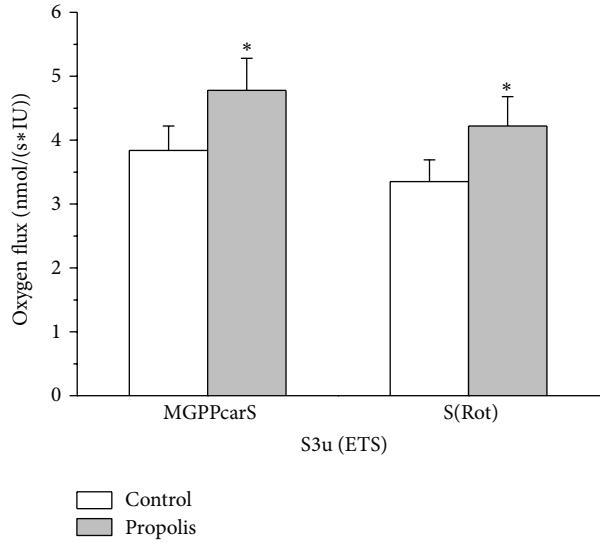

Figure 6: Oxygen consumption rates in the state S3u in permeabilized spermatozoa. Oxygen consumption rates in the state S3u (ETS) in permeabilized spermatozoa measured under control conditions (control) and with propolis extract added (propolis) in the presence of FCCP and substrates providing electrons to complex I, ETF, and complex II. M = malate, G = glutamate, P = pyruvate, Pcar = palmitoylcarnitine, S = succinate, and complex I inhibitor rotenone (Rot). Oxygen fluxes were corrected for residual oxygen consumption and expressed per IU citrate synthase activity. $^{*}P < 0.05$, compared to the respective control value.

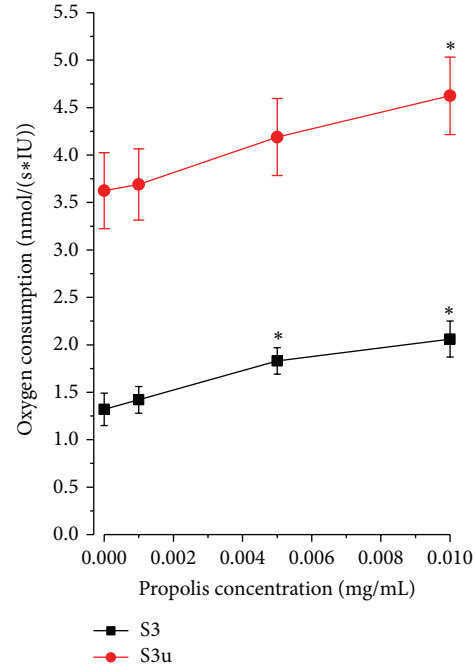

Figure 7: Dose response relationship between oxygen consumption and final propolis concentration. State S3 (OXPHOS) = oxygen consumption rate in permeabilized spermatozoa measured with malate, glutamate, pyruvate, succinate, and ADP. State S3u = oxygen consumption rate in permeabilized spermatozoa measured after sequential addition of malate, glutamate, ADP, pyruvate, succinate, and FCCP. Oxygen fluxes were corrected for residual oxygen consumption and expressed per IU citrate synthase activity. $^{*}P < 0.05$, compared to the respective value without propolis.

inhibitors, and uncouplers required to determine high resolution respirometry (Figure 8).

3.5. Sperm Flow Cytometry Evaluation. Depolarization of the mitochondrial membrane is a sensitive indicator of mitochondrial damage. JC-1 is a membrane-permeable fluorescent probe aggregating in the mitochondrial matrix and then emitting red fluorescence, if $\Delta\Psi m$ is high. In case of mitochondrial depolarization, the monomeric form of JC-1 cannot accumulate in the mitochondrial matrix and produce green fluorescence in the cytoplasm. In the spermatozoa, loss of $\Delta\Psi m$ could serve as a marker of early apoptosis and sperm dysfunction [24]. In our experiments, incubation of the sperm samples with propolis (60 minutes) had no significant effect on $\Delta\Psi m$ (Figure 9). In the control samples, the percentage of cells with high $\Delta\Psi m$ was 98.43 ± 1.07% and it even slightly increased in the propolis-treated spermatozoa reaching 99.33 ± 0.25%.

3.6. Citrate Synthase Activity. In the control samples, citrate synthase activity was 6.58 ± 0.84 mIU/10^7 cells and it was not significantly affected by propolis (6.08 ± 0.84 mIU/10^7 cells) and by the substances (substrates, inhibitors, media) added during the respirometric measurements, as tested in separate controls.

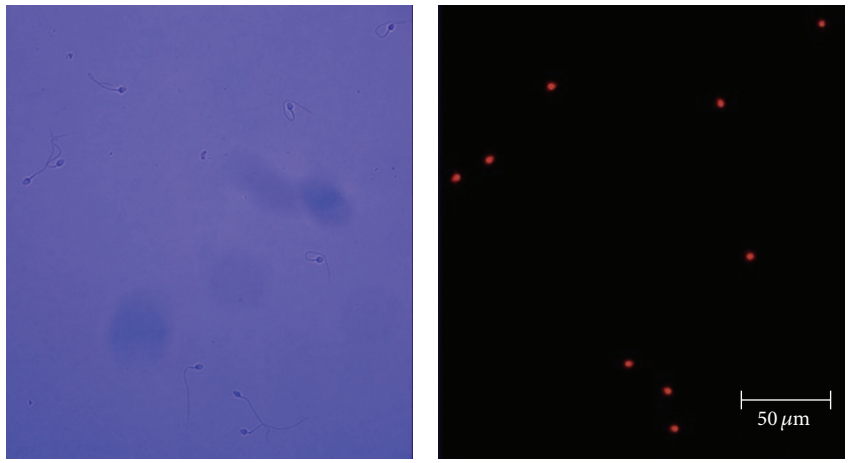

Figure 8: Effect of digitonin treatment on spermatozoa. (a) Micrograph of human spermatozoa and (b) fluorescent micrograph of the same optical field after treatment with the nonpermeable nuclear dye propidium iodide.

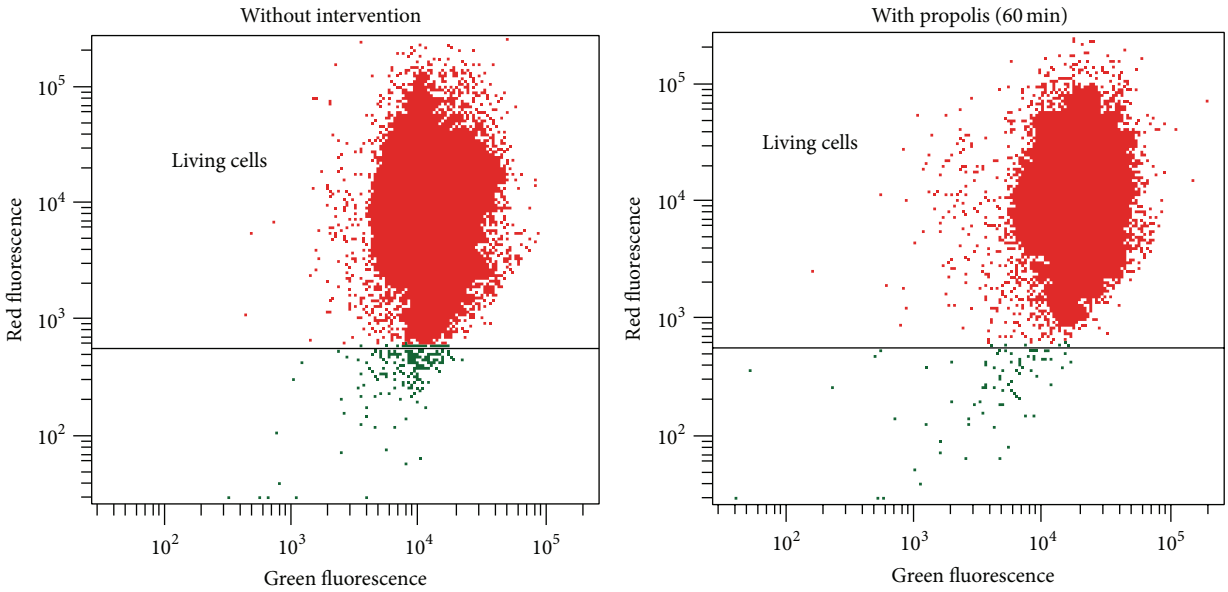

Figure 9: Typical double fluorescence dot plots of flow cytometry analysis. Mitochondrial membrane potential was determined with MitoProbe JC-1 Assay Kit (Life Technologies). R-phycoerythrin = red fluorescence, normal cells; Alexa Fluor 488 dye = green fluorescence, reduced mitochondrial membrane potential.

4. Discussion

This is the first study showing chemical composition of propolis collected in the Czech Republic. Bee glue has a very complex chemical composition that depends on a number of factors including diversity of plants and geographical location from which bees collect it. Although the region of collection of the tested sample of propolis is situated in the northern temperate zone where the "poplar" type propolis is a typical bee product [3], the tree structure within the mentioned locality is composed of coniferous trees (90%), birch (6%), alder (2%), beech (1%), and oak (1%) [25]. However, the tested sample contained chrysin, the reference flavonoid in poplar propolis, and phenolic acids and other flavonoids typically found in bee glue extracts originating from similar geographical regions and reported to be responsible for various beneficial effects of propolis [26]. Among them, ferulic acid, coumaric acid, and kaempferol were present in the highest concentrations in the Czech propolis extract. Caffeic acid phenethyl ester, naringenin, and quercetin—substances frequently contained in the poplar propolis [2, 3] and widely tested for their anti-inflammatory, anticancer, and antioxidant activities in recent years [27]—have not been detected in the Czech propolis. The factors that could contribute to the above mentioned differences could include not only diversity of plant species growing around

the hive, but also season, illumination, altitude, collector type, and food availability [28]. It should be noted that the search for a single substance or a particular substance class that could be responsible for the beneficial actions of propolis has not been successful to date. Scientific studies demonstrated that biological activity of propolis could be almost identical (i.e., antimicrobial, antitumor, antioxidant, anti-inflammatory, etc.) in samples from different climatic zones and of completely different chemical composition [3]. Most probably, a combination of substances is essential for the biological activity of bee glue [29].

The present study describes the effects of propolis on the sperm motility, mitochondrial membrane potential, and mitochondrial respiratory activity assessed by high-resolution respirometry allowing determination of individual respiratory states in a sequential manner on the same sample, thus allowing complex evaluation of the mitochondrial function close to the situation in vivo. In addition, high sensitivity of the method enables determination of respirometric activity of individual mitochondrial complexes in a relatively small amount of cells [30]. In our experiments, we have used the purified spermatozoa that were subjected to membrane permeabilization by mild nonionic detergent digitonin, the dose of which was carefully titrated to permeabilize the cell membrane without damaging the mitochondrial function. To date, oxygen consumption by human sperm mitochondria has been determined mostly by traditional oxygraphy in the germ cells subjected to hypotonic swelling [13, 31–33]. However, in the spermatozoa of several mammalian species, hypotonic challenge could substantially influence the activity of various protein kinases (PK), including PKA, PKC, and protein-tyrosine kinase via osmosensitive K^+ and Cl^- channels in the process called regulatory volume decrease requiring energy supply [34].

The major finding of the present study is that propolis enhances the activity of mitochondrial respiratory complexes II and IV without affecting the coupling of the electron transport to ATP synthesis and/or mitochondrial membrane potential in permeabilized human spermatozoa in vitro. In the coupled state, propolis enhanced oxygen consumption with complex I and complex II substrates by ~50%. This increase was attributed to complex II, since the activity of complex I alone was not affected by propolis. In addition, the ratio P_{I+II}/P_I was significantly higher in the propolis-treated samples. Similarly, in the uncoupled state (S3u, E), oxygen consumption was significantly (by ~25%) higher after propolis, both in the presence of substrates of complexes I and II and after inhibition of complex I by rotenone. Activity of the complex IV was increased to the same extent (~27%).

The data available on the effects of propolis and its major compounds on mitochondrial respiration or activity of individual mitochondrial enzymes involved in the electron-transport convergent system are scarce. The most frequent finding is that this effect is negligible in normal somatic cells (cardiomyocytes, neurons, and hepatocytes), but becomes beneficial in the cells challenged by toxic stimuli where oxidative phosphorylation is compromised [16, 35, 36]. In contrast, in various types of tumor cells, propolis extract or its constituents inhibit oxidative phosphorylation and trigger release of cytochrome c and subsequent apoptosis [15, 17]. In view of this, the action of propolis on the cellular respiration is not easily predictable and depends on the cell type.

Some studies suggested that propolis or its phenolic constituents might influence mitochondrial membrane potential via increased permeability of the inner mitochondrial membrane [14]. This issue was addressed in the experiments with MitoProbe JC-1 Assay Kit that clearly showed that in the human spermatozoa, mitochondrial membrane potential was not affected by propolis. In addition, oligomycin-induced respiratory state (LEAK) that reflects compensation for the proton leak, proton slip, electron slip, and cation cycling [30] was not affected by propolis. Thus, the decrease in the LEAK control ratio after propolis could be attributed to the increased efficiency of the electron transport through complex II. The putative molecular mechanism of complex II activation was suggested in study of Cimen et al. [37], where propolis constituent kaempferol increased deacetylation of succinate dehydrogenase thus increasing its activity.

To date, the effects of propolis or propolis compounds on the sperm characteristics have been rarely studied. The whole propolis extract was used in studies conducted by Yousef and collaborators on rats and rabbits that were treated with propolis for 10 to 12 weeks [38, 39]. Administration of propolis resulted in an increased sperm count and motility, plasma testosterone levels, and a decreased dead and abnormal sperm count. A single study documented positive effect of the propolis compound chrysin on the sperm motility, sperm concentration, and serum testosterone levels [40]. Ferulic acid was also reported to enhance sperm motility and viability [41]. All these findings were attributed to the activity of propolis as antioxidant and none of these studies dealt with the action of propolis or its constituents on mitochondrial energy production. Our study describes a novel beneficial effect of propolis on the sperm characteristics.

Recent experimental evidence suggests that oxidative phosphorylation in the human spermatozoa plays a crucial role in gaining energy for the sperm motility and indicates that asthenozoospermia might be related to the impaired mitochondrial functionality [42]. High-resolution respirometry could provide new data in search for substances that could positively affect human sperm motility and thus improve sperm fertilizing ability. In addition, detailed analysis of respiratory efficiency of individual mitochondrial enzymatic complexes under coupled and uncoupled conditions could provide better insight into pathophysiology of asthenozoospermia.

5. Conclusions

This study demonstrates, for the first time, that ethanolic extract of propolis increases activities of mitochondrial respiratory complexes II and IV without affecting mitochondrial membrane potential. The obtained data suggest that propolis improves the total mitochondrial respiratory efficiency in the human spermatozoa in vitro thereby having potential to improve the sperm motility.

Conflict of Interests

The authors declare that they have no conflict of interests regarding the publication of this paper.

Authors' Contribution

Miroslava Cedikova and Jitka Kuncova contributed equally to this work.

Acknowledgments

This work was supported by the Project ED2.1.00/03.0076 from European Regional Development Fund, the Charles University Research Fund (Project no. P36), the Specific Student Research Project no. 260048/2014 of the Charles University in Prague and by the Grant from Charles University Grant Agency no. 696212.

References

[1] M. Viuda-Martos, Y. Ruiz-Navajas, J. Fernández-López, and J. A. Pérez-Álvarez, "Functional properties of honey, propolis, and royal jelly," *Journal of Food Science*, vol. 73, no. 9, pp. R117–R124, 2008.

[2] V. Bankova, M. Popova, S. Bogdanov, and A. G. Sabatini, "Chemical composition of European propolis: expected and unexpected results," *Zeitschrift für Naturforschung C: A Journal of Biosciences*, vol. 57, no. 5-6, pp. 530–533, 2002.

[3] V. Bankova, "Chemical diversity of propolis and the problem of standardization," *Journal of Ethnopharmacology*, vol. 100, no. 1-2, pp. 114–117, 2005.

[4] A. Russo, R. Longo, and A. Vanella, "Antioxidant activity of propolis: role of caffeic acid phenethyl ester and galangin," *Fitoterapia*, vol. 73, supplement 1, pp. S21–S29, 2002.

[5] A. M. Gómez-Caravaca, M. Gómez-Romero, D. Arráez-Román, A. Segura-Carretero, and A. Fernández-Gutiérrez, "Advances in the analysis of phenolic compounds in products derived from bees," *Journal of Pharmaceutical and Biomedical Analysis*, vol. 41, no. 4, pp. 1220–1234, 2006.

[6] M. L. Khalil, "Biological activity of bee propolis in health and disease," *Asian Pacific Journal of Cancer Prevention*, vol. 7, no. 1, pp. 22–31, 2006.

[7] A. H. Banskota, Y. Tezuka, and S. Kadota, "Recent progress in pharmacological research of propolis," *Phytotherapy Research*, vol. 15, no. 7, pp. 561–571, 2001.

[8] M. Králícková, P. Síma, and Z. Rokyta, "Role of the leukemia-inhibitory factor gene mutations in infertile women: the embryo-endometrial cytokine cross talk during implantation—a delicate homeostatic equilibrium," *Folia Microbiologica*, vol. 50, no. 3, pp. 179–186, 2005.

[9] J. C. St. John, D. Sakkas, and C. L. R. Barratt, "A role for mitochondrial DNA and sperm survival," *Journal of Andrology*, vol. 21, no. 2, pp. 189–199, 2000.

[10] W. C. L. Ford, "Glycolysis and sperm motility: does a spoonful of sugar help the flagellum go round?" *Human Reproduction Update*, vol. 12, no. 3, pp. 269–274, 2006.

[11] R. M. Turner, "Moving to the beat: a review of mammalian sperm motility regulation," *Reproduction, Fertility and Development*, vol. 18, no. 1-2, pp. 25–38, 2006.

[12] V. Y. Rawe, R. Hermes, F. N. Nodar, G. Fiszbajn, and H. E. Chemes, "Results of intracytoplasmic sperm injection in two infertile patients with abnormal organization of sperm mitochondrial sheaths and severe asthenoteratozoospermia," *Fertility and Sterility*, vol. 88, no. 3, pp. 649–653, 2007.

[13] A. Ferramosca, R. Focarelli, P. Piomboni, L. Coppola, and V. Zara, "Oxygen uptake by mitochondria in demembranated human spermatozoa: a reliable tool for the evaluation of sperm respiratory efficiency," *International Journal of Andrology*, vol. 31, no. 3, pp. 337–345, 2008.

[14] S. Das, J. Das, A. Samadder, N. Boujedaini, and A. R. Khuda-Bukhsh, "Apigenin-induced apoptosis in A375 and A549 cells through selective action and dysfunction of mitochondria," *Experimental Biology and Medicine*, vol. 237, no. 12, pp. 1433–1448, 2012.

[15] V. Chen, R. E. Staub, S. Baggett et al., "Identification and analysis of the active phytochemicals from the anti-cancer botanical extract Bezielle," *PLoS ONE*, vol. 7, no. 1, Article ID e30107, 2012.

[16] R. Lagoa, I. Graziani, C. Lopez-Sanchez, V. Garcia-Martinez, and C. Gutierrez-Merino, "Complex I and cytochrome *c* are molecular targets of flavonoids that inhibit hydrogen peroxide production by mitochondria," *Biochimica et Biophysica Acta*, vol. 1807, no. 12, pp. 1562–1572, 2011.

[17] R. D. Yeh, J. C. Chen, T. Y. Lai et al., "Gallic acid induces G_0/G_1 phase arrest and apoptosis in human leukemia HL-60 cells through inhibiting cyclin D and E, and activating mitochondria-dependent pathway," *Anticancer Research*, vol. 31, no. 9, pp. 2821–2832, 2011.

[18] J. S. Bonvehí and A. L. Gutiérrez, "The antimicrobial effects of propolis collected in different regions in the Basque Country (Northern Spain)," *World Journal of Microbiology and Biotechnology*, vol. 28, no. 4, pp. 1351–1358, 2012.

[19] M. Barbarić, K. Mišković, M. Bojić et al., "Chemical composition of the ethanolic propolis extracts and its effect on HeLa cells," *Journal of Ethnopharmacology*, vol. 135, no. 3, pp. 772–778, 2011.

[20] WHO, "WHO laboratory manual for the examination and processing of human semen," 2010, http://www.who.int/reproductivehealth/publications/infertility/9789241547789/en/.

[21] E. Gnaiger, G. Méndez, and S. C. Hand, "High phosphorylation efficiency and depression of uncoupled respiration in mitochondria under hypoxia," *Proceedings of the National Academy of Sciences of the United States of America*, vol. 97, no. 20, pp. 11080–11085, 2000.

[22] A. V. Kuznetsov, D. Strobl, E. Ruttmann, A. Königsrainer, R. Margreiter, and E. Gnaiger, "Evaluation of mitochondrial respiratory function in small biopsies of liver," *Analytical Biochemistry*, vol. 305, no. 2, pp. 186–194, 2002.

[23] S. Larsen, J. Nielsen, C. N. Hansen et al., "Biomarkers of mitochondrial content in skeletal muscle of healthy young human subjects," *The Journal of Physiology*, vol. 590, no. 14, pp. 3349–3360, 2012.

[24] G. Barroso, S. Taylor, M. Morshedi, F. Manzur, F. Gaviño, and S. Oehninger, "Mitochondrial membrane potential integrity and plasma membrane translocation of phosphatidylserine as early apoptotic markers: a comparison of two different sperm subpopulations," *Fertility and Sterility*, vol. 85, no. 1, pp. 149–154, 2006.

[25] Č. R. Lesy, s. p., http://www.lesycr.cz/ls229/charakteristika-lesni-spravy/Stranky/default.aspx.

[26] R. D. Wojtyczka, A. Dziedzic, D. Idzik et al., "Susceptibility of Staphylococcus aureus clinical isolates to propolis extract alone

or in combination with antimicrobial drugs," *Molecules*, vol. 18, no. 8, pp. 9623–9640, 2013.

[27] G. Ozturk, Z. Ginis, S. Akyol, G. Erden, A. Gurel, and O. Akyol, "The anticancer mechanism of caffeic acid phenethyl ester (CAPE): review of melanomas, lung and prostate cancers," *European Review for Medical and Pharmacological Sciences*, vol. 16, no. 15, pp. 2064–2068, 2012.

[28] V. C. Toreti, H. H. Sato, G. M. Pastore, and Y. K. Park, "Recent progress of propolis for its biological and chemical compositions and its botanical origin," *Evidence-Based Complementary and Alternative Medicine*, vol. 2013, Article ID 697390, 13 pages, 2013.

[29] A. Kujumgiev, I. Tsvetkova, Y. Serkedjieva, V. Bankova, R. Christov, and S. Popov, "Antibacterial, antifungal and antiviral activity of propolis of different geographic origin," *Journal of Ethnopharmacology*, vol. 64, no. 3, pp. 235–240, 1999.

[30] D. Pesta and E. Gnaiger, "High-resolution respirometry: OXPHOS protocols for human cells and permeabilized fibers from small biopsies of human muscle," *Methods in Molecular Biology*, vol. 810, pp. 25–58, 2012.

[31] M. Piasecka and J. Kawiak, "Sperm mitochondria of patients with normal sperm motility and with asthenozoospermia: Morphological and functional study," *Folia Histochemica et Cytobiologica*, vol. 41, no. 3, pp. 125–139, 2003.

[32] M. Piasecka, M. Laszczyńska, and D. Gaczarzewicz, "Morphological and functional evaluation of spermatozoa from patients with asthenoteratozoospermia," *Folia Morphologica*, vol. 62, no. 4, pp. 479–481, 2003.

[33] A. Stendardi, R. Focarelli, P. Piomboni et al., "Evaluation of mitochondrial respiratory efficiency during in vitro capacitation of human spermatozoa," *International Journal of Andrology*, vol. 34, no. 3, pp. 247–255, 2011.

[34] A. M. Petrunkina, R. A. P. Harrison, M. Tsolova, E. Jebe, and E. Töpfer-Petersen, "Signalling pathways involved in the control of sperm cell volume," *Reproduction*, vol. 133, no. 1, pp. 61–73, 2007.

[35] R. Barros Silva, N. A. G. Santos, N. M. Martins et al., "Caffeic acid phenethyl ester protects against the dopaminergic neuronal loss induced by 6-hydroxydopamine in rats," *Neuroscience*, vol. 233, pp. 86–94, 2013.

[36] K. S. Kumaran and P. S. M. Prince, "Caffeic acid protects rat heart mitochondria against isoproterenol-induced oxidative damage," *Cell Stress and Chaperones*, vol. 15, no. 6, pp. 791–806, 2010.

[37] H. Cimen, M. J. Han, Y. Yang, Q. Tong, H. Koc, and E. C. Koc, "Regulation of succinate dehydrogenase activity by SIRT3 in mammalian mitochondria," *Biochemistry*, vol. 49, no. 2, pp. 304–311, 2010.

[38] M. I. Yousef and A. F. Salama, "Propolis protection from reproductive toxicity caused by aluminium chloride in male rats," *Food and Chemical Toxicology*, vol. 47, no. 6, pp. 1168–1175, 2009.

[39] M. I. Yousef, K. I. Kamel, M. S. Hassan, and A. M. A. El-Morsy, "Protective role of propolis against reproductive toxicity of triphenyltin in male rabbits," *Food and Chemical Toxicology*, vol. 48, no. 7, pp. 1846–1852, 2010.

[40] O. Ciftci, I. Ozdemir, M. Aydin, and A. Beytur, "Beneficial effects of chrysin on the reproductive system of adult male rats," *Andrologia*, vol. 44, no. 3, pp. 181–186, 2012.

[41] R. Zheng and H. Zhang, "Effects of ferulic acid on fertile and asthenozoospermic infertile human sperm motility, viability, lipid peroxidation, and cyclic nucleotides," *Free Radical Biology and Medicine*, vol. 22, no. 4, pp. 581–586, 1997.

[42] A. Ferramosca, S. P. Provenzano, L. Coppola, and V. Zara, "Mitochondrial respiratory efficiency is positively correlated with human sperm motility," *Urology*, vol. 79, no. 4, pp. 809–814, 2012.

Hindawi Publishing Corporation
Evidence-Based Complementary and Alternative Medicine
Volume 2014, Article ID 285356, 6 pages
http://dx.doi.org/10.1155/2014/285356

Research Article

Astragalus Polysaccharide Protects Astrocytes from Being Infected by HSV-1 through TLR3/NF-κB Signaling Pathway

Lihong Shi,[1] Fengling Yin,[2] Xiangui Xin,[3] Shumei Mao,[1] Pingping Hu,[1] Chunzhen Zhao,[1] and Xiuning Sun[4]

[1] *Department of Pharmacology, Weifang Medical University, 7166 Baotong West Street, Weifang 261053, China*
[2] *Hospital of Weifang Medical University, 7166 Baotong West Street, Weifang 261053, China*
[3] *The Affiliated Hospital of Shandong Traditional Chinese Medicine Junior College, 508 Binhai East Road, Yantai 264199, China*
[4] *Department of Parasitology, Weifang Medical University, 7166 Baotong West Street, Weifang 261053, China*

Correspondence should be addressed to Xiuning Sun; sxn321@163.com

Received 17 April 2014; Revised 10 June 2014; Accepted 12 June 2014; Published 26 June 2014

Academic Editor: Shi-Biao Wu

Astragalus polysaccharide (APS) is the most immunoreactive substance in Astragalus. APS can regulate the body's immunity and is widely used in many immune related diseases. However, till now, there is little information about its contribution to the protection of astrocytes infected by virus. Toll-like receptor 3 (TLR3) is a key component of the innate immune system and has the ability to detect virus infection and trigger host defence responses. This study was undertaken to elucidate the protective effect of APS on herpes simplex virus (HSV-1) infected astrocytes and the underlying mechanisms. The results showed that APS protected the astrocytes from HSV-1 induced proliferation inhibition along with increasing expression of tumor necrosis factor-α (TNF-α) and interleukin-6 (IL-6) markedly. Moreover, APS significantly promoted the expression of Toll-like receptor 3 (TLR3) and the activation of nuclear factor-κB (NF-κB) in astrocytes. In addition, while astrocytes were pretreated with TLR3 antibody before adding HSV-1 and APS, the expression of TLR3, TNF-α, and IL-6 and the activation of NF-κB decreased sharply. These results indicate that APS can protect astrocytes by promoting immunological function provoked by HSV-1 through TLR3/NF-κB pathway.

1. Introduction

Herpes simplex encephalitis (HSE) is the most common sporadic and nonepidemic viral encephalitis in both children and adults. Untreated HSE can result in prolonged neuroinflammation and compromised brain function or death [1–4]. Furthermore, the majority of treated patients would suffer various degrees of sequela despite the improvements in diagnosis and therapy [5]. HSV-1 infection of the brain results in devastating necrotizing encephalitis. Murine model of herpes simplex encephalitis showed that HSV-1 infection triggered a robust immune response including infiltration of leukocytes, production of proinflammatory mediators, activation of resident microglial cells, and focal tissue damage.

Toll-like receptor is an important class of immune recognition receptors that can recognize pathogens molecules, activate the innate immune response and invoke the releasing of cytokines, and initiate adaptive immunity [6, 7]. As an important member of the Toll-like receptor family, TLR3 can recognize double-stranded RNA (dsRNA) of viruses and induce related signal pathway to play important role in host defense against viruses [8, 9]. It is a remarkable fact that TLR3 is vital for natural immunity to HSV-1 in the central nervous system [10, 11].

Astrocytes are the most abundant cells in the central nervous system (CNS). The main function of astrocytes is to provide nutrition and support. In addition, astrocytes can secrete cytokines and neurotrophic factors to regulate the immune function [12, 13]. When mice embryos were infected by HSV-1, neuronal injury and necrosis accompanied by pathological changes of astrocytes would occur [14]. Recently, Furr et al. reported that astrocytes increased expression of DNA-dependent activator of interferon-regulatory factors (DAI) as an important innate immune mechanism underlying the rapid and potentially lethal inflammation associated with HSV-1 infection [15]. Our previous studies revealed

that when astrocytes were infected by HSV-1, NF-κB was activated through Toll-like receptor 3 (TLR3) and then the activated NF-κB would translocate from the cytoplasm to the nucleus so as to promote the production of TNF-α and IL-6 to play antiviral roles [16]. These results demonstrate that astrocytes play significant roles in the inflammatory responses of resident CNS cells to HSV-1 challenge.

Astragalus is a traditional Chinese medicine which contains polysaccharides, saponins, flavonoids, amino acids, linoleic acid, alkaloids, and so forth. Astragalus polysaccharide (APS) is the most immunoreactive substance in Astragalus which can regulate the body immunity. APS has been identified as a class of macromolecules that can profoundly affect the immune system and is widely used as an immune adjuvant in China. APS can induce the expression of surface antigens on lymphocytes, promote the production of antibodies, affect the secretion of cytokines, and even stimulate cell proliferation [17, 18]. Previous studies proved the effective immunostimulatory roles of APS against various viruses [17, 19, 20].

In this paper, based on our previous research, the antiviral effect of APS on the HSV-1 infected astrocytes was investigated. Furthermore, the immunoregulatory effect and the possible immunization mechanisms of APS were evaluated.

2. Materials and Methods

2.1. Laboratory Animals, Cells, and Virus. The BALB/c mice were purchased from Medicine Animal Center of Shandong University. HSV-1 SM44 strain was kept in Central Laboratory of Weifang Medical University at −80°C. The rabbit anti-mouse antibody TLR3, NF-κB, and β-actin were from Invitrogen; Nuclear and Cytoplasmic Protein Extraction Kit were from Beyotime Institute of Biotechnology; MTT kit was purchased from Sigma; 96T enzyme-linked immunosorbent assay (ELISA) kit was purchased from ADL; APS was purchased from Tianjin Sino Pharmaceutical Company; batch number is 120102.

This research was conducted in strict accordance with the recommendations in the Guide for the Care and Use of Laboratory Animals of the National Institutes of Health. Surgery was performed under sodium pentobarbital anesthesia; all efforts were made to minimize suffering. The protocol was approved by the Committee on the Ethics of Animal Experiments of Weifang Medical University (number 2012-056).

2.2. HSV-1 Multiplication and Tittering. The HSV-1 strain SM44 propagated in Vero cells; the supernatant was collected when cytopathic effect (CPE) was in confluence to 75%. By freezing in −80°C and thawing for three times, HSV-1 particles were released. By centrifuging for 8 min with 1200 rpm, the supernatant was collected as inoculum and stocked in freezer. All of the HSV-1 samples used in this study were of the same batch. In following research, final concentration of HSV-1 : $TCID_{50}$ was 10^{-6} mL^{-1}.

2.3. Astrocytes Culture and Purification. Newborn BALB/c mice in day 1 to day 3 were taken and cells culture and purification were performed according to McNaught's protocol [21]. Take the 3rd generation of astrocytes for experimental research according to our team's protocol [16].

2.4. MTT Cell Proliferation Assay, Calculating the Median Effective Concentration (EC_{50}) of APS. Astrocytes (1×10^6 mL^{-1}) were cultured in DMEM/F12 media in the presence of HSV-1 (final $TCID_{50}$: 10^{-6} mL^{-1}) with APS (0, 50, 100, 200, and 300 $\mu g\,mL^{-1}$), 5 repeating groups for each concentration. 20 μL MTT solution (5 mg mL^{-1}) was added to cell media at various time points (6, 12, 18, and 24 h) after the addition of HSV-1 and APS, incubated for 4 h, and then supernatants were gently removed and 200 μL dimethyl sulfoxide was added into each pore. After 10 minutes' vibration, the absorbance (OD value) was measured at a wavelength of 492 nm by enzyme-linked immunosorbent detector. OD value is proportional to the proliferation of living cells and is an indicator of cell proliferation.

The mean and standard deviation of OD values for each concentration of APS at every action time point were calculated. The results showed that cell proliferation is the most exuberant at 12 h time point for every concentration of APS, so 12 h is the detection time point in the following assays. EC_{50} of APS was 120 $\mu g\,mL^{-1}$, so in the following research, the final concentration of APS was 120 $\mu g\,mL^{-1}$. The formula to calculated EC_{50} is

$$\text{effect}\% = \frac{OD_{drug} - OD_{model}}{OD_{control} - OD_{model}} \times 100\%. \quad (1)$$

2.5. Grouping and Detecting the Effect of APS on Astrocytes Proliferation by MTT Assay. Astrocytes were seeded at density of 1×10^6 mL^{-1} into 24-well plates; four groups were set up according to the different intervention conditions: HSV-1 group, HSV-1 + APS group, TLR3 antibody + HSV-1 + APS group, and blank control group. In HSV-1 groups, all flask cells were inoculated with viral suspension (final $TCID_{50}$: 10^{-6} mL^{-1}); in HSV-1 + APS group, all flask cells were inoculated with viral suspension (final $TCID_{50}$: 10^{-6} mL^{-1}) and APS (final concentration: 120 $\mu g\,mL^{-1}$); in TLR3 antibody + HSV-1 + APS group, TLR3 antibody (final concentration: 10 $\mu g\,mL^{-1}$) was used to pretreat cells for 30 min, and then viral suspension (final $TCID_{50}$: 10^{-6} mL^{-1}) and APS (final concentration: 120 $\mu g\,mL^{-1}$) were added to cells; in blank control group, the same volume of cell culture medium as the aforementioned groups was added into each flask cells. For each group, 3 repeating experiments were performed. The proliferation rate of cells was assayed by MTT after culturing for 12 h.

2.6. Determination of the Levels of TNF-α and IL-6 by ELISA. Astrocytes were seeded at density of 1×10^6 mL^{-1} into 12 flasks (25 cm^2). Grouping and treatment were performed as previously mentioned. Supernatants were collected and filtered. TNF-α and IL-6 in the supernatant were measured

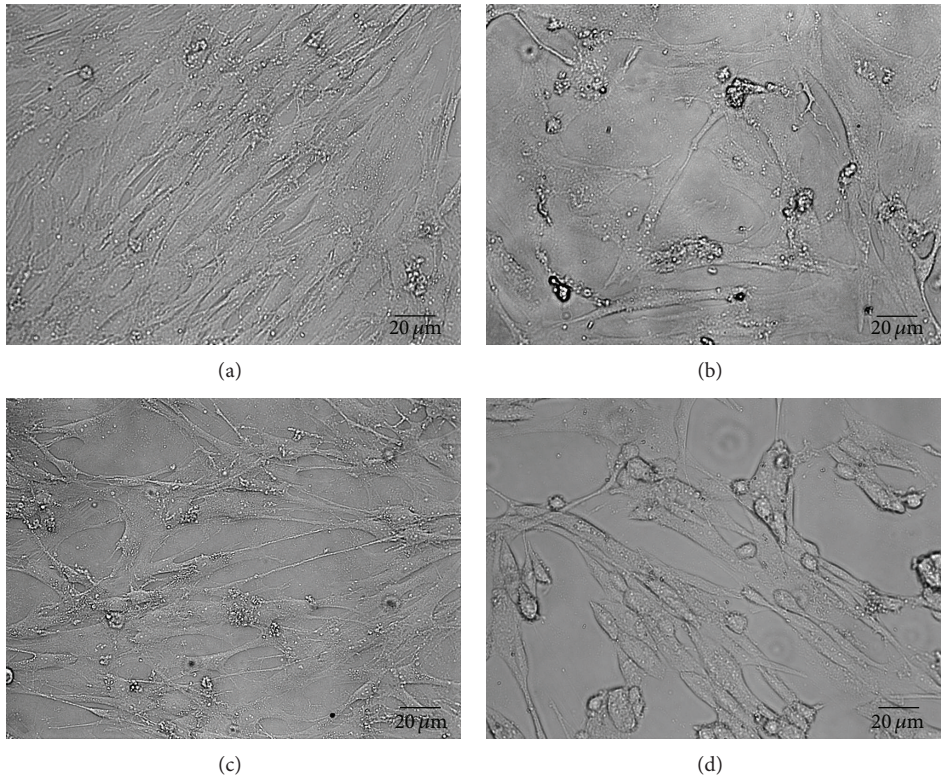

(a) (b) (c) (d)

Figure 1: Effect of APS on the growth and proliferation of astrocytes. (a) Blank control group: the astrocytes grew in good condition with active proliferation. (b) HSV-1 group: 12 h after infection with HSV-1, the proliferation of astrocytes was significantly inhibited and the infected astrocytes' bodies were gradually swollen into round and giant appearance. (c) HSV-1 + APS group: the proliferation inhibitory effect of HSV-1 could be suppressed by APS, and most astrocytes grew in good conditiosn. (d) TLR3 antibody + HSV-1 + APS group: when astrocytes were pretreated with TLR3 antibody, the proliferation of astrocytes reduced markedly, and some infected astrocytes' bodies were swollen into round appearance. Scale bar: 20 μm.

by ELISA. The absorbance (OD value) was determined using a microplate reader at a wavelength of 450 nm. For each sample, the measurement was repeated 3 times and the average concentration of TNF-α and IL-6 was set as the final result.

2.7. Detection of TLR3 Protein in Cells and NF-κB Protein in Cell Nuclei by Western Blot. In brief, total protein and nuclear protein were extracted following the reagent company's instruction. Protein samples were separated by SDS-PAGE, transferred to polyvinylidene difluoride membranes, immunoblotted using the appropriate primary and the HRP conjugated secondary antibodies, and visualized by using enhanced chemiluminescence reagents ECL. Anti-β-actin or LMNB1 monoclonal antibody was used as loading control. The intensities of bands in Western blots were quantified by densitometry analysis using AlphaImager HP (Alpha Innotech, USA) and NIH Image J software (Rockville, MD, USA). Western blot data shown in the paper are representatives of three independent experiments.

2.8. Statistical Analysis. All data were analyzed using the SPSS 13.0 statistical software. Values were expressed as mean ± standard deviation ($\overline{X} \pm S$). The significance of differences between groups was determined using the one-way ANOVA. Statistical significance was accepted for P values <0.05.

3. Result

APS promotes the growth and proliferation of astrocytes infected by HSV-1. Observation under microscope showed that, in the blank control group, the uninfected astrocytes were in thin and flat appearance with good refraction and grew in good condition with active proliferation (Figure 1(a)); in the HSV-1 group, the proliferation of astrocytes was significantly inhibited and the infected astrocytes' bodies were gradually swollen into round and giant appearance (Figure 1(b)); the inhibited proliferation of astrocytes infected by HSV-1 could be rescued by APS apparently in HSV-1 + APS group (Figure 1(c)); when astrocytes were pretreated with TLR3 antibody and then exposed to HSV-1 and APS concurrently, the proliferation of astrocytes reduced markedly compared with the HSV-1 + APS group (Figure 1(d)).

MTT analysis (Figure 2) showed that when astrocytes were exposed to HSV-1, the proliferation of astrocytes was significantly inhibited compared to the blank control group. The inhibited proliferation of astrocytes infected by HSV-1 could be rescued by APS apparently in the HSV-1 + APS

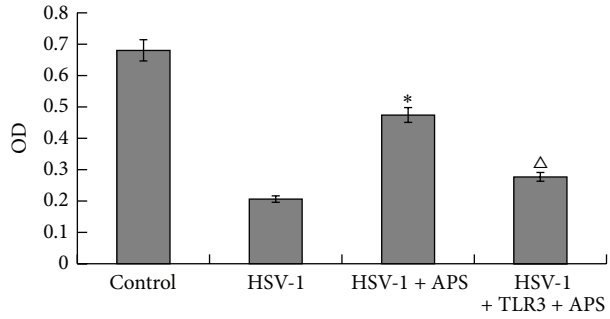

Figure 2: Astrocytes proliferation detected by MTT. $^{*}P < 0.01$ versus the HSV-1 group. $^{\Delta}P < 0.05$ versus the TLR3 antibody + HSV-1 + APS group. $n = 3$.

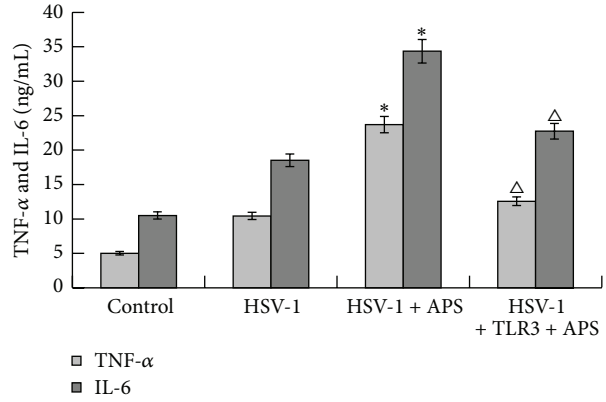

Figure 3: Concentration of TNF-α and IL-6 ($\mathrm{ng\,mL^{-1}}$) in cell culture medium detected by ELISA. $^{*}P < 0.01$ versus the HSV-1 group. $^{\Delta}P < 0.05$ versus the TLR3 antibody + HSV-1 + APS group. $n = 3$.

group. In the presence of APS, the proliferation of astrocytes increased to some extent and the OD value of HSV-1 + APS group was greater than that of the HSV-1 group ($P < 0.01$), which suggests that APS can protect astrocytes from HSV-1 induced proliferation inhibition. Interestingly, when astrocytes were pretreated with TLR3 antibody before adding HSV-1 and APS, the proliferation of astrocytes decreased markedly when compared to the HSV-1 + APS group ($P < 0.05$). This result indicates that the protective effect of APS against HSV-1 infection may be associated with TLR3 pathway.

Secretion levels of TNF-α and IL-6 in culture supernatant were detected by ELISA (Figure 3). The concentrations of TNF-α and IL-6 were very low in culture supernatant of the blank control group, whereas in culture supernatant of the HSV-1 group, the concentrations of both TNF-α and IL-6 increased obviously ($P < 0.01$). In the presence of APS, HSV-1 infected astrocytes expressed higher amount of TNF-α and IL-6 than that of the HSV-1 group. Remarkably, pretreatment of astrocytes with TLR3 antibody decreased the expression of TNF-α and IL-6 in the TLR3 antibody + HSV-1 + APS group ($P < 0.05$).

Western blot analysis showed that the expression level of TLR3 and the activation of NF-κB were low in the control group (Figure 4). In the HSV-1 group, after being exposed to HSV-1 for 12 h, astrocytes expressed higher level of TLR3 than the control group. At the same time, HSV-1 infection induced the activation of NF-κB significantly. Moreover, in the presence of APS, the expression level of TLR3 and the activation level of NF-κB were obviously higher than those of the HSV-1 group. However, when astrocytes were pretreated with TLR3 antibody before addition of HSV-1 and APS, astrocytes reduced the expression of TLR3 and the activation of NF-κB significantly. Considering the different secretion levels of TNF-α and IL-6 in different groups, these results indicate that APS may activate NF-κB which leads to the production of TNF-α and IL-6 through TLR3 pathway ($P < 0.05$).

4. Discussion

Recent studies have confirmed that many herbs have effects of modulating immunity and inhibiting and killing pathogenic microorganisms [22, 23]. As one of the bioactive ingredients from the natural traditional Chinese medicinal herb *Astragalus membranaceus*, APS is used widely as an immunomodulator in China. Evidences indicate that APS can enhance lymphocyte blastogenesis and stimulate macrophage activation without cytotoxic effects [7, 8]. APS cannot inhibit virus directly but it can activate the immune system and induce the production of cytokines to initiate an antiviral response [24, 25]. Consistent with these previous reports, the current study showed that HSV-1 infection induced the secretion of TNF-α and IL-6 in astrocytes and the secretion notably increased in response to APS. These results indicate that APS can promote immunomodulatory effects of astrocytes.

In addition, we also found that HSV-1 infection induced a higher expression of TLR3 and decreased the proliferation of astrocytes; these results are in accordance with previous reports which showed that high expression of TLR3 impaired cell proliferation and inhibited cell cycle progress [26, 27]. Furthermore, we found that APS was capable of promoting the proliferation of astrocytes infected by HSV-1. This result squares with what we already know about the role of APS on cell proliferation [18, 28, 29]. Although the potential mechanism is still to be clarified, regarding the current understanding of TLR3 signaling function, we infer that the effect of APS on proliferation of astrocytes may not be associated with its effect on TLR3.

Antiviral innate immunity depends on different sensor systems that recognize viral-pathogen-associated molecular patterns (PAMPs) and affect specific signaling pathways, including those leading to the activation of NF-κB. Recent studies demonstrate that TLR3 is also present in cells as a sensor to recognize the structure of the pathogens and participate in the adaptive immune response directly [30]. TLR3 can recognize the dsRNA of viruses, initiates intracellular signal transduction pathway, and then induces the activation of NF-κB [30, 31]. Activated NF-κB translocates from cytoplasm to the nucleus, combines with target genes to trigger gene transcriptions, and increases the production of certain

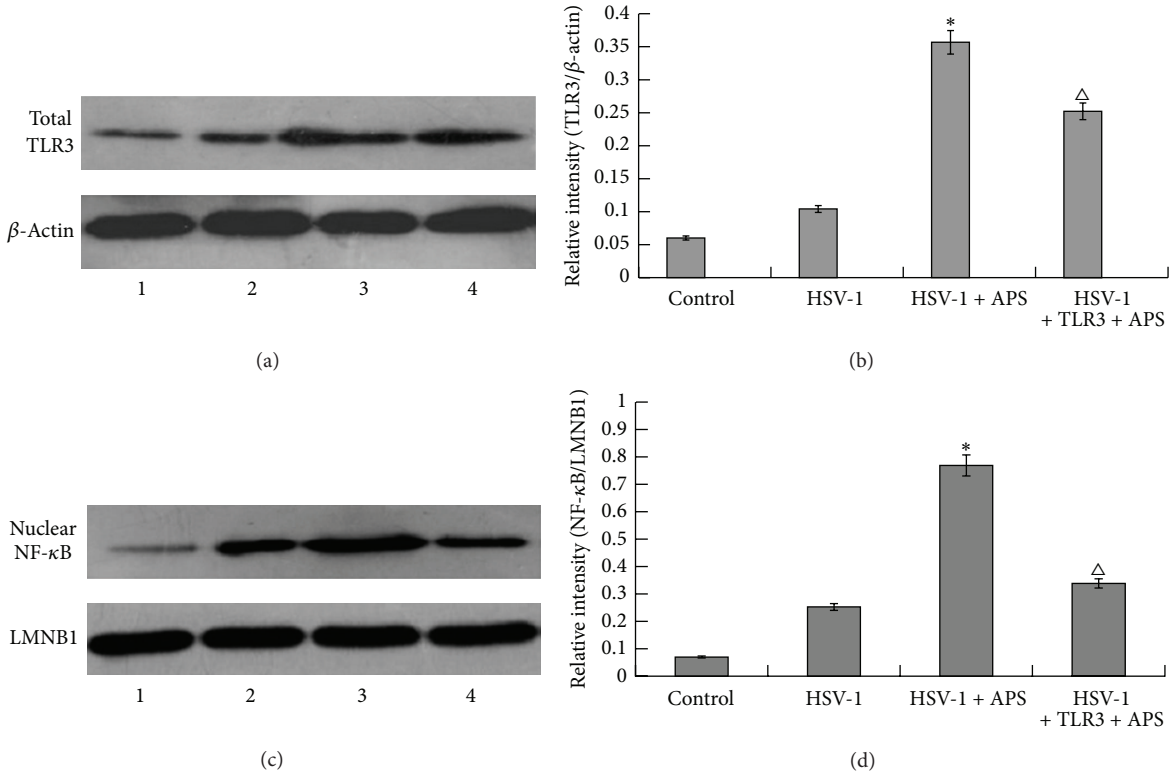

Figure 4: Western blot analysis of expression levels of total TLR3 and nuclear NF-κB (activated NF-κB). (a) Expression levels of total TLR3 protein in blank control group, HSV-1 group, HSV-1 + APS group, and TLR3 antibody + HSV-1 + APS group. β-Actin was used as a loading control. (b) The relative intensity of total TLR3 protein as analyzed by Western blot. (c) Expression levels of nuclear NF-κB protein (activated NF-κB) in blank control group, HSV-1 group, HSV-1 + APS group, and TLR3 antibody + HSV-1 + APS group. LMNB1 was used as a loading control. (d) The relative intensity of nuclear NF-κB protein (activated NF-κB) as analyzed by Western blot. $^{*}P < 0.01$ versus the HSV-1 group. $^{\Delta}P < 0.05$ versus the TLR3 antibody + HSV-1 + APS group. The results of Western blot were from a representative of at least three repeated experiments. $n = 3$.

antiapoptotic proteins and proinflammatory cytokines [26–28]. Our previous study revealed that when astrocytes were infected by HSV-1, the NF-κB was activated through TLR3 and the generation of TNF-α and IL-6 increased obviously [5]. In this paper, we further confirmed that TLR3 and NF-κB positively contribute to the immune response to HSV-1 infection. Moreover, we showed that, for HSV-1 infected astrocytes, APS could promote the expression of TLR3 and the activation of NF-κB which elicits the secretion of inflammatory cytokines TNF-α and IL-6, indicating that APS can protect astrocytes by promoting immunological function provoked by HSV-1 through TLR3/NF-κB pathway.

5. Conclusion

In conclusion, APS can protect the astrocytes against HSV-1 induced proliferation inhibition and enhance the immunological function of astrocytes by upregulating the TLR3/NF-κB signaling pathway along with increasing expression of TNF-α and IL-6. The study suggests that APS has potential in the treatment of HSV-1 infectious diseases in central nervous system.

Conflict of Interests

The authors declare that there is no conflict of interests regarding the publication of this paper.

Acknowledgments

This work was supported by a Project of Shandong Province High Educational Science and Technology Program (no. J12LK04), Traditional Chinese Medicine Science and Technology Research Projects of Shandong Province (nos. 2013-140, 2013-236, and 2013-240), the Natural Science Foundation of Shandong Province (nos. ZR2011HL047 and ZR2011HL066), and Natural Science Foundation of China (81341137).

References

[1] R. N. Aravalli, S. Hu, T. N. Rowen, J. M. Palmquist, and J. R. Lokensgard, "Cutting edge: TLR2-mediated proinflammatory cytokine and chemokine production by microglial cells in response to herpes simplex virus," *Journal of Immunology*, vol. 175, no. 7, pp. 4189–4193, 2005.

[2] A. G. Armien, S. Hu, M. R. Little et al., "Chronic cortical and subcortical pathology with associated neurological deficits ensuing experimental herpes encephalitis," *Brain Pathology*, vol. 20, no. 4, pp. 738–750, 2010.

[3] C. P. Marques, M.-C. Cheeran, J. M. Palmquist, S. Hu, S. L. Urban, and J. R. Lokensgard, "Prolonged microglial cell activation and lymphocyte infiltration following experimental herpes encephalitis," *The Journal of Immunology*, vol. 181, no. 9, pp. 6417–6426, 2008.

[4] J. Kavouras, E. Prandovszky, K. Valyi-Nagy et al., "Herpes simplex virus type 1 infection induces oxidative stress and the release of bioactive lipid peroxidation by-products in mouse P19N neural cell cultures," *Journal of NeuroVirology*, vol. 13, no. 5, pp. 416–425, 2007.

[5] R. J. Whitley and J. W. Gnann, "Viral encephalitis: familiar infections and emerging pathogens," *The Lancet*, vol. 359, no. 9305, pp. 507–513, 2002.

[6] J. M. Thompson and A. Iwasaki, "Toll-like receptors regulation of viral infection and disease," *Advanced Drug Delivery Reviews*, vol. 60, no. 7, pp. 786–794, 2008.

[7] K. Tabeta, P. Georgel, E. Janssen et al., "Toll-like receptors 9 and 3 as essential complonents of innate immune defense against mouse cytomegalovirus infection," *Proceedings of the National Academy of Sciences of the United States of America*, vol. 101, no. 10, pp. 3516–3521, 2004.

[8] K. Fukuda, T. Tsujita, M. Matsumoto et al., "Analysis of the interaction between human TLR3 ectodomain and nucleic acids.," *Nucleic Acids Symposium Series*, no. 50, pp. 249–250, 2006.

[9] Z.-Y. Lu, S. P. Yu, J.-F. Wei, and L. Wei, "Age-related neural degeneration in nuclear-factor κB p50 knockout mice," *Neuroscience*, vol. 139, no. 3, pp. 965–978, 2006.

[10] S. Zhang, E. Jouanguy, S. Ugolini et al., "TLR3 deficiency in patients with herpes simplex encephalitis," *Science*, vol. 317, no. 5844, pp. 1522–1527, 2007.

[11] J. Tabiasco, E. Devêvre, N. Rufer et al., "Human effector $CD8^+$ T lymphocytes express TLR3 as a functional coreceptor," *The Journal of Immunology*, vol. 177, no. 12, pp. 8708–8713, 2006.

[12] C. S. Jack, N. Arbour, J. Manusow et al., "TLR signaling tailors innate immune responses in human microglia and astrocytes," *The Journal of Immunology*, vol. 175, no. 7, pp. 4320–4330, 2005.

[13] K. R. Jessen, "Glial cells," *International Journal of Biochemistry and Cell Biology*, vol. 36, no. 10, pp. 1861–1867, 2004.

[14] W. Schäbitz, C. Berger, R. Kollmar et al., "Effect of brain-derived neurotrophic factor treatment and forced arm use on functional motor recovery after small cortical ischemia," *Stroke*, vol. 35, no. 4, pp. 992–997, 2004.

[15] S. R. Furr, V. S. Chauhan, M. J. Moerdyk-Schauwecker, and I. Marriott, "A role for DNA-dependent activator of interferon regulatory factor in the recognition of herpes simplex virus type 1 by glial cells," *Journal of Neuroinflammation*, vol. 8, article no. 99, 2011.

[16] Z. Liu, Y. Guan, X. Sun et al., "HSV-1 activates NF-kappaB in mouse astrocytes and increases TNF-alpha and IL-6 expression via Toll-like receptor 3," *Neurological Research*, vol. 35, no. 7, pp. 755–762, 2013.

[17] J. Li, Y. Zhong, H. Li et al., "Enhancement of Astragalus polysaccharide on the immune responses in pigs inoculated with foot-and-mouth disease virus vaccine," *International Journal of Biological Macromolecules*, vol. 49, no. 3, pp. 362–368, 2011.

[18] X. Kong, Y. Hu, R. Rui, D. Wang, and X. Li, "Effects of Chinese herbal medicinal ingredients on peripheral lymphocyte proliferation and serum antibody titer after vaccination in chicken," *International Immunopharmacology*, vol. 4, no. 7, pp. 975–982, 2004.

[19] K. Lim, S. D. Jazayeri, S. K. Yeap et al., "Co-administration of avian influenza virus H5 plasmid DNA with chicken IL-15 and IL-18 enhanced chickens immune responses," *BMC Veterinary Research*, vol. 8, article 132, 2012.

[20] H. Chen, Y. Shang, H. Yao et al., "Immune responses of chickens inoculated with a recombinant fowlpox vaccine coexpressing HA of H9N2 avain influenza virus and chicken IL-18," *Antiviral Research*, vol. 91, no. 1, pp. 50–56, 2011.

[21] K. S. McNaught and P. Jenner, "Extracellular accumulation of nitric oxide, hydrogen peroxide, and glutamate in astrocytic cultures following glutathione depletion, complex I inhibition, and/or lipopolysaccharide-induced activation," *Biochemical Pharmacology*, vol. 60, no. 7, pp. 979–988, 2000.

[22] S. E. Dorman and S. M. Holland, "Interferon-γ and interleukin-12 pathway defects and human disease," *Cytokine and Growth Factor Reviews*, vol. 11, no. 4, pp. 321–333, 2000.

[23] Z. Zhuge, Y. Zhu, P. Liu et al., "Effects of astragalus polysaccharide on immune responses of porcine PBMC stimulated with PRRSV or CSFV," *PLoS ONE*, vol. 7, no. 1, Article ID e29320, 2012.

[24] X. Du, X. Chen, B. Zhao et al., "Astragalus polysaccharides enhance the humoral and cellular immune responses of hepatitis B surface antigen vaccination through inhibiting the expression of transforming growth factor β and the frequency of regulatory T cells," *FEMS Immunology and Medical Microbiology*, vol. 63, no. 2, pp. 228–235, 2011.

[25] S. Makino, S. Ikegami, H. Kano et al., "Immunomodulatory effects of polysaccharides produced by *Lactobacillus delbrueckii* ssp. bulgaricus OLL1073R-1," *Journal of Dairy Science*, vol. 89, no. 8, pp. 2873–2881, 2006.

[26] M. Yang, Z. Xiao, Q. Lv et al., "The functional expression of TLR3 in EPCs impairs cell proliferation by induction of cell apoptosis and cell cycle progress inhibition," *International Immunopharmacology*, vol. 11, no. 12, pp. 2118–2124, 2011.

[27] C. Meyer, R. Pries, and B. Wollenberg, "Established and novel NF-κB inhibitors lead to downregulation of TLR3 and the proliferation and cytokine secretion in HNSCC," *Oral Oncology*, vol. 47, no. 9, pp. 818–826, 2011.

[28] C. J. Xu, X. C. Jian, F. Guo, Q. P. Gao, J. Y. Peng, and X. P. Xu, "Effect of astragalus polysaccharides on the proliferation and ultrastructure of dog bone marrow stem cells induced into osteoblasts in vitro," *Hua Xi Kou Qiang Yi Xue Za Zhi*, vol. 25, no. 5, pp. 432–436, 2007.

[29] Y. Liu, W. J. Wang, W. H. Chen, and J. Yin, "Effects of Astragalus polysaccharides on proliferation and differentiation of 3T3-L1 preadipocytes," *Zhong Xi Yi Jie He Xue Bao*, vol. 5, no. 4, pp. 421–426, 2007.

[30] K. A. Fitzgerald, S. M. McWhirter, K. L. Faia et al., "IKKE and TBKI are essential components of the IRF3 signalling pathway," *Nature Immunology*, vol. 4, no. 5, pp. 491–496, 2003.

[31] Y. Y. Wang, L. Li, K. J. Han, Z. Zhai, and H. B. Shu, "A20 is a potent inhibitor of TLR3- and Sendai virus-induced activation of NF-κB and ISRE and IFN-β promoter," *FEBS Letters*, vol. 576, no. 1-2, pp. 86–90, 2004.

Hindawi Publishing Corporation
Evidence-Based Complementary and Alternative Medicine
Volume 2014, Article ID 894515, 12 pages
http://dx.doi.org/10.1155/2014/894515

Research Article

Rabdosia japonica var. *glaucocalyx* Flavonoids Fraction Attenuates Lipopolysaccharide-Induced Acute Lung Injury in Mice

Chun-jun Chu,[1] Nai-yu Xu,[1] Xian-lun Li,[1] Long Xia,[1] Jian Zhang,[1] Zhi-tao Liang,[2] Zhong-zhen Zhao,[2] and Dao-feng Chen[3]

[1] *College of Pharmaceutical Science, Soochow University, Suzhou 215123, China*
[2] *School of Chinese Medicine, Hong Kong Baptist University, Kowloon, Hong Kong*
[3] *Department of Pharmacognosy, School of Pharmacy, Fudan University, Shanghai 201203, China*

Correspondence should be addressed to Jian Zhang; jianzhang@suda.edu.cn and Dao-feng Chen; dfchen@shmu.edu.cn

Received 15 April 2014; Accepted 18 May 2014; Published 11 June 2014

Academic Editor: Shi-Biao Wu

Rabdosia japonica var. *glaucocalyx* (Maxim.) Hara, belonging to the *Labiatae* family, is widely used as an anti-inflammatory and antitumor drug for the treatment of different inflammations and cancers. *Aim of the Study*. To investigate therapeutic effects and possible mechanism of the flavonoids fraction of *Rabdosia japonica* var. *glaucocalyx* (Maxim.) Hara (RJFs) in acute lung injury (ALI) mice induced by lipopolysaccharide (LPS). *Materials and Methods*. Mice were orally administrated with RJFs (6.4, 12.8, and 25.6 mg/kg) per day for 7 days, consecutively, before LPS challenge. Lung specimens and the bronchoalveolar lavage fluid (BALF) were isolated for histopathological examinations and biochemical analysis. The level of complement 3 (C3) in serum was quantified by a sandwich ELISA kit. *Results*. RJFs significantly attenuated LPS-induced ALI via reducing productions of the level of inflammatory mediators (TNF-α, IL-6, and IL-1β), and significantly reduced complement deposition with decreasing the level of C3 in serum, which was exhibited together with the lowered myeloperoxidase (MPO) activity and nitric oxide (NO) and protein concentration in BALF. *Conclusions*. RJFs significantly attenuate LPS-induced ALI *via* reducing productions of proinflammatory mediators, decreasing the level of complement, and reducing radicals.

1. Introduction

Acute lung injury (ALI) and its more severe form, acute respiratory distress syndrome (ARDS), are the critical pathological condition especially in some severe infectious respiratory diseases [1]. Both of them are characterized by alveolar-capillary membrane disruption, extensive leukocyte infiltration, and releasing of proinflammatory mediators, pulmonary edema associated with proteinaceous alveolar exudates and deterioration of gas exchange, and finally respiratory failure [2]. In addition, the pathogenesis of ALI/ARDS involves the immunity damage and the overactivation of complement system [3]. It reported that complement 3 (C3) is involved in lung injury, and inhibition of complement activation might be a potential therapeutic strategy [4, 5]. Despite recent advances in many new strategies for treatment, the mortality of ALI still remains more than 40% [6]. The development of efficient agents is still urgently needed.

Rabdosia japonica var. *glaucocalyx* (Maxim.) Hara, a plant belonging to *genus Rabdosia* in family Labiatae, is used as traditional medicinal herb for centuries in China with low toxicity [7]. In the folk medicine, it is found to be effective in colds, fever, hepatitis, gastritis, mastitis, tonsillitis, liver cancer, and breast cancer [8]. Recently, its modern pharmacological properties were also reported, such as antibacterial and anti-ischemic properties [9, 10]. The main compounds, such as luteolin, quercetin-3-methylether, apigenin, quercetin, luteolin-7-methylether, rutin, isoquercitrin,

glaucocalyxin A, glaucocalyxin B, glaucocalyxin C, oleanic acid, and ursolic acid, had been isolated and identified from the herb [11–13].

In our previous study, the ethanol extract of *Rabdosia japonica* var. *glaucocalyx* (Maxim.) Hara was found to contain a lot of flavonoids compounds; furthermore, ten flavonoids were characterized as anticomplementary agents *in vitro* [11–13]. However, whether the flavonoidsfractionof *Rabdosia japonica* var. glaucocalyx (Maxim.) Hara (RJFs) attenuates LPS-induced ALI and the possible mechanisms are still unknown. In the present study, we investigate therapeutic effects and possible mechanism of RJFs on ALI induced by LPS in mice.

2. Materials and Methods

2.1. Reagents. LPS (*Escherichia coli* 055:B5) was purchased from Sigma-Aldrich Co., Ltd (St. Louis, MO, USA). Dexamethasone (DXM) acetate tablets (number. H33020822) were purchased from Zhejiang Xianju Pharmaceutical Co., Ltd. (Hangzhou, Zhejiang, China). Mouse TNF-α, IL-6, and IL-1β ELISA kits (number B1007233) were purchased from Shanghai Chuanfu Biotechnology Co., Ltd. (Shanghai, China). Nitric oxide (NO) and bicinchoninic acid (BCA) protein assay kit, myeloperoxidase (MPO), and superoxide dismutase (SOD) determination kits were purchased from Nanjing Jiancheng Bioengineering Institute (Nanjing, Jiangsu, China). The trifluoroacetic acid was purchased from Fluka. β-galactosidase and β-glucosidase were purchased from Sigma-Aldrich Co., Ltd. Polymyxin B sulfate was purchased from Amresco. Polyclonal rabbit anti-human C3c complement (RS-0367R) was purchased from Shanghai Ruiqi Biological Technology Co., Ltd. (Shanghai, China). The solvents, acetonitrile, and methanol were of HPLC grade from E. Merck (Darmstadt, Germany) and formic acid with a purity of 96% was also in HPLC grade (Tedia, U.S.A.). Water was obtained from a Milli-Q water purification system (Millipore, Bedford, MA, USA). AB-8 macroporous adsorption resins were purchased from Baoen Adsorption-material Technology Co., Ltd (Cangzhou, Hebei, China). All other reagents were of the highest quality available.

2.2. Plant Materials and Preparation of RJFs. *Rabdosia japonica* var. *glaucocalyx* (Maxim.) Hara was purchased from Baihe Forest, Taoshan Forestry Administration, Tieli, Heilongjiang Province of China, in October of 2008. The plant material was authenticated by Prof. Zhenyue Wang, Heilongjiang University of Chinese Medicine, and the voucher specimen (number 081008) was deposited at the Herbarium of Materia Medica, Heilongjiang University of Chinese Medicine, Heilongjiang, P. R. China. The extraction and purification of RJFs were carried out according to our previous studies. The dried leaves and stems of *Rabdosia japonica* var. *glaucocalyx* (Maxim.) Hara (100 g) were extracted under reflux with 80% EtOH (1000 mL) for 2 h, repeated twice. After filtration, the combined 80% EtOH extracts were evaporated to dryness under vacuum at 60°C. The solution of extract (0.32 g/mL) was added into column loading-treated AB-8 macroreticular resin for adsorption at 36 mL/min, and then washed with water to get rid of polar impurities. RJFs in the column were eluted with 60% EtOH, and the eluting solution was evaporated to dryness at 60°C until yellow powders were achieved.

2.3. Complementary Activity through the Classical Pathway. Based on Mayer's modified method [14], sensitized erythrocytes (EAs) were prepared by incubation of 2% sheep erythrocytes (4.0×10^8 cells/mL) with rabbit anti-sheep erythrocyte antibody (1 : 1000) in VBS^{2+} (containing 0.5 mM Mg^{2+} and 0.15 mM Ca^{2+}). Samples were dissolved in VBS^{2+}. Guinea pig serum was used as the complement source. The 1 : 60 diluted Guinea pig serum was chosen to give submaximal lysis in the absence of complement inhibitors. In brief, various dilutions of tested samples (200 μL) were mixed with 200 μL of Guinea pig serum, and 200 μL of EAs was added, and then the mixture was incubated at 37°C for 30 min. The different assay controls were incubated in the same conditions: (1) vehicle control: 200 μL EAs in 400 μL VBS^{2+}; (2) 100% lysis: 200 μL EAs in 400 μL ultrapure water; (3) samples background: 200 μL dilution of each sample in 400 μL VBS^{2+}. The reacted mixture was centrifuged immediately at 4°C after incubation. Optical density of the supernatant was measured at 405 nm on well scan (Labsystems Dragon). Results were indicated in percentage of hemolytic inhibition. Inhibition of lysis (%) = $100 - 100 \times (OD_{\text{sample}} - OD_{\text{sample background}}) \div OD_{100\% \text{ lysis}}$.

2.4. Ultra High Performance Liquid Chromatography-Mass Spectrometry (UHPLC-MS) Analysis of RJFs. The UHPLC was performed on an Agilent 6540 accurate-mass Q-TOF LC/MS system (Agilent Technologies, USA). A UPLC C18 analytical column (2.1 mm × 100 mm, I.D. 1.7 μm, ACQUITY UPLC BEH, Waters, USA) was conducted for separation, coupled with a C18 precolumn (2.1 mm × 5 mm, I.D. 1.7 μm, Van Guard TM BEH, Waters, USA) at room temperature of 20°C. The mobile phase was a mixture of water (A) and acetonitrile (B), both containing 0.1% formic acid, using a gradient elution (0 min: 5% B, 8 min: 25% B, 18 min: 75% B, 25 min: 100% B, 28 min: 100% B) with 3 min of balance back to 5% B. The injection volume was 1 μL, and the flow rate was set at 0.4 mL/min. Mass spectra were obtained in positive mode, and the source parameters were set as follows: Gas Temp 300°C, Gas Flow 8 L/min, Nebulizer 40 psi, Vcap 3500, Nozzle Voltage (V) 500, and Fragmentor 120. Reference masses were used at m/z 121.0509 (purine) and 922.0098 (hexakis phosphazine).

Reference compounds (>95% by HPLC) isolated in our laboratory were solved in pure methanol solution, and the concentration of each standard solution was made as follows: quercetin 336 μg/mL, luteolin 308 μg/mL, vitexin 143 μg/mL, isoquercitrin 336 μg/mL, and GLA 500 μg/mL. Then a stock solution of mixed reference compounds was prepared for calibration, containing 67.2 μg/mL quercetin, 61.6 μg/mL luteolin, 28.6 μg/mL vitexin, 67.2 μg/mL isoquercitrin, and 100.0 μg/mL GLA.

Data analysis was performed on Agilent MassHunter Workstation software-Qualitative Analysis (version B.04.00,

Build 4.0.479.5, Service Pack 3, Agilent Technologies, Inc. 2011). It was applied in positive ion mode with the following settings: extraction restrict retention time of 2–20 min, peaks with height ≥100 counts to be used, charge state of 1, and peak spacing tolerance of 0.0025 *m/z*, plus 5.0 ppm; compound relative height ≥2.5%, and absolute height ≥1000 counts; elements of C, H, O, N, from 3–60, 0–120, 0–30, 0–30, respectively, to generate formulae. Results are shown by base peak chromatogram (BPC with *m/z* range 100–950).

2.5. The Contents of Glaucocalyxin A (GLA), Quercetin, and Luteolin in RJFs by High Performance Liquid Chromatographic (HPLC) Analysis. HPLC quantitative analysis was performed using an Agilent Infinity 1260 system with a YMC C18 column (4.6 × 250 mm, 5 μm). The HPLC was performed with the mobile phase, which was a mixture of 50% water (A) and 50% methanol (B), both containing 0.1% formic acid. The injection volume was 20 μL and the flow rate was set at 1.0 mL/min, and peaks were monitored at 230 and 365 nm. Calibration curves consisted of 0.064–2.001 mg/mL GLA, 0.063–2.206 mg/mL quercetin, and 0.063–2.006 mg/mL luteolin standard solutions. Peaks were identified by congruent retention times compared with standards. Analyses were performed in triplicate.

2.6. Determination of Total Flavonoid Content in RJFs. Total flavonoids in RJFs were determined using a slightly modified colorimetric method described previously [15]. A 13 mL methanol of diluted sample solution was mixed with 1 mL of a 5% $NaNO_2$ solution. After 6 min, 1 mL of a 10% $AlCl_3$ solution was added and allowed to stand for 6 min then 10 mL of a 4% NaOH solution was added to the mixture and left to stand for another 15 min. The absorbance of the mixture was determined at 510 nm, and luteolin was used as the standard.

2.7. Animals. Male Kunming mice, about 24–28 g, were purchased from the Center of Experimental Animals Soochow University (Suzhou, Jiangsu, China). The mice were kept in a specific pathogen free condition and received food and water *ad libitum*. Laboratory temperature was 24 ± 1°C, and relative humidity was 40–80%. Before experimentation, the mice were allowed to adapt to the experimental environment for a minimum of 3 days. The experimental protocols shown in this study were approved by the Animal Ethical Committee of School of Pharmacy at Soochow University.

2.8. Establishment of the ALI Model and Preventive Regimen [16–24]. RJFs were ground and suspended in distilled water containing 0.5% sodium carboxymethyl cellulose (CMC-Na) for administration to mice.

The mice were randomly divided into seven groups (n = 20): control group, RJFs group (RJFs treated at 25.6 mg/kg without LPS), model (LPS, 2 mg/kg) group, RJFs-pretreated groups (RJFs at 6.4, 12.8, and 25.6 mg/kg with LPS, resp.), and positive group (DXM, 5 mg/kg).

RJFs and RJFs-pretreated groups received an intragastric injection of RJFs at given doses, each mouse was administered orally once per day for 7 days, consecutively. Positive group received DXM only on day 7. Mice from control, model, and positive groups received the equal volume distilled water instead of RJFs. The doses of these drugs we chose were on the basis of our preliminary experiments. On day 7, 2 h after RJFs and DXM treatment, mice were slightly anesthetized with a 20% urethane (4 mL/kg) given intraperitoneally. Then, in experimental groups, 2 mg/kg LPS was instilled intratracheally (i.t.) in 50 μL NS to induce lung injury. Mice from control and RJFs groups were given a 50 μL NS i.t. instillation without LPS. It took about 5-6 min per mouse to induce lung injury. Animals recovered quickly from the procedure with only mild discomfort.

6 h after LPS challenge, half of the mice of each group (n = 10) were sacrificed and the blood samples were collected (each one was approximately 1 mL). The right lung was used to collect BALF, which was lavaged three times with 0.8 mL of autoclaved NS. The left lung was used to obtain the lung W/D ratio. 24 h after LPS challenge, the rest of the mice were sacrificed. The inferior lobe of right lung was used for histopathologic evaluation. The superior lobes of right lung were used to collect BALF. The left lung was homogenized using a homogenizer.

2.9. NO and Protein Analysis. BALF was collected as previously described. At 6 h after LPS challenge, mice were sacrificed by exsanguination. BALF was obtained by intratracheal instillation, each sample was centrifuged (4°C, 1400 ×g, 10 min) and its supernatants were stored at −80°C for analysis of NO and protein levels. The content of NO and protein in the supernatants of the BALF (6 h) were measured by NO and BCA protein assay kits according to the manufacturer's instructions strictly.

2.10. Lung W/D Ratio. Mice were sacrificed by exsanguination at 6 h after LPS challenge. The left lung was excised, blotted dry, and weighed to obtain the "wet" weight and then placed in an oven at 80°C for 48 h to obtain the "dry" weight. The ratio of the wet lung to the dry lung was calculated to assess tissue edema.

2.11. Complement 3 (C3) in Serum Analysis. At 6 h after LPS challenge, the blood of mice was collected. Blood samples were coagulated at room temperature for 10 min and then centrifuged (4°C, 1400 ×g, 20 min), its supernatants (serum) were stored at −80°C for subsequent analysis. The level of complement 3 in serum was quantified by the sandwich ELISA kit, according to the manufacturer's instructions strictly.

2.12. Assays for SOD and MPO Activities. At 24 h after LPS challenge, the left lungs were homogenized using a homogenizer, then they were prepared to 10% lung tissue homogenate. The tissue homogenate generated was assayed for MPO activity, which was measured by MPO determination kit using commercially available reagents according to the manufacturer's instructions. The homogenate was then centrifuged at 1400 ×g for 10 min at 4°C. The supernatants

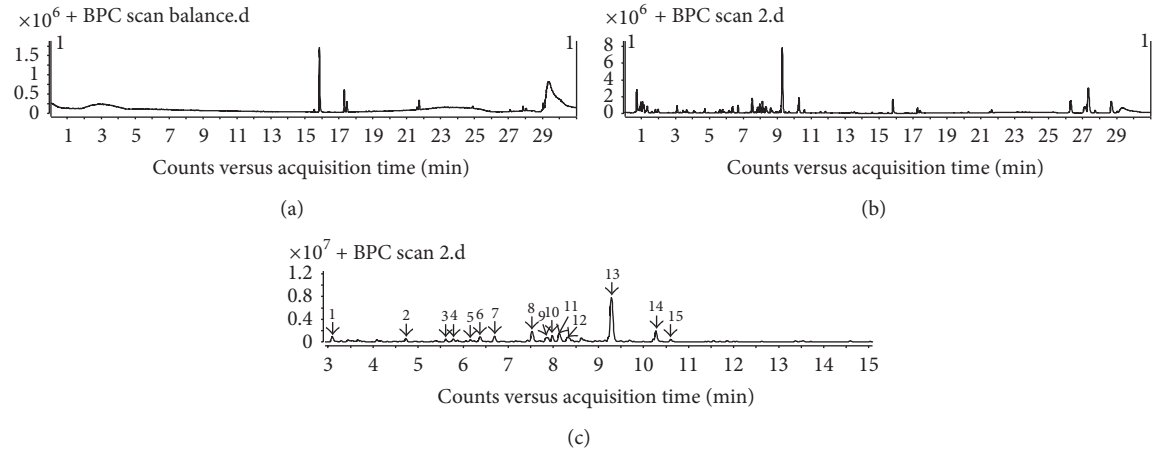

Figure 1: LC-MS base peak chromatograms of RJFs. The peak numbers referred to Table 1. (a) Methanol. (b) RJFs (0–30 min). (c) RJFs (3–15 min).

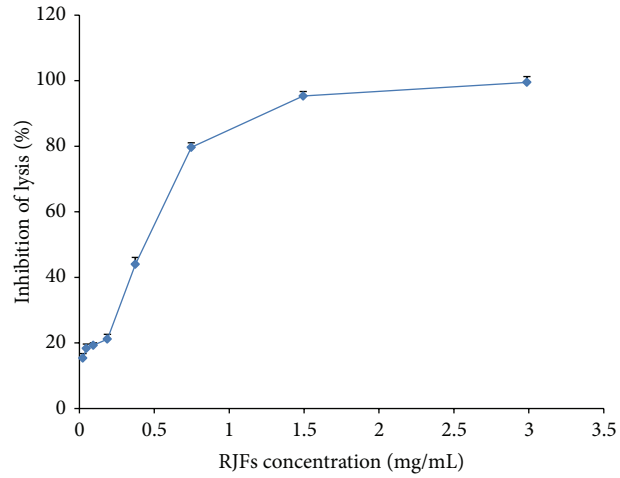

Figure 2: Inhibition of the classical pathway-mediated hemolysis by RJFs. Lysis of sheep erythrocytes in 1 : 60 diluted Guinea pig serum in the presence of increasing amounts of RJFs. Data are listed as mean ± S.D. ($n = 3$).

obtained were used for assay of SOD activity. SOD activity was expressed as units per milligram of protein.

2.13. Cytokine Analysis. The levels of cytokine TNF-α, IL-6, and IL-1β in the supernatants of the BALF (24 h) were quantified in duplication by the sandwich ELISA kit using commercially available reagents, according to the manufacturer's instructions strictly.

2.14. Histological Studies of Lung. After mice were sacrificed, inferior lobe of right lung tissue was immediately harvested and fixed in 4% formaldehyde. Then lung tissue was dehydrated and embedded in paraffin. Paraffin sections were stained with hematoxylin and eosin (H&E) according to the regular staining method. Images were observed under an Olympus microscope at an original magnification of 400x.

For the detection of complement deposits, the 5 μm sections were deparaffinized, rehydrated, and incubated with rabbit anti-human C3c overnight at 4°C. Slices were visualized using chromogenic substrate solution 3,3′-diaminobenzidine (DAB). All slides were imaged with CoolPix 4500 camera (Nikon) matched on a CX21 microscope (Olympus) at an original magnification of 400x.

2.15. Statistical Analysis. All values were expressed as mean ± S.D. To perform statistical analysis, one-way analysis of variance (ANOVA) was used. If any significant changes were found, post hoc comparisons were performed using Fisher's PLSD. Statistical significance was accepted at $P < 0.05$.

3. Results

3.1. Chemical Profiling of RJFs. A previous study has demonstrated that *Rabdosia japonica* var. *glaucocalyx* (Maxim.) Hara primarily contains flavonoids and terpenoids [11–13]. AB-8 macroporous adsorption resins were used for flavonoid and diterpenoids enrichment of RJFs. By UHPLC-Q-TOF-MS analysis, a total of 15 well-separated chromatographic peaks in RJFs could be found in the BPC of RJFs (Figure 1). In LC-MS analysis, five peaks can be achieved via comparison of the reference standards' retention data and MS spectra. Other detected peaks were tentatively identified by their accurate mass data in comparison with reported references. RJFs mainly contain flavonoid compounds. As shown in Table 1, peaks 3, 4, 5, 6, 7, 8, 12, 13, and 15 were tentatively identified to be flavonoids and peaks 9 and 14 were tentatively identified to be terpenoids. In our previous study, we had isolated some compounds such as peaks 1, 3, 5, 9, 13, 14, and 15 [11–13]. The results indicated that the GLA, quercetin, and luteolin contents were 2.90%, 0.308%, and 0.291% of RJFS, respectively, by HPLC analysis. The total flavonoids content were 12.90% of RJFs by colorimetric method.

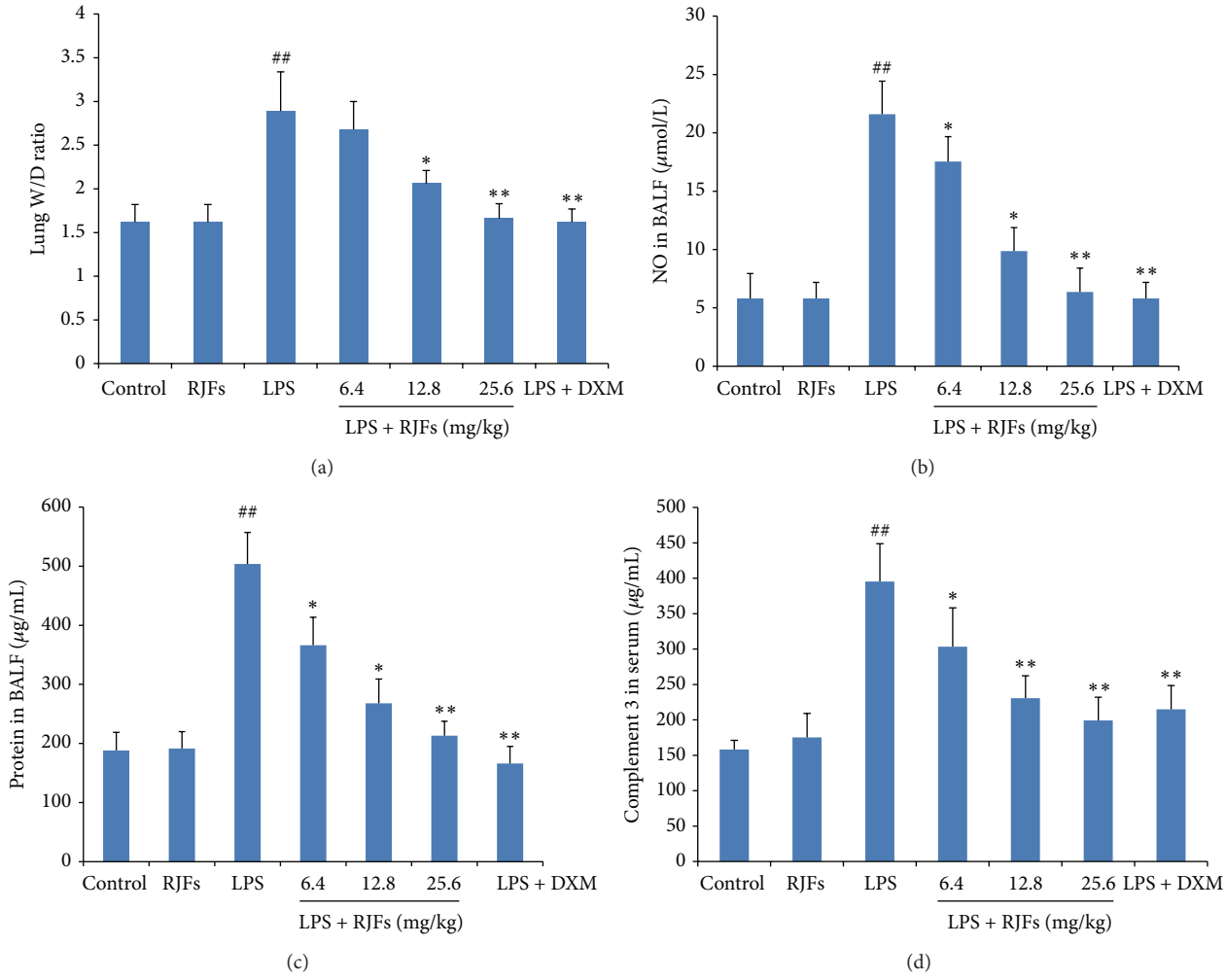

Figure 3: Effects of RJFs on the lung W/D ratio, NO, total protein concentration in BALF, and the level of C3 in serum of mice. 2 h after RJFs pretreatment on day 7, mice were slightly anesthetized, and then 2 mg/kg LPS was instilled intratracheally (i.t.) to induce lung injury. The lung W/D ratio was determined at 6 h after LPS challenge; BALF and the serum were collected at 6 h following LPS challenge. NO and total protein concentration in the supernatant of BALF were determined by kits. C3 activity in serum was determined by mouse C3 ELISA kit. Data expressed as means ± S.D. ($n = 10$); $^{\#\#}P < 0.01$ compared with control, $^{*}P < 0.05$ and $^{**}P < 0.01$ compared with vehicle treated ALI model group.

3.2. In Vitro Anticomplementary Activity of RJFs. As shown in Figure 2, RJFs significantly inhibited hemolysis in sheep erythrocytes induced by Guinea pig serum ($CP_{50} = 0.354 \pm 0.066$ mg/mL).

3.3. Effects of RJFs on Lung W/D Ratio, NO, and Total Protein Concentration in BALF of Mice. As shown in Figure 3, the lung W/D ratio, NO, and the total protein concentration in BALF were found to be significantly higher after LPS challenge compared with those of the control group ($P < 0.01$), while RJFs (25.6 mg/kg) gavage itself did not cause significant changes.

Compared with vehicle treated ALI model group, pretreatment with RJFs markedly decreased the NO and the total protein concentration ($P < 0.05$) in BALF of mice (Figures 3(b) and 3(c)). RJFs at 12.8 and 25.6 mg/kg significantly decreased the lung W/D ratio ($P < 0.05$) (Figure 3(a)). DXM also significantly decreased the lung W/D ratio, NO, and the total protein concentration.

3.4. Effect of RJFs on C3 Production in Serum of LPS-Induced ALI. As shown in Figure 3(d), the level of C3 was significantly higher after LPS challenge compared with those of the control group ($P < 0.01$), while RJFs (25.6 mg/kg) gavage itself did not cause significant changes. Compared with vehicle treated ALI model group, pretreatment with RJFs markedly decreased the level of C3 ($P < 0.05$) in serum of mice. RJFs at 12.8 and 25.6 mg/kg significantly decreased the

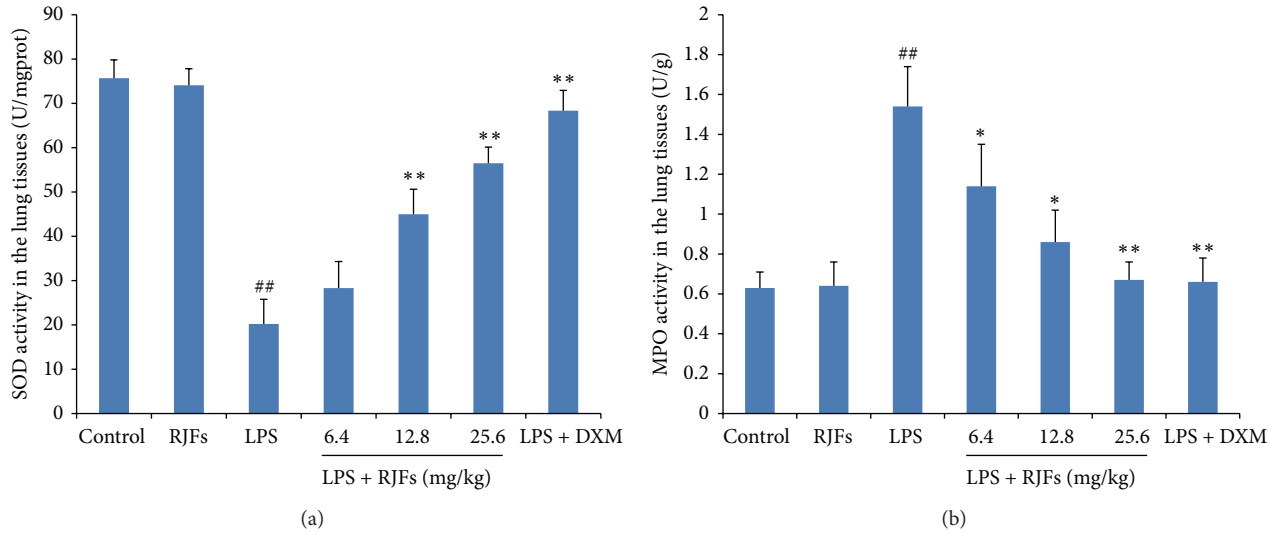

Figure 4: Effects of RJFs on SOD and MPO activities of lung tissue in mice. 2 h after RJFs pretreatment on day 7, mice were slightly anesthetized, and then 2 mg/kg LPS was instilled intratracheally (i.t.) to induce lung injury. Lung homogenates were prepared at 24 h after LPS challenge. SOD and MPO activities were determined by kits. Data expressed as means ± S.D. ($n = 10$); $^{\#\#}P < 0.01$ compared with control, $^{*}P < 0.05$ and $^{**}P < 0.01$ compared with vehicle treated ALI model group.

Table 1: Characteristics of chemical components of RJFs by UHPLC-Q-TOF-MS.

Peaks number	Retention time (min)	Mass ions (m/z)	Molecular formula	Identification
1	3.104	198.0755 $[M + H_2O]^+$	$C_9H_8O_4$	Caffeic acid
2	4.731	351.1248 $[M + H]^+$	$C_{20}H_{30}O_5$	RabdoloxinB
3	5.882	434.2496 $[M + 2H]^+$	$C_{21}H_{20}O_{10}$	Vitexin
4	5.915	451.2321 $[M + H + H_2O]^+$	$C_{21}H_{20}O_{10}$	Isovitexin
5	6.240	437.1120 $[M + H–CO]^+$	$C_{21}H_{20}O_{12}$	Isoquercitrin
6	6.374	317.2116 $[M–H]^+$	$C_{15}H_{10}O_8$	Myricetin
7	6.691	283.7185 $[M–H]^+$	$C_{16}H_{12}O_5$	Baicalein-methylether
8	7.525	340.2600 $[M–H + Na]^+$	$C_{15}H_{10}O_8$	Quercetagetin
9	7.859	351.2127 $[M + H]^+$	$C_{20}H_{30}O_5$	Kamebakaurin
10	7.975	745.3335 $[2M + Na]^+$	$C_{18}H_{16}O_7$	Methyl-6-dehydroxyl rosmarinate
11	8.125	396.8057 $[M + Na–H]^+$	$C_{19}H_{18}O_8$	Methyl rosmarinate
12	8.317	426.2526 $[M + H + Na]^+$	$C_{20}H_{18}O_9$	Apigenin-7-arabinoside
13	9.293	285.1869 $[M–H]^+$	$C_{15}H_{10}O_6$	Luteolin
14	10.277	333.2062 $[M + H]^+$	$C_{20}H_{28}O_4$	Glaucocalyxin A
15	10.611	785.4507 $[2M–H + 2HCOONa + 2Na]^+$	$C_{15}H_{10}O_7$	Quercetin

level of C3 ($P < 0.01$). DXM also significantly decreased the level of C3.

3.5. Effects of RJFs on SOD and MPO Activities in Lung Tissues of LPS-Induced ALI. As shown in Figure 4, LPS challenge resulted in significant decreases of SOD activity and significant increases of MPO activity in the lungs compared with the control group ($P < 0.01$), while RJFs (25.6 mg/kg) gavage itself did not cause significant changes.

RJFs at 12.8 and 25.6 mg/kg significantly increased SOD activity ($P < 0.01$) (Figure 4(a)), while RJFs at 25.6 mg/kg decreased MPO activity ($P < 0.01$) (Figure 4(b)). DXM also significantly increased SOD activity and decreased MPO activity.

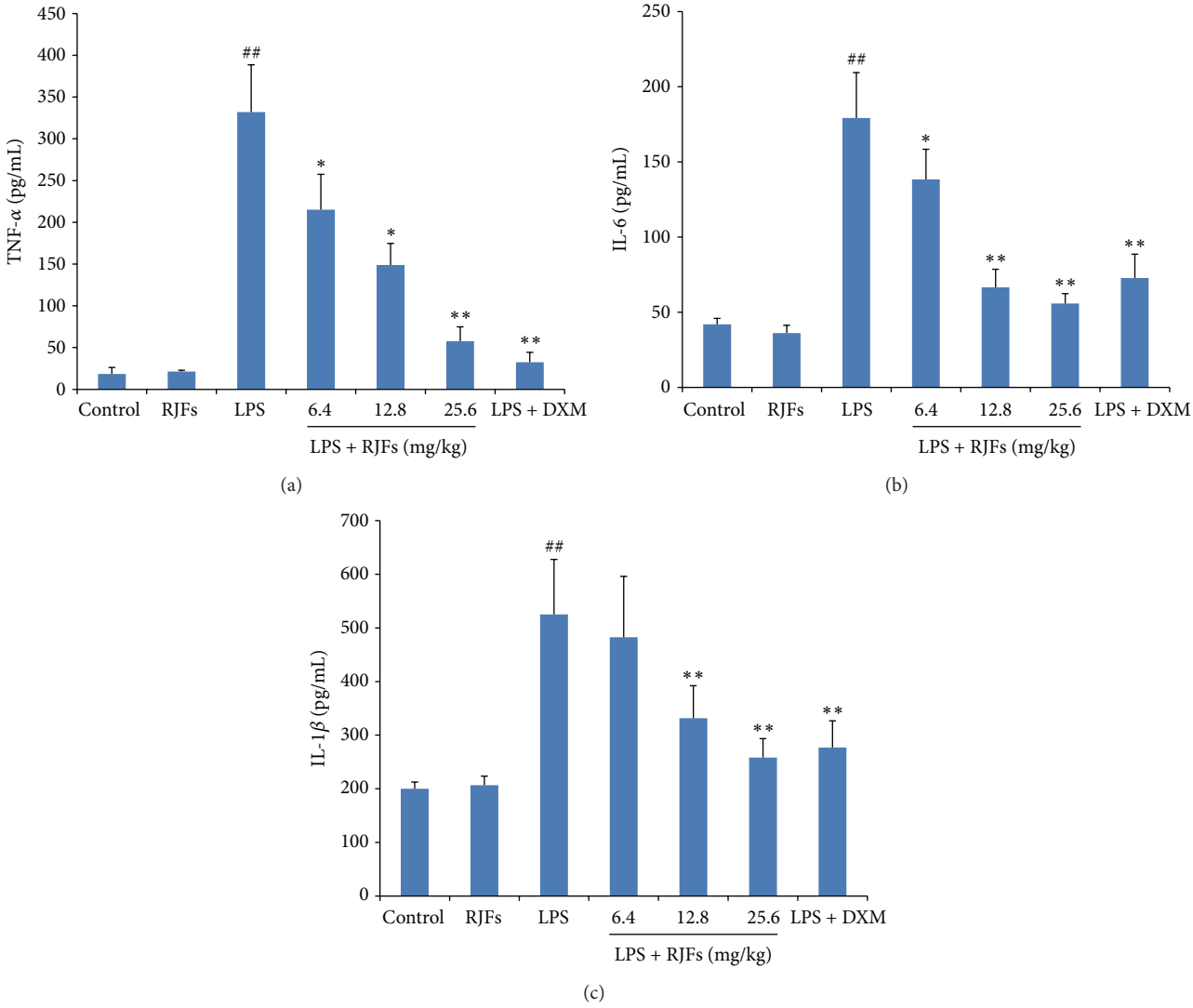

FIGURE 5: Effects of RJFs on production of inflammatory cytokine TNF-α, IL-6, and IL-1β in BALF of mice. 2 h after RJFs pretreatment on day 7, mice were slightly anesthetized, and then 2 mg/kg LPS was instilled intratracheally (i.t.) to induce lung injury. BALF was collected at 24 h following LPS challenge. The levels of TNF-α, IL-6, and IL-1β in the supernatants of BALF were determined by mouse ELISA kits. Data expressed as means ± S.D. ($n = 10$); $^{\#\#}P < 0.01$ compared with control, $^{*}P < 0.05$ and $^{**}P < 0.01$ compared with vehicle treated ALI model group.

3.6. Effects of RJFs on TNF-α, IL-6, and IL-1β Production in BALF. As shown in Figure 5, LPS significantly increased TNF-α, IL-6, and IL-1β production compared with the control group ($P < 0.01$), while RJFs (25.6 mg/kg) gavage itself did not cause significant changes.

Compared with vehicle treated ALI model group, pretreatment with RJFs markedly decreased the level of TNF-α in the BALF of mice ($P < 0.05$) (Figure 5(a)). RJFs at 12.8 and 25.6 mg/kg significantly reduced the level of IL-6 and IL-1β in the BALF ($P < 0.01$) (Figures 5(b) and 5(c)). DXM also significantly decreased TNF-α, IL-6, and IL-1β production.

3.7. Effect of RJFs on Lung Histology. Histopathological changes of each group were observed by histochemical staining with H&E. Histopathological changes such as lung edema, increased alveolar wall thickness, inflammatory cells aggregation, and pulmonary hemorrhage were observed in model group mice induced by LPS given intratracheally. As shown in Figure 6, these lesions were not apparent in control group stimulated with only NS. Pretreatment with RJFs markedly ameliorated the pulmonary injury.

For vehicle treated ALI model group, immunohistochemistry of lung tissue sections showed a patchy dense immunoperoxidase indicative of complement deposition. Complement appeared by bulk deposition and was mainly deposited in lung tissue. In contrast, mice in control group had little complement deposition in lung tissue. Pretreatment with RJFs markedly decreased complement deposition (Figure 6).

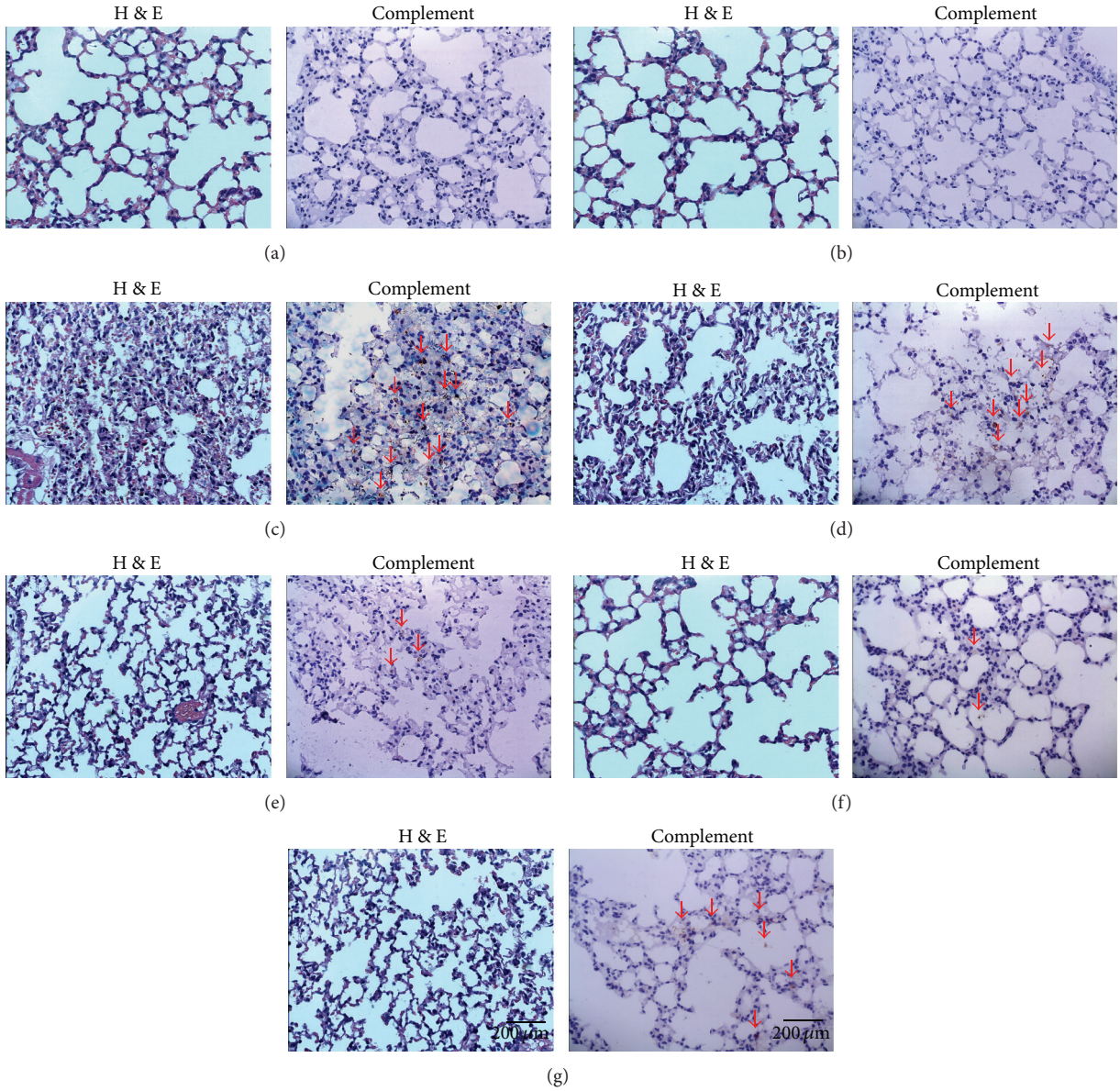

Figure 6: Hematoxylin and eosin-stained (H&E) (400x) and immunohistochemistry of lung tissue (400x). Lungs from each group were processed for histological evaluation at 24 h after LPS challenge: Section of control (a) and RJFs (b) groups mice: normal lung tissue sections (H&E and complement). Section of a LPS-induced ALI model (c) group mouse: note increased alveolar wall thickness, inflammatory cells aggregation, pulmonary hemorrhage (H&E), and a patchy dense immunoperoxidase indicative of complement deposition marked with red arrows (complement). Section from 6.4, 12.8, and 25.6 mg/kg RJFs-pretreated ((d), (e), and (f), resp.) and DXM-treated (g) groups mouse: note mild alveolar wall thickness, reduced inflammatory cells aggregation, little pulmonary hemorrhage (H&E), and little complement deposition marked with red arrows (complement).

4. Discussion

Rabdosia japonica var. *glaucocalyx* (Maxim.) Hara was used as a folk medicine for a long time and contained mainly diterpenoids, flavonoids, and steroids [11–13]. In our previous study, we found the flavonoids (such as quercetin, luteolin, isoquercetin, rutin, etc.) and the phenylpropionic acid (such as caffeic acid and caffeic acid ethylene ester) have anticomplementary activity in the test of complementary activity through the classical pathway, but the diterpenoids (such as GLA) did not have anticomplementary activity [13]. Therefore, RJFs were prepared for study and the results showed it exhibited a high anticomplementary activity.

The UHPLC-Q-TOF-MS analysis indicated RJFs had mainly flavonoids, fewer terpenoids, and the phenylpropionic acid. In this study, we demonstrated that RJFs significantly alleviated the LPS-induced ALI in mice by reducing the production of inflammatory mediators and downregulation of the complement level.

LPS, a large molecule consisting of a lipid and a polysaccharide joined by a covalent bond, is the major component of the outer membranes of Gram-negative bacteria, acts as endotoxins, and elicits strong inflammatory and immune response in animals [18, 19]. It is an important inducer of lung injury which can be employed in the investigation of ALI [20–22]. Therefore, an animal model of direct ALI was established and used by i.t. instillation of LPS in mice in our study. Glucocorticoids can cause neutrophilic granulocyte and alveolar macrophages, that are used to alleviate respiratory in the clinical treatment of ALI/ARDS [23, 24]. Therefore, DXM was used as a positive control to evaluate the anti-inflammatory efficiency of RJFs in LPS-induced ALI.

In our present investigation, we evaluated the lung wet-to-dry weight ratio to quantify the magnitude of pulmonary edema, which is a typical symptom of inflammation and a major characteristic of ALI [1, 25, 26]. Here, RJFs decreased the lung W/D ratio, which indicated that RJFs could inhibit the leakage of serous fluid into lung tissue and attenuate the development of pulmonary edema. As other indexes of epithelial and endothelial permeability in ALI, we measured the total protein content in the BALF [27]. As expected, mice exposed to LPS presented high protein content in the BALF, which were inhibited by RJFs.

NO has well been demonstrated in the pathophysiology and development of ALI induced by LPS, although its role in the pathogenesis of ALI has not been clearly elucidated [28]. LPS is well demonstrated to stimulate iNOS expression and NO overproduction in many pulmonary cell types, including lung endothelial cells, epithelial cells, macrophages, and neutrophils [29]. In our experiment, RJFs reduced the productions of NO in BALF, which might contribute to the amelioration of inflammatory response and the lessened lung damage.

Oxidative stress plays an important role in the development of LPS-induced ALI. MPO was released by neutrophils, which could act as an index to reflect the activation, adhesion, and recruitment of neutrophils into lung [30]. Neutrophils excrete MPO in the extracellular medium, bringing about an accumulation of H_2O_2-Cl and several other reactive oxygen derivatives and leading to an oxidative modification of proteins or cellular structures [31]. The present study showed that LPS induced a significant enhancement of MPO activity in mice lung parenchyma after LPS challenge in comparison to control mice, indicating a significant recruitment of neutrophils in lung parenchyma. RJFs inhibited pulmonary parenchymal MPO activity and were consistent with decreased number of neutrophils in the BALF, suggesting a mechanism by which RJFs inhibited LPS-induced ALI. SOD is an enzyme that exists in cells removing oxyradicals, whose activity variation may represent the degree of tissue injury [32]. In this study, RJFs enhanced SOD activity, suggesting RJFs may effectively scavenge oxyradicals during the inflammatory response to LPS-induced ALI.

LPS is known to induce the production of several inflammatory and chemotactic cytokines. TNF-α, which mainly originate from macrophages, damage vascular endothelial cells and increase their permeability, resulting in leukocyte adhesion, granulocyte degranulation, leukocyte migration into inflammatory positions, and lung lesion [33, 34]. Proinflammatory cytokines TNF-α, IL-6, and IL-1β appear in the early phase of an inflammatory response, play a critical role in the pathophysiology of inflammation in ALI, and contribute to the severity of lung injury [22, 35]. High levels of TNF-α, IL-6, and IL-1β in the BALF have been noted in patients with ALI/ARDS, and the persistent elevation of proinflammatory cytokines in humans with ALI or sepsis has been associated with more severe outcomes [36]. According the changes of inflammatory mediators in BALF and serum following intrapulmonary challenge with LPS in our previous studies, we chose to detect the inflammatory mediators in BALF at 24 h. In the present study, LPS induced the production of large amounts of TNF-α, IL-6, and IL-1β in the BALF of mice; RJFs lowered TNF-α, IL-6, and IL-1β secretion at 24 h after LPS challenge. Therefore, RJFs may protect against LPS-induced ALI by decreasing the production of these proinflammatory cytokines.

The levels of TNF-α, IL-6, and IL-1β are regulated by the activation of transcription factor NF-κB, which plays a crucial role in immune and inflammatory responses [37, 38]. It reported that total flavonoids of *Mosla scabra* (MF) leaves could attenuate pulmonary inflammation in mice with LPS-induced ALI, and the protective effect of MF in ALI might be related to its suppression of NF-κB and MAPK activation and, subsequently, caused a remarkable reduction in inflammatory cell infiltration and inflammatory cytokine secretion in lung tissues [39]. Also, luteolin suppresses inflammatory mediator expression by blocking the Akt/NFκB pathway in acute lung injury induced by lipopolysaccharide [40]. Moreover, luteolin attenuates the pulmonary inflammatory response which involves abilities of antioxidation and inhibition of MAPK and NF-κB pathways in mice with endotoxin-induced acute lung injury in mice [41]. The most important fraction of the RJFs is flavonoid, so the potential mechanisms of flavonoid in the treatment of acute lung injury are also associated with NF-κB pathways possibly.

Activation of the complement system plays a key role in normal inflammatory response to injury but may cause substantial injury when activated inappropriately. The complement system consists of more than 30 serum and cellular proteins, including positive and negative regulators, linked in three biochemical cascades, the classical, alternative and lectin complement pathways [42, 43]. C3 activation leads to the entry of the final common pathway resulting in the formation of the membrane attack complex (MAC, C5b-9) [44]. Animal model of ALI studies demonstrated alterations of complement 3 levels in ALI [5]. Pretreatment of wild type mice with humanized cobra venom factor, which inactivates C3, decreased polymorphonuclear neutrophil (PMN) in BAL cells and reduces C3 deposition in the lung [4]. Therefore, complement 3 plays an important role in activating complement system of ALI. As we detected the changes of C3-level in serum following intrapulmonary challenge with LPS, we found that it increased significantly at 6 h. In this research, the level of C3 in serum increased obviously at 6 h after LPS challenge; then, at 24 h, immunohistochemistry of lung tissue sections showed overactivation of complement with abundantly complement deposition in vehicle treated ALI

model group. RJFs markedly decreased complement deposition and the level of C3 in serum which might contribute to the attenuation of lung injury. We thought that inhibitors of complement may be potential adjunctive treatments for LPS-induced ALI.

Rabdosia japonica var. *glaucocalyx* (Maxim.) Hara is used as traditional medicinal herb for centuries in China with low toxicity [7]. In this study, RJFs (25.6 mg/kg) gavage itself did not cause significant changes; therefore, RJFs are effective with low toxicity, indicating them as a potential therapeutic agent for ALI.

5. Conclusion

In conclusion, RJFs attenuated LPS-induced lung injury, including reduction of lung W/D ratio, inhibition of protein level, and NO overproduction in BALF. In addition, RJFs lowered TNF-α, IL-6, and IL-1β level in BALF in ALI mice. The increased SOD activity and inhibited MPO activity in lung tissue were also observed in RJFs-pretreated ALI mice. Histological examination showed that RJFs significantly ameliorated lung injury by improving lung morphology and decreasing complement deposition. Meantime, RJFs obviously reduced the level of C3 in serum in ALI mice. The effects of RJFs against ALI were related with the inhibition on the production of proinflammatory mediators and decreasing the level of complement.

Abbreviations

RJ:	*Rabdosia japonica* var. *glaucocalyx* (Maxim.) Hara
RJFs:	The Flavonoids Fraction of *Rabdosia japonica* var. *glaucocalyx* (Maxim.) Hara
LPS:	Lipopolysaccharide
ALI:	Acute Lung Injury
BALF:	The Bronchoalveolar Lavage Fluid
C3:	Complement 3
ELISA:	Enzyme Linked Immunosorbent Assay
Lung W/D ratio:	Lung Wet-to-Dry Weight Ratio
MPO:	Myeloperoxidase
SOD:	Superoxide Dismutase
BCA:	Bicinchoninic Acid
ARDS:	Acute Respiratory Distress Syndrome
DXM:	Dexamethasone
NO:	Nitric Oxide
VBS:	Veronal Buffer Saline
EAs:	Sensitized Erythrocytes
H&E:	Hematoxylin and Eosin
GLA:	Glaucocalyxin A
BPC:	Base Peak Chromatograms
UHPLC-MS:	Ultra High Performance Liquid Chromatography-Mass Spectrometry
Q-TOF-MS:	Quadrupole Time of Flight Tandem Mass Spectrometry.

Ethical Approval

This study received permission from the Animal Ethical Committee of School of Pharmacy at Soochow University, China.

Conflict of Interests

The authors declare that there is no conflict of interests.

Acknowledgments

The authors acknowledge Mr. Alan Ho from the School of Chinese Medicine, Hong Kong Baptist University, for his technical supports. This work was financially supported by the Natural Science Fund for Colleges and Universities in Jiangsu Province (no. 10KJB350004), Suzhou Application Foundation Research Project (no. SYS201206), and the Priority Academic Program Development of Jiangsu Higher Education Institutions (PAPD). The authors are grateful to Dr. Hong Li at Department of Pharmacology of Fudan University for her valuable suggestion to improve the paper.

References

[1] J. Yang, J.-M. Qu, H. Summah, J. Zhang, Y.-G. Zhu, and H.-N. Jiang, "Protective effects of imipramine in murine endotoxin-induced acute lung injury," *European Journal of Pharmacology*, vol. 638, no. 1-3, pp. 128–133, 2010.

[2] H.-Q. Zhang, H.-D. Wang, D.-X. Lu et al., "Berberine inhibits cytosolic phospholipase A2 and protects against LPS-induced lung injury and lethality independent of the α2-adrenergic receptor in mice," *Shock*, vol. 29, no. 5, pp. 617–622, 2008.

[3] M. A. Flierl, D. Rittirsch, J. Vidya Sarma, M. Huber-Lang, and P. A. Ward, "Adrenergic regulation of complement-induced acute lung injury," *Advances in Experimental Medicine and Biology*, vol. 632, pp. 93–103, 2008.

[4] K. Takahashi, D. Saha, I. Shattino et al., "Complement 3 is involved with ventilator-induced lung injury," *International Immunopharmacology*, vol. 11, no. 12, pp. 2138–2143, 2011.

[5] M. Bosmann and P. A. Ward, "Role of C3, C5 and anaphylatoxin receptors in acute lung injury and in sepsis," *Advances in Experimental Medicine and Biology*, vol. 946, pp. 147–159, 2012.

[6] M. Zambon and J.-L. Vincent, "Mortality rates for patients with acute lung injury/ARDS have decreased over time," *Chest*, vol. 133, no. 5, pp. 1120–1127, 2008.

[7] T. T. Cui, L. J. Zhao, Y. Liu, and W. Jiang, "Toxicological studies on *Rabdosia japonica* var. *glaucocalyx*," *Guide of China Medicine*, vol. 8, no. 19, pp. 246–249, 2010.

[8] Z. K. Yan and W. L. Li, *China Changbai Mountain Medicinal Plant Colour Atlas*, 1997.

[9] L.-D. Liu, L.-K. Ye, D.-J. Pan, Y.-D. Jiang, T.-Z. Zhang, and H. Yang, "Effects of varglaucocalyx on c-fos gene expression during global myocardial ischemia-reperfusion in rat," *China Journal of Chinese Materia Medica*, vol. 28, no. 4, pp. 358–361, 2003.

[10] Z. M. Jin, W. Sha, and X. Y. Hu, "Study on bacteriostasis of the extracts of *Isodon japonica* (Burm. f.) Hara var. *glaucocalyx* (Maxim.) Hara," *Guangxi Sciences*, vol. 14, no. 2, pp. 160–162, 2007.

[11] J. Zhang, B. Wang, and N. Zhang, "Study on flavonoids from *Rabdosia japonica*," *Chinese Traditional and Herbal Drugs*, vol. 37, no. 8, pp. 1142–1144, 2006.

[12] X. D. Shen, B. Wang, C. Y. Liu, and J. Zhang, "Study on chemical constituents from *Rabdosia japonica* I," *Chinese Traditional and Herbal Drugs*, vol. 40, no. 12, pp. 35–37, 2009.

[13] S. Yao, N.-Y. Xu, C.-J. Chu, J. Zhang, and D.-F. Chen, "Chemical constituents of *Rabdosia japonica* var. *glaucocalyx* and their anti-complementary activity," *China Journal of Chinese Materia Medica*, vol. 38, no. 2, pp. 199–203, 2013.

[14] M. M. Mayer, "Complement and complement fixation," in *Experimental Immunochemistry*, E. A. Kabat and M. M. Mayer, Eds., pp. 133–240, Springfield Publications, 1961.

[15] Y. Wang, Y. Y. Xie, J. H. Sun, R. J. Wang, and D. Yuan, "Quantitative determination of the total flavonoids andorganicacids of *Chrysanthemum morifolium* extract," *Journal of Shenyang Pharmaceutical University*, vol. 28, no. 2, pp. 124–129, 2011.

[16] L. Liu, H. Xiong, J. Ping, Y. Ju, and X. Zhang Xuemei, "*Taraxacum officinale* protects against lipopolysaccharide-induced acute lung injury in mice," *Journal of Ethnopharmacology*, vol. 130, no. 2, pp. 392–397, 2010.

[17] C. W. Han, M. J. Kwun, K. H. Kim et al., "Ethanol extract of *Alismatis Rhizoma* reduces acute lung inflammation by suppressing NF-κB and activating Nrf2," *Journal of Ethnopharmacology*, vol. 146, no. 1, pp. 402–410, 2013.

[18] J. Saluk-Juszczak and B. Wachowicz, "The proinflammatory activity of lipopolysaccharide," *Postepy Biochemii*, vol. 51, no. 3, pp. 280–287, 2005.

[19] B. Pulendran, P. Kumar, C. W. Cutler, M. Mohamadzadeh, T. Van Dyke, and J. Banchereau, "Lipopolysaccharides from distinct pathogens induce different classes of immune responses *in vivo*," *Journal of Immunology*, vol. 167, no. 9, pp. 5067–5076, 2001.

[20] Y. Wu, M. Singer, F. Thouron, M. Alaoui-El-Azher, and L. Touqui, "Effect of surfactant on pulmonary expression of type IIA PLA2 in an animal model of acute lung injury," *The American Journal of Physiology—Lung Cellular and Molecular Physiology*, vol. 282, no. 4, pp. L743–L750, 2002.

[21] J.-Y. Xie, H.-Y. Di, H. Li, X.-Q. Cheng, Y.-Y. Zhang, and D.-F. Chen, "*Bupleurum chinense* DC polysaccharides attenuates lipopolysaccharide-induced acute lung injury in mice," *Phytomedicine*, vol. 19, no. 2, pp. 130–137, 2012.

[22] G. Chi, M. Wei, X. Xie, L. W. Soromou, F. Liu, and S. Zhao, "Suppression of MAPK and NF-κB pathways by limonene contributes to attenuation of lipopolysaccharide-induced inflammatory responses in acute lung injury," *Inflammation*, vol. 36, no. 2, pp. 501–511, 2013.

[23] P. von Bismarck, K. Klemm, C.-F. García Wistädt, S. Winoto-Morbach, S. Schütze, and M. F. Krause, "Selective NF-κB inhibition, but not dexamethasone, decreases acute lung injury in a newborn piglet airway inflammation model," *Pulmonary Pharmacology and Therapeutics*, vol. 22, no. 4, pp. 297–304, 2009.

[24] G. Umberto Meduri, E. A. Tolley, G. P. Chrousos, and F. Stentz, "Prolonged methylprednisolone treatment suppresses systemic inflammation in patients with unresolving acute respiratory distress syndrome: evidence for inadequate endogenous glucocorticoid secretion and inflammation-induced immune cell resistance to glucocorticoids," *The American Journal of Respiratory and Critical Care Medicine*, vol. 165, no. 7, pp. 983–991, 2002.

[25] G. Kalyan Kumar, R. Dhamotharan, N. M. Kulkarni, M. Y. A. Mahat, J. Gunasekaran, and M. Ashfaque, "Embelin reduces cutaneous TNF-α level and ameliorates skin edema in acute and chronic model of skin inflammation in mice," *European Journal of Pharmacology*, vol. 662, no. 1–3, pp. 63–69, 2011.

[26] K. Tureyen, K. Bowen, J. Liang, R. J. Dempsey, and R. Vemuganti, "Exacerbated brain damage, edema and inflammation in type-2 diabetic mice subjected to focal ischemia," *Journal of Neurochemistry*, vol. 116, no. 4, pp. 499–507, 2011.

[27] B. D. Beck, J. D. Brain, and D. E. Bohannon, "An *in vivo* hamster bioassay to assess the toxicity of particulates for the lungs," *Toxicology and Applied Pharmacology*, vol. 66, no. 1, pp. 9–29, 1982.

[28] L. J. Huffman, D. J. Prugh, L. Millecchia, K. C. Schuller, S. Cantrell, and D. W. Porter, "Nitric oxide production by rat bronchoalveolar macrophages or polymorphonuclear leukocytes following intratracheal instillation of lipopolysaccharide or silica," *Journal of Biosciences*, vol. 28, no. 1, pp. 29–37, 2003.

[29] H. M. Razavi, F. W. Le, S. Weicker et al., "Pulmonary neutrophil infiltration in murine sepsis: role of inducible nitric oxide synthase," *The American Journal of Respiratory and Critical Care Medicine*, vol. 170, no. 3, pp. 227–233, 2004.

[30] S. J. Klebanoff, "Myeloperoxidase: friend and foe," *Journal of Leukocyte Biology*, vol. 77, no. 5, pp. 598–625, 2005.

[31] P. V. Antwerpen, F. Dufrasne, M. Lequeux et al., "Inhibition of the myeloperoxidase chlorinating activity by non-steroidal anti-inflammatory drugs: flufenamic acid and its 5-chloro-derivative directly interact with a recombinant human myeloperoxidase to inhibit the synthesis of hypochlorous acid," *European Journal of Pharmacology*, vol. 570, no. 1–3, pp. 235–243, 2007.

[32] H. Macarthur, T. C. Westfall, D. P. Riley, T. P. Misko, and D. Salvemini, "Inactivation of catecholamines by superoxide gives new insights on the pathogenesis of septic shock," *Proceedings of the National Academy of Sciences of the United States of America*, vol. 97, no. 17, pp. 9753–9758, 2000.

[33] J. Guan, D.-D. Jin, L.-J. Jin, and Q. Lu, "Apoptosis in organs of rats in early stage after polytrauma combined with shock," *Journal of Trauma—Injury, Infection and Critical Care*, vol. 52, no. 1, pp. 104–111, 2002.

[34] C. D. Yeo, C. K. Rhee, I. K. Kim et al., "Protective effect of pravastatin on lipopolysaccharide-induced acute lung injury during neutropenia recovery in mice," *Experimental Lung Research*, vol. 39, no. 2, pp. 99–106, 2013.

[35] I. A. J. Giebelen, D. J. Van Westerloo, G. J. LaRosa, A. F. De Vos, and T. Van Der Poll, "Local stimulation of α7 cholinergic receptors inhibits LPS-induced TNF-α release in the mouse lung," *Shock*, vol. 28, no. 6, pp. 700–703, 2007.

[36] T. Minamino and I. Komuro, "Regeneration of the endothelium as a novel therapeutic strategy for acute lung injury," *Journal of Clinical Investigation*, vol. 116, no. 9, pp. 2316–2319, 2006.

[37] T. Lawrence and C. Fong, "The resolution of inflammation: anti-inflammatory roles for NF-κB," *International Journal of Biochemistry and Cell Biology*, vol. 42, no. 4, pp. 519–523, 2010.

[38] M. Terblanche, Y. Almog, R. S. Rosenson, T. S. Smith, and D. G. Hackam, "Statins and sepsis: multiple modifications at multiple levels," *Lancet Infectious Diseases*, vol. 7, no. 5, pp. 358–368, 2007.

[39] J. Chen, J.-B. Wang, C.-H. Yu, L.-Q. Chen, P. Xu, and W.-Y. Yu, "Total flavonoids of *Mosla scabra* leaves attenuates lipopolysaccharide-induced acute lung injury via down-regulation of inflammatory signaling in mice," *Journal of Ethnopharmacology*, vol. 148, no. 3, pp. 835–841, 2013.

[40] Y.-C. Li, C.-H. Yeh, M.-L. Yang, and Y.-H. Kuan, "Luteolin suppresses inflammatory mediator expression by blocking the Akt/NFκB pathway in acute lung injury induced by lipopolysaccharide in mice," *Evidence-Based Complementary and Alternative Medicine*, vol. 2012, Article ID 383608, 8 pages, 2012.

[41] M.-Y. Kuo, M.-F. Liao, F.-L. Chen et al., "Luteolin attenuates the pulmonary inflammatory response involves abilities of antioxidation and inhibition of MAPK and NFκB pathways in mice with endotoxin-induced acute lung injury," *Food and Chemical Toxicology*, vol. 49, no. 10, pp. 2660–2666, 2011.

[42] S. Thiel, T. Vorup-Jensen, C. M. Stover et al., "A second serine protease associated with mannan-binding lectin that activates complement," *Nature*, vol. 386, no. 6624, pp. 506–510, 1997.

[43] S. C. Makrides, "Therapeutic inhibition of the complement system," *Pharmacological Reviews*, vol. 50, no. 1, pp. 59–87, 1998.

[44] R. Yanai, A. Thanos, and K. M. Connor, "Complement involvement in neovascular ocular diseases," *Advances in Experimental Medicine and Biology*, vol. 946, pp. 161–183, 2012.

Hindawi Publishing Corporation
Evidence-Based Complementary and Alternative Medicine
Volume 2014, Article ID 369204, 32 pages
http://dx.doi.org/10.1155/2014/369204

Review Article

Jatropha gossypiifolia L. (Euphorbiaceae): A Review of Traditional Uses, Phytochemistry, Pharmacology, and Toxicology of This Medicinal Plant

Juliana Félix-Silva,[1] Raquel Brandt Giordani,[2] Arnóbio Antonio da Silva-Jr,[1] Silvana Maria Zucolotto,[2] and Matheus de Freitas Fernandes-Pedrosa[1]

[1] *Laboratório de Tecnologia & Biotecnologia Farmacêutica (TecBioFar), Programa de Pós-graduação em Ciências Farmacêuticas (PPgCF), Universidade Federal do Rio Grande do Norte (UFRN), Rua General Cordeiro de Farias, s/n, Petrópolis, 59012-570 Natal, RN, Brazil*
[2] *Laboratório de Farmacognosia, Departamento de Farmácia, Universidade Federal do Rio Grande do Norte (UFRN), Rua General Cordeiro de Farias, s/n, Petrópolis, 59012-570 Natal, RN, Brazil*

Correspondence should be addressed to Matheus de Freitas Fernandes-Pedrosa; mpedrosa31@uol.com.br

Received 24 February 2014; Revised 1 May 2014; Accepted 1 May 2014; Published 5 June 2014

Academic Editor: Shi-Biao Wu

Jatropha gossypiifolia L. (Euphorbiaceae), widely known as "*bellyache bush,*" is a medicinal plant largely used throughout Africa and America. Several human and veterinary uses in traditional medicine are described for different parts and preparations based on this plant. However, critical reviews discussing emphatically its medicinal value are missing. This review aims to provide an up-to-date overview of the traditional uses, as well as the phytochemistry, pharmacology, and toxicity data of *J. gossypiifolia* species, in view of discussing its medicinal value and potential application in complementary and alternative medicine. Pharmacological studies have demonstrated significant action of different extracts and/or isolated compounds as antimicrobial, anti-inflammatory, antidiarrheal, antihypertensive, and anticancer agents, among others, supporting some of its popular uses. No clinical trial has been detected to date. Further studies are necessary to assay important folk uses, as well as to find new bioactive molecules with pharmacological relevance based on the popular claims. Toxicological studies associated with phytochemical analysis are important to understand the eventual toxic effects that could reduce its medicinal value. The present review provides insights for future research aiming for both ethnopharmacological validation of its popular use and its exploration as a new source of herbal drugs and/or bioactive natural products.

1. Introduction

The Euphorbiaceae family, which is considered one of the largest families of Angiosperms, covers about 7,800 species distributed in approximately 300 genera and 5 subfamilies worldwide. These species occur preferentially in tropical and subtropical environments [1, 2].

Among the main genera belonging to this family, there is *Jatropha* L., which belongs to the subfamily Crotonoideae, Jatropheae tribe and is represented by about 200 species. This genus is widely distributed in tropical and subtropical regions of Africa and the Americas [1]. The name "*Jatropha*" is derived from the Greek words "*jatros,*" which means "doctor" and "*trophe,*" meaning "food," which is associated with its medicinal uses [3]. The *Jatropha* genus is divided into two subgenera, *Jatropha* and *curcas,* from which the subgenus *Jatropha* has the widest distribution, with species found in Africa, India, South America, West Indies, Central America, and the Caribbean [4]. *Jatropha* species are used in traditional medicine to cure various ailments in Africa, Asia, and Latin America or as ornamental plants and energy crops [3]. Several known species from genus *Jatropha* have been reported for their medicinal uses, chemical constituents, and biological activities such as *Jatropha curcas*, *Jatropha elliptica*,

Jatropha gossypiifolia, and *Jatropha mollissima*, among others [3].

From these species, *Jatropha gossypiifolia* L. (Figure 1) is discussed here. It is a vegetal species widely known as "*bellyache bush*" and is a multipurpose medicinal plant largely used in folk medicine for the treatment of various diseases [3, 5, 6]. It is widely distributed in countries of tropical, subtropical, and dry tropical weather and tropical semiarid regions of Africa and the Americas [7]. In Brazil, it predominates in the Amazon, Caatinga, and Atlantic Forest and is distributed throughout the country in the North, Northeast, Midwest, South, and Southeast regions [8].

Several human and veterinary uses in traditional medicine are described for different parts (leaves, stems, roots, seeds, and latex) and preparations (infusion, decoction, and maceration, among others) based on this plant, by different routes (oral or topical). The most frequent reports concern its antihypertensive, anti-inflammatory, antiophidian, analgesic, antipyretic, antimicrobial, healing, antianemic, antidiabetic, and antihemorrhagic activities, among many other examples [3, 5, 7, 9]. Other uses are also related to this plant, such as biodiesel production, pesticide, insecticide, vermifuge, ornamentation, and even its use in religious rituals [3, 6, 10–13].

An important feature of *J. gossypiifolia* species is that, due to its important potential medicinal applications, in Brazil, it is included in the National List of Medicinal Plants of Interest to the Brazilian Public Health System (*Relação Nacional de Plantas Medicinais de Interesse ao Sistema Único de Saúde Brasileiro—RENISUS*), which is a report published by the Brazilian Health Ministry in February 2009 that includes 71 species of medicinal plants that have the potential to generate pharmaceutical products of interest to public health of Brazil [14].

Regarding its phytochemical constitution, alkaloids, coumarins, flavonoids, lignoids, phenols, saponins, steroids, tannins, and terpenoids were already detected in different extracts from different parts of this plant [15].

Among the main activities already studied for this species (including various types of extracts from different parts of the plant), the antihypertensive, antimicrobial, anti-inflammatory, antioxidant, and antineoplasic activities mainly stand out, supporting some of its popular uses [3, 16].

Some toxicity studies have shown that despite the known toxicity of *Jatropha* species, *J. gossypiifolia* presented low toxicity in some *in vitro* and *in vivo* experiments. However, some studies have indicated that ethanolic extract from the leaves, in acute oral use, is safe for rats, but with chronic use, it could be toxic [17–19].

So, in view of the potential applications of this plant, this review aims to provide an up-to-date overview of the traditional uses, phytochemistry, pharmacology, and toxicity data of different parts from *J. gossypiifolia*, which could be significant in providing insights for present and future research aimed at both ethnopharmacological validation of its popular use, as well as its exploration as a new source of herbal drugs and/or bioactive natural products. The medicinal value and pharmacological and/or biotechnological potential of this species are also discussed in this paper.

2. Methodology

An extensive review of the literature was undertaken in different national and international scientific sources, such as Centre for Reviews and Dissemination (http://www.crd.york.ac.uk/CRDWeb/), The Cochrane Library (http://www.thecochranelibrary.com), PubMed (http://www.ncbi.nlm.nih.gov/pubmed/), Science Direct (http://www.sciencedirect.com/), Scopus (http://www.scopus.com/), Lilacs (http://lilacs.bvsalud.org/), Scielo (http://www.scielo.org/php/index.php), Web of Knowledge (http://apps.webofknowledge.com), and the Brazilian database of thesis and dissertations "Domínio Público" (http://www.dominiopublico.gov.br/pesquisa/PesquisaPeriodicoForm.jsp). The study database included original articles, theses, books, and other reports that preferentially had been judged for academic quality (peer-reviewed), covering several aspects of the vegetal species (botany, phytochemistry, traditional uses, pharmacology, or toxicology), dating from 1967 (first scientific report) to November 2013, without language restriction. The search strategy was constructed based on the scientific name, synonyms, and main popular names of the species identified by the botanical databases "Flora do Brasil" (http://floradobrasil.jbrj.gov.br), Tropicos (http://www.tropicos.org), The Plant List (http://www.theplantlist.org), and NCBI Taxonomy Browser (http://www.ncbi.nlm.nih.gov/taxonomy). The search strategy contained the combination of the following terms: "*Jatropha gossypiifolia*" OR "*Jatropha gossypifolia*" OR "*Jatropha gossipyifolia*" OR "*Manihot gossypiifolia*" OR "*Adenoropium gossypiifolium*" OR "*Adenoropium elegans*" OR "*Jatropha elegans*" OR "*Jatropha staphysagriifolia*" OR *"pinhão roxo"* OR *"pinhão-roxo"* OR *"pião roxo"* OR *"pião-roxo"* OR *"peão-roxo"* OR *"peão roxo"* OR *"batata-de-teu"* OR *"bata de teu"* OR *"erva-purgante"* OR *"erva purgante"* OR *"jalapão"* OR *"mamoninha"* OR *"raiz-de-teiú"* OR *"raiz de teiú"* OR *"peão-curador"* OR *"peão curador"* OR *"peão-pajé"* OR *"peão pajé"* OR *"pião-caboclo"* OR *"pião caboclo"* OR *"black physicnut"* OR *"bellyache bush"*. The Endnote X.3.0.1 reference manager was used. The software ACD/ChemSketch Freeware Version 12.01 was used to draw the chemical structures.

3. Botanic Information

Jatropha gossypiifolia Linneus is a Euphorbiaceae plant popularly known worldwide as *"bellyache bush"* or *"black physicnut"*. It is a pantropical species originating from South America that is cultivated in tropical countries throughout the world [20–22].

In Brazil, it is known by various popular names and the most common are "*pinhão-roxo,*" "*pião-roxo,*" "*peão-roxo,*" "*batata-de-teu,*" "*erva-purgante,*" "*jalapão,*" "*mamoninha,*" "*raiz-de-teiú,*" "*peão-curador,*" "*peão-pajé,*" "*pião-caboclo,*" and "*pião-preto,*" among others [5, 8, 23]. There are also the following vernacular names for *J. gossypiifolia*: "*frailecillo,*" "*frailejón,*" "*purga de fraile*" (Colômbia); "*frailecillo*" (Costa Rica); "*frailecillo,*" "*San Juan Del Cabre,*" "*túatúa,*" "*tuba tuba*" (Cuba); "*baga*" (Malinké et Dioula); "*higuereta cimarrona,*" "*túatúa*" (Puerto Rico); "*túatúa*" (Santo

(a) (b)

Figure 1: *Jatropha gossypiifolia* L. (a) aerial parts of plant. (b) flowers detail. Photography by Juliana Félix-Silva.

Domingo); "*frailecillo,*" "*sibidigua,*" "*tuatuá*" (Venezuela); "*pignut,*" "*fignut,*" "*lapalapa,*" "*binidasugu,*" "*oluluidi,*" "*botuje red,*" "*botuge pupa*" (Nigeria); "*athalai,*" "*lal bherenda*" (India); "*parroty grass*" (Nicaragua); "*babatidjin*" (Africa); "*piñón,*" "*piñon-colorado,*" "*piñón negro,*" "*piñon-rojo,*" "*purga de huane*" (Spanish); "*herbe à mal de ventre,*" "*medicinier cathartique,*" "*medicinier sauvage*" (French); "*bellyachebuhs,*" "*bellyache bush,*" "*bellyache nettlespurge,*" "*black physicnut,*" "*purge nut,*" "*red fig-nut flower,*" "*wild cassada*" (English); "*babatidjin,*" "*balautandoiong,*" "*cassava marble,*" "*cotton-leaf physicnut,*" "*figus nut,*" "*kishka,*" "*lansi-lansinaan,*" "*médicinier bâtard,*" "*médicinier noir,*" "*médicinier rouge,*" "*quelite de fraile,*" "*sosori,*" "*tagumbau-a-nalabaga,*" "*tatua,*" "*tauataua,*" "*tautuba,*" "*tuatúa blanca,*" "*tuatúa morada,*" "*tubang morado,*" "*tuba sa buaia,*" "*tuba-tuba*" (Achanti); "*satamân*" (Bambara) [22, 24–31].

The complete taxonomy of the species is Eukaryota; Viridiplantae; Streptophyta; Streptophytina; Embryophyta; Tracheophyta; Euphyllophyta; Spermatophyta; Magnoliophyta; eudicotyledons; core eudicotyledons; rosids; fabids; Malpighiales; Euphorbiaceae; Crotonoideae; Jatropheae; *Jatropha;* and *Jatropha gossypiifolia* [32]. *Adenoropium gossypiifolium* (L.) Pohl, *Manihot gossypiifolia* (L.) Crantz, *Adenoropium elegans* Pohl, *Jatropha elegans* Kl., *Jatropha staphysagriifolia* Mill., *Jatropha gossypifolia,* and *Jatropha gossipyifolia* are botanical synonymous of *J. gossypiifolia* species [8, 32–34].

J. gossypiifolia is a small shrub with dark green or more frequently purplish-red dark leaves, with 16–19 cm of length per 10–12.9 cm of width; they are alternate, palmate, and pubescent, with an acuminate apex, cordate base, and serrated margin. The flowers are unisexual, purple, and in cymose summits, with the calyx having five petals, which in male flowers may form a petaloid tube. The fruit is capsular, with three furrows, containing a dark seed with black spots [5, 35, 36]. Regarding the microscopic aspect of the plant leaves, some studies have shown key and important features for botanical identification of this species among other *Jatropha* species [21, 35–37].

4. Chemical Constituents

Various chemical constituents have been detected in extracts from different parts of *J. gossypiifolia*, the literature having reported, in general, the presence of fatty acids, sugars, alkaloids, amino acids, coumarins, steroids, flavonoids, lignans, proteins, saponins, tannins, and terpenoids, as can be seen in Table 1.

Accordingly reviewed by Zhang et al. [15], the main compounds isolated from *Jatropha* genus are the terpenoids. In fact, many of them were isolated from different parts of *J. gossypiifolia*. Another very important class from *J. gossypiifolia* is the lignoids, since a good number of them was already isolated and identified.

However, it is important to note that most of the phytochemical studies found in literature are not about isolation of compounds, but only about the phytochemical screening of the major classes through chemical qualitative reactions or more sensitive and specific methods such as thin layer chromatography (TLC). Relative to other *Jatropha* species, few studies have isolated chemical compounds from *J. gossypiifolia* (Table 2). In addition, up till now it is not clear which are the major bioactive compounds in the plant, since only a few studies were conducted by bioassay-guided isolation.

Additionally, to the best of our knowledge, there are no phytochemical studies regarding the use of water as solvent for the extraction of *J. gossypiifolia* constituents. This is important to note since popular use occurs more frequently with infusions or decoctions, and little is known about the constitution of this type of extract. In this context, it is important to conduct studies to evaluate the phytochemical constitution of these extracts. More commonly, the studies use solvents or mixtures of solvents with nonpolar characteristics, which could contribute to further characterization of nonpolar compounds, such as terpenoids and lignoids. Polar compounds such as flavonoids, tannins, and sugars are poorly described in the species so far, probably due to this fact.

5. Traditional Uses

Various medicinal properties for the species *J. gossypiifolia* are reported by traditional medicine, as shown in Table 3. Some properties related to *J. gossypiifolia* are also common to other species of the *Jatropha* genus [3, 9, 25], where human and veterinary uses are described. Different parts of this plant, such as leaves, stems, roots, seeds, and latex, are used

Table 1: Chemical constituents of *Jatropha gossypiifolia* L. described in the literature.

Plant part	Classification	Compound	Extract type and/or preparation	Reference
Whole plant	Coumarin-lignoids	Propacin	Isolated from dichloromethane : methanol (1 : 1, v/v) extract after successive column chromatography on silica gel	[38]
		Venkatasin	Not specified*	[39]
	Diterpenes	Citlalitrione	Isolated from dichloromethane : methanol (1 : 1, v/v) extract after successive column chromatography on silica gel	[40]
		Jatrophenone	Isolated from dichloromethane : methanol (1 : 1, v/v) extract after successive column chromatography on silica gel	[41]
Stem, roots, and seeds	Coumarin-lignoids	Arylnaphthalene lignan	Isolated from petrol ether extract after successive column chromatography on silica gel	[42]
		Gadain	Isolated from petrol ether extract after successive column chromatography on silica gel	[43]
		Jatrophan	Isolated from petrol ether extract	[44]
Aerial parts	Flavonoids	—	Detected by phytochemical screening reactions of ethanol extract	[19, 45]
	Lignans	Gossypifan	Isolated from petrol ether extract after successive column chromatography on silica gel	[46]
		Gossypiline	Isolated from dichloromethane : methanol (1 : 1, v/v) extract after successive column chromatography on silica gel	[47]
	Phenols	—	Quantitative analysis showed that the petrol ether, chloroform, ethyl acetate, and *n*-butanol extracts presented, respectively, 45.0 ± 1.0, 106.0 ± 2.3, 296.0 ± 3.5, and 128.5 ± 1.1 mg of gallic acid equivalents/g of crude extract	[48]
	Steroids	—	Detected by phytochemical screening reactions of ethanol extract	[19, 45]
	Tannins	—	Detected by phytochemical screening reactions of ethanol extract	[23, 45]
	Triterpenoids	—	Detected by phytochemical screening reactions of ethanol extract	[45]
Leaves	Alkaloids	Ricinine	Compound isolated from ethyl acetate extract from senescent leaves	[49]
		—	Detected by phytochemical screening reactions of chloroform and methanol extracts	[50]
		—	Quantitative analysis showed 2.81% on leaves	[51]
		—	Not specified	[30]
	Cardiac glycosides	—	Identified on leaves by qualitative phytochemical screening reactions	[52]
	Flavonoids	Apigenin	Identified in ether fraction from ethanol extract	[53]
		Isovitexin	Identified in ethyl acetate and methyl ethyl ketone fractions from ethanol extract	[53]
		Orientin/isoorientin	Isomers identified in different types of extracts from leaves	[54]
		Schaftoside/isoschaftoside	Isomers identified in different types of extracts from leaves	[54]
		Vitexin	Identified in ethyl acetate fraction from ethanol extract	[53]
		Vitexin/isovitexin	Isomers identified in different types of extracts from leaves	[54]
		—	Identified on leaves by qualitative phytochemical screening reactions	[52]
		—	Quantitative analysis showed 7.4% on leaves	[55]
		—	Quantitative analysis showed 2.41% on leaves	[51]
	Phenols	—	Quantitative analysis showed 8.6% on leaves	[55]
		—	Quantitative analysis showed 0.26% on leaves	[51]
	Phlobotannins	—	Detected by phytochemical screening reactions of chloroform and methanol extracts	[50]
		—	Identified on leaves by qualitative phytochemical screening reactions	[52]
	Proteins	—	Leaves obtained by micropropagation were macerated in liquid nitrogen and extracted at 4°C for 6 h with 0.1 M NaCl. The material was centrifuged and the limpid supernatant was dialyzed against water at low temperature in a cellulose membrane to remove nonprotein compound with molecular mass below 3.5 kDa	[56]

Table 1: Continued.

Plant part	Classification	Compound	Extract type and/or preparation	Reference
	Reducing sugars	—	Identified on leaves by qualitative phytochemical screening reactions	[52]
	Saponins	—	Identified on leaves by qualitative phytochemical screening reactions	[52]
		—	Quantitative analysis showed 4.15% on leaves	[51]
	Steroids	—	Identified on leaves by qualitative phytochemical screening reactions	[52]
	Tannins	—	Detected by phytochemical screening reactions of methanol extract	[50]
		—	Detected on leaves by qualitative phytochemical screening reactions	[52]
		—	Quantitative analysis showed 5.14% on leaves	[51]
	Terpenoids	—	Detected on leaves by qualitative phytochemical screening reactions	[52]
	Triterpenes	(2α, 13α, 14β, 20S)-2,24,25-Trihydroxylanost-7-en-3-one	Isolated from the ethanol extract after successive partitions procedures and column chromatography on silica gel and preparative TLC	[57]
		(13α, 14β, 20S)-2,24,25-Trihydroxylanosta-1,7-dien-3-one	Isolated from the ethanol extract after successive partition procedures and column chromatography on silica gel and preparative TLC	[57]
Stems	Alkaloids	—	Quantitative analysis showed 2.16% of alkaloid on stems	[51]
	Coumarin-lignoids	4′-*O*-Demethyl retrochinensin	Not specified	[58]
		Cleomiscosin A	Compound isolated from ethyl acetate fraction stems after successive column chromatography on silica gel	[59]
		Gossypidien	Compound isolated from hexane extract from dried stems after successive column chromatography on silica gel	[60]
		Isogadain	Not specified*	[61]
		Jatrodien	Compound isolated from petrol ether extract after successive column chromatography on silica gel	[62]
		Prasanthaline	Not specified*	[63]
	Flavonoids	—	Quantitative analysis showed 1.2% on stems	[51]
	Phenols	—	Quantitative analysis showed 0.13% on stems	[51]
	Saponins	—	Quantitative analysis showed 2.18% on stems	[51]
	Tannins	—	Quantitative analysis showed 1.36% on stems	[51]
Roots	Alkaloids	—	Quantitative analysis showed 1.6% on roots	[51]
	Diterpenes	2α-Hydroxyjatrophone	Isolated from petrol ether extract after successive column chromatography on silica gel	[64]
		2β-Hydroxy-5,6-isojatrophone	Isolated from petrol ether extract after successive column chromatography on silica gel	[64]
		2β-Hydroxyjatrophone	Isolated from petrol ether extract after successive column chromatography on silica gel	[64]
		Citlalitrione	Isolated from petrol ether fraction from the methanol extract after successive column chromatography on silica gel	[13]
		Falodone	Isolated from petrol ether fraction from the methanol extract after successive column chromatography on silica gel	[13]
		Jatropholone A	Not specified*	[65]
		Jatropholone B	Not specified*	[65]
		Jatrophone	Isolated from ethanol extract	[66]
	Flavonoids	—	Quantitative analysis showed 1.75% on roots	[51]
	Phenols	—	Quantitative analysis showed 0.24% on roots	[51]
	Saponins	—	Quantitative analysis showed 2.83% on roots	[51]
	Tannins	—	Quantitative analysis showed 2.73% on roots	[51]

Table 1: Continued.

Plant part	Classification	Compound	Extract type and/or preparation	Reference
Seeds	Alkaloids	—	Quantitative analysis showed 2.36% on seeds	[51]
	Amino acids	—	Not specified*	[67]
	Carbohydrates	—	Quantitative analysis showed 30.32% on seeds	[68]
		—	Not specified*	[67]
	Esters	12-Deoxy-16-hydroxylphorbol	Isolated from hydrophilic fraction from the ether extract, by countercurrent chromatography	[69]
	Fatty acids	Arachidic acid	Identified in petrol ether extract	[68, 70]
		Caprilic acid	Identified in petrol ether extract	[68, 70]
		Lauric acid	Identified in petrol ether extract	[68, 70]
		Lignoceric acid	Identified in petrol ether extract	[68, 70]
		Linoleic acid	Identified in petrol ether extract	[68, 70]
		Myristic acid	Identified in petrol ether extract	[68, 70]
		Oleic acid	Identified in petrol ether extract	[68, 70]
		Palmitic acid	Identified in petrol ether extract	[68, 70]
		Palmitoleic acid	Identified in petrol ether extract	[68, 70]
		Ricinoleic acid	Identified in petrol ether extract	[68, 70]
		Stearic acid	Identified in petrol ether extract	[68, 70]
		Vernolic acid	Identified in petrol ether extract	[68, 70]
	Fibers	—	Quantitative analysis showed 9.25% on seeds	[68]
	Flavonoids	—	Quantitative analysis showed 2.26% on seeds	[51]
	Phenols	—	Quantitative analysis showed 0.18% on seeds	[51]
	Proteins	—	Quantitative analysis showed 13.40% on seeds	[68]
	Saponins	—	Quantitative analysis showed 2.37 on seeds	[51]
		—	Quantitative analysis showed 6 g/kg on seeds	[68]
	Tannins	—	Quantitative analysis showed 3.52% on seeds	[51]
Latex	Proteins	Cyclogossine A	Not specified	[71]
		Cyclogossine B	Isolated from ethyl acetate extract by gel filtration column chromatography	[20]
Not specified	Alkaloids	Imidazole alkaloid	Isolated from the plant exudates*	[72]
		Piperidine	Isolated from the plant exudates*	[72]
	Diterpenoids	Abiodone	Not specified*	[73]

*The complete version of the paper was not accessible, so the information was obtained from its abstract.

Table 2: Main isolated compounds from *Jatropha gossypiifolia* L. described in the literature.

Classification	Compound	Plant part	Biological activity	Reference
Alkaloids	Ricinine 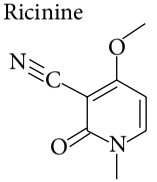	Leaves	Insecticide *in vitro*	[49]
	Imidazole alkaloid	Not specified	—	[72]
	Piperidine 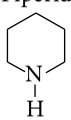	Not specified	—	[72]
	4′-*O*-demethyl retrochinensin	Stems	—	[58]
	Arylnaphthalene lignan 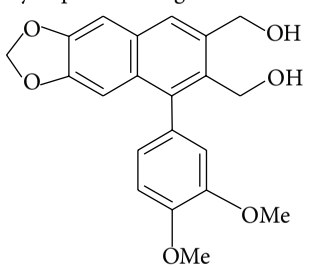	Stems, roots, and seeds	—	[42]
	Cleomiscosin A 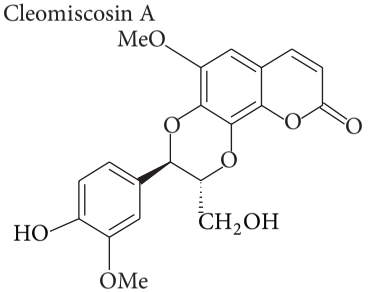	Stems	—	[59]

Table 2: Continued.

Classification	Compound	Plant part	Biological activity	Reference
Coumarin-lignoids	Gadain 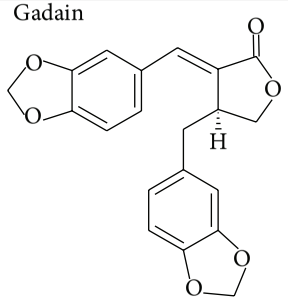	Stems, roots, and seeds	—	[43]
	Gossypidien 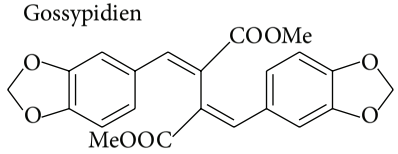	Stems	—	[60]
	Isogadain 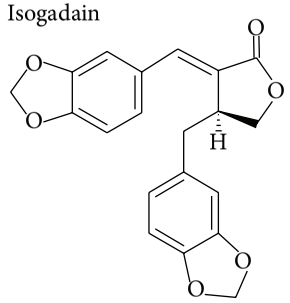	Stems	—	[61]
	Jatrodien 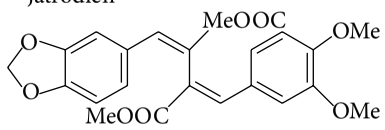	Stems	—	[62]

Table 2: Continued.

Classification	Compound	Plant part	Biological activity	Reference
	Jatrophan 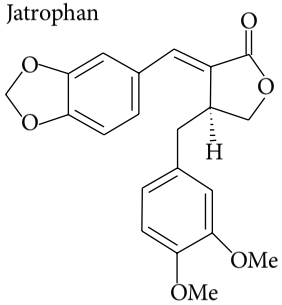	Stems, roots, and seeds	—	[44]
	Prasanthaline 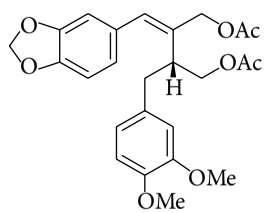	Stems	—	[63]
	Propacin 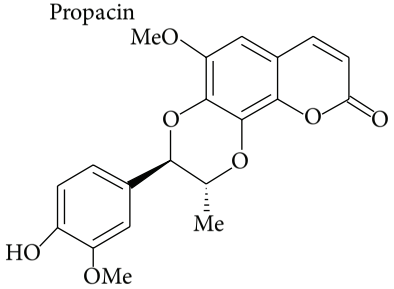	Whole plant	—	[38]
	Venkatasin	Whole plant	—	[39]
	2α-Hydroxyjatrophone 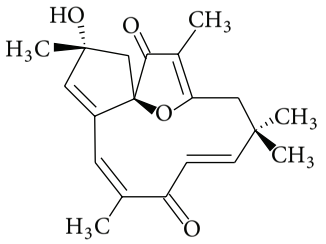	Roots	Antileukemic *in vitro* and *in vivo*	[64]

Table 2: Continued.

Classification	Compound	Plant part	Biological activity	Reference
Diterpenes	2β-Hydroxy-5, 6-isojatrophone 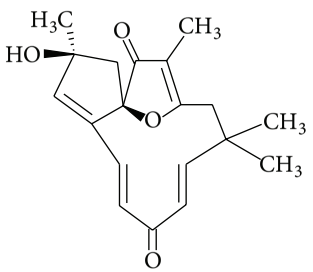	Roots	Antileukemic *in vitro* and *in vivo*	[64]
	2β-Hydroxyjatrophone 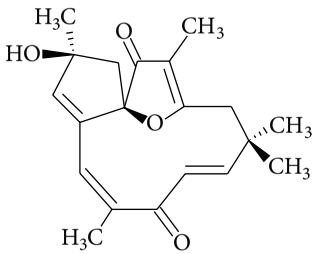	Roots	Antileukemic *in vitro* and *in vivo*	[64]
	Abiodone	Not specified	Anticancer *in vitro*	[73]
	Citlalitrione 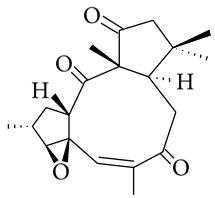	Roots	—	[13]
		Whole plant	—	[40]
	Falodone 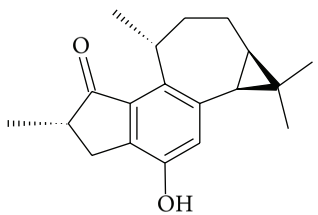	Roots	Anticancer *in vitro*	[13]

Table 2: Continued.

Classification	Compound	Plant part	Biological activity	Reference
	Jatrophenone 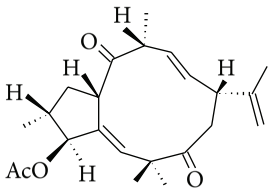	Whole plant	Antibacterial *in vitro*	[41]
	Jatropholone A 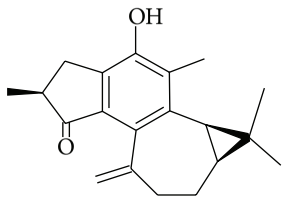	Roots	—	[65]
	Jatropholone B 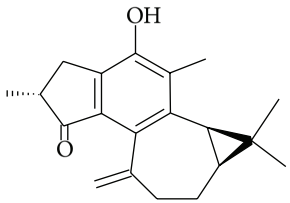	Roots	—	[65]
	Jatrophone 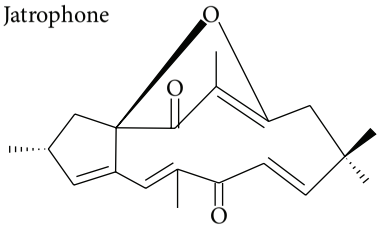	Roots	Anticancer *in vitro* and *in vivo*	[66]

Table 2: Continued.

Classification	Compound	Plant part	Biological activity	Reference
Esters	12-Deoxy-16-hydroxylphorbol 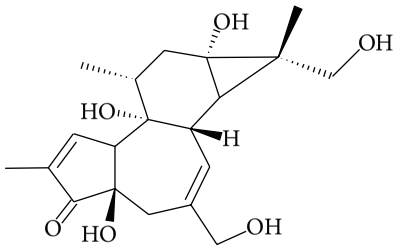	Seeds	Irritant to mouse ear	[69]
Lignans	Gossypifan 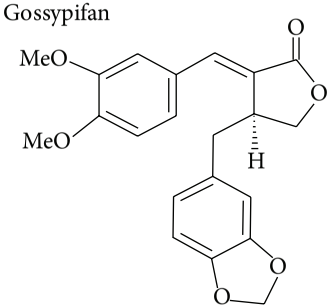	Aerial parts	—	[46]
	Gossypiline 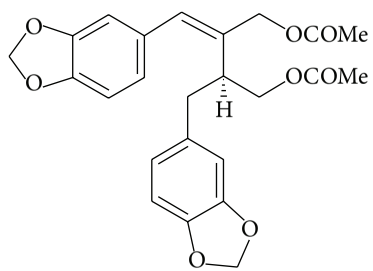	Aerial parts	—	[47]
Proteins	Cyclogossine A 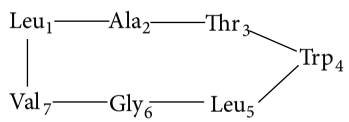	Latex	—	[15, 71]

Table 2: Continued.

Classification	Compound	Plant part	Biological activity	Reference
	Cyclogossine B 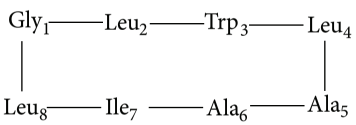 	Latex	—	[15, 20]
Triterpenes	(13α, 14β, 20S)-2,24,25-Trihydroxylanosta-1, 7-dien-3-one 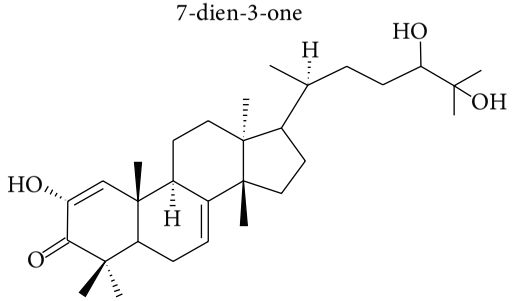 	Leaves	—	[57]
	(2α, 13α, 14β, 20S)-2,24,25-Trihydroxylanost-7-en-3-one 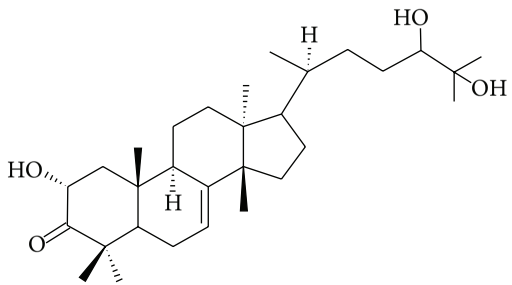 	Leaves	—	[57]

in different forms of preparation (infusion, decoction, and maceration, among others), by different routes and forms (oral, topical, baths, etc.). The most frequent reports refer to its anti-inflammatory, antidiarrheal, antiophidian, analgesic, antipyretic, antimicrobial, healing, antianemic, antidiabetic, and antihemorrhagic activities, among many other examples [3, 5, 7, 9].

Some properties are attributed to specific parts of the plant, while others are assigned to different parts. Interestingly, in some cases certain uses may appear contradictory, such as antidiarrheal and laxative or its use as anticoagulant and antihemorrhagic. One hypothesis is that this difference may be related with the dose used, since, for example, the laxative effect is an effect commonly related with toxic events with this plant.

6. Pharmacological Activities

Despite the grand variety of popular uses and the data from *Jatropha* species, *J. gossypiifolia* has been scarcely studied regarding biological activities (Table 4). Studies showing the biological potential of aqueous extract are rare so far, which is important to be mentioned since the most popular use of this plant is as a tea (decoction or infusion). Among the main activities that have been studied the antihypertensive, anticancer, antimicrobial, healing, anti-inflammatory, and analgesic activities stand out.

6.1. Antihypertensive Action. Based on popular use of teas from *J. gossypiifolia* roots and aerial parts, the hypotensive and vasorelaxant effects of the ethanolic extract of aerial parts of the plant were tested by Abreu et al. [45]. The study revealed that the extract (125 and 250 mg/kg/day, over 4 weeks, by oral route in rats), in a dose-dependent manner, produced a reduction of systolic blood pressure in conscious normotensive animals. This hypotensive effect could be attributed to its vasorelaxant action, since it produced concentration-dependent relaxant effect in rat isolated endothelium-deprived mesenteric artery precontracted with norepinephrine or calcium. Moreover, it inhibited, in a concentration-dependent and noncompetitive manner, the contractile response induced by norepinephrine or $CaCl_2$ in the same preparation [45].

6.2. Antimicrobial Action. The antibiotic activity of different extracts from *J. gossypiifolia* is frequently reported, as observed in Table 4. In general, some extent of antibacterial, antifungal, antiparasitic, and antiviral activity was observed. The only report of *J. gossypiifolia* isolated compound with antimicrobial activity is of the macrocyclic diterpene jatrophenone, which presented significant *in vitro* antibacterial activity against *Staphylococcus aureus* [41].

6.3. Anti-Inflammatory and/or Analgesic Action. Many important popular uses of *J. gossypiifolia* are related to inflammatory process. Bhagat et al. [28] showed that the methanolic extract of leaves of this species has significant systemic acute and chronic anti-inflammatory activity. The extract, at 500 and 1000 mg/kg oral doses, was able to inhibit the acute carrageenan-induced paw edema in rats and at 50 and 100 mg/kg oral doses inhibited the chronic cotton pellet-induced granuloma formation in rats. Additionally, the *J. gossypiifolia* leaf paste (0.5 and 1 mg/ear) showed significant reduction in TPA-induced local inflammatory changes in mouse ear edema model [28].

In another study, the anti-inflammatory and analgesic properties of the methanol and petrol ether extracts of aerial parts of *J. gossypiifolia* were demonstrated in mice [92]. At 100 and 200 mg/kg/day, during 7 days, by oral route, only the methanol extract presented significant analgesic activity in Eddy's hot plate and tail-flick models and anti-inflammatory activity in carrageenan-induced paw edema [92]. The anti-inflammatory activity of the bark from *J. gossypiifolia* (methanol and petrol ether extracts) was also demonstrated in carrageenan-induced paw edema in rats [115].

In a recent study, using the *in vitro* human red blood cell membrane stabilization method, Nagaharika et al. [118] suggested that ethanol and water extracts from *J. gossypiifolia* leaves have anti-inflammatory activity. According to the authors, since human red blood cell membranes are similar to the lysosomal membrane components, the prevention of hypotonicity-induced membrane lysis of these cells could be taken as a measure in estimating the anti-inflammatory property of compounds [118].

The analgesic activity of the methanol extract from the leaves of *J. gossypiifolia* was evaluated in acetic acid-induced writhing test in mice, where highly significant inhibition was seen of 67.56 and 65.14% at 200 and 400 mg/kg oral doses, respectively [111]. Similar results were observed in the methanolic extract from fruits [110].

6.4. Healing Action. The healing action of the ethanol crude extract of *J. gossypiifolia* (plant part not specified) was evaluated in suture healing of ventral abdominal wall of rats, through tensiometric measurement and macro- and microscopic aspect of postoperative period. The extract, which was administered by an intraperitoneal instillation of 100 mg/kg single dose in the peritoneal cavity, presented more intense adhesion on macroscopic examination and greater strain evaluation and vascular neoformation. However, a greater inflammatory process was also observed, and other histological parameters were similar to the control group, indicating that, in general, the extract presented poor wound healing properties in the used model [124].

Another study evaluated the healing action of the hydroethanolic crude extract from leaves of *J. gossypiifolia* in the healing process of sutures performed on the bladder of rats, and similar results were presented, although some improvement might have been observed in some parameters. In general, the authors concluded that no favorable healing effect was observed with the administration of single intraperitoneal dose of *J. gossypiifolia* L. [108]. In another study analyzing the morphological aspects of the healing process occurring in open skin lesions in rats under topical administration of raw extract from *J. gossypiifolia* (details

Table 3: Popular medicinal uses of *Jatropha gossypiifolia* L. described in the literature.

Plant part	Popular use	Preparation and/or mode of use	Reference
Whole plant	Analgesic (headache)	Leaves anointed with "*Sebo de Holanda*" (mutton tallow) and heated in the fire are used as compress for headaches	[5]
	Analgesic (toothache)	Not specified	[3]
	Antimicrobial	Not specified	[3]
	Antipyretic	Decoction	[20]
	Dyscrasia	Not specified	[3]
	Dysphonia	Not specified	[3]
	Wound healing	Not specified	[74, 75]
Aerial parts	Antianemic (malaria treatment)	Decoction, used by oral route	[76]
	Abscess	Bath	[77]
	Alopecia	Ash leaves	[25]
	Analgesic (eye pain)	Not specified	[78]
	Analgesic (headache)	Not specified	[78]
	Analgesic (headache and otitis)	Not specified	[79]
	Analgesic (pain in general)	Decoction or infusion	[80]
	Analgesic (toothache)	Decoction or infusion	[80]
	Antianemic	Decoction	[81]
		Decoction by oral route	[82]
	Anticancer	Ash of leaves	[25]
		Decoction of the association of leaves of *J. gossypiifolia* with leaves of *Petiveria alliacea* and aerial parts of *Stachytarpheta jamaicensis*, by oral route	[29]
		Not specified	[3]
	Anticonvulsivant	Not specified	[83]
	Antidiabetic	Decoction	[84, 85]
		Decoction by oral route	[30]
	Antidiarrheal	Decoction by oral route	[30]
		Not specified	[3]
	Antihemorrhagic	Decoction by oral route	[30]
		Fresh crushed leaves are used in cases of cutaneous and nasal bleeding	[86]
	Anti-infective	Decoction by oral route	[30]
		Not specified	[87, 88]
	Anti-inflammatory	Not specified	[78]
	Antipyretic	Decoction	[81]
		"Tea"	[5]
		Not specified	[88]
	Antiseptic	Bath prepared from the leaves	[5]
	Antithrombotic	Decoction or infusion	[80]
	Antiulcerogenic	Decoction by oral route	[30]
		Leaf juice	[89]
	Boils	Application of the pounded leaves	[90]

Table 3: Continued.

Plant part	Popular use	Preparation and/or mode of use	Reference
Leaves	Burns	Ash of leaves	[25]
		Used in association with seeds of *Gossypium arboreum*, sugar, honey bee, and fat of ram, prepared by grinding, applied topically	[29]
	Contraceptive and oxitotoxic	Not specified	[79]
	Depurative	Squeezed, the juice obtained is drunk	[91]
	Detoxificant	Not specified	[92]
	Eczema	Ash of leaves	[25]
	Emetic	Squeezed, the juice obtained is drunk	[91]
	Gastrointestinal disorders	Not specified	[79]
	Gingivitis	Leaf juice	[89]
	Gonorrhoea	Ash of leaves	[25]
	Healing	Bath prepared from the leaves	[5]
		Decoction	[30]
		Decoction or infusion	[80]
	Hemorrhoids	Used in association with leaves of *Nicotiana tabacum* and copper sulphate, boiled in water, and used as steam directed at the anal region	[93]
	Hemostatic	Decoction or infusion	[80]
	Hepatitis	Not specified	[12]
	Itching skin	Application of the pounded leaves	[90]
	Leprosy	Leaf juice	[89]
	Malaria	Decoction	[81]
		Decoction by oral route	[82]
		Used in association with leaves of *Azadirachta indica* and *Combretum* sp., boiled, for steam baths and by oral route	[94]
		Used in association with leaves of *Combretum ghasalense* and whole plant of *Ocimum canum*, by oral route or for steam baths	[94]
	Mastitis	Pounded leaves applied on swollen breasts	[90]
	Mycosis	Ash of leaves	[25]
	Psychoactive	Not specified	[79]
	Purgative	Not specified	[3, 88]
	Rheumatism	Ash of leaves	[25]
	Scabies	Ash of leaves	[25]
	Skin diseases	Not specified	[3]
	Stomachic	Decoction by oral route	[30]
		Not specified	[88, 92]
	Syphilis	Ash of leaves	[25]
	Thrush (oral candidiasis)	Ash of leaves	[25]
	Treatment of "cultural syndromes," "*derrame*," "*quebrante*," "*espante*," "*vento-caído*," "*panema*," "*doença-do-ar*," "*mãe-do-corpo*"	Not specified	[79]
	Vaginal infection	Slightly boiled, used as vaginal wash	[91]
	Veneral diseases	Not specified	[92]
	Vermifuge	Ash of leaves	[25]
	Vertigo	Not specified	[3]

Table 3: Continued.

Plant part	Popular use	Preparation and/or mode of use	Reference
	Wounds and rashes	Bath of the leaves	[24]
		Decoction by oral route	[30]
		Decoction used as baths for cleaning wounds in dogs	[95]
	Wound disinfectant	Slightly boiled, used as wound wash	[91]
Stem	Analgesic (toothache)	Not specified	[96]
	Antianemic	Decoction by oral route	[82]
	Anticancer	Decoction by oral or topical route	[26]
	Emmenagogue	Decoction of barks	[70, 92]
	Malaria	Decoction by oral route	[82]
	Rheumatism	Not specified	[77]
	Thick blood	Not specified	[77]
Roots	Anticancer	Decoction by oral or topical route	[26]
		Root bark used for cancer of the lungs	[73]
	Anticonvulsivant	Not specified	[83]
	Antidiarrheal	Not specified	[89]
	Antimicrobial	Root bark used in bacterial infections	[73]
	Impotence	Decoction of the association of roots of *J. gossypiifolia*, *Chiococca alba*, *Citrus aurantifolia*, *Desmodium canum*, *Roystonea regia*, *Senna occidentalis*, *Stachytarpheta jamaicensis*, and *Waltheria indica* with the whole plant of *Commelina erecta*, *Cyperus rotundus*, and sugar, by oral route	[29]
	Leprosy	Not specified	[3, 92]
	Snakebites	Not specified	[22, 92, 97, 98]
	Urinary pain	Not specified	[92]
	Uterus diseases	Decoction by oral route	[99, 100]
Seeds	Analgesic (body pain)	Not specified	[101]
	Analgesic (headache)	Not specified	[79]
	Antigripal	Used in strong colds	[5]
	Antihemorrhagic	Not specified	[9]
	Antiulcerogenic	Seed oil	[3]
	Contraceptive and oxitotoxic	Not specified	[79]
	Depurative	Not specified	[91]
	Emetic	Not specified	[70, 91, 101]
	Gastrointestinal disorders	Not specified	[79]
	Leprosy	Seed oil	[3]
	Mycosis	Seed oil	[3]
	Psychoactive	Not specified	[79]
	Purgative	Not specified	[3, 9, 101, 102]
	Treatment of "cultural syndromes," "*derrame*," "*quebrante*," "*espante*," "*vento-caído*," "*panema*," "*doença-do-ar*," "*mãe-do-corpo*"	Not specified	[79]
	Vaginal infection	Slightly boiled, used as vaginal wash	[91]
	Wound infection	Slightly boiled, used as wound wash	[91]

Table 3: Continued.

Plant part	Popular use	Preparation and/or mode of use	Reference
Fruits	Analgesic	Massaging pregnant women's bellies with tea or *garrafada** when they are in pain	[77]
	Analgesic (headache)	Tea or *garrafada**	[77]
	Analgesic (toothache)	Tea or *garrafada**	[77]
	Laxative	Ingestion *in natura* of the powder fruit	[102]
	Numbness after bug stings	Tea or *garrafada**	[77]
Latex	Alopecia	Not specified	[25]
	Analgesic (eye pain)	Not specified	[78]
	Analgesic (pain in general)	Drink or massage the affected area with latex	[80]
	Analgesic (toothache)	Cotton soaked with latex kept in contact with the sore tooth	[103]
		Drink or massage the affected area with latex	[80]
	Anticancer	Not specified	[25]
	Antihemorrhagic	Not specified	[9, 24, 86, 95]
	Antithrombotic	Oral route	[80]
	Antiulcerogenic	Not specified	[20, 89]
	Bite of venomous animals	Application of fresh latex at the affected site	[5]
	Diuretic	A few drops of fresh latex in water	[6]
	Eczema	Not specified	[25]
	Gingivitis	Not specified	[89]
	Gonorrhea	Not specified	[25]
	Hemostatic	Not specified	[25, 80]
	Infected wounds	Application of fresh latex at the affected site	[5, 20]
	Leprosy	Not specified	[89]
	Mycosis	Not specified	[25]
	Purgative	A few drops of fresh latex in water	[6]
		Not specified	[9]
	Rheumatism	Not specified	[25]
	Scabies	Not specified	[25]
	Skin burns	Application of fresh latex at the affected site	[104]
		Not specified	[25]
	Stop of itching of cuts and scratches	Not specified	[95]
	Syphilis	Not specified	[25]
	Thrush (oral candidiasis)	Not specified	[25]
	Vermifuge	Not specified	[25]
	Wound healing	Application of latex at the affected site	[5]
		Drink or massage the affected site with latex	[80]
		Not specified	[74, 75]
Resin	Toothache	Toothpowder	[27]
	Wounds in lips and tongue	Topical application	[27]
Oil	Arthritis	Applied locally	[89]
	Purgative	Not specified	[89]
	Skin disease	Applied locally	[89]

Table 3: Continued.

Plant part	Popular use	Preparation and/or mode of use	Reference
Not specified	Alopecia	Tea applied locally in dogs	[105]
	Analgesic	Not specified	[13]
		Poultices	[95]
	Anticancer	Not specified	[13, 66]
	Antidiarrheal	Not specified	[28, 45, 106]
	Antihypertensive	Not specified	[45]
	Anti-inflammatory	Not specified	[13, 28]
	Antipyretic	Not specified	[28]
	Antiseptic	Not specified	[45]
	Antiulcerogenic	Not specified	[28]
	Coughs and colds	Bark juice (4 spoonfuls, 3 times a day) by oral route	[107]
	Detoxication	Not specified	[28]
	Diuretic	Not specified	[45]
	Eczema	Not specified	[28]
	Gum infection	Not specified	[28]
	Healing	Not specified	[45, 108]
	Hydropsy	Not specified	[5]
	Leprosy	Not specified	[28]
	Obstructions of the abdominal tract	Not specified	[5]
	Purgative	Not specified	[5]
	Regulate menses	Not specified	[109]
	Rheumatism	Not specified	[5]
	Snake and scorpion bites	Not specified	[3, 22]
	Stomach pain	Not specified	[28]
	Venereal diseases	Not specified	[28]
	Wounds	Poultices	[95]
		Used as bath	[28]

* *Garrafada*: preparation done by macerating plant parts in alcohol or hydroalcoholic mediums, in general, brandies.

Table 4: Pharmacological studies of *Jatropha gossypiifolia* L. described in the literature.

Pharmacological activity	Plant part	Extract/compounds	Detail	Reference
Analgesic	Aerial parts	Methanol and petrol ether extracts	At 100 and 200 mg/kg/day, over 7 days, by oral route in mice, only the methanol extract presented significant analgesic activity in Eddy's hot plate and tail-flack models	[92]
	Fruits	Methanol extract	At 200 and 400 mg/kg, by oral route in mice, highly significantly inhibited the writhing responses induced by acetic acid	[110]
	Leaves	Methanol extract	At 200 and 400 mg/kg, by oral route in mice, significantly inhibited the writhing responses induced by acetic acid	[111]
Antibacterial	Latex	Crude latex	At 100 μL volume inhibited *in vitro Listeria monocytogenes, Salmonella tyhimurium*, *Salmonella typhi*, and *Staphylococcus aureus*	[112]
	Latex	Not specified	Presented bactericidal effect *in vitro* against *Shigella dysenteriae* and *Staphylococcus aureus**	[113]
	Leaves	Fractions obtained by sequential extraction of the vegetal material with petrol ether, benzene, chloroform, acetone, ethanol, methanol, and water	Petrol ether fraction was inactive against *Escherichia coli* and *Bacillus subtilis*. Benzene fraction was the most active, against both microorganisms. Chloroform and methanol fractions were active only against *Bacillus subtilis*. Acetone and ethanol fractions were active only against *Escherichia coli*. Aqueous fraction was active against both microorganisms, although to a much lesser degree than the other fractions.	[52]
		Methanol, chloroform, and water extracts	All extracts were active *in vitro* against *Shigella dysenteriae**	[113]
		Petrol ether and ethyl acetate fractions from ethanol : dichloromethane (1 : 1, v/v) extract	The petrol ether fraction (1 mg/mL) inhibited *in vitro Pseudomonas aeruginosa*, *Staphylococcus epidermidis,* and *Salmonella typhimurium.* The ethyl acetate fraction (1 mg/mL) was active against *Staphylococcus aureus*	[87]
	Whole plant	Jatrophenone	Presented *in vitro* antibacterial activity against *Staphylococcus aureus* comparable to penicillin	[41]
	Aerial parts	Water and ethyl acetate fractions from methanol extract	Both fractions, at 1 mg, did not produce zones of inhibition for *Escherichia coli*, *Staphylococcus aureus*, *Saccharomyces cerevisiae,*nor *Candida albicans*	[114]
	Leaves	Chloroform extract	Presented antibacterial activity against *Salmonella typhi*, *Pseudomonas aeruginosa*,,and *Staphylococcus aureus* and antifungal activity against *Candida albicans*. Did not produce inhibition zones against *Escherichia coli, Bacillus subtilis, Proteus mirabilis, Corynebacterium diptheriae, Shigella dysenteriae,*and *Streptococcus penumoniae*	[50]
		Dichloromethane : methanol (1 : 1, v/v) extract	At 0.5 and 1 mg/mL, showed significant antibacterial activity *in vitro* against *Bacillus cereus* var *mycoides*, *Bacillus pumilus*, *Bacillus subtilis*, *Bordetella bronchiseptica*, *Micrococcus luteus*, *Staphylococcus aureus, Staphylococcus epidermidis, Klebsiella pneumoniae,* and *Streptococcus faecalis* and antifungal activity *in vitro* against *Candida albicans*	[88]
	Leaves	Methanol extract	Presented antibacterial activity against *Salmonella typhi*, *Pseudomonas aeruginosa,* and *Staphylococcus aureus* and antifungal activity against *Candida albicans*. Did not produce inhibition zones against *Escherichia coli, Bacillus subtilis, Proteus mirabilis, Corynebacterium diptheriae, Shigella dysenteriae,*and *Streptococcus penumoniae*	[50]

Table 4: Continued.

Pharmacological activity	Plant part	Extract/compounds	Detail	Reference
Antibacterial and antifungal	Not specified	Extracts obtained by sequential extraction of the vegetal material with *n*-hexane, chloroform, acetone, methanol, and water	*n*-Hexane extract had inhibitory activity *in vitro* against *Escherichia coli*, *Salmonella typhi*, *Pseudomonas aeruginosa*, *Bacillus cereus*, *Klebsiella aerogenes*, and *Candida albicans* but was inactive against *Shiguella boydi*, *Aspergillus fumigatus*, *Aspergillus flavus,* and *Aspergillus niger*. Chloroform extract inhibited *in vitro Salmonella typhi*, *Pseudomonas aeruginosa*, *Bacillus cereus,*and *Candida albicans* but was inactive against *Escherichia coli, Staphylococcus aureus, Shiguella boydi, Aspergillus fumigatus, Aspergillus flavus*, and *Aspergillus niger.* Acetone extract inhibited *in vitro Escherichia coli, Pseudomonas aeruginosa, Staphylococcus aureus, Klebsiella aerogenes, Proteus vulgaris,*and *Candida albicans* but was inactive against *Salmonella typhi, Aspergillus fumigatus, Aspergillus flavus,*and *Aspergillus niger.* Methanol extract inhibited *in vitro Escherichia coli, Salmonella typhi, Pseudomonas aeruginosa, Staphylococcus aureus, Bacillus cereus,*and *Candida albicans* but was inactive against *Aspergillus fumigatus, Aspergillus flavus,*and *Aspergillus niger.* Water extract was active *in vitro* against *Escherichia coli, Salmonella typhi, Pseudomonas aeruginosa, Staphylococcus aureus, Bacillus cereus, Klebsiella aerogenes, Proteus vulgaris,*and *Candida albicans* but was inactive against *Aspergillus fumigatus, Aspergillus flavus,* and *Aspergillus niger*	[89]
		Methanol and petrol ether extracts from bark	At 200 μg/100 μL, only the methanol extract showed *in vitro* antibacterial activity upon *Staphylococcus aureus*, *Streptococcus pyogenes,* and *Escherichia coli* and antifungal activity upon *Aspergillus niger*, *Candida albicans*, *Penicillium notatum,* and *Saccharomyces cerevisiae*	[115]
Anticholinesterase	Latex	Lyophilized latex	Inhibited time- and dose-dependently the acetylcholinesterase enzyme in nervous tissue of freshwater air breathing fish *Channa marulius*	[116]
	Leaves	Fractions obtained by sequential extraction of the vegetal material with ethyl acetate and methanol	At 2 mg/mL concentration, the ethyl acetate and methanol fractions presented inhibitory activities *in vitro* of 71 and 100%. The methanol fraction presented IC_{50} of 0.05 mg/mL	[117]
Antidiarrheal	Fruits	Methanol extract	At 200 and 400 mg/kg, by oral route in mice, inhibited the castor oil induced diarrhea	[110]
	Leaves	Methanol extract	At 200 and 400 mg/kg, by oral route in mice, inhibited the castor oil induced diarrhea	[111]
Antifungal (antidermatophytic fungi)	Aerial parts	Water and ethyl acetate fractions from methanol extract	The minimal concentration producing 75% of inhibition or higher against *Microsporus canis,* for both fractions, was 1 μg/mL. For the fungus *Microsporus gypseum, Microsporus fulvum,*and *Microsporus gallinae,* none of the fraction presented inhibitory activity	[114]

Table 4: Continued.

Pharmacological activity	Plant part	Extract/compounds	Detail	Reference
Anti-inflammatory	Aerial parts	Methanol and petrol ether extracts	At 100 and 200 mg/kg/day, over 7 days, by oral route in mice, only the methanol extract presented significant anti-inflammatory activity on carrageenan-induced paw edema	[92]
	Leaves	Aqueous extract	At 100 and 200 μg/mL, significantly prevented the lysis of human red blood cells in membrane stabilization method *in vitro*	[118]
		Ethanol extract	At 100 μg/mL, significantly prevented the lysis of human red blood cells in membrane stabilization method *in vitro*	[118]
		Methanol extract and leaf paste	At 500 and 1000 mg/kg, by oral route in rats, inhibited the carrageenan-induced paw edema. At 50 and 100 mg/kg, by oral route in rats, inhibited the cotton pellet induced granuloma formation in rats. At 0.5 and 1 mg/ear, the leaf paste reduced the inflammation response in mouse ear edema model	[28]
	Not specified	Methanol and petrol ether extracts from bark	At 200 mg/kg, by oral route in rats, both extracts reduced the carrageenan-induced paw edema	[115]
Antimalarial	Leaves	Aqueous extract	30 μg inhibited *in vitro* the growth of *Plasmodium falciparum*	[31]
		Dichloromethane extract	Active *in vitro* against *Plasmodium falciparum*, with IC_{50} of about 35 μg/mL	[81]
Antineoplasic	Roots	Ethanolic extract and jatrophone	The ethanol extract, as well as jatrophone, exhibited significant inhibitory activity *in vitro* against cells derived from human carcinoma of the nasopharynx and lymphocytic leukemia P-388 and *in vivo* against four standard animal tumor systems	[66]
		Falodone	Showed potent proliferation inhibitory activity against A-549 human cancer cell line, with IC_{50} of 120 μg/mL	[13]
		2α-Hydroxyjatrophone, 2β-hydroxy-5,6-isojatrophone and 2β-hydroxyjatrophone, diterpenes isolated from petrol ether extract	Presented antineoplasic activity upon P-388 lymphocytic leukemia test system both *in vivo* and *in vitro*, as well as for the Eagle's carcinoma of the nasopharynx test system *in vitro*	[64]
	Not specified	Abiodone	Not specified*	[73]
Antioxidant	Leaves	Methanol, ethyl acetate, and aqueous extract	All extracts showed significant antioxidant activity *in vitro* in DPPH free radical, ferric thiocyanate, and nitric oxide scavenging methods*	[55]
	Whole plant	Petrol ether, chloroform, ethyl acetate, and *n*-butanol extracts	All extracts showed only poor DPPH scavenging activity. The total antioxidant capacity was higher in ethyl acetate and *n*-butanol extracts, having the petrol ether and chloroform showing only poor activity. The lipid peroxidation was inhibited only partially by the extracts, with the ethyl acetate being the most active and the petrol ether being the least	[48]
Antispasmodic	Aerial parts	Ethanol extract, fractions, and subfractions	At 500, 1000, and 2000 mg/kg, by oral route in mice, showed significant antispasmodic activity in mouse intestinal transit model and at 0.5, 1.0, and 2.0 mg/mL inhibited *in vitro* the acetylcholine and calcium-induced contractions of isolated rat jejunum. Only the organic fraction of the extract had a calcium-antagonist effect, whereas both chloroformic and aqueous fractions had anticholinergic effect	[119]

Table 4: Continued.

Pharmacological activity	Plant part	Extract/compounds	Detail	Reference
Antiviral	Aerial parts	Water and ethyl acetate fractions from methanol extract	At 1, 10, and 100 μg/mL, both fractions presented 100% of inhibition of plaque-forming ability of *Sindbis virus* in treatment preinfection protocol ($IC_{50} < 1\,\mu$g/mL), while in treatment postinfection, the IC_{50} of water fraction increased to 512 and acetate fraction increased to 37 μg/mL. For murine cytomegalovirus, IC_{50} of 1.7 and 1.5 to water and ethyl acetate fractions were observed, respectively, in treatment preinfection protocol. In the treatment postinfection, however, no inhibition was observed in this microorganism	[114]
	Not specified	Methanol extract from barks	Partially active against *Sindbis virus* and herpes simplex virus-l. Inactive against human poliovirus	[107]
Bronchodilator	Stems	Aqueous extract	The extract was inactive in bronchodilator activity in guinea pigs	[120]
Contraceptive	Leaves	Ethanol extract	At 450 mg/kg/day, over 21 days, by oral route, caused an antifertility activity in female mice	[121]
Healing	Aerial parts	Ethanol 70% extract	At 1 mL/kg dose, by intraperitoneal route in rats, presented beneficial activity in healing process of colonic anastomosis	[122]
	Aerial parts	Ethanol 70% extract	At 200 mg/kg, by intraperitoneal route in rats, favored the healing process of gastrorrhaphies and reduced the acute inflammatory reaction *in vivo*	[123]
	Leaves	Hydroethanol extract	At 200 mg/kg, by intraperitoneal route, decreased the inflammation and increased vascular neoformation and collagen deposition when compared to the control group in healing process of sutures performed on the bladder of rats. However, in general, no favorable healing effect was observed.	[108]
	Not specified	Ethanolic extract	Although some improvement could be observed in suture healing of ventral abdominal wall of rats treated with 100 mg/kg of extract (intraperitoneal instillation intraperitoneal cavity), in general, only a poor healing activity was observed.	[124]
		Not specified	At 0.1 mL volume, by topical application, the crude extract presented significant differences concerning the macroscopic and microscopic aspects of healing process occurring in open skin lesions in rats	[125]
Hemostatic	Latex	Crude fresh latex	Decreased clotting and bleeding time in healthy subjects	[101]
Hepatoprotective	Aerial parts	Petrol ether, methanol, and water extracts	At 200 mg/kg/day, over 7 days, by oral route in rats, both extracts presented hepatoprotective activity in carbon tetrachloride induced liver damage, with the petrol ether being the most active and the methanol being the least	[126]
Hypotensive and vasorelaxant	Aerial parts	Ethanolic extract	At 125 and 250 mg/kg/day, over 4 weeks, by oral route in rats, in a dose-dependent manner, reduced the systolic blood pressure and produced a concentration-dependent relaxant effect in rat isolated (*ex vivo*) endothelium-deprived mesenteric artery precontracted with norepinephrine or $CaCl_2$	[45]
Immunomodulatory	Whole plant	Petrol ether extract	At 100, 200, and 400 μg/mL increased the proliferation of mouse spleen cell *in vitro*	[127]
Local anesthetic	Not specified	Methanol and aqueous extracts	Both extracts presented significant local anesthetic activity by plexus anesthesia in frogs*	[128]

Table 4: Continued.

Pharmacological activity	Plant part	Extract/compounds	Detail	Reference
Relaxant effect on uterine smooth muscle (tocolytic activity)	Aerial parts	Ethanolic extract and chloroformic and aqueous fractions	At 0.5 and 1.0 mg/mL, the ethanolic extract reduced the calcium-evoked contractile response of the uterine smooth muscle, as well as the chloroformic fraction. The aqueous fraction presented only slight effect	[129]
Sedative and anxiolytic	Fruits	Methanol extract	At 200 and 400 mg/kg, by oral route in mice, presented sedative effect in the hole cross test; At 200 mg/kg, presented anxiolytic activity in hole board test; At 400 mg/kg, presented anxiolytic activity in elevated plus-maze test	[110]
	Leaves	Methanol extract	At 200 and 400 mg/kg, by oral route in mice, presented sedative effect in the hole cross test; At 200 mg/kg, presented anxiolytic activity in hole board test; At 400 mg/kg, presented anxiolytic in elevated plus-maze test	[111]

*The complete version of the paper was not accessible, so the information was obtained from its abstract.
IC_{50}: concentration that inhibits 50% of the referred activity.

about extract preparation and plant part not specified), the authors also observed an absence of healing action, although some histological improvement was shown [125].

However, studying the influence of *J. gossypiifolia* on the healing process of colonic anastomosis in rats, Servin et al. showed that the administration of 1 mL/kg single dose of the hydro alcoholic extract from aerial parts has beneficial effect on the healing process [122]. However, according to these authors, on the seventh day of the experiment, there was a decrease in the action of the extract, suggesting that the extract, in this experiment, was less active in later stages of healing process [122]. A plausible hypothesis, not raised by the authors, could be the fact that the extract was administered in a single dose, which may not have been sufficient to maintain the effect throughout the time of the experiment. Additionally, Vale et al. showed that the ethanolic extract from aerial parts of *J. gossypiifolia*, at single intraperitoneal dose of 200 mg/kg, favored the healing process of gastrorrhaphies and reduced the acute inflammatory reaction *in vivo* [123].

6.5. Hemostatic Action. The use of *J. gossypiifolia*, especially the latex, is widespread as a hemostatic agent for preventing bleeding disorders. The results of whole blood clotting time using Lee and White method and bleeding time using Ivy's method were significantly reduced when stem latex was introduced, suggesting procoagulant activity [101]. Regarding the possible mechanism of action, based on experiments that show the precipitating action of the latex upon bovine albumin, the authors suggest that the latex precipitates clotting factors thereby bringing the coagulation factors into close contact, and then the activation of coagulation cascade leads to the generation of thrombin and formation of a clot takes place in a matter of seconds when compared to the control experiment, which took minutes to complete coagulation [101]. It is important to emphasize that, to the best of our knowledge, this is the only study performed on human subjects.

6.6. Anticholinesterase Action. Based on the cholinergic hypothesis, acetylcholinesterase inhibitors are widely used to treat Alzheimer's disease. *J. gossypiifolia* presented an important anticholinesterase activity since the methanolic extract from leaves showed an IC_{50} of 0.05 mg/mL [117]. Another study showed that the lyophilized latex of the plant was able to inhibit time- and dose-dependently the acetylcholinesterase enzyme in nervous tissue of freshwater air breathing fish *Channa marulius* [116].

6.7. Antioxidant Action. The antioxidant activity of extracts from *J. gossypiifolia* was evaluated by Kharat et al. [55]. In this work the high content of phenols, tannins, and flavonoids in the leaves prompted the authors to evaluate the antioxidant activity of the leaves. DPPH free radical, ferric thiocyanate, and nitric oxide scavenging methods were used to analyze the antioxidant activity *in vitro* of methanol, ethyl acetate, and aqueous extracts, demonstrating positive results. The authors attributed the free radical scavenging activity to the presence of flavonoids [55]. On the other hand, a study showed that different extracts (petrol ether, chloroform, ethyl acetate, and *n*-butanol) from whole plant of *J. gossypiifolia* had only partial antioxidant activity in DPPH scavenging, total antioxidant capacity, and lipid peroxidation tests [48]. Among them, the ethyl acetate extract was the most active, which correlates positively with its higher content of phenolic compounds in comparison with the other extracts [48].

6.8. Contraceptive Action. Based on its popular use, *J. gossypiifolia* was assessed for its antifertility activity, as an alternative to oral contraceptive agents. *J. gossypiifolia* leaf extract, by oral route, altered the major hormones involved in estrous cycle regulation, indicating its antifertility effect on mice [121]. Evaluating other parameters (estrogenic and early abortifacient activities) the anti-infertility effect of the extract was once more demonstrated later [130].

6.9. Tocolytic Action. Based on the ethnopharmacological application of the plant as tocolytic remedy, the effects on calcium-evoked uterine smooth muscle contraction of the ethanolic extract and fractions were evaluated [129]. The crude extract and, to a higher extent, the chloroformic fraction reduced the calcium-evoked contractile response of the uterine smooth muscle, promoting a rightward displacement of calcium cumulative curves, as well as reducing the maximal contractions [129].

6.10. Antineoplasic Action. One of the most well-known pharmacological activities of *J. gossypiifolia* is its antineoplasic action, which is frequently associated with the content of lignoids and terpenoids. One of the first reports was made by Kupchan et al. [66], when the authors found that the ethanolic extract from roots, as well as the isolated diterpene jatrophone, exhibited significant inhibitory activity *in vitro* against cells derived from human carcinoma of the nasopharynx and lymphocytic leukemia P-388 and *in vivo* against four standard animal tumor systems, such as sarcoma 180, Lewis lung carcinoma, P-388 lymphocytic leukemia, and Walker 256 intramuscular carcinosarcoma [66]. Later, three new antitumor derivatives of jatrophone were isolated from petrol ether extracts from roots of *J. gossypiifolia*: 2α-hydroxyjatrophone, 2β-hydroxy-5,6-isojatrophone, and 2β-hydroxyjatrophone [64]. Recently, two other diterpenes with potent antineoplasic activity were isolated from *J. gossypiifolia*: falodone and abiodone. Falodone was isolated from methanol extract from roots and showed potent proliferation inhibitory activity against A-549 human cancer cell line [13]. Abiodone, a lathyrane diterpenoid compound, was isolated from *J. gossypiifolia* and presented potent anticancer activity [73].

6.11. Local Anesthetic Action. The local anesthetic action of *J. gossypiifolia* was evaluated by plexus anaesthesia in frogs [128]. The authors observed that the aqueous and methanol extract (plant part not specified) presented significant anesthetic action when compared to control group.

6.12. Neuropharmacological Action. The neuropharmacological action of the methanol extract of the leaves of *J. gossypiifolia* was evaluated by Apu et al. [111]. The authors observed that in hole cross test the extract at 200 and 400 mg/kg, by oral route, showed significant sedative effect in mice. In hole board test, the extract showed highly significant anxiolytic activity at a dose of 200 mg/kg, whereas the same activity was observed at 400 mg/kg dose in elevated plus-maze test [111]. Similar results were observed in the methanolic extract from fruits [110].

6.13. Antidiarrheal Action. Although it may seem contradictory as shown in Table 3, *J. gossypiifolia* species is popularly used both as purgative and as antidiarrheal remedy. However, in literature, there are interesting results about the antidiarrheal properties of different extracts of this species.

At 200 and 400 mg/kg oral doses in mice, the methanol extract of *J. gossypiifolia* leaves produced highly significant antidiarrheal activity upon castor oil-induced diarrhea, decreasing the mean number of stool and total weight of fecal output when compared to control group [111]. Similar results were observed in the methanolic extract from fruits [110].

Aiming to determine the possible action mechanism of *J. gossypiifolia* aerial parts ethanol extract as antidiarrheal agent, Silva et al. [119] have investigated the effect of this extract on intestinal transit velocity and on isolated rat jejunum. At 500, 1000, and 2000 mg/kg, by oral route in mice, the extract showed significant antispasmodic activity in mouse intestinal transit model when compared to control. At 0.5, 1.0, and 2.0 mg/mL, the crude extract inhibited *in vitro* the acetylcholine and calcium-induced contractions of isolated rat jejunum. The chloroform and aqueous fractions were obtained and it was observed that only the chloroform fraction of the extract had a calcium-antagonist effect, whereas both chloroformic and aqueous fractions had anticholinergic effect, suggesting that the antispasmodic effect of *J. gossypiifolia* may be due to a combination of anticholinergic and calcium-antagonist mechanisms [119].

6.14. Immunomodulatory Action. The immunomodulatory action of synthetic lignan compounds was evaluated by the assay of proliferation of mouse spleen cell *in vitro* and compared with petrol ether extract of whole plant of *J. gossypiifolia*, since it is a natural source of this kind of compound [127]. The authors showed that both synthetic and naturally occurring 1-phenylnaphthalene lignans could positively modulate the immunity of the host, since they significantly increased the proliferation of mouse spleen cell *in vitro* [127].

6.15. Hepatoprotective Action. Despite some studies having shown the hepatotoxic potential of *J. gossypiifolia*, a study was performed to analyze the possible hepatoprotective action of extracts of this plant in carbon tetrachloride-induced liver damage in rats [126]. In fact, the petrol ether, methanol, and water extracts from the aerial parts of *J. gossypiifolia* presented significant hepatoprotective action in this model, substantially restoring towards normalization the serum levels of serum glutamate oxaloacetate transaminase, serum glutamate pyruvate transaminase, serum alkaline phosphatase, total bilirubin, superoxide dismutase, and catalase [126]. The authors also discuss the close relationship between the hepatoprotective action observed and the possible antioxidant mechanism present in the extracts.

7. Other Actions and Biotechnological Applications

In addition to studies demonstrating scientific evidences of the pharmacological properties of *J. gossypiifolia*, several studies have demonstrated the potential of this species to obtain molecules with various applications, thus showing its multipurpose character.

Among the main applications described, the use of *J. gossypiifolia* seed oil for biodiesel production could be mentioned. *Jatropha* species has drawn the attention of researchers in recent years due to its emergence as a highly suitable feedstock plant for biodiesel production [11]. Among the species, *J. gossypiifolia*, *J. curcas,* and *J. pohliana* produce seeds with high oil content [11]. In a study investigating the potential of two plants of the *Jatropha* genus (including *J. gossypiifolia*), the authors observed that the studied physicochemical properties of the produced biodiesel are in the acceptable range for use as biodiesel in diesel engines, showing a promising economic exploitation of these raw materials [131].

Studies have shown the potential of the species for the development of new tools for biochemical analysis. A recent study showed that the diluted fresh latex *J. gossypiifolia* can be used as precipitating agent for biochemical determination of proteins in plasma, urine, and cerebrospinal fluid, with values comparable to those obtained from the conventional protein precipitants sodium tungstate and trichloroacetic acid [24]. According to the authors, the precipitating potential could be related to the capacity of the latex to form clots when applied to a bleeding sore or wound when it is used in folk medicine [24]. Another study showed the potentiality of the juice extracted from the fresh leaves of *J. gossypiifolia* as an anticoagulant for haematological analyses [86]. 0.1 mL of extract per mL of blood proved to be suitable for obtaining plasmas for biochemical analysis comparable with conventional anticoagulants [86]. However, the authors emphasize that the extract must be purified to remove interfering substances for it to be perfectly suitable for biochemical analysis [86].

Some studies have demonstrated the potentiality of *J. gossypiifolia* as a source of pesticide biomolecules. Bullangpoti et al. [49] isolated ricinine from the ethyl acetate extract from senescent leaves, the main compound responsible for the toxicity of the crude extract in *Spodoptera exigua* larvae, thus demonstrating that it could be an alternative choice to chemical insecticides. In another study, Bullangpoti et al. [132] showed that the ethanol extract of *J. gossypiifolia* in association with the ethanol extract of *Melia azedarach* was toxic and inhibited some enzymes from *Spodoptera*

frugiperda larvae, demonstrating once more the potentiality of the species as insecticide agent. Calatayud et al. [56] showed the presence of proteins of about 100 kDa with toxic activity upon *Phenacoccus herreni,* another type of insect. In this work, the authors performed a strategy of extraction that eliminated nonprotein compounds, being able to demonstrate the potential of the species to obtain insecticidal proteins [56]. Leaf extract of *J. gossypiifolia* reduced the fecundity and egg viability against stored product insect pests *Tribolium castaneum* [133].

The potential molluscicidal activity of *J. gossypiifolia* has also been evaluated as an alternative mode of prevention of schistosomiasis. Sukumaran et al. [134] showed that the methanol and *n*-butanol extracts from unripened seeds of *J. gossypiifolia* was toxic against eggs and adults of two species of freshwater snails, *Lymnaea luteola* and *Indoplanorbis exustus*. The results indicated that *n*-butanol extract was the most effective and that the eggs were more susceptible than adults [134].

8. Toxicology

Species of *Jatropha* are notably known for their toxic potential [135, 136]. This toxicity is related primarily to latex and seeds. The latex is released from the aerial parts of the plant by mechanical injury and it is extremely caustic and irritating to skin and mucous membranes. The seeds are rich in toxalbumins that cause agglutination and hemolysis to erythrocytes as well as damage to other cell types and contain a lipoid resin complex that can cause dermatitis [3, 12, 135]. The symptomatology consists, in general, of gastrointestinal disorders (abdominal pain, nausea, vomiting, and diarrhea). Additionally, the clinical course can bring cardiovascular, neurological, and renal complications [136]. Cases of poisoning in humans usually occur by eating fruit and seeds because of its similarity to edible chestnuts [136].

Some toxicological studies have demonstrated the toxic properties of *J. gossypiifolia*, while others show the absence of toxicity. However, it is important to observe the models used, doses administrated, and types of extract employed (solvent and plant part), among other aspects, to make the proper conclusions about the toxicity.

The study of experimental poisoning in sheep showed that the intake of fresh plant leaves in a single dose of 40 g/kg was lethal to these animals [137]. The clinical and pathological picture in the experimental sheep was characterized by digestive, lung, and heart disturbances and also by slight regressive changes evidenced in hepatic and renal histological examinations [137]. However, as observed by Mariz et al. [7], it is important to note that the medicinal use of the plant is rarely *in natura*, but instead by different preparations, such as infusions or decoctions, sometimes of the dried material, which could inactivate the possible toxic components. However, this is only a hypothesis, and so the toxicity of extracts from leaves cannot be discarded.

One of the first studies relating the identification of the constituents responsible for the toxic effects of the *Jatropha* species was published by Adolf et al. [69]. In this work, by a bioguided isolation, the irritant polyunsaturated ester 12-deoxy-16-hydroxylphorbol was isolated from the ether extract from the seeds of *J. gossypiifolia* by countercurrent chromatography [69]. The irritant activity was visualized in mouse ear after 24 h of the application of the fractions and isolated compounds [69].

The *in vitro* cytotoxicity assay using brine shrimp larvae test revealed that ethanol and methanol extracts (plant organ unspecified) showed low toxicity [138]. An earlier study showed that the water and ethyl acetate fraction of a methanol extract from aerial parts of *J. gossypiifolia* did not present toxicity against the same organisms [114].

A study performed in Wistar rats evaluated the toxicity of the ethanolic root extract of *J. gossypiifolia* at 10, 20, and 30 mg/kg by oral route [139]. The authors observed that the extract was toxic to the kidney and caused increased urea retention in the blood, as observed by histological studies and biochemical analysis of blood [139].

A preclinical toxicological assessment of the crude ethanol extract from *J. gossypiifolia* leaves showed that the extract presents relatively low oral acute toxicity in Wistar rats [18, 19]. Rats treated with single doses of 1.2–5.0 g/kg by oral route were observed for 14 days, and the most important signs of toxicity were ptosis, reduction of body weight, and hind limb paralysis. Other significant alterations occurred only in males treated with 5.0 g/kg dose: increase in creatinine, aspartate aminotransferase, sodium and potassium seric levels, reduction of urea and albumin, leucopenia and small alteration in color, and consistency of viscera. The median lethal dose (LD_{50}) was higher than 4.0 g/kg for males and higher than 5.0 g/kg for females [19]. In the histopathological evaluation some alteration was observed in liver and lung only at 5.0 g/kg, suggesting the relatively low toxicity of the extract [18]. However, in the chronic toxicological study (thirteen weeks of treatment), this extract showed significant oral chronic toxicity in rats [17]. The most significant toxic signs indicated a reduction of the activity in the central nervous system and digestive disturbances. The histopathological analysis revealed hepatotoxicity and pulmonary damages. The lethality was 46.6% and 13.3% among males and females under the higher tested dose (405 mg/kg), respectively [17]. Based on this, Mariz et al. [7] discussed that the development of herbal medicine based on this species needs to prioritize the chemical refinement of the crude extracts to obtain less toxic fractions, which should be tested for their safety and therapeutic efficacy.

Another study, on the other hand, evaluating the oral acute toxicity of the aqueous and ethanol extracts from leaves of *J. gossypiifolia*, did not show any sign of toxicity in up to 2 g/kg in rats, enabling the authors to conclude that this extract could be considered safe [118]. This is an interesting result since in most cases the plant is used popularly as tea (aqueous extract).

The toxicity of the stem latex of *J. gossypiifolia* was studied in Wistar rats by applying different doses of crude latex on incised skin daily for 18 days, based on the popular use of the latex as hemostatic agent in skin lesions [140]. The authors observed that the application of the latex did not produce any significant difference in results of biochemical

and hematological parameters obtained from the control and experimental animals, leading to the conclusion that the stem latex has no harmful effects [140].

9. Conclusions

As demonstrated by this review, *J. gossypiifolia* presents an important potential for the generation of pharmacological and/or biotechnological products, based on popular uses and biological studies scientifically showing its properties. However, regarding specifically its medicinal properties, further studies are still necessary to assay important folk uses of the species and characterize the major compounds responsible for the bioactivity. Thus, studies of bioprospecting could prioritize this species, since many popular uses for various medical purposes are reported, demonstrating a great potential to originate bioactive molecules with pharmacological relevance. Furthermore, future phytochemical studies of this plant are important to obtain the best knowledge of the chemical composition of different extracts of the plant, in order to recognize the really important compounds in the pharmacological actions, aspiring to the chemical refinement of the products to eliminate the eventual toxic effects that could reduce the medicinal value of the species. In conclusion, the data presented in this review could provide insights for future research aimed at both ethnopharmacological validation of the popular use of *J. gossypiifolia* and its exploration as a new source of bioactive molecules for herbal drugs and/or bioactive natural products for potential application in complementary and alternative medicine.

Conflict of Interests

The authors declare that there is no conflict of interests regarding the publication of this paper.

Acknowledgments

The authors thank BNB, CNPq, and CAPES (Brazil) for the financial support. Matheus de Freitas Fernandes-Pedrosa gives thanks to CNPq for Scholarship in Research Productivity. The authors also thank Andrew Alastair Cumming for editing this paper for the English revision.

References

[1] G. L. Webster, "Classification of the euphorbiaceae," *Annals of the Missouri Botanical Garden*, vol. 81, pp. 3–143, 1994.

[2] M. V. Alves, "Checklist das espécies de Euphorbiaceae Juss. ocorrentes no semi-árido pernambucano, Brasil," *Acta Botância Brasileira*, vol. 12, no. 3, pp. 485–495, 1998.

[3] C. W. Sabandar, N. Ahmat, F. M. Jaafar, and I. Sahidin, "Medicinal property, phytochemistry and pharmacology of several *Jatropha* species (Euphorbiaceae): a review," *Phytochemistry*, vol. 85, pp. 7–29, 2013.

[4] C. K. A. Leal and M. D. F. Agra, "Estudo farmacobotânico comparativo das folhas de *Jatropha molissima* (Pohl) Baill," *Acta Farmaceutica Bonaerense*, vol. 24, no. 1, pp. 5–13, 2005.

[5] L. C. Di Stasi and C. A. Hiruma-Lima, *Plantas medicinais na Amazônia e na Mata Atlântica*, UNESP, São Paulo, Brazil, 2nd edition, 2002.

[6] M. D. F. Agra, K. N. Silva, I. J. L. D. Basílio, P. F. De Freitas, and J. M. Barbosa-Filho, "Survey of medicinal plants used in the region Northeast of Brazil," *Brazilian Journal of Pharmacognosy*, vol. 18, no. 3, pp. 472–508, 2008.

[7] S. R. Mariz, A. C. R. Borges, M. F. F. Melo-Diniz, and I. A. Medeiros, "Possibilidades terapêuticas e riscos toxicológicos de *Jatropha gossypiifolia* L.: uma revisão narrativa," *Revista Brasileira De Plantas Medicinais*, vol. 12, no. 3, pp. 346–357, 2010.

[8] I. Cordeiro and R. Secco, "*Jatropha gossypiifolia* L. Lista de espécies da flora do Brasil," *Jardim Botânico do Rio de Janeiro*, http://floradobrasil.jbrj.gov.br/jabot/floradobrasil/FB17581.

[9] U. P. de Albuquerque, P. M. de Medeiros, A. L. S. de Almeida et al., "Medicinal plants of the caatinga (semi-arid) vegetation of NE Brazil: a quantitative approach," *Journal of Ethnopharmacology*, vol. 114, no. 3, pp. 325–354, 2007.

[10] U. P. Albuquerque, L. H. C. Andrade, and J. Caballero, "Structure and floristics of homegardens in Northeastern Brazil," *Journal of Arid Environments*, vol. 62, no. 3, pp. 491–506, 2005.

[11] S. A. Ceasar and S. Ignacimuthu, "Applications of biotechnology and biochemical engineering for the improvement of Jatropha and Biodiesel: a review," *Renewable and Sustainable Energy Reviews*, vol. 15, no. 9, pp. 5176–5185, 2011.

[12] U. P. de Albuquerque, J. M. Monteiro, M. A. Ramos, and E. L. C. de Amorim, "Medicinal and magic plants from a public market in northeastern Brazil," *Journal of Ethnopharmacology*, vol. 110, no. 1, pp. 76–91, 2007.

[13] A. Falodun, Q. Sheng-Xiang, G. Parkinson, and S. Gibbons, "Isolation and characterization of a new anticancer diterpenoid from *Jatropha gossypifolia*," *Pharmaceutical Chemistry Journal*, vol. 45, no. 10, pp. 636–639, 2012.

[14] BRASIL, "Fitoterapia: plantas de interesse ao SUS," *Brazilian Health Ministry*, http://portal.saude.gov.br/portal/arquivos/pdf/RENISUS.pdf.

[15] X.-P. Zhang, M.-L. Zhang, X.-H. Su, C.-H. Huo, Y.-C. Gu, and Q.-W. Shi, "Chemical constituents of the plants from genus Jatropha," *Chemistry and Biodiversity*, vol. 6, no. 12, pp. 2166–2183, 2009.

[16] S. K. Sharma and H. Singh, "A review on pharmacological significance of genus *Jatropha* (Euphorbiaceae)," *Chinese Journal of Integrative Medicine*, vol. 18, no. 11, pp. 868–880, 2012.

[17] S. R. Mariz, G. S. Cerqueira, W. C. Araújo et al., "Chronic toxicologic study of the ethanolic extract of the aerial parts of *Jatropha gossypiifolia* in rats," *Revista Brasileira de Farmacognosia*, vol. 22, no. 3, pp. 663–668, 2012.

[18] S. R. Mariz, M. S. T. Araujo, G. S. Cerqueira et al., "Histopathological evaluation in rats after acute treatment with the ethanol extract from aerial parts of *Jatropha gossypiifolia* L," *Revista Brasileira De Farmacognosia*, vol. 18, no. 2, pp. 213–216, 2008.

[19] S. R. Mariz, G. S. Cerqueira, W. C. Araújo et al., "Estudo toxicológico agudo do extrato etanólico de partes aéreas de *Jatropha gossypiifolia* L. em ratos," *Revista Brasileira de Farmacognosia*, vol. 16, no. 3, pp. 372–378, 2006.

[20] C. Auvin-Guette, C. Baraguey, A. Blond, J. L. Pousset, and B. Bodo, "Cyclogossine B, a cyclic octapeptide from *Jatropha gossypifolia*," *Journal of Natural Products*, vol. 60, pp. 1155–1157, 1997.

[21] V. S. Parvathi, B. S. Jyothi, T. Lakshmi, P. S. Babu, and R. Karthikeyan, "Morpho-anatomical and physicochemical studies of *Jatropha gossypifolia* (L.)," *Der Pharmacia Lettre*, vol. 4, no. 1, pp. 256–262, 2012.

[22] M. N. S. Rios and F. Pastore Junior, *Plantas da Amazônia: 450 Espécies de Uso Geral*, Universidade de Brasília—Biblioteca Central, Brasília, 2011.

[23] S. R. Mariz, *Estudo toxicológico pré-clínico de Jatropha gossypiifolia L. [Ph.D. thesis]*, Universidade Federal da Paraíba, João Pessoa, Brazil, 2007.

[24] O. G. Adeosun, T. Oduola, F. A. Fagbomedo et al., "Suitability of stem latex of *Jatropha gossypifolia* as a protein precipitant for biochemical analysis," *Indian Journal of Clinical Biochemistry*, vol. 29, no. 2, pp. 210–212, 2014.

[25] F. O. A. Ajose, "Some Nigerian plants of dermatologic importance," *International Journal of Dermatology*, vol. 46, no. 1, pp. 48–55, 2007.

[26] J. S. Ashidi, P. J. Houghton, P. J. Hylands, and T. Efferth, "Ethnobotanical survey and cytotoxicity testing of plants of South-western Nigeria used to treat cancer, with isolation of cytotoxic constituents from Cajanus cajan Millsp. leaves," *Journal of Ethnopharmacology*, vol. 128, no. 2, pp. 501–512, 2010.

[27] M. Ayyanar and S. Ignacimuthu, "Ethnobotanical survey of medicinal plants commonly used by Kani tribals in Tirunelveli hills of Western Ghats, India," *Journal of Ethnopharmacology*, vol. 134, no. 3, pp. 851–864, 2011.

[28] R. Bhagat, S. D. Ambavade, A. V. Misar, and D. K. Kulkarni, "Anti-inflammatory activity of *Jatropha gossypifolia* L. leaves in albino mice and Wistar rat," *Journal of Scientific and Industrial Research*, vol. 70, no. 4, pp. 289–292, 2011.

[29] J. H. Cano and G. Volpato, "Herbal mixtures in the traditional medicine of Eastern Cuba," *Journal of Ethnopharmacology*, vol. 90, no. 2-3, pp. 293–316, 2004.

[30] F. G. Coe and G. J. Anderson, "Screening of medicinal plants used by the Garífuna of Eastern Nicaragua for bioactive compounds," *Journal of Ethnopharmacology*, vol. 53, no. 1, pp. 29–50, 1996.

[31] M. Gbeassor, Y. Kossou, K. Amegbo, C. De Souza, K. Koumaglo, and A. Denke, "Antimalarial effects of eight African medicinal plants," *Journal of Ethnopharmacology*, vol. 25, no. 1, pp. 115–118, 1989.

[32] National Center for Biotechnology Information, "*Jatropha gossypiifolia*," *Taxonomy Browser*, http://www.ncbi.nlm.nih.gov/Taxonomy/Browser/wwwtax.cgi?id=454931.

[33] Tropicos, "*Jatropha gossypiifolia* L.," http://www.tropicos.org/NamePrint.aspx?nameid=12802174&tab=details.

[34] The Plant List, "*Jatropha gossypiifolia* L.," http://www.theplantlist.org/tpl/record/kew-104621.

[35] M. S. Khyade and N. P. Vaikos, "Pharmacognostical and phytochemical evaluation of leaf of *Jatropha gossypifolia* L.," *International Journal of Research in Ayurveda & Pharmacy*, vol. 2, no. 1, pp. 177–180, 2011.

[36] D. O. Aworinde, D. U. Nwoye, A. A. Jayeola, A. O. Olagoke, and A. A. Ogundele, "Taxonomic significance of foliar epidermis in some members of euphorbiaceae family in Nigeria," *Research Journal of Botany*, vol. 4, no. 1, pp. 17–28, 2009.

[37] J. D. Olowokudejo, "Comparative epidermal morphology of West African species of Jatropha L. (Euphorbiaceae)," *Botanical Journal of the Linnean Society*, vol. 111, no. 2, pp. 139–154, 1993.

[38] B. Das and B. Venkataiah, "A minor coumarino-lignoid from *Jatropha gossypifolia*," *Biochemical Systematics and Ecology*, vol. 29, no. 2, pp. 213–214, 2001.

[39] B. Das, B. Venkataiah, and A. Kashinatham, "Venkatasin, a new coumarino-lignoid from *Jatropha gossypifolia*," *Natural Product Letters*, vol. 13, no. 4, pp. 293–297, 1999.

[40] B. Das and B. Venkataiah, "A rare diterpene from *Jatropha gossypifolia*," *Biochemical Systematics and Ecology*, vol. 27, no. 7, pp. 759–760, 1999.

[41] N. Ravindranath, B. Venkataiah, C. Ramesh, P. Jayaprakash, and B. Das, "Jatrophenone, a novel macrocyclic bioactive diterpene from *Jatropha gossypifolia*," *Chemical and Pharmaceutical Bulletin*, vol. 51, no. 7, pp. 870–871, 2003.

[42] B. Das and J. Banerji, "Arylnaphthalene lignan from *Jatropha gossypifolia*," *Phytochemistry*, vol. 27, no. 11, pp. 3684–3686, 1988.

[43] J. Banerji, B. Das, A. Chatterjee, and J. N. Shoolery, "Gadain, a lignan from *Jatropha gossypifolia*," *Phytochemistry*, vol. 23, no. 10, pp. 2323–2327, 1984.

[44] A. Chatterjee, B. Das, C. Pascard, and T. Prange, "Crystal structure of a lignan from *Jatropha gossypifolia*," *Phytochemistry*, vol. 20, no. 8, pp. 2047–2048, 1981.

[45] I. C. Abreu, A. S. S. Marinho, A. M. A. Paes et al., "Hypotensive and vasorelaxant effects of ethanolic extract from *Jatropha gossypiifolia* L. in rats," *Fitoterapia*, vol. 74, no. 7-8, pp. 650–657, 2003.

[46] B. Das and R. Das, "Gossypifan, a lignan from *Jatropha gossypifolia*," *Phytochemistry*, vol. 40, no. 3, pp. 931–932, 1995.

[47] R. Das, B. Das, and A. Kashinatham, "Gossypiline, a new lignan from *Jatropha gossypifolia*," *Natural Product Sciences*, vol. 4, no. 4, pp. 238–240, 1998.

[48] D. Shahwar, S.-U. Shafiq, N. Ahmad, S. Ullah, and M. A. Raza, "Antioxidant activities of the selected plants from the family Euphorbiaceae, Lauraceae, Malvaceae and Balsaminaceae," *African Journal of Biotechnology*, vol. 9, no. 7, pp. 1086–1096, 2010.

[49] V. Bullangpoti, N. Khumrungsee, W. Pluempanupat, Y. Kainoh, and U. Saguanpong, "Toxicity of ethyl acetate extract and ricinine from *Jatropha gossypifolia* senescent leaves against *Spodoptera exigua* Hubner (Lepidoptera: Noctuidae)," *Journal of Pesticide Science*, vol. 36, no. 2, pp. 260–263, 2011.

[50] A. O. Ogundare, "Antimicrobial effect of *Tithonia diversifolia* and *Jatropha gossypifolia* leaf extracts," *Trends in Applied Sciences Research*, vol. 2, no. 2, pp. 145–150, 2007.

[51] N. Nwokocha, A. Blessing, I. O. Agbagwa, and B. E. Okoli, "Comparative phytochemical screening of *Jatropha* L. Species in the Niger Delta," *Research Journal of Phytochemistry*, vol. 5, no. 2, pp. 107–114, 2011.

[52] R. Seth and R. Sarin, "Analysis of the phytochemical content and anti-microbial activity of *Jatropha gossypifolia* L.," *Archives of Applied Science Research*, vol. 2, no. 5, pp. 285–291, 2010.

[53] S. Sankara Subramanian, S. Nagarajan, and N. Sulochana, "Flavonoids of the leaves of *Jatropha gossypifolia*," *Phytochemistry*, vol. 10, no. 7, p. 1690, 1971.

[54] A. C. Pilon, R. L. Carneiro, F. Carnevale Neto, V. S. Bolzani, and I. Castro-Gamboa, "Interval multivariate curve resolution in the dereplication of HPLC-DAD data from *Jatropha gossypifolia*," *Phytochemical Analysis*, vol. 24, no. 4, pp. 401–406, 2013.

[55] A. R. Kharat, A. K. Dolui, and S. Das, "Free radical scavenging potential of *Jatropha gossypifolia*," *Asian Journal of Chemistry*, vol. 23, no. 2, pp. 799–801, 2011.

[56] P.-A. Calatayud, D. F. Munera, S. Calatayud, A. Valencia-Jimenez, and A. C. Bellotti, "*Jatropha gossypiifolia* (Euphorbiaceae), a source of proteins toxic to *Phenacoccus herreni* (Sternorryncha: Pseudococcidae)," *Florida Entomologist*, vol. 94, no. 3, pp. 649–654, 2011.

[57] W. F. Tinto, L. M. D. John, W. F. Reynolds, and S. McLean, "Triterpenoids of *Jatropha gossypiifolia*," *Journal of Natural Products*, vol. 55, no. 6, pp. 807–809, 1992.

[58] R. Das, K. Venkateswarlu, V. Saidi Reddy, and B. Das, "4′-*O*-demethyl retrochinensin a minor new lignan from *Jatropha gossypifolia*," *Indian Journal of Heterocyclic Chemistry*, vol. 14, no. 2, pp. 169–170, 2004.

[59] B. Das, A. Kashinatham, B. Venkataiah, K. V. N. S. Srinivas, G. Mahender, and M. R. Reddy, "Cleomiscosin A, a coumarino-lignoid from *Jatropha gossypifolia*," *Biochemical Systematics and Ecology*, vol. 31, no. 10, pp. 1189–1191, 2003.

[60] B. Das and G. Anjani, "Gossypidien, a lignan from stems of *Jatropha gossypifollia*," *Phytochemistry*, vol. 51, no. 1, pp. 115–117, 1999.

[61] B. Das, S. P. Rao, and K. V. Srinivas, "Isolation of isogadain from *Jatropha gossypifolia*," *Planta Medica*, vol. 62, no. 1, article 90, 1996.

[62] B. Das, S. P. Rao, K. V. N. S. Srinivas, and R. Das, "Jatrodien, a lignan from stems of *Jatropha gossypifolia*," *Phytochemistry*, vol. 41, no. 3, pp. 985–987, 1996.

[63] A. Chatterjee, B. Das, R. Chakrabarti et al., "Prasanthaline: a new lignan from *Jatropha gossypifolia* Linn.," *Indian Journal of Chemistry*, vol. 27, pp. 740–741, 1988.

[64] M. D. Taylor, A. B. Smith III, G. T. Furst et al., "New antileukemic jatrophone derivatives from *Jatropha gossypiifolia* structural and stereochemical assignment through nuclear magnetic resonance Spectroscopy," *Journal of the American Chemical Society*, vol. 105, no. 10, pp. 3177–3183, 1983.

[65] K. K. Purushothaman, S. Chandrasekharan, A. F. Cameron et al., "Jatropholones A and B, new diterpenoids from the roots of *Jatropha gossypiifolia* (Euphorbiaceae)—crystal structure analysis of Jatropholone B," *Tetrahedron Letters*, vol. 20, no. 11, pp. 979–980, 1979.

[66] S. M. Kupchan, C. W. Sigel, M. J. Matz, J. A. S. Renauld, R. C. Haltiwanger, and R. F. Bryan, "Jatrophone, a novel macrocyclic diterpenoid tumor inhibitor from *Jatropha gossypiifolia*," *Journal of the American Chemical Society*, vol. 92, no. 14, pp. 4476–4477, 1970.

[67] Y. R. Prasad, G. S. J. G. Alankararao, and P. Baby, "Constituents of the seeds of *Jatropha gossypifolia*," *Fitoterapia*, vol. 64, no. 4, p. 376, 1993.

[68] O. Ogbobe and V. Akano, "The physico-chemical properties of the seed and seed oil of *Jatropha gossypifolia*," *Plant Foods for Human Nutrition*, vol. 43, no. 3, pp. 197–200, 1993.

[69] W. Adolf, H. J. Opferkuch, and E. Hecker, "Irritant phorbol derivatives from four *Jatropha* species," *Phytochemistry*, vol. 23, no. 1, pp. 129–132, 1984.

[70] K. M. Hosamani and K. S. Katagi, "Characterization and structure elucidation of 12-hydroxyoctadec-cis-9-enoic acid in *Jatropha gossypifolia* and *Hevea brasiliensis* seed oils: a rich source of hydroxy fatty acid," *Chemistry and Physics of Lipids*, vol. 152, no. 1, pp. 9–12, 2008.

[71] S. F. A. J. Horsten, A. J. J. Van Den Berg, J. J. Kettenes-Van Den Bosch, B. R. Leeflang, and R. P. Labadie, "Cyclogossine A: a novel cyclic heptapeptide isolated from the latex of *Jatropha gossypifolia*," *Planta Medica*, vol. 62, no. 1, pp. 46–50, 1996.

[72] M. U. Ahmad, M. R. Islam, A. H. Mirza, B. H. Chowdhury, and N. Nahar, "Alkaloids of *Jatropha gossypifolia* Linn," *Indian Journal of Chemistry B: Organic Chemistry Including Medicinal Chemistry*, vol. 31, no. 1, pp. 67–69, 1992.

[73] A. Falodun, U. Kragl, S.-M. T. Touem, A. Villinger, T. Fahrenwaldt, and P. Langer, "A novel anticancer diterpenoid from *Jatropha gossypifolia*," *Natural Product Communications*, vol. 7, no. 2, pp. 151–152, 2012.

[74] G. D. Wadankar, S. N. Malode, and S. L. Sarambekar, "Traditionally used medicinal plants for ound healing in the Washim district, Maharashtra (India)," *International Journal of PharmTech Research*, vol. 3, no. 4, pp. 2080–2084, 2011.

[75] B. Kumar, M. Vijayakumar, R. Govindarajan, and P. Pushpangadan, "Ethnopharmacological approaches to wound healing-Exploring medicinal plants of India," *Journal of Ethnopharmacology*, vol. 114, no. 2, pp. 103–113, 2007.

[76] K. Koudouvo, D. S. Karou, K. Kokou et al., "An ethnobotanical study of antimalarial plants in Togo Maritime Region," *Journal of Ethnopharmacology*, vol. 134, no. 1, pp. 183–190, 2011.

[77] M. Coelho-Ferreira, "Medicinal knowledge and plant utilization in an Amazonian coastal community of Marudá, Pará State (Brazil)," *Journal of Ethnopharmacology*, vol. 126, no. 1, pp. 159–175, 2009.

[78] F. C. S. Oliveira, R. F. M. Barros, and J. M. Moita Neto, "Plantas medicinais utilizadas em comunidades rurais de Oeiras, semiárido piauiense," *Revista Brasileira de Plantas Medicinais*, vol. 12, no. 3, pp. 282–301, 2010.

[79] J. D. F. L. Santos, E. Pagani, J. Ramos, and E. Rodrigues, "Observations on the therapeutic practices of riverine communities of the Unini River, AM, Brazil," *Journal of Ethnopharmacology*, vol. 142, no. 2, pp. 503–515, 2012.

[80] S. L. Cartaxo, M. M. de Almeida Souza, and U. P. de Albuquerque, "Medicinal plants with bioprospecting potential used in semi-arid northeastern Brazil," *Journal of Ethnopharmacology*, vol. 131, no. 2, pp. 326–342, 2010.

[81] O. Jansen, L. Angenot, M. Tits et al., "Evaluation of 13 selected medicinal plants from Burkina Faso for their antiplasmodial properties," *Journal of Ethnopharmacology*, vol. 130, no. 1, pp. 143–150, 2010.

[82] M. H. Yetein, L. G. Houessou, T. O. Lougbégnon, O. Teka, and B. Tente, "Ethnobotanical study of medicinal plants used for the treatment of malaria in plateau of Allada, Benin (West Africa)," *Journal of Ethnopharmacology*, vol. 146, no. 1, pp. 154–163, 2013.

[83] L. J. Quintans Junior, J. R. G. S. Almeida, J. T. Lima et al., "Plants with anticonvulsivant properties—a review," *Revista Brasileira de Farmacognosia*, vol. 18, pp. 798–819, 2008.

[84] A. Diallo, M. S. Traore, S. M. Keita et al., "Management of diabetes in Guinean traditional medicine: an ethnobotanical investigation in the coastal lowlands," *Journal of Ethnopharmacology*, vol. 144, no. 2, pp. 353–361, 2012.

[85] S. O. Olabanji, A. C. Adebajo, O. R. Omobuwajo et al., "PIXE analysis of some Nigerian anti-diabetic medicinal plants (II)," *Nuclear Instruments and Methods in Physics Research B: Beam Interactions With Materials and Atoms*, vol. 318, pp. 187–190, 2014.

[86] T. Oduola, O. G. Avwioro, and T. B. Ayanniyi, "Suitability of the leaf extract of *Jatropha gossypifolia* as an anticoagulant for biochemical and haematological analyses," *African Journal of Biotechnology*, vol. 4, no. 7, pp. 679–681, 2005.

[87] C. M. Chariandy, C. E. Seaforth, R. H. Phelps, G. V. Pollard, and B. P. S. Khambay, "Screening of medicinal plants from Trinidad and Tobago for antimicrobial and insecticidal properties," *Journal of Ethnopharmacology*, vol. 64, no. 3, pp. 265–270, 1999.

[88] V. P. Kumar, N. S. Chauhan, H. Padh, and M. Rajani, "Search for antibacterial and antifungal agents from selected Indian

medicinal plants," *Journal of Ethnopharmacology*, vol. 107, no. 2, pp. 182–188, 2006.

[89] R. Dabur, A. Gupta, T. K. Mandal et al., "Antimicrobial activity of some medicinal plants," *African Journal of Traditional, Complementary and Alternative Medicines*, vol. 4, no. 3, pp. 313–318, 2007.

[90] H. C. Ong and M. Nordiana, "Malay ethno-medico botany in Machang, Kelantan, Malaysia," *Fitoterapia*, vol. 70, no. 5, pp. 502–513, 1999.

[91] J. Sanz-Biset, J. Campos-de-la-Cruz, M. A. Epiquién-Rivera, and S. Cañigueral, "A first survey on the medicinal plants of the Chazuta valley (Peruvian Amazon)," *Journal of Ethnopharmacology*, vol. 122, no. 2, pp. 333–362, 2009.

[92] B. B. Panda, K. Gaur, M. L. Kori et al., "Anti-inflammatory and analgesic activity of *Jatropha gossypifolia* in experimental animal models," *Global Journal of Pharmacology*, vol. 3, no. 1, 2009.

[93] S. S. Ningthoujam, A. D. Talukdar, K. S. Potsangbam, and M. D. Choudhury, "Traditional uses of herbal vapour therapy in Manipur, North East India: an ethnobotanical survey," *Journal of Ethnopharmacology*, vol. 147, no. 1, pp. 136–147, 2013.

[94] A. Asase, A. A. Oteng-Yeboah, G. T. Odamtten, and M. S. J. Simmonds, "Ethnobotanical study of some Ghanaian anti-malarial plants," *Journal of Ethnopharmacology*, vol. 99, no. 2, pp. 273–279, 2005.

[95] C. Lans, T. Harper, K. Georges, and E. Bridgewater, "Medicinal and ethnoveterinary remedies of hunters in Trinidad," *BMC Complementary and Alternative Medicine*, vol. 1, article 10, 2001.

[96] L. Rasingam, S. Jeeva, and D. Kannan, "Dental care of Andaman and Nicobar folks: medicinal plants use as tooth stick," *Asian Pacific Journal of Tropical Biomedicine*, vol. 2, no. 2, pp. S1013–S1016, 2012.

[97] P. J. Houghton and I. M. Osibogun, "Flowering plants used against snakebite," *Journal of Ethnopharmacology*, vol. 39, no. 1, pp. 1–29, 1993.

[98] M. Molander, C. H. Saslis-Lagoudakis, A. K. Jäger, and N. Rønsted, "Cross-cultural comparison of medicinal floras used against snakebites," *Journal of Ethnopharmacology*, vol. 139, no. 3, pp. 863–872, 2012.

[99] A. Jain, S. S. Katewa, B. L. Chaudhary, and P. Galav, "Folk herbal medicines used in birth control and sexual diseases by tribals of southern Rajasthan, India," *Journal of Ethnopharmacology*, vol. 90, no. 1, pp. 171–177, 2004.

[100] A. Jain, S. S. Katewa, P. K. Galav, and P. Sharma, "Medicinal plant diversity of Sitamata wildlife sanctuary, Rajasthan, India," *Journal of Ethnopharmacology*, vol. 102, no. 2, pp. 143–157, 2005.

[101] T. Oduola, G. O. Adeosun, T. A. Oduola, G. O. Avwioro, and M. A. Oyeniyi, "Mechanism of action of Jatropha gossypifolia stem latex as a haemostatic agent," *European Journal of General Medicine*, vol. 2, no. 4, pp. 140–143, 2005.

[102] D. Garcia, M. V. Domingues, and E. Rodrigues, "Ethnopharmacological survey among migrants living in the Southeast Atlantic Forest of Diadema, São Paulo, Brazil," *Journal of Ethnobiology and Ethnomedicine*, vol. 6, article 29, 2010.

[103] S. S. Hebbar, V. H. Harsha, V. Shripathi, and G. R. Hegde, "Ethnomedicine of Dharwad district in Karnataka, India—plants used in oral health care," *Journal of Ethnopharmacology*, vol. 94, no. 2-3, pp. 261–266, 2004.

[104] S. B. Kosalge and R. A. Fursule, "Investigation of ethnomedicinal claims of some plants used by tribals of Satpuda Hills in India," *Journal of Ethnopharmacology*, vol. 121, no. 3, pp. 456–461, 2009.

[105] R. A. Ritter, M. V. B. Monteiro, F. O. B. Monteiro et al., "Ethnoveterinary knowledge and practices at Colares island, Pará state, eastern Amazon, Brazil," *Journal of Ethnopharmacology*, vol. 144, no. 2, pp. 346–352, 2012.

[106] S. K. Dash and S. Padhy, "Review on ethnomedicines for diarrhoea diseases from Orissa: prevalence versus culture," *Journal of Human Ecology*, vol. 20, no. 1, pp. 59–64, 2006.

[107] R. S. L. Taylor, J. B. Hudson, N. P. Manandhar, and G. H. N. Towers, "Antiviral activities of medicinal plants of southern Nepal," *Journal of Ethnopharmacology*, vol. 53, pp. 97–104, 1996.

[108] J. M. A. Maia, N. G. Czeczko, J. M. R. Filho et al., "Estudo da cicatrização de suturas na bexiga urinária de ratos com e sem utilização de extrato bruto de *Jatropha gossypiifolia* L. intraperitoneal," *Acta Cirúrgica Brasileira*, vol. 21, no. 2, pp. 23–30, 2006.

[109] A. L. Ososki, P. Lohr, M. Reiff et al., "Ethnobotanical literature survey of medicinal plants in the Dominican Republic used for women's health conditions," *Journal of Ethnopharmacology*, vol. 79, no. 3, pp. 285–298, 2002.

[110] A. S. Apu, F. Hossain, F. Rizwan et al., "Study of pharmacological activities of methanol extract of *Jatropha gossypifolia* fruits," *Journal of Basic and Clinical Pharmacy*, vol. 4, no. 1, pp. 20–24, 2013.

[111] A. S. Apu, K. Ireen, S. Hossan Bhuyan et al., "Evaluation of analgesic, neuropharmacological and anti-diarrheal potential of *Jatropha gossypifolia* (Linn.) leaves in mice," *Journal of Medical Sciences*, vol. 12, no. 8, pp. 274–279, 2012.

[112] F. A. G. Rocha and L. I. S. Dantas, "Atividade antimicrobiana *in vitro* do látex do aveloz (*Euphorbia tirucalli* L.), pinhão bravo (*Jatropha mollissima* L.) e pinhão roxo (*Jatropha gossypiifolia* L.) sobre microrganismos patogênicos," *Holos*, vol. 25, no. 4, 2009.

[113] O. M. David and J. O. Oluyege, "*In vitro* susceptibility of selected pathogenic bacteria to leaf extracts and latex of *Jatropha gossypiifolia*(L) and *Jatropha curcas* (L)," *Biosciences Biotechnology Research Asia*, vol. 3, no. 1, pp. 91–94, 2006.

[114] W. D. MacBae, J. B. Hudson, and G. H. N. Towers, "Studies on the pharmacological activity of amazonian euphorbiaceae," *Journal of Ethnopharmacology*, vol. 22, no. 2, pp. 143–172, 1988.

[115] M. C. Purohit and R. Purohit, "Evaluation of antimicrobial and anti-inflammatory activities of bark of *Jatropha gossypifolia*," *World Journal of Science and Technology*, vol. 1, no. 10, pp. 1–5, 2011.

[116] D. Singh and A. Singh, "The toxicity of four native Indian plants: effect on AChE and acid/alkaline phosphatase level in fish *Channa marulius*," *Chemosphere*, vol. 60, no. 1, pp. 135–140, 2005.

[117] C. M. Feitosa, R. M. Freitas, N. N. N. Luz, M. Z. B. Bezerra, and M. T. S. Trevisan, "Acetylcholinesterase inhibition by somes promising Brazilian medicinal plants," *Brazilian Journal of Biology*, vol. 71, no. 3, pp. 783–789, 2011.

[118] Y. Nagaharika, V. Kalyani, S. Rasheed, and R. Karthikeyan, "Anti-inflammatory activity of leaves of *Jatropha gossypifolia* L. by HRBC membrane stabilization method," *Journal of Acute Disease*, vol. 2, no. 2, pp. 156–158, 2013.

[119] S. D. N. Silva, I. C. Abreu, S. M. D. F. Freire et al., "Antispasmodic effect of *Jatropha gossypiifolia* is mediated through dual blockade of muscarinic receptors and Ca^{2+} channels," *Brazilian Journal of Pharmacognosy*, vol. 21, no. 4, pp. 715–720, 2011.

[120] D. Carabajal, A. Casaco, L. Arruzazabala, R. Gonzalez, and V. Fuentes, "Pharmacological screening of plant decoctions commonly used in Cuban folk medicine," *Journal of Ethnopharmacology*, vol. 33, no. 1-2, pp. 21–24, 1991.

[121] S. Jain, G. P. Choudhary, and D. K. Jain, "Pharmacological evaluation of anti-fertility activity of ethanolic extract of *Jatropha gossypifolia* leaf in female albino mice," *Asian Pacific Journal of Tropical Biomedicine*, vol. 2, no. 3, pp. S1671–S1674, 2012.

[122] S. C. N. Servin, O. J. M. Torres, J. E. F. Matias et al., "Ação do extrato de *Jatropha gossypiifolia* L., (pião roxo) na cicatrização de anastomose colônica: estudo experimental em ratos," *Acta Cirúrgica Brasileira*, vol. 21, no. 3, pp. 89–96, 2006.

[123] J. R. Vale, N. G. Czeczko, J. U. Aquino et al., "Estudo comparativo da cicatrização de gastrorrafias com e sem o uso do extrato de *Jatropha gossypiifolia* L., (pião roxo) em ratos," *Acta Cirúrgica Brasileira*, vol. 21, no. 3, pp. 40–48, 2006.

[124] J. U. Aquino, N. G. Czeczko, O. Malafaia et al., "Avaliação fitoterápica da *Jatropha gossypiifolia* L. na cicatrização de suturas na parede abdominal ventral de ratos," *Acta Cirúrgica Brasileira*, vol. 21, no. 2, pp. 61–66, 2006.

[125] M. F. D. S. Santos, N. G. Czeczko, P. A. N. Nassif et al., "Avaliação do uso do extrato bruto de *Jatropha gossypiifolia* L. na cicatrização de feridas cutâneas em ratos," *Acta Cirúrgica Brasileira*, vol. 21, no. 3, pp. 2–7, 2006.

[126] B. B. Panda, K. Gaur, R. K. Nema, C. S. Sharma, A. K. Jain, and C. P. Jain, "Hepatoprotective activity of Jatropha gossypifolia against carbon tetrachloride- induced hepatic injury in rats," *Asian Journal of Pharmaceutical and Clinical Research*, vol. 2, no. 1, pp. 50–54, 2009.

[127] S. S. Deo, T. M. Chaudhari, and F. Inam, "Evaluation of the immunomodulatory effects of 1-phenylnaphthalene and pericarbonyl lactone lignan compounds," *Der Pharma Chemica*, vol. 4, no. 2, pp. 771–776, 2012.

[128] S. K. Rasheed, S. Kunapareddy, and R. Karthikeyan, "Local anesthetic activity of *Jatropha gossypifolia* L. on frogs," *Biomedical and Pharmacology Journal*, vol. 5, no. 2, pp. 395–397, 2012.

[129] A. M. A. Paes, A. L. Camara, S. M. F. Freire, and M. O. R. Borges, "Relaxant effect of *Jatropha gossypiifolia* L. on uterine smooth muscle," *International Journal of Phytomedicine*, vol. 4, no. 3, pp. 310–313, 2012.

[130] S. J. Jain, G. P. Choudhary, and D. K. Jain, "Pharmacological evaluation and antifertility activity of *Jatropha gossypifolia* in rats," *BioMed Research International*, vol. 2013, Article ID 125980, 5 pages, 2013.

[131] J. S. de Oliveira, P. M. Leite, L. B. de Souza et al., "Characteristics and composition of *Jatropha gossypiifolia* and *Jatropha curcas* L. oils and application for biodiesel production," *Biomass and Bioenergy*, vol. 33, no. 3, pp. 449–453, 2009.

[132] V. Bullangpoti, E. Wajnberg, P. Audant, and R. Feyereisen, "Antifeedant activity of *Jatropha gossypifolia* and *Melia azedarach* senescent leaf extracts on *Spodoptera frugiperda* (Lepidoptera: Noctuidae) and their potential use as synergists," *Pest Management Science*, vol. 68, no. 9, pp. 1255–1264, 2012.

[133] S. N. K. Jilani, W. Islam, and M. Kamsh, "Potential of pyrethroid insecticides and plant extracts on fecundity and egg viability of tribolium castaneum (Herbst)," *Journal of Bio-Science*, vol. 19, no. 1, pp. 95–97, 2011.

[134] D. Sukumaran, B. D. Parashar, and K. M. Rao, "Toxicity of *Jatropha gossypiifolia* and *Vaccaria pyramidata* against freshwater snails vectors of animal schistosomiasis," *Fitoterapia*, vol. 66, no. 5, pp. 393–398, 1995.

[135] R. K. Devappa, H. P. S. Makkar, and K. Becker, "*Jatropha* toxicity—a review," *Journal of Toxicology and Environmental Health B: Critical Reviews*, vol. 13, no. 6, pp. 476–507, 2010.

[136] E. P. Schenkel, M. Zannin, L. A. Mentz, S. A. L. Bordignon, and B. Irgang, "Plantas tóxicas," in *Farmacognosia: Da Planta ao Medicamento*, C. M. O. Simões, E. P. Schenkel, G. Gosmann, J. C. P. Mello, L. A. Mentz, and P. R. Petrovick, Eds., pp. 959–993, Editora da UFRGS/UFSC, Porto Alegre, Brazil, 3d edition, 2007.

[137] L. I. Oliveira, F. F. Jabour, V. A. Nogueira, and E. M. Yamasaki, "Intoxicação experimental com as folhas de *Jatropha gossypifolia*(Euphorbiaceae) em ovinos," *Pesquisa Veterinária Brasileira*, vol. 28, no. 6, pp. 275–278, 2008.

[138] P. I. A. Awachie and F. O. Ugwu, "Preliminary investigation of the antimicrobial and brine shrimp lethality properties of some nigerian medicinal plants," *International Journal of Pharmacognosy*, vol. 35, no. 5, pp. 338–343, 1997.

[139] L. J. Medubi, V. O. Ukwenya, O. T. Aderinto et al., "Effects of administration of ethanolic root extract of *Jatropha gossypiifolia* and prednisolone on the kidneys of Wistar rats," *Electronic Journal of Biomedicine*, vol. 2, pp. 41–48, 2010.

[140] T. Oduola, G. B. Popoola, G. O. Avwioro et al., "Use of *Jatropha gossypifolia* stem latex as a haemostatic agent: how safe is it?" *Journal of Medicinal Plants Reasearch*, vol. 1, no. 1, pp. 14–17, 2007.

Hindawi Publishing Corporation
Evidence-Based Complementary and Alternative Medicine
Volume 2014, Article ID 247595, 12 pages
http://dx.doi.org/10.1155/2014/247595

Research Article

The Spectroscopy Study of the Binding of an Active Ingredient of *Dioscorea* Species with Bovine Serum Albumin with or without Co^{2+} or Zn^{2+}

He-Dong Bian,[1,2] Xia-Lian Peng,[2] Fu-Ping Huang,[2] Di Yao,[2] Qing Yu,[2] and Hong Liang[2]

[1] *Key Laboratory of Development and Application of Forest Chemicals of Guangxi, Guangxi University of Nationalities, Nanning 530006, China*
[2] *Key Laboratory for the Chemistry and Molecular Engineering of Medicinal Resources (Ministry of Education of China), School of Chemistry and Pharmaceutical Sciences of Guangxi Normal University, Guilin 541004, China*

Correspondence should be addressed to He-Dong Bian; gxunchem@163.com and Hong Liang; gxnuchem312@aliyun.com

Received 30 March 2014; Revised 6 May 2014; Accepted 15 May 2014; Published 4 June 2014

Academic Editor: Shi-Biao Wu

Diosgenin (DIO) is the active ingredient of *Dioscorea* species. The interaction of DIO with bovine serum albumin (BSA) was investigated through spectroscopic methods under simulated physiological conditions. The fluorescence quenching data revealed that the binding of DIO to BSA without or with Co^{2+} or Zn^{2+} was a static quenching process. The presence of Co^{2+} or Zn^{2+} both increased the static quenching constants K_{SV} and the binding affinity for the BSA-DIO system. In the sight of the competitive experiment and the negative values of ΔH^0 and ΔS^0, DIO bound to site I of BSA mainly through the hydrogen bond and Van der Waals' force. In addition, the conformational changes of BSA were studied by Raman spectra, which revealed that the secondary structure of BSA and microenvironment of the aromatic residues were changed by DIO. The Raman spectra analysis indicated that the changes of conformations, disulfide bridges, and the microenvironment of Tyr, Trp residues of BSA induced by DIO with Co^{2+} or Zn^{2+} were different from that without Co^{2+} or Zn^{2+}.

1. Introduction

Dioscoreaceae mainly distributes Guangdong, Sichuan, and Zhejiang provinces in China. Diosgenin (DIO), 3β-hydroxy-5-spirostene (Figure 1), one of the active ingredients of *Dioscorea* species, is derived from the tubers of *Dioscorea* species. The previous studies have indicated that DIO can retard the progression of osteoporosis [1] and attenuate plasma cholesterol [2], possess anti-inflammatory [3] and inhibition of vasoconstriction [4] effects, and so on.

Serum albumin (SA) is composed of three structurally homologous domains (I–III); each domain contains two subdomains (A and B). It is the major transport protein, which can act as a carrier of endogenous and exogenous ligands [5]. The transportation and distribution of the drugs in vivo are related to their interaction with serum albumin. On the other hand, the binding of drugs also can change the conformation function of serum albumin. So it is important to investigate the interaction between drugs and serum albumin. Bovine serum albumin (BSA) has similar structure and property with human serum albumin (HSA); the major difference between these two serum albumins was that there was only one Trp residue in HSA, but in BSA there were two Trp residues (^{134}Trp and ^{212}Trp). Compared with HSA, BSA was always selected as a model protein due to its low cost, unusual ligand-binding properties. The study of the interaction between drugs and BSA plays an important role in pharmacology and pharmacodynamics [6].

Blood plasma contains many metal ions which play important roles in the biochemical processes. The previous reports of interactions between serum albumin and several metal ions suggested that many metal ions have special binding sites on proteins [7–9]. The binding of drugs with serum albumin in the presence of metal ions was also extensively studied [10, 11]. The previous studies indicated that the presence of metal ions would not only affect the interaction

of serum albumin with drugs, but also the conformational changes of serum albumin induced by drugs. The metal ions of Co^{2+} and Zn^{2+} are abundant essential elements in organism which possess many biochemical functions. It is necessary to investigate the interaction of BSA-DIO in the presence of Co^{2+} or Zn^{2+}.

In this paper, we studied the binding of DIO with BSA under simulated physiological conditions of pH = 7.43. Fluorescence spectra and Raman spectra were employed to investigate the binding process and the changes of protein structure in the absence and presence of Co^{2+} or Zn^{2+}.

2. Materials and Methods

2.1. Materials. DIO (98%, purchased from Aladdin Reagent Company) was dissolved in ethanol to prepare a stock solution of 1×10^{-3} mol·L^{-1}. 0.05 mol·L^{-1} phosphate buffer solution (PBS) of pH = 7.43, contained 0.1 mol·L^{-1} NaCl. BSA (98%, fatty acid free, and globulin free, Sigma) was dissolved in PBS to prepare stock solution of 1×10^{-3} mol·L^{-1} and stored at 277 K, diluted before used. Ibuprofen and ketoprofen were dissolved in ethanol to prepare stock solution of 1×10^{-3} mol·L^{-1}, respectively. Sodium chloride, ethanol, zinc chloride, cobalt(II) chloride hexahydrate, and other experimental drugs are analytically pure reagents. Double distilled water was used throughout.

2.2. Fluorescence Spectrum. Fluorescence spectra were carried out on a RF-5301 fluorescence spectrophotometer (Japan Shimadzu Company). A solution of 5.0×10^{-7} mol·L^{-1} BSA was added in a 1.0 cm quartz cell; metal ions or DIO were then gradually added into BSA by microinjector. Scan the solution of BSA in the absence and presence of DIO or metal ions in the wavelength range of 300–500 nm, respectively. The slit widths were 5 nm/5 nm; the excitation wavelength was 280 nm. The reaction temperatures for DIO-BSA system without metal ions were controlled at 291 K, 298 K, and 306 K, respectively. The reaction temperatures for DIO-BSA system with Co^{2+} or Zn^{2+} were controlled at 298 K. For site marker experiment, BSA and site markers were mixed in equimolar concentrations at room temperature for 2 h, and then DIO was gradually added into the solution, scan the fluorescence spectra of the solution.

2.2.1. The Quenching Mechanism. In order to confirm the quenching mechanism induced by DIO, the fluorescence quenching was described by Stern-Volmer equation [12]:

$$\frac{F_0}{F} = 1 + k_q \tau_0 [Q] = 1 + K_{SV} [Q], \quad (1)$$

where F_0 and F are the fluorescence intensity in the absence and presence of quencher, respectively. k_q is the quenching rate constant. τ_0 is the average fluorescence lifetime of the biomolecule in the absence of quencher. $[Q]$ is the concentration of quencher. K_{SV} is the Stern-Volmer quenching constant. Since the fluorescence lifetime of the biopolymer is 10^{-8} s [13], K_{SV} and k_q can be obtained according to the slopes of the Stern-Volmer plots.

2.2.2. The Quenching Mechanism and the Binding Constant. The binding constants of the static quenching were calculated according to the modified Stern-Volmer equation [14]:

$$\frac{F_0}{(F_0 - F)} = \frac{1}{f} + \frac{1}{(Kf[Q])}, \quad (2)$$

where f is the fraction of accessible fluorescence and K is the effective quenching constant for the accessible fluorophores, which are analogous to associative binding constants.

2.2.3. Thermodynamic Parameters. The enthalpy change (ΔH^0) was regarded as a constant when the temperature changed little, then enthalpy change (ΔH^0) and entropy change (ΔS^0) can be obtained from Van't Hoff equation [15]:

$$\ln K = -\frac{\Delta H^0}{RT} + \frac{\Delta S^0}{R}, \quad (3)$$

$$\Delta G^0 = \Delta H^0 - T\Delta S^0 = -RT \ln K, \quad (4)$$

where R was the gas constant and ΔG^0 was the standard free energy change.

2.2.4. Energy Transfer Calculation. According to Forster's nonradiative energy transfer theory [16, 17], the energy transfer efficiency is decided not only by the distance between the acceptor and donor, but also the critical energy transfer distance (R_0); that is [18],

$$E = 1 - \frac{F}{F_0} = \frac{R_0^6}{R_0^6 + r^6}, \quad (5)$$

where r is the distance between acceptor and donor and R_0 is the critical distance in the case of the transfer efficiency is 50%

$$R_0^6 = 8.8 \times 10^{-25} K^2 n^{-4} \Phi J, \quad (6)$$

where K^2 is the spatial orientation factor of the dipole, n is the refractive index of the medium, Φ is the fluorescence quantum yield of donor, and J is the overlap integral of fluorescence emission spectrum of donor and absorption spectrum of acceptor

$$J = \frac{\sum F(\lambda) \varepsilon(\lambda) \lambda^4 \Delta\lambda}{\sum F(\lambda) \Delta\lambda}, \quad (7)$$

where $F(\lambda)$ is the fluorescence intensity of the donor at wavelength λ and $\varepsilon(\lambda)$ is the molar absorption coefficient of the acceptor at wavelength λ.

2.3. Raman Spectrum. The Raman spectra were recorded on a Renishaw Invia+Plus FT-Raman spectrometer using an Ar^+ laser with excitation wavelength of 514 nm. The laser power was 3 mW; the recording range was 200–2000 cm^{-1} with spectral resolution of 1 cm^{-1}. Scan the Raman spectra of 5×10^{-4} mol·L^{-1} BSA in the absence and presence of DIO and metal ions of the same concentration under the room

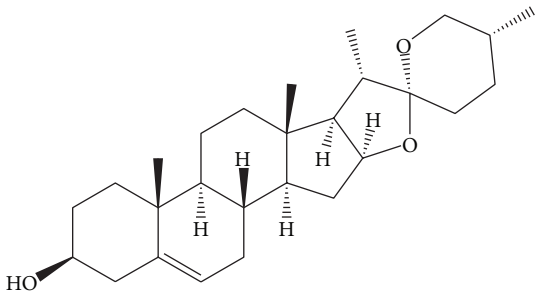

Figure 1: The chemical structure of diosgenin.

temperature. In Raman experiment, DIO was first dissolved in ethanol/water (1 : 9) and then mixed with BSA, metal ions solution to prepare Raman scanning sample. The curve fitting of Raman spectral regions was analysed by the curve-fitting procedure (Peak Analyzer module of Origin 8.0, Microcal Origin, USA) using Gaussian curves.

3. Results and Discussion

3.1. The Influence of DIO on the Fluorescence of BSA without or with Co^{2+} or Zn^{2+}. For macromolecules, the fluorescence measurements can give information of the binding of small molecule substances to protein. When excited at 280 nm, the intrinsic fluorescence of BSA was mainly contributed by Trp residues [19, 20]. The fluorescence of BSA quenched by DIO in the presence and absence of Co^{2+} or Zn^{2+} of the same concentration was shown in Figure 2. Figure 2(a) showed that the fluorescence intensity of BSA decreased regularly with increasing DIO. Meanwhile, the small blue shift observed with increasing DIO concentration indicated a more hydrophobic environment of the fluorescence chromophore of BSA [21]. Figures 2(b) and 2(c) showed that the fluorescence intensity decreased after adding Co^{2+} or Zn^{2+} with the same concentration. These indicated that the metal ions bind with BSA which is in accordance with our previous work. When DIO was added into BSA solution containing equimolar Co^{2+} or Zn^{2+}, the fluorescence intensity decreased regularly with blue shift. The shapes of spectra were similar to those in the absence of Co^{2+} or Zn^{2+}, while the fluorescence intensity in the presence of Co^{2+} or Zn^{2+} was weaker than those without Co^{2+} or Zn^{2+}. The result obtained suggested that the fluorescence was quenched not only by the metal ions but also by DIO. The interaction occurred among BSA, DIO, and the metal ions.

3.2. The Quenching Mechanism and the Binding Constant. Fluorescence quenching is classified as dynamic quenching and static quenching. Usually, static quenching is due to the formation of ground-state complex between fluorophore and quencher. The static quenching constant will decrease with increasing temperature, because higher temperature will lower the stability of the complex. Dynamic quenching results from collision between fluorophore and quencher, as higher temperatures result in larger diffusion coefficients, so the reverse effect is observed [22–24].

To confirm the quenching mechanism, the fluorescence quenching data were analyzed according to the Stern-Volmer equation (1). The Stern-Volmer plots of different temperatures and the corresponding results were shown in Figure 3 and Table 1. The results showed that K_{SV} decreased with increasing temperature, and k_q were much greater than 2.0×10^{10} L·mol^{-1}·s^{-1}, indicating a static quenching mechanism between BSA and DIO [25]. The quenching constants K_{SV} were both increased in the presence of Co^{2+} or Zn^{2+}, indicating that the presence of Co^{2+} or Zn^{2+} increased the fluorescence quenching effect of DIO. Meanwhile, the k_q values in the presence of Co^{2+} or Zn^{2+} suggest a static quenching mechanism for the binding of DIO to BSA with Co^{2+} or Zn^{2+}.

In order to obtain the binding constants, the experimental data were also analyzed according to the modified Stern-Volmer equation (2). Figure 4 showed the modified Stern-Volmer plots at different temperatures, and the calculated binding constants K for BSA-DIO system were listed in Table 2. The K values for the binding of DIO with BSA were decreased with increasing temperature, which further suggested that the binding of DIO with BSA was static quenching. The binding constants K for BSA-DIO system in the presence of Co^{2+} or Zn^{2+} were calculated to be 2.10×10^5 L·mol^{-1} and 1.94×10^5 L·mol^{-1}, respectively. The binding constants K for BSA-DIO system were both increased in the presence of Co^{2+} or Zn^{2+}, implying stronger binding of DIO to BSA in the present of Co^{2+} or Zn^{2+}.

3.3. The Nature of the Binding Forces. Generally, small organic molecules bound to biomolecules mainly through four types of acting forces: hydrogen bond, van der Waals' force, electrostatic force, and hydrophobic interaction, and so forth [26]. The force type can be determined by three thermodynamic parameters, enthalpy (ΔH^0), free-energy change (ΔG^0), and the entropy change (ΔS^0). These parameters for the interaction between DIO and BSA were calculated by Van't Hoff equation (3) and thermodynamic equation (4). The Van't Hoff plots were shown in Figure 5, and the thermodynamic parameters were listed in Table 2. The negative ΔG^0 suggested that the reactions between DIO and BSA were spontaneous. DIO bound to BSA mainly through the hydrogen bond and Van der Waals' force as evidenced by the negative value of ΔH^0 and ΔS^0 [27].

3.4. Energy Transfer between Drugs and BSA. The overlap of the absorption spectrum of DIO and the fluorescence emission spectrum of BSA is shown in Figure 6. For BSA, $K^2 = 2/3$, $\Phi = 0.15$, and $n = 1.336$ [28]; then we can obtain the following results: $J = 8.36 \times 10^{-14}$ cm^3·L·mol^{-1}, $R_0 = 3.64$ nm, and $r = 5.36$ nm. The distance between BSA and DIO was smaller than 8 nm, which suggested that the quenching of BSA by DIO was static quenching, which was in accordance with the results above.

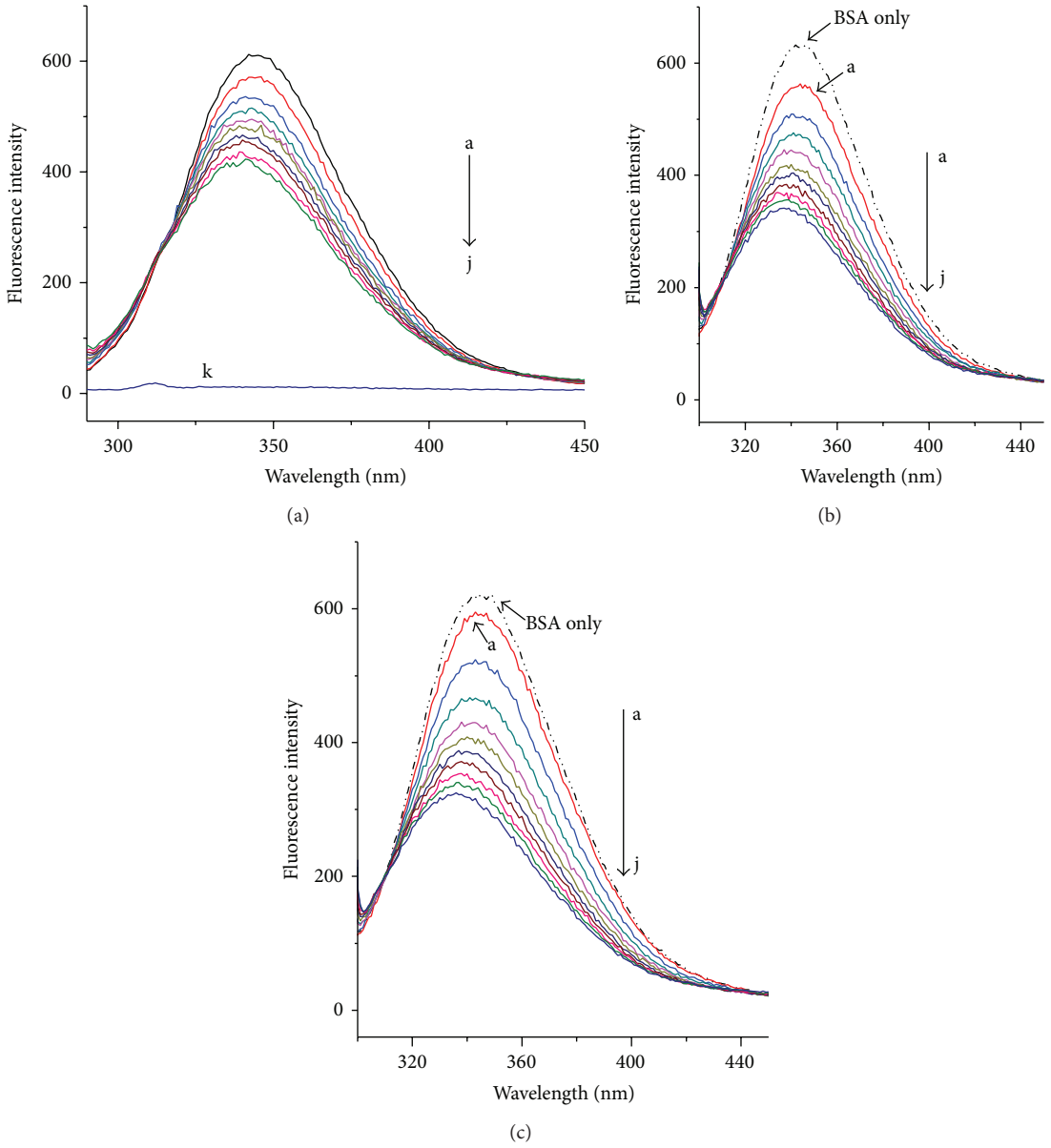

Figure 2: The fluorescence spectra of BSA by DIO in the absence and presence of Co^{2+} or Zn^{2+}. (a) BSA-DIO system; (b) BSA-DIO-Co^{2+} system; (c) BSA-DIO-Zn^{2+} system. From a to j, the concentration of DIO was varied from 0 to 9×10^{-6} mol·L^{-1} at increments of 1×10^{-6} mol·L^{-1}. k: DIO only, 9×10^{-6} mol·L^{-1}. [BSA] = [Co^{2+}] = [Zn^{2+}] = 5×10^{-7} mol·L^{-1}, T = 298 K.

Table 1: The Stern-Volmer quenching constants of DIO with BSA.

	T (K)	K_{SV} ($\times 10^4$·mol^{-1})	k_q ($\times 10^{12}$ L·mol^{-1}·s^{-1})	R^a	S.D.[b]
DIO-BSA	291	7.47	7.47	0.9928	0.03
	298	5.23	5.23	0.9947	0.02
	306	4.31	5.23	0.9964	0.01
BSA-DIO-Co^{2+}	298	7.83	4.31	0.9958	0.02
BSA-DIO-Zn^{2+}	298	9.58	7.83	0.9923	0.04

[a] R is the correlation coefficient; [b] S.D. is the standard deviation for the K_{SV} values.

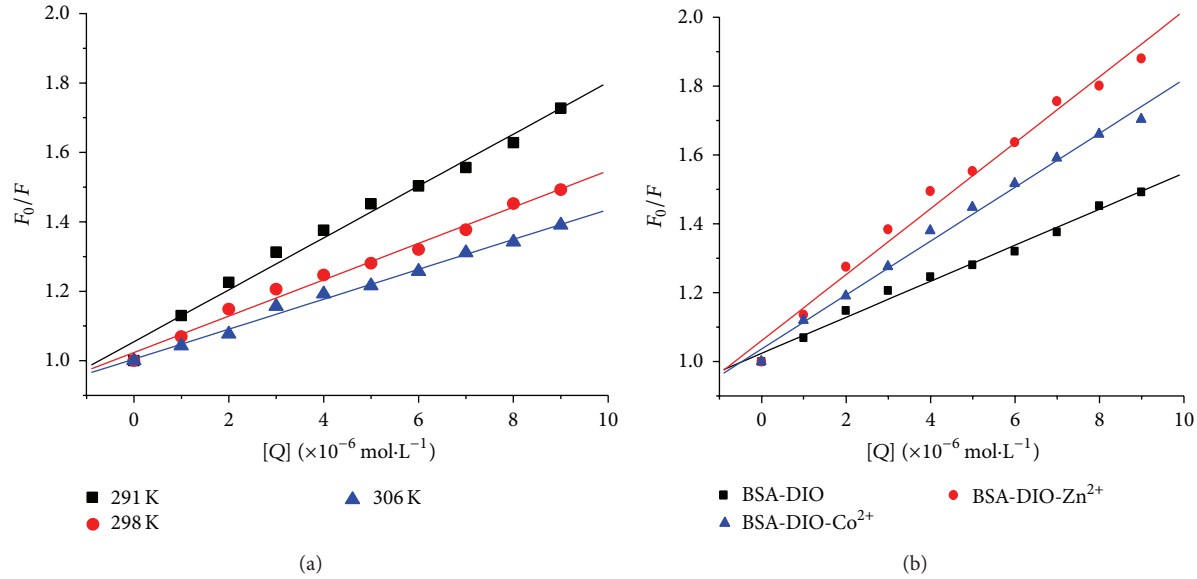

Figure 3: The Stern-Volmer plots for the binding of DIO with BSA at different temperatures (a) and in the absence and presence of Co^{2+} or Zn^{2+}, T = 298 K (b).

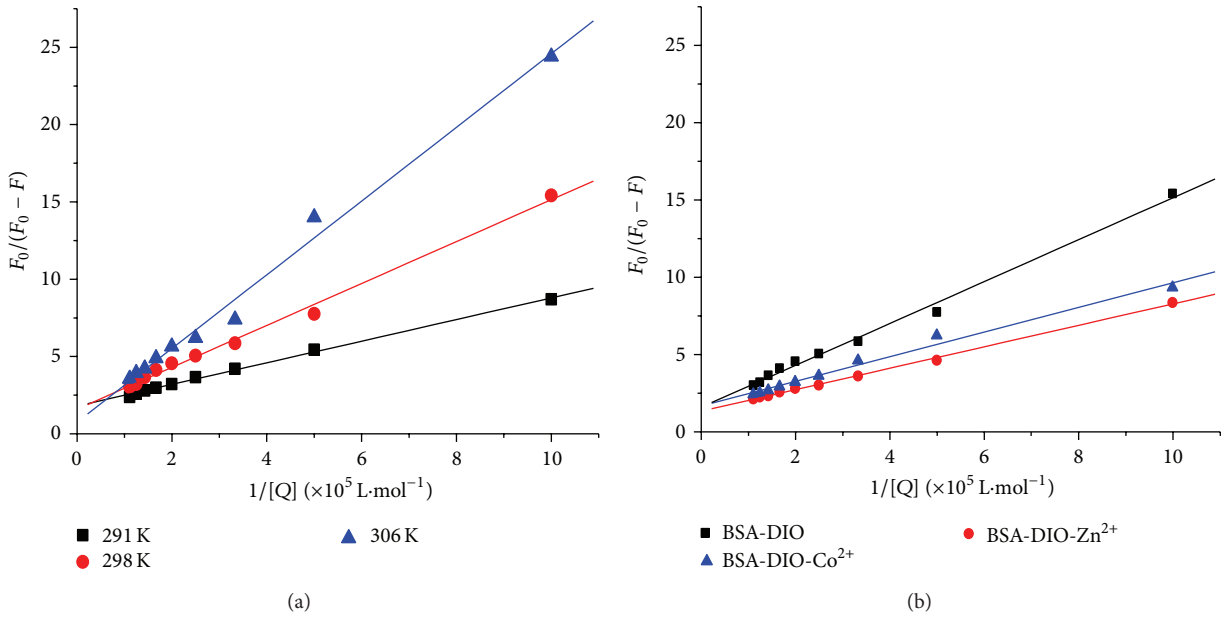

Figure 4: The modified Stern-Volmer plots for the binding of DIO with BSA at different temperatures (a) and in the absence and presence of Co^{2+} or Zn^{2+}, T = 298 K (b).

Table 2: The static binding constants K and thermodynamic parameters of DIO with BSA at different temperatures.

	T (K)	K ($\times 10^5$ L·mol^{-1})	R^a	ΔG^0 (kJ·mol^{-1})	ΔS^0 (J·mol^{-1}·K^{-1})	ΔH^0 (kJ·mol^{-1})
DIO-BSA	291	2.57	0.9985	−30.31	−252.48	−103.78
	298	1.17	0.9971	−28.54		
	306	0.32	0.9948	−26.52		

[a] R is the correlation coefficient for the K values.

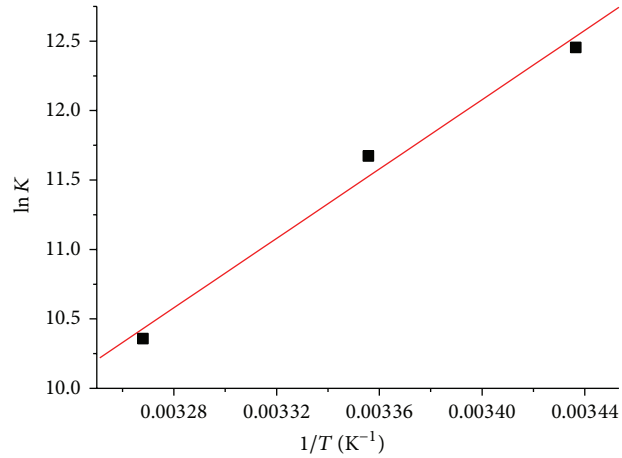

Figure 5: Van't Hoff plots for the binding of DIO with BSA.

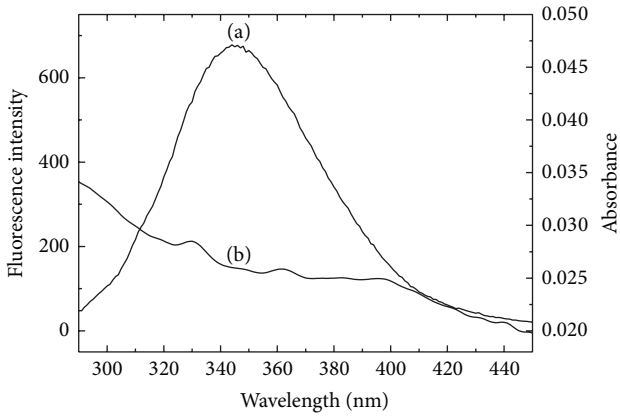

Figure 6: Spectral overlap between the fluorescence emission spectrum of BSA and the absorption spectrum of DIO. (a) fluorescence emission spectrum of BSA (5.0×10^{-7} mol·L^{-1}); (b) absorption spectrum of DIO (5.0×10^{-7} mol·L^{-1}).

3.5. The Binding of Site Maker Probes. There were two major binding sites for drugs on albumin which were known as Sudlow sites I and II. Site I is formed as a pocket in subdomain IIA and involves the lone tryptophan of the protein (^{212}Trp). Site I is adaptable and binds kinds of ligands with very different chemical structures. Site II locate at subdomain IIIA. It can bind smaller ligands because it is smaller, less flexible, and narrower than site I [29, 30]. Site I showed affinity for warfarin, ketoprofen, and so forth, and site II for ibuprofen, flufenamic acid, and so forth [31–33]. In order to determine the binding sites of DIO to BSA, the competitive displacement experiments were carried out using different site probes of ketoprofen for site I and ibuprofen for site II, respectively. The results showed that the binding constants of DIO to BSA were surprisingly changed from 2.57 to 1.304×10^5 L·mol^{-1} in the presence of ketoprofen, while the K values almost remained the same in the case of ibuprofen (2.47×10^5 L·mol^{-1}). The results indicated that ketoprofen exhibited

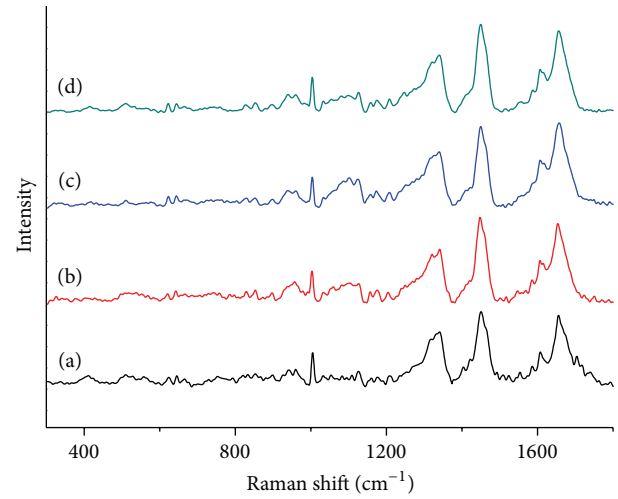

Figure 7: Raman spectra of (a) free BSA; (b) DIO-BSA system; (c) DIO-BSA-Co^{2+} system; (d) DIO-BSA-Zn^{2+} system. [BSA] = [DIO] = [Co^{2+}] = [Zn^{2+}] = 5×10^{-4} mol·L^{-1}.

significant displacement of DIO. However, ibuprofen was not displaced by DIO obviously. These meant that the binding site of DIO to BSA was site I.

3.6. Analysis of BSA Conformational Changes. Raman spectroscopy has emerged as a useful method to investigate the conformational changes of protein secondary structure and the microenvironment of amino acid residues [34]. In order to study the effects of DIO on the conformation of BSA, we analyzed the amide I and the regions of aromatic amino acid residues of Raman spectra. In Raman spectra, the peaks that appeared in the region of 1550–1620 cm^{-1} were the ring vibration bands of aromatic residues [35]. The amide I band (1700–1630 cm^{-1}) originated mainly from peptide C=O stretching [36, 37]. Figure 7 displayed the Raman spectra of BSA and BSA-DIO system in the absence and presence of Co^{2+} and Zn^{2+}. In the amide I band of BSA, the major band of BSA around 1648–1658 cm^{-1} was the characterization of α-helix; while the band of 1630–1640 cm^{-1} represented short segment chains connecting the α-helix, the bands of β-turn were centered at 1680–1700 cm^{-1}, respectively [38–42]. Figure 8 was the curve fitting of Raman amide I; the corresponding results were listed in Table 3. The results showed that native BSA contains major α-helix conformation (55.71%), which are consistent with the previous ones reported for BSA by Raman, infrared, and CD spectroscopy [43–45]. The α-helix contents decreased to 47.58% due to the binding of DIO. Meanwhile, the content of β-turn increased while the content of short segment decreased. The results indicated that the secondary structure of BSA was changed by DIO. Competing with the BSA-DIO system, the decreased extent of α-helix content was lower in the presence of Zn^{2+}, while for Co^{2+} there was an increase. The results indicated that the presence of Co^{2+} or Zn^{2+} affects the changes of BSA secondary structure.

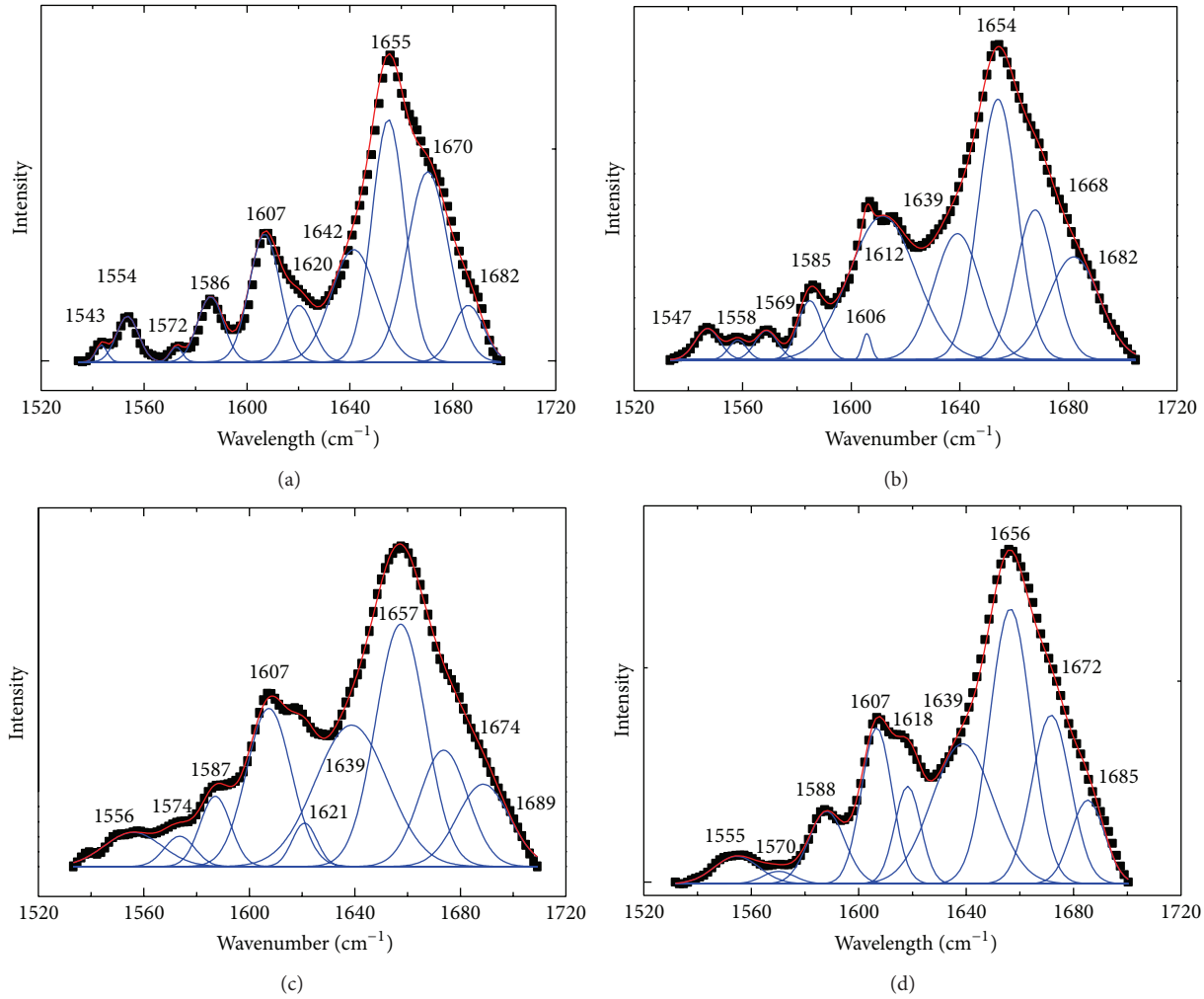

FIGURE 8: The curve fitting of Raman amide I of (a) free BSA; (b) DIO-BSA system; (c) DIO-BSA-Co^{2+} system; (d) DIO-BSA-Zn^{2+} system. The experimental spectra (black dots); the fitting curves (solid line).

TABLE 3: The curve fitting results of Raman amide *I* of BSA.

System		α-Helix	Short segment	β-Turn
BSA	Frequency (cm^{-1})	1655	1642	1682
	Content (%)	55.71	34.51	9.78
BSA-DIO	Frequency (cm^{-1})	1654	1639	1682
	Content (%)	47.58	27.70	24.72
BSA-DIO-Co^{2+}	Frequency (cm^{-1})	1657	1639	1689
	Content (%)	45.55	38.52	15.93
BSA-DIO-Zn^{2+}	Frequency (cm^{-1})	1657	1639	1685
	Content (%)	51.48	38.30	10.22

The conformation of 17 disulphide bridges of serum albumin molecule can be sensitively determined by Raman spectroscopy. The disulphide bridges of BSA have three conformations: gauche-gauche-gauche (g-g-g, peaks around 510 cm^{-1}), gauche-gauche-trans or trans-gauche-gauche (g-g-t or t-g-g, peaks around 525 cm^{-1}), and trans-gauche-trans (t-g-t, peaks around 540 cm^{-1}) [46]. Figure 9 was the analysis of the S-S bands; the conformations of 17 disulphide bridges were obtained according to the fitting results. As shown in Table 4, the major conformation of disulphide bridges in native BSA was g-g-g conformations. After binding DIO, there were 7 S-S bridges converted conformations, while 3

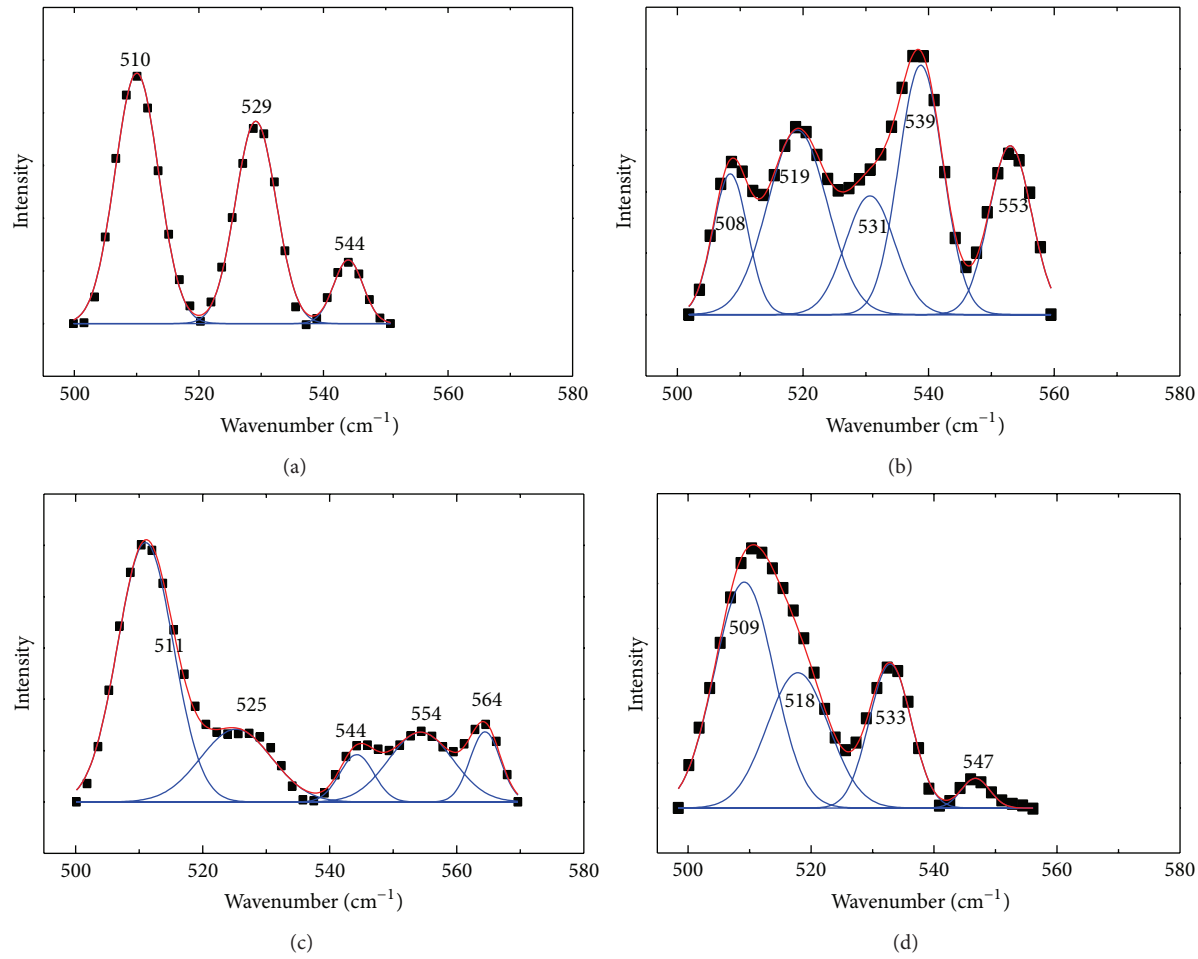

Figure 9: The analysis of the S-S bands of (a) free BSA; (b) DIO-BSA system; (c) DIO-BSA-Co^{2+} system; (d) DIO-BSA-Zn^{2+} system. The experimental spectra (black dots), the fitting curves (solid line).

Table 4: The conformation of the 17 disulfide bridges of BSA.

System	g-g-g	g-g-t or t-g-g	t-g-t	change
BSA	9	7	1	—
BSA-DIO	2	9	6	7
BSA-DIO-Co^{2+}	12	4	1	3
BSA-DIO-Zn^{2+}	8	5	4	3

Table 5: The analysis of the Tyr and Trp side chains.

System	BSA	BSA-DIO	BSA-DIO-Co^{2+}	BSA-DIO-Zn^{2+}
I_{850}/I_{830}	1.7180	1.0352	2.1477	2.1645
I_{1363}/I_{1340}	0.0409	0.0461	0.0502	0.0574

conformations of S-S bridges were changed in the presence of Co^{2+} or Zn^{2+}, which indicated the presence of Co^{2+} or Zn^{2+} decreased the changed of DIO to S-S bridges.

The tyrosyl doublet around 850 and 830 cm^{-1}, so-called "Fermi-resonance Tyr-doublet, was due to the symmetric ring-breathing vibration and the out-of-plane ring-bending vibration. The bands at 850 and 830 cm^{-1} are extremely sensitive to hydrogen bonding of the phenolic OH-groups, and the intensity ratio of this doublet (I_{850}/I_{830}) is an indicator of the microenvironment of tyrosine residues. The value of this ratio between 0.3 and 0.5 indicated that the tyrosyl residues were "buried." On the other hand, the tyrosine residues were "exposed," when the values range from 1.25 to 1.40 [47, 48]. The analysis of the Tyr side chains was displayed in Figure 10; the results in Table 5 showed that the value of I_{850}/I_{830} decreased after the addition of DIO. But I_{850}/I_{830} for BSA-DIO-Co^{2+} and BSA-DIO-Zn^{2+} systems were both increased in the presence of Co^{2+} or Zn^{2+}, and the values were larger than that of free BSA. The results indicated that the buriedness of Tyr residues in protein was increased by DIO, but the presence of Co^{2+} or Zn^{2+} decreased the buriedness of Tyr residues [49].

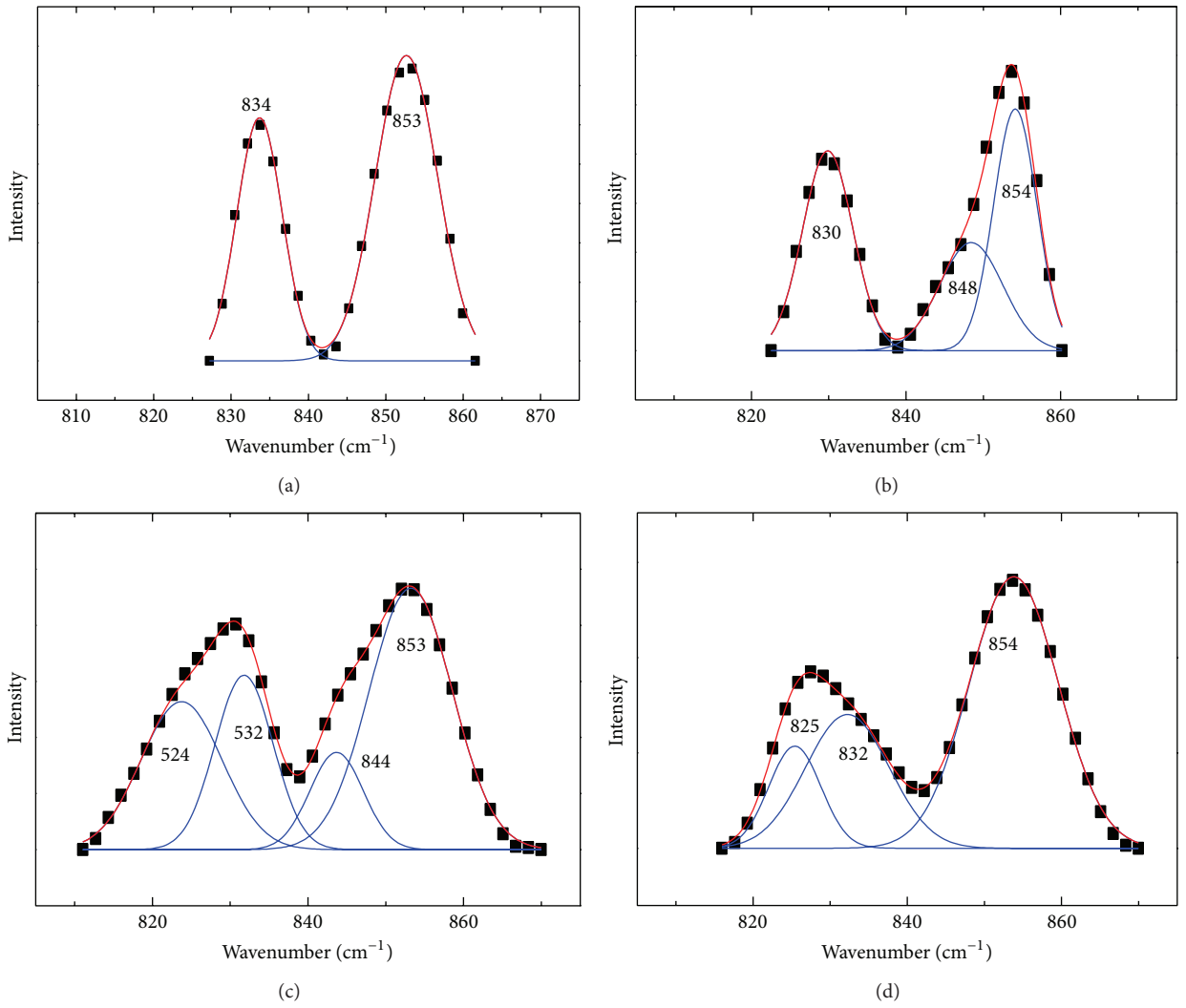

FIGURE 10: The analysis of the Tyr side chains of (a) free BSA; (b) DIO-BSA system; (c) DIO-BSA-Co^{2+} system; (d) DIO-BSA-Zn^{2+} system. The experimental spectra (black dots), the fitting curves (solid line).

The band appeared around 1340 cm^{-1} and the weak shoulder around 1363 cm^{-1} owing to the Fermi-resonance doublet bands of Trp residues. Their intensity ratio I_{1363}/I_{1340} can also be used to investigate the overall hydrophobicity of the environment surrounding tryptophan residues [50, 51]. Figure 11 was the analysis of the Trp side chains; the results were listed in Table 5. The intensity ratio of I_{1363}/I_{1340} increased from 0.0409 to 0.0461 due to the addition of DIO, while greater changes were found in BSA-DIO-Co^{2+} and BSA-DIO-Zn^{2+} systems. The results indicated that the hydrophobicity around the Trp residues increased due to the binding of DIO; the hydrophobicity increased more in the presence of Co^{2+} and Zn^{2+} [51].

4. Conclusions

In summary, we simulated the interaction of DIO with BSA in vitro by spectroscopic investigations. The experimental results indicated that the drugs could bind with BSA to form a DIO-BSA complex. The binding reaction was spontaneous. DIO bound to site I of BSA mainly through the hydrogen bond and Van der Waals' force. The presence of Co^{2+} or Zn^{2+} increased the quenching effect and the binding affinity of DIO to BSA. Otherwise, the analysis of conformation change confirmed that the binding of DIO induced the unfolding of protein secondary structure. Although the changes of BSA secondary structure caused by DIO in the presence of Co^{2+} or Zn^{2+} were different from those without metal ions, they all major led to the decrease of α-helix conformation. The addition of DIO changed 7 conformations of S-S bridges of BSA, while the changes were both reduced to 3 in the presence of Co^{2+} or Zn^{2+}. Besides, DIO increased the buriedness of Tyr residues in protein, but the effects were opposite for BSA-DIO-Co^{2+} and BSA-DIO-Zn^{2+} systems. Meanwhile, the hydrophobicity around the tryptophan residues was all increased due to the binding of DIO in the absence and presence of Co^{2+} or Zn^{2+}.

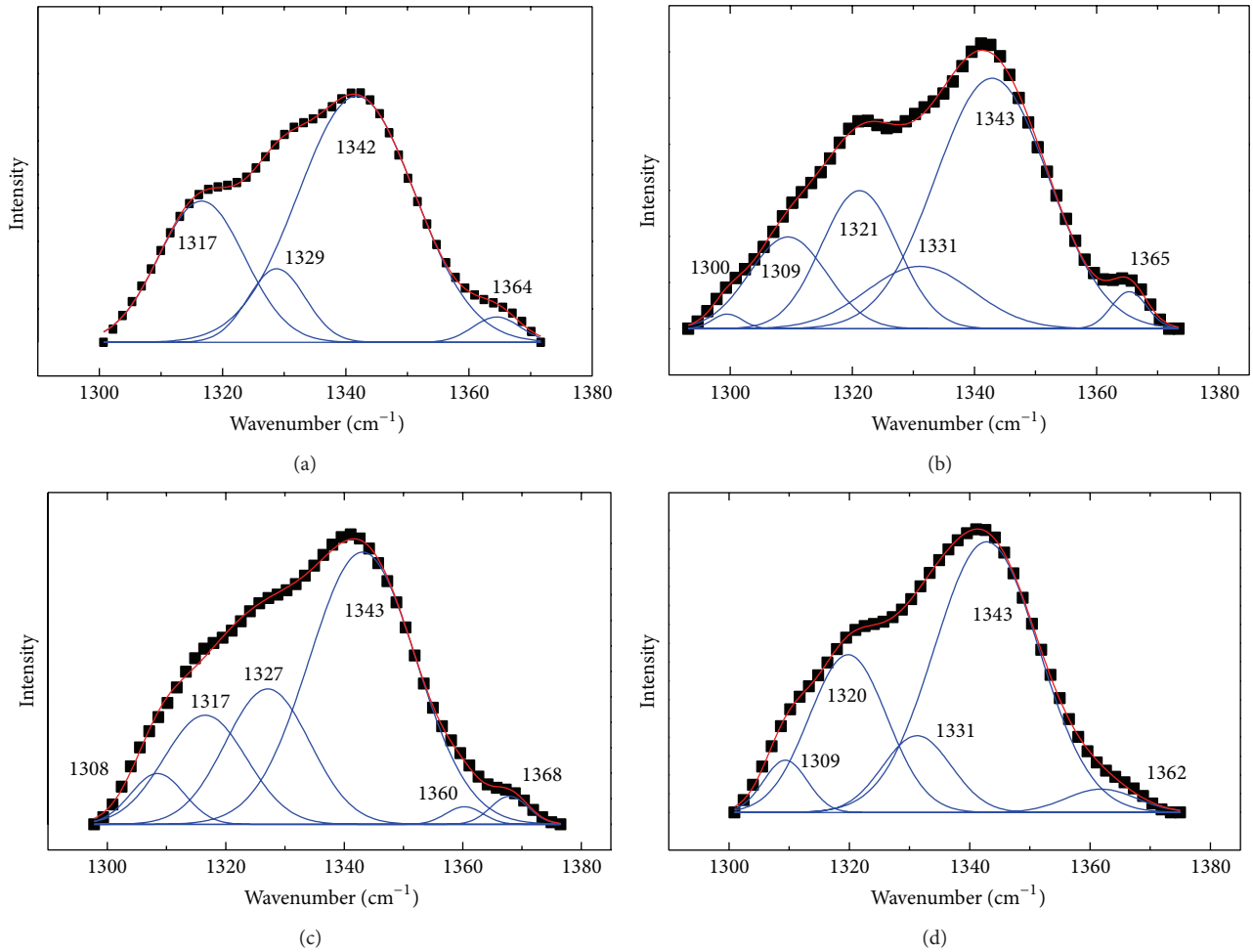

FIGURE 11: The analysis of the Trp side chains of (a) free BSA; (b) DIO-BSA system; (c) DIO-BSA-Co^{2+} system; (d) DIO-BSA-Zn^{2+} system. The experimental spectra (black dots), the fitting curves (solid line).

Conflict of Interests

The authors declare that there is no conflict of interests regarding the publication of this paper.

Acknowledgments

The authors gratefully acknowledge the National Natural Science Foundation of China (21061002, 21361003, and 21101035), the Scientific Research Foundation for the Returned overseas Chinese Scholars, the Guangxi Natural Science Foundation of China (2011GXNSFC018009, 2012GXNSFAA053035), Talent's Small Highland project of Guangxi Medicinal Industry (1201), and the Foundation of Key Laboratory for Chemistry and Molecular Engineering of Medicinal Resources.

References

[1] K. Higdon, A. Scott, M. Tucci et al., "The use of estrogen, dhea, and diosgenin in a sustained delivery setting as a novel treatment approach for osteoporosis in the ovariectomized adult rat model," *Biomedical Sciences Instrumentation*, vol. 37, pp. 281–286, 2001.

[2] R. E. Temel, J. M. Brown, Y. Ma et al., "Diosgenin stimulation of fecal cholesterol excretion in mice is not NPC1L1 dependent," *Journal of Lipid Research*, vol. 50, no. 5, pp. 915–923, 2009.

[3] T. Yamada, M. Hoshino, T. Hayakawa et al., "Dietary diosgenin attenuates subacute intestinal inflammation associated with indomethacin in rats," *The American Journal of Physiology: Gastrointestinal and Liver Physiology*, vol. 273, no. 2, pp. G355–G364, 1997.

[4] K. L. G. Dias, N. D. A. Correia, K. K. G. Pereira et al., "Mechanisms involved in the vasodilator effect induced by diosgenin in rat superior mesenteric artery," *European Journal of Pharmacology*, vol. 574, no. 2-3, pp. 172–178, 2007.

[5] Z. Yu, D. Li, B. Ji, and J. Chen, "Characterization of the binding of nevadensin to bovine serum albumin by optical spectroscopic technique," *Journal of Molecular Structure*, vol. 889, no. 1–3, pp. 422–428, 2008.

[6] U. R. Chatterjee, S. Ray, V. Micard et al., "Interaction with bovine serum albumin of an anti-oxidative pectic arabinogalactan from *Andrographis paniculata*," *Carbohydrate Polymers*, vol. 101, pp. 342–348, 2014.

[7] X. Xu, L. Zhang, D. Shen, H. Wu, and Q. Liu, "Oxygen-dependent oxidation of Fe(II) to Fe(III) and interaction of Fe(III) with bovine serum albumin, leading to a hysteretic effect on the fluorescence of bovine serum albumin," *Journal of Fluorescence*, vol. 18, no. 1, pp. 193–201, 2008.

[8] H. Liang, B. Xin, X. Wang, Y. Yuan, Y. Zhou, and P. Shen, "Equilibrium dialysis study on the interaction between Cu(II) and HSA or BSA," *Chinese Science Bulletin*, vol. 43, no. 5, pp. 404–409, 1998.

[9] H. Liang, J. Huang, C.-Q. Tu, M. Zhang, Y.-Q. Zhou, and P.-W. Shen, "The subsequent effect of interaction between Co^{2+} and human serum albumin or bovine serum albumin," *Journal of Inorganic Biochemistry*, vol. 85, no. 2-3, pp. 167–171, 2001.

[10] S. M. T. Shaikh, J. Seetharamappa, P. B. Kandagal, and D. H. Manjunatha, "Antioxidant Chinese yam polysaccharides and its pro-proliferative effect on endometrial epithelial cells," *International Journal of Biological Macromolecules*, vol. 41, no. 1, pp. 81–86, 2007.

[11] P. N. Naik, S. A. Chimatadar, and S. T. Nandibewoor, "Interaction between a potent corticosteroid drug—dexamethasone with bovine serum albumin and human serum albumin: a fluorescence quenching and fourier transformation infrared spectroscopy study," *Journal of Photochemistry and Photobiology B: Biology*, vol. 100, no. 3, pp. 147–159, 2010.

[12] Y. Q. Wang, H. M. Zhang, G. C. Zhang, W. H. Tao, and S. H. Tang, "Binding of rare earth metal complexes with an ofloxacin derivative to bovine serum albumin and its effect on the conformation of protein," *Journal of Luminescence*, vol. 126, pp. 211–218, 2007.

[13] Y. Ni, G. Liu, and S. Kokot, "Fluorescence spectrometric study on the interactions of isoprocarb and sodium 2-isopropylphenate with bovine serum albumin," *Talanta*, vol. 76, no. 3, pp. 513–521, 2008.

[14] S. S. Lehrer, "Solute perturbation of protein fluorescence. The quenching of the tryptophyl fluorescence of model compounds and of lysozyme by iodide ion," *Biochemistry*, vol. 10, no. 17, pp. 3254–3263, 1971.

[15] W. He, Y. Li, C. Xue, Z. Hu, X. Chen, and F. Sheng, "Effect of Chinese medicine alpinetin on the structure of human serum albumin," *Bioorganic and Medicinal Chemistry*, vol. 13, no. 5, pp. 1837–1845, 2005.

[16] T. Förster and O. Sinanoglu, *Modern Quantum Chemistry*, Academic Press, New York, NY,USA, 1966.

[17] J. R. Lakowicz, *Principles of Fluorescence Spectroscopy*, Plenum Press, New York, NY, USA, 1983.

[18] W. D. Horrocks Jr. and A. Peter Snyder, "Measurement of distance between fluorescent amino acid residues and metal ion binding sites. Quantitation of energy transfer between tryptophan and terbium(III) or europium(III) in thermolysin," *Biochemical and Biophysical Research Communications*, vol. 100, no. 1, pp. 111–117, 1981.

[19] P. B. Kandagal, J. Seetharamappa, S. Ashoka, S. M. T. Shaikh, and D. H. Manjunatha, "Study of the interaction between doxepin hydrochloride and bovine serum albumin by spectroscopic techniques," *International Journal of Biological Macromolecules*, vol. 39, no. 4-5, pp. 234–239, 2006.

[20] A. Sułkowska, M. Maciazek-Jurczyk, B. Bojko et al., "Competitive binding of phenylbutazone and colchicine to serum albumin in multidrug therapy: a spectroscopic study," *Journal of Molecular Structure*, vol. 881, no. 1–3, pp. 97–106, 2008.

[21] T. Yuan, A. M. Weljie, and H. J. Vogel, "Tryptophan fluorescence quenching by methionine and selenomethionine residues of calmodulin: orientation of peptide and protein binding," *Biochemistry*, vol. 37, no. 9, pp. 3187–3195, 1998.

[22] D. Ran, X. Wu, J. Zheng et al., "Study on the interaction between florasulam and bovine serum albumin," *Journal of Fluorescence*, vol. 17, no. 6, pp. 721–726, 2007.

[23] M. Xu, F.-J. Chen, L. Huang, P.-X. Xi, and Z.-Z. Zeng, "Binding of rare earth metal complexes with an ofloxacin derivative to bovine serum albumin and its effect on the conformation of protein," *Journal of Luminescence*, vol. 131, no. 8, pp. 1557–1565, 2011.

[24] J. R. Lakowicz, *Principles of Fluorescence Spectroscopy*, Kluwer Academic/Plenum, New York, NY, USA, 2nd edition, 1999.

[25] P. Banerjee, S. Pramanik, A. Sarkar, and S. C. Bhattacharya, "Deciphering the fluorescence resonance energy transfer signature of 3-pyrazolyl 2-pyrazoline in transport proteinous environment," *The Journal of Physical Chemistry B*, vol. 113, no. 33, pp. 11429–11436, 2009.

[26] S. N. Timaseff, "Thermodynamics of protein interactions," in *Proteins of Biological Fluids*, H. Peeters, Ed., pp. 511–519, Pergamon Press, Oxford, UK, 1972.

[27] P. D. Ross and S. Subramanian, "Thermodynamics of protein association reactions: forces contributing to stability," *Biochemistry*, vol. 20, no. 11, pp. 3096–3102, 1981.

[28] X.-Z. Feng, Z. Lin, L.-J. Yang, C. Wang, and C.-L. Bai, "Investigation of the interaction between acridine orange and bovine serum albumin," *Talanta*, vol. 47, no. 5, pp. 1223–1229, 1998.

[29] T. Peters, *All about Albumin: Biochemistry, Genetics, and Medical Applications*, Academic Press, San Diego, CA, USA, 1996.

[30] U. Krach-Hansen, V. T. G. Chuang, and M. Otagiri, "Practical aspects of the ligand-binding and enzymatic properties of human serum albumin," *Biological and Pharmaceutical Bulletin*, vol. 25, no. 6, pp. 695–704, 2002.

[31] C. E. Petersen, C.-E. Ha, S. Curry, and N. V. Bhagavan, "Probing the structure of the warfarin-binding site on human serum albumin using site-directed mutagenesis," *Proteins: Structure, Function and Genetics*, vol. 47, no. 2, pp. 116–125, 2002.

[32] X. M. He and D. C. Carter, "Atomic structure and chemistry of human serum albumin," *Nature*, vol. 358, no. 6383, pp. 209–215, 1992.

[33] H. Greige-Gerges, R. A. Khalil, E. A. Mansour, J. Magdalou, R. Chahine, and N. Ouaini, "Cucurbitacins from *Ecballium elaterium* juice increase the binding of bilirubin and ibuprofen to albumin in human plasma," *Chemico-Biological Interactions*, vol. 169, no. 1, pp. 53–62, 2007.

[34] A. Misiunas, Z. Talaikyte, G. Niaura, V. Razumas, and T. Nylander, "Thermomyces lanuginosus lipase in the liquid-crystalline phases of aqueous phytantriol: X-ray diffraction and vibrational spectroscopic studies," *Biophysical Chemistry*, vol. 134, no. 3, pp. 144–156, 2008.

[35] C. David, S. Foley, C. Mavon, and M. Enescu, "Reductive unfolding of serum albumins uncovered by Raman spectroscopy," *Biopolymers*, vol. 89, no. 7, pp. 623–634, 2008.

[36] W. K. Surewicz, H. H. Mantsch, and D. Chapman, "Determination of protein secondary structure by fourier transform infrared spectroscopy: a critical assessment," *Biochemistry*, vol. 32, no. 2, pp. 389–394, 1993.

[37] A. I. Ivanov, E. A. Korolenko, E. V. Korolik et al., "Chronic liver and renal diseases differently affect structure of human serum albumin," *Archives of Biochemistry and Biophysics*, vol. 408, no. 1, pp. 69–77, 2002.

[38] J. T. Pelton and L. R. McLean, "Spectroscopic methods for analysis of protein secondary structure," *Analytical Biochemistry*, vol. 277, no. 2, pp. 167–176, 2000.

[39] B. M. Smith and S. Franzen, "Single-pass attenuated total reflection fourier transform infrared spectroscopy for the analysis of proteins in H_2O solution," *Analytical Chemistry*, vol. 74, no. 16, pp. 4076–4080, 2002.

[40] J. Fontecha, J. Bellanato, and M. Juarez, "Infrared and Raman spectroscopic study of casein in cheese: effect of freezing and frozen storage," *Journal of Dairy Science*, vol. 76, no. 11, pp. 3303–3309, 1993.

[41] H. Fabian and P. Anzenbacher, "New developments in Raman spectroscopy of biological systems," *Vibrational Spectroscopy*, vol. 4, no. 2, pp. 125–148, 1993.

[42] J. Wang, S. Li, X. L. Peng et al., "Multi-spectroscopic studies on the interaction of human serum albumin with astilbin: binding characteristics and structural analysis," *Journal of Luminescence*, vol. 136, pp. 422–429, 2013.

[43] Q. Yang, J. Liang, and H. Han, "Probing the interaction of magnetic iron oxide nanoparticles with bovine serum albumin by spectroscopic techniques," *The Journal of Physical Chemistry B*, vol. 113, no. 30, pp. 10454–10458, 2009.

[44] B. I. Baello, P. Pancoska, and T. A. Keiderling, "Enhanced prediction accuracy of protein secondary structure using hydrogen exchange fourier transform infrared spectroscopy," *Analytical Biochemistry*, vol. 280, no. 1, pp. 46–57, 2000.

[45] D. Li, M. Zhu, C. Xu, and B. Ji, "Characterization of the baicalein-bovine serum albumin complex without or with Cu^{2+} or Fe^{3+} by spectroscopic approaches," *European Journal of Medicinal Chemistry*, vol. 46, no. 2, pp. 588–599, 2011.

[46] H. E. Van Wart, A. Lewis, H. A. Scheraga, and F. D. Saeva, "Disulfide bond dihedral angles from Raman spectroscopy," *Proceedings of the National Academy of Sciences of the United States of America*, vol. 70, no. 9, pp. 2619–2623, 1973.

[47] Z. Jurasekova, G. Marconi, S. Sanchez-Cortes, and A. Torreggiani, "Spectroscopic and molecular modeling studies on the binding of the flavonoid luteolin and human serum albumin," *Biopolymers*, vol. 91, no. 11, pp. 917–927, 2009.

[48] P. R. Carey, *Biochemical Applications of Raman and Resonance Raman Spectroscopics*, Academic Press, New York, NY, USA, 1982.

[49] N.-T. Yu, B. H. Jo, and D. C. O'Shea, "Laser Raman scattering of cobramine B, a basic protein from cobra venom," *Archives of Biochemistry and Biophysics*, vol. 156, no. 1, pp. 71–76, 1973.

[50] T. Miura, H. Takeuchi, and I. Harada, "Characterization of individual tryptophan side chains in proteins using Raman spectroscopy and hydrogen-deuterium exchange kinetics," *Biochemistry*, vol. 27, no. 1, pp. 88–94, 1988.

[51] I. Harada, T. Miura, and H. Takeuchi, "Origin of the doublet at 1360 and 1340 cm^{-1} in the Raman spectra of tryptophan and related compounds," *Spectrochimica Acta A: Molecular Spectroscopy*, vol. 42, no. 2-3, pp. 307–312, 1986.

Hindawi Publishing Corporation
Evidence-Based Complementary and Alternative Medicine
Volume 2014, Article ID 372503, 7 pages
http://dx.doi.org/10.1155/2014/372503

Research Article

Generation of the Bovine Viral Diarrhea Virus E0 Protein in Transgenic *Astragalus* and Its Immunogenicity in Sika Deer

Yugang Gao, Xueliang Zhao, Pu Zang, Qun Liu, Gongqing Wei, and Lianxue Zhang

College of Traditional Material Medicine, Jilin Agricultural University, Changchun 130118, China

Correspondence should be addressed to Lianxue Zhang; lianxuezhang863@sina.com

Received 24 March 2014; Revised 29 April 2014; Accepted 6 May 2014; Published 22 May 2014

Academic Editor: Shi-Biao Wu

The bovine viral diarrhea virus (BVDV), a single-stranded RNA virus, can cause fatal diarrhea syndrome, respiratory problems, and reproductive disorders in herds. Over the past few years, it has become clear that the BVDV infection rates are increasing and it is likely that an effective vaccine for BVDV will be needed. In this study, transgenic *Astragalus* was used as an alternative productive platform for the expression of glycoprotein E0. The immunogenicity of glycoprotein E0 expressed in transgenic *Astragalus* was detected in deer. The presence of pBI121-E0 was confirmed by polymerase chain reaction (PCR), transcription was verified by reverse transcription- (RT-) PCR, and recombinant protein expression was confirmed by ELISA and Western blot analyses. Deer that were immunized subcutaneously with the transgenic plant vaccine developed specific humoral and cell-mediated immune responses against BVDV. This study provides a new method for a protein with weak immunogenicity to be used as part of a transgenic plant vaccine.

1. Introduction

Bovine viral diarrhea (BVD) is a widespread disease that affects cattle [1]. The causative agent is the bovine viral diarrhea virus (BVDV), a *Pestivirus* of the family Flaviviridae. BVDV infection presents a wide spectrum of diseases, ranging from mild acute infection to fatal mucosal disease [2]. The virus is known to damage the immune system of the infected animals, which can make the animals more susceptible to other diseases and causes significant loss to the livestock industry [3–5]. The virus can infect and be transmitted between a variety of animals, such as cattle, sheep, and whitetail deer [6–9]. In our previous study, a new single strain of BVDV named CCSYD was isolated and verified from sika deer [10].

Different strategies are available to control the spread of BVDV in a herd, such as vaccination and test-and-cull schemes. Among these strategies, test-and-cull schemes have been very successfully applied in areas with low cattle densities and low BVDV prevalence, such as Scandinavia [11, 12]. But in the areas with high cattle densities and high BVDV prevalence, the program will bring huge economic loss. Vaccine research is considered to be a promising alternative to prevent BVDV spread. Inactivated vaccines generally possess inadequate efficacy and do not induce sufficient protective immunity. Although modified live vaccines provide certain protection against homologous strains, the intrinsic risk of virulence reversion remains a concern [13, 14]. Due to the poor immunogenicity of inactivated vaccines and the safety concerns surrounding the use of modified live vaccine, an effective subunit vaccine for BVDV has become the subject of increasing research interest [15].

BVDV is a single-stranded RNA virus and has approximately 12.5 kb RNA genome [16] and the genomes of BVDV are translated and processed into eleven mature proteins. After infection or vaccination, cattle elicit antibodies to the three envelope proteins E0, E1, and E2 and against the nonstructural protein NS_3 [17]. Glycoprotein E2 is the major target of the protective immune response triggered against BVDV infection and is widely used for subunit vaccines [18, 19]. However, the highly variable sequence of E2 protein often leads to immune failure [20, 21].

E0 is a conserved protein and shows less antigenic diversity than E2 [22]. Nevertheless, the BVDV E0 expressed in prokaryotes system produced neutralizing antibodies but at low titers that could not efficiently neutralize virus, which was attributed to a misfolding of E0 [17]. In view that eukaryotic expression could maintain the correct folding and glycosylation of proteins, eukaryotic expression has become the research focus in the study of subunit vaccine. Last year, Gao et al. [23] successfully constructed a prokaryotic expression vector PVAX1-E0 and identified its antigen activity in rabbits. The result shows that the recombined PVAX1-E0 could produce specific humoral and cellular immune response in rabbits. Transgenic plants are new eukaryotic expression-delivery systems that have become attractive bioreactors in the production of high-value medical peptides and proteins [24]. Up to now, several types of plant species have been used as antigen-delivery systems for subunit vaccines [25, 26]. For example, the truncated glycoprotein BVDV E2 has been expressed in *N. tabacum* leaves and subsequently showed high reactivity in virus neutralization test [27].

Another strategy to improve the immune activity of vaccine is the use of adjuvant [28]. Vaccine adjuvant can stimulate the immune system to an increased specific antibody response. *Radix Astragali* (*Astragalus*) is a plant used as a traditional herb medicine in China, and it is known for its antiviral activity and immunity-boosting properties [29–31]. *Astragalus* polysaccharides can improve the function of macrophages, enhance macrophage phagocytosis, and increase the activity of natural killer (NK) cells [32]. *Astragalus* as host plants can play a role in the immune adjuvant to enhance the immune level.

In this study, plant expression vector pBI121-E0 was constructed and transferred into *Astragalus*. The immunogenicity and protective efficacy of the recombinant proteins were demonstrated in deer. The aim of this study was to develop a transgenic *Astragalus* vaccine for bovine viral diarrhea.

2. Materials and Methods

2.1. Reagents, Bacteria, and Plasmids. The plasmid pMD18-T-E0 was developed in our previous work [23]. The *E. coli* strain DH5α was purchased from Invitrogen (Shanghai, China). Plasmid pBI121 (Novagen, Darmstadt, Germany) was used for recombinant protein expression. Restriction enzymes, Taq DNA polymerase, TriPure Kit, and T4 ligase were purchased from TaKaRa Biotechnology Co., Dalian, China.

2.2. Plasmid Construction. The BVDV E0 open reading frame was amplified from plasmid pMD18-T-E0 which contains the complete gene with the forward primer (5′-CCG GAT CCA CCA TGG AAA ACA TAA CAC AGT GG-3′, *BamHI* site underlined) and the reverse primer (5′-GCG AGC TCT TAA GCG TAT GCT CCA AAC CAC GT-3′, *SacI* site underlined). The PCR product was digested with *BamHI* and *SacI* and inserted into plant expression vector pBI121 digested with the same enzymes to create the recombinant plasmid pBI121-E0.

2.3. Plant Transformation and Genetic Analysis. The *Astragalus membranaceus* (Fisch.) Bungevar. *mongholicus* (Bunge) P. K. Hsiao cultivated in our laboratory was used as the host plant. The transformation experiment was carried out in the middle of July. After 20 h artificial pollination [33], 150 μL plasmid pBI121-E0 (1-2 ng/μL) was applied to the stigmas evenly using a micropipette. At maturity stage, seeds were harvested and stored at room temperature. The transgenic seedlings were identified by PCR and RT-PCR analysis with the forward primer 5′-CCG GAT CCA CCA TGG AAA ACA TAA CAC AGT GG-3′ and the reverse primer 5′-GCG AGC TCT TAA GCG TAT GCT CCA AAC CAC GT-3′.

2.4. Protein Extraction. Protein isolation was conducted using 0.5 g fresh leaves of regeneration seedlings that were quickly ground in liquid nitrogen. The resulting powder was resuspended in 1 mL extraction buffer (0.24 g/L KH_2PO_4, 1.44 g/L Na_2HPO_4, 0.2 g/L KCl, 8 g/L NaCl, 10 μg/mL leupeptin, 5 mM PMSF, 50 mM EDTA, and pH 7.0–7.2) as previously described [27]. The mixture was centrifuged at 12,000 g for 20 min at 4°C, and the protein concentration was measured by the Bradford protein assay [34] in 1 mL of the supernatant using bovine serum albumin (BSA) as a standard.

2.5. Enzyme-Linked Immunosorbent Assay (ELISA). To illustrate the expression of glycoprotein E0, the ELISA was carried out. ELISA assay plates were coated at 4°C overnight with 90 μL protein samples (containing 30 μg total protein extracted from transgenic *Astragalus*) diluted in 10 μL coating buffer (pH = 8.0). After removing the liquid, the plates were washed three times with phosphate-buffered saline (PBS) with Tween 20 (PBST) and blocked with 10% horse serum at 37°C for 1 h. Then, BVDV-positive bovine serum (1 : 20 dilution) was added to the plates and incubated for 1 h at 37°C. Then, the plates were incubated for 1 h at 37°C with horseradish peroxidase (HRP) conjugated rabbit anti-bovine IgG (1 : 5,000 dilution) as the secondary antibody. Substrate was added for colour reaction at 37°C for 15 min and reaction was terminated by adding 2 M H_2SO_4 (50 μL/well). The absorbance was examined using an ELISA reader at 490 nm.

2.6. Western Blot Analysis. To further demonstrate the immune activity of the glycoprotein E0 expressed in transgenic lines, the recombinant proteins were detected by Western blot analysis. The total soluble proteins (60 μg) extracted from fresh leaves of transgenic *Astragalus* were subjected to electrophoresis on a 12% sodium dodecyl sulfate polyacrylamide gel (SDS-PAGE) and transferred to a nitrocellulose membrane (GE Healthcare, USA). Western blot was carried out using BVDV-positive bovine serum (1 : 100 dilution) and HRP-conjugated rabbit anti-bovine IgG (1 : 5000 dilution, Southern Biotechnology, USA) as the primary and secondary antibodies, respectively. The total proteins were extracted from wild-type *Astragalus* as negative control and glycoprotein E0 was expressed in the baby hamster kidney- (BHK-) 21 cells [23] as a positive control.

2.7. Ethics Statement. All the deer were obtained from DongDa Deer Industry Co., Ltd. The deer care and maintenance at the sika deer farm of Jilin Agricultural University and permission to undertake this work were granted by the Management Bureau of Animal Husbandry in Jilin Province (Shaoxian Liu, Director). The research was also approved by the animal ethics committees of Jilin Agricultural University and the National Deer Industry Association of China Animal Agriculture Association (CAAA). We anesthetized all deer prior to sampling. The blood samplings were performed by veterinarians, biologists, or technicians with previous training and experience in these procedures. We collected up to 2 mL of blood via the jugular vein. All surgery was performed under sodium pentobarbital and all efforts were made to minimize suffering. Finally, all the deer were not sacrificed.

2.8. Immunization Schedule. Thirty healthy one-month-old young male sika deer were randomly divided into five groups (six deer per group). The vaccines were prepared as previously described [27]. Briefly, montanide ISA 70 SEPPIC and Al $(OH)_3$ hydrogel were used as the adjuvant in oil vaccine and in aqueous vaccine. And the ratios of antigen to adjuvant were 40 : 60 and 90 : 10, respectively. The deer in group one were immunized subcutaneously with 1 mL formulated oil vaccine containing 100 μg total protein extracted from transgenic *Astragalus*; group two was immunized s.c. with 1 mL formulated aqueous vaccine containing the same dose of the protein extracted from transgenic *Astragalus*. Group three and group four acted as negative groups; deer in the two groups were immunized s.c. with 1 mL oil vaccine and aqueous vaccine containing 100 μg total protein extracted from wild-type *Astragalus*, respectively. Group five was injected s.c. with 100 $TCID_{50}$ of inactivated BVDV vaccine (purchased from Chinese Veterinary Drug Control Room). The second immunization was carried out in all groups on day 14. Blood samples were collected at the time of immunization (day 0) and on the days 7, 14, 21, 28, 35, and 42 after the first immunization. The blood sera were used for lymphocyte blastogenesis assay and ELISA assay.

2.9. Determination of Specific Antibodies in Immunized Deer. The blood taken from sika deer was diluted (1 : 40) with coating buffer (pH = 8.0) and added into microtiter plates (100 μL/well). The microtiter plates were coated for 2 h at 37°C. After removing the liquid, the plates were washed three times with PBST and blocked with 10% horse serum for 2 h at 37°C. Then, 100 μL soluble whole virus antigen (containing 100 μg viral proteins) extracted from the $C_{24}V$ BVDV (purchased from the China Institute of Veterinary Drug Control) was added to the plates and incubated for 2 h at 37°C. The plates were then washed three times with PBST and incubated for 1 h at 37°C with 100 μL BVDV-positive bovine serum (1 : 200 dilution). HRP-conjugated rabbit anti-bovine IgG (1 : 5000 dilution) was used as the secondary antibody. Substrate was added to facilitate the color reaction at 37°C for 15 min and the reaction was terminated by the addition of 2 M H_2SO_4 (50 μL/well). The optical density (OD) was assessed at 490 nm.

2.10. Lymphocyte Blastogenesis Assay. Peripheral blood mononuclear cells were isolated from anticoagulated jugular blood as previously reported (see Figure 4) [35]. More than 95% of the cells were lymphocytes. The cell viability was checked with a trypan blue dye exclusion assay and the cells were resuspended in Roswell Park Memorial Institute medium (RPMI) 1640, supplemented with 10% fetal bovine serum, 100 IU/mL penicillin (Sigma), and 100 mg/mL streptomycin (Sigma). The cells were placed into 96-well round-bottom plates at a concentration of 4×10^6 cells/well (100 μL) and incubated with or without BVDV (10^4 TCID50/well) in hexaplicate at 37°C under 5% CO_2. Phytohaemagglutinin(PHA) (Sigma) at 5 mg/mL was used as a positive control. After 40 to 48 h incubation at 37°C under 5% CO_2, 3-(4,5-dimethylthiazol-2-yl)-2, 5-diphenyltetrazolium bromide (MTT) was added to each well and the cells were cultured for 4 h. After the addition of 100 μL dimethyl sulfoxide (DMSO) to each well to stop the colour development, plates were tested at 570 nm.

2.11. Statistical Analysis. Multiple group comparisons were performed using one way analysis of variance (ANOVA) followed by Tukey's test in order to detect intergroup differences. GraphPad Prism software (Version 5.0; GraphPad Software, Inc., San Diego, CA) was used to perform the statistical analysis. A value of $P < 0.05$ was considered statistically significant.

3. Results

3.1. Genetic Identification of the Transgenic Astragalus. To confirm the integration of the E0 gene into the chromosome of transgenic seedlings, genomic DNA and total RNA were isolated from transgenic *Astragalus* and tested by PCR and RT-PCR. As expected, specific bonds of 706 bp were detected in all groups except for the negative control groups (Figures 1(a) and 1(b)).

3.2. Expression of E0 Protein in Transgenic Astragalus Seedlings. The ELISA assay was used to determine the expression of glycoprotein E0 in transgenic *Astragalus*. The OD490 values of transgenic *Astragalus* groups were similar to the positive groups but significantly higher than the negative groups (Figure 2(a)). That reveals glycoprotein E0 was highly expressed in transgenic *Astragalus*. To further confirm the immune activity of E0 protein, the Western blot analysis was carried out. A specific band of 50 kDa corresponding to glycoprotein E0 was detected in coomassie blue gel analysis (Figure 2(b)) and Western blot for both the samples and the positive control was shown in Figure 2(c). As expected, it was not detected in the negative controls.

3.3. Detection of Deer Serum Antibody and Cellular Immune Level. The serum antibody levels of immune deer were detected by ELISA and the results are shown in Figure 3. Before immunization, no significant difference was found among all groups. But, in the serum of immunized deer for the first seven days, the serum antibodies in oil vaccine

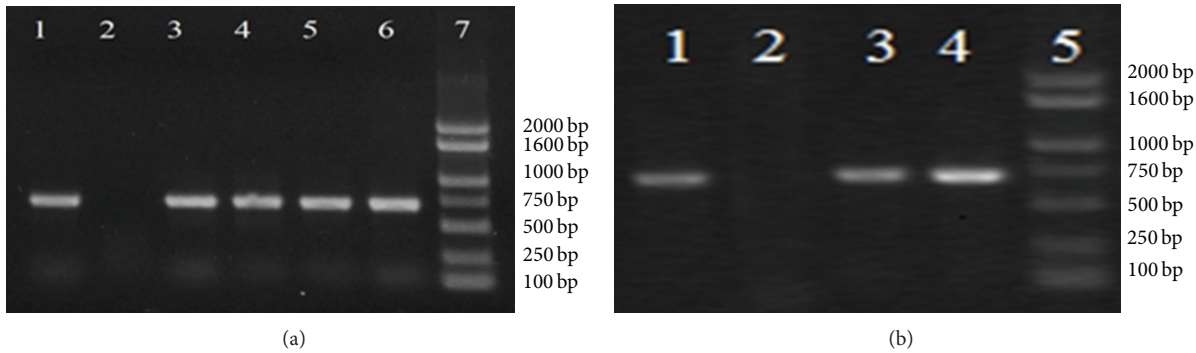

(a) (b)

Figure 1: Genetic identification of the transgenic *Astragalus*. The genomic DNA and total RNA were extracted from the leaves of transgenic *Astragalus* for PCR (a) and RT-PCR (b) identification, respectively. (a) PCR analysis of the transgenic *Astragalus*. Total genomic DNAs were extracted from the leaves of different transgenic *Astragalus* spp. (lanes 3–6) and untransformed wild-type *Astragalus* (lane 2 as negative control). Lane 1 is indicated as the positive control by using pBI121-E0 plasmid DNA as PCR template. The left showed the DNA molecular mass marker (lane 5); (b) RT-PCR analysis. DNA fragment was *amplified* from the transformed plant with E0 specific primers. Lane 1: PCR product from the plasmid pBI121-E0. Lane 2: RT-PCR product from nontransformed *Astragalus*. Lanes 3-4: RT-PCR product from different transgenic *Astragalus* spp. Lane 5 showed the DNA molecular mass marker.

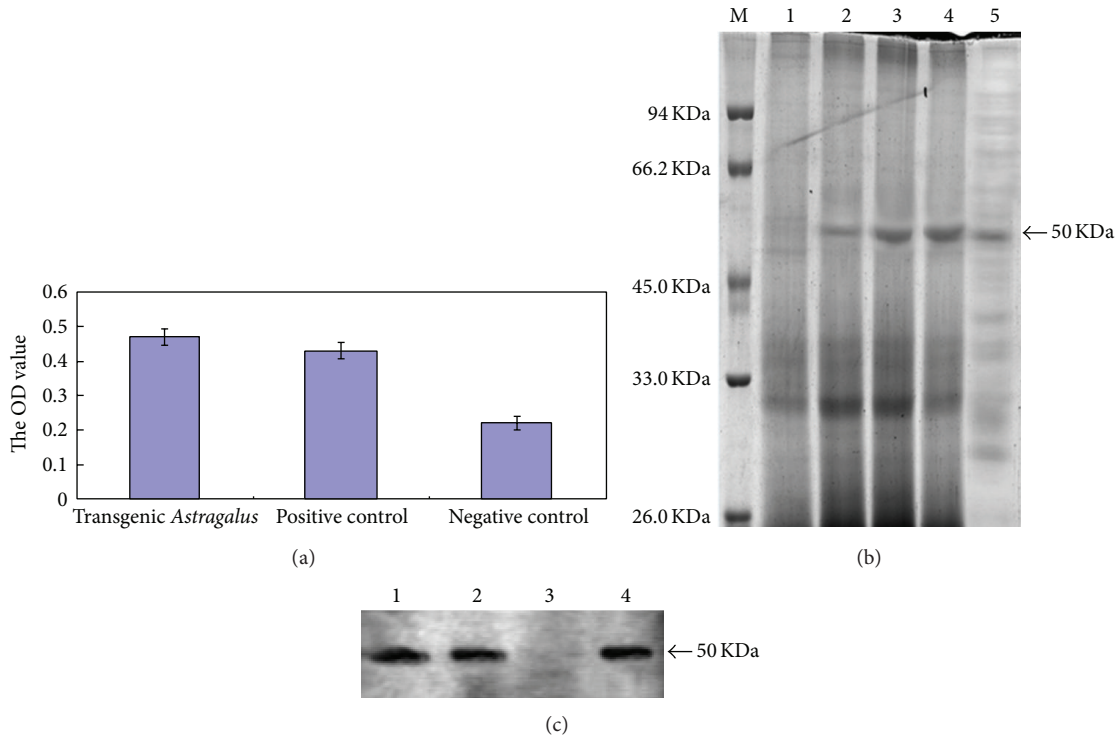

(a) (b) (c)

Figure 2: Protein analysis in transgenic *Astragalus* extract. (a) ELISA test to determine the presence of the antigen E0 in transgenic *Astragalus* leaves extract. ELISA protocol was described in methods section. Transgenic *Astragalus* group (the recombinant proteins extracted from transgenic *Astragalus* leaves); positive control (E0 protein expressed in BHK-21 cells); negative control (proteins extracted from wild-type *Astragalus*). (b) Coomassie brilliant blue staining of protein extracted from transgenic *Astragalus* leaves analyzed by 12% of SDS-PAGE. M: protein markers, 1: negative control, 2–4: transgenic *Astragalus* groups, 5: positive control. (c) Western blot analysis showing immune activity of the E0 protein expressing in transgenic *Astragalus*. In transgenic *Astragalus* group (lanes 1, 4) and positive control (lane 2 E0 protein expressed in BHK-21 cells) a specific band of 50 kDa was detected. Lane 3: negative control (proteins extracted from wild-type *Astragalus*).

group, aqueous vaccine group, and inactivated BVDV vaccine group were significantly higher than negative groups ($P < 0.05$). The antibody levels increased with the immune time in all groups, except for negative groups. With the increasing of the immune time, the antibody levels of deer BVDV inactivated vaccine group reached the peak value after 35 days of immunization, while oil vaccine group and aqueous vaccine group reached the peak value after 42 days. This revealed that oil vaccine and aqueous vaccine gave the deer longer protection from BVDV infection.

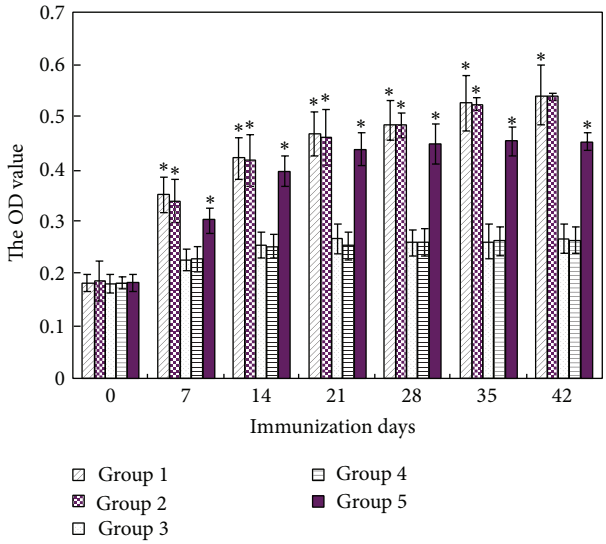

Figure 3: Specific humoral response in deer following vaccination. The deer were immunized subcutaneously with transgenic *Astragalus* oil vaccine (group 1), transgenic *Astragalus* aqueous vaccine (group 2), oil negative control (group 3), aqueous negative control (group 4), and inactivated BVDV vaccine (group 5). Serum samples used to assess the humoral immune response were collected on days 0, 7, 14, 21, 28, 35, and 42 after primary immunization and detected at 490 nm. *The difference between aqueous negative control (group 4) and other groups at the same days after primary immunization is significant ($P < 0.05$).

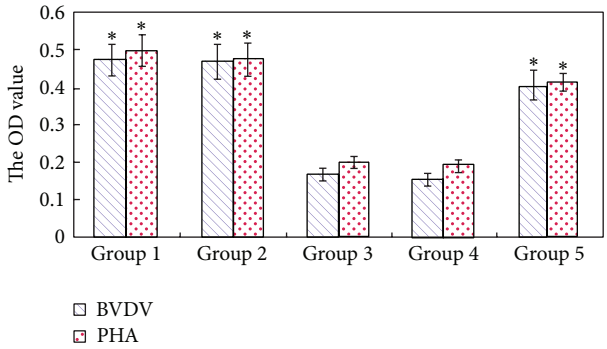

Figure 4: Lymphocyte blastogenesis assay. The blood was collected from each deer on day 42 after the immunization. Group 1: transgenic *Astragalus* oil vaccine; group 2: transgenic *Astragalus* aqueous vaccine; group 3: oil negative control; group 4: aqueous negative control; group 5: inactivated BVDV vaccine. *The difference between aqueous negative control (Group 4) and other groups is significant ($P < 0.05$).

To evaluate the cell-mediated immune responses, blood samples were collected on the 42nd day after immunization and tested for lymphocyte proliferative responses. As shown in Figure 3, the results indicated that lymphocytes present in blood from deer that received transgenic *Astragalus* plants proliferated substantially upon restimulation with BVDV antigens (Figure 3). This specific proliferation was absent in the negative groups that received nontransformed leaves (Figure 3). The result is corresponding to the result of PHA-induced lymphocyte proliferation. This suggested that BVDV-E0 specific prolonged cell-mediated immune responses in deer subcutaneously immunized with E0 transgenic *Astragalus* plant leaves were present.

4. Discussion

BVDV infection is an important cause of morbidity and economical losses in cattle worldwide. It is estimated that BVD generates a negative economic impact in dairy operations (between $20 and $160 per adult cow per year) [36]. Developing effective and inexpensive vaccines is critical for protecting animals against BVDV infection. With the development of genetic molecular biology and plant biotechnology, plants have emerged as a new platform for the production and delivery of antigenic proteins as plant-based vaccines. Plant-based vaccines offer several advantages over traditional vaccine such as ease of delivery, mucosal efficacy, safety, rapid scalability, and low cost. However, there are still no reports about the expression of E0 glycoprotein in plants. This experiment successfully acquired glycoprotein E0 of BVDV in transgenic *Astragalus* through pollen-tube pathway. This is the first report on the expression of E0 glycoprotein in a medicinal plant.

The glycoprotein E0 has several functions, such as virus attachment and entry to target cells and the production of neutralizing antibodies, as well as having effects on the pathogenicity of BVDV [37, 38]. The glycoprotein E0 consists of 227 amino acids and isoelectric point is 7.61 [39]. As a conserved protein, E0 shows less antigenic diversity than E2. However, as antigen for BVDV, E0 still has many defects. For example, E0 has many glycosylation sites that are important for proper folding and activity maintenance of protein, and it also exhibits weak immunogenicity. In this study, the transgenic *Astragalus* was successfully used as a platform for production of the glycoprotein E0, which allowed us to overcome the above shortcomings. *Astragalus* extracted as vaccine adjuvant significantly improves immune activity of E0 subunit vaccine. As such, the plant-made glycoprotein E0 has the ability to generate an immune response in sika deer. This study provides a new method for proteins with weak immunogenicity to be used as transgenic vaccine candidates by use of a plant system.

The use of transgenic plants as new antigen-delivery systems for subunit vaccines has been increasingly explored [40]. *Astragalus* has immunomodulatory effects and *Astragalus* as host plants can play a role in the immune adjuvant to enhance the immune level. Plants can be mass-produced, inexpensive source of antigens, and an ideal system for subunit vaccine. The research provided new ideas for the development of transgenic medicinal plants vaccines.

5. Conclusions

In summary, glycoprotein E0 was effectively expressed in transgenic *Astragalus*. Deer immunized subcutaneously

(s.c.) with the transgenic plant vaccine could develop specific humoral and cell-mediated immune responses against BVDV. The research provides new ideas for the development of medicinal plants vaccine.

Conflict of Interests

The authors declare that there is no conflict of interests regarding the publication of this paper.

Authors' Contribution

Yugang Gao and Xueliang Zhao contributed equally to this work.

Acknowledgments

The authors gratefully acknowledge the financial support provided by the National Natural Science Foundation of China (31070316), Ministry of Science and Technology of China (2011BAT03B01), and Science and Technology Department of Jilin Province (2010B10010945, 20110228, and 20112101).

References

[1] G. J. Gunn, H. W. Saatkamp, R. W. Humphry, and A. W. Stott, "Assessing economic and social pressure for the control of bovine viral diarrhoea virus," *Preventive Veterinary Medicine*, vol. 72, no. 1-2, pp. 149–162, 2005.

[2] W. Z. Xue, D. Mattick, L. Smith, J. Umbaugh, and E. Trigo, "Vaccination with a modified-live bovine viral diarrhea virus (BVDV) type 1a vaccine completely protected calves against challenge with BVDV type 1b strains," *Vaccine*, vol. 29, no. 1, pp. 70–76, 2010.

[3] M. Al-Haddawi, G. B. Mitchell, M. E. Clark, R. D. Wood, and J. L. Caswell, "Impairment of innate immune responses of airway epithelium by infection with bovine viral diarrhea virus," *Veterinary Immunology and Immunopathology*, vol. 116, no. 3-4, pp. 153–162, 2007.

[4] I. M. G. A. Berends, W. A. J. M. Swart, K. Frankena, J. Muskens, T. J. G. M. Lam, and G. van Schaik, "The effect of becoming BVDV-free on fertility and udder health in Dutch dairy herds," *Preventive Veterinary Medicine*, vol. 84, no. 1-2, pp. 48–60, 2008.

[5] E. Peterhans, T. W. Jungi, and M. Schweizer, "How the bovine viral diarrhea virus outwits the immune system," *Deutsche Tierarztliche Wochenschrift*, vol. 113, no. 4, pp. 124–129, 2006.

[6] H. Yilmaz, E. Altan, J. Ridpath, and N. Turan, "Genetic diversity and frequency of bovine viral diarrhea virus (BVDV) detected in cattle in Turkey," *Comparative Immunology, Microbiology and Infectious Diseases*, vol. 35, no. 5, pp. 411–416, 2012.

[7] T. Passler, P. H. Walz, S. S. Ditchkoff, M. D. Givens, H. S. Maxwell, and K. V. Brock, "Experimental persistent infection with bovine viral diarrhea virus in white-tailed deer," *Veterinary Microbiology*, vol. 122, no. 3-4, pp. 350–356, 2007.

[8] S. Juliá, M. I. Craig, L. S. Jiménez, G. B. Pinto, and E. L. Weber, "First report of BVDV circulation in sheep in Argentina," *Preventive Veterinary Medicine*, vol. 90, no. 3-4, pp. 274–277, 2009.

[9] T. Passler, P. H. Walz, S. S. Ditchkoff et al., "Cohabitation of pregnant white-tailed deer and cattle persistently infected with Bovine viral diarrhea virus results in persistently infected fawns," *Veterinary Microbiology*, vol. 134, no. 3-4, pp. 362–367, 2009.

[10] Y. G. Gao, S. J. Wang, R. Du et al., "Isolation and identification of a bovine viral diarrhea virus from sika deer in China," *Virology Journal*, vol. 8, article 83, 2011.

[11] I. Greiser-Wilke, B. Grummer, and V. Moennig, "Bovine viral diarrhoea eradication and control programmes in Europe," *Biologicals*, vol. 31, no. 2, pp. 113–118, 2003.

[12] A.-F. Viet, C. Fourichon, and H. Seegers, "Simulation study to assess the efficiency of a test-and-cull scheme to control the spread of the bovine viral-diarrhoea virus in a dairy herd," *Preventive Veterinary Medicine*, vol. 76, no. 3-4, pp. 151–166, 2006.

[13] R. W. Fulton, J. F. Ridpath, A. W. Confer, J. T. Saliki, L. J. Burge, and M. E. Payton, "Bovine viral diarrhoea virus antigenic diversity: impact on disease and vaccination programmes," *Biologicals*, vol. 31, no. 2, pp. 89–95, 2003.

[14] C. L. Kelling, "Evolution of bovine viral diarrhea virus vaccines," *Veterinary Clinics of North America—Food Animal Practice*, vol. 20, no. 1, pp. 115–129, 2004.

[15] C. Thomas, N. J. Young, J. Heaney, M. E. Collins, and J. Brownlie, "Evaluation of efficacy of mammalian and baculovirus expressed E2 subunit vaccine candidates to bovine viral diarrhoea virus," *Vaccine*, vol. 27, no. 17, pp. 2387–2393, 2009.

[16] M. Schweizer, P. Mätzener, G. Pfaffen, H. Stalder, and E. Peterhans, ""Self" and "nonself" manipulation of interferon defense during persistent infection: bovine viral diarrhea virus resists alpha/beta interferon without blocking antiviral activity against unrelated viruses replicating in its host cells," *Journal of Virology*, vol. 80, no. 14, pp. 6926–6935, 2006.

[17] S. R. Bolin, "Immunogens of bovine viral diarrhea virus," *Veterinary Microbiology*, vol. 37, no. 3-4, pp. 263–271, 1993.

[18] P. Andrea, S. A. María, A. Alejandra et al., "Safety and efficacy of an E2 glycoprotein subunit vaccine produced in mammalian cells to prevent experimental infection with bovine viral diarrhoea virus in cattle," *Veterinary Research Communications*, vol. 36, no. 3, pp. 157–164, 2012.

[19] M. K. Baxi, D. Deregt, J. Robertson, L. A. Babiuk, T. Schlapp, and S. K. Tikoo, "Recombinant bovine adenovirus type 3 expressing bovine viral diarrhea virus glycoprotein E2 induces an immune response in cotton rats," *Virology*, vol. 278, no. 1, pp. 234–243, 2000.

[20] T. Rümenapf, G. Unger, J. H. Strauss, and H.-J. Thiel, "Processing of the envelope glycoproteins of pestiviruses," *Journal of Virology*, vol. 67, no. 6, pp. 3288–3294, 1993.

[21] W. Xue, F. Blecha, and H. C. Minocha, "Antigenic variations in bovine viral diarrhea viruses detected by monoclonal antibodies," *Journal of Clinical Microbiology*, vol. 28, no. 8, pp. 1688–1693, 1990.

[22] R. W. Fulton, D. L. Step, J. F. Ridpath et al., "Response of calves persistently infected with noncytopathic bovine viral diarrhea virus (BVDV) subtype 1b after vaccination with heterologous BVDV strains in modified live virus vaccines and *Mannheimia haemolytica* bacterin-toxoid," *Vaccine*, vol. 21, no. 21-22, pp. 2980–2985, 2003.

[23] Y. G. Gao, Y. J. Wang, R. Du et al., "A recombinant E0 gene of bovine viral diarrhea virus protects against challenge with bovine viral diarrhea virus of sika deer," *African Journal of Microbiology Research*, vol. 5, no. 9, pp. 1012–1017, 2011.

[24] Z.-Q. Yang, Q.-Q. Liu, Z.-M. Pan, H.-X. Yu, and X.-A. Jiao, "Expression of the fusion glycoprotein of newcasstle disease

virus in transgenic rice and its immunogenicity in mice," *Vaccine*, vol. 25, no. 4, pp. 591–598, 2007.

[25] H.-F. Chen, M.-H. Chang, B.-L. Chiang, and S.-T. Jeng, "Oral immunization of mice using transgenic tomato fruit expressing VP1 protein from enterovirus 71," *Vaccine*, vol. 24, no. 15, pp. 2944–2951, 2006.

[26] Z.-J. Guan, B. Guo, Y.-L. Huo, Z.-P. Guan, and Y.-H. Wei, "Overview of expression of hepatitis B surface antigen in transgenic plants," *Vaccine*, vol. 28, no. 46, pp. 7351–7362, 2010.

[27] G. Nelson, P. Marconi, O. Periolo, J. L. Torre, and M. A. Alvarez, "Immunocompetent truncated E2 glycoprotein of bovine viral diarrhea virus (BVDV) expressed in Nicotiana tabacum plants: a candidate antigen for new generation of veterinary vaccines," *Vaccine*, vol. 30, no. 30, pp. 4499–4504, 2012.

[28] V. E. J. C. Schijns and E. C. Lavelle, "Trends in vaccine adjuvants," *Expert Review of Vaccines*, vol. 10, no. 4, pp. 539–550, 2011.

[29] Y. U. Ling, J. Z. Li, and H. Y. Wang, "Progress in the study of the treatment of nephropathy with *Astragalus* and Angelica and their therapeutic mechanism," *Chinese Journal of Integrated Traditional and Western Medicine*, vol. 21, no. 5, pp. 396–399, 2001.

[30] L. Y. Qi and H. X. li, "The study of chemical composition and pharmacological function on *Astragalus*," *Journal of Baoding Teachers College*, vol. 17, no. 4, pp. 40–42, 2004.

[31] W. Zhao, Y.-F. Ren, and J.-H. Fan, "Study on effects of *Astragalus* aksuensis against virus," *Chinese Pharmaceutical Journal*, vol. 36, no. 1, pp. 23–25, 2001.

[32] S. L. Yuan, X. S. Piao, D. F. Li, S. W. Kim, H. S. Lee, and P. F. Quo, "Effects of dietary *Astragalus* polysaccharide on growth performance and immune function in weaned pigs," *Animal Science*, vol. 82, no. 4, pp. 501–507, 2006.

[33] S. Q. Wu and M. L. Mei, "Study on pollination characteristic of *Radix astragali*," *Journal of Anhui Agricultural Sciences*, vol. 36, no. 21, pp. 9184–9303, 2008.

[34] M. M. Bradford, "A rapid and sensitive method for the quantitation of microgram quantities of protein utilizing the principle of protein dye binding," *Analytical Biochemistry*, vol. 72, no. 1-2, pp. 248–254, 1976.

[35] A. Summerfield, S. M. Knötig, and K. C. McCullough, "Lymphocyte apoptosis during classical swine fever: implication of activation-induced cell death," *Journal of Virology*, vol. 72, no. 3, pp. 1853–1861, 1998.

[36] H. Houe, "Epidemiological features and economical importance of bovine virus diarrhoea virus (BVDV) infections," *Veterinary Microbiology*, vol. 64, no. 2-3, pp. 89–107, 1999.

[37] T. Rumenapf, R. Stark, G. Meyers, and H.-J. Thiel, "Structural proteins of hog cholera virus expressed by vaccinia virus: further characterization and induction of protective immunity," *Journal of Virology*, vol. 65, no. 2, pp. 589–597, 1991.

[38] R. Schneider, G. Unger, R. Stark, E. Schneider-Scherzer, and H.-J. Thiel, "Identification of a structural glycoprotein of an RNA virus as a ribonuclease," *Science*, vol. 261, no. 5125, pp. 1169–1171, 1993.

[39] Y. G. Gao, F. Y. Li, H. Yang, R. Du, and P. Zang, "Analysis on BVDV gene of E0 protein's character in Chinese sika deer," *Journal of Biology*, vol. 27, no. 5, pp. 1–3, 2010.

[40] M. Hernández, J. L. Cabrera-Ponce, G. Fragoso et al., "A new highly effective anticysticercosis vaccine expressed in transgenic papaya," *Vaccine*, vol. 25, no. 21, pp. 4252–4260, 2007.

Hindawi Publishing Corporation
Evidence-Based Complementary and Alternative Medicine
Volume 2014, Article ID 580483, 6 pages
http://dx.doi.org/10.1155/2014/580483

Research Article

Cytotoxicity of Aporphine, Protoberberine, and Protopine Alkaloids from *Dicranostigma leptopodum* (Maxim.) Fedde

Ruiqi Sun,[1] Haiyan Jiang,[2] Wenjuan Zhang,[3] Kai Yang,[3] Chengfang Wang,[4] Li Fan,[4] Qing He,[1] Jiangbin Feng,[4] Shushan Du,[3] Zhiwei Deng,[1] and Zhufeng Geng[1]

[1] *Analytic and Testing Center, Beijing Normal University, No. 19 Xinjiekouwai Street, Haidian District, Beijing 100875, China*
[2] *College of Pharmacy, Liaoning University of Traditional Chinese Medicine, Dalian, Liaoning 116600, China*
[3] *State Key Laboratory of Earth Surface Processes and Resource Ecology, Beijing Normal University, Beijing 100875, China*
[4] *Key Laboratory of Radiological Protection and Nuclear Emergency, Chinese Center for Disease Control and Prevention, Haidian District, Beijing 100875, China*

Correspondence should be addressed to Zhufeng Geng; gengzhufeng@bnu.edu.cn

Received 10 April 2014; Revised 2 May 2014; Accepted 2 May 2014; Published 21 May 2014

Academic Editor: Shi-Biao Wu

Nine alkaloids with three different structural skeletons were isolated from *Dicranostigma leptopodum* (Maxim.) Fedde (Papaveraceae) by repeated silica gel column chromatography. Their chemical structures were identified on the basic of physicochemical and spectroscopic data. Among them, 10-*O*-methylhernovine (**1**), nantenine (**2**), corytuberine (**3**), lagesianine A (**4**), and dihydrocryptopine (**9**) were first isolated from this plant. With a series of cytotoxic tests, compounds **2**, **3**, and **7** displayed cytotoxicity against SMMC-7721 with IC_{50} values of 70.08 ± 4.63, 73.22 ± 2.35, and 27.77 ± 2.29 μM, respectively.

1. Introduction

It was reported that nearly three-fifths of currently used anticancer agents were obtained from natural sources [1–3]. Therefore, utilization of ethnopharmacology is an important channel of discovering new biologically active compounds. *Dicranostigma* is a genus in the poppy family Papaveraceae, which is widely distributed in highland areas, especially in Western China. The plants of *Dicranostigma* have been used in folk medicine for treatment of tonsillitis, hepatitis, and inflammation in China for a long time [4–7]. With development of natural product chemistry, recent researches showed that *D. leptopodum* had more excellent biological activities. Extractsof *D. leptopodum* have been reported to exhibit antimicrobial activity [7], antiviral [8], antitumor [9], and anti-liver fibrosis activity [10], and anti-inflammatory activity [11]. Several compounds including alkaloids and terpenes have been reported from *D. leptopodum* [5–7]. But further investigation is necessary to find the chemical basis of activities in this plant. This work aimed to identify the active compounds by assessing the cytotoxic activity of alkaloids isolated from whole plant of *Dicranostigma leptopodum* (Maxim.) Fedde on selected cell lines. And the structural evidence related to cytotoxicity is also discussed.

2. Results and Discussion

Six aporphine alkaloids along with one protoberberine alkaloid and two protopine alkaloids were isolated and characterized from the crude extract. They were 10-*O*-methylhernovine (**1**), nantenine (**2**), corytuberine (**3**), lagesianine A (**4**), corydine (**5**), isocorydine (**6**), dihydrosanguinarine (**7**), protopine (**8**), and dihydrocryptopine (**9**). The structures of compounds **1**–**9** were showed in Figure 1. Among them, compounds **1**–**4** and **9** were isolated from this plant for the first time.

In order to obtain their potential pharmacological activities, compounds **1**–**9** were evaluated for their cytotoxicities against H1299, MCF-7, and SMMC-7721 tumor cell lines by the CCK-8 assay. The results were listed in Table 1.

Compound **2**, **3**, and **7** showed their cytotoxicity against SMCC-7721. It was reported that promising effects of extracts

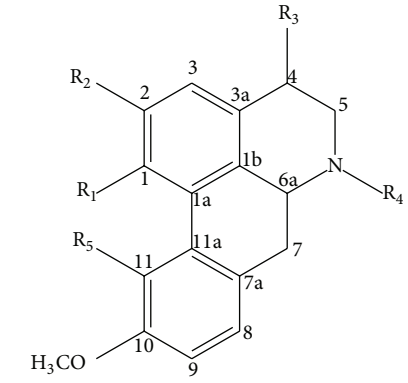

	R_1	R_2	R_3	R_4	R_5
1	OCH_3	OH	H	H	OCH_3
3	OH	OCH_3	H	CH_3	OH
4	OCH_3	OCH_3	OH	CH_3	OH
5	OH	OCH_3	H	CH_3	OCH_3
6	OCH_3	OCH_3	H	CH_3	OH

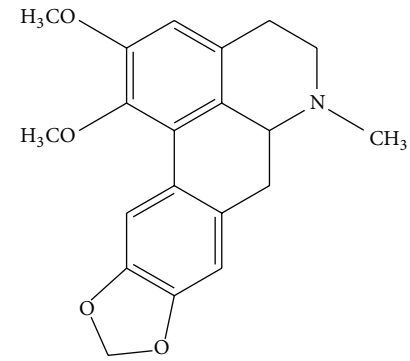

Nantenine (**2**)

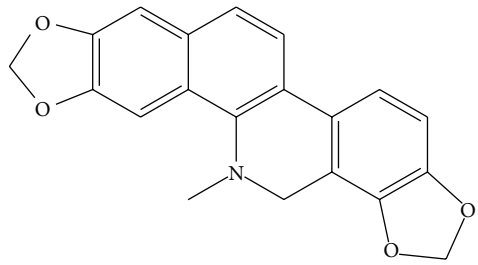

Dihydrosanguinarine (**7**)

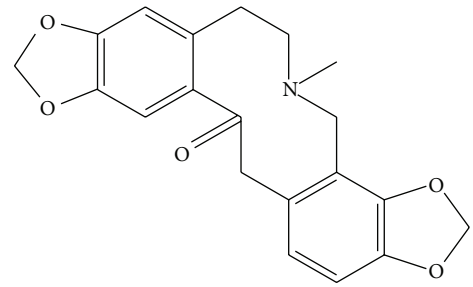

Protopine (**8**)

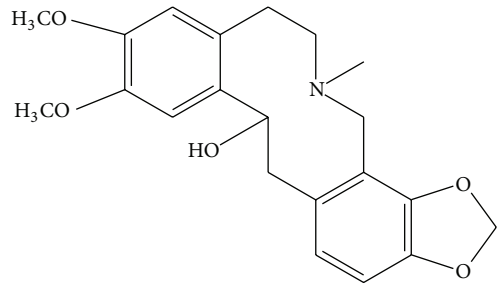

Dihydrocryptopine (**9**)

Figure 1: The structures of compounds **1**–**9**.

of *D. leptopodum* were determined both in vitro and in vivo on antiproliferating of SMCC-7721 cells [12]. Therefore, the cytotoxicity showed in the report [12] might mainly relate with these constituents.

Other compounds (**1**, **4**–**6**, **8**, and **9**) did not show cytotoxicity against the tested cell lines. However, there were some other biological activities of these compounds reported in the literature. This was the first time that cytotoxicity of compound **1** was reported. Compound **4** has been tested in vitro against human poliovirus and was found to be active with selectivity indices >14 [13]. Compounds **5** and **6** were reported to have weak cytotoxicity, such as nontoxic to KB cells, but showed activities in inhibiting cell proliferation of hepatocellular carcinoma [14–18]. The result was consistent with the literature that compound **7** often showed better cytotoxicity than compound **8** against cancer cell lines such as A549, HT-29, KB, and P-388 [19–21].

In aporphine type alkaloids, compounds **2** and **3** showed cytotoxicities to selected cell lines. It has been reported that compound **2** has cytotoxicity against human colon cancer (HCT-116, Caco-2) and normal colon (CCD-18Co) cell lines [22]. And compound **3** was reported to show strong activities in inhibiting the T or B cell proliferation and exhibited strong analgesic effects [23].

Table 1: Cytotoxicities of compounds **1–9** from *Dicranostigma leptopodum* (Maxim.) Fedde.

Compound	IC_{50} (μM)[a,b]		
	H1299	MCF-7	SMMC-7721
Aporphine alkaloids			
1	>100	>100	>100
2	>100	>100	70.08 ± 4.63
3	53.58 ± 5.47	72.30 ± 1.72	73.22 ± 2.35
4	>100	>100	>100
5	>100	>100	>100
6	>100	>100	>100
Protoberberine alkaloids			
7	28.22 ± 1.03	28.34 ± 2.00	27.77 ± 2.29
Protopine alkaloids			
8	>100	>100	>100
9	>100	>100	>100
DOX[c]	11.70 ± 1.53	7.82 ± 0.89	2.74 ± 0.34

[a]IC_{50} value was the 50% inhibition concentration and calculated from regression lines using five different concentrations in replicate experiments for six times. [b]Solvent used in the cytotoxicity test was DMSO, and purity of compounds under the test is above 90%. [c]Doxorubicin was used as the positive control.

Both compounds **3** and **6** have 10-CH_3 and 11-OH. It has been reported that aporphine alkaloids with a 10-CH_3 substitution was negative to its activity related to D2 receptor, despite the presence of the critical 11-OH [24]. In addition, it was found that cytotoxicity of compound **3** with 1-OH was stronger than compound **6** with 1-OCH_3. It could be inferred that cytotoxicity of aporphine alkaloids with 1-OH was stronger than those with 1-OCH_3. And the potential drug targets of these compounds in cell might related with D2 receptor [25].

From the view of structure-activity relationship [26], it could be inferred that 1-OH together with 11-OH is necessary to exhibit cytotoxicity among aporphine alkaloids. For example, compound **3**, having these two hydroxyl substitutions, showed certain cytotoxicity. Indeed, other aporphine compounds above showed weaker cytotoxicity against selected cell lines in this work.

3. Conclusions

Among compounds **1–9**, it was obviously that protoberberine-type alkaloids had stronger cytotoxicity than protopine and aporphine-type ones. From the perspective of structure-activity relationship, it was expected that both 1-OH and 11-OH groups in aporphine alkaloids might be important to exhibit cytotoxic against selected cell lines while 1-OCH_3 exhibits a negative effect to the cytotoxic. The D2 receptor in cell might be the potential drug targets of these compounds. Moreover, further study is needed to investigate the internal mechanism of alkaloids obtained from *D. leptopodum*. This may become potential basis for new antitumor drugs.

4. Material and Methods

4.1. General. ^{1}H and ^{13}C-NMR spectra were recorded on Bruker Avance DRX 500 NMR spectrometer using $CDCl_3$ (D: 99.8%, CLV, Germany) as the solvent with TMS as the internal standard. ESI-MS spectra were obtained from Bruker Q-TOF mass spectrometer. Silica gel (160–200 mesh, 200–300 mesh, Branch of Qingdao Haiyang Chemical Co., Ltd, Qingdao, China) used for column chromatography and Sephadex LH-20 was supplied by Amersham Pharmacia Biotech (Beijing, China). Analytical grade solvents were produced by Beijing Chemical Works (Beijing, China).

4.2. Plant Material. The whole plant (3.0 kg) of *D. leptopodum* was collected from Pingliang, Gansu Province, China (35.30°N, 107.03°E), September 2011, and identified by Dr. Liu Q.R., College of Life Sciences, Beijing Normal University. Voucher specimens (BNU-HSL-Dushushan-2011-9-25) were deposited at the herbarium (BNU) in the College of Resources Sciences, Beijing Normal University.

4.3. Extraction and Isolation. The dried powder (3.0 kg) was extracted by using ultrasound for three times (each for 30 minutes) with chloroform methanol ($CHCl_3$/CH_3OH) (6 L). The crude extract (160.0 g) was obtained by solvent evaporation under reduced pressure. Then silica gel column chromatography (160–200 mesh, 10.0 × 33 cm, 1000 g) was used on fractionation. Chloroform methanol solvent system (v/v ratio of chloroform, 50 : 1, 30 : 1, 10 : 1, and methanol) was used to obtain 50 fractions. Fr.42 (0.70 g) was purified by silica gel column from $CHCl_3$/CH_3OH (8 : 1) to give crystalline compound **6** (32 mg) and compound **5** (13 mg). Silica gel column chromatography (160–200 mesh, 2.0 × 35 cm, 100 g) of Fr.43 (1.26 g) eluting $CHCl_3$/CH_3OH (30 : 1) gave thirty subfractions (43.1–43.30). Fr.43-5 was subjected to silica gel column (160–200 mesh, 1.5 × 30 cm, 48 g) eluted with $CHCl_3$/CH_3OH (8 : 1) to afford compound **4** (5.5 mg) and compound **1** (4.5 mg). Fr.43-12 was subjected to silica gel column (160–200 mesh, 1.5 × 30 cm, 48 g) eluted with $CHCl_3$/CH_3OH (20 : 1) to afford compound **7** (5 mg) and $CHCl_3$/CH_3OH (10 : 1) to obtain compound **8** (8.3 mg). Fr.43-14 was separated by silica gel column (160–200 mesh, 1.5 × 30 cm, 48 g) eluted with $CHCl_3$/CH_3OH (10 : 1) to afford compound **2** (5 mg). Fr.43-15 was subjected to silica gel column (160–200 mesh, 1.5×30 cm, 48 g) eluted with $CHCl_3$/CH_3OH (15 : 1) to obtain subfraction Fr.43-15-1 to afford compound **9** (6.0 mg) and eluted with $CHCl_3$/CH_3OH (10 : 1) to obtain subfraction Fr.43-15-4 purified with $CHCl_3$/CH_3OH (8 : 1), yielding compound **3** (5 mg).

*10-O-Methylhernovine (**1**).* Light brown powder, soluble in chloroform, is with Dragendorff's test positive. ^{1}H-NMR (500 MHz, $CDCl_3$) δ ppm: 6.74 (1H, s, H-3), 3.07 (2H, d, J = 12.5 Hz, H-4), 2.86 (2H, d, J = 12.5 Hz, H-5), 3.29 (1H, m, H-6a), 2.60 (1H, m, H-7), 3.17 (1H, m, H-7), 6.83 (1H, d, J = 7.9 Hz, H-8), 6.86 (1H, d, J = 7.9 Hz, H-9), 3.92 (3H, s, 1-OCH_3), 8.86 (1H, br, s, 2-OH), 3.74 (1H, s, 10-OCH_3), 3.92 (1H, s, 11-OCH_3). ^{13}C-NMR (125 MHz, $CDCl_3$) δ ppm: 142.6

(C-1), 126.0 (C-1a), 119.8 (C-1b), 152.2 (C-2), 111.3 (C-3), 130.9 (C-3a), 128.8 (C-3b), 27.4 (C-4), 41.8 (C-5), 53.6 (C-6a), 36.5 (C-7), 128.2 (C-7a), 119.4 (C-8), 111.5 (C-9), 149.8 (C-10), 144.3 (C-11), 56.0 (1-OCH_3), 62.2 (10-OCH_3), 56.2 (11-OCH_3). Its NMR spectral data were in accord with the reported data [27].

*Nantenine (**2**)*. Yellow needle crystals, soluble in chloroform, exhibited a positive Dragendorff's test. ^{1}H-NMR (500 MHz, $CDCl_3$) δ ppm: 6.63 (1H, s, H-3), 4.51 (2H, s, H-7), 6.95 (1H, d, J = 8.0 Hz, H-8), 7.07 (1H, s, H-9), 6.92 (1H, d, J = 8.0 Hz, H-11), 3.88 (3H, s, 1-OCH_3), 3.87 (3H, s, 2-OCH_3), 2.95 (3H, s, N-CH_3), 5.97 (2H, s, –OCH_2–). ^{13}C-NMR (125 MHz, $CDCl_3$) δ ppm: 145.7 (C-1), 125.0 (C-1a), 121.5 (C-1b), 151.2 (C-2), 112.9 (C-3), 127.7 (C-3a), 128.2 (C-3b), 29.7 (C-4), 54.9 (C-5), 63.8 (C-6a), 38.8 (C-7), 130.9 (C-7a), 106.7 (C-8), 148.8 (C-9), 147.4 (C-10), 108.6 (C-11), 60.9 (1-OCH_3), 55.9 (2-OCH_3), 43.5 (N-CH_3), 101.6 (9, 10-OCH_2O–). The ^{1}H- and ^{13}C-NMR spectral data were consistent with the reported data [28].

*Corytuberine (**3**)*. Colorless columnar crystals, soluble in chloroform, were positive to Dragendorff's test. ^{1}H-NMR (500 MHz, $CDCl_3$) δ ppm: 6.71 (1H, s, H-3), 3.18 (1H, td, J = 14, 4 Hz, H-4), 2.69 (1H, dd, J = 14, 4 Hz, H-4), 3.05 (1H, m, H-5), 2.54 (1H, m, H-5), 2.99 (1H, d, J = 13 Hz, H-6a), 3.04 (1H, m, H-7), 2.44 (1H, d, J = 13 Hz, H-7), 7.01 (1H, d, J = 7.5 Hz, H-8), 6.92 (1H, d, J = 7.5 Hz, H-9), 3.92 (3H, s, 2-OCH_3), 2.57 (3H, s, N-CH_3), 3.76 (3H, s, 10-OCH_3). ^{13}C-NMR (125 MHz, $CDCl_3$) δ ppm: 141.8 (C-1), 124.3 (C-1a), 130.9 (C-1b), 148.8 (C-2), 111.4 (C-3), 125.2 (C-3a), 118.9 (C-3b), 28.9 (C-4), 52.8 (C-5), 62.7 (C-6a), 35.2 (C-7), 127.9 (C-7a), 125.1 (C-8), 114.7 (C-9), 148.2 (C-10), 142.2 (C-11), 62.0 (1-OCH_3), 44.0 (N-CH_3), 62.5 (10-OCH_3). The ^{1}H- and ^{13}C-NMR spectral data were identical with the literature data [29].

*Lagesianine A (**4**)*. Colorless columnar crystals, soluble in chloroform, gave a positive visualization to Dragendorff's test. ^{1}H-NMR (500 MHz, $CDCl_3$) δ ppm: 7.05 (1H, s, H-3), 4.59 (1H, br, s, H-4), 3.22 (1H, br, dd, J = 12, 1.7 Hz, H-5), 2.80 (1H, dd, J = 13, 3.1 Hz, H-5), 3.06 (1H, m, H-6a), 3.10 (1H, dd, J = 13, 3.1 Hz, H-7), 2.62 (1H, m, H-7), 6.86 (1H, d, J = 8 Hz, H-8), 6.89 (1H, d, J = 8 Hz, H-9), 3.98 (3H, s, 1-OCH_3), 3.76 (3H, s, 2-OCH_3), 2.67 (3H, s, N-CH_3), 3.94 (3H, s, 10-OCH_3), 8.76 (1H, s, 11-OH). ^{13}C-NMR (125 MHz, $CDCl_3$) δ ppm: 144.2 (C-1), 128.3 (C-1a), 119.3 (C-1b), 152.2 (C-2), 111.8 (C-3), 131.9 (C-3a), 125.8 (C-3b), 62.1 (C-4), 60.1 (C-5), 66.4 (C-6a), 35.1 (C-7), 128.8 (C-7a), 119.9 (C-8), 111.2 (C-9), 149.7 (C-10), 143.7 (C-11), 63.1 (1-OCH_3), 55.9 (2-OCH_3), 43.3 (N-CH_3), 56.1 (10-OCH_3). The above data were in accord with the literature data [30].

*Corydine (**5**)*. It is colorless columnar crystals.^{1}H-NMR (500 MHz, $CDCl_3$) δ ppm: 6.71 (1H, s, H-3), 3.21 (1H, td, J = 13.4, 6.5 Hz, H-4), 2.71 (1H, m, H-4), 3.09 (1H, dd, J = 7, 3.5 Hz, H-5), 2.57 (1H, m, H-5), 3.06 (1H, m, H-6a), 3.08 (1H, m, H-7), 2.48 (1H, t, J = 13 Hz, H-7), 7.11 (1H, d, J = 8.3 Hz, H-8), 6.90 (1H, d, J = 8.3 Hz, H-9), 8.73 (1H, s, 1-OH), 3.93 (3H, s, 2-OCH_3), 2.58 (3H, s, N-CH_3), 3.94 (3H, s, 10-OCH_3), 3.76 (3H, s, 11-OCH_3). ^{13}C-NMR (125 MHz, $CDCl_3$) δ ppm: 142.4 (C-1), 123.8 (C-1a), 130.7 (C-1b), 149.3 (C-2), 111.4 (C-3), 126.4 (C-3a), 119.3 (C-3b), 28.8 (C-4), 52.7 (C-5), 62.7 (C-6a), 35.4 (C-7), 127.7 (C-7a), 124.4 (C-8), 111.0 (C-9), 151.9 (C-10), 143.9 (C-11), 56.0 (2, 10-OCH_3), 43.7 (N-CH_3), 62.0 (11-OCH_3). The ^{1}H- and ^{13}C-NMR spectral data were consistent with the literature data [31].

*Isocorydine (**6**)*. It is colorless columnar crystals. ^{1}H-NMR (500 MHz, $CDCl_3$) δ ppm: 6.73 (1H, s, H-3), 3.20 (1H, m, H-4), 2.72 (2H, d, J = 17 Hz, H-4), 3.02 (1H, m, H-5), 2.49 (1H, t, J = 12 Hz, H-5), 2.89 (1H, d, J = 12 Hz, H-6a), 3.06 (1H, dd, J = 13.5, 3.1 Hz, H-7), 2.45 (1H, q, J = 13.5 Hz, H-7), 6.86 (1H, d, J = 8.0 Hz, H-8), 6.88 (1H, d, J = 8.0 Hz, H-9), 3.72 (3H, s, 1-OCH_3), 3.94 (3H, s, 2-OCH_3), 2.55 (3H, s, N-CH_3), 3.92 (3H, s, 10-OCH_3), 8.85 (1H, s, 11-OH). ^{13}C-NMR (125 MHz, $CDCl_3$) δ ppm: 142.2 (C-1), 126.0 (C-1a), 120.1 (C-1b), 151.3 (C-2), 111.1 (C-3), 129.0 (C-3a), 130.0 (C-3b), 29.4 (C-4), 52.8 (C-5), 62.9 (C-6a), 35.9 (C-7), 130.0 (C-7a), 119.0 (C-8), 111.0 (C-9), 149.5 (C-10), 144.0 (C-11), 62.1 (1-OCH_3), 56.1 (2-OCH_3), 43.9 (N-CH_3), 56.0 (10-OCH_3). The ^{1}H- and ^{13}C-NMR spectral data were identical with published data [32].

*Dihydrosanguinarine (**7**)*. It is pale yellow needles. ^{1}H-NMR (500 MHz, $CDCl_3$) δ ppm: 7.13 (1H, s, H-1), 7.69 (1H, s, H-4), 4.22 (2H, s, H-6), 6.87 (1H, d, J = 8.0 Hz, H-9), 7.32 (1H, d, J = 8.0 Hz, H-10), 7.71 (1H, d, J = 8.5 Hz, H-11), 7.50 (1H, d, J = 8.5 Hz, H-12), 6.08 (2H, s, 2, 3-OCH_2O–), 6.30 (2H, s, 7, 8-OCH_2O–), 2.64 (3H, s, N-CH_3). ^{13}C-NMR (125 MHz, $CDCl_3$) δ ppm: 104.3 (C-1), 148.1 (C-2), 147.5 (C-3), 100.7 (C-4), 126.5 (C-4a), 142.5 (C-4b), 48.5 (C-6), 113.6 (C-6a), 144.6 (C-7), 147.1 (C-8), 107.2 (C-9), 116.2 (C-10), 127.3 (C-10a), 124.4 (C-10b), 120.4 (C-11), 123.9 (C-12), 130.8 (C-12a), 101.0 (2, 3-OCH_2O–), 101.3 (7, 8-OCH_2O–), 41.6 (N-CH_3). The ^{1}H- and ^{13}C-NMR spectral data were in accord with published data [33].

*Protopine (**8**)*. It is colorless columnar crystals. ^{1}H-NMR (500 MHz, $CDCl_3$) δ ppm: 6.66 (1H, s, H-1), 6.93 (1H, s, H-4), 6.71 (1H, d, J = 7.7 Hz, H-11), 6.68 (1H, d, J = 7.7 Hz, H-12), 5.97 (2H, s, 2, 3-OCH_2O–), 5.95 (2H, s, 9, 10-OCH_2O–), 2.00 (3H, s, N-CH_3). ^{13}C-NMR (125 MHz, $CDCl_3$) δ ppm: 110.3 (C-1), 148.0 (C-2), 146.2 (C-3), 108.0 (C-4), 135.6 (C-4a), 31.4 (C-5), 57.7 (C-6), 51.1 (C-8), 117.5 (C-8a), 146.0 (C-9), 145.9 (C-10), 106.8 (C-11), 124.9 (C-12), 128.6 (C-12a), 46.1 (C-13), 197.5 (C-14), 132.3 (C-14a), 101.2 (2, 3-OCH_2O–), 100.9 (9, 10-OCH_2O–), 41.6 (N-CH_3). The ^{1}H- and ^{13}C-NMR spectral data were consistent with published data [34].

*Dihydrocryptopine (**9**)*. It is white powder. ESI-MS m/z: 372.5 $[M + H]^+$. ^{1}H-NMR (500 MHz, $CDCl_3$) δ ppm: 7.04 (1H, s, H-1), 6.63 (1H, s, H-4), 6.63 (1H, s, H-4), 3.65 (2H, m, H-5), 3.40 (1H, m, H-6), 3.33 (1H, m, H-6), 4.31 (2H, s H-8), 6.93 (1H, d, J = 8.6 Hz, H-11), 6.88 (1H, d, J = 8.6 Hz, H-11), 3.18 (2H, m, H-13), 3.05 (1H, m, H-14), 3.86 (3H, s, 2-OCH_3), 3.87 (3H, s, 3-OCH_3), 5.97 (2H, s, 9, 10-OCH_2O–), 6.30 (1H, br, s, 14-OH), 2.62 (3H, s, N-CH_3). ^{13}C-NMR (125 MHz, $CDCl_3$) δ ppm: 107.4 (C-1), 151.3 (C-2), 146.1 (C-3), 109.0 (C-4), 130.9 (C-4a), 63.9 (C-5), 55.5 (C-6), 54.1 (C-8), 123.8 (C-8a), 147.0 (C-9), 148.5 (C-10), 125.7 (C-11), 112.3 (C-12), 124.3 (C-12a), 55.4 (C-13), 42.0 (C-14), 126.9 (C-14a), 60.8 (2-OCH_3),

55.8 (3-OCH_3), 101.5 (9, 10-OCH_2O–), 42.6 (N-CH_3). The spectrum matched the previous report [35].

4.4. Cytotoxicity Assay. The cytotoxicity of compounds **1**–**9** was determined by the CCK-8 assay [36]. H1299 (nonsmall lung carcinoma), MCF-7 (breast cancer), and SMMC-7721 (liver cancer) were purchased from the Chinese Academy of Medical Sciences (Beijing, China). Doxorubicin (DOX, Adriamycin, Actavis Italy S.p.A., Beijing, China) was the positive control. All cells were grown and maintained in RPMI 1640 (Sigma, St. Louis, MO, USA) medium supplemented with 10% fetal bovine serum (Grand Island, NY, USA), 100 IU/mL penicillin (Flow Lab, Beijing, China), and 100 μg/mL streptomycin (Flow Lab, Beijing, China) at 37°C, 5% CO_2, and 90% humidity. Cancer cells were seeded in the growth medium (100 μL) into 96-well microtiter plate (5×10^3 cells per each well). After 4–6 h preincubation in the incubator (Forma Series II Water Jacket) to allow cellular attachment, various concentrations of test solution were added and cells were incubated for 36 h. At the end of the incubation, CCK-8 reagent (Cell Counting Kit-8, Dojindo, Kumamoto, Japan, 10 μL) was added into each well followed by further incubation for 2 h. The optical density (OD) was measured at 450 nm using a multiscan microplate reader (Thermo, Shanghai, China) [37]. Each determination represented the average mean of six replicates. The half-maximal growth inhibitory concentration (IC_{50}) value was calculated by the line equation of the dose-dependent curve of each compound. The equation to calculate the inhibition rate was

$$R_{\text{Inhibition}} = 1 - \frac{\left(R_{\text{dosing cell group}} - R_{\text{control group}}\right)}{\left(R_{\text{cell control group}} - R_{\text{control group}}\right)} - R_{\text{sovlent}}. \quad (1)$$

Disclosure

Samples of the crude extracts and pure compounds are available from the authors.

Conflict of Interests

The authors declare no conflict of interests.

Acknowledgments

This project was supported by the State Key Laboratory of Earth Surface Processes and Resource Ecology and the National Natural Science Foundation of China (no. 81374069).

References

[1] G. M. Cragg and D. J. Newman, "Natural product drug discovery in the next millennium," *Pharmaceutical Biology*, vol. 39, supplement 1, pp. 8–17, 2001.

[2] S.-B. Wu, J.-J. Su, L.-H. Sun et al., "Triterpenoids and steroids from the fruits of *Melia toosendan* and their cytotoxic effects on two human cancer cell lines," *Journal of Natural Products*, vol. 73, no. 11, pp. 1898–1906, 2010.

[3] S.-B. Wu, F. Pang, Y. Wen, H.-F. Zhang, Z. Zhao, and J.-F. Hu, "Antiproliferative and apoptotic activities of linear furocoumarins from *Notopterygium incisum* on cancer cell lines," *Planta Medica*, vol. 76, no. 1, pp. 82–85, 2010.

[4] H. Guinaudeau, M. Lebœuf, and A. Cavé, "Aporphinoid alkaloids, V," *Journal of Natural Products*, vol. 57, no. 8, pp. 1033–1135, 1994.

[5] Y. Dang, H. F. Gong, J. X. Liu, and S. J. Yu, "Alkaloid from *Dicranostigma leptopodum* (Maxim) Fedde," *Chinese Chemical Letters*, vol. 20, no. 10, pp. 1218–1220, 2009.

[6] F. Wang and Y.-M. Li, "New hopane triterpene from *Dicranostigma leptopodum* (Maxim) Fedde," *Journal of Asian Natural Products Research*, vol. 12, no. 1, pp. 94–97, 2010.

[7] Q. Zhao, T. Wang, S. Yu et al., "Determination of antibacterial activities of *Dicranostigma leptodum* (Maxim.) Fedde's alkaloid," *Chinese Journal of Veterinary Science and Technolo*, vol. 12, pp. 1098–1101, 2008.

[8] D. Yan, M. A. Zhi-Hong, G. Xiang-Zheng et al., "Antiviral test on *Dicranostigma leptopodum* (Maxim) Fedde of water soluble preparation for external use," *Journal of Animal Science and Veterinary Medicine*, vol. 32, no. 1, pp. 3–5, 2013.

[9] J. Li and H. Sun, "Agent for selectively killing tumor stem cells and use thereof," Google Patents CN, 102657653 A, 2012.

[10] "Novel application of dicranostigma leptopodum or extracts of dicranostigma leptopodum," Google Patents CN, 102697864 A, 2013.

[11] W. Tingpu and Z. Qiang, "Research progress on chemical constituents and anti-inflammatory effects of medicinal plant *Dicranostigma leptodum* (Maxim.) Fedde," *Journal of Food Safety and Quality*, vol. 4, no. 5, pp. 1323–1328, 2013.

[12] W.-H. Zhang, M.-H. Lv, J. Hai, Q.-P. Wang, and Q. Wang, "*Dicranostigma leptopodum* (Maxim) Fedde induced apoptosis in SMMC-7721 human hepatoma cells and inhibited tumor growth in mice," *Natural Science*, vol. 2, no. 5, pp. 457–463, 2010.

[13] J. Boustie, J.-L. Stigliani, J. Montanha, M. Amoros, M. Payard, and L. Girret, "Antipoliovirus structure-activity relationships of some aporphine alkaloids," *Journal of Natural Products*, vol. 61, no. 4, pp. 480–484, 1998.

[14] H. Sun, H. Hou, P. Lu et al., "Isocorydine inhibits cell proliferation in hepatocellular carcinoma cell lines by inducing G2/M cell cycle arrest and apoptosis," *PLoS ONE*, vol. 7, no. 5, Article ID e36808, 2012.

[15] P. Lu, H. Sun, L. Zhang et al., "Isocorydine targets the drug-resistant cellular side population through PDCD4-related apoptosis in hepatocellular carcinoma," *Molecular Medicine*, vol. 18, pp. 1136–1146, 2012.

[16] C.-M. Chiou, C.-T. Lin, W.-J. Huang et al., "Semisynthesis and myocardial activity of thaliporphine N-homologues," *Journal of Natural Products*, vol. 76, no. 3, pp. 405–412, 2013.

[17] Y. Liu, J. Liu, D. Di, M. Li, and Y. Fen, "Structural and mechanistic bases of the anticancer activity of natural aporphinoid alkaloids," *Current Topics in Medicinal Chemistry*, vol. 13, no. 17, pp. 2116–2126, 2013.

[18] C. W. Wright, S. J. Marshall, P. F. Russell et al., "In vitro antiplasmodial, antiamoebic, and cytotoxic activities of some monomeric isoquinoline alkaloids," *Journal of Natural Products*, vol. 63, no. 12, pp. 1638–1640, 2000.

[19] K. W. Bentley, "β-phenylethylamines and the isoquinoline alkaloids," *Natural Product Reports*, vol. 20, no. 3, pp. 342–365, 2003.

[20] L. Grycová, J. Dostál, and R. Marek, "Quaternary protoberberine alkaloids," *Phytochemistry*, vol. 68, no. 2, pp. 150–175, 2007.

[21] J.-J. Chen, C.-Y. Duh, and I.-S. Chen, "New tetrahydroprotoberberine *N*-oxide alkaloids and cytotoxic constituents of *Corydolis tashiroi*," *Planta Medica*, vol. 65, no. 7, pp. 643–647, 1999.

[22] S. Ponnala, S. Chaudhary, A. González-Sarrias, N. P. Seeram, and W. W. Harding, "Cytotoxicity of aporphines in human colon cancer cell lines HCT-116 and Caco-2: an SAR study," *Bioorganic & Medicinal Chemistry Letters*, vol. 21, no. 15, pp. 4462–4464, 2011.

[23] Y.-N. Zhang, X.-G. Zhong, Z.-P. Zheng, X.-D. Hu, J.-P. Zuo, and L.-H. Hu, "Discovery and synthesis of new immunosuppressive alkaloids from the stem of *Fissistigma oldhamii* (Hemsl.) Merr.," *Bioorganic & Medicinal Chemistry*, vol. 15, no. 2, pp. 988–996, 2007.

[24] J. G. Cannon, S. T. Moe, and J. P. Long, "Enantiomers of 11-hydroxy-10-methylaporphine having opposing pharmacological effects at 5-HT_{1A} receptors," *Chirality*, vol. 3, no. 1, pp. 19–23, 1991.

[25] A. Zhang, Y. Zhang, A. R. Branfman, R. J. Baldessarini, and J. L. Neumeyer, "Advances in development of dopaminergic aporphinoids," *Journal of Medicinal Chemistry*, vol. 50, no. 2, pp. 171–181, 2007.

[26] X. Wang, C. A. Ohlin, Q. Lu, Z. Fei, J. Hu, and P. J. Dyson, "Cytotoxicity of ionic liquids and precursor compounds towards human cell line HeLa," *Green Chemistry*, vol. 9, no. 11, pp. 1191–1197, 2007.

[27] M. S. Buchanan, A. R. Carroll, D. Pass, and R. J. Quinn, *Aporphine Alkaloids from the Chinese Tree Neolitsea aurata var. paraciculata*, Natural Product Communications, 2007.

[28] H. Guinaudeau, M. Leboeuf, and A. Cavé, "Aporphine alkaloids. II," *Journal of Natural Products*, vol. 42, no. 4, pp. 325–360, 1979.

[29] T. Kametani and M. Ihara, "Alkaloid formation through *N*-oxide intermediates; regioselective synthesis of (±)-corytuberine by redox reaction," *Journal of the Chemical Society, Perkin Transactions 1*, pp. 629–632, 1980.

[30] M. L. R. Ferreira, I. C. de Pascoli, I. R. Nascimento, J. Zukerman-Schpector, and L. M. X. Lopes, "Aporphine and bisaporphine alkaloids from *Aristolochia lagesiana* var. *intermedia*," *Phytochemistry*, vol. 71, no. 4, pp. 469–478, 2010.

[31] D. L. Galinis, D. F. Wiemer, and J. Cazin Jr., "Cissampentin: a new bisbenzylisoquinoline alkaloid from *Cissampelos fasciculata*," *Tetrahedron*, vol. 49, no. 7, pp. 1337–1342, 1993.

[32] M.-H. Yang, A. V. Patel, G. Blunden, C. H. Turner, M. J. O'Neill, and J. A. Lewist, "Crabbine, an aporphine alkaloid from *Corydalis lutea*," *Phytochemistry*, vol. 33, no. 4, pp. 943–945, 1993.

[33] S. M. Oechslin, G. M. König, K. Oechslin-Merkel et al., "An NMR study of four benzophenanthridine alkaloids," *Journal of Natural Products*, vol. 54, no. 2, pp. 519–524, 1991.

[34] C. Seger, S. Sturm, E.-M. Strasser, E. Ellmerer, and H. Stuppner, "^{1}H and ^{13}C NMR signal assignment of benzylisoquinoline alkaloids from *Fumaria officinalis* L. (Papaveraceae)," *Magnetic Resonance in Chemistry*, vol. 42, no. 10, pp. 882–886, 2004.

[35] S. G. Davies, C. L. Goodfellow, J. M. Peach, and A. Waller, "Stereoselective and regioselective functionalisation of protopine alkaloids: the synthesis of 1-substituted O-methyldihydrocryptopines," *Journal of the Chemical Society, Perkin Transactions 1*, no. 5, pp. 1019–1025, 1991.

[36] S.-B. Wu, Y.-P. Ji, J.-J. Zhu et al., "Steroids from the leaves of Chinese *Melia azedarach* and their cytotoxic effects on human cancer cell lines," *Steroids*, vol. 74, no. 9, pp. 761–765, 2009.

[37] S.-B. Wu, Q.-Y. Bao, W.-X. Wang et al., "Cytotoxic triterpenoids and steroids from the bark of *Melia azedarach*," *Planta Medica*, vol. 77, no. 9, pp. 922–928, 2011.

Hindawi Publishing Corporation
Evidence-Based Complementary and Alternative Medicine
Volume 2014, Article ID 573745, 10 pages
http://dx.doi.org/10.1155/2014/573745

Research Article

Cardioprotective Effect of Betulinic Acid on Myocardial Ischemia Reperfusion Injury in Rats

Anzhou Xia,[1] Zhi Xue,[1] Yong Li,[2] Wei Wang,[1] Jieyun Xia,[1] Tiantian Wei,[1] Jing Cao,[1] and Weidong Zhou[3]

[1] *Department of Pharmacology, Xuzhou Medical College, Xuzhou, Jiangsu 221004, China*
[2] *Department of Gastrointestinal Surgery, Xuzhou Central Hospital, Xuzhou, Jiangsu 221006, China*
[3] *Department of Cardiology, The People's Hospital of Suining, Suining, Xuzhou, Jiangsu 221200, China*

Correspondence should be addressed to Weidong Zhou; xzd211xz@sina.com

Received 18 March 2014; Accepted 1 May 2014; Published 21 May 2014

Academic Editor: Shi-Biao Wu

Objectives. This study aims to investigate the effect of betulinic acid (BA) on myocardial ischemia reperfusion/injury in an open-chest anesthetized rat model. *Methods*. The model was induced by 30 minutes left anterior descending occlusion followed by 2 hours reperfusion. There are six groups in our present study: sham operation group, ischemia/reperfusion group, low-dosage BA group, medium-dosage BA group, high-dosage BA group, and fosinopril sodium group. Rats in the latter four groups were administrated with BA (50, 100, and 200 mg/kg, i.g.) or fosinopril sodium (10 mg/kg, i.g.) once a day for 7 days before operation, respectively. Rats in the former two groups were given the same volume of vehicle (0.5% CMC-Na, i.g.). During the operation, cardiac function was continuously monitored. Serum LDH and CK were measured with colorimetric assays. The expression of Bcl-2 and Bax and the apoptosis of cardiomyocytes were investigated with western blot and TUNEL assay, respectively. *Results*. Pretreatment with BA improved cardiac function and attenuated LDH and CK activities compared with IR group. Further investigation demonstrated that the expression of Bcl-2 and Bax and TUNEL assay was in line with the above results. *Conclusion*. BA may reduce the release of LDH and CK, prevent cardiomyocytes apoptosis, and eventually alleviate the extent of the myocardial ischemia/reperfusion injury.

1. Introduction

In China, cardiovascular diseases (CVDs) are the leading cause of death and a major health problem. According to the report on cardiovascular diseases in China, approximately 3 million Chinese people die from CVD every year, accounting for 40% of all causes of death [1], of which ischemic heart disease accounts for a large percentage. Ischemic heart disease is a major cause of morbidity and mortality in both the developing and the developed world now [2]. Myocardial ischemia/reperfusion injury (MIRI) was first postulated in 1960 by Jennings et al. [3], which refers to a phenomenon that timely restoring coronary blood flow after myocardial ischemia induces severe myocardium injury, although at the same time it could reduce myocardial infarct size and improve the clinical outcomes. The underlying mechanisms are complex, and the present main proposals include Ca^{2+} overload, excessive reactive oxygen species (ROS) generation, inflammation, and apoptosis [4]. These modalities interact with each other, and apoptosis plays a pivotal role in the progress of MIRI and, thus, influences the outcomes. Apoptosis is usually triggered by intracellular Ca^{2+} overload, which induces the processing of procaspase-8 into active caspase-8 and the activation of Bax, which lead to the release of the apoptosis-inducing factor, Smac, and cytochrome-c from mitochondria. Apoptosis-inducing factor translocates into the nucleus and facilitates nonspecific DNA fragmentation. Smac inactivates X chromosome-linked inhibitor of apoptosis protein, which inhibits caspase-3, and cytochrome-c forms an apoptosome complex with procaspase-9 and apoptotic protease-activating factor-1, which activates caspase-9. Taken together, these cascades ultimately contribute to irreversible cellular dysfunction [4].

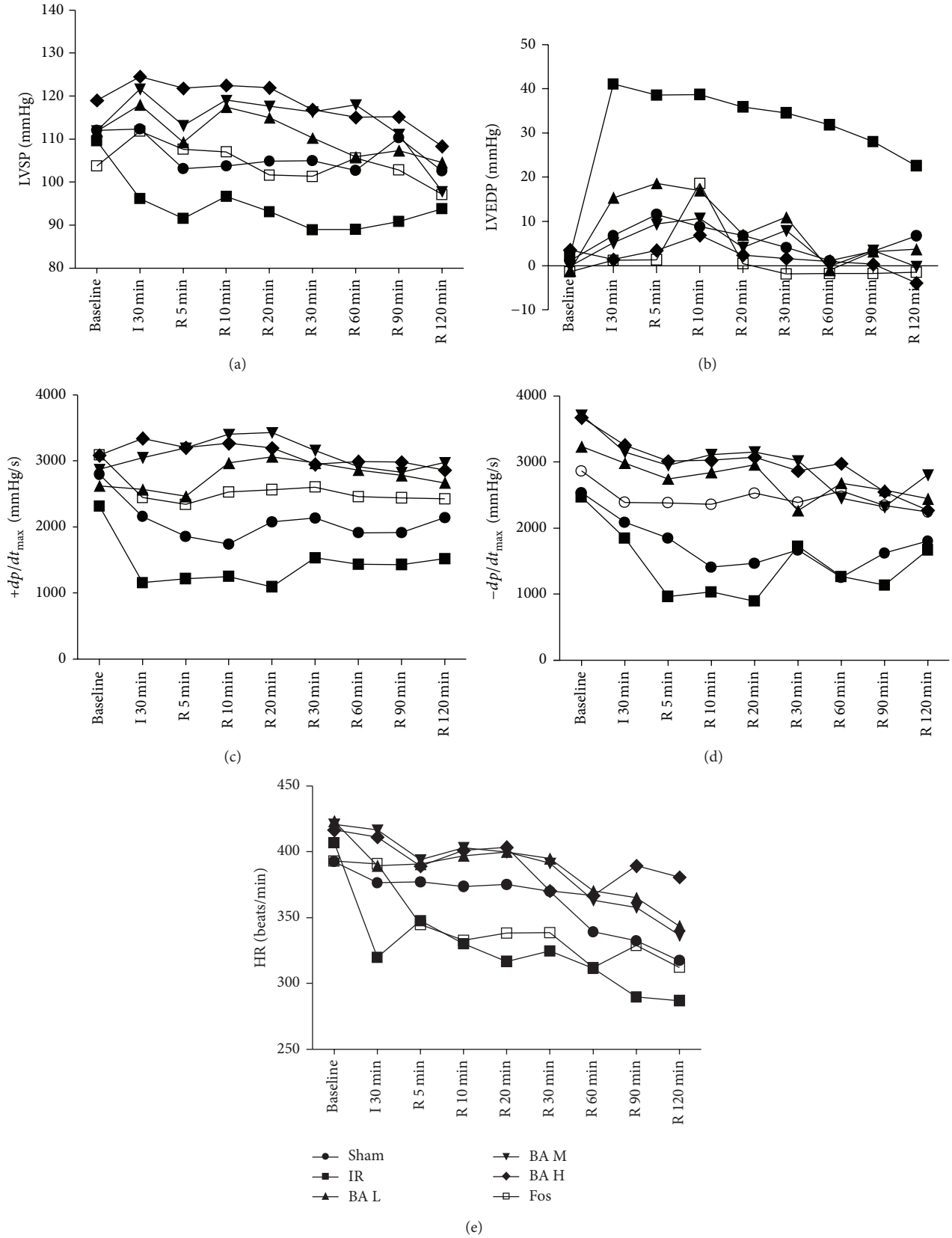

Figure 1: Hemodynamic parameters during the experiments (mean, $n = 8$). LVSP: left ventricular systolic pressure; LVEDP: left ventricular end-diastolic pressure; $\pm dp/dt_{max}$: the rate in rise and fall of ventricular pressure; HR: heart rate.

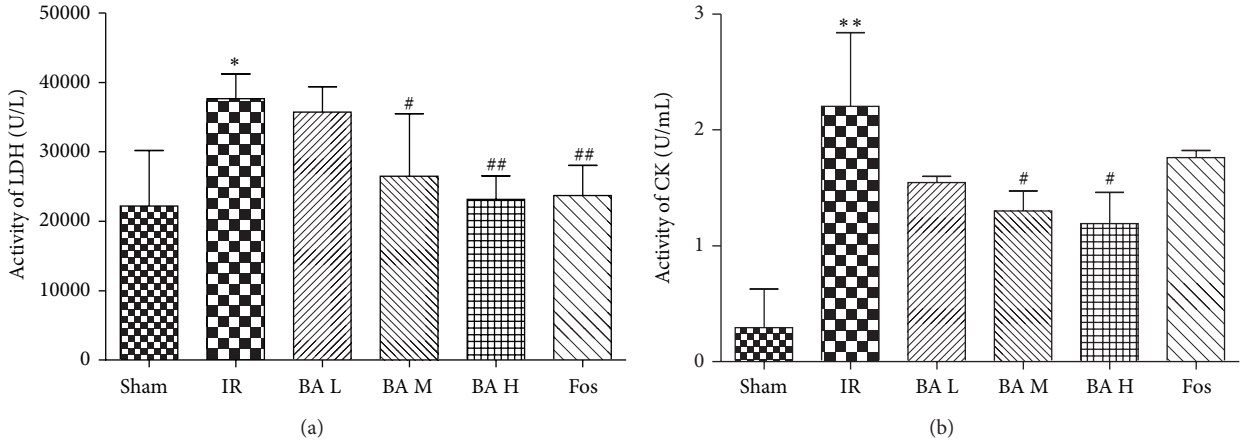

Figure 2: Activities of serum LDH (a) and CK (b) in different groups (mean ± SD, $n = 8$). LDH: lactate dehydrogenase; CK: creatine kinase. $^{*}P < 0.05$, $^{**}P < 0.01$ versus Sham group; $^{\#}P < 0.05$, $^{\#\#}P < 0.01$ versus IR group.

As a result of this paradoxical phenomenon, studies in this area focus on how to eliminate or at least partly diminish the injury, and, fortunately, ischemic preconditioning and ischemic postconditioning were documented as effective strategies to reduce MIRI. Both of these pathways, however, have ethical questions. Recently, lots of pharmacological agents, such as adenosine, bradykinin, opioids, glucagon-like peptide 1, atrial natriuretic peptide, insulin, volatile anesthetics, nitroglycerin atorvastatin, nicorandil, and ciclosporin, have also been verified that they could protect myocardium from MIRI [2], and it is termed as pharmacological preconditioning/postconditioning.

Betulinic acid, serving as a pentacyclic triterpene, has several botanical sources, and it can also be derived chemically from betulin, a substance found in abundance in the outer bark of white birch trees (*Betula alba*) [5, 6]. The compound is mainly known for its antitumor [7–9] and anti-inflammatory [10, 11] activities. Recent studies have shown that BA protects against cerebral [12] and renal [6] ischemia reperfusion injuries. However, effect of BA on myocardial ischemia reperfusion injury has not been demonstrated yet. Thus, the objectives of our study were (1) whether BA protects against myocardial ischemia/reperfusion and (2) if BA actually has cardioprotective activity, what are the underlying mechanisms?

2. Materials and Methods

2.1. Animals and Reagents. Male Sprague-Dawley (SD) rats (Laboratory Animal Centre, Xuzhou Medical College, Xuzhou, China), weighing 220–240 g, were used for these experiments. The animals were housed on a 12 h light/dark cycle under controlled temperature (23 ± 1°C) and relative humidity (65–70%). The animals were randomly divided into specified experimental groups. The procedures in this study were conducted in accordance with the Chinese Council on Animal Care and Institutional Care Committee of Xuzhou Medical College.

BA (purity > 98%) was purchased from Nanjing Spring & Autumn Biological Engineering Co., Ltd. (Jiangsu, China). Fos was purchased from China and American Shanghai Squibb Company (Shanghai, China). All other reagents were of standard analytical grade.

2.2. Experimental Protocols. Forty-eight SD rats were randomly divided into six groups as follows: (1) Sham operation group (Sham, $n = 8$); (2) IR group (heart subjected to ischemia/reperfusion, $n = 8$); (3) BA L group (heart subjected to ischemia/reperfusion treated with low-dose betulinic acid, 50 mg/kg/d, $n = 8$); (4) BA M group (heart subjected to ischemia/reperfusion treated with medium-dose betulinic acid, 100 mg/kg/d, $n = 8$); (5) BA H group (heart subjected to ischemia/reperfusion treated with high-dose betulinic acid, 200 mg/kg/d, $n = 8$); (6) Fos group (heart subjected to ischemia/reperfusion treated with fosinopril sodium, 10 mg/kg/d, $n = 8$). Rats in latter four groups were administrated with drug (once a day, i.g., 1 mL/100 g) for 7 days before the operation. And rats in the Sham group and IR group were given equal volumes of 0.5% CMC-Na at the same time. Prior to surgical procedure, rats were anesthetized by intraperitoneal injection of 10% chloral hydrate (350 mg/kg). IR model was induced by ligating the left anterior descending (LAD) for 30 min followed by reperfusion for 2 h in anesthetized rats. The significant fall of the ST segment of the ECG was selected as the reperfusion criterion. Rats in the Sham group underwent the same surgical procedures except that the suture placed under the LAD was not tied.

2.3. Hemodynamic Measurement. Cardiac function was continuously monitored before and during the entire IR procedure by PowerLab 16/30 data acquisition system (AD Instrument, Germany). And the data at baseline, 30 min of ischemia, and 30, 60, 90, and 120 min of reperfusion were analyzed. Left ventricular systolic pressure (LVSP), left ventricular end-diastolic pressure (LVEDP), heart rate, and the rate in rise and fall of ventricular pressure ($\pm dp/dt_{\max}$) were recorded as left ventricular functional parameters.

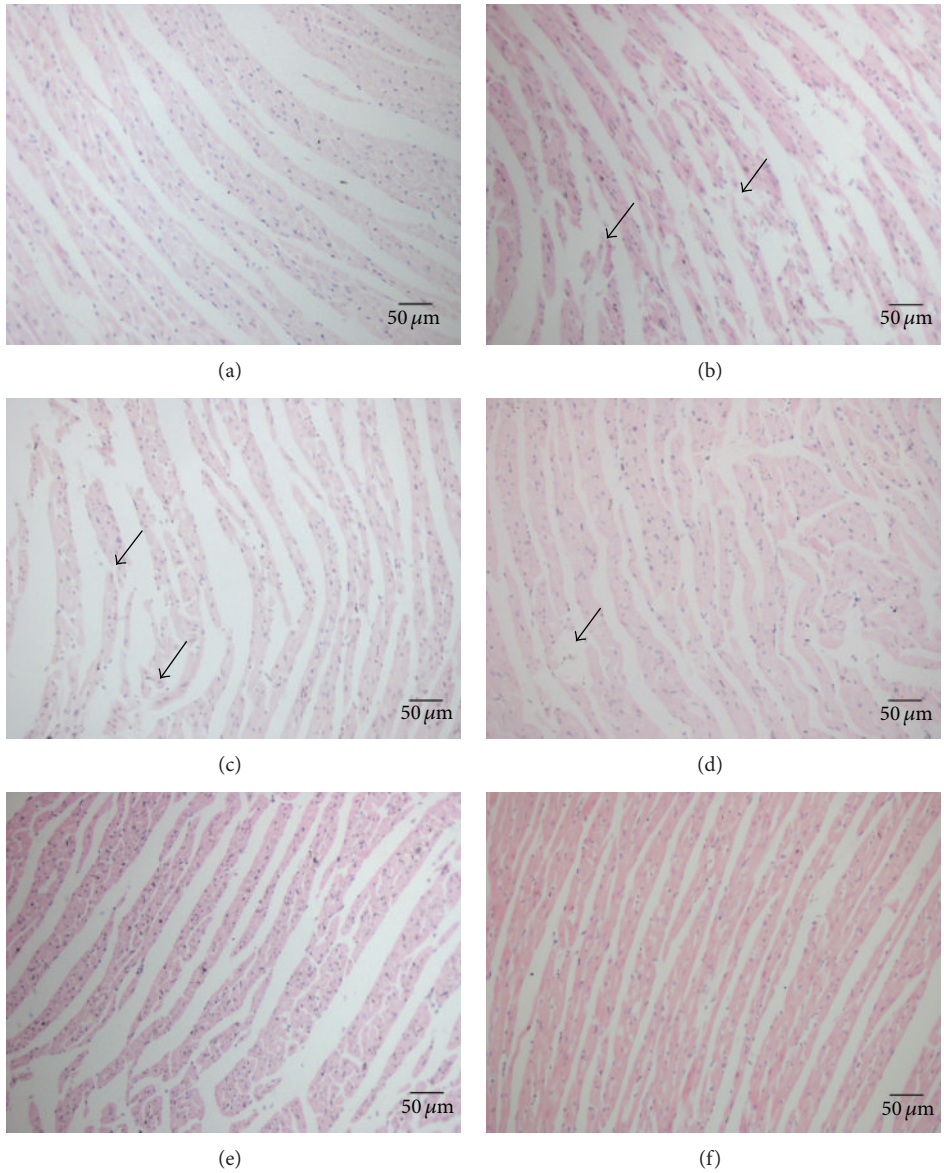

Figure 3: HE staining (×200). (a) Sham group, (b) IR group, (c) BA L group, (d) BA M group, (e) BA H group, and (f) Fos group. The black arrows represent the inflammatory cells.

2.4. Measurement of Serum LDH and CK Activities. Blood was collected from abdominal aorta immediately after reperfusion for 2 hours. Lactate dehydrogenase (LDH) and creatine kinase (CK) assay kits (Jiancheng Bioengineering Institute, Nanjing, China) were used to detect their activities. All procedures were according to the manufacturer's protocol.

2.5. Histologic Examination. The heart was fixed in 10% neutral-buffered formalin, embedded in paraffin, and cut into 4 μm sections. The sections were stained using hematoxylin and eosin (H&E) for histochemistry. All histopathological changes were evaluated in a blinded fashion by two investigators, and the main observation indexes including intercellular space, edema of cardiomyocytes, and inflammatory cell infiltration were assessed under microscope (OLYMPUS, Japan).

2.6. Assessment of Apoptosis. Apoptosis was detected by the terminal deoxyribonucleotide transferase- (TdT-) mediated dUTP nick end labeling (TUNEL) detection kit (Roche, Germany) according to the manufacturer's protocol. In this method, the TUNEL-positive brown-colored cells were considered to be apoptotic cells. The results were scored semiquantitatively by averaging the number of apoptotic cells/field at 400x magnification. Five fields were evaluated per tissue sample, and the cardiomyocytes apoptosis was represented as apoptosis index (AI) calculated as follows: AI = the number of TUNEL-positive cells/the total number of cells.

2.7. Western Blot Assay for Bcl-2 and Bax Expression. The samples were ground with RIPA buffer and the mixture was centrifuged at 12,000 g for 15 min at 4°C. The supernatants

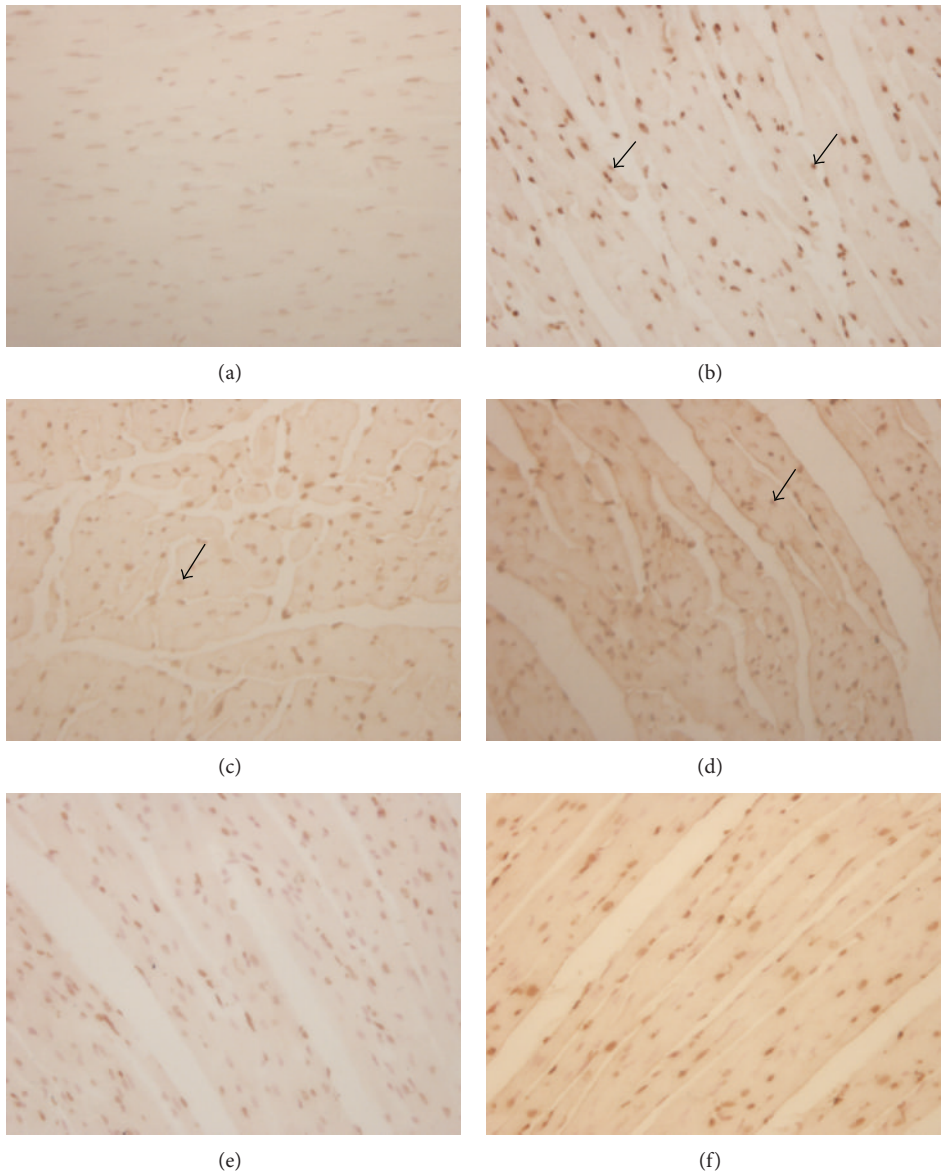

Figure 4: Representative photomicrographs of TUNEL assay (×400). (a) Sham group, (b) IR group, (c) BA L group, (d) BA M group, (e) BA H group, and (f) Fos group. The black arrows represent positive apoptotic cells.

were stored at −20°C and the protein concentration was measured using bicinchoninic acid (BCA) protein assay kit (Beyotime Institute of Biotechnology). Totally, 100 μg of proteins was separated using 12% sodium dodecyl sulfate polyacrylamide gel electrophoresis (SDS-PAGE). The proteins were transferred to nitrocellulose membranes. The membranes were treated with blocking buffer (3% BSA) for 2 h and incubated with the primary antibodies against Bcl-2 (1 : 100, Beijing Golden Bridge Biotechnology Company, China), Bax (1 : 100, Beijing Golden Bridge Biotechnology Company, China), or GAPDH (1 : 6000, Bioworld, China) at 4°C overnight, respectively. After five times of washing for 5 min with washing buffer, the membranes were incubated with anti-rabbit IgG (Beijing Golden Bridge Biotechnology Company, China) at a ratio of 1 : 1000 at room temperature for 2 h. After another five times of washing for 5 min with washing buffer the membranes were shown by NBT/BCIP. The protein bands were scanned and quantified using Image J software.

2.8. Statistical Analysis. Data were presented as means ± SD; statistical analysis was performed with SPSS 13.0. Statistical significance ($P < 0.05$) for each variable was estimated by Student's unpaired t-test or one-way analysis of variance (ANOVA) followed by a Bonferroni post hoc correction between all groups.

3. Results

3.1. Effects of Betulinic Acid on Left Ventricular Function. The hemodynamic data including left ventricular systolic pressure

(LVSP), left ventricular end-diastolic pressure (LVEDP), the rate in rise and fall of ventricular pressure $\pm dp/dt_{max}$), and heart rate (HR) were summarized in Table 1 and Figure 1. During ischemia/reperfusion, IR group rats showed lower LVSP than Sham group at R 90 min (Table 1, $P < 0.01$) and BA M group showed increased LVSP at R 30 min and R 60 min (Table 1, $P < 0.05$ versus IR group); however, BA H group increased HR in the phase of I 30 min to R 60 min (Table 1, $P < 0.05$ versus IR group). The LVEDP of IR group was higher than that of Sham group throughout the experimental period (Table 1, $P < 0.001$); interestingly, other groups decreased LVEDP pronouncedly compared with IR group at the same time points (Table 1, $P < 0.001$). $+dp/dt_{max}$ of rats in IR group was lower than that of Sham group at I 30 min (Table 1, $P < 0.05$). BA groups exert more robust protection against augmentation of $+dp/dt_{max}$ than Fos group when compared with IR group, but there are no pronouncedly differences between three BA groups. $-dp/dt_{max}$ of rats in IR group was lower than that of Sham group (Table 1, $P > 0.05$). $-dp/dt_{max}$ of rats in BA M and BA H groups was higher than that of IR group during almost all the experimental periods (Table 1, $P < 0.05$ or $P < 0.01$). Throughout ischemia/reperfusion experimental period, HR was not significantly different between Sham and IR groups (Table 1, $P > 0.05$). However, BA and Fos increased HR when compared with IR group. BA played strong roles at both ischemia and reperfusion phases, whereas Fos played a role mainly at the end of ischemia (Table 1, $P < 0.05$). Most importantly, at the end of reperfusion, only BA H group markedly increased HR compared with IR group (Table 1, $P < 0.01$).

3.2. Effects of Betulinic Acid on LDH and CK Activities. LDH and CK had low activities in Sham group rats serum, but rats subjected to IR injury showed 1.7-fold LDH activities (Figure 2(a), $P < 0.05$) and 7.5-fold CK activities (Figure 2(b), $P < 0.01$) higher than Sham group. In contrast, BA M and BA H groups of rats exhibited decreased both LDH activities (Figure 2(a), $P < 0.05$ or $P < 0.01$) and CK activities (Figure 2(b), $P < 0.05$) compared with IR group. Especially, BA H (200 mg/kg) group decreased LDH and CK to 1.04-fold and 4.06-fold higher than Sham group, respectively.

3.3. Effects of Betulinic Acid on Histology. Rats in the Sham group showed normal architecture of myocardium, cardiomyocytes presented normal size, clear boundaries and arranged regularly, whereas, in IR group, cardiomyocytes arranged irregularly, presented extensive edema, intercellular space enlarged, and inflammatory cell infiltration increased. The changes of the myocardium in the BA-treated and Fos-treated groups were significantly relieved compared with those of the IR group, cardiomyocytes ranked in order, presented mild edema and inflammatory cell infiltration reduced markedly (Figure 3).

3.4. Effects of Betulinic Acid on Cardiomyocyte Apoptosis. The presence of apoptotic cells was documented by the TUNEL assay (Figure 4). In Sham group, only scattered TUNEL-positive cells were observed. The hearts of animals that were subjected to myocardial ischemia reperfusion exhibited severe tissue damage appeared to have increased number of TUNEL-positive cells (Figure 5, 48.67 ± 4.27% versus 5.33 ± 1.37%, $P < 0.001$). In contrast, BA and Fos groups of rats demonstrated a marked reduction of TUNEL-positive cells compared with IR group (Figure 5, BA L: 39.83 ± 3.97%, $P < 0.01$; BA M: 38.50 ± 3.73%, $P < 0.01$; BA H: 27.83 ± 4.45%, $P < 0.001$; Fos: 32.00 ± 5.37%, $P < 0.001$).

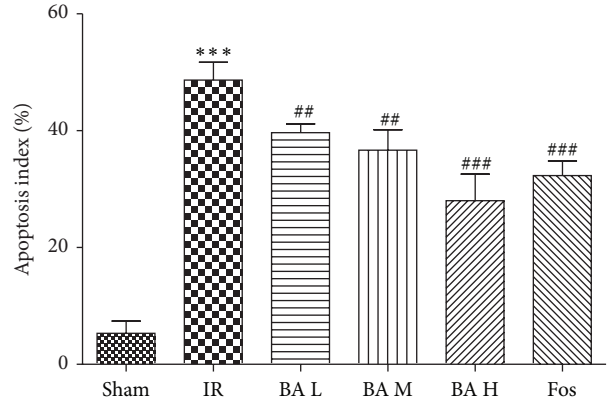

Figure 5: Apoptosis index of the six groups (mean ± SD, $n = 8$). $^{***}P < 0.001$ versus Sham group; $^{\#\#}P < 0.01$, $^{\#\#\#}P < 0.001$ versus IR group. Apoptosis index (AI) = the number of positively stained apoptotic myocytes/the total number of myocytes counted × 100%.

3.5. Effects of Betulinic Acid on the Expression of Bcl-2 and Bax. Sham group demonstrated basic expression of both Bcl-2 and Bax and IR induced downregulated Bcl-2 and upregulated Bax (Figures 6(c) and 6(d), $P < 0.05$). Pretreating with BA (especially high dosage) increased the expression of Bcl-2 (Figure 6(c), $P < 0.05$) and decreased the expression of Bax (Figure 6(d), $P < 0.01$) and, consequently, upregulated Bcl-2/Bax ratio compared with IR group (Figure 6(e), $P < 0.001$).

4. Discussion

It has been verified that BA possesses antitumor and anti-inflammatory activities and recently cerebral and renal ischemia reperfusion injuries protection. However, effects of BA on myocardial ischemia reperfusion injury have not been elucidated clearly yet. In the present study, we showed the *in vivo* evidence for the first time that BA reduces the release of LDH and CK, suppresses myocardial apoptosis, alleviates ischemia/reperfusion injury, and therefore improves left ventricular function. These results suggest that pretreatment with BA may play an important role in reducing myocardial ischemia/reperfusion injury in rats.

Ischemic preconditioning was documented as effective strategies to reduce MIRI, but this pathway has ethical questions. Preconditioning has two protection stages: early stage which starts in 30 min to several hours and late stage which lasts between 2 and 3 days. For the early stage, it is caused

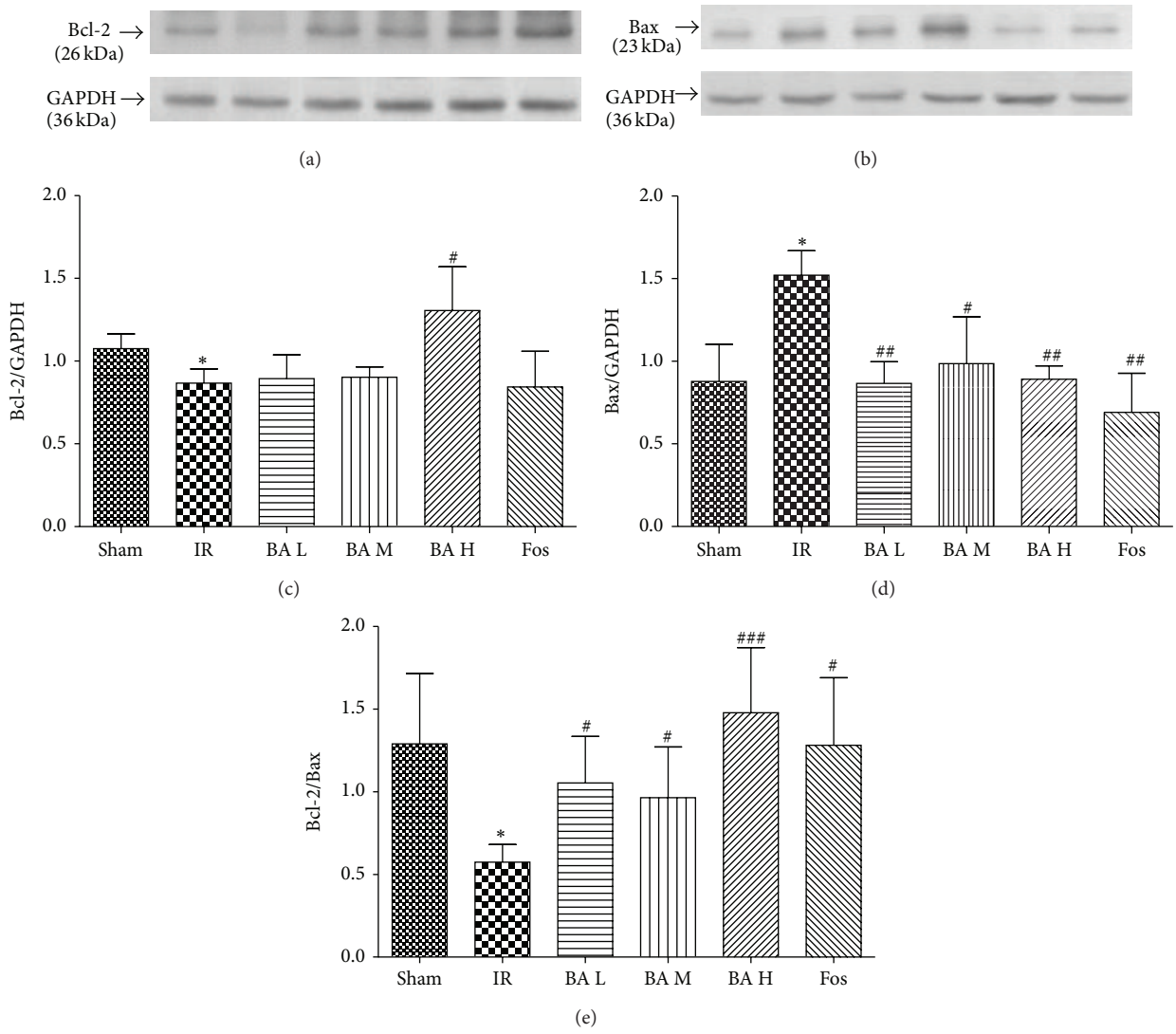

Figure 6: Expression of Bcl-2 (a) and Bax (b) by Western blot analysis. (c) Quantification of the Bcl-2/GAPDH. (d) Quantification of the Bax/GAPDH. (e) Quantification of the Bcl-2/Bax (mean ± SD, $n = 3$). $^{*}P < 0.05$ versus Sham group; $^{\#}P < 0.05$, $^{\#\#}P < 0.01$, $^{\#\#\#}P < 0.001$ versus IR group.

by immediate signal transduction through opioid receptor [13], bradykinin [14], and adenosine receptor [15]. However, the late stage is induced by transcription and translation. Previous studies indicate that BA pretreatment could alleviate the myocardial injury, suppress cardiomyocyte apoptosis, and improve cardiac function; obviously it could induce the early stage protection against MIRI. It was suggested that the late stage protection of preconditioning is associated with the activity of endogenous antioxidant enzymes, such as SOD, catalase, and the level of HSP 70. BA has significantly antioxidant activity which could reduce the consumption of endogenous antioxidant enzymes, so it also could induce the late stage protection of preconditioning. Moreover antiapoptotic properties of BA pretreatment also contribute to the late stage protection against ischemia/reperfusion insult.

Left ventricular remodeling which starts immediately after acute myocardial infarction and evolves in the chronic phase of heart failure associates with decrease in cardiac function and ventricular dilation [16]. Impairment of ventricular function is the most common fatal complication secondary to ischemic heart diseases. Therefore, improvement of cardiac function and attenuation of ventricular dilation are vital for the treatment of ischemic heart diseases [17]. The present study demonstrated that BA, especially the high dose of BA (200 mg/kg), could increase LVSP, HR, and $\pm dp/dt_{\max}$ but decrease LVEDP (Table 1 and Figure 1). It is known that LVSP and $+dp/dt_{\max}$ represent ventricular systolic function and LVEDP and $-dp/dt_{\max}$ refer to ventricular diastolic function. We indicated that BA could improve recovery of left ventricular function from improving both systolic and diastolic functions.

It has been shown that LDH and CK are reliable markers of cellular necrosis [18–20] and CK was also well known to be a golden criterion of cardiomyocyte injury; CK measurement

Table 1: Hemodynamic parameters during the experiments ($\overline{x} \pm s, n = 8$).

Parameters	Baseline	I 30 min	R 30 min	R 60 min	R 90 min	R 120 min
LVSP (mmHg)						
Sham	112.04 ± 4.14	112.38 ± 6.94	105.00 ± 10.49	102.73 ± 11.59	110.35 ± 6.59	102.69 ± 15.56
IR	109.60 ± 8.79	96.16 ± 8.26	88.96 ± 5.55	89.00 ± 7.92	90.88 ± 9.97**	93.84 ± 4.41
BA L	111.83 ± 16.32	117.98 ± 17.12	110.28 ± 20.84	105.87 ± 26.25	107.31 ± 16.88	104.59 ± 18.16
BA M	111.94 ± 12.05	121.68 ± 5.66	116.31 ± 16.24$^{\#}$	118.04 ± 18.63$^{\#}$	111.18 ± 21.05	97.89 ± 10.58
BA H	119.00 ± 9.99	124.58 ± 9.48$^{\#}$	116.89 ± 16.53$^{\#}$	115.06 ± 11.78$^{\#}$	115.18 ± 18.72	108.35 ± 21.23
Fos	103.75 ± 18.86	111.85 ± 6.00	101.37 ± 22.47	105.61 ± 16.36	102.85 ± 20.80	97.17 ± 20.11
LVEDP (mmHg)						
Sham	1.17 ± 5.06	6.83 ± 1.88	4.10 ± 3.69	1.13 ± 2.92	3.29 ± 6.03	6.76 ± 5.43
IR	2.40 ± 0.67	41.09 ± 5.01***	34.56 ± 4.41***	31.89 ± 3.52***	28.08 ± 3.02***	22.65 ± 2.47***
BA L	−1.10 ± 1.88	15.35 ± 4.29$^{\#\#\#}$	10.99 ± 2.73$^{\#\#\#}$	−0.97 ± 1.30$^{\#\#\#}$	3.22 ± 1.51$^{\#\#\#}$	3.73 ± 1.08$^{\#\#\#}$
BA M	−0.12 ± 0.88	5.18 ± 0.99$^{\#\#\#}$	7.95 ± 4.73$^{\#\#\#}$	−0.14 ± 1.54$^{\#\#\#}$	3.52 ± 0.82$^{\#\#\#}$	−0.17 ± 0.55$^{\#\#\#}$
BA H	3.57 ± 0.79	1.44 ± 0.38$^{\#\#\#}$	1.68 ± 0.63$^{\#\#\#}$	0.96 ± 0.29$^{\#\#\#}$	0.39 ± 1.84$^{\#\#\#}$	−3.85 ± 4.78$^{\#\#\#}$
Fos	−1.36 ± 3.46	1.22 ± 4.72$^{\#\#\#}$	−1.89 ± 1.20$^{\#\#\#}$	−1.79 ± 0.74$^{\#\#\#}$	−1.78 ± 1.81$^{\#\#\#}$	−1.49 ± 2.36$^{\#\#\#}$
$+dp/dt_{max}$ (mmHg/s)						
Sham	2796.99 ± 747.48	2159.27 ± 616.19	2133.73 ± 664.39	1913.15 ± 746.26	1914.93 ± 740.10	2140.04 ± 904.89
IR	2314.22 ± 523.11	1158.08 ± 126.28*	1530.25 ± 457.50	1436.53 ± 335.40	1431.64 ± 396.76	1516.97 ± 301.25
BA L	2622.34 ± 554.96	2567.47 ± 783.53$^{\#\#}$	2966.97 ± 727.40$^{\#\#}$	2862.31 ± 929.28$^{\#\#}$	2780.30 ± 676.20$^{\#\#}$	2669.20 ± 607.90$^{\#}$
BA M	2872.46 ± 900.11	3050.93 ± 530.30$^{\#\#\#}$	3163.21 ± 549.83$^{\#\#\#}$	2912.10 ± 761.54$^{\#\#}$	2827.94 ± 631.95$^{\#\#}$	2974.98 ± 607.48$^{\#\#}$
BA H	3084.91 ± 652.90	3340.11 ± 416.84$^{\#\#\#}$	2952.91 ± 562.36$^{\#\#}$	2992.94 ± 266.80$^{\#\#\#}$	2982.98 ± 418.88$^{\#\#\#}$	2860.16 ± 626.23$^{\#\#}$
Fos	2671.93 ± 811.72	2445.77 ± 495.77$^{\#\#}$	2604.37 ± 1088.58$^{\#}$	2459.49 ± 906.66	2440.16 ± 593.09	2425.22 ± 520.44
$-dp/dt_{max}$ (mmHg/s)						
Sham	2538.50 ± 842.98	2088.54 ± 804.64	1667.45 ± 538.83	1255.24 ± 521.60	1621.34 ± 727.98	1804.14 ± 766.69
IR	2470.82 ± 710.12	1851.84 ± 511.17	1724.73 ± 154.39	1263.52 ± 202.00	1137.58 ± 215.10	1670.25 ± 353.45
BA L	3235.65 ± 907.33	2985.13 ± 649.47$^{\#\#}$	2264.23 ± 654.76	2681.89 ± 918.39$^{\#\#\#}$	2574.89 ± 615.74$^{\#\#\#}$	2444.46 ± 570.20
BA M	3716.18 ± 615.38$^{\#\#}$	3155.59 ± 305.19$^{\#\#\#}$	3020.08 ± 527.96$^{\#\#}$	2455.59 ± 427.79$^{\#\#}$	2321.44 ± 448.27$^{\#\#}$	2809.39 ± 734.00$^{\#\#}$
BA H	3673.42 ± 396.67$^{\#\#}$	3258.30 ± 416.35$^{\#\#\#}$	2869.15 ± 466.16$^{\#\#}$	2978.49 ± 297.56$^{\#\#\#}$	2550.87 ± 756.55$^{\#\#\#}$	2270.48 ± 612.49
Fos	2864.85 ± 610.09	2390.76 ± 677.84	2391.93 ± 718.98	2564.15 ± 514.71$^{\#\#}$	2346.04 ± 577.70$^{\#\#}$	2247.83 ± 513.18
HR (beats/min)						
Sham	392.58 ± 66.04	376.55 ± 35.80	370.02 ± 44.77	339.31 ± 42.13	332.37 ± 56.53	317.47 ± 72.61
IR	406.84 ± 30.06	319.83 ± 70.13	324.68 ± 32.55	311.47 ± 38.66	289.73 ± 58.39	286.94 ± 49.31
BA L	423.22 ± 33.79	389.34 ± 26.38$^{\#}$	394.86 ± 15.99$^{\#}$	370.48 ± 35.85	365.28 ± 26.74$^{\#}$	343.66 ± 34.22
BA M	421.08 ± 34.06	416.78 ± 15.23$^{\#\#\#}$	391.48 ± 25.79	363.22 ± 26.80	357.79 ± 39.67	336.57 ± 42.96
BA H	416.65 ± 35.79	411.22 ± 29.49$^{\#\#}$	370.43 ± 25.76	366.98 ± 35.70	389.45 ± 50.12$^{\#\#\#}$	380.80 ± 54.36$^{\#\#}$
Fos	393.02 ± 57.07	390.88 ± 40.24$^{\#}$	338.62 ± 59.94	312.03 ± 67.08	328.87 ± 35.22	312.22 ± 57.54

LVSP: left ventricular systolic pressure; LVEDP: left ventricular end-diastolic pressure; $\pm dp/dt_{max}$: the rate in rise and fall of ventricular pressure; HR: heart rate. I: ischemia; R: reperfusion. All data were expressed as the mean ± SD. $^{*}P < 0.05$, $^{**}P < 0.01$, $^{***}P < 0.001$ versus Sham; $^{\#}P < 0.05$, $^{\#\#}P < 0.01$, $^{\#\#\#}P < 0.001$ versus IR.

plays a vital role in early diagnosis of myocardial infarction and other diseases, and it is more reliable than ECG analysis. In our study, determining two kinases associated with cardiomyocytes injury has two purposes: (1) to make sure successful establishment of IR model and (2) wonder if BA exerts its cardioprotective effect through attenuating the LDH and CK activities. Our results were in accordance with the two objectives mentioned above (Figure 2).

Myocardial ischemia and reperfusion injury leads to cell death [21]. And accumulated evidence indicated that apoptosis, a complex series of ordered cell-autonomous biochemical events, contributes significantly to myocardial cell death, suggesting that therapeutic interventions that inhibit apoptotic cell death may attenuate ischemic-induced heart injury [16, 22]. The Bcl-2 family consists of pro- and antiapoptotic members. The family consists of both cell death promoters such as Bax and Bad and cell death inhibitors, which include Bcl-2 and Bcl-X. It has been demonstrated that the high ratio of Bax/Bcl-2 is associated with greater vulnerability to apoptotic activation [17, 23–26]. The balance

between proapoptotic and antiapoptotic proteins determines the possibility of cells to either survive or undergo apoptosis after a certain stimulus or injury [27]. Since inhibition of the apoptotic processes has been shown to prevent the myocardial ischemia/reperfusion injury, we next studied the effect of BA on apoptosis through TUNEL assay (Figures 4 and 5). As shown in Figure 4, we found that BA could inhibit myocardial cells apoptosis, expressed as decreased number of TUNEL-positive cardiomyocytes. Furthermore, we suggested that the myocardial apoptosis which we examined is early apoptosis and it can initiate extensive loss of cardiomyocytes, contribute to the pathogenesis of MIRI, and ultimately deteriorate cardiac function. Meanwhile, the expressions of Bax and Bcl-2 were measured by Western blot (Figure 6), and the results show that BA may upregulate the expression of Bcl-2 while downregulating Bax expression, therefore increasing the ratio of Bcl-2 to Bax (Figure 6). Interestingly, treatment with 200 mg/kg of BA significantly prevents myocardial cells undergoing apoptosis after ischemia/reperfusion insult in this study based on statistical analysis.

Our study has some limitations. Firstly, mechanisms underlying the cardioprotective effect of BA need further investigations. It has been reported that BA could suppress oxidant stress. Here, we only focus on Bcl-2/Bax ratio, a classical pathway in apoptosis research, but if there are other signaling pathways involved in the cardioprotection of BA? We do not know whether it has reached to your magazine's standard. Secondly, we did not show infarct size (IS) measurement results. IS measurement is a common and direct item to weigh cardioprotective effect, but rats in our present study were limited; we plan to measure it in our further researches.

Based on the above results, we suggested that BA ameliorates myocardial ischemia/reperfusion injury in rats by inhibiting the release of LDH and CK, suppressing myocyte apoptosis. This may provide insight into the role of BA in MIRI.

Conflict of Interests

The authors declared no potential conflict of interests with respect to the research, authorship, and/or publication of this paper.

Authors' Contribution

Anzhou Xia, Zhi Xue, and Yong Li contributed equally to this work.

Acknowledgments

This work was supported by the Postgraduate Scientific Innovation Research of Jiangsu Province Grants (CXLX12_0999) and by Bureau of Science and Technology of Xuzhou Grant (XM12B069).

References

[1] J. Fan, G. Q. Li, J. Liu et al., "Impact of cardiovascular disease deaths on life expectancy in chinese population," *Biomedical and Environmental Sciences*, vol. 27, no. 3, pp. 162–168, 2014.

[2] V. Sivaraman and D. M. Yellon, "Pharmacologic therapy that simulates conditioning for cardiac ischemic/reperfusion injury," *Journal of Cardiovascular Pharmacology and Therapeutics*, vol. 19, no. 1, pp. 83–96, 2014.

[3] R. B. Jennings, H. M. Sommers, G. A. Smyth, H. A. Flack, and H. Linn, "Myocardial necrosis induced by temporary occlusion of a coronary artery in the dog," *Archives of Pathology*, vol. 70, pp. 68–78, 1960.

[4] S. Sanada, I. Komuro, and M. Kitakaze, "Pathophysiology of myocardial reperfusion injury: preconditioning, postconditioning, and translational aspects of protective measures," *American Journal of Physiology: Heart and Circulatory Physiology*, vol. 301, no. 5, pp. H1723–H1741, 2011.

[5] S. Alakurtti, T. Mäkelä, S. Koskimies, and J. Yli-Kauhaluoma, "Pharmacological properties of the ubiquitous natural product betulin," *European Journal of Pharmaceutical Sciences*, vol. 29, no. 1, pp. 1–13, 2006.

[6] E. Ekşioğlu-Demiralp, E. R. Kardaş, S. Özgül et al., "Betulinic acid protects against ischemia/reperfusion-induced renal damage and inhibits leukocyte apoptosis," *Phytotherapy Research*, vol. 24, no. 3, pp. 325–332, 2010.

[7] F. B. Mullauer, J. H. Kessler, and J. P. Medema, "Betulinic acid, a natural compound with potent anticancer effects," *Anti-Cancer Drugs*, vol. 21, no. 3, pp. 215–227, 2010.

[8] W. Ding, M. Sun, S. Luo et al., "A 3D QSAR study of betulinic acid derivatives as anti-tumor agents using topomer CoMFA: model building studies and experimental verification," *Molecules*, vol. 18, no. 9, pp. 10228–10241, 2013.

[9] S. Chintharlapalli, S. Papineni, P. Lei, S. Pathi, and S. Safe, "Betulinic acid inhibits colon cancer cell and tumor growth and induces proteasome-dependent and -independent downregulation of specificity proteins (Sp) transcription factors," *BMC Cancer*, vol. 11, article 371, 2011.

[10] V. Viji, B. Shobha, S. K. Kavitha, M. Ratheesh, K. Kripa, and A. Helen, "Betulinic acid isolated from Bacopa monniera (L.) Wettst suppresses lipopolysaccharide stimulated interleukin-6 production through modulation of nuclear factor-κB in peripheral blood mononuclear cells," *International Immunopharmacology*, vol. 10, no. 8, pp. 843–849, 2010.

[11] Y. Yun, S. Han, E. Park et al., "Immunomodulatory activity of betulinic acid by producing pro-inflammatory cytokines and activation of macrophages," *Archives of Pharmacal Research*, vol. 26, no. 12, pp. 1087–1095, 2003.

[12] Q. Lu, N. Xia, H. Xu et al., "Betulinic acid protects against cerebral ischemia-reperfusion injury in mice by reducing oxidative and nitrosative stress," *Nitric Oxide*, vol. 24, no. 3, pp. 132–138, 2011.

[13] S. Dragasis, E. Bassiakou, N. Iacovidou et al., "The role of opioid receptor agonists in ischemic preconditioning," *European Journal of Pharmacology*, vol. 720, no. 1–3, pp. 401–408, 2013.

[14] Z. Sheng, Y. Yao, Y. Li, F. Yan, J. Huang, and G. Ma, "Bradykinin preconditioning improves therapeutic potential of human endothelial progenitor cells in infarcted myocardium," *PloS ONE*, vol. 8, no. 12, Article ID e81505, 2013.

[15] Z. Yang, W. Sun, and K. Hu, "Adenosine A1 receptors selectively target protein kinase C isoforms to the caveolin-rich plasma

membrane in cardiac myocytes," *Biochimica et Biophysica Acta*, vol. 1793, no. 12, pp. 1868–1875, 2009.

[16] R. Rossini, M. Senni, G. Musumeci, P. Ferrazzi, and A. Gavazzi, "Prevention of left ventricular remodelling after acute myocardial infarction: an update," *Recent Patents on Cardiovascular Drug Discovery*, vol. 5, no. 3, pp. 196–207, 2010.

[17] S. Chen, J. Liu, X. Liu et al., "Panax notoginseng saponins inhibit ischemia-induced apoptosis by activating PI3K/Akt pathway in cardiomyocytes," *Journal of Ethnopharmacology*, vol. 137, no. 1, pp. 263–270, 2011.

[18] J. Zhang, A. Liu, R. Hou et al., "Salidroside protects cardiomyocyte against hypoxia-induced death: a HIF-1α-activated and VEGF-mediated pathway," *European Journal of Pharmacology*, vol. 607, no. 1–3, pp. 6–14, 2009.

[19] C. Deng, Z. Sun, G. Tong et al., "alpha-Lipoic acid reduces infarct size and preserves cardiac function in rat myocardial ischemia/reperfusion injury through activation of PI3K/Akt/Nrf2 pathway," *PloS ONE*, vol. 8, no. 3, Article ID e58371, 2013.

[20] M. M. Zhao, J. Y. Yang, X. B. Wang, C. S. Tang, J. B. Du, and H. F. Jin, "The PI3K/Akt pathway mediates the protection of SO(2) preconditioning against myocardial ischemia/reperfusion injury in rats," *Acta Pharmacologica Sinica*, vol. 34, no. 4, pp. 501–506, 2013.

[21] R. A. Gottlieb, K. O. Burleson, R. A. Kloner, B. M. Babior, and R. L. Engler, "Reperfusion injury induces apoptosis in rabbit cardiomyocytes," *The Journal of Clinical Investigation*, vol. 94, no. 4, pp. 1621–1628, 1994.

[22] P. Caroppi, F. Sinibaldi, L. Fiorucci, and R. Santucci, "Apoptosis and human diseases: mitochondrion damage and lethal role of released cytochrome c as proapoptotic protein," *Current Medicinal Chemistry*, vol. 16, no. 31, pp. 4058–4065, 2009.

[23] D. Sun, J. Huang, Z. Zhang et al., "Luteolin limits infarct size and improves cardiac function after myocardium ischemia/reperfusion injury in diabetic rats," *PloS ONE*, vol. 7, no. 3, Article ID e33491, 2012.

[24] B. Wu, H. Cui, X. Peng et al., "Dietary nickel chloride induces oxidative stress, apoptosis and alters Bax/Bcl-2 and caspase-3 mRNA expression in the cecal tonsil of broilers," *Food and Chemical Toxicology*, vol. 63, pp. 18–29, 2014.

[25] Y. K. Verma, P. K. Raghav, H. G. Raj, R. P. Tripathi, and G. U. Gangenahalli, "Enhanced heterodimerization of Bax by Bcl-2 mutants improves irradiated cell survival," *Apoptosis*, vol. 18, no. 2, pp. 212–225, 2013.

[26] J. Xu, M. Zhou, J. Ouyang et al., "Gambogic acid induces mitochondria-dependent apoptosis by modulation of Bcl-2 and Bax in mantle cell lymphoma JeKo-1 cells," *Chinese Journal of Cancer Research*, vol. 25, no. 2, pp. 183–191, 2013.

[27] Y. H. Liao, N. Xia, S. F. Zhou et al., "Interleukin-17A contributes to myocardial ischemia/reperfusion injury by regulating cardiomyocyte apoptosis and neutrophil infiltration," *Journal of the American College of Cardiology*, vol. 59, no. 4, pp. 420–429, 2012.

Hindawi Publishing Corporation
Evidence-Based Complementary and Alternative Medicine
Volume 2014, Article ID 614273, 8 pages
http://dx.doi.org/10.1155/2014/614273

Research Article

Anticoagulant Activity of Polyphenolic-Polysaccharides Isolated from *Melastoma malabathricum* L.

Li Teng Khoo,[1] Faridah Abas,[2,3] Janna Ong Abdullah,[1] Eusni Rahayu Mohd Tohit,[4] and Muhajir Hamid[1,3]

[1] *Department of Microbiology, Faculty of Biotechnology and Biomolecular Sciences, Universiti Putra Malaysia, 43400 Serdang, Selangor, Malaysia*
[2] *Department of Food Science, Faculty of Food Science and Technology, Universiti Putra Malaysia, 43400 Serdang, Selangor, Malaysia*
[3] *Institute of Biosciences, Universiti Putra Malaysia, 43400 Serdang, Selangor, Malaysia*
[4] *Department of Pathology, Faculty of Medicine and Health Sciences, Universiti Putra Malaysia, 43400 Serdang, Selangor, Malaysia*

Correspondence should be addressed to Muhajir Hamid; muhajir@upm.edu.my

Received 23 March 2014; Revised 18 April 2014; Accepted 26 April 2014; Published 20 May 2014

Academic Editor: Shi-Biao Wu

Melastoma malabathricum Linn. is a perennial traditional medicine plants that grows abundantly throughout Asian countries. In this study, *M. malabathricum* Linn. leaf hot water crude extract with anticoagulant activity was purified through solid phase extraction cartridge and examined for the bioactive chemical constituents on blood coagulation reaction. The SPE purified fractions were, respectively, designated as F1, F2, F3, and F4, and each was subjected to the activated partial thromboplastin time (APTT) anticoagulant assay. Active anticoagulant fractions (F1, F2, and F3) were subjected to chemical characterisation evaluation. Besides, neutral sugar for carbohydrate part was also examined. F1, F2, and F3 were found to significantly prolong the anticoagulant activities in the following order, F1 > F2 > F3, in a dose dependent manner. In addition, carbohydrate, hexuronic acid, and polyphenolic moiety were measured for the active anticoagulant fractions (F1, F2, and F3). The characterisation of chemical constituents revealed that all these three fractions contained acidic polysaccharides (rhamnogalacturonan, homogalacturonan, and rhamnose hexose-pectic type polysaccharide) and polyphenolics. Hence, it was concluded that the presence of high hexuronic acids and polysaccharides, as well as polyphenolics in traditional medicinal plant, *M. malabathricum*, played a role in prolonging blood clotting in the intrinsic pathway.

1. Introduction

Melastoma malabathricum Linn. is a small shrub belonging to the Melastomataceae family [1]. This evergreen plant grows wildly and abundantly in open fields, lowlands, and mountainous forests throughout the tropical and subtropical regions. In Malaysia, *M. malabathricum* Linn. is known as "senduduk," and this species is widely accepted as a traditional medicinal plant [2].

The whole *M. malabathricum* Linn. plant has been reported to be used as a folklore medicine. Decoction from the leaves is the most favourable as it is believed to be able to treat diarrhoea and dysentery and heal wounds and other ailments [3]. Besides, scientific reports have shown that the leaf crude extract of *M. malabathricum* Linn. exhibited antidiarrheal [4] as well as antinociceptive, anti-inflammatory, and antipyretic activities [5, 6].

Manicam et al. [7] have shown that *M. malabathricum* Linn. hot water extract has an outstanding anticoagulant activity. To our best knowledge, however, there has been no report on the chemical constituents of *M. malabathricum* Linn.hot water extract, which exhibits anticoagulant activity. Previous literature has also proven that the anticoagulant activity of *Lythrum salicaria* and *Porana volubilis* is contributed by acidic polysaccharides and polyphenolic compounds [8, 9]. In this study, it was hypothesised that the fractions from hot water extract of *M. malabathricum* Linn. leaf contain similar chemical constituents which demonstrate

similar anticoagulant activity that is probably better than other higher plants such as *L. salicaria* and *P. volubilis*. Thus, in continuum with the previous study, the hot water crude extract of *M. malabathricum* Linn. leaf was fractionated, and anticoagulant activities of fractionated fractions were evaluated. At the same time, carbohydrate, hexuronic acid, and polyphenolic moiety in the active anticoagulant fractions were also measured. Overall, this study revealed that the fractions of *M. malabathricum* Linn. contained high amounts of carbohydrate, hexuronic acid, and polyphenolic, which are responsible for the anticoagulant activity. Such a discovery is crucial information as it provides clues for potential treatment of blood coagulant disorders.

2. Material and Methods

2.1. Materials. Standard human normal pooled plasma, STA-PTT automated reagent, and 0.025 M calcium chloride were purchased from Diagnostica Stago (Asnieres-sur-Seine, France), while sodium bicarbonate, sodium borohydride, gallic acid, carbazole, glucuronic acid, arabinose, galactose, mannose, rhamnose, xylose, dextran standards, trifluoroacetic acid (TFA), and heparin sodium salt were bought from Sigma-Aldrich (Missouri, USA). Phenol, acetonitrile, ammonium hydroxide, glacial acetic acid, acetic anhydride, dimethyl sulfoxide (DMSO), and Folin-Ciocalteu's reagent were purchased from Merck (New Jersey, USA). Concentrated sulphuric acid and glucose were purchased from Fisher Scientific (Massachusetts, UK), and sodium borate de carbohydrate was purchased from Biobasic (Ontario, Canada).

2.2. Plant Material. Fresh matured *M. malabathricum* Linn. leaves were collected between September and October 2009 from Lebuh Silikon, Universiti Putra Malaysia, in Serdang, Selangor, Malaysia. The samples were identified by a botanist and a voucher specimen was deposited at the Herbarium Biodiversity Unit, Institute of Biosciences, Universiti Putra Malaysia, under the reference number SK 1717/09.

2.3. Extraction and Fractionation of the Plant Material. The hot water extraction from the leaf of *M. malabathricum* was performed according to the method described by Manicam et al. [7]. Briefly, fine pieces of *M. malabathricum* leaves (500 g) were refluxed for 5 h at 100°C with 1 L deionised water. After 5 h, the hot water extract was filtered using Whatman Grade number 1 filter paper (Whatman, US), concentrated into dryness, lyophilised, and stored at −20°C until further analysis. Next, lyophilised crude extract (0.5 g) was dissolved in 100% deionised water and loaded into 10 g of C_{18}, Sep-Pak Cartridge (Water, Massachusetts, USA). Four different ratios of water to acetonitrile (95 : 5, 90 : 10, 80 : 20, and 50 : 50, v/v) were passed through the cartridge. The analysts of interests for each fraction were collected, dried and lyophilized. Four fractions designated as F1, F2, F3, and F4 were obtained. Each fraction was reconstituted with distilled water at different concentrations for anticoagulant activity assay and chemical characterisation.

2.4. Anticoagulant Assay. In vitro intrinsic anticoagulant pathway was measured by activated partial thromboplastin time (APTT). Standard human normal pooled plasma was spiked with equal volume of different concentrations of *M. malabathricum* crude extract and fractions (1 mg/mL, 500 μg/mL, 250 μg/Ml, and 125 μg/mL). Meanwhile, STA-PTT automated reagent was reconstituted and subjected to APTT assay, together with 0.025 M calcium chloride. The APTT assay was analysed using STA Compact coagulation analyser (Diagnostica Stago, Asnieres-sur-Seine, France) according to the manufacturer's protocol. The anticoagulant activity was measured by using a parallel standard curve based on the standard calibration curve for heparin sodium salt (140 IU/mg).

2.5. Chemical Characterisation. Total carbohydrate content was determined by using a modified phenol-sulphuric acid assay [10]. Absorbance was measured on Mindray microplate reader (Shenzhen, China) and glucose was used as a standard. Total phenolic content was measured by using a modified Folin-Ciocalteu method [11]. The content of hexuronic acid was determined by carbazole assay [12]. Absorbances of total phenolic and hexuronic acid contents were measured on Novaspec II visible spectrophotometer (Nicosia, Greek). Gallic acid and glucuronic acid were used as standards, respectively. Infrared spectrum was recorded with Perkin-Elmer Spectrum 100 FT-IR infrared spectrometer (Massachusetts, USA) and 16 scans were recorded with 4 cm^{-1} resolution. The ^{1}H NMR spectra were obtained from 500 MHz Varian INOVA NMR spectrometer (California, USA). All the ^{1}H NMR samples were dissolved in deuterium oxide (D_2O).

2.6. Monosaccharide Compositions Analysis. Neutral sugar compositions were identified and quantified through gas chromatography (GC) analysis. Polysaccharides were subjected to hydrolysation, reduction, and acetylation [13, 14]. Active anticoagulant samples (5 mg) were hydrolysed with 2 M TFA at 100°C for 2 h and dried. This was followed by reconstituting the samples with 200 μL water and adding 20 μL allose as an internal standard. Next, 20 μL of 15 M ammonium hydroxide and 1 mL of 0.5 M sodium borohydride solution in dimethyl sulfoxide were added. The samples were then left overnight at 4°C after being incubated in 40°C water bath for 90 min. On the following day, the samples were prewarmed at 40°C for 5 min. Subsequently, 100 μL of glacial acetic acid, 200 μL of 1-methylimidazole, and 1 mL of acetic anhydride were added. The samples were incubated at 40°C for 10 min to allow completion of acetylation. Finally, 2.5 mL of water and 1 mL of dichloromethane were added and centrifuged at 1000 ×g for 10 min. The lower dichloromethane part was analysed using GC. Meanwhile, arabinose, glucose, galactose, mannose, rhamnose, and xylose were used as standards. Aditol hexa-acetates were analysed using Agilent 6890 gas chromatography (Santa Clara, USA) with BPX-70 column (30 m × 0.32 mm I.D., 0.25 μm film thicknesses, SGE, Australia). Helium was used as gas carrier on column injection and flame ionisation detector was utilized as a detector. The temperature was programmed at 50°C and

maintained for 30 s, increased to 170°C at 50°C/min and finally to 230°C at 2°C/min before it was maintained for 5 min. The inlet temperature was 250°C, with a flow rate of 1 mL/min.

2.7. Molecular Mass Determination. Molecular mass of active anticoagulant samples was determined through Jasco high performance liquid chromatography (HPLC LC-1500 series) with refractive index detector (Maryland, USA). Phenomenex polysep-GFC-P-4000 (California, USA) was used with the flow rate at 0.8 mL/min, while the mobile phase was deionised water. Dextran standards of various molecular masses from 5 kDa to 270 kDa were used as standards for calibration.

2.8. Statistical Analysis. Data are shown as mean ± S.E.M. ($n = 3$) and analysis was performed using one-way analysis of variance (ANOVA), followed by *post hoc* Dunnett's multiple range tests to determine the means of significance from the control (Prism 5.0, GraphPad Software Inc., California, USA). Significant differences for all the data sets were measured and designated as $^{*}P < 0.05$, $^{**}P < 0.01$, and $^{***}P < 0.001$.

3. Results and Discussion

A previous study by Manicam et al. [7] showed that *M. malabathricum* Linn. leaf hot water extract exhibited an excellent anticoagulant activity. Therefore, in this study, the hot water extract of *M. malabathricum* Linn. leaf was fractionated, while the anticoagulant activity of each fraction was evaluated. Chemical compositions of active anticoagulant fractions were also elucidated.

The dark brown material (lyophilised crude extract) was fractionated into four fractions with increasing solvent polarity. The fractions were labelled as F1, F2, F3, and F4. The anticoagulant activity of each fraction was determined by automated partial thromboplastin time (APTT) assay. This is in continuum with Manicam et al.'s report, which showed that *M. malabathricum* Linn. leaf hot water extract possessed outstanding prolongation blood clotting time verified by the APTT assay. APTT is able to measure the inhibition of intrinsic factors of blood coagulation pathway such as F XII, XI, IX, VIII, and V [15]. Overall, all the fractions showed significant prolonged intrinsic blood clotting time, except for F4 (Figure 1). Hence, F4 was not considered for further chemical characteristics evaluation. Meanwhile, F1 was shown to be the most active anticoagulant fraction as it significantly prolonged APTT at a concentration as low as 125 μg/mL. It is noteworthy to highlight that F1 was more active compared to the crude extract. Specifically, the clotting time for F1 was about 273.33 ± 3.28 s ($P < 0.001$) and 264.15 ± 2.34 s ($P < 0.001$) compared to the crude extract, which exhibited 252.51 ± 2.01 s ($P < 0.001$) and 255.56 ± 3.68 s ($P < 0.001$) at 500 μg/mL and 1 mg/mL, respectively. Similarly, F2 also showed a similar anticoagulant characteristic as F1. It significantly prolonged the blood clotting time at a concentration as low as 125 μg/mL. The prolonged clotting time at 1 mg/mL for F2 was 249.37 ± 3.45 s ($P < 0.001$).

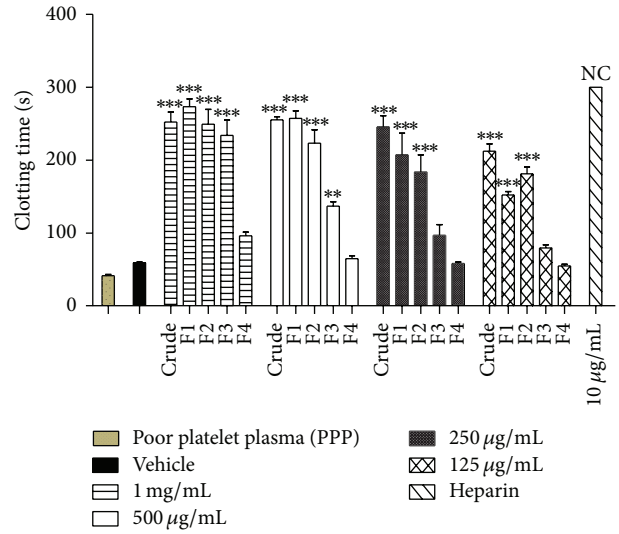

Figure 1: Activated partial thromboplastin time (APTT) of *Melastoma malabathricum* Linn. leaf extract purified via solid phase extraction (SPE) into F1, F2, F3, and F4. Crude extract and fractions (1 mg/mL, 500 μg/mL, 250 μg/mL, and 125 μg/mL) were tested on human normal pooled plasma. Heparin sodium salt from porcine intestinal mucosa (140 USP units mg^{-1}) was used as a positive control. Data represent means ± S.E.M. of three independent experiments. Significant differences compared to the control group (normal pooled plasma with deionised water, vehicle) are designated as $^{**}P < 0.05$ and $^{***}P < 0.001$. NC: no coagulation.

However, F3 was only able to significantly inhibit blood clotting at 1 mg/mL and 500 μg/mL, with 234.14 ± 0.99 s ($P < 0.001$) and 137.11 ± 0.58 s ($P < 0.05$), respectively.

The anticoagulant activity for all the fractions was subsequently measured using the standard calibration curve of unfractionated heparin (140 IU/mg). As summarised in Figure 2, the anticoagulant activities for F1, F2, and F3 were 0.90 IU/mg, 0.89 IU/mg, and 0.77 IU/mg, respectively. The two fractions exhibited more active anticoagulant profiles compared to *Lythrum salicaria* (0.17 IU/mg) and *Filipendula ulmaria* (0.5 IU/mg) and were therefore reported as anticoagulant medicinal higher plants [16].

The chemical characterisation was carried out to have a better understanding of the chemical compositions for active anticoagulant fractions (F1, F2, and F3). F1 was a dark brown gum, while F2 was a brown material, and F3 was a light brown material. The yields for F1, F2, and F3 were 54.17%, 14.97%, and 8.8% (w/w) of dry crude extract, respectively.

Generally, carbohydrates, phenolic acids, and uronic acids were presented and they served as the main constituents for F1, F2, and F3 (Table 1). It is interesting to note that all active anticoagulant fractions were rich in carbohydrate contents. The *M. malabathricum* Linn. hot water extract which was fractionated with increasing solvent polarity had decreased carbohydrate compositions in the F1, F2, and F3. From the results, F1 with the most potent anticoagulant fraction yielded the highest compositions of carbohydrate and uronic acid contents. The occurrences of carbohydrate and uronic acid compositions of fractions were correlated

Table 1: Chemical compositions of active anticoagulant fractions of F1, F2, and F3 were purified through solid phase extraction (SPE) from *Melastoma malabathricum* Linn. leaf hot water extract. Carbohydrate content was measured by using phenol-sulphuric acid, while glucose was used as a standard. Phenolic acid was measured by using the Folin-Ciocalteu method, and gallic acid was used as a standard. Uronic acid was measured by carbazole assay, and glucuronic acid was used as a standard. Values are expressed as mean ± S.E.M. ($n = 3$).

	Total yield (%)	Carbohydrate content (wt%)	Phenolic acid content (wt%)	Uronic acid content (wt%)
F1	54.17	78 ± 2.29	4.59 ± 0.49	31.71 ± 3.96
F2	14.97	46.34 ± 3.86	34.76 ± 0.53	22.85 ± 3.60
F3	8.8	14.98 ± 1.96	65.12 ± 0.78	15.42 ± 2.37

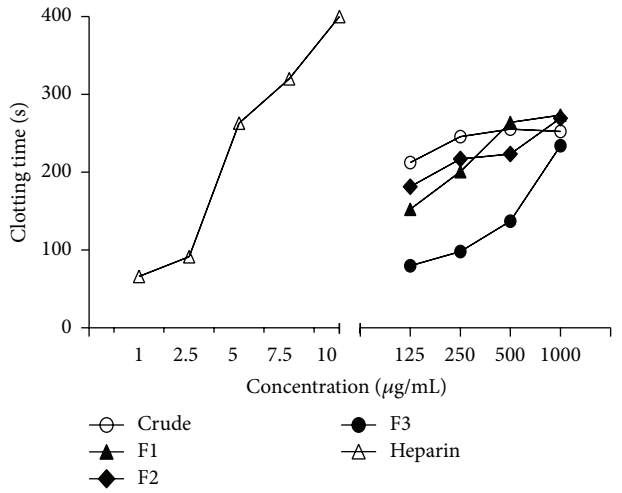

Figure 2: Anticoagulant activities of *Melastoma malabathricum* Linn. leaf crude extract, F1, F2, and F3, in comparison with the activity of heparin sodium salt (140 IU/mg), measured by activated partial thromboplastin time (APTT). F1, F2, and F3 were purified by solid phase extraction (SPE) from *M. malabathricum* Linn. leaf hot water crude extract. Data represent means of three independent experiments.

with the anticoagulant activities. The anticoagulant activities of the fractions decreased as the carbohydrate and uronic acid contents decreased in the following sequence F1, F2, and F3.

On the other hand, F3 with moderate amounts of carbohydrate and uronic acid contents compared to F1 and F2 also displayed significant anticoagulant activity. This might be due to the presence of high percentage of phenolic acids in F3. Phenolic acids together with carbohydrates and uronic acids had been suggested to play a role in anticoagulant activities by Pawlaczyk et al. [17, 18] and Mozzicafreddo et al. [19].

Besides, three types of neutral sugars were being identified from F1, F2, and F3 active anticoagulant fractions. These findings suggest that rhamnogalacturonan, homogalacturonan, and rhamnose hexose types of pectic polysaccharide were presented. However, these neutral sugars occurred in small amounts only (Table 2).

Table 2: Neutral sugar compositions of active anticoagulant fractions of F1, F2, and F3 were purified through solid phase extraction (SPE) from the hot water extract of *Melastoma malabathricum* Linn. leaf. Neutral sugar compositions of the samples were determined by using the GC-FID analysis. Values are expressed as mean ± S.E.M. ($n = 3$).

	Neutral sugar compositions		
	Glu (wt%)	Gal (wt%)	Rhamn (wt%)
F1	2.39 ± 0.15	n.d.	2.39 ± 0.11
F2	1.05 ± 0.10	1.83 ± 0.22	6.01 ± 0.27
F3	n.d.	7.05 ± 0.09	n.d.

Glucose is labelled as Glu; galactose is labelled as Gal; rhmanose is labelled as Rhamn; not detected is labelled as n.d.

Table 3: Molecular mass of active anticoagulant fractions of F1, F2, and F3 was purified through solid phase extraction (SPE) from *Melastoma malabathricum* Linn. leaf hot water extract. Molecular mass was determined by gel permeable chromatography. There were three distinguishable peaks identified from the gel permeable chromatogram of each fraction and which was labelled as Peak 1, Peak 2, and Peak 3. A set of dextran standards was used for molecular mass determination of the three peaks. Values are expressed as mean ± S.E.M. ($n = 3$).

	Molecular mass 10^3 (kDa)		
	Peak 1	Peak 2	Peak 3
F1	280.08 ± 3.57	168.60 ± 3.57	82.05 ± 3.22
F2	267.48 ± 0.66	224.85 ± 1.28	177.36 ± 1.63
F3	271.24 ± 0.39	240.23 ± 0.04	183.49 ± 0.31

The HPLC molecular mass analysis of F1, F2, and F3 showed broad and incomplete separated peaks. These unresolved molecular mass distribution patterns are typical profiles for polysaccharide conjugates that comprise mixtures of similar building fragments [17]. Besides, the three active anticoagulant fractions were the polydispersity fractions, with the molecular masses between 82 and 281 kDa (Table 3).

F1 was the first fraction purified from the SPE extraction, which had been eluted with 95% water and 5% acetonitrile. The highest yield was obtained for F1, with 54.17% (w/w) of dry crude extract. From the HPLC molecular mass determination analysis, three major not well-separated peaks were identified. The molecular masses were ~280.08 ± 3.57 kDa, ~168.60 ± 3.57 kDa, and ~82.05 ± 3.22 kDa. However, the distinct peak at a retention time of 12.35 min could not be identified by using the set of dextran standards (data not shown). Molecular masses of sample analytes were separated based on the size. Larger molecular mass of analyte was eluted out first, followed by analyte with smaller molecular mass. In addition, retention time for 5 kDa of dextran standard was 10.94 min, while retention time for 27 kDa was 8.20 min. Therefore, this distinct peak with retention time at 12.35 min was postulated to have a molecular mass less than 5 kDa. Besides, fractionation through high water compositions of solvent resulted in the highest amounts of carbohydrates and uronic acids, with 78 ± 2.29% and 31.71 ± 3.96%, respectively. In spite of these, the phenolic acids content was the least

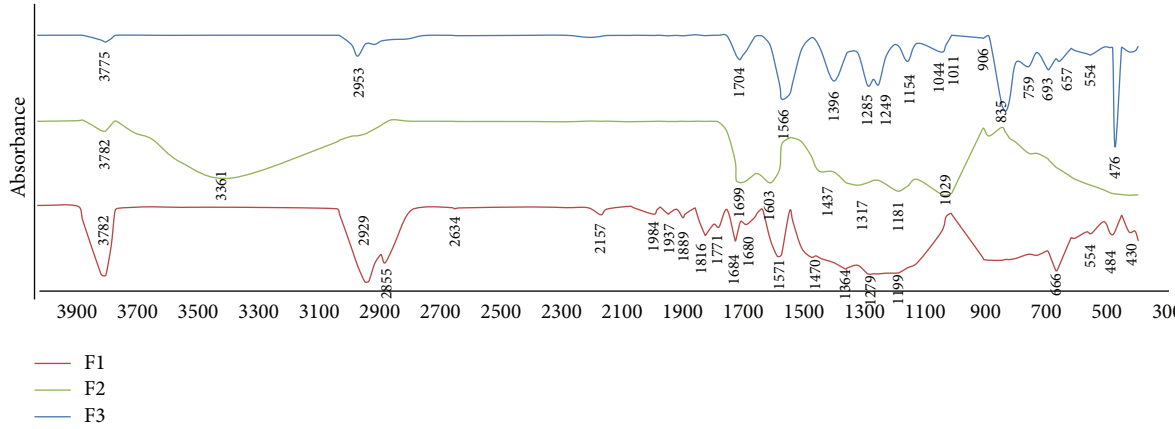

Figure 3: FT-IR spectrum of F1, F2, and F3. Active anticoagulant fractions F1, F2, and F3 were purified by solid phase extraction (SPE) from *Melastoma malabathricum* Linn. leaf hot water crude extract, and fractions were determined to have significantly prolonged activated partial thromboplastin time (APTT). Red line represented F1. Green line represented F2. Blue line represented F3.

abundant in F2 and F3. The percentage for phenolic acids present in F1 was 4.50 ± 0.49%. Meanwhile, F1 contained 2.39 ± 0.11% of rhamnose and 2.39 ± 0.15% of glucose. These results indicated the presence of rhamnose-hexose type polysaccharide.

F2 was fractionated with 90% of water and 10% of acetonitrile containing 14.97% of the total mass. The molecular mass determination analysis for F2 revealed that F2 contains higher molecular mass components than F1. The average molecular mass of two dominant peaks was about ~267.48 ± 0.66 kDa and ~177.36 ± 1.63 kDa. Another distinguishable shoulder tailing peak was about ~224.85 ± 1.28 kDa. The presence of carbohydrates, phenolic acids, and uronic acids pointed out that F2 was a polyphenolic glycoconjugate. There were 46.34 ± 3.86% of carbohydrates, 34.76 ± 0.53% of phenolic acids, and 22.85 ± 3.60% of uronic acids found in F2. The neutral sugars compositions for F2 contained rhamnogalacturonan, homogalacturonan, and rhamnose-hexose types of pectic polysaccharides. The most dominant neutral sugar presence in F2 was rhamnose which was 6.01 ± 0.27%.

F3 was purified with higher compositions of nonpolar solvent, with 80% of water and 20% of acetonitrile, and yielded 8.8% of the total dry weight of the crude extract. The HPLC molecular mass analyses for both F2 and F3 were alike. F3 also contained two dominants and one shoulder tailing peaks with ~271.24 ± 0.39 kDa, ~240.23 ± 0.04 kDa, and 183.49 ± 0.31 kDa, respectively. Phenolic acids were most likely distributed and extracted by higher compositions of nonpolar solvent. Therefore, F3 was rich in phenolic acids compared to F1 and F2. There was 65.12 ± 0.78% of phenolic acids found in F3. On the other hand, the carbohydrates and uronic acids compositions were the least abundant in F3, with 14.98 ± 1.96% and 15.42 ± 2.37%, respectively. Besides, there was only one neutral sugar-galactose found in F3. The percentage of galactose for F3 was 7.05 ± 0.09%, and type of pectic polysaccharide was suggested as homogalacturonan.

The FT-IR spectrum of each active anticoagulant fraction (Figure 3) demonstrated a characteristic carbohydrate group with the signal band at region 3782–3361 cm^{-1}. This spectral shape was identified as a stretching vibration of intramolecular hydrogen on hydroxyl (OH) group in carbohydrate [20, 21]. Besides, the band spectra of active anticoagulant fractions (F1, F2, and F3) were found at 2953–2855 cm^{-1}. These regions corresponded to the stretch vibration of aliphatic C–H groups derived from the methyl (CH_3) group [8, 22]. In addition, the characteristic bands of uronic acids or phenolic acids region-carbonyl stretching mode were observed for all three active anticoagulant fractions [23] at 1771–1566 cm^{-1}. Stretching of phenolics C–C for F1, F2, and F3 was observed at the bands at 1470–1437 cm^{-1}. In addition, the spectra band at 1396–1249 cm^{-1} indicated the presence of phenolic acids in the fractions. These bands were signature bands for phenolics C–O (H) stretching [24].

The FT-IR spectrum of F1 further proved that F1 did contain high amounts of carbohydrates and uronic acids. As shown in Figure 3, F1 spectrum displayed three discrete and intense bands at 3782 cm^{-1}, 2929 cm^{-1}, and 2855 cm^{-1}. The band spectrum at 3782 cm^{-1} was a signature band for carbohydrates. Carbohydrates were also abundantly found at strong signal bands of 1279–1199 cm^{-1}. These bands could be due to the ring vibration of carbohydrates overlapping with stretching vibration of OH group and glycosidic vibration [25]. The bands at 2929 cm^{-1} and 2855 cm^{-1} showed the stretching vibration of aliphatic carbon and hydrogen (C–H). The intensive band at 1470 cm^{-1} presented the characteristic of carboxylic functional group for uronic acids or phenolic acids.

The characteristic of carbohydrates, phenolic acids, and uronic acids was displayed at F2 FT-IR spectrum. Broad band signal was exhibited at region 3361 cm^{-1}. This band corresponded to the interaction of hydroxyl (O–H) group of carbohydrates and phenolic acids. Meanwhile, the intensive signals at 1699–1603 cm^{-1} demonstrated the stretching vibration of carboxylic group of uronic acids or phenolic acids in asymmetric and symmetric modes. Typical galacturonopyranose backbone of pectic polysaccharides was also presented at region 1181 cm^{-1}.

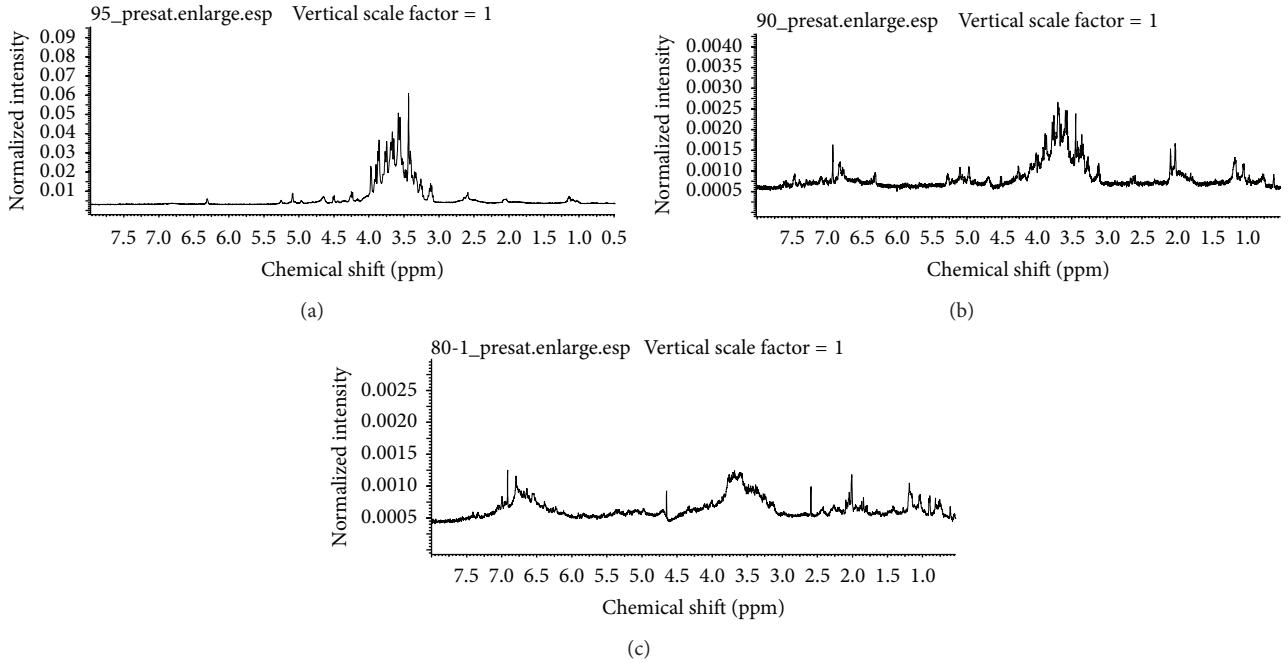

Figure 4: ^{1}H NMR spectrum of F1 (a), F2 (b), and F3 (c). Active anticoagulant fractions F1, F2, and F3 were purified by solid phase extraction (SPE) from *Melastoma malabathricum* Linn. leaf hot water crude extract and were determined with significantly prolonged activated partial thromboplastin time (APTT).

F3, with the least abundance of carbohydrate moiety, did not have intense signal bands at the carbohydrate regions. Nevertheless, F3 did display a distinct band at 1566 cm^{-1}. This region matched the characteristic of uronic acids or phenolic acids. Signals at region 1285–1249 cm^{-1} matched the FT-IR spectrum for phenolic acids. Moreover, spectra bands at 1044–1011 cm^{-1} displayed the stretching vibration of C–O for phenolic acids [26].

In agreement with the general chemical characteristics and FT-IR spectra, the ^{1}H NMR spectra for active anticoagulant fractions (F1, F2, and F3) also revealed the presence of carbohydrates and phenolic acids. Overall, the ^{1}H NMR spectra were shown to be complex and displayed broad hump signals. These were due to the complex nature of F1, F2, and F3. The not well-resolved spectra were also caused by the overlapping of many chemical constituents within the samples. From Figure 4, carbohydrate moieties were observed for F1, F2, and F3, and the carbohydrate regions were observed at δ 5.30–3.0 ppm.

The ^{1}H NMR spectrum for F1 was slightly different from that of ^{1}H NMR of F2 and F3. F1, which was rich in carbohydrate contents, only displayed a complex signal at δ 5.30–3.0 ppm. This suggests the presence of C2–C6 atoms attached at the carbohydrate pyranose ring [18]. Other than that, both F2 and F3 showed the existence of phenolic acids within the fractions at δ 8.0–6.5 ppm. Both consisted of higher phenolic acids contents compared to F1. Furthermore, with the highest amount of phenolic acids, F3 was translated into having a more complicated signal than F2. The additional ^{1}H NMR signals at δ 2.1–1.9 observed for F2 and F3 could be due to the substitution of acetyl, ethyl, or methyl groups for carbohydrates [27].

Generally, F1, F2, and F3 showed significant prolonged blood clotting time, especially in the intrinsic pathway. The anticoagulant activities of the fractions were in an increasing manner of F1 > F2 > F3. These fractions were purer and they gave better anticoagulant activity profile compared to the crude extract. Taken altogether, and with all the chemical analyses, the results showed that active anticoagulant *M. malabathricum* Linn. fractions had high polydispersity of macromolecules. The active principles of the anticoagulant activity of these fractions were acidic polysaccharides and polyphenolics. This result further proved that the anticoagulant activities for *M. malabathricum* Linn. fractions were high when the polysaccharide and hexuronic acids contents were high. A plausible explanation for the anticoagulant activities is the presence of carboxylic acid from the uronic acids, which provided negative charge properties to the fractions [18]. Hence, the results of this study are in agreement with several reported works, whereby higher plants such as *Lythrum salicaria, Erigeron canadensis,* and *Porana volubilis* have been found to contain polyphenolic polysaccharide conjugates as negative charged macromolecules for anticoagulant activity [9, 18]. Even though the hexuronic acid and polysaccharides contents were moderate for F3, its anticoagulant activity is still promising. Mozzicafreddo et al. [19], Guglielmone et al. [28], and Dong et al. [29] reported that polyphenolic demonstrated anticoagulant activity through prolongation of activated partial thromboplastin time (APTT). In this regard, we postulate that probably the anticoagulant activity of F3 could be due to its high polyphenolic contents.

4. Conclusion

All in all, the presence of negative charged polyphenolic-polysaccharides were suggested to have played a role in the anticoagulant activity, especially prolonging blood coagulation in the intrinsic pathway, as exhibited by the purified *M. malabathricum* Linn. hot water leaf extract. This discovery opens up the avenue that the simple preparation of fractions and the abundant availability of *M. malabathricum* Linn. plant materials could lead to the development of *M. malabathricum* Linn. active anticoagulant fractions as safe and cheap natural oral anticoagulant agents. A further study to isolate single anticoagulant bioactive compound from active anticoagulant SPE purified fractions (F1, F2, and F3) and an investigation into the action of single bioactive compound in blood coagulation pathway can be carried out.

Conflict of Interests

The authors declare that there is no conflict of interests regarding the publication of this paper.

Acknowledgment

The authors would like to thank the financial support granted under the ScienceFund (Grant no. 02-01-04-SF1275)from the Ministry of Science, Technology and Innovation, Malaysia.

References

[1] I. H. Burkill, W. Birtwistle, F. W. Foxworthy et al., *A Dictionary of the Economic Products of the Malay Peninsula*, Governments of Malaysia and Singapore by the Ministry of Agriculture and Cooperatives, Kuala Lumpur, Malaysia, 1966.

[2] T. C. Whitmore, *Tree Flora of Malaya*, Longman, Kuala Lumpur, Malaysia, 1972.

[3] H. C. Ong and J. Norzalina, "Malay herbal medicine in Gemencheh, Negeri Sembilan, Malaysia," *Fitoterapia*, vol. 70, no. 1, pp. 10–14, 1999.

[4] J. A. J. Sunilson, K. Anandarajagopal, A. V. A. G. Kumari, and S. Mohan, "Antidiarrhoeal activity of leaves of *Melastoma malabathricum* Linn," *Indian Journal of Pharmaceutical Sciences*, vol. 71, no. 6, pp. 691–695, 2009.

[5] M. R. Sulaiman, M. N. Somchit, D. A. Israf, Z. Ahmad, and S. Moin, "Antinociceptive effect of *Melastoma malabathricum* ethanolic extract in mice," *Fitoterapia*, vol. 75, no. 7-8, pp. 667–672, 2004.

[6] Z. A. Zakaria, R. N. R. M. Nor, G. H. Kumar et al., "Antinociceptive, anti-inflammatory and antipyretic properties of *Melastoma malabathricum* leaves aqueous extract in experimental animals," *Canadian Journal of Physiology and Pharmacology*, vol. 84, no. 12, pp. 1291–1299, 2006.

[7] C. Manicam, J. O. Abdullah, E. R. M. Tohit et al., "In vitro anticoagulant activities of *Melastoma malabathricum* Linn. aqueous leaf extract: a preliminary novel finding," *Journal of Medicinal Plants Research*, vol. 4, no. 14, pp. 1464–1472, 2010.

[8] I. Pawlaczyk, P. Capek, L. Czerchawski et al., "An anticoagulant effect and chemical characterization of *Lythrum salicaria* L. glycoconjugates," *Carbohydrate Polymers*, vol. 86, no. 1, pp. 277–284, 2011.

[9] S.-J. Yoon, M. S. Pereira, M. S. G. Pavão, J.-K. Hwang, Y.-R. Pyun, and P. A. S. Mourão, "The medicinal plant *Porana volubilis* contains polysaccharides with anticoagulant activity mediated by heparin cofactor II," *Thrombosis Research*, vol. 106, no. 1, pp. 51–58, 2002.

[10] T. Masuko, A. Minami, N. Iwasaki, T. Majima, S.-I. Nishimura, and Y. C. Lee, "Carbohydrate analysis by a phenol-sulfuric acid method in microplate format," *Analytical Biochemistry*, vol. 339, no. 1, pp. 69–72, 2005.

[11] H. K. Ju, H. W. Chung, S.-S. Hong, J. H. Park, J. Lee, and S. W. Kwon, "Effect of steam treatment on soluble phenolic content and antioxidant activity of the Chaga mushroom (*Inonotus obliquus*)," *Food Chemistry*, vol. 119, no. 2, pp. 619–625, 2010.

[12] K. A. Taylor and J. G. Buchanan-Smith, "A colorimetric method for the quantitation of uronic acids and a specific assay for galacturonic acid," *Analytical Biochemistry*, vol. 201, no. 1, pp. 190–196, 1992.

[13] N. P. Brunton, T. R. Gormley, and B. Murray, "Use of the alditol acetate derivatisation for the analysis of reducing sugars in potato tubers," *Food Chemistry*, vol. 104, no. 1, pp. 398–402, 2007.

[14] L. D. Melton and B. G. Smith, "Curent protocol in food analytical chemistry," in *Determination of Neutral Sugars by Gas Chromatography of Their Alditol Acetates*, L. D. Melton and B. G. Smith, Eds., pp. E3.2.1–E3.2.13, John Wiley & Sons, New Jersey, NJ, USA, 2001.

[15] S. M. Bates and J. I. Weitz, "Coagulation assays," *Circulation*, vol. 112, no. 4, pp. E53–E60, 2005.

[16] L. A. Liapina and G. A. Kovalchuk, "A comparative study of the action on the hemostatic system of extracts from the flowers and seeds of the meadowsweet (*Filipendula ulmaria* L.) Maxim," *Izvestiia Akademii Nauk: Seriia Biologicheskaia*, vol. 4, pp. 625–628, 1993.

[17] I. Pawlaczyk, M. Lewik-Tsirigotis, P. Capek et al., "Effects of extraction condition on structural features and anticoagulant activity of *F. vesca* L. conjugates," *Carbohydrate Polymer*, vol. 92, no. 1, pp. 741–750, 2013.

[18] I. Pawlaczyk, L. Czerchawski, J. Kańska et al., "An acidic glycoconjugate from *Lythrum salicaria* L. with controversial effects on haemostasis," *Journal of Ethnopharmacology*, vol. 131, no. 1, pp. 63–69, 2010.

[19] M. Mozzicafreddo, M. Cuccioloni, A. M. Eleuteri, E. Fioretti, and M. Angeletti, "Flavonoids inhibit the amidolytic activity of human thrombin," *Biochimie*, vol. 88, no. 9, pp. 1297–1306, 2006.

[20] N. Abidi, L. Cabrales, and C. H. Haigler, "Changes in the cell wall and cellulose content of developing cotton fibers investigated by FTIR spectroscopy," *Carbohydrate Polymers*, vol. 100, pp. 9–16, 2014.

[21] W. B. Fischer and H. H. Eysel, "Raman and FTIR spectroscopic study on water structural changes in aqueous solutions of amino acids and related compounds," *Journal of Molecular Structure*, vol. 415, no. 3, pp. 249–257, 1997.

[22] Q. Peng, X. Lv, Q. Xu et al., "Isolation and structural characterization of the polysaccharide LRGP1 from *Lycium ruthenicum*," *Carbohydrate Polymers*, vol. 90, no. 1, pp. 95–101, 2012.

[23] A. S. Sivam, D. Sun-Waterhouse, C. O. Perera, and G. I. N. Waterhouse, "Exploring the interactions between blackcurrant polyphenols, pectin and wheat biopolymers in model breads; a FTIR and HPLC investigation," *Food Chemistry*, vol. 131, no. 3, pp. 802–810, 2012.

[24] X.-H. Guan, C. Shang, and G.-H. Chen, "ATR-FTIR investigation of the role of phenolic groups in the interaction of

some NOM model compounds with aluminum hydroxide," *Chemosphere*, vol. 65, no. 11, pp. 2074–2081, 2006.

[25] S. Posé, A. R. Kirby, J. A. Mercado, V. J. Morris, and M. A. Quesada, "Structural characterization of cell wall pectin fractions in ripe strawberry fruits using AFM," *Carbohydrate Polymers*, vol. 88, no. 3, pp. 882–890, 2012.

[26] S. D. Silva, R. P. Feliciano, L. V. Boas et al., "Application of FTIR-ATR to Moscatel dessert wines for prediction of total phenolic and flavonoid contents and antioxidant capacity," *Food Chemistry*, vol. 150, pp. 489–493, 2014.

[27] I. Pawlaczyk, L. Czerchawski, W. Kuliczkowski et al., "Anticoagulant and anti-platelet activity of polyphenolic-polysaccharide preparation isolated from the medicinal plant *Erigeron canadensis* L," *Thrombosis Research*, vol. 127, no. 4, pp. 328–340, 2011.

[28] H. A. Guglielmone, A. M. Agnese, S. C. N. Montoya, and J. L. Cabrera, "Anticoagulant effect and action mechanism of sulphated flavonoids from *Flaveria bidentis*," *Thrombosis Research*, vol. 105, no. 2, pp. 183–188, 2002.

[29] H. Dong, S.-X. Chen, R. M. Kini, and H.-X. Xu, "Effects of tannins from *Geum japonicum* on the catalytic activity of thrombin and factor Xa of blood coagulation cascade," *Journal of Natural Products*, vol. 61, no. 11, pp. 1356–1360, 1998.

Hindawi Publishing Corporation
Evidence-Based Complementary and Alternative Medicine
Volume 2014, Article ID 950817, 7 pages
http://dx.doi.org/10.1155/2014/950817

Research Article

Antiviral Activity of Total Flavonoid Extracts from *Selaginella moellendorffii* Hieron against Coxsackie Virus B3 *In Vitro* and *In Vivo*

Dan Yin,[1,2] Juan Li,[1] Xiang Lei,[1] Yimei Liu,[1] Zhanqiu Yang,[3] and Keli Chen[1]

[1] *Key Laboratory of TCM Resource and TCM Compound Co-Constructed by Hubei Province and Ministry of Education, Hubei University of Traditional Chinese Medicine, Wuhan 430065, China*
[2] *Wuhan Bioengineering Institute, Wuhan 430415, China*
[3] *State Key Laboratory of Virology, School of Medicine, Institute of Medical Virology, Wuhan University, Wuhan 430071, China*

Correspondence should be addressed to Juan Li; lz198207@126.com and Keli Chen; kelichen@126.com

Received 11 February 2014; Revised 22 April 2014; Accepted 30 April 2014; Published 19 May 2014

Academic Editor: Shi-Biao Wu

The antiviral activity of total flavonoid extracts from *Selaginella moellendorffii* Hieron and its main constituents amentoflavone were investigated against coxsackie virus B3 (CVB3). When added during or after viral infection, the extracts and amentoflavone prevented the cytopathic effect (CPE) of CVB3, as demonstrated in a 3-(4,5-dimethylthiazol-2-yl)-2,5-diphenyl tetrazolium bromide (MTT) colorimetric assay, with a 50% inhibitory concentration (IC50) from 19 ± 1.6 to 41 ± 1.2 μg/mL and 25 ± 1.2 to 52 ± 0.8 μg/mL, respectively. KM mice were used as animal models to test the extracts' activity *in vivo*. Oral administration of the total flavonoid extracts at 300 mg/kg/day significantly reduced mean viral titers in the heart and kidneys as well as mortality after infection for 15 days. The experimental results demonstrate that *in vitro* and *in vivo* the model mice infected with CVB3 can be effectively treated by the total flavonoid extracts from *Selaginella moellendorffii* Hieron.

1. Introduction

Group B coxsackieviruses have been associated with a wide range of human diseases, such as encephalitis, common cold, cardiomyopathy, diabetes, inflammation, and neurological disorders [1–3]. Among them, CVB3 is the leading cause of viral myocarditis. Because proper infection control practices are still not fully available for CVB3 infection, patients with myocarditis often progress into chronic dilated cardiomyopathy and finally die of heart failure [4]. So far, in China, attempts have been made to incorporate natural herbal medicine into treatment of viral infections [5–7].

Selaginella moellendorffii Hieron, a medicinal plant of genus *Selaginella* (Selaginellaceae), has been used in traditional Chinese folk medicine for treatment of jaundice, gonorrhea, bleeding, and acute hepatitis [8]. The primary bioactive constituents of *S. moellendorffii* are reported to be flavones, such as amentoflavone, robustaflavone, biapigenin, hinokiflavone, podocarpusflavone A, and ginkgetin, which have antioxidant, antivirus, and antitumor properties [8–11].

In our previous study, it was found that the total flavonoid extracts of *Selaginella moellendorffii* (TFE) showed strong inhibition effects on CVB3 *in vitro* [12]. In this study, the antiviral activity of amentoflavone (the main constituent of *S. moellendorffii*) and TFE against CVB3 *in vitro* and *in vivo* is systematically investigated.

2. Materials and Methods

2.1. Plant Materials and Chemicals. The whole herbs of *Selaginella moellendorffii* Hieron were collected during September 2010 from the Wuduhe town of Yichang (Hubei, China). Identification of specimen was confirmed by Dr. Dingrong Wan, South Central University for Nationalities (Wuhan, China), and a voucher specimen was deposited in the herbarium of Hubei University of Chinese Medicine, China.

Acyclovir (ACV) was produced in Wuhan Changlian Laifu pharmaceutical Limited Liability Company (Wuhan, Hubei, China). RPMI 1640, trypsin, and fetal calf serum (FCS) were purchased from GIBCO (Grand Island, NY, USA). MTT and dimethyl sulfoxide (DMSO) were from Sigma (St. Louis, MO, USA). Deionized water was prepared using a Millipore Milli Q plus system. All other chemicals not mentioned here were of analytical grade from standard sources.

2.2. Preparation of Samples. Ethyl acetate extracts of *S. moellendorffii* (EAE): the air-dried and powdered *S. moellendorffii* (50 g) were extracted twice with petroleum ether and then were filtered. The residues were extracted twice with ethyl acetate (500 mL) and then were filtered. Then the solution was dried using a rotary evaporator. The purity of EAE was about 8.9%.

TFE were prepared in our key laboratory according to their preparation technology and quality standard [13, 14]. The content of total flavonoids and the main constituent amentoflavone were not less than 50.0% and 35.0%, respectively. The content of TFE and amentoflavone in EAE was about 17.4% and 5.6%, respectively.

Amentoflavone, as chemical reference substance, was refined from *S. moellendorffii* in the key laboratory with a purity of 99.7% [15, 16].

The above four samples (ACV, EAE, TFE, and amentoflavone) were dissolved in DMSO and stored at −20°C for the assay *in vitro*. Final concentrations for different experiments were prepared by diluting with complete medium. The final maximum DMSO concentration was 0.05%, which showed no effect on cell cultures. The blank control received the carrier solvent. For *in vivo* assay, TFE and ACV were suspended uniformly in distilled water with ultrasonic waves before use.

2.3. Cell Cultures and Viruses. HEp-2 (human laryngeal carcinoma) cells and CVB3 were maintained at Institute of Medical Virology, Wuhan University. HEp-2 cells were grown in RPMI 1640 supplemented with 10% fetal calf serum (FCS), 0.1% L-glutamine, 100 U/mL penicillin, and 0.1 mg/mL streptomycin. The test medium used for the cytotoxic assay as well as for antiviral assays contained 2% of FCS in the above medium. The virus was stored in small aliquots at −80°C until use.

2.4. Virus Titration. Virus titration was performed by the limited dilution method using a 96-well plate. The virus titer was estimated from cytopathogenicity of cells infected with CVB3 and expressed as 50% tissue culture infectious doses/mL ($TCID_{50}$/mL) [17].

2.5. Cytotoxicity and Virus Growth Inhibition Assay. The cytotoxicity and antiviral effect of the samples were determined by quantitative colorimetric MTT method [18, 19]. Briefly, HEp-2 cells (2×10^4/well) were seeded in 96-well plates. After the removal of growth medium, cells were incubated with various concentrations of extract. The plates were incubated at 37°C, and the development of cytopathic effect was monitored daily by light microscopy until the virus-infected, untreated cells showed CPE up to 80%. At this time point, MTT solution (5 mg/mL in phosphate-buffered saline, PBS) was added to each well after the removal of the medium and incubated for an additional 4 h. The formazan crystal formed was dissolved with DMSO. The optical densities (ODs) were then detected at double wavelengths of 540 and 690 nm from the microplate spectrophotometer. The data was expressed as a percentage of OD value of treated cell cultures relative to untreated ones. The 50% cytotoxic concentrations (CC50) and IC50 of the samples were determined. Then, therapeutic index (TI) of the samples by CC50/IC50 was obtained. Each dilution was tested in triplicate.

2.6. Treatment of Sample before Virus Infection. The dilutions of the samples were dissolved in RPMI-1640 and incubated with HEp-2 cells in 96-well microtiter plates for 24 h at 37°C in a 5% CO_2 atmosphere. The cells were washed with PBS and infected with 0.1 mL of CVB3 ($100TCID50/mL : 10^{-5}$) after removal of the samples. The cells were rinsed with PBS after a 1 h incubation and then incubated with test medium until typical CPE was obvious [20]. The inhibition of the virus induced CPE was observed by light microscopy and measured by the MTT assay. Virus controls, normal controls, and ACV controls were included in all assays. All the results of experiments were measured in triplicate.

2.7. Virucidal Assay. Viral suspensions were cocultured with the dilutions of the samples at 37°C for 1 h in a 5% CO_2 atmosphere. Then they were added to the HEp-2 cells in 96-well plates. The solutions containing both samples and viruses were removed after a 1 h incubation and the cells were washed carefully with PBS and then incubated with test medium. The experiment was performed according to the above operation. The antiviral effect was determined using CPE observation and viral titer evaluation following the procedures described above.

2.8. Sample Treatment after Virus Infection. The HEp-2 cells were infected with 0.1 mL viruses ($100TCID50/mL : 10^{-5}$) for 1 h at 37°C in a 5% CO_2 atmosphere. The cells were washed with PBS and added with different doses of the samples. The assay was performed according to the above operation as well.

2.9. CVB3 Infections in Mice. Specific-pathogen-free male Kunming mice (10 ± 2 g), obtained from Animal Center of Wuhan University, were used in the study. Sixty mice (10 mice/group, six groups) were used in this experiment. Fifty mice were infected with CVB3 intraperitoneally, and the remaining 10 were used as normal control and injected intraperitoneally with the same volume of PBS. After infection for 24 hours, mice were treated by oral gavage (p.o.) with 0.2 mL of total flavonoids extracts from *S. moellendorffii* at 100, 300, and 900 mg/kg body weight/day, respectively, and treatment was continued daily for 15 days unless otherwise indicated. The mice of ACV control group were administered with ACV orally at 10 mg/kg. The virus and normal control group received water instead of samples.

Table 1: Cytotoxicity (CC50: μg/mL), *in vitro* antiviral activity (IC50: μg/mL), and therapeutic index (TI) for each sample.

Samples	CC50[a]	Treating before infection		Treating during infection		Treating after infection	
		IC50[a]	TI	IC50[a]	TI	IC50[a]	TI
TFE	85 ± 1.7	NA	NA	41 ± 1.2	2.07	19 ± 1.6	4.47
EAE	60 ± 2.1	NA	NA	36 ± 1.9	1.67	16 ± 1.9	3.75
Amentoflavone	53 ± 0.9	NA	NA	52 ± 0.8	1.02	25 ± 1.2	2.12
ACV	>500	NA	NA	NA	NA	NA	NA

CC50: the half of the cytotoxic concentration; IC50: the inhibitory concentration required to reduce viral replication by 50%; TI: the ratio of CC50/IC50; NA: no activity in the assayed concentrations; ACV: acyclovir; EAE: ethyl acetate extracts of *S. moellendorffii*; TFE: total flavonoid extracts of *S. moellendorffii*.
[a]Mean ± SD values are shown from three independent experiments.

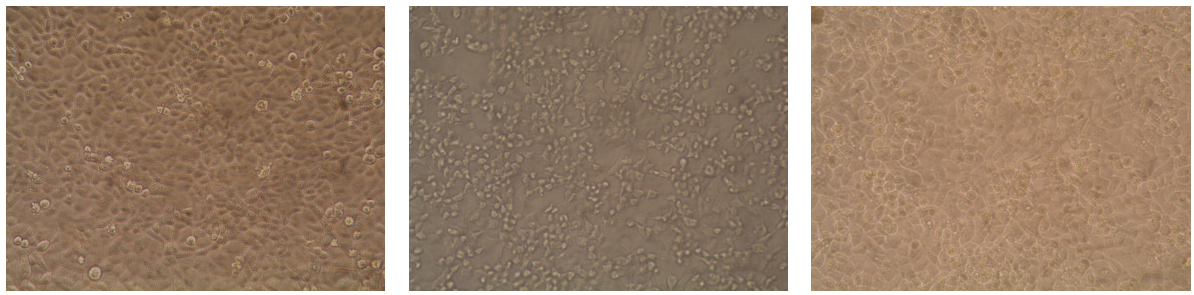

(a) (b) (c)

Figure 1: Morphology changes of HEp-2 cells infected with CVB3. (a) Normal control demonstrated that these HEp-2 cells were typical with normal morphology. (b) Viral control demonstrated that most of the HEp-2 cells lost their normal morphology and appeared to be round in shape. Most of them were detached. (c) TFE group demonstrated that some HEp-2 cells had normal morphology and quantity.

Three mice from each group were sacrificed by cervical dislocation on day 10 after viral exposure. We recorded the body weights of the mice daily until the animals were killed. The kidneys and hearts were harvested from the mice of each group, which were further homogenized to 10% (weight/volume) suspensions in test medium. The homogenates were frozen and thawed twice to release the virus and then centrifuged at 3,000 rpm for 15 min. Virus titration was determined by the limited dilution method. The remaining animals of each group were observed every day for changes in body weight and for any deaths. We obtained the tissue samples from the kidneys and heart until animals of each group were sacrificed on day 15 after viral exposure for pathological examination (HE staining).

2.10. Statistical Analysis. The data were analyzed by SPSS 18.0 software. Results were expressed as mean ± standard deviation for three independent experiments. Survival rates of the mice were compared by Kaplan-Meier Survival analysis (log-rank test). A P value of <0.05 was considered statistically significant.

3. Results

3.1. Cellular Cytotoxicity and Antiviral Potential of Samples from S. moellendorffii against CVB3 In Vitro. ACV, EAE, TFE, and amentoflavone were examined for cytotoxicity and antiviral potential by MTT assay. A cellular toxicity of 85 ± 1.7 μg/mL was recorded for TFE on HEp-2 cells, followed by EAE (60 ± 2.1 μg/mL) and amentoflavone (53 ± 0.9 μg/mL); ACV which was the positive sample had no toxicity in the rage of experimental concentration. The level of cytotoxicity was as follows: ACV < TFE < EAE < amentoflavone (Table 1).

Different concentrations of samples from *S. moellendorffii* were subjected to the HEp-2 cells before/after the CVB3 infection or directly mixed with virus as described in Materials and Methods. All samples could not prevent HEp-2 cells from CVB3 infection in the pretreatment assay. There was no significant difference between sample-treated groups and the untreated virus control group, and HEp-2 cells showed typical virus disease which is growth disorders, becoming round or elongated, increasing particles and refraction, and shed or died finally (Figure 1).

However, direct virucidal activity of EAE, TFE, and amentoflavone was observed (Table 1) and the average viral suppression rate of different concentrations of each sample was detected (Figure 2). Also, inhibitory activity of EAE, TFE, and amentoflavone was observed when samples were added after HEp-2 cells had been infected with CVB3 (Table 1) and the average viral suppression rate of various concentrations of each sample was detected (Figure 3). In the assayed concentrations, no virucidal activity of ACV was observed before/after the CVB3 infection or directly mixed with virus.

The level of TI was as follows: TFE > EAE > amentoflavone. There was no significant difference in antiviral activity between EAE and TFE group. However, there was statistically significant difference in amentoflavone group and TFE or EAE group.

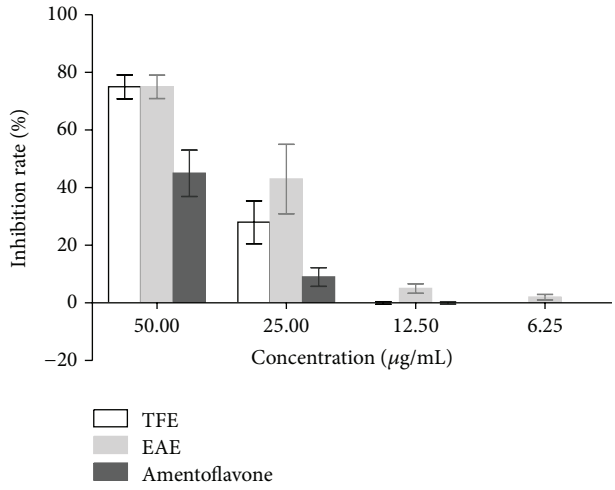

Figure 2: Direct virucidal activity of EAE, TFE, and amentoflavone. The average viral inhibition rate of samples (%) was detected by MTT assay, when they were treated during infection. Viral suspensions were cocultured with the dilutions of the samples (50–6.25 μg/mL) at 37°C for 1 h in a 5% CO_2 atmosphere.

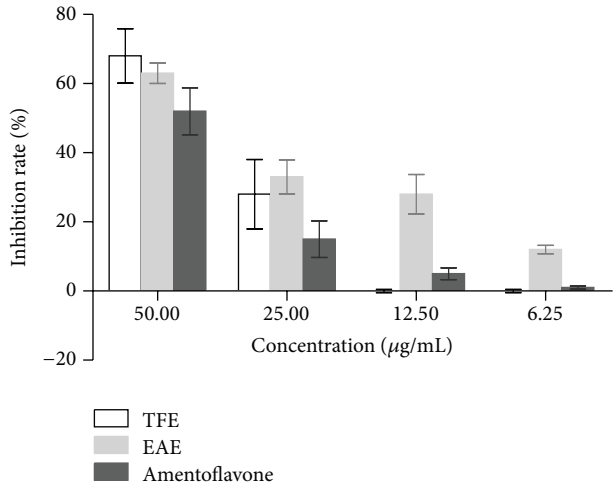

Figure 3: Virucidal activity of EAE, TFE, and amentoflavone after the CVB3 infection. The average viral inhibition rate of samples (%) was detected by MTT assay. The HEp-2 cells were infected with viruses for 1 h at 37°C in a 5% CO_2 atmosphere. Then cells were washed with PBS and added with different doses of the samples (50–6.25 μg/mL).

3.2. Antiviral Effects of TFE against CVB3 in Mice

3.2.1. Clinical Observations. In the viral control and ACV group, on day 6 after infection it was observed that animals showed ruffled fur, a tendency to huddle, diminished vitality, and weight loss (Figure 4). On day 7, this group of animals began to die, and, by day 15, all of them had died. In the TFE-treated group, the animals receiving 100 mg/kg/day began to die on day 9 after challenge, and 15-day mortality was 50%. There was no significant difference in body weight between normal control and TFE 300 mg/kg/day group. The animals

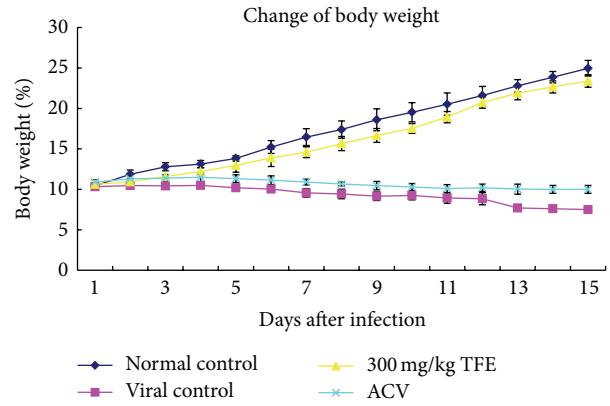

Figure 4: The body weight of CBV3-infected mice during the 15-day period. KM mice were infected intraperitoneally with CVB3 (10^5TCID$_{50}$/0.2 mL). 24 h after infection, mice were treated by oral gavage with 300 mg/kg/day TFE for 15 days. The virus control group and the normal control group received water instead of the chemicals. Body weight was recorded daily.

Table 2: Cure and mortality rate in CBV3-infected mice.

	Cure rate (%)	Mortality rate (%)
Normal control	100	0
Viral control	0	100
TFE-100 mg/kg[b]	30 ± 8**	50 ± 16**
TFE-300 mg/kg[b]	50 ± 12**	20 ± 5**
TFE-900 mg/kg[b]	70 ± 17**	10 ± 12**
ACV-10 mg/kg	0	100

[b]If the body weight of the remaining mice in the TFE-treated group was with no continuous growth, they were considered to be uncured. ** $P < 0.01$, compared with the virus control group.

receiving 300 mg/kg/day and the normal control animals did not show abnormalities during the 15-day period, the body weight of animals was gradually increased in the normal control group (Figure 4), and 15-day mortality reduced to 20%. The 15-day mortality decreased to 10% in mice treated with TFE 900 mg/kg/day (Table 2). The cure rates in mice treated with TFE at the doses of 100, 300, and 900 mg/kg/day were 30%, 50%, and 70%, respectively (Table 2).

3.2.2. Pathological Evaluation. We obtained the tissue samples from the kidneys and heart until animals of each group were sacrificed on day 15 after viral exposure for pathological examination. As shown microscopically, inflammatory cell infiltration and glomerular atrophy were in the viral control and ACV group animals, which also showed hyperemia and edema with massive infiltration of the inflammatory cell. Tissue samples from the animals of TFE-treated group did not have obvious changes (Figure 5).

3.2.3. Virological Evaluation. The changes of the virus titers in heart and kidneys of the CVB3-infected mice from different groups at day 10 were shown in Table 3. The virus titers of kidneys and heart were significantly lower in mice receiving

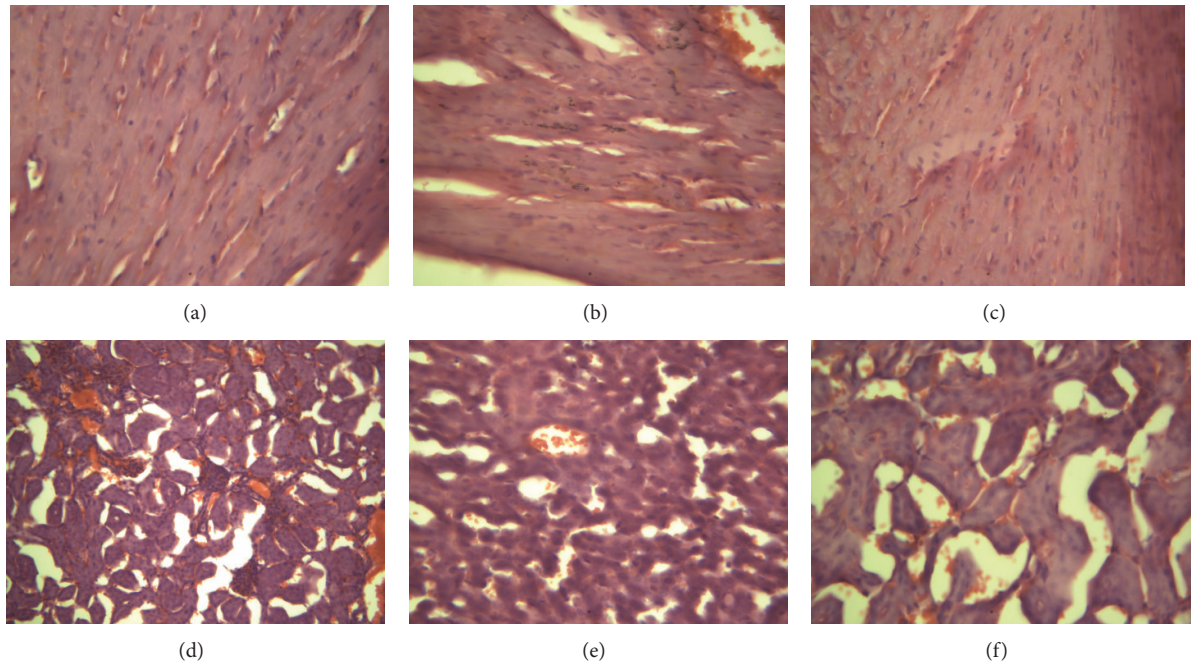

Figure 5: Pathologic features of hearts and kidneys (HE staining, ×200). (a) Normal control of heart tissue; (b) infected control of heart tissue; (c) TFE-treated group of heart tissue; (d) normal control of kidney tissue; (e) infected control of kidney tissue; (f) TFE-treated group of kidney tissue. Animals of each group were sacrificed on day 15 after viral exposure for pathological examination.

oral administration of TFE at three doses for 10 days than in the viral control group and ACV group ($P < 0.05$).

4. Discussion

S. moellendorffii has been used in traditional Chinese folk medicine for treatment of various inflammatory diseases such as pneumonia, acute tonsillitis, conjunctivitis, mastitis, and icteric hepatitis [8]. In addition, *S. moellendorffii* has been made into medicinal tablets in China, and it has good effect on idiopathic and secondary thrombocytopenic purpura and various bleeding ailments. The chemical constituents of this plant are reported to be biflavonoids, aliphatic acids, sitosterols, coumarins, and lignanosides [21, 22]. EAE contains amentoflavone, hinokiflavone, podocarpusflavone A, robustaflavone, and ginkgetin [8, 16]. Ginkgetin, hinokiflavone, and robustaflavone had antivirus activity, beside amentoflavone [23].

In this study, the antiviral activity of total flavonoids against CVB3 *in vitro and in vivo* was investigated. TFE, EAE, and amentoflavone treatments during and after injection exhibit 2~3-fold difference in activities, and the level of TI was as follows: TFE > EAE > amentoflavone; the level of cytotoxicity was as follows: TFE < EAE < amentoflavone. These results showed that single compound with higher cytotoxicity showed relatively weaker antiviral activity than extracts. These indicated that other compounds might have synergistic effect, or the compound showing strong antiviral activity against CVB3 might not be amentoflavone, despite being the main constituent of *S. moellendorffii.* Therefore, further study of amentoflavone *in vivo* was not investigated, and the single compound amentoflavone used in practice might not be a good choice.

Table 3: Virus titers of heart and kidney in CBV3-infected mice (-lgTCID50).

Groups	Heart	Kidney
Normal control	0	0
Virus control	4.3 ± 0.3	5.3 ± 0.4
TFE-100 mg/kg	3.5 ± 0.3*	3.9 ± 0.3**
TFE-300 mg/kg	1.9 ± 0.2**	2.4 ± 0.1**
TFE-900 mg/kg	1.2 ± 0.1**	1.6 ± 0.2**
ACV-10 mg/kg	4.2 ± 0.2	5.4 ± 0.3

All the viral titers data present in a format of -lgTCID$_{50}$. Values are means ± SD ($n = 10$). $^{*}P < 0.05$ and $^{**}P < 0.01$, compared with the virus control group.

When primarily cultured HEp-2 cells infected with CVB3 were treated with TFE by different methods, TFE was found to present potent antiviral activity against CVB3 when added during and after infection. These data demonstrated that TFE could induce durable antiviral activity in host cells, not only inactivating CVB3 but also inhibiting viral replication. Humans medically use biflavonoid especially for antioxidant, anti-inflammatory, and anticarcinogenic. As an antioxidant, amentoflavone inhibits production of NO, which inactivates NF-κB, while, as anti-inflammatory, amentoflavone and ginkgetin inhibit inflammation that induces iNOS and COX-2 at macrophage RAW 264.7. However, the mechanism of antiviral activity needed further study.

The mouse model infected with CVB3 was established to further study whether TFE possessed antiviral action against

CVB3 *in vivo*. The infected mice display some symptoms of circulatory failure such as cyanosis and lack of blood perfusion in the tails, and there was evidence of virus replication in the heart and kidneys. Pathological findings also confirmed the results, and all viral control mice died on the 15th day after infection. Thus, CVB3 infection in KM mice was a suitable *in vivo* antiviral activity. The mice orally administered TFE 100, 300, or 900 mg/kg/day after infection with CVB3 for 15 days significantly enhanced survival rate compared to the virus group and revealed clear dose-effect relationship. The virus yields were reduced and the pathological abnormalities were released in kidneys and hearts.

ACV, the positive control sample, has been successfully used to treat myocarditis associated with Epstein-Barr and varicella virus, but there was no obvious evidence demonstrating that ACV was effective in CVB3 induced myocarditis.

5. Conclusions

In summary, the total flavonoid extracts from *S. moellendorffii* have been found to exhibit an effective antiviral activity against CVB3 infection *in vitro* and *in vivo*. This provides new therapeutic candidates for CVB-induced myocarditis treatment. However, further experiments are required to determine the mechanism and target of action.

Abbreviations

ACV: Acyclovir
CC50: The half of the cytotoxic concentration
CPE: Cytopathic effect
CVB3: Coxsackievirus B3
DMSO: Dimethyl sulfoxide
EAE: Ethyl acetate extracts of *S. moellendorffii*
FCS: Fetal calf serum
HEp-2: Human laryngeal carcinoma cells
IC50: The inhibitory concentration required to reduce viral replication by 50%
MTT: 3-(4,5-Dimethylthiazol-2-yl)-2,5-diphenyl tetrazolium bromide
ODs: Optical densities
TFE: Total flavonoid extracts of *Selaginella moellendorffii*
TI: Therapeutic index (the ratio of CC50/IC50).

Conflict of Interests

The authors declare no conflict of interests regarding the publication of this paper.

Authors' Contribution

Dan Yin and Juan Li contributed equally to the work.

Acknowledgments

This work was supported by the National Natural Science Foundation Project (30470193), the Science and Technology Research Project of Hubei Province of China (2006AA301B01), and the Scientific Research Foundation Project of the Education Department of Hubei Province (Q20142007).

References

[1] L. C. Archard, M. A. Khan, B. A. Soteriou et al., "Characterization of coxsackie B virus RNA in myocardium from patients with dilated cardiomyopathy by nucleotide sequencing of reverse transcription-nested polymerase chain reaction products," *Human Pathology*, vol. 29, no. 6, pp. 578–584, 1998.

[2] M. Esfandiarei and B. M. McManus, "Molecular biology and pathogenesis of viral myocarditis," *Annual Review of Pathology: Mechanisms of Disease*, vol. 3, no. 3, pp. 127–155, 2008.

[3] M. S. Horwitz, L. M. Bradley, J. Harbertson, T. Krahl, J. Lee, and N. Sarvetnick, "Diabetes induced by Coxsackie virus: initiation by bystander damage and not molecular mimicry," *Nature Medicine*, vol. 4, no. 7, pp. 781–785, 1998.

[4] Z. Liu, F. Wei, L. J. Chen et al., "*In vitro* and *in vivo* studies of the inhibitory effects of emodin isolated from *Polygonum cuspidatum* on Coxsakievirus B4," *Molecules*, vol. 18, no. 10, pp. 11842–11858, 2013.

[5] H. R. Xiong, Y. Y. Shen, L. Lu et al., "The inhibitory effect of *Rheum palmatum* against coxsackievirus B3 *in vitro* and *in vivo*," *American Journal of Chinese Medicine*, vol. 40, no. 4, pp. 801–812, 2012.

[6] X. Q. Wei, "Effect evaluation of treating viral myocarditis by Jiawei Buxin Jiedu decoction," *China Medicine and Pharmacy*, vol. 2, no. 20, pp. 88–89, 2012.

[7] P. F. Zhao, Y. H. Yang, and S. L. Bai, "103 cases of treating viral myocarditis by Honeysuckle soup," *Nei Mongol Journal of Traditional Chinese Medicine*, vol. 15, pp. 22–23, 2012.

[8] S. Shi, H. Zhou, Y. Zhang, and K. Huang, "Hyphenated HSCCC-DPPH for rapid preparative isolation and screening of antioxidants from *Selaginella moellendorffii*," *Chromatographia*, vol. 68, no. 3-4, pp. 173–178, 2008.

[9] S. Li, M. Zhao, Y. Li et al., "Preparative isolation of six antitumour biflavonoids from *Selaginella doederleinii* Hieron by high-speed counter-current chromatography," *Phytochemical Analysis*, vol. 25, no. 2, pp. 127–133, 2014.

[10] S.-C. Ma, P. P. But, V. E. Ooi et al., "Antiviral amentoflavone from *Selaginella sinensis*," *Biological and Pharmaceutical Bulletin*, vol. 24, no. 3, pp. 311–312, 2001.

[11] H. Liu, H. Peng, Z. Ji et al., "Reactive oxygen species-mediated mitochondrial dysfunction is involved in apoptosis in human nasopharyngeal carcinoma CNE cells induced by *Selaginella doederleinii* extract," *Journal of Ethnopharmacology*, vol. 138, no. 1, pp. 184–191, 2011.

[12] D. Yin and K. L. Chen, "Study on the inhibitory action on CVB3 replication *in vitro* by the extracts from *Selaginella moellendorfii* Hieron," *Chinese Hospital Pharmaceutical Journal*, vol. 29, no. 4, pp. 262–264, 2009.

[13] D. Yin and K. L. Chen, "Optimization of the extraction technology of total flavonoids from *Selaginella tamarisciana* by orthogonal experiment," *China Pharmacy*, vol. 21, no. 15, pp. 1368–1370, 2010.

[14] D. Yin and K. L. Chen, "Purification technology of total flavonoids from *Selaginella moellendorfii* Hieron withmacroporous adsorption resin," *Chinese Journal of Pharmaceutical Analysis*, vol. 30, no. 11, pp. 2040–2043, 2010.

[15] X.-L. Fan, J.-C. Xu, X.-H. Lin, and K.-L. Chen, "Study on biflavonoids from *Selaginella uncinata* (Desv.) Spring," *Chinese Pharmaceutical Journal*, vol. 44, no. 1, pp. 15–19, 2009.

[16] X.-P. Jiang and K.-L. Chen, "Study on biflavonoids from *Selaginella moellendorjii* Hieron," *Chinese Pharmaceutical Journal*, vol. 44, no. 2, pp. 96–98, 2009.

[17] A. F. Reed, "A left superior vena cava draining the blood from a closed coronary sinus," *Journal of Anatomy*, vol. 73, no. 1, pp. 195–197, 1938.

[18] Y. Li, P. P. But, and V. E. Ooi, "Antiviral activity and mode of action of caffeoylquinic acids from *Schefflera heptaphylla* (L.) Frodin," *Antiviral Research*, vol. 68, no. 1, pp. 1–9, 2005.

[19] A. Garozzo, C. C. Cutri, A. Castro et al., "Anti-rhinovirus activity of 3-methylthio-5-aryl-4-isothiazolecarbonitrile derivatives," *Antiviral Research*, vol. 45, no. 3, pp. 199–210, 2000.

[20] A. Kujumgiev, I. Tsvetkova, Y. Serkedjieva, V. Bankova, R. Christov, and S. Popov, "Antibacterial, antifungal and antiviral activity of propolis of different geographic origin," *Journal of Ethnopharmacology*, vol. 64, no. 3, pp. 235–240, 1999.

[21] C. M. Sun, W. J. Syu, Y. T. Huang et al., "Selective cytotoxicity of ginkgetin from *Selaginella moellendorffii*," *Jounal of Natural Products*, vol. 60, no. 4, pp. 382–384, 1997.

[22] X. K. Zheng, K. K. Li, Y. Z. Wang, and W. S. Feng, "A new dihydrobenzofuran lignanoside from *Selaginella moellendorffii* Hieron," *Chinese Chemical Letters*, vol. 19, no. 1, pp. 79–81, 2008.

[23] A. D. Setyawan, "Review: natural products from genus *Selaginella* (Selaginellaceae)," *Nusantara Bioscience*, vol. 3, no. 1, pp. 44–58, 2011.

Hindawi Publishing Corporation
Evidence-Based Complementary and Alternative Medicine
Volume 2014, Article ID 569594, 7 pages
http://dx.doi.org/10.1155/2014/569594

Research Article

Bioactivities of Compounds from *Elephantopus scaber*, an Ethnomedicinal Plant from Southwest China

Jianjun Wang,[1] Ping Li,[1] Baosai Li,[2] Zhiyong Guo,[1] Edward J. Kennelly,[1,3] and Chunlin Long[1,4]

[1] *College of Life and Environmental Sciences, Minzu University of China, 27 Zhong-Guan-Cun South Avenue, Haidian District, Beijing 100081, China*
[2] *School of Chinese Materia Medica, Beijing University of Chinese Medicine, 11 Third Ring Road, Chaoyang District, Beijing 100029, China*
[3] *Department of Biological Science, Lehman College, and Graduate Center, City University of New York, 250 Bedford Park Boulevard West, Bronx, NY 10468, USA*
[4] *Kunming Institute of Botany, Chinese Academy of Sciences, 132 Lanhei Road, Kunming 650201, China*

Correspondence should be addressed to Chunlin Long; long@mail.kib.ac.cn

Received 2 April 2014; Accepted 30 April 2014; Published 19 May 2014

Academic Editor: Shi-Biao Wu

Elephantopus scaber is an ethnomedicinal plant used by the Zhuang people in Southwest China to treat headaches, colds, diarrhea, hepatitis, and bronchitis. A new δ-truxinate derivative, ethyl, methyl 3,4,3′,4′-tetrahydroxy-δ-truxinate (**1**), was isolated from the ethyl acetate extract of the entire plant, along with 4 known compounds. The antioxidant activity of these 5 compounds was determined by ABTS radical scavenging assay. Compound **1** was also tested for its cytotoxicity effect against HepG2 by MTT assay (IC_{50} = 60 μM), and its potential anti-inflammatory, antibiotic, and antitumor bioactivities were predicted using target fishing method software.

1. Introduction

Elephantopus is a genus comprised of about 30 species worldwide, mainly distributed in South America, with only 2 species *E. scaber* and *E. tomentosus* found in Southwest China [1]. From 2008 to 2012, our ethnobotanical investigation in the traditional medicinal market, held during the Dragon-Boat Festival in the fifth month of the Chinese lunar calendar with a history of over 700 years, found that *Elephantopus scaber* L. (Asteraceae) is a common medicinal plant used by the Zhuang people in Jingxi County of Southwest China. The local Zhuang people use *E. scaber* commonly as a traditional herbal medicine to treat many ailments including headaches, colds, diarrhea, hepatitis, and bronchitis.

To date, 30 compounds have been reported from *E. scaber*, including 4 sesquiterpene lactones, 9 triterpenes, and 5 flavones. Previous bioactivity studies on *E. scaber* demonstrated that the extracts or compounds from this species have antibiosis, antivirus, and cytotoxicity activities [2]. The sesquiterpene lactones in particular have been explored for their anti-inflammatory and hepatoprotective activities [3], which partially proved the traditional knowledge of *E. scaber*.

In this paper, the isolation and structure elucidation of a new ethyl, methyl 3,4,3′,4′-tetrahydroxy-δ-truxinate (**1**, Figure 1) is reported, together with 4 known compounds, 5-*O*-caffeoylquinic acid (**2**) [4], chlorogenic acid methyl ester (**3**) [5], deoxyelephantopin (**4**), and isoscarbertopin (**5**) [6]. The radical scavenging activity of these 5 compounds was conducted using the ABTS method. The cytotoxicity effect against HpeG2 cell line of the new compound was determined by MTT assay, and the IC_{50} value (24.0 μg/mL) was obtained. In addition, the potential activity of **1**, calculated with target fishing, which used 3D structures of compounds to identify their interacting proteins by virtual screening [7], is also presented.

2. Materials and Method

2.1. Plant Material. The whole plant of *E. scaber* was collected from the traditional medicinal market during the

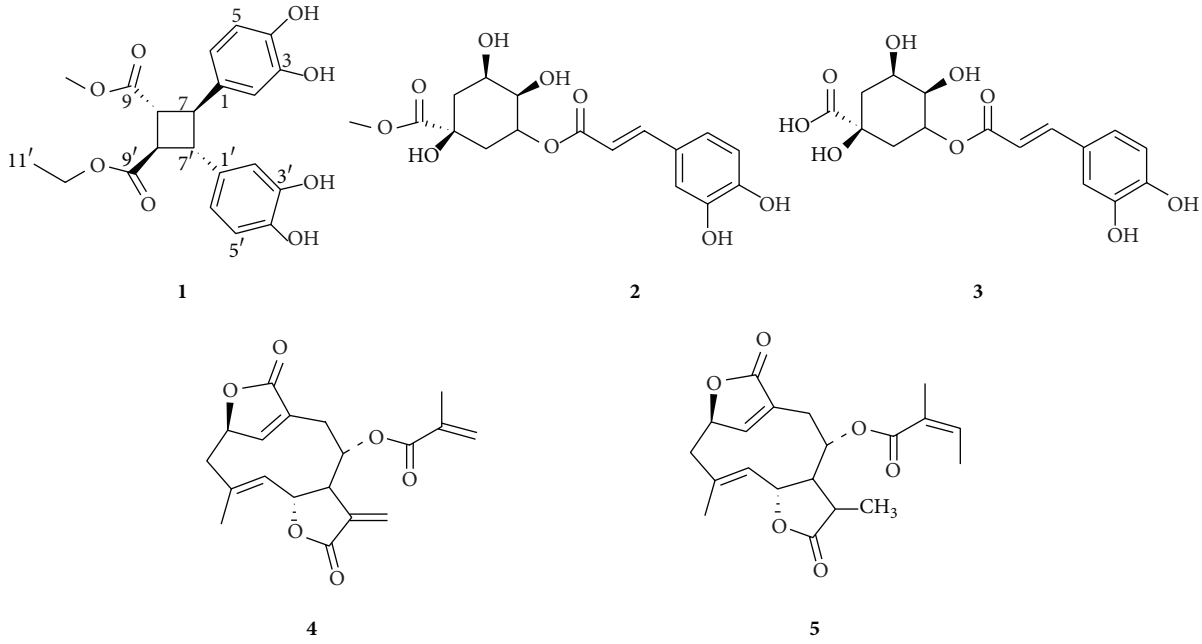

Figure 1: The chemical structures of compounds obtained from *Elephantopus scaber*.

Dragon-Boat Festival of Jingxi County (Guangxi), Southwest China, and identified by Professor Chunlin Long. A voucher specimen was deposited in the Herbarium of Minzu University of China, numbered 201006023.

2.2. Extraction and Isolation. The air-dried and ground whole plant of *E. scaber* (4.0 kg) was extracted with EtOH : H_2O (90 : 10) at reflux for 3 × 3 h. The solvent was evaporated under reduced pressure to yield dark brown material (372.4 g). The latter was suspended in H_2O (3 L) and individually partitioned with petroleum ether (3 × 3 L), Chloroform (2 × 3 L), EtOAc (3 × 3 L), and *n*-BuOH (3 × 3 L) to obtain petroleum ether (169.4 g), Chloroform (33.8 g), EtOAc (46.9 g), and *n*-BuOH (122.3 g) phase.

The EtOAc phase was separated by silica gel column chromatography (CC) eluted with $CHCl_3$: CH_3OH in order of increasing polarity to give seven fractions on the basis of TLC. Fraction 3 was subjected to MCI CC eluted with CH_3OH : H_2O to seven fractions A_1–A_7. Fraction A_1 was isolated by Sephadex LH-20, ODS CC (CH_3OH : H_2O = 44 : 56), and Si gel CC ($CHCl_3$: CH_3OH = 14 : 1) successively to afford compound **1** (24.0 mg). Fraction A_2 was purified with Sephadex LH-20 to give six subfractions. Subfraction 2 was subjected to ODS CC (CH_3OH : H_2O = 30 : 70) and silica gel CC ($CHCl_3$: CH_3OH = 12 : 1) successively to give compound **3** (17.0 mg). Subfraction 3 was subjected to ODS CC (CH_3OH : H_2O = 48 : 52) and Sephadex LH-20 to afford compound **2** (27.0 mg).

The petroleum ether phase was separated by silica gel CC eluted with petroleum ether : EtOAc (100 : 1–0 : 100) to give ten fractions. Fraction 8 was purified by MCI CC using CH_3OH : H_2O (60 : 100–100 : 0) to afford four fractions B_1–B_4. Fraction B_2 was subjected to Sephadex LH-20 and ODS CC (CH_3OH : H_2O = 83 : 17) to give compound **4** (9.0 mg). Fraction B_3 was isolated by ODS CC (CH_3OH : H_2O = 80 : 20) and Sephadex LH-20 to give compound **5** (7.0 mg).

2.3. Antioxidant Assay. The antioxidant activity of compounds **1**–**5** was evaluated with ABTS radical scavenging assay as described previously [8]. The IC_{50} was expressed as millimoles per liter (mM).

2.4. Cytotoxicity Assay. Compound **1** was tested for cytotoxicity using a slightly modified MTT method [9]. Briefly 150 μL (10 μM, 20 μM, 30 μM, and 40 μM) of samples was added to 96-well plate containing a confluent HepG2 cell monolayer in sextuplicate; 10 μg/mL of norcantharidin (NCTD) and blank medium were used as the positive and control group, respectively. After a 72 h incubation at 37°C, 100 μL MTT solution (5 mg/mL phosphate buffered saline) was added to each well, which was further incubated for 4 h for the formation of the formazan product. After removing the medium, 150 μL DMSO was added to dissolve the formazan crystals. The optical density (OD) was measured at 550 nm with a microplate reader. The rate of inhibition was calculated by the following formula: rate of inhibition = (1 − sample OD)/control OD. The concentration causing inhibition of viable cells by 50% (IC_{50}) was determined from a dose-response curve, which was based on triplicate measurements.

2.5. Virtual Screening. The potential activity of compound **1** was predicted by the "Target Fishing" functional model software (Discovery Studio). The target fishing process was conducted as follows. The DockScore energy function was utilized to minimize the energy of compound **1** conformation. Setting full minimization as minimization gave the smart conformation of compound **1**. Then, pharmacophore search

was set to be screened and profiled. Screen and profile was set to be ligand profiler. PharmaDB pharmacophores were set to be all. Conformation generation was set to be the best. Maximum conformation was set to be 200. Energy threshold was set to be 10. Saved conformations were set to be true, and other parameters were set to be default.

Top 14 candidate receptors were ranked according to the fit value (as shown in Table 2), which is based on force field approximation and specifically examined the compound internal energy and the compound-receptor interaction energy, which is taken as the sum of van der Waal force and electrostatic energy [10].

2.6. Ethyl, Methyl 3,4,3′,4′-tetrahydroxy-δ-truxinate. Light yellow oil; $[\alpha]_D$ −2.0° (*c* 0.018, MeOH); UV (in MeOH): λ_{max} 284 and 228 nm; IR ν_{max} ATR (cm^{-1}): 3436, 2924, 2854, 1736, and 1600–1450; HRESIMS (*m/z*): 403.1286 $[M+H]^+$; ^1H NMR (300 MHz, CD_3OD): δ_H 6.73 (4H, d-like), 6.62 (1H, t, *J* = 6.0, 3.0 Hz), 6.59 (1H, t, *J* = 6.0, 3.0 Hz), 4.19 (2H, q, *J* = 7.1 Hz), 3.73 (3H, s), 3.43 (1H, d-like, *J* = 2.9 Hz), 3.40 (1H, d-like, *J* = 2.5 Hz), 3.30 (1H, d-like, *J* = 3.1 Hz), 3.27 (1H, d-like, *J* = 3.5 Hz), and 1.26 (3H, t, *J* = 14.2, 7.1 Hz). ^{13}C NMR (75 MHz, CD_3OD): δ_C 173.5, 173.0, 145.0, 144.1, 132.8, 117.6, 115.0, 113.5, 60.7, 51.2, 50.2, 50.0, 46.2, 45.8, and 13.2.

3. Results

Compound **1** (28.0 mg) was separated from the ethyl acetate extract of *E. scaber* whole plant as a light yellow oil. The molecular formula $C_{21}H_{22}O_8$ was determined by the molecular ion observed at *m/z* 403.1359 $[M+H]^+$ in the LC-TOF-MS (positive mode), which requires 11 degrees of unsaturation. The IR spectrum presented bands in the 1600–1450 cm^{-1}, 1736 cm^{-1}, 2854 cm^{-1}, 2924 cm^{-1}, and 3436 cm^{-1} region, which corresponded to aromatic, ester, methyl or methylene, and phenolic hydroxyl groups, respectively. The structure of compound **1** was further elucidated by examination of its 1D ^{13}C (75 MHz), DEPT (90° and 135°), and ^1H (300 MHz) NMR spectra and HMQC, HMBC, COSY, and NOESY spectra in MeOH-d_4. Only 13 carbon resonance signals and the other two carbon signals overlapped by the solvent carbon signals were found in ^{13}C NMR and DEPT spectra, respectively, which suggested that there are many identical parts in this molecule. Further analysis of the ^{13}C NMR spectrum of compound **1** suggested each signal of δ_C 145.0, 144.1, 132.8, 117.6, 115.0, and 113.5 is comprised of two overlapping carbon signals [δ_C 145.0 (C-3 and C-3′), 144.1 (C-4 and C-4′), 132.8 (C-1 and C-1′), 117.6 (C-6 and C-6′), 115.0 (C-5 and C-5′), and 113.5 (C-2 and C-2′)]; the other signals were assigned to two carbonyl carbon atoms [δ 173.5 (C-9) and 173.0 (C-9′)], one methoxy group (δ_C 60.7, C-10), one submethoxy (δ_C 51.2, C-10′), methyl (δ_C 13.2, C-11′), and four methine carbons [δ_C 50.2 (C-7′), 50.0 (C-7), 46.2 (C-8′), and 45.8 (C-8)]. From the number of unsaturations and carbons, these four methane carbons were deduced to be cyclobutane ring. From the analysis of ^1H NMR spectrum of compound **1**, two phenylpropanoid units were presented at δ_H 6.73 (4H, d-like, H-2, H-5, H-2′, H-5′), δ_H 6.62 (1H, t, *J* = 6.0, 3.0 Hz, H-6/H-6′), and 6.59 (1H, t, *J* = 6.0, 3.0 Hz, H-6′/H-6). Four methane carbons of the cyclobutane ring were observed at δ_H 3.43 (1H, d-like, *J* = 2.9 Hz, H-7), 3.40 (1H, d-like, *J* = 2.5 Hz, H-7′), 3.30 (1H, d-like, *J* = 3.1 Hz, H-8′), and 3.27 (1H, d-like, *J* = 3.5 Hz, H-8), and the relative configuration of the cyclobutane ring was determined by comparing the chemical shift of compound **1** with reported ^1H NMR data of other δ-truxinate derivatives [11]. Other signals of ^1H NMR spectra were assigned to submethoxy [δ_H 4.19 (2H, q, *J* = 7.1 Hz, H-10′)], methoxy [δ_H 3.73 (3H, s, H-10)], and methyl [δ_H 1.26 (3H, t, *J* = 14.2, 7.1 Hz, H-11′)]. Meanwhile, the HMBC spectrum of compound **1** presented the correlations from H-10 to C-9, H-8 to C-9 and C-8′, H-7 to C-2 and C-6, H-11′ to C-10′, from C-10′ to H-9′ and H-11′, from C-8′ to C-9′, and from C-7′ to H-2′ and H-6′, respectively (Figure 2). Consequently, the structure of compound **1** was deduced to be ethyl, methyl 3,4,3′,4′-tetrahydroxy-δ-truxinate, which was further confirmed by HMQC, COSY, and NOESY spectra. This paper reports a new δ-truxinate derivative in *Elephantopus* genus for the first time. Compounds **2**–**5** were identified, respectively, as 5-*O*-caffeoylquinic acid (**2**), chlorogenic acid methyl ester (**3**), deoxyelephantopin (**4**), and isoscarbertopin (**5**) by comparing their NMR and MS data with reported literature values.

Table 1: The radical scavenging activity of 5 compounds from *Elephantopus scaber*.

Compound	Name	IC_{50} (mM)[a]
1	Ethyl, methyl 3, 4, 3′, 4′-tetrahydroxy-δ-truxinate	0.44 ± 0.039
2	5-*O*-caffeoylquinic acid	0.96 ± 0.096
3	Chlorogenic acid methyl ester	0.89 ± 0.140
4	Deoxyelephantopin	NR
5	Isoscarbertopin	NR
6[b]	Trolox	1.33 ± 0.187

[a]The inhibition was recorded at 10 min of reaction (ABTS method) and IC_{50} value was measured using PROBIT model: PROBIT (*p*) = intercept + *BX* (covariates *X* are transformed using the base 10.000 logarithm). Each value corresponds to the mean and standard deviation of duplicates at five concentrations.
[b]Positive control group.
NR: No reaction at the conditions discribed.

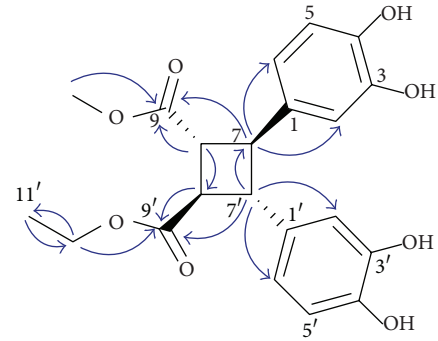

Figure 2: Selected HMBC (proton to carbon) correlations of compound **1**.

The antioxidant activity of 5 compounds isolated from *E. scaber* was evaluated by the ABTS radical scavenging assay, and the results are presented as IC_{50} in Table 1.

Table 2: The potential bioactivity screening results of compound **1**.

Pharmacophore	Name of pharmacophore	Type	Fit value	Biological function(s)	Reference
2zb8-01-s	Prostaglandin reductase 2	Protein	4.05271	Inflammation	[14]
3kjs-01	Dihydrofolate reductase-thymidylate synthase	Protein	3.9615	Malarial parasites, anticancer, and inflammation	[15–17]
2uue-01	Cell division protein kinase 2	Protein	3.60758	Cell division	[18, 19]
2w4i-01-s	Glutamate racemase	Protein	3.55547	Antibiotics	[20–24]
3k6l-01	Peptide deformylase	Protein	3.51102	Antibiotic	[25, 26]
3md7-01	*beta*-lactamase-like	Protein	3.41887	Antibiotic	[27, 28]
2ovy-01	Phosphodiesterase 10A	Protein	3.41834	Schizophrenia and nervous system	[29–31]
3ac8-01	Protooncogene tyrosine-protein kinase LCK	Protein	3.39142	Antitumor	[32, 33]
3f7z-01	G17 glycogen synthase kinase-3-*beta*	Protein	3.30076	Antitumor and neurodegenerative disease	[34]
3cgy-01	Virulence sensor histidine kinase phoQ	Protein	3.28695	Antibiotic	[35, 36]
2qe5-01	RNA-directed RNA polymerase	Protein	3.28198	Antivirus	[37, 38]
1dvx-01	Transthyretin	Protein	3.27421	Antitumor and obesity	[39, 40]
2brc-01	ATP-dependent molecular chaperone HSP90	Protein	3.26648	Antitumor and antivirus	[41, 42]
1c1b-01-s	HIV-1 reverse transcriptase (A-chain)	Protein	3.25549	Anti-HIV	[43–45]

The most active radical scavengers were the new compound ethyl, methyl 3,4,3′,4′-tetrahydroxy-δ-truxinate (IC_{50} = 0.44 ± 0.039 mM). The other 2 quinic acid derivatives 5-*O*-caffeoylquinic acid and chlorogenic acid methyl ester also showed radical scavenging potential (IC_{50} = 0.96 ± 0.096 and 0.89 ± 0.140 mM, resp.), while the antioxidant activity of the other 2 sesquiterpene lactone compounds deoxyelephantopin and isoscabertopin was not detected. Comparing the structures of these 5 compounds, the different antioxidant activities were attributed to the existence of phenolic hydroxyl groups in compounds, which were supported by the previous reports [12].

Compound **1** was also tested for *in vitro* cytotoxicity against HepG2 cell line with norcantharidin (NCTD, 60 μM) as positive control at 72 h incubation (Figure 3). Compound **1** exhibited a dose-response inhibition curve from 27% growth inhibition at 10 μg/mL to 81% at 40 μg/mL, demonstrating that it has significant and dose-dependent inhibition on the growth of HepG2 (IC_{50} = 60 μM). Further work will be conducted on the mechanism by which compound **1** induces apoptosis.

With the rapid development of computer-aided drug design (CADD), virtual screening technique has been used more and more widely in drug design and bioactivity screening of compounds [13]. The potential bioactivities of compound **1** have been predicted by the target fishing method which was based on the Discovery Studio software and Protein Date Bank (PDB) including over twelve thousand 3D macromolecular structure data determined experimentally by X-ray crystallography and NMR. The top 14 biological molecular targets ranked as the fit value (FV) are reported (Table 2).

Theoretically, FV > 3 means this target should be explored experimentally. The strongest activity of compound **1** was predicted to be anti-inflammatory (FV = 4.05271) and anti-AIDS (FV = 3.25549), respectively (Table 2). Further experiments on the biological functions of **1** should be directed towards its potential anti-inflammatory, antibiotic, antivirus, and anticancer activities.

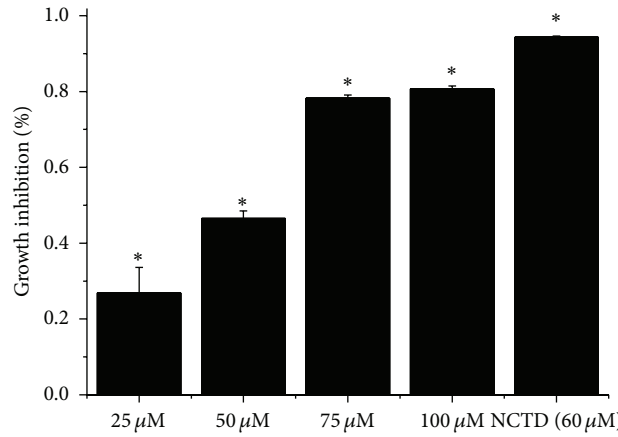

Figure 3: Growth inhibition of compound **1** on HepG2 cell lines, where each value represents mean ± standard deviation of 6 replicates (n = 6), as compared to the positive control norcantharidin (60 μM) ($^*P < 0.001$ for comparison of control cell with cells treated with compound **1** and NCTD); 72 h for the incubation period of cells after being treated with compound **1** and NCTD.

4. Discussion and Conclusion

With more and more present modern drugs discovered from traditional medical knowledge, the traditional knowledge is getting more extensive attention, which also led to the development of important drugs such as reserpine (a treatment for hypertension) podophyllotoxin (the base of an important anticancer drug), and vinblastine (used in the treatment of certain cancers) [46].

Previous studies showed that pulmonary oxidant stress can cause some disease conditions, such as acute lung injury,

radiation injury, COPD (chronic obstructive pulmonary disease), and inflammation [47]. Meanwhile, previous clinical and experimental studies described that antioxidant supplementation including flavonoids and vitamins may inverse the oxidant-mediated cough depression by modulating the inflammatory process in lung disease [48, 49]. Interestingly, our work using ABTS assay demonstrated that compounds **1**–**3** showed strong antioxidant activity, especially compound **1** (IC_{50} = 0.44 ± 0.039 mM). Moreover, *E. scaber* was also reported as the source of a number of sesquiterpene lactones, such as compounds **4** and **5**, which have shown significant contribution to the anti-inflammatory activity of plants [50]. Some of the sesquiterpenes from the genus *Elephantopus* have demonstrated significant anti-inflammatory as well as hepatoprotective activities and are being considered as drug lead compounds [3]. Based on the above analysis, we hypothesize that Zhuang people use this plant to treat headaches, bronchitis, and hepatitis,due to its anti-inflammatory and antioxidant effects.

According to the *in vitro* cytotoxicity assay with NCTD (60 μM) as control group and activity virtual screening, compound **1** exhibited good (IC_{50} = 60 μM) and dose-response inhibition on HepG2 cell line and potential anti-inflammatory, antibiotic, antivirus, and anticancer activities, which indicated that the further research of *E. scaber* could be focused on anticancer and anti-inflammatory activity. The present work further developed the usage of this traditional medicine plant.

Conflict of Interests

The authors declare that there is no conflict of interests regarding the publication of this paper.

Acknowledgments

The authors thank Vanya Petrova (City University of New York) for assistance with the antioxidant assay and Weiguo Liu (Minzu University of China) for assistance with using the Discovery Studio software. This work was supported in part by the National Natural Science Foundation of China (31161140345 and 31070288), the Ministry of Science & Technology of China (2012FY110300), the Ministry of Education of China through its 111 and 985 Projects (B08044, MUC985-9, and MUC98506-01000101), and JSPS Asian Core program (JSPS/AP/109080).

References

[1] Z. Y. Wu and P. Raven, *Flora of China*, vol. 20-21 of *Asteraceae*, Science Press, Beijing, China; Missouri Botanical Garden, St. Louis, Mo, USA, 2007.

[2] J. J. Wang, Y. J. Liu, J. X. Xu, A. Wang, Y. L. Wang, and C. L. Long, "Studies on medicinal plants of *Elephantopus* (Compositae)," *Natural Products Research and Development*, vol. 25, pp. 401–409, 2013.

[3] C. C. Huang, K. J. Lin, Y. W. Cheng, C. A. Hsu, S. S. Yang, and L. F. Shyur, "Hepatoprotective effect and mechanistic insights of deoxyelephantopin, a phyto-sesquiterpene lactone, against fulminant hepatitis," *Journal of Nutritional Biochemistry*, vol. 24, no. 3, pp. 516–530, 2013.

[4] K. Schütz, D. Kammerer, R. Carle, and A. Schieber, "Identification and quantification of caffeoylquinic acids and flavonoids from artichoke (*Cynara scolymus* L.) heads, juice, and pomace by HPLC-DAD-ESI/MSn," *Journal of Agricultural and Food Chemistry*, vol. 52, no. 13, pp. 4090–4096, 2004.

[5] X. Zhu, X. Dong, Y. Wang, P. Ju, and S. Luo, "Phenolic compounds from *Viburnum cylindricum*," *Helvetica Chimica Acta*, vol. 88, no. 2, pp. 339–342, 2005.

[6] Q. L. Liang and Z. D. Min, "Sesquiterpene lactones from *Elephantopus scaber*," *Chinese Chemical Letters*, vol. 13, no. 4, pp. 343–344, 2002.

[7] L. R. Wang and X. Q. Xie, "Computational target fishing: what should chemogenomics researchers expect for the future of *in silico* drug design and discovery?" *Future Medicinal Chemistry*, vol. 6, no. 3, pp. 247–249, 2014.

[8] S. B. Wu, K. Dastmalchhi, C. L. Long, and E. J. Kennelly, "Metabolite profiling of jaboticaba (*Myrciaria cauliflora*) and other dark-colored fruit juices," *Journal of Agriculture and Food Chemistry*, vol. 60, no. 30, pp. 7513–7525, 2012.

[9] A. L. Liu, H. D. Wang, S. M. Lee, Y. T. Wang, and G. H. Du, "Structure-activity relationship of flavonoids as influenza virus neuraminidase inhibitors and their in vitro anti-viral activities," *Bioorganic and Medicinal Chemistry*, vol. 16, no. 15, pp. 7141–7147, 2008.

[10] C. Y. C. Chen, "Virtual screening and drug design for PDE-5 receptor from traditional Chinese medicine database," *Journal of Biomolecular Structure and Dynamics*, vol. 27, no. 5, pp. 627–640, 2010.

[11] Y. Deng, Y. W. Chin, H. B. Chai et al., "Phytochemical and bioactivity studies on constituents of the leaves of *Vitex quinata*," *Phytochemistry Letters*, vol. 4, no. 3, pp. 213–217, 2011.

[12] D. Huang, O. U. Boxin, and R. L. Prior, "The chemistry behind antioxidant capacity assays," *Journal of Agricultural and Food Chemistry*, vol. 53, no. 6, pp. 1841–1856, 2005.

[13] J. H. Nettles, J. L. Jenkins, A. Bender, Z. Deng, J. W. Davies, and M. Glick, "Bridging chemical and biological space: "target fishing" using 2D and 3D molecular descriptors," *Journal of Medicinal Chemistry*, vol. 49, no. 23, pp. 6802–6810, 2006.

[14] I. Inoue, S. I. Goto, K. Mizotani et al., "Lipophilic HMG-CoA reductase inhibitor has an anti-inflammatory effect: reduction of MRNA levels for interleukin-1β, interleukin-6, cyclooxygenase-2, and p22phox by regulation of peroxisome proliferator-activated receptor α (PPARα) in primary endothelial cells," *Life Sciences*, vol. 67, no. 8, pp. 863–876, 2000.

[15] B. I. Schweitzer, A. P. Dicker, and J. R. Bertino, "Dihydrofolate reductase as a therapeutic target," *The FASEB Journal*, vol. 4, no. 8, pp. 2441–2452, 1990.

[16] L. Jiang, P. C. Lee, J. White, and P. K. Rathod, "Potent and selective activity of a combination of thymidine and 1843U89, a folate-based thymidylate synthase inhibitor, against *Plasmodium falciparum*," *Antimicrobial Agents and Chemotherapy*, vol. 44, no. 4, pp. 1047–1050, 2000.

[17] N. Sienkiewicz, S. Jarosławski, S. Wyllie, and A. H. Fairlamb, "Chemical and genetic validation of dihydrofolate reductase-thymidylate synthase as a drug target in African trypanosomes," *Molecular Microbiology*, vol. 69, no. 2, pp. 520–533, 2008.

[18] L. A. Pinna and F. Meggio, "Protein kinase CK2 ("casein kinase-2") and its implication in cell division and proliferation," *Progress in Cell Cycle Research*, vol. 3, pp. 77–97, 1997.

[19] S. Ortega, I. Prieto, J. Odajima et al., "Cyclin-dependent kinase 2 is essential for meiosis but not for mitotic cell division in mice," *Nature Genetics*, vol. 35, no. 1, pp. 25–31, 2003.

[20] M. Ashiuchi, K. Tani, K. Soda, and H. Misono, "Properties of glutamate racemase from *Bacillus subtilis* IFO 3336 producing poly-γ-glutamate," *Journal of Biochemistry*, vol. 123, no. 6, pp. 1156–1163, 1998.

[21] K. Y. Hwang, C. S. Cho, S. S. Kim, H. C. Sung, Y. G. Yu, and Y. Cho, "Structure and mechanism of glutamate racemase from *Aquifex pyrophilus*," *Nature Structural Biology*, vol. 6, no. 5, pp. 422–426, 1999.

[22] A. de Dios, L. Prieto, J. A. Martín et al., "4-substituted D-glutamic acid analogues: the first potent inhibitors of glutamate racemase (MurI) enzyme with antibacterial activity," *Journal of Medicinal Chemistry*, vol. 45, no. 20, pp. 4559–4570, 2002.

[23] G. S. Basarab, P. J. Hill, A. Rastagar, and P. J. H. Webborn, "Design of *Helicobacter pylori* glutamate racemase inhibitors as selective antibacterial agents: a novel pro-drug approach to increase exposure," *Bioorganic and Medicinal Chemistry Letters*, vol. 18, no. 16, pp. 4716–4722, 2008.

[24] B. Geng, G. Basarab, J. Comita-Prevoir et al., "Potent and selective inhibitors of *Helicobacter pylori* glutamate racemase (MurI): pyridodiazepine amines," *Bioorganic and Medicinal Chemistry Letters*, vol. 19, no. 3, pp. 930–936, 2009.

[25] C. M. Apfel, H. Locher, S. Evers et al., "Peptide deformylase as an antibacterial drug target: target validation and resistance development," *Antimicrobial Agents and Chemotherapy*, vol. 45, no. 4, pp. 1058–1064, 2001.

[26] J. A. Leeds and C. R. Dean, "Peptide deformylase as an antibacterial target: a critical assessment," *Current Opinion in Pharmacology*, vol. 6, no. 5, pp. 445–452, 2006.

[27] S. Kumar, U. Narain, S. Tripathi, and K. Misra, "Syntheses of curcumin bioconjugates and study of their antibacterial activities against β-lactamase-producing microorganisms," *Bioconjugate Chemistry*, vol. 12, no. 4, pp. 464–469, 2001.

[28] Q. Li, J. Y. Lee, R. Castillo et al., "NB2001, a novel antibacterial agent with broad-spectrum activity and enhanced potency against β-lactamase-producing strains," *Antimicrobial Agents and Chemotherapy*, vol. 46, no. 5, pp. 1262–1268, 2002.

[29] T. M. Coskran, D. Morton, F. S. Menniti et al., "Immunohistochemical localization of phosphodiesterase 10A in multiple mammalian species," *Journal of Histochemistry and Cytochemistry*, vol. 54, no. 11, pp. 1205–1213, 2006.

[30] F. S. Menniti, T. A. Chappie, J. M. Humphrey, and C. J. Schmidt, "Phosphodiesterase 10A inhibitors: a novel approach to the treatment of the symptoms of schizophrenia," *Current Opinion in Investigational Drugs*, vol. 8, no. 1, pp. 54–59, 2007.

[31] C. J. Schmidt, D. S. Chapin, J. Cianfrogna et al., "Preclinical characterization of selective phosphodiesterase 10A inhibitors: a new therapeutic approach to the treatment of schizophrenia," *The Journal of Pharmacology and Experimental Therapeutics*, vol. 325, no. 2, pp. 681–690, 2008.

[32] J. B. Bolen, R. B. Rowley, C. Spana, and A. Y. Tsygankov, "The Src family of tyrosine protein kinases in hemopoietic signal transduction," *The FASEB Journal*, vol. 6, no. 15, pp. 3403–3409, 1992.

[33] E. Buchdunger, J. Zimmermann, H. Mett et al., "Inhibition of the Abl protein-tyrosine kinase *in vitro* and *in vivo* by a 2-phenylaminopyrimidine derivative," *Cancer Research*, vol. 56, pp. 100–104, 1996.

[34] P. Mishra, S. Senthivinayagam, A. Rana, and B. Rana, "Glycogen synthase kinase-3β regulates snail and β-catenin during gastrin-induced migration of gastric cancer cells," *Journal of Molecular Signaling*, vol. 5, article 9, 2010.

[35] D. Beier and R. Gross, "Regulation of bacterial virulence by two-component systems," *Current Opinion in Microbiology*, vol. 9, no. 2, pp. 143–152, 2006.

[36] W. J. Gooderham, S. L. Gellatly, F. Sanschagrin et al., "The sensor kinase PhoQ mediates virulence in *Pseudomonas aeruginosa*," *Microbiology*, vol. 155, no. 3, pp. 699–711, 2009.

[37] T. Dalmay, A. Hamilton, S. Rudd, S. Angell, and D. C. Baulcombe, "An RNA-dependent RNA polymerase gene in *Arabidopsis* is required for posttranscriptional gene silencing mediated by a transgene but not by a virus," *Cell*, vol. 101, no. 5, pp. 543–553, 2000.

[38] F. Simmer, M. Tijsterman, S. Parrish et al., "Loss of the putative RNA-directed RNA polymerase RRF-3 makes *C. elegans* hypersensitive to RNAi," *Current Biology*, vol. 12, no. 15, pp. 1317–1319, 2002.

[39] L. H. Wu and C. T. Woodbridge, "Regulation of transthyretin to treat obesity," Patent Application publication 0160394 A1, 2002.

[40] S. K. Frey, J. Spranger, A. Henze, A. F. H. Pfeiffer, F. J. Schweigert, and J. Raila, "Factors that influence retinol-binding protein 4-transthyretin interaction are not altered in overweight subjects and overweight subjects with type 2 diabetes mellitus," *Metabolism: Clinical and Experimental*, vol. 58, no. 10, pp. 1386–1392, 2009.

[41] J. Hu and C. Seeger, "Hsp90 is required for the activity of a hepatitis B virus reverse transcriptase," *Proceedings of the National Academy of Sciences of the United States of America*, vol. 93, no. 3, pp. 1060–1064, 1996.

[42] J. R. Sydor, E. Normant, C. S. Pien et al., "Development of 17-allylamino-17-demethoxygeldanamycin hydroquinone hydrochloride (IPI-504), an anti-cancer agent directed against Hsp90," *Proceedings of the National Academy of Sciences of the United States of America*, vol. 103, no. 46, pp. 17408–17413, 2006.

[43] C. Tantillo, J. Ding, A. Jacobo-Molina et al., "Locations of anti-AIDS drug binding sites and resistance mutations in the three-dimensional structure of HIV-1 reverse transcriptase. Implications for mechanisms of drug inhibition and resistance," *Journal of Molecular Biology*, vol. 243, no. 3, pp. 369–387, 1994.

[44] S. G. Sarafianos, B. Marchand, K. Das et al., "Structure and function of HIV-1 reverse transcriptase: molecular mechanisms of polymerization and inhibition," *Journal of Molecular Biology*, vol. 385, no. 3, pp. 693–713, 2009.

[45] K. M. Frey, M. Bollini, A. C. Mislak et al., "Crystal structures of HIV-1 reverse transcriptase with picomolar inhibitors reveal key interactions for drug design," *Journal of the American Chemical Society*, vol. 134, no. 48, pp. 19501–19503, 2012.

[46] M. Idu, "Current trends in ethnobotany," *Tropical Journal of Pharmaceutical Research*, vol. 8, no. 4, pp. 295–296, 2009.

[47] M. Christofidou-Solomidou and V. R. Muzykantov, "Antioxidant strategies in respiratory medicine," *Treatments in Respiratory Medicine*, vol. 5, no. 1, pp. 47–78, 2006.

[48] M. Brozmanova, J. Plevkova, V. Bartos, L. Plank, M. Javorka, and M. Tatar, "The interaction of dietary antioxidant vitamins and oxidative stress on cough reflex in guinea-pigs after long term oxygen therapy," *Journal of Physiology and Pharmacology*, vol. 57, supplement 4, pp. 45–54, 2006.

[49] M. Brozmanova, V. Bartos, L. Plank, J. Plevkova, and M. Tatar, "Dietary intake of flavonoids and hyperoxia-induced oxidative stress related cough in guinea pigs," *Bratislava Medical Journal*, vol. 108, no. 12, pp. 489–494, 2007.

[50] M. Chadwick, H. Trewin, F. Gawthrop, and C. Wagstaff, "Sesquiterpenoids lactones: benefits to plants and people," *International Journal of Molecular Sciences*, vol. 14, no. 6, pp. 12780–12805, 2013.

Hindawi Publishing Corporation
Evidence-Based Complementary and Alternative Medicine
Volume 2014, Article ID 494528, 11 pages
http://dx.doi.org/10.1155/2014/494528

Research Article

Action Mechanism of Fuzheng Fangai Pill Combined with Cyclophosphamide on Tumor Metastasis and Growth

Sheng Liu, Xiao-min Wang, and Guo-wang Yang

Oncology Department of Beijing Hospital of Traditional Chinese Medicine (TCM) affiliated to Capital Medical University, Beijing 100010, China

Correspondence should be addressed to Sheng Liu; liusheng4377@163.com and Xiao-min Wang; ntxm100@sina.com

Received 28 December 2013; Revised 11 March 2014; Accepted 28 March 2014; Published 8 May 2014

Academic Editor: Shi-Biao Wu

Fuzheng Fangai pill (FZFA), a traditional Chinese formula, is widely used for cancer treatment. Compared with other anticancer drugs, it is characterized by moderate and persistent efficacy with few side effects. The present paper emphasizes antitumor effect of FZFA combined with cyclophosphamide (CTX) on C57BL/6 mice subcutaneously injected with Lewis lung cancer cells, Comparing it with that of CTX. On the 21st day, a set of biochemical parameters were studied: the tumor weight and tumor volume, the inhibition rate of lung metastasis, the percentage and ratio of spleen $CD4^+IL\text{-}17^+$ Th17 (T helper cell 17, Th17 for short) and $CD4^+CD25^+Foxp3^+$Treg (T regulatory cell, Treg for short) cells, and the concentrations of IL-6, TGF-β, IL-17, IL-23, and IFN-γ in culture supernatants of $CD4^+$ T lymphocytes were determined. The expression of the splenic Foxp3 and RORγt mRNA and JAK2, STAT3, and SOCS3 protein as also determined. The results show that compared with the model control group and CTX group, FZFA+CTX restored the ratio of spleen $CD4^+IL\text{-}17^+$ Th17 and $CD4^+CD25^+Foxp3^+$ Treg cells, and inhibited the inflammatory response including the nuclear SOCS3/JAK-STAT pathway, regulation of interleukins TGF-β, IL-6, IL-17, IL-23, and IFN-γ, and Foxp3 and RORγt gene expression in $CD4^+$ T lymphocytes. We conclude that FZFA + CTX strongly reduced the growth and metastasis rate of Lewis lung cancer through inhibition of SOCS/JAK-STAT pathway and inflammatory cytokine responses. FZFA + CTX had greater activity than CTX alone.

1. Introduction

Tumor metastasis is closely related to the immune state of the human body [1]. During implementation of the National Natural Science Foundation of China project, we observed the effect of Fuzheng Fangai pill (FZFA) combined with cyclophosphamide (CTX) on the metastasis of several tumor types. Our results showed that FZFA with cyclophosphamide inhibited lung cancer growth and metastasis through a mechanism that involved decreased expression of $CD4^+CD25^+Foxp3^+$ regulatory T cells (Tregs) and inhibition of the expression of transcription factors and cytokines associated with these cells. In addition, recent research has shown that the expression and function of $CD4^+CD25^+Foxp3^+$Tregs and $CD4^+IL\text{-}17^+$ T helper 17 cells (Th17) are closely related. Therefore, we hypothesized that $CD4^+IL\text{-}17^+$ Th17 cells might be a key link between $CD4^+CD25^+Foxp3^+$Tregs and tumor growth and metastasis. This implicates regulation of the balance between $CD4^+CD25^+Foxp3^+$ Treg and $CD4^+IL\text{-}17^+$ Th17 as a new strategy to reverse tumor progression.

The balance between $CD4^+CD25^+Foxp3^+$Treg and $CD4^+IL\text{-}17^+$ Th17 cells plays an important role in the process of growth and metastasis. Both cell types are derived from the initial $CD4^+$ T cell population and the differentiated cells perform opposing functions to maintain homeostasis for steady state immune function in the body [2, 3]. TGF-β and IL-6 are important factors in the initial differentiation of $CD4^+$ T cells. TGF-β and IL-6 induce differentiation of $CD4^+$ T cells into $CD4^+IL\text{-}17^+$ Th17 cells, which secrete IL-17 and IL-6 involved in inflammation and tumor development. TGF-β induces differentiation of $CD4^+$ T cells into $CD4^+CD25^+Foxp3^+$Tregs, which secrete TGF-β and express Foxp3 involved in immune regulation [4]. In addition, IL-23 and Th17 promote $CD4^+$ T-cell differentiation, and IFN-γ inhibits $CD4^+$ T-cell differentiation. In tumor microenvironment, overexpression

of the above inflammatory cytokines disrupts the balance of $CD4^+CD25^+Foxp3^+$Treg and $CD4^+IL\text{-}17^+$ Th17 [4], which can generate tumor growth signals and promote the spread of tumor cells to other tissues [5]. In the present study we examined the balance of these two $CD4^+$ T-cell populations, the expression levels of proinflammatory cytokines, and the SOCS3-JAK2/STAT3 signal transduction pathway, to elucidate the mechanism underlying the effect of FZFA auxiliary treatment on the growth and metastasis of tumor.

2. Materials and Methods

2.1. Animals. This study was conducted using 6- to 8-week-old male C57BL/6 mice weighing 18–22 g. Animals were provided by The Experimental Animal Research Institute of the Chinese Academy of Medical Sciences (license number SCXK-11-00-0006). The Lewis lung cancer cell line was provided by Guanganmen Hospital of China Academy of Traditional Chinese Medicine (license number SYXK [Beijing] 2011-0001). Animals were housed under constant conditions of 23 ± 1°C and 40 ± 5% humidity and had free access to feed pellets and tap water. All animals were cared for in accordance with the policies and guidelines for animal use of the Chinese Academy of Traditional Chinese Medicine.

This study was approved by the Ethics Committee of the Chinese Academy of Traditional Chinese Medicine. All experiments were performed following the guidelines of the China Institute of Laboratory Animal Science (CALAS).

2.2. Preparation of FZFA. Tangshen (*Codonopsis pilosula*), Huangqi (*Astragalus mongholicus*), Gouqizi (medlar), Heshouwu (*Polygonum multiflorum*), Quanshen (bistort root), and Tengligen (Chinese *Actinidia* root) were purchased from Beijing Tongrentang Co. Ltd. The decoction of FZFA was composed of Tangshan (15 g), Huangqi (30 g), Gouqizi (12 g), Heshouwu (12 g), Quanshen (10 g), and Tengligen (12 g). FZFA crude powder was extracted twice using a 10-fold excess of boiling water and filtration through four-layer gauze. The combined filtrate was centrifuged at 2,000 rpm/min for 20 min and concentrated under reduced pressure. The concentrated solution was cooled to room temperature and mixed with pure alcohol to an alcohol content of 70%. The mixture was refrigerated for 24 h and filtered. The resulting sediment was vacuum-evaporated to obtain powder, which was dissolved in water immediately before oral administration. The FZFA decoction was concentrated to 1.3 g drug per milliliter. On the basis of the clinical dose for a 70 kg adult, we converted the dose for mice to 6.5 g crude drug per 100 g body weight.

2.3. Induction of Lewis Lung Cancer in Mice. The left armpit skin of the mice was disinfected with alcohol and 0.2 mL of a suspension of Lewis lung cancer cells (containing approximately 1×10^6 cells/mL by trypan blue staining and counting of living cells) was injected into subcutaneous tissue using a 1 mL syringe.

2.4. Experimental Scheme

2.4.1. Experimental Groups. Thirty-two C57BL/6 mice were randomly assigned to four groups as follows: FZFA + CTX treatment, CTX control, model control, and normal control (eight rats per group). Mice in the FZFA + CTX group received FZFA (6.5 g crude drug/100 g body weight for 3 weeks) plus cyclophosphamide (6 mg/100 g body weight), given by intraperitoneal injection within 48 h after inoculation. Mice in the CTX group received CTX (6 mg/100 g, given by intraperitoneal injection within 48 h after inoculation), while mice in the normal control groups received equivalent volumes of distilled water for 3 weeks without tumor cell injection and without drug.

2.4.2. Assessment of Initial Immune Status. Blood samples (0.2 mL) were extracted from the inner canthus and mixed with heparin to prevent clotting. 20 μL of monoclonal antibody reagents (Miltenyi Biotec, Germany) specific for $CD3^+$, $CD4^+$, $CD8^+$, and NK cells was mixed to 180 μL of blood and placed in the dark for 15 minutes. Blood cells were lysed using the Q-PREP system (Beckman-Coulter, Pasadena, CA). For each sample, the percentage of $CD3^+$, $CD4^+$, $CD8^+$, and NK cells and the ratio of $CD4^+/CD8^+$ cells among 5,000 T cells were confirmed by flow cytometry (FACS CantoII, BD Biosciences). There was no significant difference in T-cell subsets between experimental groups before treatment ($P > 0.05$).

2.4.3. Observation of Inhibition Rate of Lung Metastasis. 21 days after inoculation, the mice were sacrificed under deep anesthesia. The lungs were rinsed with physiological saline, fixed with 4% paraformaldehyde for 24 h, dehydrated in various concentrations of ethanol, and embedded in paraffin. Sections of the pulmonary lobes (3 μm thickness) were stained with hematoxylin and eosin. The number of metastases in every pulmonary lobe was counted (metastasis present as round small nodular protrusions with a circular translucent point of 2~5 mm; parts of metastases can be fused together). The inhibition rate of lung metastasis was evaluated as follows. Lung metastasis rate (%) = number of mice with metastasis/total number of mice. Inhibition rate of lung metastasis (%) = (1 − mean number of lung metastases in experimental group/mean number of lung metastases in control group) × 100.

2.4.4. Tumor Volume and Weight. The tumors were stripped and then the mice and the tumors were weighed. Tumor volume (V) was calculated as $V = \pi abc/2$ (a: height, b: length, and c: width) [6].

2.4.5. Determination of the Percentage and Ratio of Splenic $CD4^+IL\text{-}17^+$ Th17 and $CD4^+CD25^+Foxp3^+$ Treg Cells by Flow Cytometry Splenic $CD4^+CD25^+Foxp3^+$ Tregs. The spleens were removed and ground up, and spleen cells were separated from membrane and adipose tissue by filtration through a 300 mesh strainer. Spleen cells were resuspended in 2 mL PBS in a centrifuge tube and the number of cells was counted.

Table 1: Inhibition rate of lung metastasis (mean ± SE).

Group	n	Metastasis rate (%)	Number of lung metastases (n)	Inhibition rate of lung metastasis (%)
Normal group	8	\	\	\
Model group	8	100	$13.50 \pm 0.91^{\triangle}$	0
CTX group	8	75	$10.50 \pm 1.25^{*\triangle}$	26.65
FZFA + CTX group	8	62.5	$7.63 \pm 0.63^{*}$	50.94

$^{*}P < 0.05$, versus model control group; $^{\triangle}P < 0.05$, versus FZFA + CTX group.

Table 2: Volume and weight of tumor (mean ± SE).

Group	n	Body weight (g)	Tumor weight (g)	Tumor volume (cm^3)
Normal group	8	21.9 ± 1.58	0	0
Model group	8	22.8 ± 1.44	$4.53 \pm 1.03^{\triangle}$	$3.06 \pm 0.84^{\triangle}$
CTX group	8	20.4 ± 0.95	$3.43 \pm 0.93^{*\triangle}$	$2.04 + 0.55^{*\triangle}$
FZFA + CTX group	8	22.0 ± 2.01	$2.12 \pm 0.79^{*}$	$1.38 + 0.32^{*}$

$^{*}P < 0.05$, versus model control group; $^{\triangle}P < 0.05$, versus FZFA + CTX group.

Table 3: Percentage and ratio of splenic Th17 and Treg (mean ± SE).

Group	n	Thl7 (%)	Treg (%)	Th17/Treg
Normal group	8	$0.64 \pm 0.01^{*\triangle}$	$5.52 \pm 0.10^{*\triangle}$	0.114 ± 0.004
Model group	8	$1.20 \pm 0.04^{\triangle}$	$8.96 \pm 0.91^{\triangle}$	$0.132 \pm 0.012^{\times}$
CTX group	8	$1.04 \pm 0.06^{*\triangle}$	$8.25 \pm 0.34^{*\triangle}$	$0.127 \pm 0.012^{\times}$
FZFA + CTX group	8	$0.78 \pm 0.11^{*}$	$7.03 \pm 0.14^{*}$	0.111 ± 0.015

$^{*}P < 0.05$, versus model control group; $^{\triangle}P < 0.05$, versus FZFA + CTX group. $^{\times}P < 0.05$, versus the normal control group.

Table 4: Percentage and ratio of Th17 and Treg of metastasis foci (mean ± SE).

Group	n	Thl7 (%)	Treg (%)	Th17/Treg
Normal group	6	$11.40 \pm 1.15^{*}$	$2.52 \pm 0.40^{*}$	4.57 ± 1.09
Model group	6	$34.69 \pm 3.85^{\triangle}$	$11.50 \pm 0.44^{\triangle}$	$3.02 \pm 0.39^{\times}$
CTX group	6	$18.87 \pm 1.78^{*\triangle}$	$5.91 \pm 0.27^{*\triangle}$	$3.17 \pm 0.49^{\times}$
FZFA + CTX group	6	$11.40 \pm 0.08^{*}$	$2.75 \pm 0.30^{*}$	4.17 ± 0.69

$^{*}P < 0.05$, versus model control group; $^{\triangle}P < 0.05$, versus FZFA + CTX group. $^{\times}P < 0.05$, versus the normal control group.

Table 5: Content of IL-6, TGFβ, IL-17, IL-23, and IFN-γ (mean ± SE).

Group	n	IL-6 (pg/mL)	TGFβ (pg/mL)	IL-17 (pg/mL)	IL-23 (pg/mL)	IFNγ (pg/mL)
Normal group	8	$0.11 \pm 0.04^{*}$	$0.08 \pm 0.004^{*}$	$0.14 \pm 0.02^{*}$	$0.38 \pm 0.05^{*}$	$0.96 \pm 0.29^{*}$
Model group	8	$0.20 \pm 0.04^{\triangle}$	$0.17 \pm 0.03^{\triangle}$	$0.18 \pm 0.07^{\triangle}$	$0.63 \pm 0.14^{\triangle}$	$2.72 \pm 0.62^{\triangle}$
CTX group	8	$0.18 \pm 0.03^{*\triangle}$	$0.16 \pm 0.01^{\triangle}$	0.17 ± 0.02	$0.40 \pm 0.15^{*}$	$1.94 \pm 0.40^{*\triangle}$
FZFA + CTX group	8	$0.11 \pm 0.002^{*}$	$0.09 \pm 0.01^{*}$	$0.15 \pm 0.03^{*}$	$0.39 \pm 0.02^{*}$	$1.15 \pm 0.54^{*}$

$^{*}P < 0.05$, versus model control group; $^{\triangle}P < 0.05$, versus FZFA + CTX group.

Table 6: Quantitation of splenic Foxp3 and RORγt mRNA (Mean ± SE).

Group	n	Foxp3 mRNA	RORγt mRNA
Model group	8	$1.81 \pm 0.08^{\triangle}$	$1.91 \pm 0.14^{\triangle}$
Normal group	8	$1.10 \pm 0.10^{*}$	$1.19 \pm 0.06^{*}$
CTX group	8	$1.53 \pm 0.05^{*\triangle}$	$1.58 \pm 0.07^{*\triangle}$
FZFA + CTX group	8	$1.12 \pm 0.03^{*}$	$1.19 \pm 0.80^{*}$

$^{*}P < 0.05$, versus model control group; $^{\triangle}P < 0.05$, versus FZFA + CTX group.

Table 7: Protein expression of splenic JAK2, STAT3, and SOCS3 (mean ± SE).

Group	n	JAK2	STAT3	SOCS3
Model group	8	$28.96 \pm 3.71^{\triangle}$	$21.88 \pm 1.11^{\triangle}$	$3.38 \pm 0.13^{\triangle}$
Normal group	8	$12.18 \pm 1.00^{*\triangle}$	$17.40 \pm 2.10^{*}$	$10.01 \pm 1.31^{*}$
CTX group	8	$23.71 \pm 5.01^{*\triangle}$	$19.82 \pm 2.09^{*\triangle}$	$7.43 \pm 0.11^{*\triangle}$
FZFA + CTX group	8	$19.12 \pm 0.40^{*}$	$17.78 \pm 1.12^{*}$	$10.00 \pm 1.15^{*}$

$^{*}P < 0.05$, versus model control group; $^{\triangle}P < 0.05$, versus FZFA + CTX group.

Spleen cell suspension containing 1×10^6 cells was added to l00 μL PBS in a test tube, and 10 μL PerCp anti-mouse CD3mAb (Miltenyi Biotec, Germany), 2 μL FITC anti-mouse CD4mAb (Miltenyi Biotec), and 4 μL PE anti-mouse CD25mAb (Miltenyi Biotec) were added. After incubation at 4°C in the dark for 30 min, the cells were centrifuged at 1500 rpm/min for 8 min, the supernatant was discarded, and the cells were resuspended in 1 mL of freshly prepared rupture of membrane liquid (Invitrogen, American) at 4°C for 40 min. After two washes with 2 mL 1x permeabilization buffer (Invitrogen, American), 4 μL PEcy5 anti-mouse Foxp3 mAb (Miltenyi Biotec) was added and the mixture was incubated at 4°C in the dark for 30 min. For flow cytometric analysis, data were collected from 5,000 cells for each sample. With delineation of the lymphocyte group as the R1 gate and $CD4^+$cell clusters as the R2 gate, Cell Quest software (BD Bioscience) was used to determine the percentage of $CD4^+CD25^+Foxp3^+$ Treg cells in the $CD3^+CD4^+$ T cells.

Splenic $CD4^+$IL-17^+Th17. Spleen cells were isolated as above and incubated with 10 μL PerCp anti-mouseCD3 mAb (Miltenyi Biotec) and 2 μL FITC anti-mouse CD4mAb (Miltenyi Biotec) at 4°C in the dark for 30 min. Cells were centrifuged at 1500 rpm/min for 8 min, the supernatant was discarded, and the cells were resuspended in 1 mL freshly prepared rupture of membrane liquid (Invitrogen, American) at 4°C for 40 min. After two washes with 2 mL 1x permeabilization buffer, 4 μL PE anti-mouse IL-17 mAb (Miltenyi Biotec) was added and the mixture was incubated at 4°C in the dark for 30 min.Th17 cells were detected with flow cytometry (FACS CantoII, BD).

2.4.6. Determination of the Percentage and Ratio of $CD4^+$IL-17^+Th17 and $CD4^+CD25^+Foxp3^+$Treg Cells in Metastasis Foci by Immunohistochemistry. Lung tissue samples preserved in 4% paraformaldehyde solution were dehydrated and embedded in paraffin. The sections were deparaffinized and blocked with 3% peroxide-methanol at room temperature to remove endogenous peroxidase. Sections were incubated with 75 μL of rabbit anti-human polyclonal antibody specific for IL-17 or $Foxp3^+$ (Miltenyi Biotec) diluted in blocking buffer in a humidified chamber for 12 h, followed by incubation with 75 μL of secondary antibody (Miltenyi Biotec) for 1 h in a humidified chamber. Subsequent immunostaining was performed using the biotin-streptavidin-peroxidase method with diaminobenzidine as a staining material and counterstaining with methyl green (1 min) or hematoxylin. Sections were immediately dehydrated in 70% ethanol, 80% ethanol, and 100% ethanol, and the glass slides were sealed with neutral gum. The negative control was treated as described above but the primary antibody was replaced by PBS. Sections were analyzed using a computerized image analyzer (Image-ProPlus6, Media Cybernetics, American). The presence of brown granules in the cytoplasm or membrane of cells was classified as positivity; cells with no brown granules were classified as negative. Ten views were obtained for each slide, and seven slides were prepared for each organ. The percentage of positive cells was calculated as follows: (positive cells/total cells) × 100.

2.4.7. Determination of IL-6, TGF-β, IL-17, IL-23, and IFN-γ Content by Enzyme-Linked Immunosorbent Assay (ELISA). Culture supernatants of $CD4^+$ T lymphocytes were collected into a 96-well plate. Test plates containing a blank well, 50 μL of sample diluent, and standard samples were incubated at room temperature for 2 h, and then 100 μL of a working solution of enzyme conjugates (Angiotensin, American) was added, and the plates were incubated at 37°C for a further 2 h. Serum concentrations of IL-17, IL-23, and IFN-γ were determined using the enzyme mark instrument (MullikanMK3, American). Absorbance (A) value was measured with a 450–630 nm dual wavelength. A standard curve constructed using the A values for the standard concentrations was used to determine the concentration of each cytokine in each sample.

2.4.8. Quantitation of Splenic Foxp3 and RORγt mRNA by RT-PCR. Total RNA was extracted from the tissues using Trizol (Sangon, Shanghai, China) and its purity was determined using a Smart Spec TM3000 spectrophotometer (Bio-Rad, Hercules, CA, USA). cDNA was synthesized according to the manufacturer's instructions (Genechem, Shanghai). PCR was performed using a GeneAmp 9600 (Perkin Elmer, Waltham, MA, USA) with cDNA as template and TaqDNA, 10x buffer, MgCl2, dNTPs, and forward and reverse primers for GAPDH, Foxp3, and RORγ (Sangon Shanghai, China). The primer sequences used were Foxp3, forward primer 5′-CTGACCAAGGCTTCATCTGT-3′ and reverse primer 5′-AACTCTGGGAATGTGCTGTT-3′; RORγ, forward primer 5′-GGCTCCCTGGATGAATAGAATG-3′ and reverse primer 5′-AGGCGAGGCAGAAAATGTAAAG-3; GAPDH, forward primer 5′-CCTTCATTGACCTCAACTACATG-3′ and reverse primer 5′-CTTCTCCATGGTGGTGAAGAC-3′. The PCR reaction conditions were 95°C for 5 min, 40 cycles of 95°C for 25 s, 55°C for 25 s, 72°C for 50 s, and final extension at 72°C for 5 min. The reaction products were subjected to 2% agarose gel electrophoresis at 60 V for 2 h and observed under an ultraviolet lamp. Expression of Foxp3 and RORγt mRNA was determined semiquantitatively using

Fluor-S MultiImager (Bio-Rad), with *GAPDH* as an internal reference. The gray scale (or opacity degree, OD) of each band was screened and the densitometric ratio for Foxp3 and RORγ relative to *GAPDH* was calculated for each sample [7, 8].

2.4.9. Determination of Splenic JAK2, STAT3, and SOCS3 Protein by Western Blotting. Spleen tissue (100 mg) was cut into small pieces and mixed with lysate, and the suspension was homogenized and centrifuged. Protein concentration was determined by the Bradford method, and tissue was preserved at −80°C prior to testing. A 50 μg sample of tissue from each group was used for 15% SDS-PAGE. Proteins were transferred to a PVDF membrane, which was blocked in 5% nonfat milk powder for 1 h at room temperature before incubation with antibodies specific for JAK2, STAT3, and SOCS3 (Cell Signaling Technology Boston, MA, USA; diluted 1 : 2,000 in TBST buffer) at 4°C overnight. Membranes were washed twice in TBST (10 min each wash) and then visualized with electrochemiluminescence. Image analysis was performed with Image Master VDS software (Amersham Pharmacia Biotech, Uppsala, Sweden) using GAPDH as an internal control to determine the relative protein concentration.

2.5. Statistical Analysis. All data were expressed as means ± standard errors of the mean (SEMs). Number of experiments (n) is indicated in the legend of each figure. All analysis was performed using the statistical package for the social sciences (SPSS) statistical software for Windows, version 17.0 (SPSS Inc., USA). The statistical significance of differences was assessed by one-way ANOVA. $P < 0.05$ was considered to be significantly different. When ANOVA indicated a significant difference, LSD or Dunnett's T3 posthoc test was then used to assess the difference between groups.

3. Results

3.1. Tumor-Burden Mouse, Armpit Implantation Tumor, and Lungs of Tumor-Burden Mice in Each Group. See Figure 1.

3.2. Pathologic Analysis of Each Group. The lungs of mice in the normal control group had alveolar walls with structural integrity and no collapse; there was no alveolar secretion or infiltration of inflammatory cells (Figure 2(a)). Lungs of mice in the model control group had a large number of metastatic cancer cells exhibiting nuclear hyperchromatism and irregular shape; the alveolar walls were thickened and there were large numbers of infiltrative mononuclear cells (Figure 2(b)). In comparison, the range of mononuclear cell infiltration in the lungs of mice in the CTX group (Figure 2(c)) and FZFA+CTX group (Figure 2(d)) was smaller, and the alveolar structure was relatively complete. The pathology of lungs in mice in the FZFA+CTX group was less disrupted than that of the CTX group.

3.3. Inhibition Rate of Lung Metastasis of Each Group. The Number of lung metastases in the model control group was higher than that in the other groups. Number of lung metastases in the FZFA + CTX group was significantly lower than that of the CTX group ($P < 0.05$). The inhibition rate of lung metastasis in the model control group was 0. The inhibition rate of metastasis in the FZFA + CTX group was higher than that of the CTX group (Table 1).

3.4. Tumor Volume and Weight of Each Group. The volume and weight of tumors in the model control group were higher than those in the other groups. Tumor weight and volume in the FZFA + CTX group were significantly lower than those of the CTX group ($P < 0.05$) (Table 2).

3.5. Percentage and Ratio of Splenic $CD4^+IL\text{-}17^+$ Th17 and $CD4^+CD25^+Foxp3^+$ Treg Cells. The percentage of $CD4^+IL\text{-}17^+$ Th17 and $CD4^+CD25^+Foxp3^+$ Tregs in the spleen was very low in the normal control group but significantly higher in the model control group ($P < 0.05$). The percentage of splenic $CD4^+IL\text{-}17^+$ Th17 and $CD4^+CD25^+Foxp3^+$Tregs in the FZFA + CTX group was significantly lower than that of the CTX group ($P < 0.05$; Table 3, Figure 3).

More importantly, the ratio of Thl7/Treg approached normalization only in the in the FZFA + CTX group; the ratio of Thl7/Treg in the FZFA + CTX group was not significantly different from that of the normal group ($P < 0.05$; Table 3).

*3.6. $CD4^+IL\text{-}17^+$ Th17 and $CD4^+CD25^+Foxp3^+$ **Treg** in Metastasis Foci (Table 4, Figure 4).* The percentage of $CD4^+IL\text{-}17^+$ Th17 and $CD4^+CD25^+Foxp3^+$ Treg cells in the metastatic foci was very low in the normal control group but was significantly increased in the model control group ($P < 0.05$). The percentage of splenic $CD4^+IL\text{-}17^+$ Th17 and $CD4^+CD25^+Foxp3^+$Treg in the FZFA + CTX group was significantly lower than in the CTX group ($P < 0.05$) (Table 4, Figure 4).

More importantly, the ratio of Thl7/Treg approached normalization only in the FZFA+CTX group. The ratio of Thl7/Treg in the FZFA + CTX group showed no significant difference from that of the normal group ($P < 0.05$; Table 4).

3.7. Content of IL-6, TGF-β, IL-17, IL-23, and IFN-γ. The model control group showed a significant increase in serum levels of IL-17, IL-23, and IFN-γ compared with the normal control group ($P < 0.01$). Expression in the FZFA + CTX group and CTX group was significantly lower than that in the model control group ($P < 0.05$). Moreover, there was a significant difference between expression in the FZFA + CTX group and the CTX group ($P < 0.05$; Table 5).

3.8. Quantitation of Splenic Foxp3 and RORγt mRNA Expression. The mRNA expression of Foxp3 and RORγt in the spleen was very low in the normal control group but significantly higher in the model control group ($P < 0.05$). In contrast, the expression of Foxp3 and RORγt mRNA in

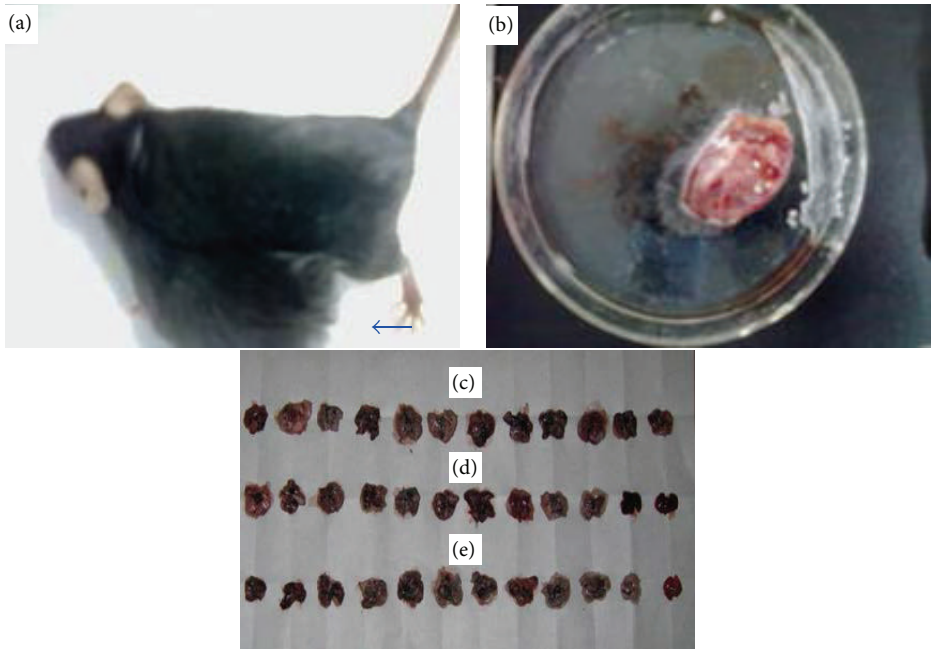

Figure 1: Judging from the appearance of armpit implantation tumor (b) in tumor-burden mouse (a), the size of armpit implantation tumors in descending order is the model control group, the CTX group, and the FZFA + CTX group. Seen with the naked eye, the lungs of tumor-burden mice were not significantly different between the model control group (c), the CTX group (d), and the FZFA + CTX group (e).

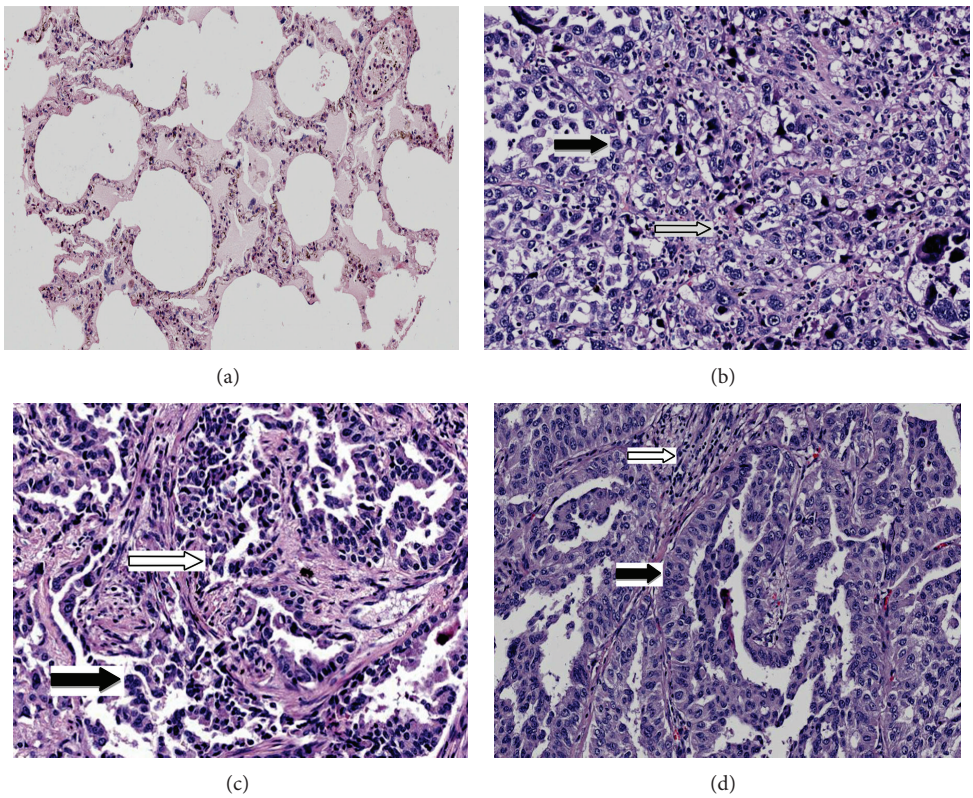

Figure 2: The pathological picture of normal control group (a), model control group (b), CTX group (c), and FZFA + CTX group (d). Lung tissues were fixed, sectioned at 4 μm thickness, stained with H&E solution, and observed under a microscope of 200 magnifications. White arrows indicate inflammatory cells and black arrows indicate the cancer cells.

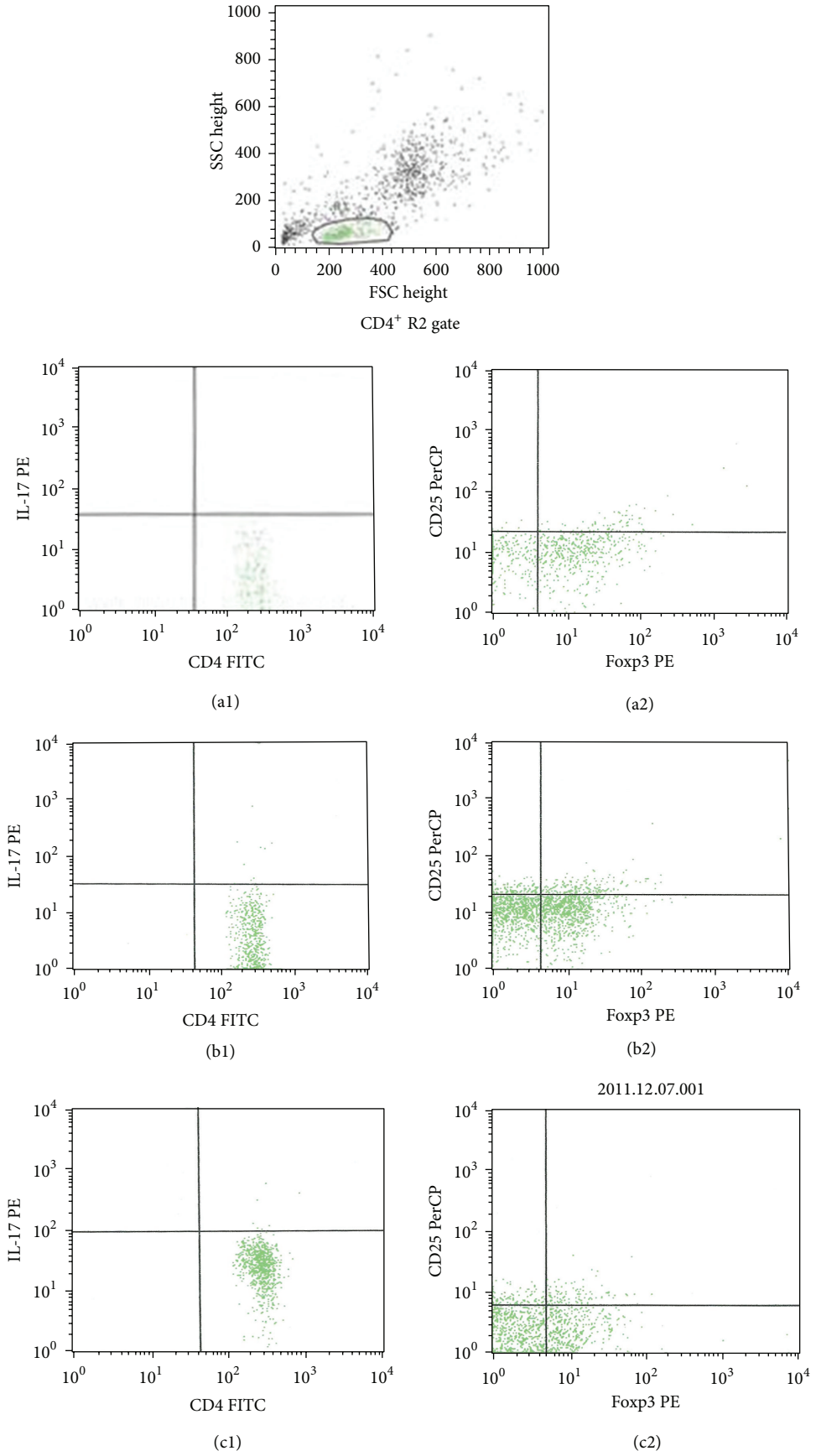

Figure 3: Continued.

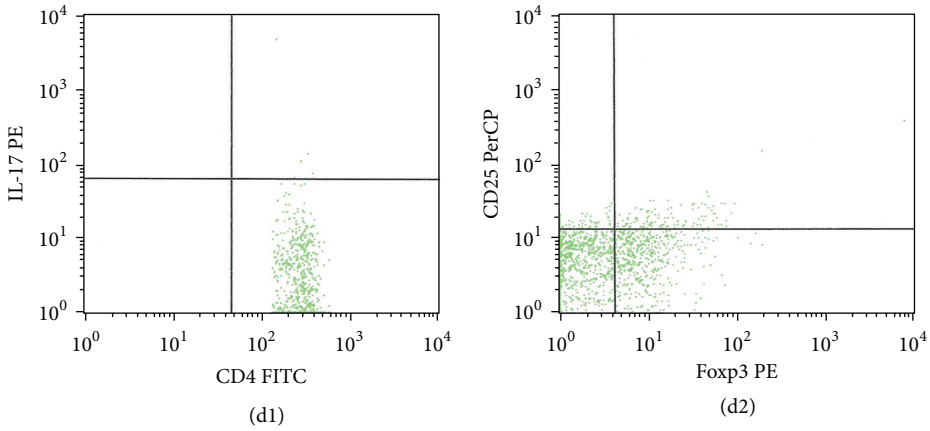

Figure 3: The distribution plot of Thl7 and Treg. Normal control group Th17 (a1), normal control group Treg (a2); model control group Th17 (b1), model control group Treg (b2); CTX group Th17 (c1), CTX group Treg (c2), FZFA + CTX group Th17 (d1), and FZFA + CTX group Treg (d2). Spleen cells were separated and labeled by antibodies and then detected by flow cytometry.

the FZFA + CTX group was significantly lower than that in the CTX group ($P < 0.05$; Table 6, Figure 5).

3.9. Protein Expression of Splenic JAK2, STAT3, and SOCS3. SOCS3 protein expression was significantly downregulated in all groups except for the normal control group ($P < 0.05$). JAK2 and STAT3 protein expression was significantly higher in the model control group than in all other groups ($P < 0.05$). The protein expression of SOCS3, JAK2, and STAT3 in the FZFA + CTX group was lower than that in the CTX group ($P < 0.05$; Table 7, Figure 6).

4. Discussion

Our previous studies showed that FZFA + CTX had greater anticancer efficacy than CTX alone, including greater inhibition of mouse cancers, longer life span, and improved survival curves [9–11]. Cytologic studies showed that FZFA + CTX had obvious inhibitory effects on cancer cells, decreasing the mitotic index and DNA content and shifting the DNA histogram to the left [9, 12].

The $CD4^+CD25^+Foxp3^+$ Treg cells that mediate immune tolerance and the $CD4^+IL\text{-}17^+$ Th17 cells that mediate the inflammatory response are derived from the initial T lymphocyte cells. Their functions and differentiation processes are opposing and under normal circumstances keeping these two cell populations in balance helps maintain immune stability [5, 13]. However, during tumor formation and development the balance of $CD4^+IL\text{-}17^+$ Th17 and $CD4^+CD25^+Foxp3^+$Treg can be disrupted by inflammatory cytokines [14]. Exploring the interaction between $CD4^+CD25^+Foxp3^+$Treg and $CD4^+IL\text{-}17^+$ Th17 cells has great implications for understanding regulation of the immune inflammatory microenvironment and for the clinical application of traditional Chinese medicine in the reversion of tumor growth and tumor immune escape.

In this study, the FZFA + CTX group exhibited less tumor growth and a lower metastasis rate of Lewis lung cancer than the other groups. The expression of $CD4^+IL\text{-}17^+$ Th17 and $CD4^+CD25^+Foxp3^+$Treg in each group showed a rising trend in all groups, but expression in the FZFA+CTX group was significantly lower than that in the other groups ($P < 0.05$). Moreover, the ratio of $CD4^+IL\text{-}17^+$ Th17 to $CD4^+CD25^+Foxp3^+$Treg was unbalanced in all groups except for the FZFA + CTX group. Overall, the percentage of $CD4^+IL\text{-}17^+$ Th17 and $CD4^+CD25^+Foxp3^+$Treg was concordant with the extent of disease.

RORγt and Foxp3 are specific nuclear transcription factors for $CD4^+IL\text{-}17^+$ Th17 and $CD4^+CD25^+Foxp3^+$Treg, respectively [15]. SOCS3-JAK2/STAT3 is the main signal transduction pathway mediating the differentiation of $CD4^+CD25^+Foxp3^+$Treg and $CD4^+IL\text{-}17^+$ Th17 [16]. The expression of IL-6, TGF-β, IL-17, and IL-23 was directly proportional to the levels of $CD4^+IL\text{-}17^+$ Th17 and $CD4^+CD25^+Foxp3^+$Treg, whereas expression of IFN-γ showed an inverse relationship. Moreover, changes in expression of the transcription factors except for SOCS3, the Foxp3, RORγt, and the signaling molecules JAK2 and STAT3 also corresponded with changes in $CD4^+IL\text{-}17^+$ Th17 and $CD4^+CD25^+Foxp3^+$ Treg expression.

5. Conclusion

Traditional Chinese medicine combined with chemotherapy inhibited the tumor growth, metastasis, and the immune inflammatory response more efficiently than chemotherapy alone. Therefore, FZFA+CTX and CTX alone had inhibitory effects on the tumor growth and metastasis, but FZFA+CTX had greater activity than CTX alone.

Conflict of Interests

All authors have no competing interests to declare regarding the publication of this paper.

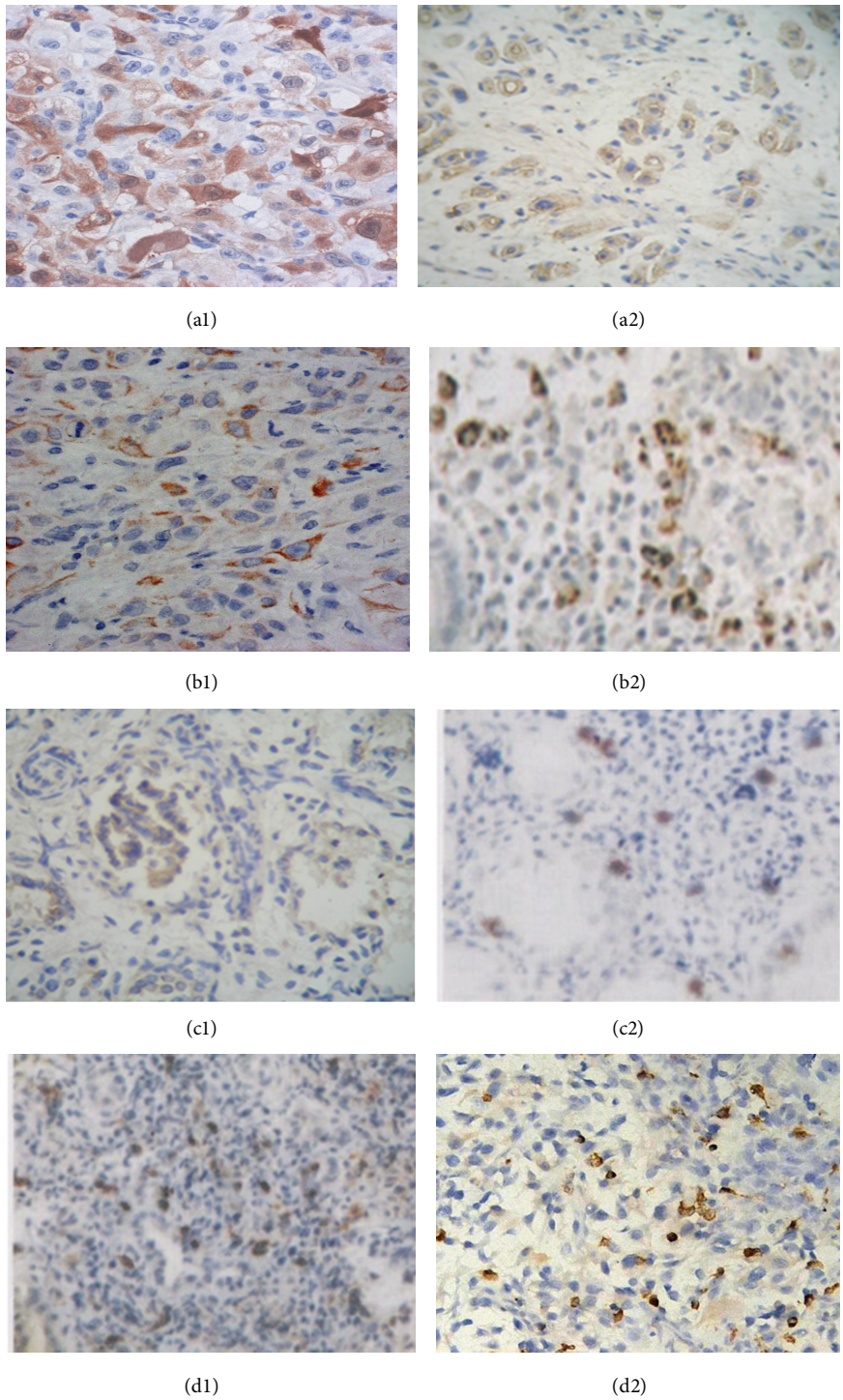

Figure 4: The Th17 and Treg of metastasis foci detected by immunohistochemistry. Normal control group Th17 (a1), normal control group Treg (a2); model control group Th17 (b1), model control group Treg (b2); CTX group Th17 (c1), CTX group Treg (c2), FZFA+CTX group Th17 (d1), and FZFA+CTX group Treg (d2). Lung tissues were fixed, sectioned at 4 μm thickness, and incubated with primary antibody and secondary antibody; then the percentage of positive cells was calculated under a microscope of 400 magnifications.

Acknowledgments

This study was in part supported by the National Natural Science Foundation of China (nos. 81273614 and 81072970).

We thank the authors for their contributions to this special issue. The authors also would like to express their sincere gratitude and appreciation to the reviewers for their valuable comments on the manuscript.

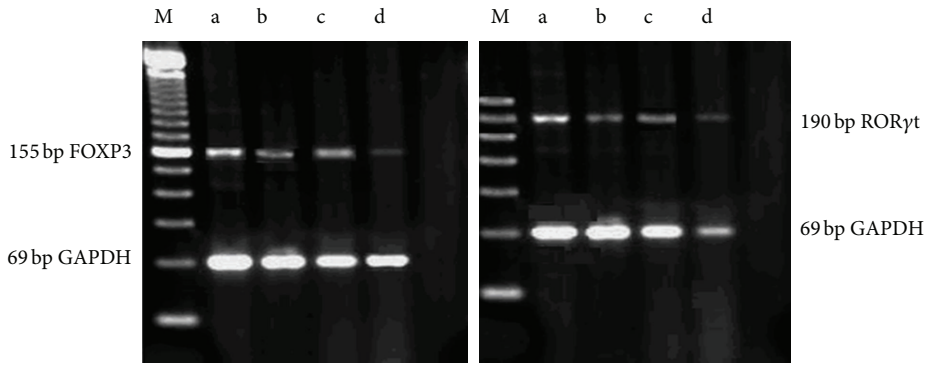

Figure 5: The Foxp3 and RORγt mRNA electrophoresis by RT-PCR. Model control group (a), normal control group (b), CTX group (c), FZFA+CTX group (d), and M: marker. GAPDH as internal reference.

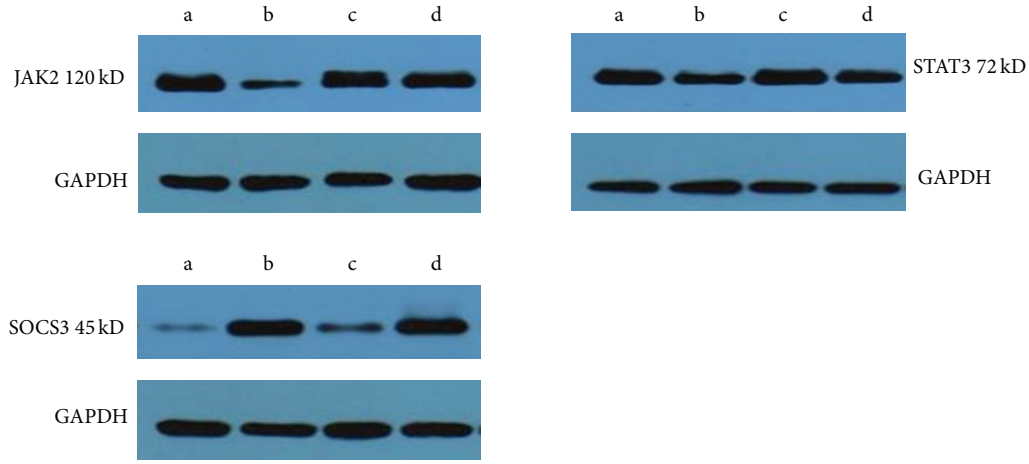

Figure 6: The JAK2, STAT3, and SOCS3 protein electrophoresis by Western blotting. Model control group (a), normal control group (b), CTX group (c), and FZFA + CTX group (d). GAPDH as internal reference.

References

[1] L. M. Coussens and Z. Werb, "Inflammation and cancer," *Nature*, vol. 420, no. 6917, pp. 860–867, 2002.

[2] L. M. Liu, C. Zhen, P. F. Chen et al., "The traditional Chinese medicine in the treatment of malignant tumor," *Journal of Traditional Chinese Medicine*, vol. 48, no. 9, pp. 776–779, 2007.

[3] M. W. Yu, G. Z. Sun, D. R. Li et al., "The role of Hematoxylin, SuMu Astragalus on Lewis lung cancer bearing mice spleen dendritic cells of traditional Chinese medicine," *Chinese Journal of Integrative Medicine*, vol. 27, no. 11, pp. 2284–2287, 2009.

[4] X. M. Chen, "Effect of inflammation on the biological behavior of malignant tumor," *Basic and Clinical Tumor*, vol. 21, no. 3, pp. 271–273, 2008.

[5] W. W. Wang and Q. Shen, "Th17 cells and its relationship with development of tumors," *Tumor*, vol. 29, no. 7, pp. 700–703, 2009.

[6] Z. J. He and X. X. Chen, "Comparison of different calculation methods of tumor volume," *Chinese Journal of Comparative Medicine*, vol. 19, no. 9, pp. 47–49, 2009.

[7] G. Chen, "Liver lipid molecules induce PEPCK-C gene transcription and attenuate insulin action," *Biochemical and Biophysical Research Communications*, vol. 361, no. 3, pp. 805–810, 2007.

[8] W. L. De, H. W. Lim, Q. Liang et al., "Targeted inhibition of calcineurin attenuates cardiac hypertrophy in vivo," *Proceedings of the National Academy of Sciences*, vol. 98, no. 6, pp. 3322–3327, 2001.

[9] G. Z. Sun, G. M. Wang, C. H. Chen et al., "Fuzhengfangai liquid combined with chemotherapy in treatment of advanced gastrointestinal cancer clinical and experimental research," *Journal of Surgery Combined with Traditional Chinese Medicine and Western Medicine Chinese*, vol. 11, no. 5, pp. 266–268, 1995.

[10] P. X. Zhang, G. Q. Yu, B. K. Pu et al., "The regulation of Feiliuping and righting anti-cancer plaster on serum ascorbate free radical in mice," *Journal of Surgery Combined with Traditional Chinese Medicine and Western Medicine China*, vol. 2, no. 6, pp. 393–395, 1996.

[11] Y. P. Xue, "Clinical and experimental studies of adjuvant treatment for colon cancer liver metastasis fuzhengfangai liquid Chinese folk therapy," *China's Naturopathy*, vol. 21, no. 5, pp. 59–62, 2013.

[12] P. T. Zhang, G. Z. Sun, S. J. Duan, M. Gao, and Z. Yang, "Scavenging effects of Fuzheng anticancer ointment on the enzymatic and non enzymatic system of hydroxyl free radical and superoxide anion," *Chinese Journal of Pharmaceuticals*, vol. 29, no. 11, pp. 657–660, 1994.

[13] C. Infante-Duarte, H. F. Horton, M. C. Byrne, and T. Kamradt, "Microbial lipopeptides induce the production of IL-17 in Th cells," *Journal of Immunology*, vol. 165, no. 11, pp. 6107–6115, 2000.

[14] X. M. Chen, "Effect of inflammation on the biological behavior of malignant tumor," *Basic and Clinical Tumor*, vol. 21, no. 3, pp. 271–274, 2008.

[15] I. I. Ivanov, B. S. McKenzie, L. Zhou et al., "The orphan nuclear receptor RORγt directs the differentiation program of pro-inflammatory IL-17$^+$ T helper cells," *Cell*, vol. 126, no. 6, pp. 1121–1133, 2006.

[16] J. H. Yu, K. H. Kim, and H. Kim, "SOCS 3 and PPAR-γ ligands inhibit the expression of IL-6 and TGF-β1 by regulating JAK2/STAT3 signaling in pancreas," *International Journal of Biochemistry and Cell Biology*, vol. 40, no. 4, pp. 677–688, 2008.

Hindawi Publishing Corporation
Evidence-Based Complementary and Alternative Medicine
Volume 2014, Article ID 573801, 10 pages
http://dx.doi.org/10.1155/2014/573801

Research Article

Anti-Inflammatory Effects of the Bioactive Compound Ferulic Acid Contained in *Oldenlandia diffusa* on Collagen-Induced Arthritis in Rats

Hao Zhu,[1] Qing-Hua Liang,[1] Xin-Gui Xiong,[1] Jiang Chen,[2] Dan Wu,[1] Yang Wang,[1] Bo Yang,[1] Yang Zhang,[1] Yong Zhang,[1] and Xi Huang[1]

[1] *Institute of Combined Traditional Chinese and Western Medicine, Xiangya Hospital, Central South University, Changsha, Hunan 410008, China*
[2] *Center of Telemedicine, Xiangya Hospital, Central South University, Changsha, Hunan 410008, China*

Correspondence should be addressed to Xin-Gui Xiong; xiongxg07@gmail.com

Received 22 January 2014; Revised 17 March 2014; Accepted 7 April 2014; Published 4 May 2014

Academic Editor: Shi-Biao Wu

Objectives. This study aimed to identify the active compounds in *Oldenlandia diffusa* (OD) decoction and the compounds absorbed into plasma, and to determine whether the absorbed compounds derived from OD exerted any anti-inflammatory effects in rats with collagen induced arthritis (CIA). *Methods*. The UPLC-PDA (Ultra Performance Liquid Chromatography Photo-Diode Array) method was applied to identify the active compounds both in the decoction and rat plasma. The absorbable compound was administered to the CIA rats, and the effects were dynamically observed. X-ray films of the joints and HE stain of synovial tissues were analyzed. The levels of IL-1β and TNF-α in the rats from each group were measured by means of ELISA. The absorbed compound in the plasma of CIA rats was identified as ferulic acid (FA), following OD decoction administration. Two weeks after the administration of FA solution or OD decoction, the general conditions improved compared to the model group. The anti-inflammatory effect of FA was inferior to that of the OD decoction ($P < 0.05$), based on a comparison of IL-1β TNF-α levels. FA from the OD decoction was absorbed into the body of CIA rats, where it elicited anti-inflammatory responses in rats with CIA. *Conclusions*. These results suggest that FA is the bioactive compound in OD decoction, and FA exerts its effects through anti-inflammatory pathways.

1. Introduction

Rheumatoid arthritis (RA) is a heterogeneous systemic autoimmune disease with the main clinical manifestation of symmetrical panarthritis. Currently, there is a lack of effective cure or prevention [1]. Up to now, the cause and pathogenesis of this disease have been unclear. Accumulating evidence indicates that certain cytokine interleukins, such as tumor necrosis factor (TNF) alpha, could be induced and synergized to promote the induction of IL-1β and IL-6 in target cells [2], culminating in the production of factors such as matrix metalloproteinases and reactive oxygen species that drive erosive arthritis [3]. Consistent with the role of inflammatory cytokines in the pathogenesis of RA, the treatment of RA has largely focused on these cytokines, with the development of biological agents targeting inflammatory cytokines such as TNF [4]. The single-target method applied by Western medicine has faced many challenges. Chinese traditional medicine could be more effective due to its multitarget approach [5]. bizhongxiao decoction (BZXD), an empirical formula based on long-term RA treatment in our ward, has been shown to be very effective [5]. This formula was formed by combining several Chinese traditional herbs, including *Oldenlandia diffusa* [6]. It has been reported that the high levels of TNF-α and IL-1β typically found in patients with RA can be significantly reduced by the administration of BZXD [7, 8]. In addition, BZXD appears to have a positive effect on RA patients by inhibiting joint bone destruction

and protecting joint function [6]. Because BZXD contains multiple herbs, in order to learn about this formula, we studied the herbs individually, starting with the most important one. *Oldenlandia diffusa* (OD) is the principal component of BZXD, and it has a very important medicinal role. Its pharmacodynamic properties have been the focus of research in traditional Chinese medicine (TCM) [9]. Previous studies have indicated that OD contains many chemicals, including triterpenoids, ferulic acid, sterols, iridoid glycosides, polypeptides, flavonoids, ursolic acids, oleanolic acids, and polysaccharides [10], some of which have multiple effects such as anti-inflammatory, antioxidative, and immunoregulatory [11, 12]. Sodium ferulate has been reported to have a beneficial effect on adjuvant arthritis treatment by reducing the level of IL-15 and IL-23 [13] and to have a curative effect on RA by influencing the expression of serum VEGF and TNF-α [14]. However, it is unknown which of the above compounds can be absorbed into the blood, resulting in a high false-positive rate. Therefore, to clarify the pharmacodynamic basis of OD's antirheumatism effect, we believe it is necessary to first identify the compounds absorbable in rat plasma by tracing the pathway of the compounds using a research strategy based in bioethnopharmaceutical analytical pharmacology [15].

2. Materials and Methods

2.1. Using the UPLC-PDA Method, We Identified the Active Compounds in OD and the Compounds Absorbable in Rat Plasma after Intragastric Administration of OD Decoction to Rats. The purity of all reference compounds was >99%. Acetonitrile and methanol (HPLC grade) were obtained from the Tedia Company, Inc, Fairfield, Ohio (USA). The Chinese herbal drug OD was purchased from the TCM Dispensary of Xiangya Hospital of Central South University. First, the drug was ground into a powder, then purified water was added to it in a ratio of 1 : 8. Next, the mixture was boiled twice for 30 min each; the mixture was filtered to extract the liquid; low-pressure rotary evaporation was carried out at a temperature of 60°C to get the concentrated OD decoction. The liquid was then processed into freeze-dried powder with a freeze dryer, with a yield rate of 18.56%, and the freeze-dried powder was sealed and stored in a refrigerator at a temperature of 4°C for future use. Ursolic acid, oleanolic acid, kaempferol, p-coumaric acid, FA, rutin, scopolamine lactone, and caffeic acid controls were purchased from Shanghai Yuanye Bio-Technology Co, Ltd, China. The purity of all reference compounds was >99%. The rats were with a body mass of 150±30 g, provided by the Laboratory Animal Center of Hunan Provincial People's Hospital. The rats were fed ad lib and were exposed to a 12 h/12 h light/dark cycle (lighting time: 6:00–18:00). The background noise was 40 ± 10 dB, and the ambient temperature was 20 ± 3°C during a one-week adaptation period.

Chromatography column: ACQUITY UPLC BEH C18 (2.1 ∗ 50 mm 1.7 μm); mobile phase: acetonitrile (A) and 0.5% acetic acid solution (B); detection wavelength: 190–400 nm; flow rate: 0.5 mL/min; column temperature: 40°C; sample volume: 5 μmL; analysis time: 15 min. The OD test solution was injected into the device for detection. We also examined the linear relationship of the test solution and the day-to-day and intraday precision, stability, and repeatability, as well as the sample recovery rate.

Although OD contains many more chemical components, we have identified the following 8 compounds, through a literature search, as mainly reported: ursolic acid, oleanolic acid, kaempferol, p-coumaric acid, FA, rutin, scopolamine lactone, and caffeic acid. All of these substances were placed in methanol for ultrasonic dissolving to obtain the control stock solutions, the concentrations of which were 0.326 mg/mL, 0.334 mg/mL, 0.413 mg/mL, 0.294 mg/mL, 0.32 mg/mL, 0.336 mg/mL, 0.22 mg/mL, and 0.464 mg/mL, respectively. All of the solutions were sealed and then stored in a refrigerator at a temperature of 4°C. Purified water was used to ultrasonically dissolve the freeze-dried OD powder, which was then centrifuged and filtered to obtain the test solution of OD at a concentration of 86.22 mg (crude drug)/mL. The mother solution was then mixed with all of the 8 references at a ratio of 1 : 1 : 1 : 1 : 1 : 1 : 1 : 1.

Normal Sprague-Dawley (SD) rats were divided into an OD intragastric administration group and a control group. The rats in the OD group were administered the OD decoction intragastrically at a dose of 1.35 g/kg (crude drug/weight) (converted according to the body surface area of an adult human weighing 70 kg [16]); the rats in the control group were administered purified water intragastrically at the same volume. After 3 days of intragastric administration, the rats were fasting for 12 h. This was followed by a final administration, after which the rats were anesthetized and decapitated, and their plasma was extracted. A pipette was used to remove 2 mL of plasma and mixed evenly with 4 mL of acetonitrile, 2 mL of ethyl acetate, and 1.2 mL of acetone, in that order, to precipitate protein and extract the active compound. The mixture was then dissolved ultrasonically for 20 min and centrifuged at a speed of 3000 r/min for 20 min. Next, the supernatant was pipetted and blow-dried with nitrogen gas in a water bath at room temperature then redissolved with 50 μL of acetic acid solution (20%) and 50 μL of methanol and centrifuged at a speed of 12000 r/min for 20 min. The supernatant was pipetted once again, and the plasma sample was set aside to be analyzed. Exactly 50 μL of plasma sample was injected into the UPLC system for analysis.

We also anesthetized and decapitated the rats from control group and extracted their plasma. The plasma were processed following the method above then divided in duplicate. For a better accuracy and reliability of the results, plasma A was tested as blank plasma. Plasma B was added with mother solution and then tested as positive control plasma.

2.2. Selection of Concentrations of FA for Intragastric Administration. Based on the clinical dose of OD and the FA content of OD, the concentration of FA administrated to rats was adjusted to match the equivalent human dose [16]. Another 4 concentrations were also used, which were half, two times, four times, and eight times the converted concentration.

Therefore, a total of 5 intervention doses were administered, namely, 0.32, 0.64, 1.28, 2.56, and 5.12 μg/g/d, which were, respectively, dose 1, dose 2, dose 3, and dose 4 groups. The purpose was to find the optimal dose of FA to intervene CIA.

25 of 30 healthy male SD rats were randomly selected for the purpose of CIA model replication, according to the modeling procedure of Chondrex. Bovine collagen type II (BIIC) solutions containing CFA or IFA were prepared and subcutaneously injected in the tail root, back, and sole of each rat on the 1st and 7th days, respectively. The other 5 rats were designed as control group.

Fourteen days after the immunization injection, all rats received intragastrically administered FA. The rats in the model group were intragastrically injected with purified water, while those in the normal group were permitted to drink freely.

The rats were anesthetized and decapitated on day 42, and the levels of IL-1β and TNF-α in their serum were measured to select the optimal dose of FA for intervention in the CIA rats. Statistical analysis of all data was accomplished with the SPSS 15.0 software package.

2.3. Effect of the Optimal Dose of FA on CIA Rats. Eighty SD rats (half male, half female) were randomly divided into 2 groups: normal ($n = 20$) and model ($n = 60$) groups. The 60 rats belonging to the latter group were assigned to CIA model replication. Two weeks after the immunization injection, animals failing in model replication were eliminated. Then, the remaining rats in model replication were subdivided into 3 groups, namely, the OD group, the FA group, and the model group.

The OD group received intragastrically administered OD decoction at a dose of 1.35 g/kg 2 times per day. The rats in the FA group received intragastrically administered reference FA at the optimal dose of 1.28 μg/g/d 2 times per day. The rats in the model group received intragastrically administered purified water at the same volume. Those in the control group were fed normally.

2.4. Observation of General Conditions. During a period of 42 days, each rat was weighed every 2 weeks and was recorded. In 28th day, we compared with the record 14 days ago, which was in the 14th day; in the 42nd day, we compared with the record 14 days ago, which was in 28th day. After that, we calculated the difference value. In addition, the arthritis index of each rat was observed and recorded by means of arthritis index integration [17]. A score of 0–4 was assigned to each CIA rat based on the degree of joint redness and swelling, as well as joint enlargement and deformity. Zero point indicates no arthritis, 1 point indicates mild swelling after appearance of red spots, 2 points indicate moderate swelling of joints, 3 points indicate severe swelling of joints, and 4 points indicate severe swelling of joints and inability to bear weight. Every week before and after immunization, a pair of compasses (fine-angle) and a flexible ruler were used to measure the thickness (in mm) of the right rear foot of each rat [18]. Statistical analysis of all data was accomplished with SPSS 15.0 to evaluate whether there were significant differences among each group in 28th and 42nd days.

Radiographic evaluation of the joints of rats in each group was carried out every 2 weeks to observe the degree of joint destruction. With the help of the Radiology Department of Xiangya Hospital, we used a diagnostic (800 mA) X-ray apparatus (PHILIPS, Inc, USA) to take the radiographs. Under the condition of general anesthesia, we took frontal X-rays of both lower extremities of the rats.

On the 14th, 28th, and 42nd days after immunization, under general anesthesia with 10% chloral hydrate, we amputated the bilateral knee joint and the whole rear paw, including the ankle joint then fixed them in 10% neutral buffered formalin for 24 hours. They were decalcified in 14% EDTA decalcifying fluid for 5 days then neutralized in 5% sodium thiosulfate for 3 hours. They were then washed for 12 hours, embedded in dehydrated paraffin, and cut into 5-6 μm slices (longitudinal). Next, the slices were placed into a 60°C oven for 30 min then soaked in xylene for 2 times 20 min. Next, they were soaked in 95% ethanol for 3 min, dipped into 80% ethanol for 1 min, and then in distilled water for 1 min. Then, they were dyed with hematoxylin for 15 min and washed, differentiated with acid alcohol for 3 s, washed with tap water for 10 min, dyed with eosin solution for 3 min, and washed again. Finally, we used 80% ethanol, 95% ethanol, and pure ethanol, successively, for gradient dehydration and mounted the samples with neutral gum. Pathological changes were observed under an optical microscope (Leica DFC425C) at 40x magnification.

The rats from the different groups were decapitated on the 28th or the 42nd days to sample their serum. Serum IL-1β and TNF-α levels were measured by enzyme-linked immunosorbent assay (ELISA; CUSABIO BIOTECH Co., Ltd, Wu Han, China) in pg/mL. The serum samples were centrifuged at 1000 r/min for 15 min and the serum was stored at −80°C. Two ELISA kits were utilized using a flat bottom with 96-well plates. Each well was coated with protein, and the serum was incubated in a well. After 1 hour at room temperature, the serum was removed and the samples were washed off with a series of buffer rinses. Next, enzymes (peroxidase) were added to metabolize the colorless substrates into colored products for 30 min, and the colored products were placed in the wells. When the enzyme reaction was complete, the entire plate was placed into a plate reader, and the optical density was determined for each well at 405 nm. The statistical analysis of all data was accomplished with SPSS 15.0 to evaluate whether there was a significant difference between day 28 and day 42.

3. Results

3.1. Identification of the Active Compounds in OD by UPLC-PDA. Exactly 50 μL of mother solution and test solution (86.22 mg crude drug/mL) was pipetted and injected into the UPLC system according to the chromatography procedure described above. The mother solution was scanned by the PDA detector (wavelength: 190–400 nm) under 321 nm, and the results in Figure 1(b) showed that the 8 references were

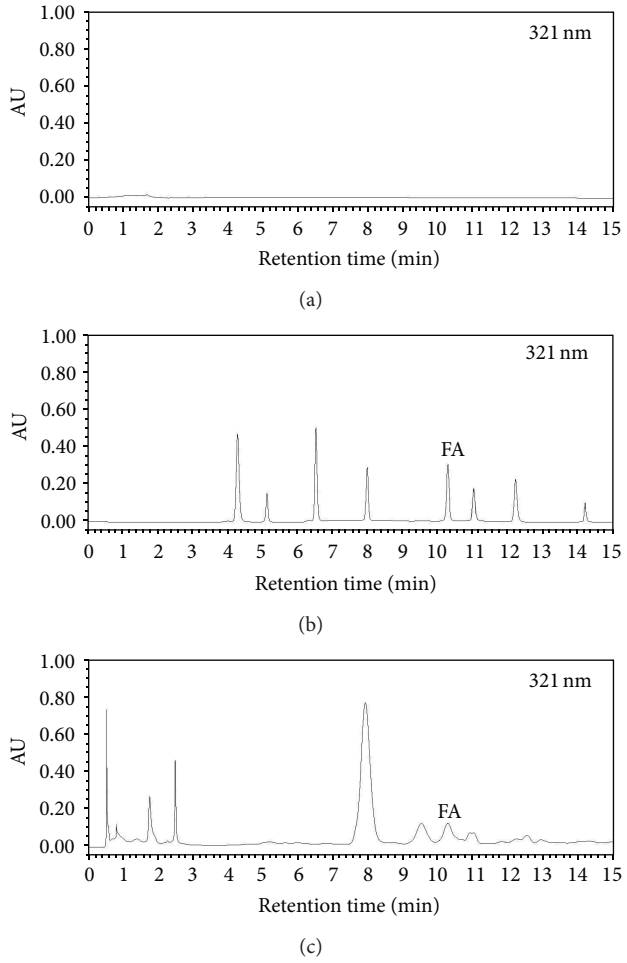

Figure 1: Typical chromatogram of samples in each group: (a) blank methanol; (b) eight reference compounds; (c) test solution of OD freeze-dried powder; FA refers to ferulic acid. All of the samples were scanned under the wavelength of 321 nm.

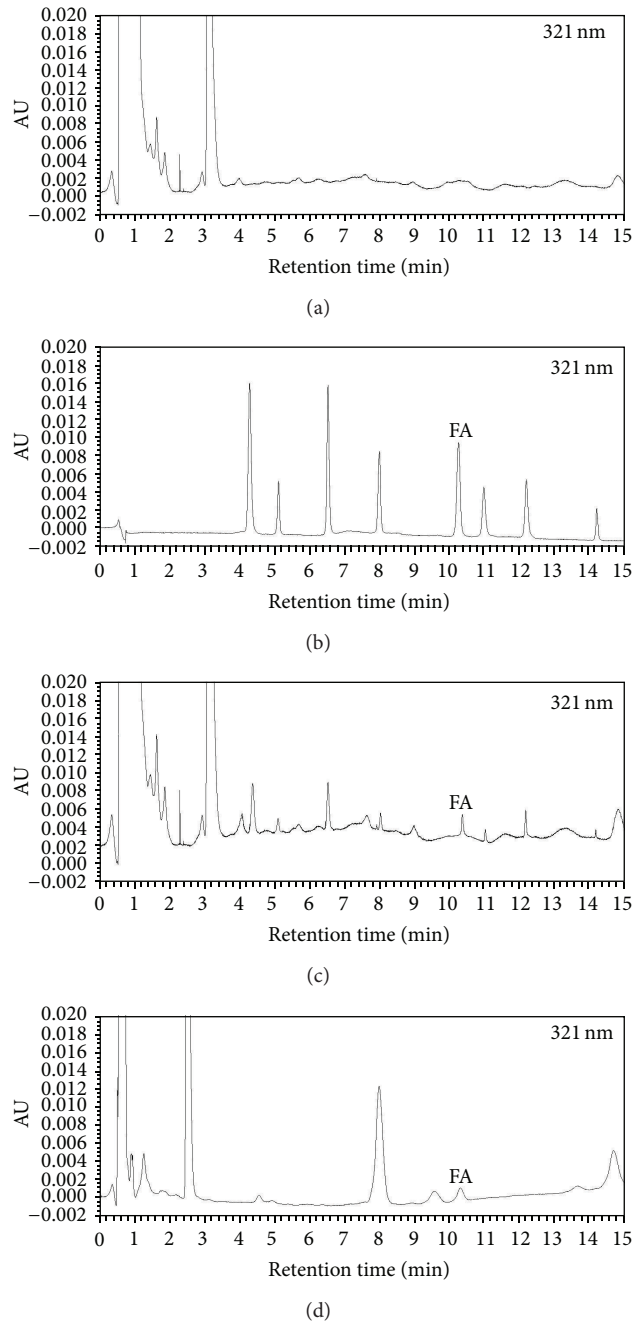

Figure 2: Typical chromatogram of samples in each group: (a) blank plasma; (b) eight reference compounds; (c) positive control; (d) plasma from rat following intragastrically administrated with OD freeze-dried powder; FA refers to ferulic acid. All of the samples were scanned under the wavelength of 321 nm.

well separated. They were ursolic acid (223 nm), oleanolic acid (224 nm), kaempferol (366 nm), p-coumaric acid (308 nm), FA (321 nm), rutin (255 nm, scopolamine lactone (228 nm), and caffeic acid (325 nm). FA was well separated at the wavelength of 321 nm after 10.29 min. On the OD test samples as shown in Figure 1(c), maximum absorption of FA was detected at the wavelength of 321 nm after 10.26 min. On the basis of these results, compared with blank methanol in Figure 1(a), we may conclude that FA is present in OD, and it is one of the chemical compounds in OD.

3.2. Detection of Absorbable Compounds in the Plasma of Rats Receiving Intragastrically Administrated OD Decoction by UPLC-PDA. Chromatography conditions were the same as tested above. As show in Figure 2(b), FA in mother solution achieved good separation at 321 nm after a time of 10.25 min. After orally administering OD to the rats, the plasma was tested, as show in Figure 2(d); maximum absorption of FA occurred at the wavelength of 321 nm after 10.29 min. Compared with blank plasma in Figure 2(a) and positive control in Figure 2(c), we found that FA could be detected in plasma of rats administrated with OD, not in blank plasma. Thus, we may safely conclude that FA could be absorbed into the blood circulation of rats, as a bioactive compound in OD. We believe that the 2 critical elements contributing to the results were the concentration of plasma and the method of preparation, which were based on a number of preliminary experiments.

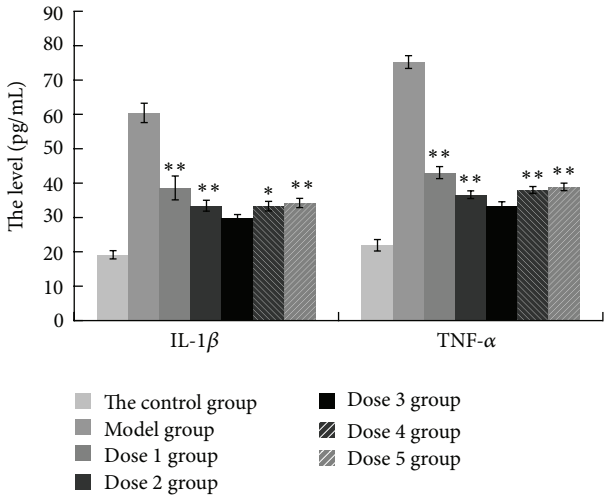

FIGURE 3: ELISA analysis of IL-1β and TNF-α in plasma of CIA rats following 5 different doses of FA (ferulic acid). And the control group and model group were also tested. The values in each group are represented as means ± SD. Statistics showing for significant difference compared with dose 3 group were marked ($^{**}P < 0.01$).

3.3. Selection of the Optimal Dose of FA for the CIA Rats. Figure 3 shows the levels of IL-1β and TNF-α in rat serum in each group: on the 42nd day, the levels of IL-1β and TNF-α in the model group were 60.41, 75.22 pg/mL, and both increased compared with the normal group, which were 19.15, 21.93 pg/mL; the levels of IL-1β and TNF-α after intervention both decreased in each group compared with the model group ($P < 0.01$); among all of the intervention groups, the levels of IL-1β and TNF-α were 29.81, 33.26 pg/mL and appeared to be the lowest in dose 3 group. Compared to dose 3 group, the levels of IL-1β and TNF-α in other dose groups were significantly higher ($P < 0.01$). According to our results, dose 3 group had the greatest effect in decreasing the level of IL-1β and TNF-α. Thus, we can conclude that the dose in 1.28 μg/g/d was the optimal dose of FA for the intervention.

3.4. Effect of Optimal FA and OD Decoction Dose on CIA Rats. The signs of arthritis appeared in the experimental rats 5–7 days after immunization. As shown in Figure 4, on the 14th day, the ankle and toe joints of rats in the model group showed more obvious redness, swelling, and hyperemia than before; redness, swelling, and hyperemia were simultaneously observed at both upper limbs of some rats. The rats in the model group were evaluated at that time; the replication rate of the CIA model reached 95%. On the 28th day, the rats in the model group were inactive and drowsy, ate and drank less, and reacted slowly when the cage was disturbed. The swelling of joints was more severe than before, and some rats had subcutaneous ecchymoses. Regarding the rats in the FA and OD groups, redness and swelling of joints of both lower limbs were reduced; hyperemic and swollen skin at the heels showed slight shrinkage; red spots and ecchymoses of joints were reduced compared to the model group. However, more pronounced changes of this kind were observed in the OD group. On the 42nd day, rats in the model group showed matted hair and increased joint symptoms; both lower limbs of some rats had reduced movement or complete loss of movement. In the FA group, redness and swelling of the joints were gradually alleviated, red spots and ecchymoses of joints faded away, and hyperemic and swollen skin at the heels showed obvious shrinkage. In the OD group, the decrease in redness and swelling of joints was more obvious than in the FA group; red spots and ecchymoses of joints also faded away, and the shrinkage on the shin was much greater than in the FA group (see Figure 4 for all the changes). On the 42nd day, compared with model group, there were no obvious redness, swelling, or hyperemia of the paw in the OD group, nor red spots or ecchymoses, only some slight skin shrinkage could be observed. All the pictures recorded in different times were shown in Figure 4.

The X-ray images showed some changes. In Figure 5(a), the control group had no swelling of soft tissues around the ankle joints, and the toe joint spaces were clear. On the 14th day, the X-ray films of rats in the model group showed swelling of tissues surrounding the ankle joints, but the joint spaces were still clear. On the 28th day, vague and narrow toe joint spaces of some rats in model group were observed, when it came to the 42nd day, the joint spaces was still unclear and even aggravated. See the change pointed out by the white arrow. In Figure 5(b), there were obvious changes between model group and FA, OD groups. When it came to the 42nd day, see the places pointed out by the white arrow in Figure 5(b), we observed that the swelling of soft tissues in OD group reduced, in comparison with the model group. And the ankle joint spaces in the FA and OD group were slightly more visible than in the model group, especially the OD group, but not as clear as in the control group. These results may indicate that both of FA and OD have the curative effect on swelling and arteriostenosis in CIA, and the OD' effect was more obvious than FA.

In HE staining test, as shown in Figure 6, the black spots refer to inflammatory cell infiltration. In Figure 6(a), no obvious abnormality was found in synovial tissues in the control group. Fourteen days after immunization, some inflammatory cell infiltration was observed in the synovial tissues of rats in the model group. On the 28th and 42nd days, a large number of inflammatory cells could be seen in the model group. In Figure 6(b), on the 28th day, no obvious inflammatory cell infiltration difference was observed among model and FA and OD groups. On the 42nd day, inflammatory cell infiltration in FA and OD groups was alleviated compared with 28th day. At the lower left of all HE pictures, a scale bar of 200 μm was marked; at the lower right, a magnified view was shown 14 times enlarged from the original. These results may indicate that FA and OD have the effect of alleviating inflammatory cell infiltration.

Each rat was weighted every 2 weeks. In the 28th day, we compared with the record in 14th day; in 42nd day, we compared with the record in 28th day. And we recorded the difference value as weigh gain. As shown in Figure 7, in 28th day, the model group got the lowest value of 8.72 g. FA group got the value of 9.22 g, which had no significant difference compared with model group ($P > 0.1$). OD group

Figure 4: General conditions of joints from 3 groups from day 0 to day 42, including the model group, FA group, OD (*Oldenlandia diffusa*) group. (a) represents the model group every 14 days. (b) represents 3 groups every 14 days.

got the value of 9.64 and had significant difference compared with model group ($P < 0.01$). In 42nd day, the model group got the lowest value of 7.91 g. FA group got the value of 8.66 g, which had significant difference compared with model group ($P < 0.05$). OD group got the value of 9.46 and had significant difference compared with model group ($P < 0.01$). In 42nd day, we compared FA group with OD group and found significant difference ($P < 0.01$). According to these results, rats in FA and OD group grew faster than model group, but it was obviously on 42nd day.

Assessment of the degree of paw swelling of rats in each group was carried out on 28th day and 42nd day. As shown in Figure 8, on 28th day, FA group got the swelling degree of 8.1 mm, and OD group was 7.45 mm. Compared with the model group of 8.48 mm, there was no significant difference ($P > 0.2$). On 42nd day, the degree of paw swelling in the FA and OD groups showed a downtrend compared with the model group, and the difference was statistically significant ($P < 0.01$); FA got 7.76 mm, OD got 6.92 mm, and the model group got 8.99 mm. Meanwhile, neither on 28th day nor 42nd day was there significant difference compared between FA group and OD group ($P > 0.08$). These results may indicate that both FA and OD had the effect of detumescence in CIA.

As shown in Figure 9, on both 28th day and 42nd day, the control group got zero degree of arthritis index. As the immune time progressed, the arthritis index integrals

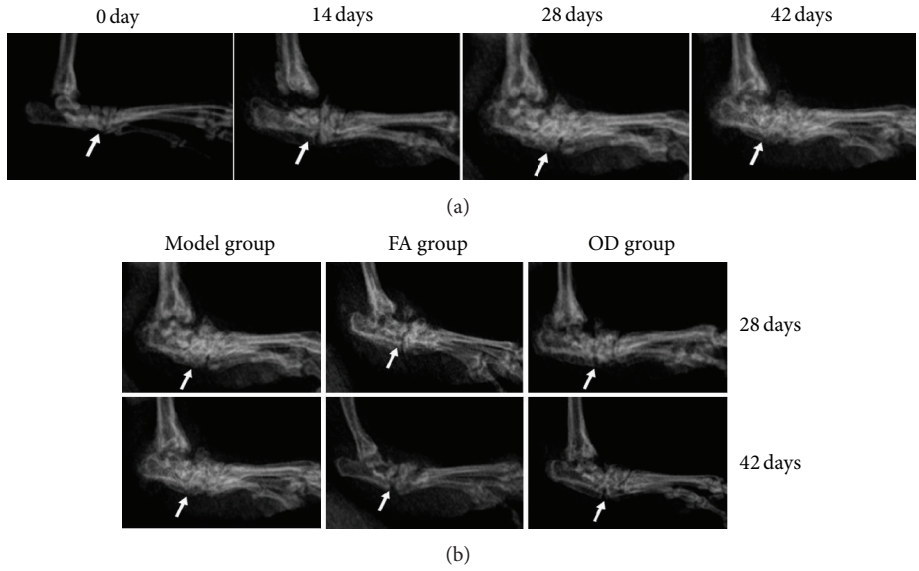

FIGURE 5: X-ray films of joints from 3 groups every 14 days. (a) represents the model group from day 0 to day 42. (b) represents 3 groups every 14 days. The joint change in each group was marked with white arrow.

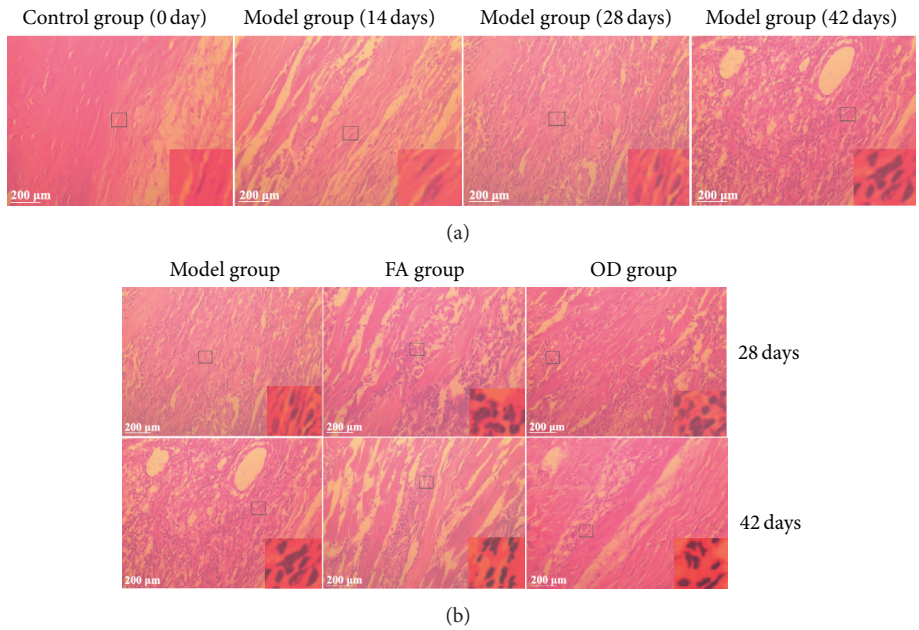

FIGURE 6: HE staining of joints from 3 groups every 14 days. (a) represents the model group from day 0 to day 42. (b) represents 3 groups every 14 days. At the left below of all HE pictures, a scale bar of 200 μm was marked; at the right below, a magnified view was shown 14 times enlarged from the original.

of the 3 groups showed an uptrend. On 28th day, the index in the model group was 8.06. FA group got 7.5. OD group got 6.95. Compared with model group, OD group had significant difference ($P < 0.01$). On 42nd day, the downtrend in FA and OD groups was significantly greater compared with the model group ($P < 0.01$); FA group got the degree of 6.55, OD group got 5.68, and model group got 7.27, and the decrease in the FA group was much more pronounced than in the OD group ($P < 0.01$).

The ELISA test of the serum of rats in each group was performed on the 28th and 42nd day to detect the inflammatory cytokines in serum (see Figure 10 for the levels of IL-1β and TNF-α in the rat serum in each group). On 28th day, the levels of IL-1β and TNF-α in the serum of the FA group were 39.13 pg/mL and 46.44 pg/mL, compared with the model group of 46.56 pg/mL and 54.74 pg/mL; FA group showed a significant downtrend ($P < 0.01$); the levels of IL-1β and TNF-α in the serum of the OD group were 32.69 pg/mL

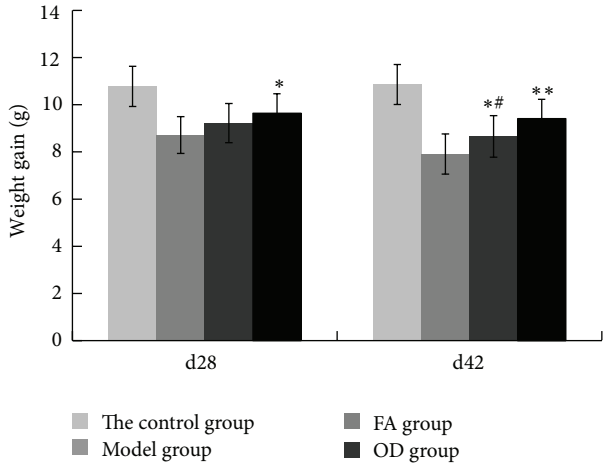

Figure 7: Weight gain records of 4 groups on 28th day and 42nd day, including control, model, FA, and OD groups. The values in each group are means ± SD. In 28th day and 42nd day, statistics in OD group are shown for significant difference ($^{*}P < 0.05$, $^{**}P < 0.01$) compared with the model group. In 42nd day, statistics in FA group are shown for significant difference ($^{\#}P < 0.05$) compared with the OD group.

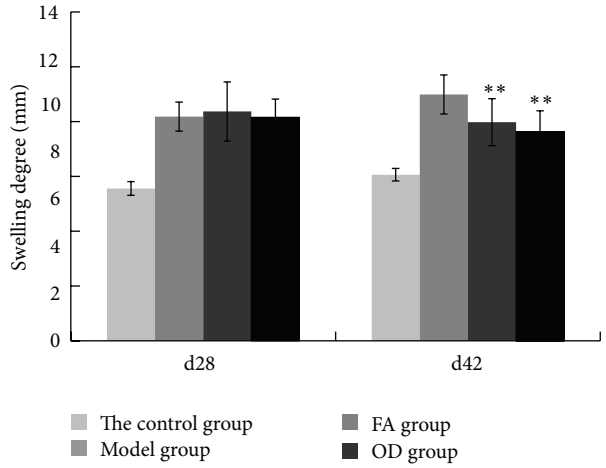

Figure 8: Degree of swelling of 4 groups on 28th day and 42nd day, including control, model, FA, and OD groups. The paws in each group are means ± SD. On 42nd day, statistics in the FA and OD groups are shown for significant difference ($^{*}P < 0.05$, $^{**}P < 0.01$) compared with the model group.

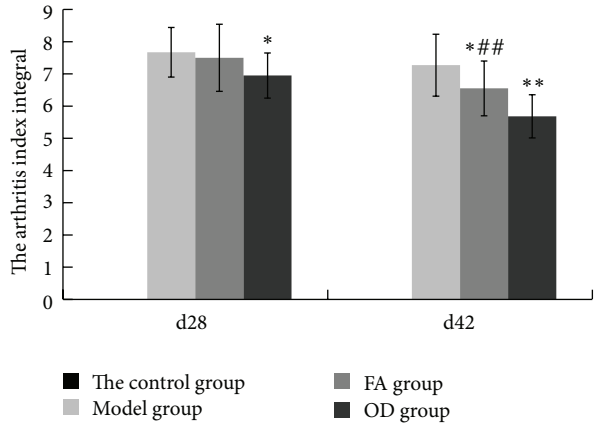

Figure 9: Arthritis index records of 4 groups on 28th day and 42nd day, including control, model, FA and OD groups. The values in each group are means ± SD. Statistics in the FA and OD groups are shown for significant difference ($^{*}P < 0.05$, $^{**}P < 0.01$) compared with the model group. On 42nd day, statistics in the FA group are shown for significant difference ($^{\#\#}P < 0.01$) compared with the OD group.

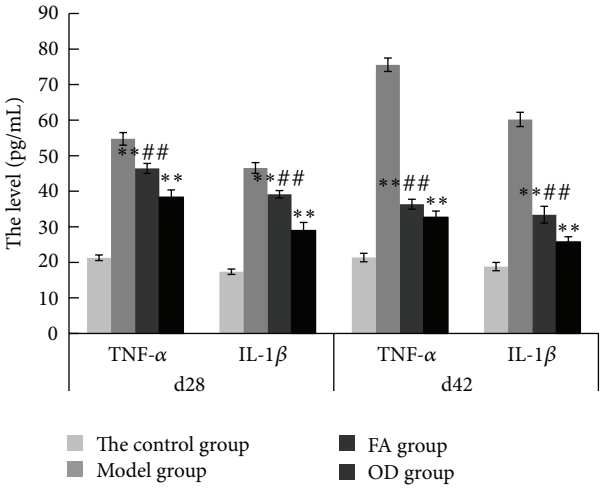

Figure 10: ELISA records of 4 groups on 28th day and 42nd day, including control, model, FA, and OD groups. The values in each group are represented as means ± SD. Statistics in the FA and OD groups are shown for significant difference ($^{**}P < 0.01$) compared with the model group. Statistics in the FA group are shown for significant difference ($^{\#\#}P < 0.01$) compared with the OD group.

and 38.31 pg/mL, compared with the model group; OD group showed a significant downtrend ($P < 0.01$). On 42nd day, the levels of IL-1β and TNF-α in the serum of the FA group were 33.40 pg/mL and 36.33 pg/mL, compared with the model group of 60.19 pg/mL and 75.58 pg/mL, FA group showed a significant downtrend ($P < 0.01$); the levels of IL-1β and TNF-α in the serum of the OD group were 25.76 pg/mL and 28.97 pg/mL, compared with the model group; OD group showed a significant downtrend ($P < 0.01$). Interestingly, on both 28th day and 42nd day, the level of inflammatory cytokines in the FA group was higher than in the OD group, and the difference was statistically significant ($P < 0.05$). This result may indicate that both FA and OD had the effect of reducing the level of IL-1β and TNF-α in CIA, and OD was more effective than FA.

4. Discussion

In clinical therapies, traditional Chinese medicines are mostly orally administered, and the bioactive compounds contained in them can take effect only after being absorbed into the blood [19]. Accordingly, it was necessary to explore the absorbable bioactive compounds. Previously, HPLC has been frequently applied in the quality control of OD [20], and the compounds detected were mostly triterpenoids,

sterols, iridoid glycosides, polypeptides, flavonoids, ursolic acids, oleanolic acids, and polysaccharides [12]. However, the metabolic processes involved in the biological action of OD have not been studied. In contrast to previous studies, which used the HPLC-method, we used the UPLC-method. UPLC significantly reduces the analysis time and solvent consumption and improves the flexibility and separation efficiency [21]. As a result, we have been able to identify the absorbable bioactive compounds contained in OD and found that FA could be absorbed into the blood of rats. As one of the mainstream approaches to study traditional Chinese medicine, this method paved a road for the following research.

In the pathological process of CIA, inflammatory cells produce reactive oxygen metabolites such as superoxide anions (e.g., O^{2-}), which induce lipid peroxidation and biomembrane damage [22] and produce inflammatory cytokines such as TNF-α and IL-1 at the same time. These substances destroy articular cartilage [23] and mediate a series of pathological reactions such as arthrocele and joint deformity [24]. As shown in Figures 4 and 5, the condition of the model group deteriorated with time, and inflammatory cells and inflammatory cytokines increased as time progressed, as shown in Figures 6 and 10. Thus, the levels of TNF-α and IL-1β in plasma may reflect the activity of inflammatory cells [25]. A previous report has indicated that FA had the ability to decrease the levels of hydrogen peroxide-induced IL-1β, TNF-α, MMP-1, and MMP-13, thereby reducing bone destruction [26], synovitis, and the erosion of cartilage in antigen-induced arthritis [27]. Because of their purported protective effects on joints, FA and OD (which contains FA) were administered to CIA rats, and, as shown in Figures 4–10, the animals' symptoms ware ameliorated, the number of inflammatory cells decreased, and the levels of IL-1β and TNF-α declined by day 28 and day 42. Both FA and OD demonstrated an anti-inflammatory effect on collagen-induced arthritis. It should be noted that a comparison of the treatment effects of FA and OD indicated that the OD group had a better therapeutic outcome, especially regarding general conditions and the level of inflammatory cytokines.

Figure 4(b) shows that the paws of the rats in the OD group had less swelling and hyperemia than those in the FA group, on both day 28 and day 42. Furthermore, statistical analysis revealed that the arthritis index was lower in the OD group on both day 28 and day 42, as shown in Figure 9. Moreover, Figure 10 shows that the levels of IL-1β and TNF-α in the OD group were lower than in the FA group on both day 28 and day 42 ($P < 0.01$). These results show that the OD group experienced a better curative effect than the FA group. We suggest that the reason for this is that OD contains multiple bioactive compounds, which act through multitarget pathways. Although our study has only demonstrated that FA was one of the bioactive compounds in OD, previous research has indicated that ursolic acid extracted from OD has a suppressive effect on rheumatoid arthritis by inhibiting paw swelling and plasma PGE(2) production [28]. In addition, hentriacontane, one of the constituent compounds of OD, exerts its anti-inflammatory effect through the regulation of the activation of nuclear factor-κB and caspase-1 [29]. Furthermore, both ursolic acid and oleanolic acid have demonstrated free radical scavenging activity [30]. Thus, OD's protective effect on joints appears to occur through multiple ways due to the various antiarthritis effects exerted by its constituent bioactive compounds. Since FA is just one of several bioactive compounds contained in OD, it exerts its effect through fewer pathways relative to OD. This can explain why OD has a better therapeutic effect than FA.

5. Conclusion

All of the above results may be related to the anti-inflammatory effects of FA contained in OD. Since FA is just one of several bioeffective compounds contained in OD, our results indicate that OD could have a better anti-inflammatory effect on the symptoms of CIA than FA. As shown in Figures 4–10, all of the results from the OD group were better than FA group, indicating that there may be several pathways through which OD exerts its effects. Such multitarget pathways may be the reason why traditional Chinese medicine has shown to be more effective than single-target Western medications in the treatment of CIA. The findings of this study offer a new direction for further studies of the pharmacodynamic bioactive compounds in OD and BZXD.

Abbreviations

OD: *Oldenlandia diffusa*
FA: Ferulic acid
CIA: Collagen induced arthritis
UPLC-PDA: Ultra performance liquid chromatography photo-diode array
RA: Rheumatoid arthritis
BZXD: Bizhongxiao decoction.

Conflict of Interests

The authors declare that there is no conflict of interests regarding the publication of this paper.

Authors' Contribution

Hao Zhu, Qing-Hua Liang, Xin-Gui Xiong, Jiang Chen, Dan Wu, Yang Wang, Bo Yang, Yang Zhang, Yong Zhang, and Xi Huang contributed equally to this paper.

Acknowledgments

This project was supported by National Natural Science Foundation of China (Grant no. 81102564), Specialized Research Fund for the Doctoral Program of Higher Education (Grant no. 20110162120004), Central South University plans to boost the freedom to explore young teachers project (Grant no. 2011QNZT154), Key-discipline construct programs of Hunan province, and SATCM.

References

[1] A. Gonzalez, H. M. Kremers, C. S. Crowson et al., "The widening mortality gap between rheumatoid arthritis patients and the general population," *Arthritis & Rheumatism*, vol. 56, no. 11, pp. 3583–3587, 2007.

[2] D.-Y. Chen, Y.-M. Chen, H.-H. Chen, C.-W. Hsieh, C.-C. Lin, and J.-L. Lan, "Increasing levels of circulating Th17 cells and interleukin-17 in rheumatoid arthritis patients with an inadequate response to anti-TNF-α therapy," *Arthritis Research & Therapy*, vol. 13, no. 4, article R126, 2011.

[3] S. L. Gaffen, "Structure and signalling in the IL-17 receptor family," *Nature Reviews Immunology*, vol. 9, no. 10, pp. 556–567, 2009.

[4] P. V. Voulgari, E. Kaltsonoudis, C. Papagoras, and A. A. Drosos, "Adalimumab in the treatment of rheumatoid arthritis," *Expert Opinion on Therapeutic Patents*, vol. 12, no. 12, pp. 1679–1686, 2012.

[5] Y. J. Guo, J. Chen, X. G. Xiong, D. Wu, and H. Zhu, "Effect of bizhongxiao decoction and its decomposed formulas on collagen-induced arthritis in rat synovial effects of IL-1 and TNF," *China Journal of Modern Medicine*, vol. 22, no. 3, pp. 6–10, 2012.

[6] X.-Q. Xun, X.-G. Xiong, J. Chen et al., "Effects of heat-clearing and detoxicating (Bizhongxiao decoction) on bone erosion of rheumatoid arthritis: Compared with combination of methotrexate and sufasalazine therapy," *Journal of Clinical Rehabilitative Tissue Engineering Research*, vol. 14, no. 41, pp. 7696–7699, 2010.

[7] A.-Y. Wang, Q.-H. Liang, J. Chen et al., "Effect of bizhongxiao decotion on TNF-alpha and interleukin-1beta in plasma of rats with C II-induced rheumatoid arthritis," *Journal of Central South University of Technology*, vol. 29, no. 3, pp. 266–269, 2004.

[8] C. Y. Li, Q. H. Liang, A. Y. Wang et al., "Effect of bizhongxiao decoction on synovial tumor necrosis factor-α gene in rats with collagen-II Induced arthritis," *Journal of TCM University of Hunan*, vol. 26, no. 6, pp. 11–14, 2006.

[9] Y. Zhao, H. H. Qu, and Q. G. Wang, "New method for analyzing pharmacodynamic material basis of traditional Chinese medicines," *China Journal of Chinese Materia Medica*, vol. 38, no. 17, pp. 2906–2910, 2013.

[10] Y.-J. Zhou, K.-S. Wu, G.-Y. Zeng et al., "Studies on constituents of oldenlandia diffusa," *China Journal of Chinese Materia Medica*, vol. 32, no. 7, pp. 590–593, 2007.

[11] C.-C. Lin, C.-L. Kuo, M.-H. Lee et al., "Extract of Hedyotis diffusa Willd influences murine leukemia WEHI-3 cells In vivo as well as promoting T- and B-cell proliferation in leukemic mice," *In Vivo*, vol. 25, no. 4, pp. 633–640, 2011.

[12] S.-J. Kim, Y.-G. Kim, D.-S. Kim et al., "Oldenlandia diffusa ameliorates dextran sulphate sodium-induced colitis through inhibition of NF-κB activation," *The American Journal of Chinese Medicine*, vol. 39, no. 5, pp. 957–969, 2011.

[13] X. P. Sun and J. Yan, "The effects of sodium ferulate on the serum expression of IL-15, IL-23, TGF- B in the adjuvant arthritis rats," *HeiLongJiang Medcine and Pharmacy*, vol. 36, no. 2, pp. 9–10, 2013.

[14] F. Li, Y. Q. Tian, F. X. Zhang, L. J. Sun, J. M. Tao, and J. H. Yao, "Effects of sodium ferulate on vascular endothelial growth factor and tumor necrosis factor-α in patients with rheumatoid arthritis," *China Pharmacy*, vol. 18, no. 23, pp. 1794–1796, 2007.

[15] X. Huang, F. Qin, H.-M. Zhang et al., "Cardioprotection by Guanxin II in rats with acute myocardial infarction is related to its three compounds," *Journal of Ethnopharmacology*, vol. 121, no. 2, pp. 268–273, 2009.

[16] W. Wei, X. M. Wu, and Y. J. Li, *Experimental Methodology of Pharmacology*, Peoples Medical Publishing House, 2010.

[17] T. R. Mikuls and J. O'Dell, "The changing face of rheumatoid arthritis therapy: results of serial surveys," *Arthritis & Rheumatism*, vol. 43, no. 2, pp. 464–465, 2000.

[18] J. S. Smolen, J. R. Kalden, D. L. Scott et al., "Efficacy and safety of leflunomide compared with placebo and sulphasalazine in active rheumatoid arthritis: a double-blind, randomised, multicentre trial," *The Lancet*, vol. 353, no. 9149, pp. 259–266, 1999.

[19] Y. Jiang, B. David, P. Tu, and Y. Barbin, "Recent analytical approaches in quality control of traditional Chinese medicines—a review," *Analytica Chimica Acta*, vol. 657, no. 1, pp. 9–18, 2010.

[20] Y. Ni, L. Zhang, J. Churchill, and S. Kokot, "Application of high performance liquid chromatography for the profiling of complex chemical mixtures with the aid of chemometrics," *Talanta*, vol. 72, no. 4, pp. 1533–1539, 2007.

[21] L. Z. Yan, Y. F. Wang, and Q. R. Yu, "HPLC-TOF-MS analysis of metabolites of diffusa effective extracts in rats," *China Journal of Chinese Materia Medica*, vol. 36, no. 10, pp. 1301–1304, 2011.

[22] J. Min, W. He, M. Z. Ao, and Y. F. Dai, "Study on anti-oxidation effect and cytokines of total saponins of panax japonicus in collagen induced arthritis rats," *Pharmacology and Clinics of Chinese*, vol. 28, no. 4, pp. 48–50, 2012.

[23] X. J. Luo, X. R. Mo, and L. L. Zhou, "The expression and activity of NF-κB and AP-1in collagen arthritis synovial tissue in mice," *Basic & Clinical Medicine*, vol. 32, no. 11, pp. 1355–1356, 2012.

[24] A. M. Vasiliev, R. N. Vasilenko, N. L. Kulikova et al., "Structural and functional properties of IL-4σ2, an alternative splice variant of human IL-4," *Journal of Proteome Research*, vol. 2, no. 3, pp. 273–281, 2003.

[25] J.-M. Dayer, "The pivotal role of interleukin-1 in the clinical manifestations of rheumatoid arthritis," *Rheumatology*, vol. 42, no. 2, pp. 3–10, 2003.

[26] M. P. Chen, S. H. Yang, C. H. Chou et al., "The chondroprotective effects of ferulic acid on hydrogen peroxide-stimulated chondrocytes: inhibition of hydrogen peroxide-induced pro-inflammatory cytokines and metalloproteinase gene expression at the mRNA level," *Inflammation Research*, vol. 59, no. 8, pp. 587–595, 2010.

[27] C. W. Kong, L. B. Chen, H. Wang et al., "Effect of sodium ferulate on antigen induced arthritis in rats," *Medical Journal of Wuhan University*, vol. 32, no. 1, pp. 40–43, 2011.

[28] S.-Y. Kang, S.-Y. Yoon, D.-H. Roh et al., "The anti-arthritic effect of ursolic acid on zymosan-induced acute inflammation and adjuvant-induced chronic arthritis models," *Journal of Pharmacy and Pharmacology*, vol. 60, no. 10, pp. 1347–1354, 2008.

[29] S.-J. Kim, W.-S. Chung, S.-S. Kim, S.-G. Ko, and J.-Y. Um, "Anti-inflammatory effect of Oldenlandia diffusa and its constituent, hentriacontane, through suppression of caspase-1 activation in mouse peritoneal macrophages," *Phytotherapy Research*, vol. 25, no. 10, pp. 1537–1546, 2011.

[30] K. M. Wójciak, R. Paduch, A. Matysik-Woźniak, P. Niedziela, and H. Donica, "The effect of ursolic and oleanolic acids on human skin fibroblast cells," *Folia Histochemica et Cytobiologica*, vol. 49, no. 4, pp. 664–669, 2011.

Hindawi Publishing Corporation
Evidence-Based Complementary and Alternative Medicine
Volume 2014, Article ID 170959, 14 pages
http://dx.doi.org/10.1155/2014/170959

Research Article

Investigation of the Chemical Changes from Crude and Processed Paeoniae Radix Alba-Atractylodis Macrocephalae Rhizoma Herbal Pair Extracts by Using Q Exactive High-Performance Benchtop Quadrupole-Orbitrap LC-MS/MS

Gang Cao,[1,2] Qinglin Li,[3] Hao Cai,[1] Sicong Tu,[4] and Baochang Cai[1,2]

[1] *College of Pharmacy, Nanjing University of Chinese Medicine, Nanjing 210023, China*
[2] *Research Center of TCM Processing Technology, Zhejiang Chinese Medical University, Hangzhou 310053, China*
[3] *Zhejiang Cancer Hospital, Hangzhou 310022, China*
[4] *Faculty of Medicine, University of New South Wales, Sydney, NSW 2031, Australia*

Correspondence should be addressed to Hao Cai; haocai_98@126.com

Received 20 January 2014; Revised 7 March 2014; Accepted 20 March 2014; Published 4 May 2014

Academic Editor: Shi-Biao Wu

The Paeoniae Radix Alba-Atractylodis Macrocephalae Rhizoma herbal pair is mainly used for regulating the functions of liver and spleen, benefiting *qi*, and nourishing blood. However, the bioactive compounds for the pharmacological activities of the crude and processed Paeoniae Radix Alba-Atractylodis Macrocephalae Rhizoma herbal pair extracts are still unclear to date. In the present study, Q Exactive high-performance benchtop quadrupole-Orbitrap LC-MS/MS was applied to identify the complicated components from crude and processed Paeoniae Radix Alba, crude and processed Atractylodis Macrocephalae Rhizoma, and their crude and processed herbal pair extracts. 123 and 101 compounds were identified in crude and processed Paeoniae Radix Alba samples, respectively. Meanwhile, 32 and 26 compounds were identified in crude and processed Atractylodis Macrocephalae Rhizoma samples, respectively. In the crude and processed Paeoniae Radix Alba-Atractylodis Macrocephalae Rhizoma herbal pair extracts, co-decoction could significantly change the chemical composition of Paeoniae Radix Alba and Atractylodis Macrocephalae Rhizoma in solution. The developed method may provide a scientific foundation for deeply elucidating the processing and compatibility mechanism of Paeoniae Radix Alba and Atractylodis Macrocephalae Rhizoma.

1. Introduction

Traditional Chinese medicine (TCM) processing is regarded as a pharmaceutical technology based on TCM theory, the requirements of different syndrome treatment, the quality nature of medicine, and different demands of clinical dispensing and preparations [1]. It is one of the characteristics in application of TCM. The compatible components of prescription are composed of prepared Chinese crude drugs after TCM processing.

The prescription compatibility and TCM processing are not only two major features of clinical medication in TCM, but are also critical to distinguish TCM from natural medicine. The research on structural features, compatible effect, and material basis of the herbal pair is the important support in the study of the prescription compatibility since the herbal pair is the minimum unit in prescription of TCM [2, 3]. They play a guidance and significant role in reveal of the compatibility rule and the scientific connotation. The herbal pair compatibility theory can explain the relationship of the prescription compatibility to some extent. The research on the relationship between the herbal pair compatibility and the prescription compatibility contributes to the elucidation of the prescription compatibility mechanism and the action mechanism of treatment. There are many herbal pairs commonly used in the clinical practice of TCM, such as the herbal pairs of Paeonia Lactiflora-Liquorice, Ginseng-Aconite, and Aconite-Rhizome Zingiberis [4, 5] besides the

Table 1: Major chemical constituents identified in crude and processed Paeoniae Radix Alba and in crude and processed Paeoniae Radix Alba-Atractylodis Macrocephalae Rhizoma herbal pair.

No.	t_R (min)	Compound name	Formula	Paeoniae Radix Alba (Measured area)		Paeoniae Radix Alba-Atractylodis Macrocephalae Rhizoma herbal pair (Measured area)	
				Crude	Processed	Crude	Processed
1	0.84	6-O-galloylsucrose	$C_{19}H_{26}O_{15}$	1.8570E + 08	1.9012E + 08	4.2870E + 07	4.4158E + 07
2	0.84	Glucogallin	$C_{13}H_{16}O_{10}$	2.9739E + 08	2.5698E + 08	1.0931E + 08	—
3	1.05	Desbenzoylpaeoniflorin	$C_{16}H_{24}O_{10}$	1.6682E + 08	1.6263E + 08	9.8500E + 07	—
4	1.06	1′-O-galloylsucrose	$C_{19}H_{26}O_{15}$	3.2574E + 08	2.9123E + 08	—	—
5	1.07	1-O-glucopyranosyl paeonisuffrone	$C_{16}H_{24}O_9$	2.8667E + 08	2.3654E + 08	1.1532E + 08	—
6	1.13	Gallic acid	$C_7H_6O_5$	4.1152E + 09	4.0736E + 09	2.7186E + 09	3.1711E + 09
7	1.18	Oxypaeoniflorin sulfonate	$C_{23}H_{28}O_{14}S$	4.9527E + 07	3.5407E + 07	6.1568E + 06	8.5010E + 07
8	1.22	Ethyl gallate	$C_9H_{10}O_5$	5.1351E + 07	6.7200E + 07	1.5592E + 07	4.8337E + 07
9	1.22	6-O-galloyl desbenzoylpaeoniflorin	$C_{23}H_{28}O_{14}$	9.9020E + 07	9.5040E + 07	5.3798E + 07	—
10	1.26	6-O-glucopyranosyl-lactinolide	$C_{16}H_{26}O_9$	1.0875E + 08	1.1180E + 08	—	3.7130E + 07
11	1.30	Paeoniflorin sulfonate I	$C_{23}H_{28}O_{13}S$	5.3777E + 07	3.6391E + 07	7.3077E + 06	7.7185E + 07
12	1.30	Mudanpioside E sulfonate	$C_{24}H_{30}O_{15}S$	5.3777E + 07	3.6391E + 07	7.3077E + 06	7.7185E + 07
13	1.43	6-O-glucopyranosyl-lactinolide	$C_{16}H_{26}O_9$	7.4342E + 08	6.5904E + 08	4.0712E + 08	3.1407E + 08
14	1.64	Mudanpioside F	$C_{16}H_{24}O_8$	6.4178E + 08	6.0980E + 08	4.0130E + 08	6.6680E + 07
15	1.76	Isomaltopaeoniflorin sulfonate	$C_{29}H_{38}O_{18}S$	1.8858E + 09	1.1382E + 09	2.6277E + 08	5.8622E + 07
16	1.81	Pedunculagin	$C_{34}H_{24}O_{22}$	4.8098E + 07	—	5.6076E + 07	1.2660E + 09
17	1.97	Paeoniflorin sulfonate I	$C_{23}H_{28}O_{13}S$	3.1881E + 10	2.3387E + 10	6.6202E + 09	5.5241E + 10
18	2.25	Oxypaeoniflorin	$C_{23}H_{28}O_{12}$	2.3173E + 09	2.4115E + 09	1.6734E + 09	1.4513E + 09
19	2.36	Gallotannin	$C_{27}H_{24}O_{18}$	2.2850E + 08	2.2458E + 08	1.6284E + 08	1.6703E + 08
20	2.37	1-O-benzoylsucrose	$C_{19}H_{26}O_{12}$	1.3761E + 08	1.3161E + 08	1.1673E + 08	8.2986E + 07
21	2.41	d-catechin	$C_{15}H_{14}O_6$	3.7822E + 09	4.2278E + 09	2.6339E + 09	2.5982E + 09
22	2.63	Methyl gallate	$C_8H_8O_5$	2.3823E + 10	2.4116E + 10	2.3388E + 10	—
23	2.63	Salicylic acid	$C_7H_6O_3$	2.3823E + 10	2.4116E + 10	2.3388E + 10	1.7399E + 10
24	2.72	Albiflorin R1	$C_{23}H_{28}O_{11}$	5.2469E + 08	5.6725E + 08	5.6329E + 08	4.5647E + 08
25	3.00	Kaempferol-3,7-di-O-glucoside	$C_{27}H_{30}O_{16}$	3.8065E + 07	2.1896E + 07	3.5719E + 07	1.5513E + 07
26	3.00	Paeonoside	$C_{27}H_{30}O_{16}$	3.8065E + 07	2.1896E + 07	3.5719E + 07	1.5513E + 07
27	3.46	Galloylpaeoniflorin	$C_{30}H_{32}O_{15}$	1.3912E + 08	1.5200E + 08	1.1501E + 08	1.0863E + 08
28	3.47	Paeonolide	$C_{20}H_{28}O_{12}$	1.0622E + 07	1.1936E + 07	9.1812E + 06	—
29	3.58	6-O-glucopyranosyl-lactinolide	$C_{16}H_{26}O_9$	2.5249E + 08	2.3834E + 08	2.2675E + 08	2.1241E + 08
30	3.68	Oxypaeoniflorin	$C_{23}H_{28}O_{12}$	1.5407E + 08	—	1.4345E + 08	1.3307E + 08
31	3.76	6-O-glucopyranosyl-lactinolide	$C_{16}H_{26}O_9$	3.2664E + 08	—	3.0588E + 08	3.1627E + 08
32	3.88	Paeonilactone B	$C_{10}H_{12}O_4$	9.0325E + 07	9.3539E + 07	5.1257E + 07	8.9597E + 07
33	3.93	Isomaltopaeoniflorin	$C_{29}H_{38}O_{16}$	1.1545E + 10	1.1941E + 10	1.2282E + 10	9.4600E + 09
34	4.07	Albiflorin	$C_{23}H_{28}O_{11}$	2.9587E + 10	2.9296E + 10	2.8430E + 10	2.8684E + 10
35	4.32	Glucopyranosylalbiorin	$C_{29}H_{38}O_{16}$	2.2813E + 09	2.4109E + 08	2.0383E + 08	1.6844E + 08
36	4.34	Galloylpaeoniflorin sulfonate	$C_{30}H_{32}O_{17}S$	7.6943E + 08	5.6793E + 08	1.5501E + 08	1.4886E + 09

Table 1: Continued.

No.	t_R (min)	Compound name	Formula	Paeoniae Radix Alba (Measured area)		Paeoniae Radix Alba-Atractylodis Macrocephalae Rhizoma herbal pair (Measured area)	
				Crude	Processed	Crude	Processed
37	4.34	Galloylpaeoniflorin isomer	$C_{30}H_{32}O_{15}$	6.7592E + 08	7.4322E + 08	6.0470E + 08	5.4051E + 08
38	4.38	1,2,3,6-tetra-O-galloylglucose	$C_{34}H_{28}O_{22}$	4.6602E + 08	3.4977E + 08	4.0697E + 08	3.6901E + 08
39	4.38	Tetragalloyl glucose A	$C_{34}H_{28}O_{22}$	4.6602E + 08	3.4977E + 08	4.0697E + 08	3.6901E + 08
40	4.56	Mudanpioside F	$C_{16}H_{24}O_8$	8.4156E + 07	8.2734E + 07	7.2666E + 07	7.9227E + 07
41	4.60	Oxypaeoniflorin isomer	$C_{23}H_{28}O_{12}$	9.6610E + 08	9.8706E + 08	9.2464E + 08	8.7359E + 08
42	4.65	Gallotannin	$C_{27}H_{24}O_{18}$	6.7737E + 07	—	—	—
43	4.77	Paeoniflorin	$C_{23}H_{28}O_{11}$	5.9556E + 10	6.1356E + 10	5.9929E + 10	5.8832E + 10
44	4.89	Paeoniflorin sulfonate II	$C_{23}H_{28}O_{13}S$	1.1095E + 08	1.4567E + 08	5.5052E + 07	2.7813E + 08
45	4.98	Isogalloylpaeoniflorin sulfonate	$C_{30}H_{32}O_{17}S$	3.6742E + 07	—	—	—
46	5.05	Ethyl gallate	$C_9H_{10}O_5$	6.0669E + 07	5.4850E + 07	1.6681E + 07	2.6790E + 07
47	5.05	Methyl salicylate	$C_8H_8O_3$	6.0669E + 07	5.4850E + 07	1.6681E + 07	2.6790E + 07
48	5.15	Benzoic acid	$C_7H_6O_2$	4.0163E + 07	4.5493E + 07	2.9695E + 07	2.9727E + 07
49	5.25	Paeonol	$C_9H_{10}O_3$	6.8567E + 07	7.4129E + 07	9.9992E + 07	6.5619E + 07
50	5.25	4-hydroxy-3-methoxy acetophenone	$C_9H_{10}O_3$	6.8567E + 07	7.4129E + 07	9.9992E + 07	6.5619E + 07
51	5.31	ortho-oxypaeoniflorin	$C_{23}H_{28}O_{12}$	1.9080E + 09	1.9263E + 09	1.8723E + 09	1.6842E + 09
52	5.63	Ethyl gallate	$C_9H_{10}O_5$	1.4627E + 08	1.2812E + 08	1.0365E + 08	8.8155E + 07
53	5.63	Methyl salicylate	$C_8H_8O_3$	1.4627E + 08	1.2812E + 08	1.0365E + 08	8.8155E + 07
54	5.66	Kaempferol-3-O-glucoside	$C_{21}H_{20}O_{11}$	1.6012E + 07	1.7385E + 07	—	—
55	5.66	Astragalin	$C_{21}H_{20}O_{11}$	1.6012E + 07	1.7385E + 07	—	—
56	6.01	Eugeniin	$C_{41}H_{30}O_{26}$	2.7483E + 08	3.0279E + 08	2.8080E + 08	3.0479E + 08
57	6.01	Dihydroxymethyl benzoyl tetragalloyl glucose	$C_{41}H_{30}O_{26}$	2.7483E + 08	3.0279E + 08	2.8080E + 08	3.0479E + 08
58	6.03	1,2,3,6-tetra-O-galloylglucose isomer A	$C_{34}H_{28}O_{22}$	1.3555E + 09	—	1.1980E + 09	1.1039E + 09
59	6.03	Tetragalloyl glucose B	$C_{34}H_{28}O_{22}$	1.3555E + 09	—	—	—
60	6.08	Astragalin	$C_{21}H_{20}O_{11}$	1.5009E + 07	1.8552E + 07	1.5922E + 07	1.4002E + 07
61	6.09	Isomaltopaeoniflorin isomer	$C_{29}H_{38}O_{16}$	7.5172E + 07	—	—	—
62	6.47	1,2,3,6-tetra-O-galloylglucose isomer B	$C_{34}H_{28}O_{22}$	1.5882E + 09	—	—	1.2570E + 09
63	6.47	Tetragalloyl glucose C	$C_{34}H_{28}O_{22}$	1.5882E + 09	—	—	1.2570E + 09
64	6.85	3,6-di-O-galloyl paeoniorin	$C_{37}H_{36}O_{19}$	7.6512E + 07	—	—	—
65	6.96	1,2,3,6-tetra-O-galloylglucose	$C_{34}H_{28}O_{22}$	4.4729E + 08	4.5825E + 08	4.0642E + 08	4.2393E + 08
66	6.96	Tetragalloyl glucose D	$C_{34}H_{28}O_{22}$	4.4729E + 08	4.5825E + 08	4.0642E + 08	4.2393E + 08
67	7.35	Galloylpaeoniflorin isomer I	$C_{30}H_{32}O_{15}$	1.2156E + 10	1.2451E + 10	1.1484E + 10	1.0962E + 10
68	7.60	1-O-glucopyranosyl-8-O-benzoyl paeonisuffrone	$C_{23}H_{28}O_{10}$	4.3983E + 07	4.5347E + 07	4.4927E + 07	3.9869E + 07
69	7.71	Glucopyranosylalbiorin isomer I	$C_{29}H_{38}O_{16}$	7.2982E + 07	7.9341E + 07	—	1.8872E + 07

Table 1: Continued.

No.	t_R (min)	Compound name	Formula	Paeoniae Radix Alba (Measured area)		Paeoniae Radix Alba-Atractylodis Macrocephalae Rhizoma herbal pair (Measured area)	
				Crude	Processed	Crude	Processed
70	8.18	1-O-glucopyranosyl-8-O-benzoyl paeonisuffrone	$C_{23}H_{28}O_{10}$	7.4648E + 07	8.3204E + 07	6.5957E + 07	5.9832E + 07
71	8.31	Ortho-oxypaeoniflorin	$C_{23}H_{28}O_{12}$	2.4469E + 07	2.4504E + 07	2.3932E + 07	2.2796E + 07
72	8.45	1,2,3,4,6-Penta-O-galloyl–D-glucopyranose	$C_{41}H_{32}O_{26}$	1.1843E + 10	1.0905E + 10	1.0518E + 10	1.0489E + 10
73	8.45	Pentagalloyl glucose	$C_{41}H_{32}O_{26}$	1.1843E + 10	1.0905E + 10	1.0518E + 10	1.0489E + 10
74	8.64	Lactiflorin	$C_{23}H_{26}O_{10}$	1.0818E + 08	1.8628E + 08	1.3689E + 08	—
75	8.80	Galloylalbiroin	$C_{30}H_{32}O_{15}$	3.2696E + 09	—	—	—
76	9.17	Astragalin	$C_{21}H_{20}O_{11}$	1.0717E + 07	1.3960E + 07	1.2843E + 07	1.0582E + 07
77	9.25	Lactinolide	$C_{10}H_{16}O_4$	2.7251E + 07	2.6105E + 07	2.1735E + 07	3.2770E + 07
78	9.29	Galloylpaeoniflorin isomer II	$C_{30}H_{32}O_{15}$	2.8831E + 09	—	2.6829E + 09	2.2850E + 09
79	9.68	Glucopyranosylalbiorin isomer II	$C_{29}H_{38}O_{16}$	2.4321E + 07	2.6804E + 07	2.2576E + 07	2.4950E + 07
80	9.84	Hexagalloyl glucose	$C_{48}H_{36}O_{30}$	4.9153E + 07	—	6.8676E + 08	5.7793E + 08
81	9.95	Oxybenzoyl-oxypaeoniflorin	$C_{30}H_{32}O_{14}$	1.4385E + 07	1.6654E + 07	1.1051E + 07	1.1345E + 07
82	10.07	1-O-glucopyranosyl-8-O-benzoylpaeonisuffrone	$C_{23}H_{28}O_{10}$	3.6916E + 09	3.5634E + 09	3.1333E + 09	3.2106E + 09
83	10.29	Albiflorin R1 isomer I	$C_{23}H_{28}O_{11}$	6.3346E + 09	6.6205E + 09	5.9528E + 09	5.8736E + 09
84	10.74	Hexagalloyl glucose	$C_{48}H_{36}O_{30}$	4.9225E + 08	2.5582E + 08	1.9395E + 09	1.5439E + 09
85	10.76	Lactiflorin	$C_{23}H_{26}O_{10}$	1.2785E + 09	3.5174E + 09	9.9713E + 08	3.4524E + 09
86	10.84	Benzoylpaeoniflorin Sulfonate	$C_{30}H_{32}O_{14}S$	9.0616E + 08	6.4075E + 08	1.5946E + 08	2.1931E + 09
87	10.88	3,6-di-O-galloyl paeoniorin	$C_{37}H_{36}O_{19}$	1.6123E + 08	—	—	—
88	10.95	Ortho-oxypaeoniflorin isomer	$C_{23}H_{28}O_{12}$	5.5563E + 07	5.8774E + 07	5.7147E + 07	5.6640E + 07
89	11.52	3,6-di-O-galloyl paeoniorin	$C_{37}H_{36}O_{19}$	3.6509E + 08	3.9290E + 08	5.2162E + 08	5.3781E + 08
90	11.72	3,6-di-O-galloyl paeoniorin isomer	$C_{37}H_{36}O_{19}$	9.7356E + 08	—	1.2523E + 09	9.5929E + 08
91	11.75	Galloylalbiroin isomer I	$C_{30}H_{32}O_{15}$	2.3457E + 08	—	—	—
92	11.84	Oxypaeoniflorin sulfonate isomer	$C_{23}H_{28}O_{14}S$	2.1063E + 07	1.9747E + 07	1.3875E + 07	1.0840E + 07
93	12.15	1-O-glucopyranosyl-8-O-benzoylpaeonisuffrone	$C_{23}H_{28}O_{10}$	7.2104E + 07	7.1468E + 07	6.7309E + 07	6.5917E + 07
94	12.15	Oxybenzoyl-oxypaeoniflorin	$C_{30}H_{32}O_{14}$	1.9982E + 08	—	—	1.6891E + 08
95	12.18	Benzoyloxypaeoniflorin	$C_{30}H_{32}O_{13}$	2.0822E + 08	—	2.0163E + 08	1.9074E + 08
96	13.42	Benzoyloxypaeoniflorin isomer	$C_{30}H_{32}O_{13}$	8.6458E + 07	6.2282E + 07	7.6048E + 07	7.2791E + 07
97	13.44	Oxybenzoyl-oxypaeoniflorin isomer I	$C_{30}H_{32}O_{14}$	1.4728E + 07	1.7389E + 07	1.5360E + 07	1.6008E + 07
98	13.85	Galloylalbiroin isomer II	$C_{30}H_{32}O_{15}$	9.6403E + 07	1.2196E + 08	1.0506E + 08	1.0272E + 08
99	14.05	Oxybenzoyl-oxypaeoniflorin isomer II	$C_{30}H_{32}O_{14}$	2.5323E + 07	2.9603E + 07	2.3556E + 07	2.8526E + 07
100	14.13	Benzoyloxypaeoniflorin	$C_{30}H_{32}O_{13}$	3.8096E + 07	3.8557E + 07	3.7499E + 07	3.5800E + 07

Table 1: Continued.

No.	t_R (min)	Compound name	Formula	Paeoniae Radix Alba (Measured area)		Paeoniae Radix Alba-Atractylodis Macrocephalae Rhizoma herbal pair (Measured area)	
				Crude	Processed	Crude	Processed
101	15.07	Benzoyloxypaeoniflorin isomer I	$C_{30}H_{32}O_{13}$	1.9827E + 07	2.3616E + 07	—	—
102	15.38	Benzoyloxypaeoniflorin isomer II	$C_{30}H_{32}O_{13}$	1.1841E + 07	1.3730E + 07	—	—
103	16.01	Oxybenzoyl-paeoniflorin	$C_{30}H_{32}O_{12}$	1.8152E + 07	—	1.8435E + 07	—
104	16.95	Isobenzoylpaeoniflorin	$C_{30}H_{32}O_{12}$	1.2225E + 10	1.3228E + 10	1.2158E + 10	1.2391E + 10
105	16.95	Oxybenzoyl-paeoniflorin isomer I	$C_{30}H_{32}O_{12}$	1.2225E + 10	1.3228E + 10	1.2158E + 10	1.2391E + 10
106	17.23	Benzoylpaeoniflorin Sulfonate	$C_{30}H_{32}O_{14}S$	1.5680E + 07	1.2235E + 07	5.6573E + 06	3.5831E + 07
107	17.48	Isobenzoylpaeoniflorin isomer I	$C_{30}H_{32}O_{12}$	5.4138E + 09	5.4432E + 09	5.2522E + 09	5.3238E + 09
108	17.48	Oxybenzoyl-paeoniflorin isomer II	$C_{30}H_{32}O_{12}$	5.4138E + 09	5.4432E + 09	5.2522E + 09	5.3238E + 09
109	17.86	Benzoyloxypaeoniflorin	$C_{30}H_{32}O_{13}$	3.4347E + 07	3.4852E + 07	3.5980E + 07	3.8814E + 07
110	18.55	Benzoyloxypaeoniflorin isomer	$C_{30}H_{32}O_{13}$	1.5397E + 07	1.7656E + 07	1.7246E + 07	1.8012E + 07
111	18.69	Albiflorin R1 isomer II	$C_{23}H_{28}O_{11}$	2.0046E + 07	1.9851E + 07	2.3462E + 07	—
112	19.30	Albiflorin R1 isomer III	$C_{23}H_{28}O_{11}$	2.9827E + 06	—	—	5.6105E + 06
113	21.79	Palbinone	$C_{22}H_{30}O_4$	8.9687E + 07	1.3174E + 08	1.2834E + 08	5.7610E + 07
114	21.93	Isobenzoylpaeoniflorin isomer II	$C_{30}H_{32}O_{12}$	4.5356E + 08	4.2874E + 07	3.4016E + 08	2.7347E + 08
115	21.93	Oxybenzoyl-paeoniflorin isomer III	$C_{30}H_{32}O_{12}$	4.5356E + 08	4.2874E + 07	3.4016E + 08	2.7347E + 08
116	22.15	Paeonilactinone	$C_{10}H_{16}O_2$	7.0423E + 06	3.7108E + 06	8.0036E + 06	6.6886E + 06
117	36.46	Hederagenin	$C_{30}H_{48}O_4$	7.6725E + 07	8.1456E + 07	9.7498E + 07	4.7332E + 07
118	37.31	23-hydroxybetulinic acid	$C_{30}H_{48}O_4$	3.9836E + 07	4.0995E + 07	3.9906E + 07	2.2611E + 07
119	38.14	Astrantiagenin D	$C_{30}H_{46}O_4$	7.8714E + 06	7.9560E + 06	1.1904E + 07	3.8958E + 06
120	43.00	Astrantiagenin D isomer	$C_{30}H_{46}O_4$	4.0450E + 06	—	3.1585E + 06	—
121	45.65	Oleanolic acid	$C_{30}H_{48}O_3$	1.1266E + 08	9.4258E + 07	7.6434E + 07	4.3295E + 07
122	46.10	Betulinic acid	$C_{30}H_{48}O_3$	6.2494E + 06	2.3289E + 07	4.0543E + 07	2.3912E + 07
123	52.48	Daucosterol	$C_{35}H_{60}O_6$	1.4060E + 07	1.9624E + 07	8.5440E + 06	6.3156E + 06

Paeoniae Radix Alba-Atractylodis Macrocephalae Rhizoma herbal pair frequently used in all China dynasties [6, 7]. Paeoniae Radix Alba nourishes blood and liver, and Atractylodis Macrocephalae Rhizoma helps invigorate spleen and eliminate dampness [8–12]. Thus, the compatibility of these two medicines could help achieve the goal of purging wood from the earth, regulating the functions of liver and spleen, benefiting *qi,* and nourishing blood [13–15]. Although the compositions of these two medicines have been extensively studied, the appropriate processing method of them, such as frying, which is believed by the practitioners of traditional medicine to have the effects for enhancing the efficacy of the medicine, and their underlying compatibility mechanism are still under investigation.

The objective of this study is to investigate the qualitative, preprocessing, and postprocessing changes in the composition and compatibility of Paeoniae Radix Alba and Atractylodis Macrocephalae Rhizoma by using Q Exactive hybrid quadrupole-Orbitrap mass spectrometer combined with high-performance quadrupole precursor selection with high-resolution and accurate-mass Orbitrap detection. The work could serve as a theoretical basis for the development of medicines from Paeoniae Radix Alba and Atractylodis Macrocephalae Rhizoma, and the reasonable clinical medication. Furthermore, it provides new insights into the investigation of the herbal pair and for the study of the appropriate processing method for Chinese herbal medicines and their underlying compatibility mechanism.

Table 2: Major chemical constituents identified in crude and processed Atractylodis Macrocephalae Rhizoma and in crude and processed Paeoniae Radix Alba-Atractylodis Macrocephalae Rhizoma herbal pair.

No.	t_R (min)	Compound name	Formula	Atractylodis Macrocephalae Rhizoma (Measured area)		Paeoniae Radix Alba-Atractylodis Macrocephalae Rhizoma herbal pair (Measured area)	
				Crude	Processed	Crude	Processed
1	1.72	Protocatechuic acid	$C_7H_6O_4$	2.0389E + 07	1.4454E + 07	2.0881E + 07	2.4383E + 07
2	2.67	Protocatechuic acid isomer I	$C_7H_6O_4$	9.6661E + 07	—	—	—
3	3.24	Caffeic acid	$C_9H_8O_4$	3.6818E + 08	1.7393E + 08	2.8796E + 08	1.2882E + 08
4	3.73	Protocatechuic acid isomer II	$C_7H_6O_4$	2.0846E + 07	—	—	1.2022E + 07
5	4.21	Dictamnoside A isomer I	$C_{21}H_{36}O_9$	1.8843E + 07	2.4981E + 07	1.0636E + 07	1.3140E + 07
6	4.70	Dictamnoside A isomer II	$C_{21}H_{36}O_9$	2.8770E + 07	3.4768E + 07	1.0395E + 07	1.4208E + 07
7	5.63	Scopoletin	$C_{10}H_8O_4$	6.1458E + 07	4.1494E + 07	6.1562E + 07	5.3342E + 07
8	5.82	Dictamnoside A	$C_{21}H_{36}O_9$	9.6195E + 07	1.1991E + 08	7.5446E + 07	9.4190E + 07
9	8.77	Atracetylentriol	$C_{14}H_{16}O_3$	1.2538E + 07	5.4052E + 06	—	—
10	9.33	Ferulic acid	$C_{10}H_{10}O_4$	1.3958E + 07	9.1214E + 06	1.1912E + 07	9.6849E + 06
11	25.81	Atractylenolide I isomer	$C_{15}H_{18}O_2$	4.5224E + 09	4.2401E + 09	5.9401E + 09	6.5277E + 09
12	25.83	Atractylenolide III	$C_{15}H_{20}O_3$	2.5549E + 09	1.8023E + 09	2.8280E + 09	3.1632E + 09
13	26.17	12-methylbutyryl-14-acetyl-2E,8EZ,10E-atractylentriol	$C_{21}H_{26}O_5$	2.4755E + 07	—	—	—
14	26.95	12-methylbutyryl-14-acetyl-2E,8EZ,10E-atractylentriol isomer	$C_{21}H_{26}O_5$	7.5991E + 07	—	—	—
15	31.10	Atractylenolide II isomer	$C_{15}H_{20}O_2$	6.7883E + 09	4.5794E + 09	7.6246E + 09	7.8814E + 09
16	31.66	Atractylenolide II	$C_{15}H_{20}O_2$	2.8279E + 10	1.9902E + 10	3.0285E + 10	3.1294E + 10
17	33.44	Atractylodin	$C_{13}H_{10}O$	6.4157E + 06	—	7.0452E + 07	—
18	35.07	Atractylenolide I isomer	$C_{15}H_{18}O_2$	8.2226E + 08	1.4781E + 09	1.0831E + 09	3.2083E + 09
19	35.94	Atractylenolide I	$C_{15}H_{18}O_2$	8.8877E + 09	7.2520E + 09	8.3857E + 09	1.2742E + 10
20	39.03	12-methylbutyryl-14-acetyl-2E,8EZ,10E-atractylentriol isomer I	$C_{21}H_{26}O_5$	3.0978E + 07	3.7863E + 07	2.9171E + 07	—
21	39.81	Dibutyl phthalate	$C_{16}H_{22}O_4$	1.1372E + 08	9.8325E + 07	1.2659E + 08	1.4865E + 08
22	40.00	12-methylbutyryl-14-acetyl 2E,8EZ,10E-atractylentriol isomer II	$C_{21}H_{26}O_5$	3.8810E + 07	7.7498E + 07	3.3885E + 07	7.0522E + 07
23	40.26	Dibutyl phthalate isomer	$C_{16}H_{22}O_4$	1.0631E + 08	5.4902E + 07	6.1958E + 07	4.6227E + 07
24	41.50	14-methylbutyryl-2E,8EZ,10Es-atractylentriol	$C_{19}H_{24}O_4$	4.9587E + 07	2.8423E + 07	5.1146E + 07	4.7855E + 07
25	46.43	Spinasteryl	$C_{29}H_{48}O$	8.6778E + 06	7.9096E + 06	1.0609E + 07	7.7832E + 06
26	47.32	Atractylon	$C_{15}H_{20}O$	7.4433E + 07	5.4063E + 07	6.6146E + 07	—
27	47.37	Biatractylolide	$C_{30}H_{38}O_4$	1.0949E + 09	9.5665E + 08	1.2797E + 09	—
28	47.96	Linoleic acid	$C_{18}H_{32}O_2$	1.8499E + 08	1.5041E + 08	1.8777E + 08	2.3743E + 08
29	48.25	Linoleic acid isomer	$C_{18}H_{32}O_2$	2.1059E + 07	—	—	—
30	48.59	Biepiasterolid isomer	$C_{30}H_{38}O_4$	9.0255E + 08	7.0863E + 08	7.4011E + 08	—
31	48.90	Atractylon isomer	$C_{15}H_{20}O$	9.5308E + 07	8.7683E + 07	8.2967E + 07	1.0132E + 08
32	49.42	Palmitic acid	$C_{16}H_{32}O_2$	2.2356E + 07	2.2942E + 07	2.5949E + 07	2.0153E + 07

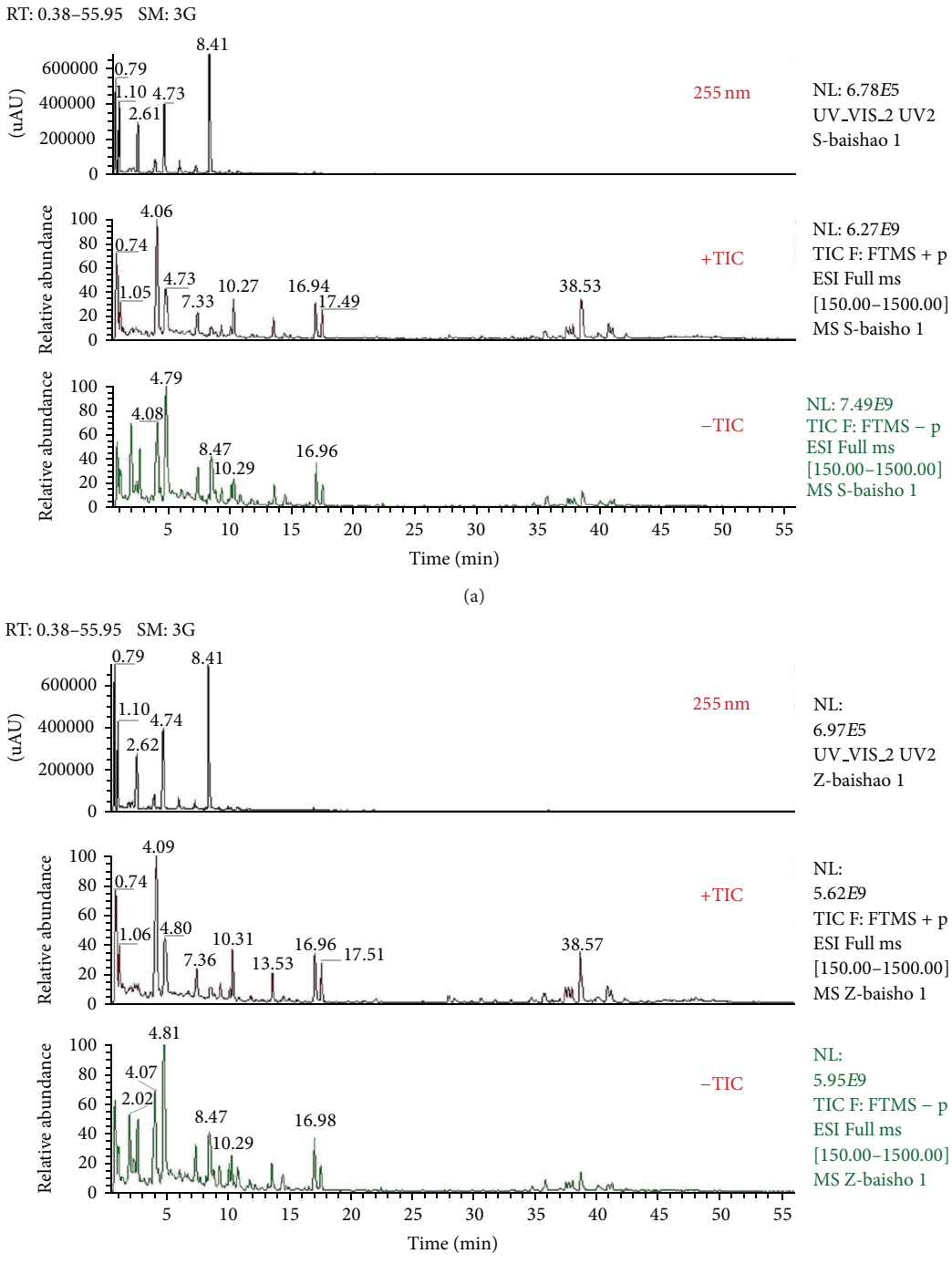

Figure 1: Total ion chromatograms of crude (a) and processed (b) Paeoniae Radix Alba obtained from both positive and negative ion modes.

2. Experimental

2.1. Chemicals, Solvents, and Herbal Materials. Paeoniae Radix Alba and Atractylodis Macrocephalae Rhizoma samples were acquired from Zhejiang suppliers. All of these herbal samples were authenticated by Professor Jianwei Chen (College of Pharmacy, Nanjing University of Chinese Medicine). HPLC-grade acetonitrile and formic acid were obtained from Merck (Darmstadt, Germany). Deionized water was purified using the Milli-Q system (Millipore, Bedford, MA, USA). All other reagents and chemicals were analytical grade.

2.2. Preparation of the Sample Solutions. The dried and powdered samples of crude and processed Paeoniae Radix Alba, crude and processed Atractylodis Macrocephalae Rhizoma, and their crude and processed herbal pair extracts (1 : 1, g/g)

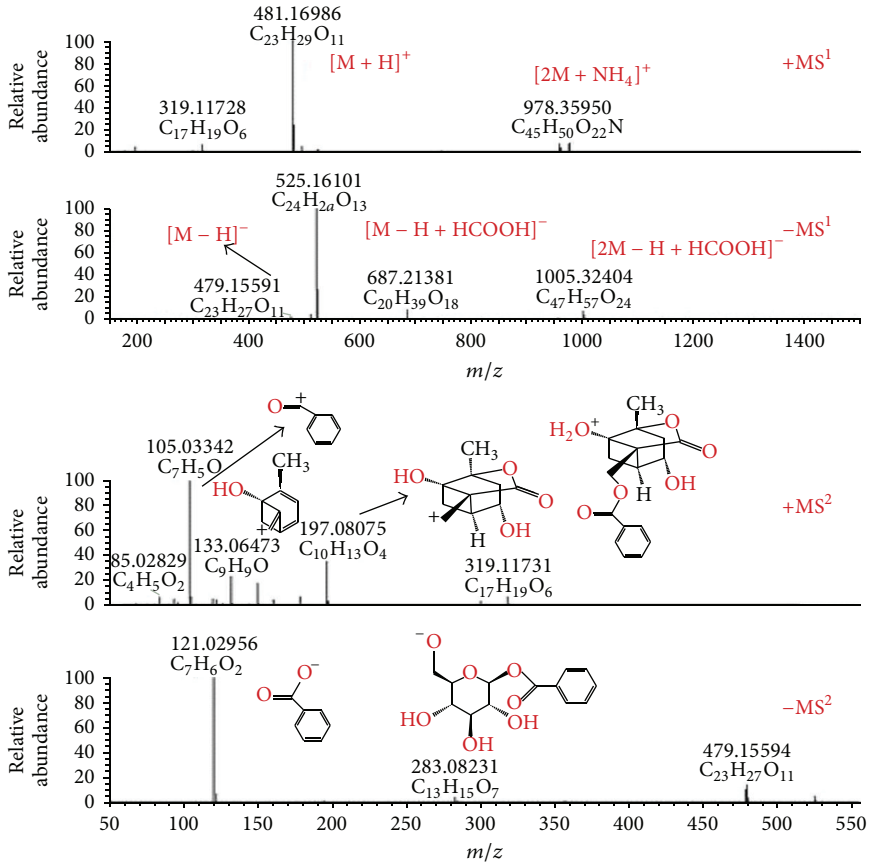

(a)

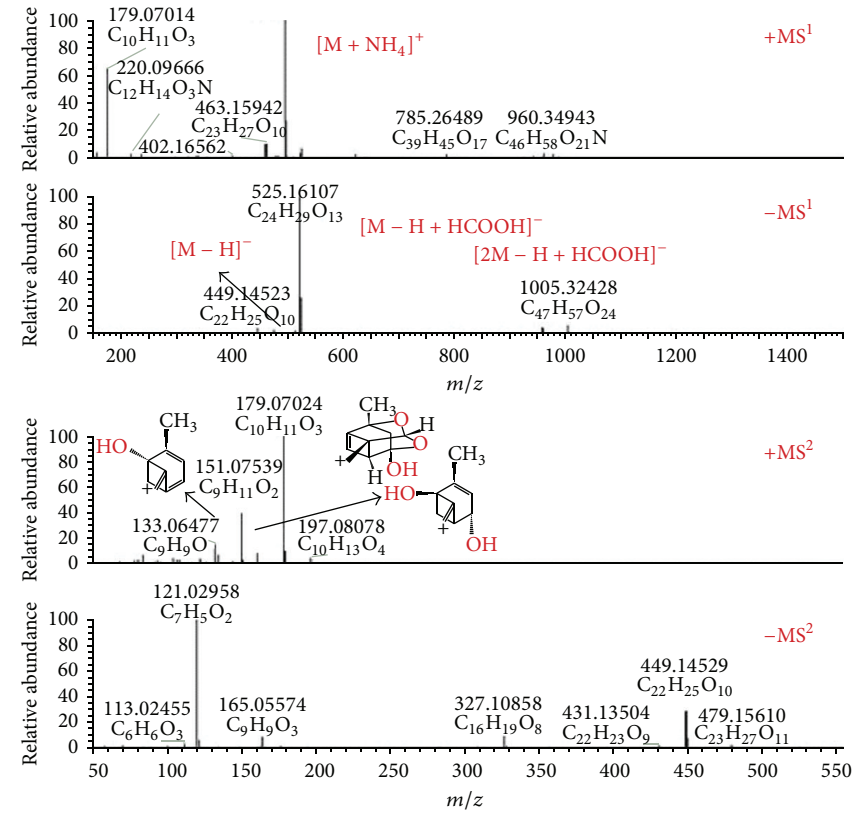

(b)

Figure 2: Continued.

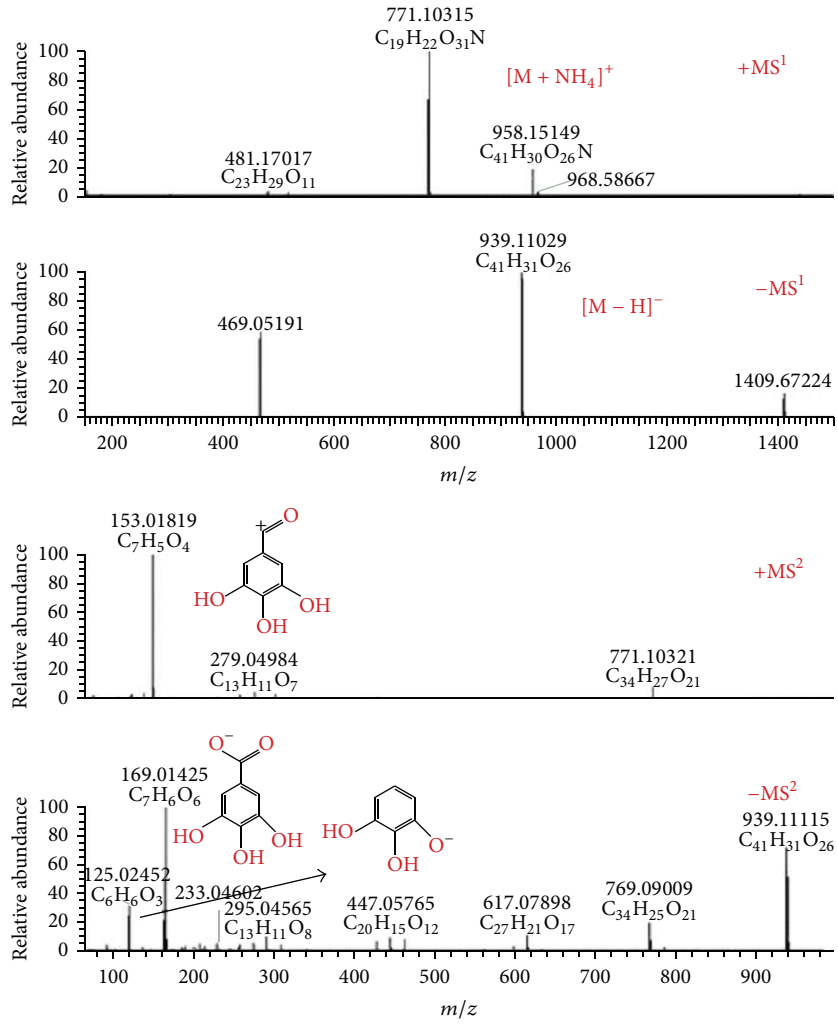

(c)

FIGURE 2: Mass spectra and proposed fragmentations of albiflorin (a), paeoniflorin (b), and 1, 2, 3, 4, 6-penta-O-galloyl-beta-D-glucopyranose (c).

were prepared. A total of 2.0 g of each sample powder was accurately weighed and transferred into a 50 mL round bottom flask with 20 mL of 70% methanol aqueous solution (v/v) and refluxed in a 80°C water bath for 1 h. The filtrate was collected after filtration and the residue was then refluxed with 20 mL of 70% methanol aqueous solution in a 80°C water bath for 1 h, the filtrate was collected again after filtration and the residue was removed. Finally, the combined filtrates were treated by rotary evaporation concentration and the resultant residue was dissolved and transferred into a 25 mL volumetric flask with 70% methanol aqueous solution to make it up to a final concentration of 0.08 g·mL^{-1}. All solutions were stored at 4°C and filtered through a 0.22 μm filter membrane before injection into the HPLC system.

2.3. Liquid Chromatography and Mass Spectrometry. Analyses were performed by using Dionex UltiMate 3000 HPLC system (Dionex, Sunnyvale, CA, USA) with a diode array detector. Detection wavelengths were set at 255 nm. A Thermo Scientific Hypersil Gold C_{18} column (100 mm × 2.1 mm, 1.9 μm) was used with a flow rate of 0.35 mL·min^{-1}. The injection volume was 5 μL, and the column temperature was maintained at 30°C. The sample separation was performed according to the previous reports with minor modification [16–18]. The mobile phase was composed of (a) aqueous formic acid (0.1%, v/v) and (b) acetonitrile under following gradient elution: 10–55% B from 0 to 40 min, 55–90% B from 40 to 51 min, 90% B from 51 to 56 min, 90–10% B from 56 to 56.1 min, and 10% B from 56.1 to 60 min. Mass spectrometry was performed on a Q Exactive high-resolution benchtop quadrupole Orbitrap mass spectrometer (Thermo Fisher Scientific, San Jose, USA) using a heated electrospray ionization (HESI-II) source for ionization of the target compounds in positive and negative ion modes. The key parameters were as follows: ionization voltage, +3.0 kV/−2.8 kV; sheath gas pressure, 35 arbitrary units; auxiliary gas, 10 arbitrary units; heat temperature, 300°C; and capillary temperature, 300°C. For

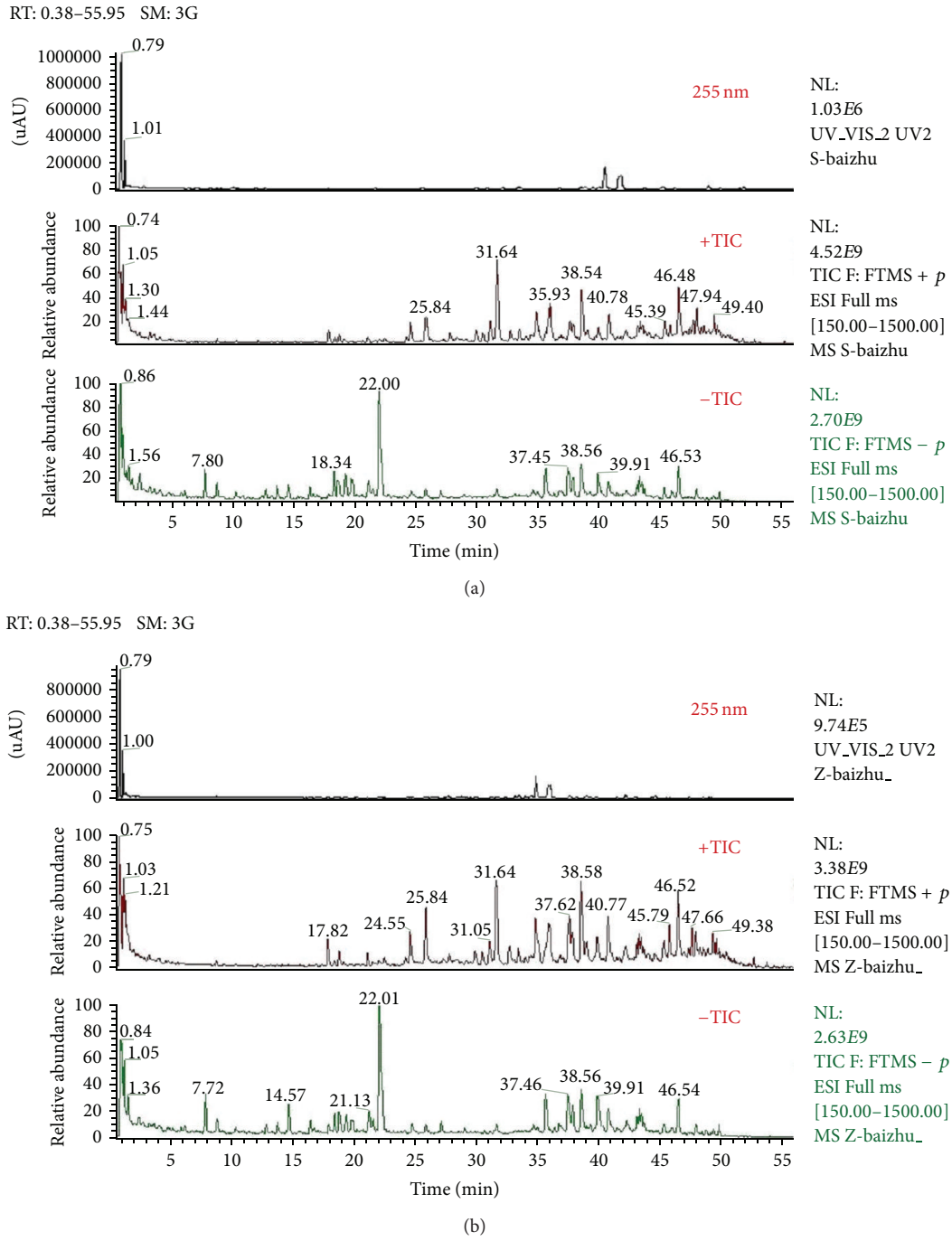

Figure 3: Total ion chromatograms of crude (a) and processed (b) Atractylodis Macrocephalae Rhizoma obtained from both positive and negative ion modes.

the compounds of interest, a scan range of m/z 150–1500 was chosen. Resolution for higher energy collisional dissociation cell (HCD) spectra was set to 17,500 at m/z 150 on the Q Exactive.

3. Results and Discussion

3.1. Identification of the Main Components in Crude and Processed Paeoniae Radix Alba. Tentative identification of the main compounds in crude and processed Paeoniae Radix Alba samples was generated based on elemental composition data determined from accurate mass measurements and comparison with the literature data. The total ion chromatograms of crude and processed Paeoniae Radix Alba samples obtained from both positive and negative ion modes were shown in Figure 1. In the preliminary study, the Q Exactive mass spectrometer was confirmed to be highly selective and sensitive. Under the present chromatographic and MS

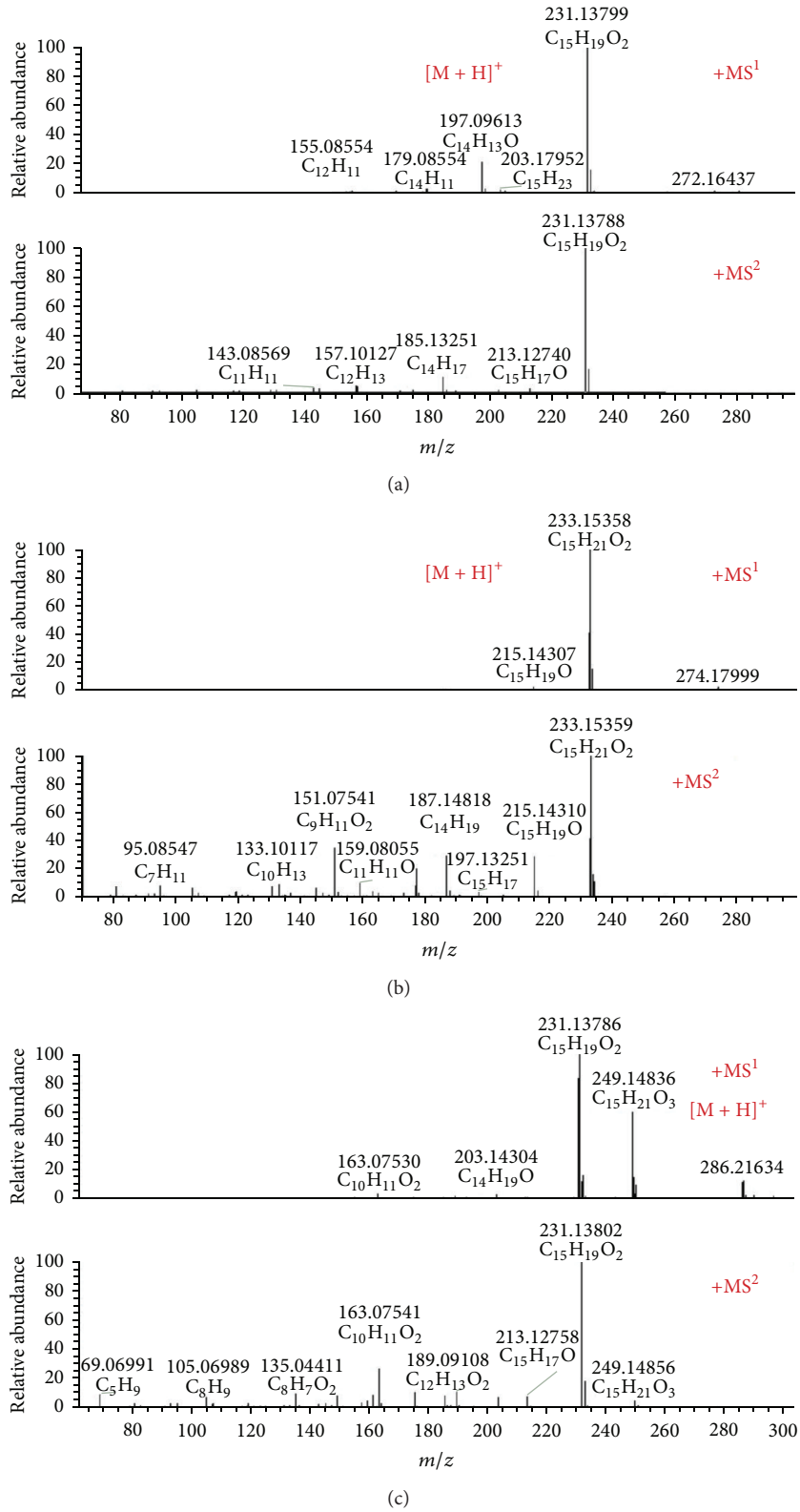

Figure 4: Mass spectra of atractylenolide I (a), atractylenolide II (b), and atractylenolide III (c).

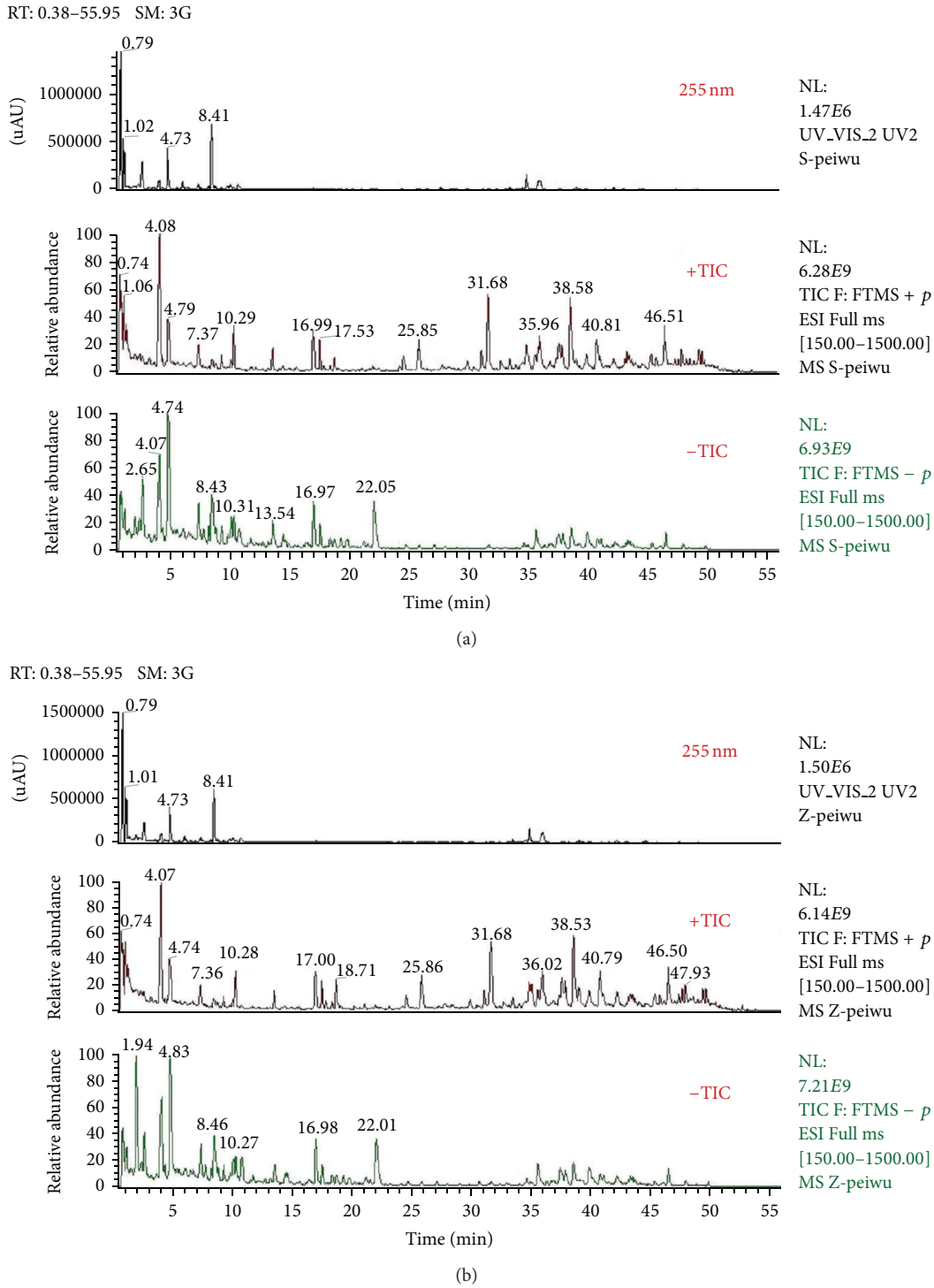

Figure 5: Total ion chromatograms of crude (a) and processed (b) Paeoniae Radix Alba-Atractylodis Macrocephalae Rhizoma herbal pair obtained from both positive and negative ion modes.

conditions, 123 and 101 compounds were identified in crude and processed Paeoniae Radix Alba samples, respectively. Compounds 16, 30, 31, 42, 45, 58, 59, 61, 62, 63, 64, 75, 78, 80, 87, 90, 91, 94, 95, 103, 112, and 120 were not detected in processed Paeoniae Radix Alba sample. Meanwhile, the ESI-MS data of crude and processed samples demonstrated that the peak areas of components 8, 113, and 122 varied significantly, and their amounts were dramatically increased in processed sample. The results were shown in Table 1.

From ESI-MS information, it was found that the sensitivities for all kinds of components in Paeoniae Radix Alba were high in both positive and negative ion modes.

In present study, we chose peaks 1, 2, and 3 to explain the identification process using Q Exactive high-performance benchtop quadrupole-Orbitrap LC-MS/MS. Peaks 1, 2, and 3 were eluted at retention times of 4.08, 4.79, and 8.47 min, respectively. Peak 1 showed the $[M+H]^+$ m/z 481.16986, $[2M+NH_4]^+$ m/z 978.35950, $[M-H]^-$ m/z 479.15591, $[M-H+HCOOH]^-$ m/z 525.16101, and $[2M-H+HCOOH]^-$ m/z 1005.32404 and the corresponding elemental compositions were $C_{23}H_{29}O_{11}$, $C_{46}H_{60}O_{22}N$, $C_{23}H_{27}O_{11}$, $C_{24}H_{29}O_{13}$, and $C_{47}H_{57}O_{24}$, respectively. On the basis of above data we deduced that the elemental composition of peak 1 was $C_{23}H_{28}O_{11}$. The molecular ion of peak 1 could lead to seven main MS^2 ions at m/z 319.11731, 197.08075, 133.06473, and 105.03342 in positive ion mode, and m/z 479.15594, 283.08231, and 121.02956 in negative ion mode. On the basis of the elemental compositions of fragment ions, peak 1 was assigned as albiflorin. Peaks 2 and 3 were therefore identified as paeoniflorin, and 1, 2, 3, 4, 6-penta-O-galloyl-beta-D-glucopyranose with above mentioned method. The mass spectra and proposed fragmentations of albiflorin, paeoniflorin, and 1, 2, 3, 4, 6-penta-O-galloyl-beta-D-glucopyranose were shown in Figure 2.

3.2. Identification of the Main Components in Crude and Processed Atractylodis Macrocephalae Rhizoma. Figure 3 showed the total ion chromatograms of crude and processed Atractylodis Macrocephalae Rhizoma samples obtained from both positive and negative ion modes. 32 and 26 compounds were identified in crude and processed Atractylodis Macrocephalae Rhizoma samples, respectively. Compounds 2, 4, 13, 14, 17, and 29 were not detected in processed Atractylodis Macrocephalae Rhizoma sample. Moreover, the amounts of compounds 3, 7, 9, 10, 21, 23, and 27 were substantially decreased, and the amounts of compounds 8, 18, and 22 were increased in processed sample compared with crude one. The results were shown in Table 2.

Atractylenolide I, atractylenolide II, and atractylenolide III are the main active compounds that belong to the sesquiterpenes in Atractylodis Macrocephalae Rhizoma. The mass spectra of atractylenolide I showed a $[M+H]^+$ ion at m/z 231.13799, which could lead to four MS^2 ions at m/z 213.12740, 185.13251, 157.10127, and 143.08569. The molecular ion of atractylenolide II ($[M+H]^+$ m/z 233.15358) could lead to six MS^2 ions at m/z 215.14310, 187.14818, 159.08055, 151.07541, 133.10117, and 95.08547. Meanwhile, the MS^2 spectrum of m/z 249.14836 from atractylenolide III contained six major fragment ions at m/z 231.13802, 213.12758, 189.09108, 163.07541, 135.04411, and 105.06989. The mass spectra of the above three compounds were shown in Figure 4.

3.3. Analysis of Chemical Changes of Paeoniae Radix Alba after Compatibility with Atractylodis Macrocephalae Rhizoma. In the present study, the Q Exactive high-performance benchtop quadrupole-Orbitrap LC-MS/MS based on chemical profiling approach was used to evaluate chemical constitution between co-decoction and single decoction of Paeoniae Radix Alba and Atractylodis Macrocephalae Rhizoma. For crude Paeoniae Radix Alba, the relative contents of most compounds were dramatically decreased except those of compounds 80, 90, 98, 113, 119, and 122 were significantly increased and 19 compounds were not detected after its compatibility with crude Atractylodis Macrocephalae Rhizoma. For processed Paeoniae Radix Alba, the relative contents of compounds 12, 36, 84, and 86 were remarkably increased except 12 compounds including pedunculagin, oxypaeoniflorin, 6-O-glucopyranosyl-lactinolide, 1, 2, 3, 6-tetra-O-galloylglucose isomer A, 1, 2, 3, 6-tetra-O-galloylglucose isomer B, tetragalloyl glucose C, galloylpaeoniflorin isomer II, hexagalloyl glucose, 3, 6-di-O-galloyl paeoniorin isomer, oxybenzoyl-oxypaeoniflorin, benzoyloxypaeoniflorin, and albiflorin R1 isomer III were newly generated and 13 compounds were not found after its compatibility with processed Atractylodis Macrocephalae Rhizoma. The results were presented in Figure 5 and Table 1.

3.4. Analysis of the Chemical Changes of Atractylodis Macrocephalae Rhizoma after Compatibility with Paeoniae Radix Alba. For crude Atractylodis Macrocephalae Rhizoma, the relative contents of compounds 17, 18, and 25 were increased clearly except those of compounds 6, 23, and 30 decreased considerably and six compounds including protocatechuic acid isomer I, protocatechuic acid isomer II, atracetylentriol, 12-methylbutyryl-14-acetyl-2E, 8EZ, 10E-atractylentriol, 12-methylbutyryl-14-acetyl-2E, 8EZ, 10E-atractylentriol isomer, and linoleic acid isomer were lost after its compatibility with crude Paeoniae Radix Alba. For processed Atractylodis Macrocephalae Rhizoma, compounds 9, 20, 26, 27, and 30 were not found except the relative contents of compounds 5, 6, and 8 were decreased while those of compounds 15, 19, 21, and 31 were increased after its compatibility with processed Paeoniae Radix Alba. Furthermore, compound 4 (protocatechuic acid isomer II) was not found in processed Atractylodis Macrocephalae Rhizoma but could be detected in processed Paeoniae Radix Alba-Atractylodis Macrocephalae Rhizoma herbal pair by using Exact Finder and MassFrontier softwares. The above results illustrated that Paeoniae Radix Alba significantly changed the components of Atractylodis Macrocephalae Rhizoma in solution when they decocted together. The corresponding results were presented in Figure 5 and Table 2.

4. Conclusions

Q Exactive high-performance benchtop quadrupole-Orbitrap LC-MS/MS is a powerful tool for discriminating the chemical changes between single herbal and co-decocting medicines. In our present study, the Q Exactive high-performance benchtop quadrupole-Orbitrap LC-MS/MS based on chemical profiling approach to investigate and evaluate chemical changes from crude and processed Paeoniae Radix Alba, crude and processed Atractylodis Macrocephalae Rhizoma, and their crude and processed herbal pair extracts was proposed. The results showed that processing and compatibility of TCM could significantly change the chemical composition of Paeoniae Radix Alba and Atractylodis Macrocephalae Rhizoma. The developed

method is considered to provide a scientific foundation for deeply elucidating the processing and compatibility mechanism of Paeoniae Radix Alba and Atractylodis Macrocephalae Rhizoma.

Conflict of Interests

The authors declare that there is no conflict of interests regarding the publication of this paper.

Authors' Contribution

Gang Cao, Qinglin Li, Hao Cai, and Sicong Tu contributed equally to this work.

Acknowledgments

This work was financially supported by the National Natural Science Foundation of China (nos. 81202918, 81173546, and 30940093), the Natural Science Foundation of Jiangsu Province, China (no. BK2009495), the International Science and Technology Cooperation Project of Jiangsu Province, China (no. BZ2011053), the Open Project of National First-Class Key Discipline for Science of Chinese Materia Medica, Nanjing University of Chinese Medicine (no. 2011ZYX2-006), the Project of Science and Technology for Chinese Medicine of Zhejiang Province, China (no. 2013KYB183), the Science and Technology Project of Hangzhou, China (nos. 20130533B68, 20131813A23), the Chinese Medicine Research Program of Zhejiang Province, China (nos. 2014ZQ008, 2008ZA002), the Project of Science Technology Department of Zhejiang Province, China (no. 2013C33SA1C0003), and the Science Foundation of Zhejiang Chinese Medical University (nos. 2011ZY25, 2013ZZ12).

References

[1] K. M. Qin, Y. C. Shu, G. Cao et al., "Thoughts and methods of Chinese materia medica processing—taking research on Rehmanniae Radix processing as an example," *Chinese Traditional and Herbal Drugs*, vol. 44, no. 11, pp. 1363–1370, 2013.

[2] K. M. Qin, L. J. Zheng, G. Cao et al., "Ideas and methods for mechanism research of traditional Chinese medicine processing—taking coffee beans roasting mechanism research as an example," *Scientia Sinica Chimica*, vol. 43, no. 7, pp. 829–839, 2013.

[3] S. L. Li, S. F. Lai, J. Z. Song et al., "Decocting-induced chemical transformations and global quality of Du-Shen-Tang, the decoction of ginseng evaluated by UPLC-Q-TOF-MS/MS based chemical profiling approach," *Journal of Pharmaceutical and Biomedical Analysis*, vol. 53, no. 4, pp. 946–957, 2010.

[4] C. Wang, Y. G. Wang, Q. D. Liang, W. Q. Rang, C. R. Xiao, and Y. Gao, "Analysis of chemical composition in combination of Aconitum and Fritillaria by UPLC/Q-TOFMS with multivariate statistical analysis," *Acta Chimica Sinica*, vol. 69, no. 16, pp. 1920–1928, 2011.

[5] Z. C. Ma, S. S. Zhou, Q. D. Liang et al., "UPLC-TOF/MS based chemical profiling approach to evaluate toxicity-attenuated chemical composition in combination of ginseng and Radix Aconiti Praeparata," *Acta Pharmaceutica Sinica*, vol. 46, no. 12, pp. 1488–1492, 2011.

[6] W. W. Peng, S. S. Liu, Y. Wang et al., "Effect of Compatibility of Radix Aconiti Lateralis Praeparate and Zingiber offiicinale Bosc. on the contents of four aconitum alkaloids," *Chinese Pharmaceutical Journal*, vol. 48, no. 4, pp. 258–261, 2013.

[7] L. J. Zheng, K. M. Qin, H. Cai, G. Cao, and B. C. Cai, "Optimization of extraction process for Baizhu Shaoyao San by multi-index orthogonal experiment," *China Journal of Chinese Materia Medica*, vol. 38, no. 10, pp. 1504–1509, 2013.

[8] X. C. Li, J. Lin, W. J. Han et al., "Antioxidant ability and mechanism of Rhizoma Atractylodes macrocephala," *Molecules*, vol. 17, no. 11, pp. 13457–13472, 2012.

[9] L. L. Yu, T. Z. Jia, and Q. Cai, "Research on the chemical references of Atractylodes Macrocephala Koidz," *Asia-Pacific Traditional Medicine*, vol. 6, no. 3, pp. 36–39, 2010.

[10] H. Cai, Z. W. Xu, S. C. Luo et al., "Study on chemical fingerprinting of crude and processed Atractylodes macrocephala from different locations in Zhejiang province by reversed-phase high-performance liquid chromatography coupled with hierarchical cluster analysis," *Pharmacognosy Magazine*, vol. 8, no. 32, pp. 300–307, 2012.

[11] S. H. Rong, H. Lin, and N. Gao, "Study on processing technology and processing principles of Atractrylodis Macrocephalae Rhizoma," *China Journal of Chinese Materia Medica*, vol. 36, no. 8, pp. 1001–1003, 2011.

[12] L. Yang, X. H. Xia, Q. Zhu, and X. P. Tan, "Study on the rule of influence of two purification methods on the chemical compositions in aqueous solution of Paeoniae Radix Alba," *Journal of Chinese Medicinal Materials*, vol. 36, no. 1, pp. 118–121, 2013.

[13] N. C. Luo, W. Ding, J. Wu et al., "UPLC-Q-TOF/MS coupled with multivariate statistical analysis as a powerful technique for rapidly exploring potential chemical markers to differentiate between radix paeoniae alba and radix paeoniae rubra," *Natural Product Communications*, vol. 8, no. 4, pp. 487–491, 2013.

[14] S. J. Huang, R. Wang, Y. H. Shi, L. Yang, Z. Y. Wang, and Z. T. Wang, "Primary safety evaluation of sulfated Paeoniae Radix Alba," *Acta Pharmaceutica Sinica*, vol. 47, no. 4, pp. 486–491, 2012.

[15] K. B. Kwon, E. K. Kim, M. J. Han et al., "Induction of apoptosis by Radix Paeoniae Alba extract through cytochrome c release and the activations of caspase-9 and caspase-3 in HL-60 cells," *Biological and Pharmaceutical Bulletin*, vol. 29, no. 6, pp. 1082–1086, 2006.

[16] Z. Q. Yu, R. M. Schmaltz, T. C. Bozeman et al., "Selective tumor cell targeting by the disaccharide moiety of bleomycin," *Journal of the American Chemical Society*, vol. 135, no. 8, pp. 2883–2886, 2013.

[17] T. Kabashima, Z. Q. Yu, C. H. Tang et al., "A selective fluorescence reaction for peptides and chromatographic analysis," *Peptides*, vol. 29, no. 3, pp. 356–363, 2008.

[18] J. Y. Pan and Z. Q. Yu, "Isolation and characterization of Hainantoxin-II, a new neurotoxic peptide from the Chinese bird spider (Haplopelma hainanum)," *Zoological Research*, vol. 31, no. 6, pp. 570–574, 2010.

Hindawi Publishing Corporation
Evidence-Based Complementary and Alternative Medicine
Volume 2014, Article ID 143286, 9 pages
http://dx.doi.org/10.1155/2014/143286

Research Article

Analysis of the Correlation between Commodity Grade and Quality of *Angelica sinensis* by Determination of Active Compounds Using Ultraperformance Liquid Chromatography Coupled with Chemometrics

Zenghui Wang, Dongmei Wang, and Linfang Huang

Institute of Medicinal Plant Development, Chinese Academy of Medical Sciences & Peking Union Medical College, Beijing 100193, China

Correspondence should be addressed to Linfang Huang; lfhuang@implad.ac.cn

Received 27 November 2013; Revised 28 February 2014; Accepted 8 March 2014; Published 14 April 2014

Academic Editor: Shi-Biao Wu

The contents of ferulic acid, senkyunolide A, butylidenephthalide, ligustilide, and n-butylphthalide were determined by UPLC analytical method; the correlation among the grade, average weight, and content was explored by correlation analysis and analysis of variance (ANOVA); the different commercial grades with average weight and content were revealed by principal component analysis (PCA) and then rationality analysis grade classification of *A. sinensis*. The results showed that various commercial grades can be distinguished by PCA analysis. And there was significant negative correlation between the commodity grades and average weight, commodity, and the content of bioactive compounds, while the content of senkyunolide A had significant negative correlation with commodity grades ($P < 0.01$). Average weight had no correlation with chemicals compounds. Additionally, there was significant positive correlation among the bioactive compounds (content of ferulic acid and phthalides) of different grades of *A. sinensis*. The content of senkyunolide A, butylidenephthalide, and ligustilide had significant positive correlation with the content of ferulic acid. The content of ligustilide and butylidenephthalide had significant positive correlation with the content of senkyunolide A. The content of ligustilide had significant positive correlation with the content of butylidenephthalide. The basis of grades classification is related with the difference levels of the bioactive compounds.

1. Introduction

Commercial specifications and grades of Chinese medicinal materials, the summary of practical experience (such as shape, size, texture, color, odor, and taste are based primarily on the human senses) for quality evaluation of traditional Chinese medicine, were the reflect of the quality of traditional Chinese medicine, which had played an important role in market circulation and ensuring clinical safety because it is easy, fast, and effective. However, most of these evaluation methods were still in the stage of experiential description which made it difficult to be inherited and applied. So far, the SFDA (State Food and Drug Administration) only issued 3 times of the commercial specification, involving 76 varieties, compared with the amount of commonly used trading of medicinal materials (more than 600 kinds); it is difficulty to satisfy the market demand [1].

Angelica sinensis (Danggui in Chinese) is one of the main exports of traditional Chinese medicine, derived from root of *Angelica sinensis* (Oliv.) Diels (Umbelliferae) [2], a well-known Chinese herbal medicine, first documented in Shennong Bencao Jing (Shennong's Classic of Materia Medica; 200–300 AD) [3, 4]. It has been used historically as a tonic, hematopoietic, and anti-inflammatory agent for the treatment of gynecological diseases such as menstrual disorders, amenorrhea, and dysmenorrheal for thousands of years in traditional Chinese Medicinal prescriptions [5, 6]. It has also been widely marketed as health food for women's care in Asia [7] and as a dietary supplement in Europe and America [8, 9]. However, quality assessment in the markets is extremely difficult and impractical when considering large number of export of this product.

Therefore, it is necessary to investigate the grades and quality assessment of *A. sinensis* [10–12]. This research took

Table 1: *A. sinensis* samples used in this study.

Commercial grades	Source	Species	Collection year
1st	Minxian, Gansu Cultivated in the normal soil for two years	*A. sinensis*	2012
1st	Minxian, Gansu Cultivated in the normal soil for two years	*A. sinensis*	2012
1st	Weiyuan, Gansu Cultivated in the normal soil for two years	*A. sinensis*	2012
1st	Minxian, Gansu Cultivated in the normal soil for two years	*A. sinensis*	2012
1st	Heqing, Yunnan Cultivated in the normal soil for two years	*A. sinensis*	2012
1st	Deyang, Sichuan Cultivated in the normal soil for two years	*A. sinensis*	2012
1st	Deyang, Sichuan Cultivated in the normal soil for two years	*A. sinensis*	2012
2nd	Dangxian, Gansu Cultivated in the normal soil for two years	*A. sinensis*	2012
2nd	Heqing, Yunnan Cultivated in the normal soil for two years	*A. sinensis*	2012
2nd	Shiyan, Hubei Cultivated in the normal soil for two years	*A. sinensis*	2012
3rd	Minxian, Gansu Cultivated in the normal soil for two years	*A. sinensis*	2012
3rd	Weiyuan, Gansu Cultivated in the normal soil for two years	*A. sinensis*	2012
3rd	Heqing, Yunnan Cultivated in the normal soil for two years	*A. sinensis*	2012
3rd	Deyang, Sichuan Cultivated in the normal soil for two years	*A. sinensis*	2012
3rd	Shiyan, Hubei Cultivated in the normal soil for two years	*A. sinensis*	2012
4th	Weiyuan, Gansu Cultivated in the normal soil for two years	*A. sinensis*	2012
4th	Deyang, Sichuan Cultivated in the normal soil for two years	*A. sinensis*	2012
4th	Weiyuan, Gansu Cultivated in the normal soil for two years	*A. sinensis*	2012
4th	Weiyuan, Gansu Cultivated in the normal soil for two years	*A. sinensis*	2012

A. sinensis as the study subject. We collected different commodity grades of *A. sinensis* in the main producing areas and determined the content of ferulic acid and ligustilides, which are thought to be the biologically active components [13–17] by UPLC method for studies of the correlation between grades and quality. The results are helpful to provide the basis for the establishment of medicinal industry standards.

2. Materials and Methods

2.1. Plant Materials. All the samples of *A. sinensis* were collected from Gansu, Yunnan, Sichuan, and Hubei province of China (Table 1, Figure 1). All the herbal samples were authenticated by Professor Lin Yulin, and the voucher specimens were deposited in the Institute of Medicinal Plant Development, Chinese Academy of Medical Sciences, Beijing, China.

2.2. Chemicals and Reagents. UPLC grade acetonitrile was from ThermoFisher, USA, analytical grade formic acid from Fisher, USA, and analytical grade method from Beijing chemical factory and deionized water was obtained from a Milli-Q water system (Millipore, Bedford, MA, USA). Ligustilide (Batch number: MUST-11072416), n-butylphthalide (Batch number: MUST-12020706), butylidenephthalide (Batch number: MUST-12071103), and senkyunolide A (Batch number: MUST-10102309) were purchased from the Chengdu Mansite, Biological Technology Co., Ltd. (all with purities > 98%).

2.3. Instrumentation. Instrumentation included Waters Acuity UPLC-PDA (Waters, USA, including quaternary solvent delivery system, vacuum degasser, autosampler, and Empower2 chromatography workstation), electronic analytical balance (Mettler, AB135-S), and Electro-Thermostatic Water Bath (Beijing Analytical Instrument Factory).

Figure 1: Different commercial grades of *A. sinensis* samples.

2.4. Preparation of Standard and Sample Solutions. The five reference compounds were accurately weighed: 1 mg dissolved in 10 mL volumetric flask with 70% methanol to produce standard stock solutions. The stock solution was diluted to yield a series of standard solution in the concentration range of 32–1722 μg/mL, 30–415 μg/mL, 156–722 μg/mL, 332–6786 μg/mL, and 33–2543 μg/mL for ferulic acid, senkyunolide, n-butylphthalide, ligustilide, and butylidenephthalide, respectively. Samples of herbal materials were ground into fine powder then passed through a 20 mesh (0.9 mm) sieve. Sample powder (0.2 g) was accurately weighed and transferred into a 60 mL round bottom flask. 70% methanol (20 mL) was added and refluxed for 30 min. When cool, the methanol was added to compensate for weight loss. After filtering through a 0.22 μm filter membrane, the filtrate was ready to be used.

2.5. Ultraperformance Liquid Chromatography. A 2 μL aliquot was analyzed on a 2.1 × 100 mm ACQUITY 1.7 μm BEH C_{18} column (Waters, Milford, MA) and maintained at 35°C using an ACQUITY UPLC system (Waters, Milford, MA). The mobile phases consisted of (a) acetonitrile and (b) water containing 0.1% formic acid. The UPLC elution conditions were optimized as follows: 95% A held for (2–4 min), 95% to 76% A (4–7 min), and 76% to 72% A (7-8 min), followed by 72% to 50% A (8–10 min), 50% to 30% A (10–12 min), 30% to 0% A (12–14 min), 0% A (held for 14-15 min), and 0% to 95% A (15-16 min). The flow rate was set at 0.30 mL/min. The column and autosampler were maintained at 35 and 5°C, respectively. The scan range for PDA was 261 nm and 281 nm. All experiments were performed in triplicate.

2.6. Validation of the UPLC Method

2.6.1. Calibration Curves. Methanol stock solutions of 5 reference compounds were prepared and diluted to appropriate concentrations for the construction of calibration curves. Six concentrations of the solution were analysed in triplicate; the calibration curves were constructed by plotting the peak areas against the concentrations of the analytes. The stock solutions mentioned above were diluted to a series of appropriate concentrations with methanol, and an aliquot of the diluted solutions were injected into UPLC-DAD for analysis. The stock solutions mentioned above were diluted to a series of appropriate concentrations with methanol, and an aliquot of the diluted solutions were injected into UPLC-DAD for analysis. The limits of determinations (LODs) and limits of quantifications (LOQs) under the present conditions were determined at signal to noise (S/N) ratio of about 3 and 10, respectively.

2.6.2. Precision, Accuracy, and Stability. Intra- and interday variations were chosen to determine the precision of the UPLC method. 0.2 g of *A. sinensis* sample was extracted and analysed as described in Sections 2.3 to 2.5. The intraday variability test was performed by triplicate extraction and analysed during a single day. The interday variability test was carried out on three different days. Variations were expressed by the relative standard deviations (R.S.D.) for intra- and interday. The recovery test was used to evaluate the accuracy of the method. Accurate amounts of ferulic acid, senkyunolide, n-butylphthalide, ligustilide, and butylidenephthalide were added to approximately 0.25 g of *A. sinensis* sample and then extracted and analysed as described in Section 2.3. The average recoveries were calculated by the following formula: recovery(%) = (amount found − regional amount)/amount spiked × 100%. For the stability test, *A. sinensis* sample was accurately weighed (approximately 0.5 g) and ultrasonic-extracted with 2.0 mL of methanol for 30 min at room temperature. The samples were then analysed at 0, 2, 4, 6, 8, 12, 24, and 36 h with the established method. The relative standard deviations (R.S.D.) of five data were used to evaluate the stability.

2.7. Statistical Methods. Spearman rank correlation analysis was carried out by SPSS system for windows release version 19.0 (SPSS Institute, Cary, NC, USA), the normality, mean, standard deviation (SD), median, and the outlier range of the *A. sinensis*; the values of the standard quality characteristics were acquired on the basis of mean ± SD.

Table 2: Calibration curves, LODs, LOQs, and precision for ferulic acid, senkyunolide A, n-butylphthalide, ligustilide, and butylidenephthalide.

Reference samples	Calibration curves	R^2	Test ranges (mg/mL)	LODs (μg/mL)	LOQs (μg/mL)
Ferulic acid	$Y = 3E + 07X + 2835.3$	0.9999	0.032~1.722	4.15	11.06
Senkyunolide A	$Y = 2E + 07X + 5256.2$	1	0.030~0.415	4.57	11.78
n-Butylphthalide	$Y = 7E + 07X + 295390$	0.999	0.156~0.722	5.33	12.56
Ligustilide	$Y = 6E + 07X + 11594$	0.9999	0.332~6.786	5.74	13.32
Butylidenephthalide	$Y = 9E + 07X + 420771$	0.9991	0.033~2.543	5.12	12.73

3. Results and Discussion

3.1. Method Optimization. In sample preparation procedure, multifarious solvents, such as different concentrations (10%, 30%, 50%, 70%, and 90%) of ethanol and methanol, were tested and 70% methanol solution was selected because of its excellent dissolving capacity for *A. sinensis* sample. For UPLC analysis, two mobile phase systems, including acetonitrile-water and methanol-water, in various proportions were compared and different mobile phase additives, such as phosphate buffer, formic acid, and acetic acid, were also investigated, and finally, 0.1% formic acid aqueous solution and acetonitrile were used as mobile phases which could provide satisfactory separation and peak shapes of investigated compounds. In addition, ferulic acid and phthalides substances absorb different wavelengths under the UV conditions. Ten times difference of response value in the same substance under different wavelengths. 281 nm was employed as the detection wavelength since the difference of response value among ferulic acid, senkyunolide A, n-butylphthalide, and ligustilide compared with the response values under the maximum absorption wavelength was not obvious, while response values under 281 nm are only 1/10 compared with 261 nm, which is difficult to observe in the chromatogram. Therefore, 261 nm was chosen as detection of butylidenephthalide wavelength.

3.2. Method Validation. The linearity, regression, and linear ranges of five analytes were determined using the developed UPLC-PDA method. The data indicated a good relationship between concentrations and peak areas of the analytes within the test ranges ($R^2 \geq 0.9990$). The LOQs and LODs of all analytes were less than 4.15 and 11.06 mg/mL. The overall RSDs of intra- and interday variations for analytes were not more than 4.49% and 6.54%, respectively. The established method also had acceptable accuracy with spike recovery of 98.33–102.22% for all analytes. As to stability test, the RSDs of the peak areas for analytes detected within 24 h were lower than 4.72% (Table 2). All these results demonstrated that the developed UPLC method was linear, sensitive, precise, accurate, and stable enough for simultaneous quantification of the five investigated compounds in *A. sinensis*.

3.3. Quality of Five Analytes in A. sinensis Samples. The developed UPLC method was successfully employed for simultaneous determination of the five major active components in 19 *A. sinensis* samples collected from different localities. Typical chromatograms of reference compounds (a) and *A. sinensis* samples (b) were shown in Figure 3. The chemical structure of the reference compounds were shown in Figure 2. The identification of the investigated compounds was carried out by comparison of their retention time and UV spectra with reference chemicals. The contents of five investigated compounds in 19 *A. sinensis* samples were summarized in Table 3.

19 batches of different region of *A. sinensis* were determined, as shown in Figure 4. The sequence of ferulic acid content is Yunnan (0.14%~0.15%) > Gansu (0.04%~0.12%) > Sichuan (0.01%~0.02%) > Hubei (0.005%~0.006%). The ferulic acid contents in Yunnan and Gansu were accorded with the quality level request in Chinese Pharmacopoeia 2010 (≥0.05%), of which the highest content of ferulic acid was Yunnan sample. While the ferulic acid content of *A. sinensis* in Sichuan and Hubei was far below the standard of Chinese Pharmacopeias, they were substandard samples.

3.4. The Correlation among the Main Chemical Compounds, Average Weight, and Grades. The grade of whole *A. sinensis* was divided into five by using grading measurement method. From the data on the correlation coefficients between the main chemical compounds, average weight versus grades in Table 4, respectively, we can see that significantly negative correlation exists between average dry weight versus grades and the content of senkyunolide A versus grades ($P < 0.01$), which indicates that the higher the grade of *A. sinensis*, the heavier the weight. From the level of 1, 2, 3, 4, to 5, the average weight decreased gradually; the result coincident with the fact. And the content of senkyunolide A decreased with the increase of grade. Average weight had no correlation with the main chemicals compounds.

Table 5 showed that 1–5 grades were analyzed by ANOVA; there were significant differences in content of ferulic acid and phthalides of different grades of *A. sinensis* (Table 5). As shown in Figure 5, the content of senkyunolide A, butylidenephthalide, and ligustilide had significant positive correlation with the content of ferulic acid. The content of ligustilide and butylidenephthalide had significant positive correlation with the content of senkyunolide A. The content of ligustilide had significant positive correlation with the content of butylidenephthalide. We found the content of ligustilide somehow related to the content of ferulic acid, senkyunolide A, and butylidenephthalide, which indicates that ligustilide and senkyunolide A serious possibility be one of the pharmacological biomarkers compounds in *A. sinensis* [18–22].

Table 3: Contents of ferulic acid, phthalides, and average weight of *A. sinensis* for different commercial grades.

Grade	Ferulic acid mg/g	Senkyunolide A mg/g	n-butylphthalide mg/g	Ligustilide mg/g	Butylidenephthalide mg/g	Average weight g
1st	1.061	0.226	0.442	3.121	1.306	28.429
1st	1.094	0.215	0.551	3.002	1.589	42.592
1st	0.842	0.099	0.194	2.540	0.847	34.265
1st	0.405	0.101	0.340	2.060	0.717	33.457
1st	1.364	0.301	0.153	3.379	1.431	54.81
1st	0.113	0.055	0.255	0.440	0.097	57.253
1st	0.059	0.054	0.284	0.400	0.121	74.985
2nd	1.198	0.086	0.468	3.215	1.309	27.598
2nd	1.496	0.235	0.244	4.243	1.603	79.09
2nd	0.056	0.020	0.343	0.431	0.103	52.095
3rd	0.622	0.141	0.365	2.695	1.295	41.63
3rd	0.836	0.829	0.411	5.551	2.146	31.045
3rd	1.389	0.142	0.226	3.582	1.362	116.31
3rd	0.15	0.052	0.258	0.588	0.065	84.52
3rd	0.049	0.019	0.313	0.497	0.083	92.35
4th	0.653	0.090	0.311	2.596	0.865	39.605
4th	0.185	0.092	0.27	0.552	0.051	56.053
4th	0.978	0.189	0.258	3.396	1.509	45.748
4th	1.085	0.077	0.310	3.081	1.053	37.943

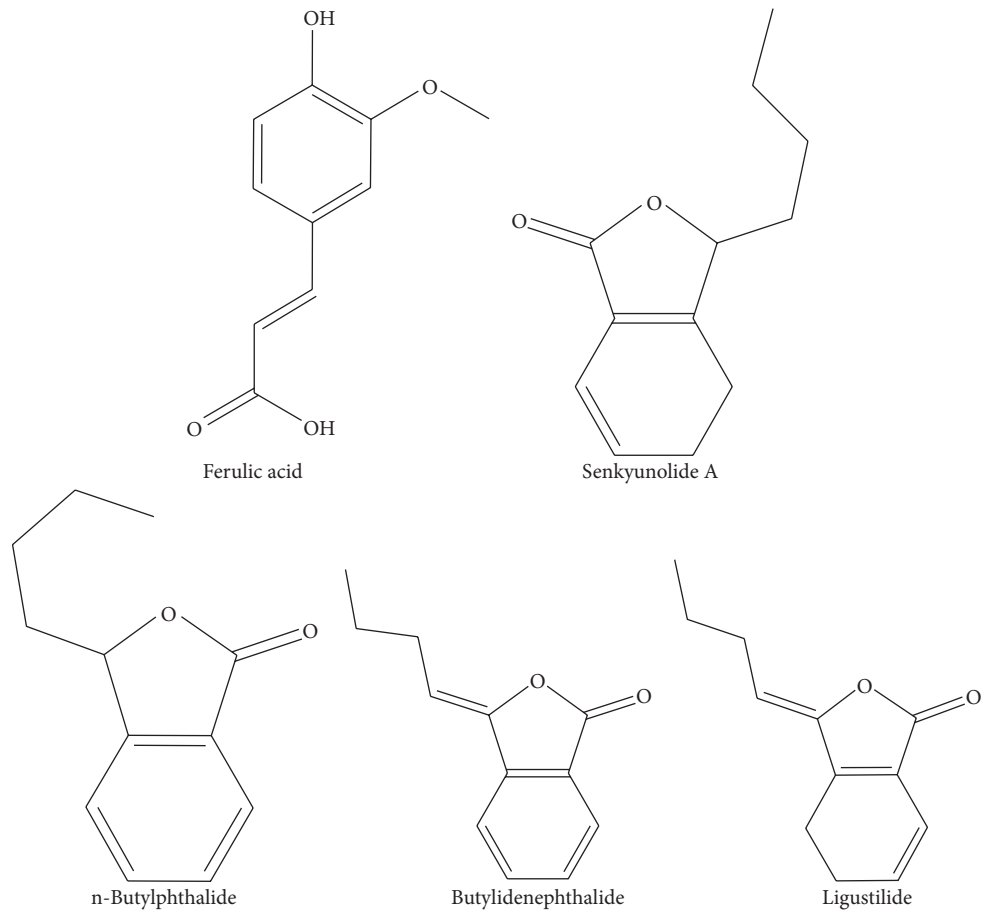

Figure 2: Chemical structures of ferulic acid and phthalides.

Table 4: The correlation among the main chemical compounds, weight, and grades of *A. sinensis*.

	Grade	Average weight	Ferulic acid	Senkyunolide	n-Butylphthalide	Ligustilide	Butylidenephthalide
Grade	1.000						
Average weight	−0.603**	1.000					
Ferulic acid	−0.089	0.01	1.000				
Senkyunolide A	−0.501*	−0.031	0.682**	1.000			
n-Butylphthalide	0.019	−0.361	−0.143	0.015	1.000		
Ligustilide	0.088	−0.012	0.863**	0.568*	0.903	1.000	
Butylidenephthalide	−0.029	−0.022	0.805**	0.582**	0.616	0.895**	1.000

**$P < 0.01$ (bilateral). The correlation is significant.
*$P < 0.05$. The correlation is significant.

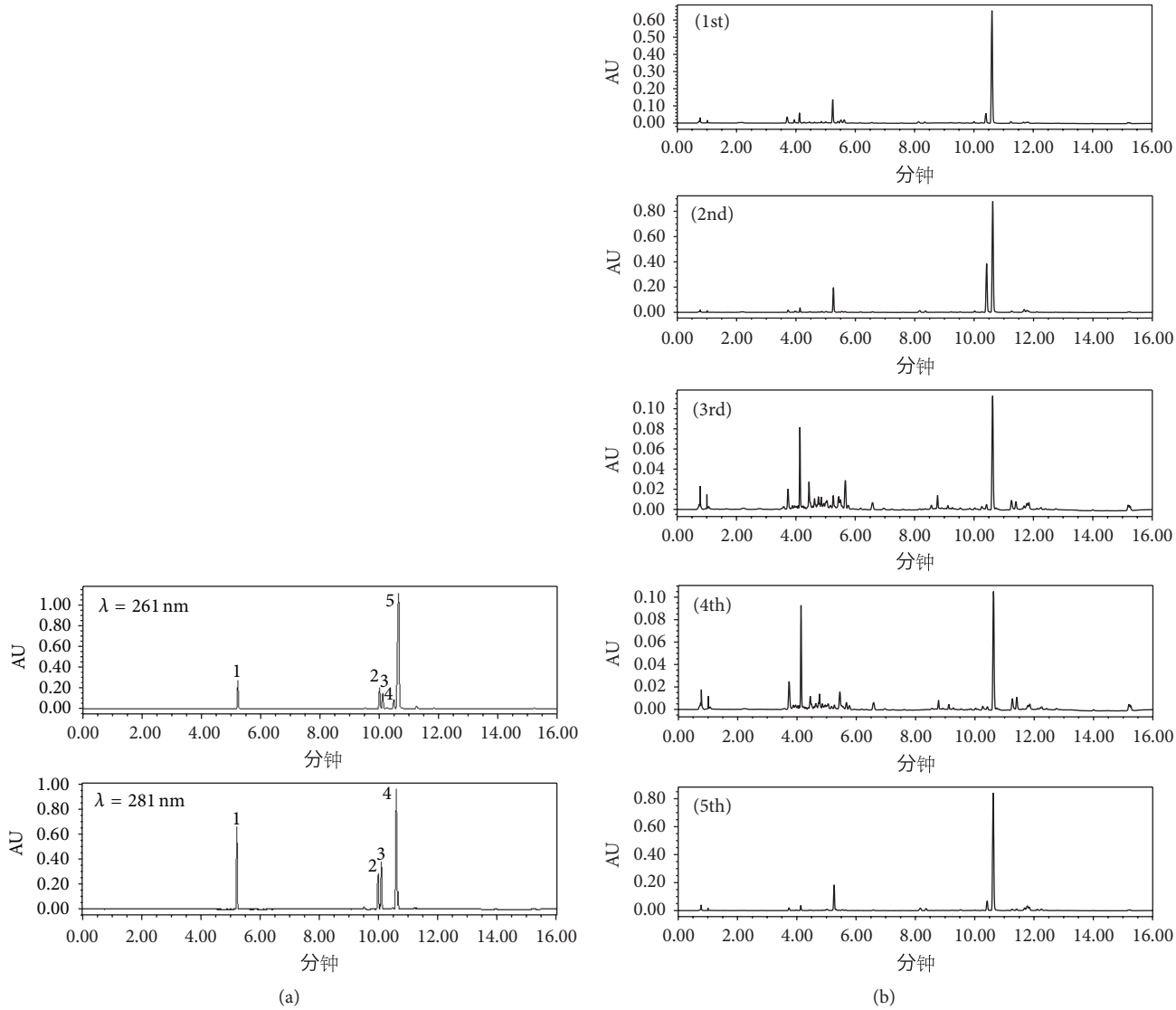

Figure 3: The UPLC chromatograms of reference standards (a) and different commercial grades *A. sinensis* samples (b). (1) Ferulic acid. (2) Senkyunolide A. (3) n-Butylphthalide. (4) Ligustilide. (5) Butylidenephthalide.

Table 5: Variance analysis of average weight, the chemical compounds, and grades.

		AVG	DF	SD	SE	P
Grade	Average weight	51.7778	18	24.5124	5.6235	0.046
	Ferulic acid	−1.7034	18	1.4675	0.3367	0.94
	Senkyunolide A	−2.2619	18	1.3978	0.3209	0.985
	n-Butylphthalide	−2.1055	18	1.4026	0.3218	0.614
	Ligustilide	−0.03321	18	1.9209	0.4406	0.619
	Butylidenephthalide	−1.4973	18	1.5016	0.3445	0.811
Average weight	Ferulic acid	53.4812	18	24.6503	5.6551	0.621
	Senkyunolide A	54.0397	18	24.6324	5.6511	0.271
	n-Butylphthalide	53.8832	18	24.6305	5.6507	0.042
	Ligustilide	51.8110	18	25.0694	5.7513	0.221
	Butylidenephthalide	53.2751	18	24.8041	5.6904	0.181
Ferulic acid	Senkyunolide A	0.5585	18	0.4661	0.1069	0.010
	Ligustilide	−1.6702	18	1.1058	0.2537	0.000
	Butylidenephthalide	−0.2061	18	0.3458	0.0793	0.000
Senkyunolide A	Ligustilide	−2.2287	18	1.3804	0.3167	0.000
	Butylidenephthalide	−0.7647	18	0.5475	0.1256	0.001
Ligustilide	Butylidenephthalide	1.4641	18	0.8750	0.2007	0.000

$P < 0.05$, significant difference.

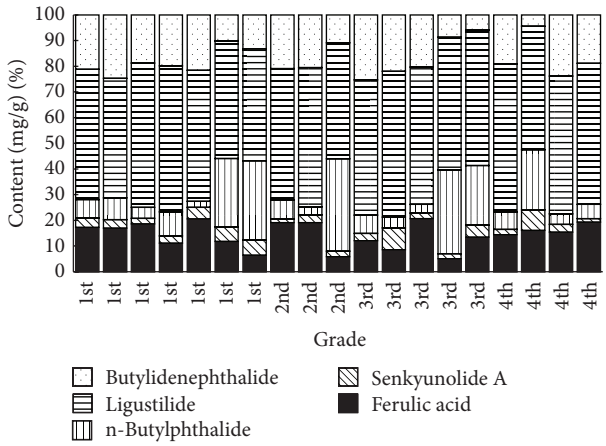

Figure 4: The content of ferulic acid, senkyunolide A, n-butylphthalide, ligustilide, and butylidenephthalide for different commercial grades of *A. sinensis* samples.

Figure 6 shows that *A. sinensis* samples were divided into 5 main clusters observed in the PCA scores plot. In Figure 6(a), such division indicated that different grades could significantly distinguish from 1st to 5th by the different average weights of *A. sinensis*, while Figure 6(b) indicated that grades were distinctly separated by different contents of the chemical compounds. This result reflected rationality of grades classification.

4. Conclusion

In summary, the contents of ferulic acid, senkyunolide A, butylidenephthalide, ligustilide, and n-butylphthalide were determined by UPLC analytical method. The correlation among the grade, average weight, and content was explored by correlation analysis and analysis of variance (ANOVA); the different commercial grades with average weight and content were revealed by principal component analysis (PCA) and then rationality analysis classification of grade and quality of *A. sinensis*. The results showed that various commercial grades can be distinguished by PCA analysis. And there were significant negative correlation between the commodity grades and average weight, commodity, and the content of bioactive compounds. While the content of senkyunolide A had significant negative correlation with commodity grades ($P < 0.01$), average weight had no correlation with chemicals compounds. Additionally, there was significant positive correlation among the bioactive compounds (content of ferulic acid and phthalides) of different grades of *A. sinensis*. The content of senkyunolide A, ligustilide, and butylidenephthalide had significant positive correlation with the content of ferulic acid. The content of ligustilide and butylidenephthalide had significant positive correlation with the content of senkyunolide A. The content of ligustilide had significant positive correlation with the content of butylidenephthalide.

Quality standards for *A. sinensis* components are described in the Chinese Pharmacopoeia, such as percentage of total ash, acid-insoluble ash, and alcoholic extract content; ferulic acid content is also described. Our results suggest

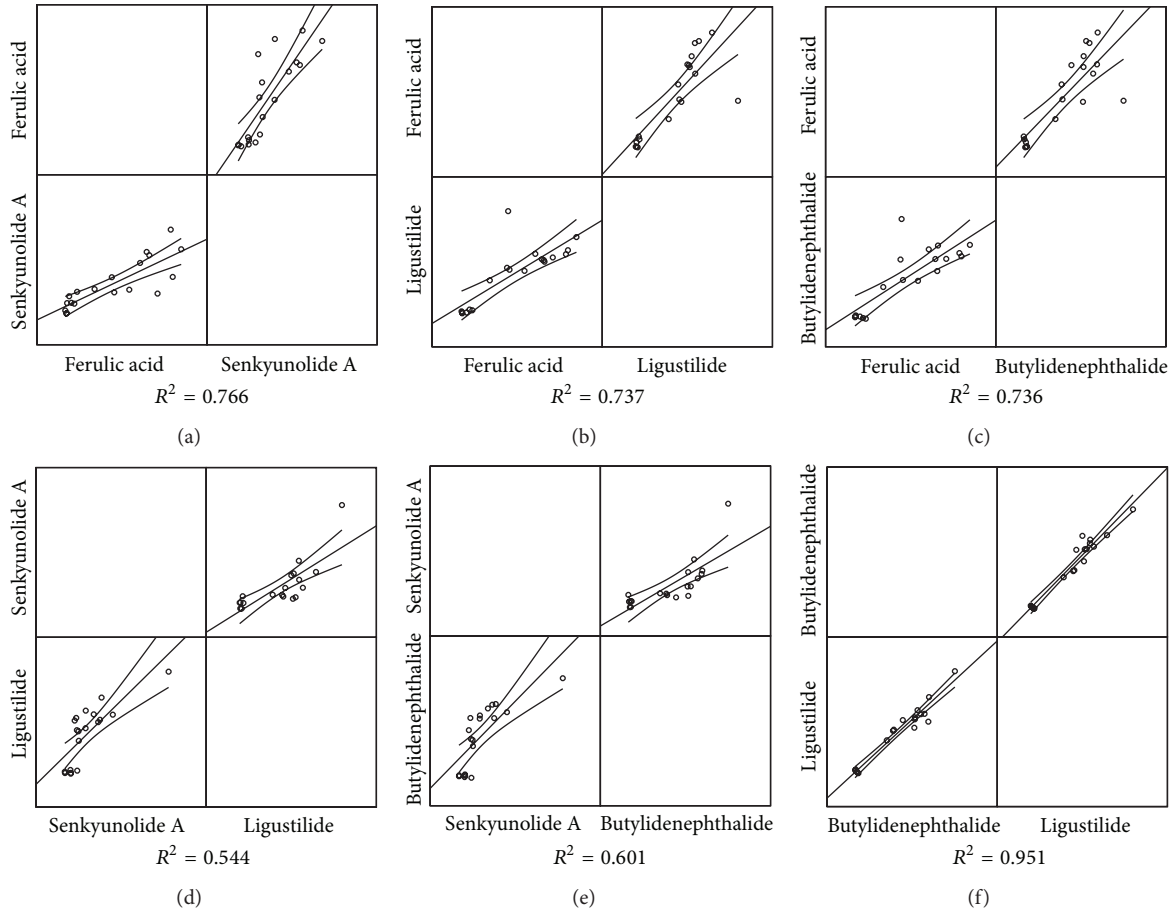

Figure 5: The correlation among chemical ingredients of *A. sinensis*.

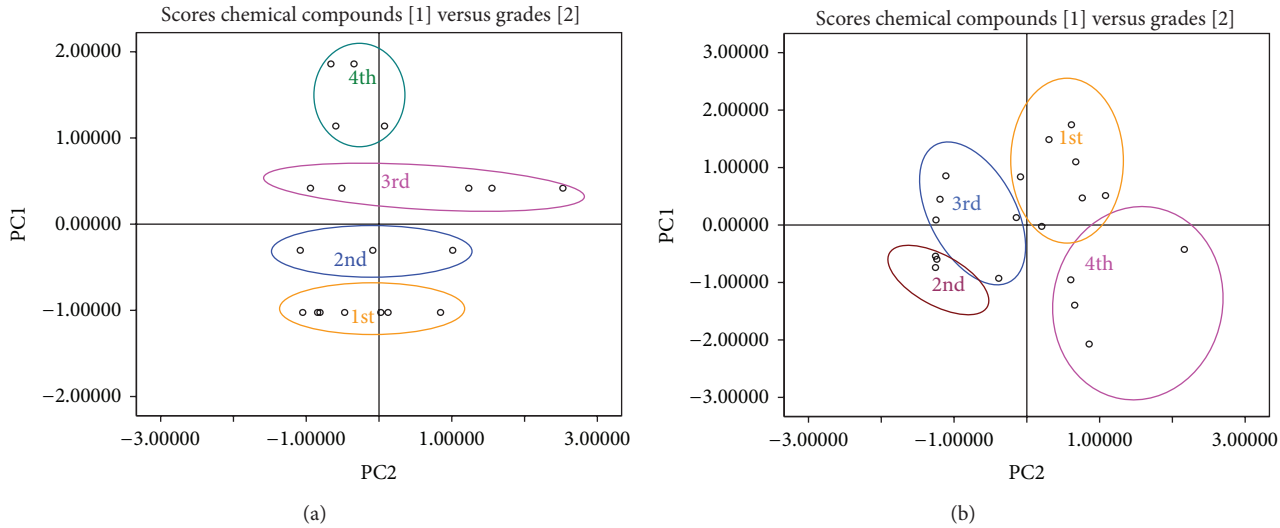

Figure 6: PCA (scores plot) of average weight versus grades (a) and chemical compounds versus grades (b) of *A. sinensis*.

that senkyunolide A is a candidate for an efficient marker to define a radix quality standard. This work will provide useful references for the quantification and standardization of quality control for *A. sinensis*.

Conflict of Interests

The authors have declared that there is no conflict of interests.

Acknowledgments

The study was supported by Grants from the National Natural Science Foundation of China (no. 81274013), Key National Natural Science Foundation of China (81130069), the Chinese National S&T Special Project on Major New Drug Innovation (2011ZX09307-002-01), and The Program for Changjiang Scholars and Innovative Research Team in University of Ministry of Education of China (IRT1150). The funders had no role in study design, data collection and analysis, decision to publish, or preparation of the paper.

References

[1] J. S. Li, B. Wu, Z. Q. Cao, and W. M. Fu, "The changes of traditional Chinese medicine commodity specification," *Capital Medicine*, vol. 2, no. 3, pp. 41–42, 2012.

[2] *State Pharmacopoeia Committee: Pharmacopoeia of the People's Republic of China 2010*, China Medical Science and Technology Press, Beijing, China, 2010.

[3] C. Liu, J. Li, F. Y. Meng et al., "Polysaccharides from the root of *Angelica sinensis* promotes hematopoiesis and thrombopoiesis through the PI3K/AKT pathway," *BMC Complementary and Alternative Medicine*, vol. 10, article 79, 2010.

[4] "Monograph. *Angelica sinensis* (Dong quai)," *Alternative Medicine Review*, vol. 9, pp. 429–433, 2004.

[5] W. Cao, X. Q. Li, X. Wang et al., "A novel polysaccharide, isolated from *Angelica sinensis* (Oliv.) Diels induces the apoptosis of cervical cancer HeLa cells through an intrinsic apoptotic pathway," *Phytomedicine*, vol. 17, no. 8-9, pp. 598–605, 2010.

[6] J. L. Lü, J. Zhao, J. A. Duan, H. Yan, Y. P. Tang, and L. B. Zhang, "Quality evaluation of *Angelica sinensis* by simultaneous determination of ten compounds using LC-PDA," *Chromatographia*, vol. 70, no. 3-4, pp. 455–465, 2009.

[7] T. L. Dog, "Menopause: a review of botanical dietary supplements," *The American Journal of Medicine*, vol. 118, no. 12, pp. 98–108, 2005.

[8] S. Deng, S. N. Chen, P. Yao et al., "Serotonergic activity-guided phytochemical investigation of the roots of *Angelica sinensis*," *Journal of Natural Products*, vol. 69, no. 4, pp. 536–541, 2006.

[9] X. Mao, L. Kong, Q. Luo, X. Li, and H. Zou, "Screening and analysis of permeable compounds in radix *Angelica sinensis* with immobilized liposome chromatography," *Journal of Chromatography B: Analytical Technologies in the Biomedical and Life Sciences*, vol. 779, no. 2, pp. 331–339, 2002.

[10] X. M. Ouyang, Y. M. He, J. R. Zhu, J. Q. He, X. Ma, and Y. H. Ding, "Primary study on the ferulic acid contents in different commercial grades of Gansu Angelica," *Chinese Pharmaceutical Affairs*, vol. 19, no. 7, pp. 423–4426, 2005.

[11] J. A. Duan, X. H. Xiao, S. L. Su, R. H. Zhao, and H. Yan, "Discussion on formation mode of TCM commodity specification," *Modern Chinese Medicine*, vol. 11, no. 6, pp. 14–17, 2009.

[12] Y. Liu, "The extraction and determination of *Angelica polysaccharides*," *Research and Practice on Chinese Medicines*, vol. 17, pp. 49–52, 2003.

[13] N. Xin, C. E. Lup, and Y. Mo, "The content comparison of ferulic acid in different levels in *Angelica*," *Journal Chinese Medicine Material*, vol. 24, no. 4, pp. 244–246, 2001.

[14] X. Yang, Y. Zhao, and Y. Lv, "*In vivo* macrophage activation and physicochemical property of the different polysaccharide fractions purified from *Angelica sinensis*," *Carbohydrate Polymers*, vol. 71, no. 3, pp. 372–379, 2008.

[15] C. X. Liu, P. G. Xiao, and D. P. Li, *Modern Research and Application of Chinese Medicinal Plants*, Hong Kong Medical Publisher, Hong Kong, China, 1st edition, 2000.

[16] J. Y. Tao, Y. P. Ruan, Q. B. Mei et al., "Studies on the antiasthmatic action of ligustilide of dang-gui, *Angelica sinensis* (Oliv.) Diels," *Acta Pharmaceutica Sinica*, vol. 198, no. 8, pp. 561–565, 1984.

[17] W. C. Ko, "A newly isolated antispasmodic—butylidenephthalide," *Japanese Journal of Pharmacology*, vol. 30, no. 1, pp. 85–91, 1980.

[18] C. M. Teng, W. Y. Chen, W. C. Ko, and C. Ouyang, "Antiplatelet effect of butylidenephthalide," *Biochimica et Biophysica Acta—General Subjects*, vol. 924, no. 3, pp. 375–382, 1987.

[19] Z. Shi, J. He, M. Zhao, and W. Chang, "Simultaneous determination of five marker constituents in traditional Chinese medicinal preparation Le-Mai granule by high performance liquid chromatography," *Journal of Pharmaceutical and Biomedical Analysis*, vol. 37, no. 3, pp. 469–473, 2005.

[20] Z. B. Dong, S. P. Li, M. Hong, and Q. Zhu, "Hypothesis of potential active components in *Angelica sinensis* by using biomembrane extraction and high performance liquid chromatography," *Journal of Pharmaceutical and Biomedical Analysis*, vol. 38, no. 4, pp. 664–669, 2005.

[21] K. J. Zhao, T. T. X. Dong, P. F. Tu, Z. H. Song, C. K. Lo, and K. W. K. Tsim, "Molecular genetic and chemical assessment of radix Angelica (Danggui) in China," *Journal of Agricultural and Food Chemistry*, vol. 51, no. 9, pp. 2576–2583, 2003.

[22] G. H. Lu, K. Chan, C. L. Chan, K. Leung, Z. H. Jiang, and Z. Z. Zhao, "Quantification of ligustilides in the roots of *Angelica sinensis* and related umbelliferous medicinal plants by high-performance liquid chromatography and liquid Chromatography-mass spectrometry," *Journal of Chromatography A*, vol. 1046, no. 1-2, pp. 101–107, 2004.